DISTRIBUTION OF URANIUM IN GRANITES AND MOBILITY OF URANIUM DURING LOW-TEMPERATURE ALTERATION PROCESSES

Submitted by Bala Bello Muhammad Dewu

to the University of Exeter

as a Dissertation for the degree of Doctor of Philosophy

in the Faculty of Science.

I certify that all material in this thesis which is not my own work has been identified and that no material is included for which a degree has previously been conferred upon me.

September, 1989

CONTENTS

Content	Page
Acknowledgements	vii
Summary	1
CHAPTER ONE: INTRODUCTION	4
1.1 Preview	4
1.2 Background	6
1.3 Objective and Scope of the Study	8
1.4 Location, Geography and Climate	10
1.5 Geology of the Areas	15
1.6 Uraniferous Mineralisation associated With the Nigerian Younger Granites.	21
CHAPTER TWO: RADIOELEMENTS IN THE NATURAL ENVIRONMENT	24
2.1 Introduction	24
2.2 Naturally Occurring Radioelements	26
2.3 Primordial Element Abundance and Distribution	29
2.4 Origin of Granites	31
2.5 Abundance and Distribution of U, Th and K in the Crust	33
2.6 Geochemical Controls on the Abundance and Distribution of U, Th and K	38

2.6.1 Radioactive Properties 38

2.6.1.1 Systematics of Nuclear Decay 38

2.6.1.2 Radioactive Decay Series 45

2.7 Chemical Properties of U 55

2.8 Interpretation 62

CHAPTER THREE: ALTERATION OF GRANITE - HYDROTHERMAL AND WEATHERING PROCESSES

3.1 Introduction 64

3.2 Hydrothermal Alteration 65

3.2.1 Introduction 65

3.2.2 Sources of Hydrothermal Solutions 66

3.2.3 Hydrothermal Convective Circulation Systems in Granites 70

3.2.4 Permeability and Fluid Movement in Hydrothermal Systems 71

3.2.5 Recharge and Alteration 82

3.2.6 Deposition of U in Hydrothermal Systems 87

3.3 Weathering Processes 90

3.3.1 Introduction 90

3.3.2 Processes in Granite Weathering 91

3.3.3 Geochemistry of Granite Weathering 99

3.3.4 Measures of Weathering 107

3.4 Conclusions 110

CHAPTER FOUR: GEOCHEMICAL BEHAVIOUR OF U IN THE NIGERIAN YOUNGER GRANITES 112

4.1 Introduction 112

4.2 Analytical Methods in Geochemistry 112

4.3 Sample Description 115

4.4 Geochemical Controls of U in Granitic Rocks 118

4.5 Sample Collection and Preparation 120

4.6 Discussion of Results 123

4.6.1 General Geochemical Features 123

4.6.2 Major Element Variation 131

4.7 Geochemical Behaviour of U in the Nigerian Younger Granites 141

4.7.1 Abundance and Distribution 141

4.7.2 Element Associations and Variation 147

4.7.3 U Mineralisation in the Granite 161

4.8 Conclusions 166

CHAPTER: 5 DISTRIBUTION OF U IN THE NIGERIAN YOUNGER GRANITES AND AND THE KAOLINISED GRANITES OF SOUTH-WEST ENGLAND

5.1 Introduction 168

5.2 Principles of Autoradiography 169

5.3 Methods and Techniques in Alpha Autoradiography 175

5.4 Location of U in granite 180

5.5 Localization of U and Th in the Nigerian Younger Granites and Kaolinised Granites from South-West England. 183

5.6 Track Registration and Developing Films 184

5.7 Track Examination and Mineral Identification 186

5.8 Discussion of Results 188

5.9 Conclusions 218

CHAPTER SIX: GAMMA-RAY SPECTROMETRY OF GRANITE AND GRANITE-RELATED MATERIALS

6.1 Introduction 221

6.2 Properties of Gamma-Rays 223

6.3 Principles of Gamma-Ray Spectrometry 230

6.4 Gamma-Ray Spectrometry and U-Series Disequilibrium 232

6.5 Gamma-Ray Spectrometric Procedures 238

6.6 Data Reduction 254

6.7 Discussion of Results 258

6.8 Conclusions 286

CHAPTER SEVEN: INVESTIGATION OF U SERIES DISEQUILIBRIUM IN GRANITE AND GRANITE-RELATED MATERIALS

7.1 Introduction 289

7.2 Secular Equilibrium 300

7.3 Secular Disequilibrium 306

7.4 Methods in Disequilibrium Studies 315

7.5 Investigation of Disequilibrium in the U Series in the Nigerian Younger Granites, and their Associated Soils, and the Kaolinised Granites of South-West England 323

7.5.1 Preparation of Sample Solution 324

7.5.2 Spiking with ^{236}U and ^{229}Th 326

7.5.3 Column Preparation and Separation of U from Th

7.5.4 Electrodeposition 332

7.5.5 Alpha-Particle Counting and Analysis 334

7.6 Results 335

7.7 Conclusions 349

CHAPTER EIGHT: KAOLINISATION AND U MOBILITY

8.1 Introduction 352

8.2 Clays and Clay Minerals 353

8.3 Kaolinisation 357

8.4 Hydrothermal activity and kaolinisation in South-West England 359

8.5 Kaolinsation Index 366

8.6 GEOCHEMISTRY OF KAOLINISATION OF GRANITES 369

8.6.1 Granite Textures 369

8.6.2 Sample Collection 372

8.6.3 Results 373

8.6.3.1 Element Variation 373

8.6.3.2 U Mobility During Kaolinisation 406

8.7 Conclusions 414

CHAPTER 9: LATERITIZATION AND U MOBILITY

9.1 Introduction 417

9.2 Processes in Soil Formation	418
9.3 Lateritization	423
9.4 Lateritization on the Jos Plateau	425
9.5 Mobility of U in Low Temperature Alteration Processes	428
9.6 Soil Survey	434
9.6.2 Sample Collection and Analysis	434
9.6.2 Sample Description	435
9.6.3 Discussion of results	436
9.6.4 Mobilisation of U During Lateritization	464
9.7 SOIL RN INVESTIGATIONS	477
9.7.1 Rn in the Natural Environment	477
9.7.2 Soil ^{222}Rn in U Exploration	481
9.7.3 ^{222}Rn Distribution in the Soils of the Jos Plateau	488
9.7.3.1 ^{222}Rn Measurements	488
9.7.3.2 Results	492
9.8 Conclusions	503
CONCLUSION AND REMARKS	506
APPENDICES	514
REFERENCES	530

ACKNOWLEDGEMENTS

A number of people have contributed to the success of the work presented here. I am particularly grateful to Dr. E. M. Durrance for supervision, criticism and invaluable assistance throughout the research period. I am also indebted to Prof. C. M. Bristow of ECC international, who provided core samples for the initial work on kaolinised granites, arranged for permission to sample Park Pit and gave valuable advice. Chemical analyses of granite from Bodmin Moor were kindly made available to me by Dr. C. S. Exley to whom I am also grateful. With thanks I appreciate the assistance of Dr. M.J. Heath in all aspects of alpha spectrometry reported in this work. I am grateful to Mr. J. R. Merefield and Mr. Ian Stone for kind assistance in all aspects of laboratory work, Mr. Brian Evans for help with sample collection in South-West England, Mr. Jeff Jones for assistance with diagrams and preparing the photographs in the thesis, Mr. Geoffry Spencer for producing the thin sections used in the study, and Mrs. Val Ellis for assistance with most of the printing of the work.

with deep gratitude I acknowledge the kind gesture by Alh. Muhammad Ruma who provided full boarding accomodation throughout my stay in Bukuru for field work on the Jos Plateau. Mr. U. M Turaki and Alh. Mohammed Audi of the Nigerian Mining Cooperation kindly made available to me most of the equipment I used for sample collection. Mr. Adamu Mohammed and Mr. Abubakar Garba were most kind in helping with sample

collection. I am also grateful to all my collegues in Nigeria who helped with domestic matters which would otherwise detracted me from my research. In particular, Alh. Umar Abdullahi assisted with the transportation of samples to England, and Mall. Nurruddeen Abba Abdullahi dealt with many various difficulties.

Support and encouragement from all the members of my family was a constant source of help over the years, and is greatly appreciated. The cooperation and patience of my wife, Halima, who had to take care of our son, Mustapha, all by herself while this thesis was being written, is hereby highly appreciated. I also wish to register my deep gratitude to Alh. Mijinyawa Dikko, Turaki Babba, for his fatherly assistance, in whose care was my wife and son were placed throughout the period of writing this thesis.

A number of my collegues made my stay in Exeter memorable. In this respect I acknowledge the companionship of Mr. A. Tehrani, Mr. M. M. Saflo, Mr. M. Aqeel, Mr. M. Abdul-Rahman, Mr. H. Nikbakht and Mr. Abdul-Munim Ali.

Finally my gratitude to the management of Ahmadu Bello University for making available the funds for this study.

SUMMARY

The Nigerian Younger Granites are significantly enriched in U. The medium-grained types are more enriched in U than the coarse-grained varieties. It was found that U and Th are well correlated in the granites with an average Th:U ratio of 2.9. Both elements increase with increasing fractionation of the granites, but U abundance was subsequently greatly modified by late- and post-magmatic alteration processes. Potash metasomatism was observed to be associated with U depletion in the granites. The high U abundance and its geochemical associations suggests that the granites form a U province with the likely occurrence of vein-controlled U mineralisation in addition to the disseminated U-Sn mineralisation.

Most of the U in the granites is held in U-rich minerals. These minerals account for over 80% of the whole-rock U. Among these, uranothorite and some Rare Earth minerals have been identified, with the possible occurrence of large amounts of uraninite. Radioactive accessory minerals that also contribute to the whole-rock U abundances in the granites are, zircon, allanite, sphene, apatite, monazite, rutile and thorite. Zircon, allanite and sphene are especially common. Most of the U in the near-surface environment has been remobilised, such that in surface samples only only resistate minerals are preserved. During weathering, U has

released from U-rich minerals and precipitated as secondary phases. As a result, the ^{238}U decay series in samples collected from rock - rock out crops is in disequilibrium.

The soils associated with the Nigerian Younger Granites are enriched in U, which is mainly of recent origin. Formation of such secondary U minerals as carnotite and tyuyamunite in the soil has occurred during pedogenic processes. Large disequilibrium in the U series was observed, with ^{238}U enriched relative to its daughters. In addition fractionation of ^{238}U and ^{234}U has taken place.

Soil gas surveys for ^{222}Rn can be used to locate U in the bedrock of the Jos Plateau. This is because the very young age of the ^{238}U means that it has not had enough time to approach secular equilibrium with ^{226}Ra. Consequently, most of the ^{222}Rn in the soil is not supported by the soil ^{238}U.

Kaolinisation in South-West England brought about both physical and chemical changes to the granites. The processes led to a reduction in the density of the granites from about $2.65gcm^{-3}$ to $2.17gcm^{-3}$, and also involved the mobilisation of many elements. Element variation patterns indicate that kaolinisation took place in two main stages. Hydrothermal circulation is considered to be the major process involved in the kaolinisation of the granites.

In the main zones of kaolinisation, U is mainly held adsorbed onto clay minerals with only some U occurring in zircon. Although the U content of the kaolinised granite is still fairly high, an average of 9ppm, it has been found that kaolinisation

caused a substantial amount of U to be removed, especially that the altered zones occupy a very large volume. This U could have been redeposited to form rich ore deposits somewhere in the vicinity of the kaolinised granites. The U presently in the kaolinised granites is young, precipitated in recent times. It is believed that modern hydrothermal circulation systems believed to be operating in the granites, are responsible for kaolinisation and remobilisation of U in the granites.

CHAPTER ONE: INTRODUCTION

1.1 Preview

There are more than 100 U-bearing minerals, and these minerals are widely distributed in a variety of geological environments. Study of the distribution of U in geological environments dates back almost to the discovery of radioactivity by Bequerel in 1896. For example, the demonstration of the distribution of radioactive minerals in pitchblende by Step and Becke in 1904 (Bowie, 1954). These studies have succeeded in determining the minerals in which U occurs, and the non-uniformity of its distribution on the Earth's surface and in geological formations. In the Earth's crust, U has been shown to be concentrated more in igneous rocks than any other lithology.

In igneous rocks, U has been found to be concentrated more in the later granitic members of the differentiation series. Recent studies of distribution of U in granites have in turn shown that most of the U is concentrated in accessory minerals such as zircon, allanite, sphene, monazite, xenotime and epidote. However, in what are termed 'fertile granites', U is found mainly in primary U minerals such as uraninite. It is largely established that in granites the major rock-forming minerals carry very little or no U.

The occurrence of high levels of U in the Nigerian Younger

Granites was established in 1949 in a study by Mackay. Sporadic occurrences of U minerals such as pitchblende, uraninite, torbernite and autunite in the granites have been noted, but the distribution of these minerals within the granites is yet to be established. The only reported information concerns the fact that U in some locations occurs in pyrochlore. Recent studies of the radioactivity of the Younger Granites have shown, not suprisingly, that they are highly radioactive. Values of U concentration much higher than that of an average granite have been confirmed. Indeed, concentrations in excess of 2% have been determined (Dewu, 1986). Because of the large area occupied by these granites, and the fact that a large number of aeroradiometric anomalies have been recorded in the granites (Dewu, 1986), further investigation of U occurrences in the granites is needed, especially the possibility of secondary concentrations brought about by lateritic weathering processes.

In the Hercynian granites of South-West England, the occurrence of high levels of U has also been well established (Basham et al., 1982b). The distribution of U in the granites has also been extensively studied. U has been found to occur in accessory minerals similar to those listed for the Nigerian granites, although in studies by Basham et al. (1982b), the widespread occurrence of U in uraninite was recognised. Although some occurrences of U mineralisation are known in the area (Dines,

1956 and Jackson et al., 1982), which suggest a genetic association with extensive kaolinisation in the granites (Durrance et al., 1982), the development of these is limited in comparison with the amount of U thought to have been mobilised during kaolinisation. Again further study of U in relation to alteration of the granites is required. This is, therefore, an investigation of U mobility during lateritic weathering and kaolinisation of granites particularly with regard to the processes of alteration and possible development of U concentration of economic significance.

1.2 Background

To study U mobilisation requires fresh material against which alteration products can be compared. However, an important difficulty occurs when sample collection is limited to within a few centimetres of the ground surface. This is because the U in even apparently fresh rock could have been greatly mobilised by processes which are to be investigated. Measurements made on such samples may therefore not give precise information of the nature of the U unaltered occurrence at depth. This problem may, however, be resolved by knowledge of disequilibrium in the U decay series.

In both areas of this study, low temperature alteration processes bring about differential mobility of the various daughters in the U decay series. For example, U occurrences with

disequilibrium favouring the ^{238}U group of nuclides, indicate recent U deposition (<10^6 yrs) must have taken place, but where disequilibrium favours the daughter nuclides, then leaching of U must have taken place within the same time frame. In both cases, with the identification of the process involved, it is possible to estimate the place of deposition and the possible mode and amount of transport involved. Another cause may be the accumulation of daughter nuclides, more especially caused by Rn. The redistribution depends on the mobility of the daughter element under the alteration process involved. By tracing these changes though materials altered to different degrees it is often possible to determine the character of the unaltered parent, even though totally fresh samples may not be available.

Because water is the main agent of low temperature alteration, the redistribution of the elements during rock-water interactions has been extensively studied in previous work on the processes of weathering and kaolinisation. Element mobility studies have been aimed at determining such parameters as the nature of transport mechanism, deposition conditions and the amount of the element involved. Methods mostly employed in such studies have included comparison of the element abundances in the ''fresh'' parent material with their abundance in product of the alteration, and leaching experiments, in which the alteration processes are simulated in the laboratory. In the former approach, the difficulty

of obtaining fresh material has been overcome by the determination of various indices of alteration, to indicate to what extent the alteration process has operated. In the laboratory simulation of the processes operative in nature, models which take into account all the various parameters involved have yet to be realised.

1.3 Objective and Scope of the Study

The study thus aimed at investigating the mineralogical distribution of U in granite, and the mobility of U during low temperature alteration processes, with particular reference to kaolinisation of the granites of South-West England and lateritization of the Nigerian Younger Granites. Also, the effect of these on the interpretation of radiometric determinations was considered. A combination of geophysical, geochemical and geological methods was employed in the study.

Airborne gamma-ray surveys of the Jos Plateau in Nigeria indicated a number of anomalies associated with the Younger Granites, as previously mentioned. It has long been argued that with the similarities that exists between the Younger Granites in Nigeria and those in Niger, which host a number of important U deposits, there is every possibility of the Nigerian Younger Granites hosting U mineralisation of economic importance. Specialised granites in the complexes of the Younger Granites have

received great attention as regards their U potential. In this study it was hoped to investigate the mode of occurrence of U in the different granites in order to specify its mobility in the soil-forming processes which affect these granites.

Kaolinisation in the granites of South-West England is also known to affect U distribution. Of particular interest is the association of deeply kaolinised zones with areas of low gamma-ray activity shown by an airborne radiometric survey of the region. In this study, the mobilisation of U during kaolinisation was investigated to determine if primary U minerals believed to be the main host of U in the granites were stable within the hydrothermal circulation systems thought to be responsible for deep kaolinisation. Knowledge of the distribution of U during kaolinisation would also lead to better understanding of the processes involved.

For the investigation of deep kaolinisation in South-West England, samples from the St. Austell granite were preliminarily investigated to develop methodology. In particular, a kaolinisation index to form the basis for assessing the degree of alteration was determined from these samples. A kaolinised zone, Park Pit, on Bodmin Moor, worked by English China Clays International was then studied in detail. The pit covered an area of about $1.7.10^4 m^2$.

For the study of the Nigerian Younger Granites, the Jos-Bukuru complex was sampled. This is an area with good exposure, and

no apparent mass movement of the soil. Many of the rock types of the Younger Granite complexes are exposed at a number of locations. In addition, the area was convenient for radiometric surveying.

However, within the the Jos - Bukuru complex a great deal of tin mining has taken place. Also the tailings left after the initial mining operations are now being reworked. These factors complicated the selection of specific sites for investigation.

1.4 Location, Geography and Climate

The Jos - Bukuru complex is one of the Younger Granite ring complexes on the Jos Plateau. Its relation to the other complexes is given in Figure 1.1. The Bodmin Moor granite is one of the major intrusions of Hercynian Granite in South-West England. In the Jos Plateau, the specific area of work is east of Bukuru, between 8^{o} 56' and 8^{o} 59'N, and 9^{o} 43' 20'' and 9^{o}. This is one of the major areas of tin production on the Jos Plateau, with important mines at Delimi and Rayfield. The northern and north-eastern parts have good outcrop and there is presently no major mining activity, except for the mine at Delimi. Small-scale mining is, however, common in this area as well as elsewhere on the Jos Plateau, with local open-cast mines along decomposed mineral veins. Around Rayfield laterite has been extensively mined for

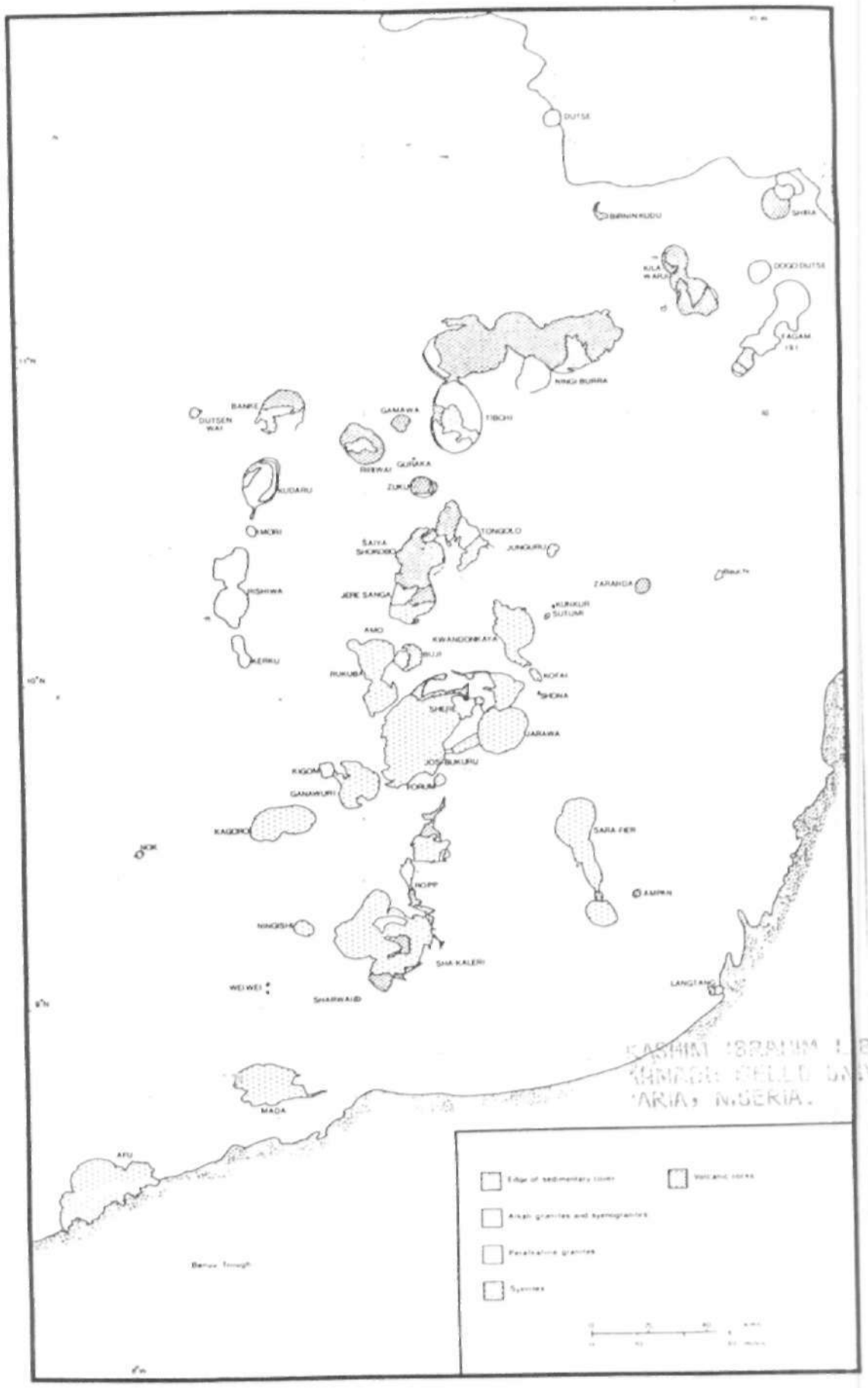


FIGURE 1.1 Location of the Jos - Bukuru complex

(From Kinnaird, 1981)

KASHIM IBRAHIM LIBR
AHMADU BELLO UNIVE
ARIA, NIGERIA.

building material. Indeed, in the ground east of Rayfield the scenery has been completely transformed by these operations, with large areas excavated to great depth. In the south, around Sabon Gida, alluvial deposits along the Bukuru river are still being mined, and a hill near Kuru is being worked for tin. Within the area, there are not many major roads, but there is a good network of minor motorable roads mostly made for the mining operations. Small streams exist in the area, the most notable being the Bukuru River, which passes through Bukuru, and the Forum River, which has been dammed at Buga da gindi. The area around Bukuru is mainly flat with ocassional hills rising above the surrounding plateau. Many of these hills provide large areas of rock outcrop. The hills at Shen, Du, and Sabon gari are at 120m, 90m and 250m above the surrounding plain, which itself stands at 1280m above sea level. To the north-east, an almost continuous hill reaches from Laminga up to Maijuju. In the north of the area rise the Shere hills, which forms the highest points on the Jos Plateau at an elevation of 1840m. These are defined by very steep slopes down the surrounding plain.

Because of its altitude, the climate of the Jos Plateau is mild for a tropical region. The change in temperature in approaching the region from the surrounding areas is quite dramatic. The average annual temperature is about $22^{o}C$, with temperatures falling as low as $5^{o}C$ in the coldest months of December to February. Rainfall averages 1387mm, second only to the

Mambila Plateau in Gongola, in the Northern part of the country. The rainy season usually starts much earlier, and ends later than in the other parts of Northern Nigeria. Some precipitation even during the dry months, is not uncommon.

Although rainfall is plentiful, there is a general absence of trees on the Plateau. Vegetation on the Jos - Bukuru complex is mainly grasses with scattered shrubs, especially on dissected hilly outcrop. Trees are mainly restricted to areas around dwelling places, where mango trees and forestry plantations have been developed. However, very little of the area is farmed because of the hardness of the ground.

The Bodmin Moor granite is one of the major intrusions of Hercynian Granite in South-West England, the others being Dartmoor, Carnmenellis, St. Austell, and Lands End. It covers an area of about 200km^2 and contains major china clay producing areas. Park Pit, investigated in this study, is situated at the southern edge of the pluton. Together with Stannon Pit, the only other pit being worked presently, it produces about 200,000 tonnes of china clay per annum (Bristow and Exley, 1988). Surrounded by farmlands, there is a general absence of outcrops around the Pit.

The climate of South-West England is mild compared to other parts of Britain with warmer summers and winters. Snow fall during the winter is generally restricted to high ground. The influence of the sea and the elevation of the moors produce localised climates,

with particularly high rainfall, strong winds and a wide temperature range experienced by much of the granite areas. Rainfall averages 1016mm annually in the low-lying area, and 2032mm on high Dartmoor (Edmonds et al., 1975). Temperatures range from -5°C in January to 22°C in the summer months.

Natural vegetation is largely determined by soil type and the weather conditions. Trees are confined to valleys, while in much of the intervening ground the vegetation is characterised by heather, bracken, gorse and tough grasses.

The high rainfall with very little evaporation provides conditions for abundant surface drainage in the form of rivers and streams. Major rivers include the Fal, Fowey, Warlegan, and De Lank. The large amount of surface drainage provides the area with an abundant water resource. Most public supplies are taken from surface waters, with reservoirs created along many of the major rivers.

1.5 Geology of the Areas

The Jos - Bukuru complex lies in the northern part of Jos Plateau and forms one of the post-orogenic intrusions of the Younger Granites. The geology of the complex is shown in Figure 1.2. Most of the rock types of the Jos Plateau are represented in this complex. The Younger Granites are dated as Jurassic, with an

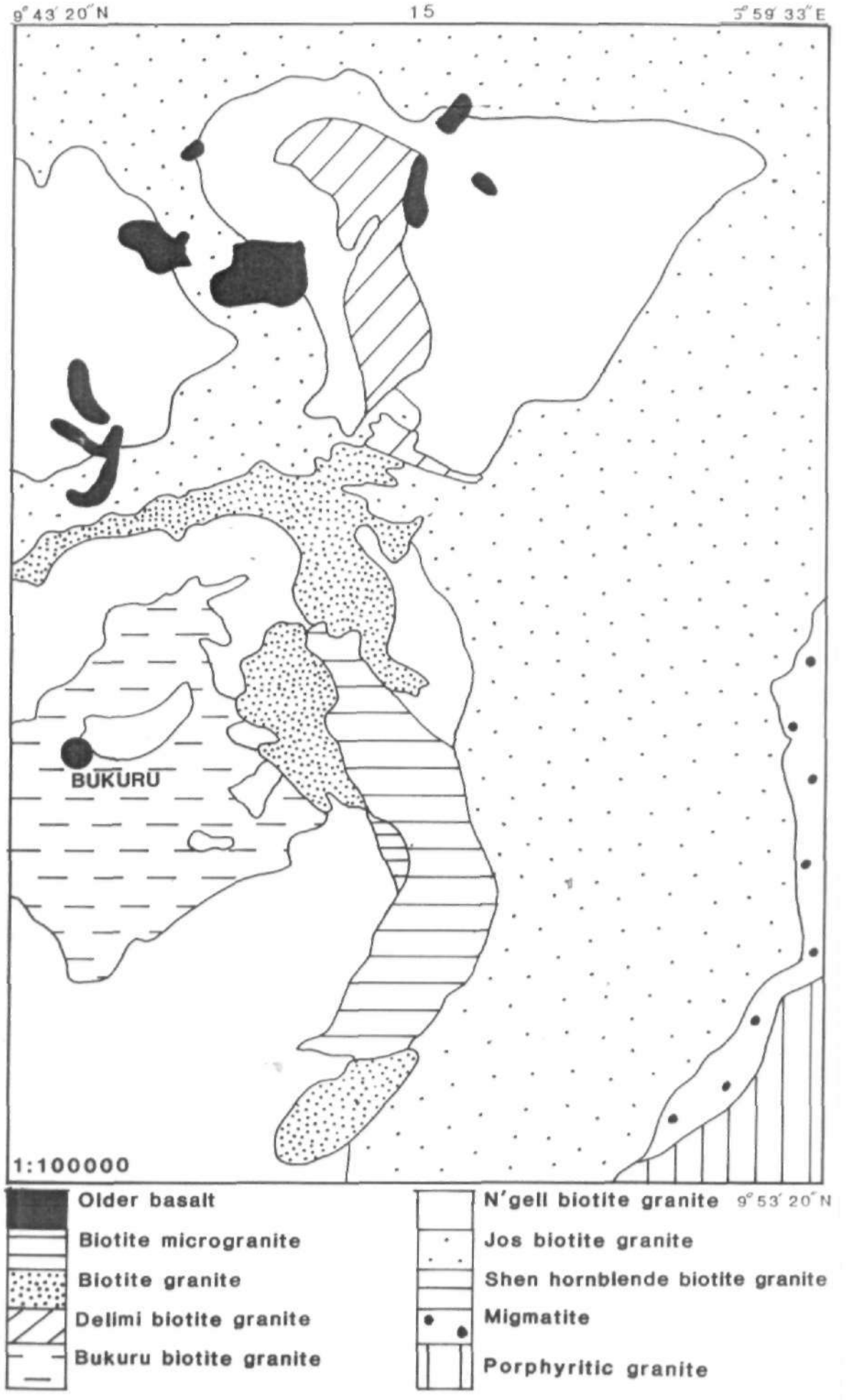


FIGURE 1.2 Geology of the area around Bukuru

age of 161Ma years for the Jos - Bukuru complex (Kinnaird et al., 1985).

The major events associated with the emplacement of the Younger Granites are believed to have taken place in three separate cycles, each cycle being responsible for certain pulse of igneous activity. The first cycle is the emplacement of an early granite porhyry, typified by the Neil's valley porphyry and the Naraguta porphyry, and some rhyolite. The second intrusive cycle of activity emplaced the early granites, as shown in the Kuru, N'ge'll and Jos biotite granites, and the riebeckite granites. The third cycle saw the emplacement of the main granites, typified by the Delimi, Sabon gida, Bukuru and Rayfield-Gona biotite granites, and the Vom microgranite. These three cycles are believed to have been preceded by a phase of emplacement of ring dykes. The distribution of these dykes has been used to delineate the tectonic history of the Younger Granites. The occurrence of the rhyolite is restricted to the northern end of the complex, while the porphyrys are confined to the western edge of the intrusion (Sheet 168: Naraguta).

The main part of the complex consist of biotite granite and biotite microgranite. The biotite granite is generally coarse-grained and contains many quartz veins with a dominant north-south trends. Pink feldspars with a diameter of about 1cm or more are common in the exposures around Laminga and Rayfield. This lithology is the most affected by weathering. The other rock types, notably

the Shen hornblende-fayalite granite, which is best exposed at Shen, are medium-grained and show more resistance to weathering -the large hill at Shen extending for about 5km with no sign of decomposition, and its contact with the surrounding plain is generally steep. The granites of this cycle are found associated with dykes, especially at Delimi and between Tin-Tin and Dogo na Hauwa. Generally these dykes are doleritic and are usually steeply dipping (Macleod, 1977). The later intrusive events produced important mineralisation, as shown by the association of columbite and cassiterite mineralisation with the biotite granites and the biotite-microgranites. The cassiterite mineralisation occurs in veins and stringers embedded within the granites. These veins are found to contain a wide spectrum of ore minerals. In addition to the vein mineralisation, the granites are also enriched with disseminated ore minerals. These form concentrations with tin minerals in the decomposed granites. The richest concentrations of cassiterite have been observed to occur towards the roof of the intrusions, with the highest concentrations being found in the most shallowly eroded intrusions. Two processes are believed to be responsible for the mineralisation: (1) late-stage magmatic dissemination, and (2) hydrothermal circulation. Pastor and Turaki (1985) identified hydrothermal quartz-sulphide-cassiterite and quartz-wolframite-cassiterite veins occurring as fissure infillings in the biotite granites. Moreover, where hydrothermal process are

extensive, vein deposits of Sn, Zn, W, and Nb with Cu, Fe, Bi, U and the Rare earth elements have been recognised (Kinnaird, 1985). This hydrothermal activity has also been found to be responsible for the concentration of ore minerals in the albitized granites. In the biotite granites, evidence of hydrothermal alteration includes greisens and quartz veins with halos of kaolinised channels (for example, in the area around Buga da gindi).

Bodmin Moor forms one of the surface expression of the granite batholith which underlies much of South-West England (Figure 1.3). The batholith, believed to have been emplaced during the Variscan orogeny, has been dated at 290-280Ma. The tectonic events that operated during the orogeny are believed to be largely due to north-south compression. This produced northward transport of nappes over the southerly dipping thrusts. Unroofing of the batholith exposed the individual granite plutons. The granites have been classified into six main groups (Exley and Stone, 1982; Exley et al., 1983). The six groups are (1) basic microgranite (type-A), (2) coarse-grained megacrystic biotite granite (type-B), (3) fine-grained biotite granite (type-C), (4) megacrystic Li-mica granite (type-D), (5) equigranular Li-mica granite (type-E), and (6) fluorite granite (type-F). The granites typified by the type-B shows much textural variation even within single intrusions but generally they are much coarser than the other granite types. Differences are also noted in the sizes and concentrations of

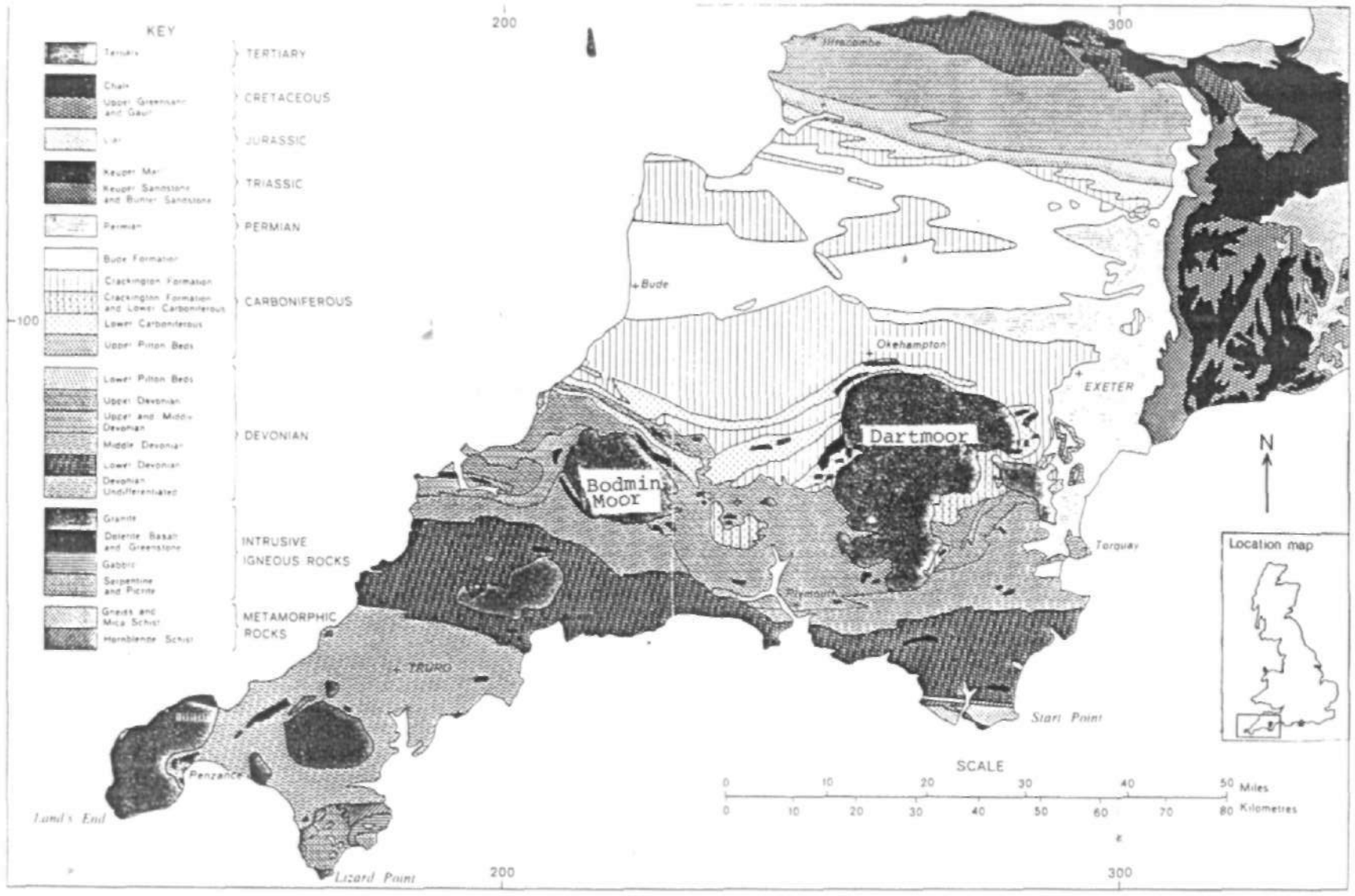


FIGURE 1.3 Geology of South-West England

megacryst among the various granite intrusions in the region. The Bodmin Moor granite is composed mainly of type-B. Post-magmatic events have played a great role in the mineralisation observed in these plutons. These events are believed to have taken place in stages, each stage contributing to the evolution of the province. In the early stages, hydrothermal activity was mainly associated with magmatic fluids. This has been identified as being responsible for sheeted vein deposits. This stage was characterised by mineralising solutions of temperatures of about 350^{o}C and salinities in the range of 19 to 27 eq. wt% NaCl (Alderton, 1978; Shepherd, et al., 1985). Following this was an extended period of hydrothermal mineralisation by fluids derived mainly from meteoric water. For these circulation systems episodes of enhanced mantle heat flow were supplemented by a continuous output of radiogenic heat from the granites themselves. This activity is believed to have started in the Permian and may still be operational (Durrance, 1983). It is this ongoing circulation which is thought to be responsible for the origin of the deep kaolinisation deposits in the region.

1.6 Uraniferous Mineralisation associated With the Nigerian Younger Granites.

U in the Nigerian Younger Granite have often been associated with pyrochlore. This mineral is found widely distributed in the riebeckite granite and related rock types in the ring complexes other occurrences of U in a number of localities associated with the Nigerian Younger Granites have also been reported. The earliest note of the occurrence of radioactive minerals associated with the Nigerian Younger Granites was the in investigation of Mackay (1949). The author described the widespread occurrence of Th-bearing minerals, chiefly thorite, uranothorite, monazite and orangite. Thorite was found to be associated with columbite in these granites with abundances increasing towards the roof zones of the granites. Large concentrates of thorite are obtained as a by-products of tin mining. It was found that although the thorite recorded in the granites is not U-rich, U follows Th in its distribution in the granites.

Mackay (1952) investigated the occurrence of U in the albite-riebeckite granites, and found U to be concentrated in pyrochlore. The albite-riebeckite granites, carry this mineral in a large proportion, but there is a general absence of thorite and monazite. Mackay's report, based on investigations of occurrences in the Kaffo valley, Dorowa, Teria and Kigom Hills albite-

riebeckite granites, noted an average U content of 0.012% U_3O_8. In the pyrochlore the U average is 3.1% U_3O_8.

U in the Nigerian Younger Granites occurs in both primary and secodary U minerals. On the Jos Plateau, later mineralisation mostly occurs in the albite-riebeckite granites, although occasionally some is found in the biotite granites.

Recently, identified minerals containing U include uraninite, torbernite, autunite, thorite and minerals typical of the accessory phase in a granite, such as monazite, xenotime, allanite and zircon. Pyrochlore was found to be exclusively associated with the albite-riebeckite granites, where it occurs as common accessory. Beer (1952) has described the occurrence of pyrochlore in the Nigerian Younger Granites. Although not one of the primary U minerals, pyrochlore has been found to contain U as one of its major constituents. The occurrence of uraninite in a pegmatite associated with greisen at Saiya Shokobo has been reported by Kinnaird (1985). Similar pegmatites occur on the Jos Plateau. Where they are found below the zone of weathering, the occurrence of uraninite may be widespread. Elsewhere, in the old basement rocks, vein-controlled U mineralisation has been reported. Oshin and Rahman (1986) described the occurrence of pitchblende, tobernite and autunite along silicified fault zones. In addition, abundant occurrences of thorite, zircon, monazite and xenotime as accessories containing U and Th in substantial amounts, in the

biotite granites, and fergusonite in the hornblende granites, have been reported. In the Bauchi plains around Gombe, the Nigerian Uranium Mining Company (NUMCO), a subsidiary of the Nigerian mining coorporation (NMC) was engaged in the exploration for U deposits which might have an origin in the Younger Granites.

CHAPTER TWO: RADIOELEMENTS IN THE NATURAL ENVIRONMENT

2.1 Introduction

The Earth's Crust contains most of the elements of importance to Man and much is accessible with the present-day technology. An understanding of the mechanisms by which elements become concentrated in the Crust is important if exploration is to be successful at a time when the less easily discovered deposits are to be found. However, for this, it is important to make some assessment of the initial composition of the Earth. In this Chapter, the original element abundances and distribution are considered together with the mechanisms of differentiation that have operated since the Earth was formed.

Many attempts have been made to determine the original abundances and distribution of the elements in the Earth, but our understanding is still hazy. Partly this is because there is still no universally accepted view on the formation of the planets. However, the nebula cold accretion theory has wide and popular acceptance among many in that field of study. Within the context of this theory, the nearest to the possible composition of the Earth at the time of its formation that we can get is the composition of the meteorites. But this is not without problems because the meteorites themselves have different compositions. Thus

the choice of meteorite type is very significant. Another approach which can be used is the composition of the outer atmosphere of the Sun as given by absorption lines in the solar spectrum. Urey (1968) has discussed arguments regarding this subject, but most workers are content with assuming that the class of meteorite known as carbonaceous chondrites are close to the composition of the primitive solar nebula from which the Earth accreted. However, even these meteorites are deficient in the lightest volatile elements that must have had high abundance in the nebula. The most important control in redistributing elements in the Crust is excercised by the geochemical properties of the elements. Certain elements have been recognised as preferentially forming bonds with O_2. These are known as lithophile elements and comprise most of the rock-forming minerals in the Crust. Strongly lithophile elements which are also incompatible (that is they are not an essential part of the main rock-forming minerals) tend to become concentrated in the end-products of magmatic differentiation - granites. Thus U and Th in igneous rocks are found mainly concentrated in granites and granite-related materials because they are both strongly lithophile and highly incompatible. Other events which have been found to redistribute the elements in the Earth Crust are weathering and the transport and deposition of sediments, and deep hydrothermal circulation.

In the second part of the Chapter, the natural occurrence of the radioactive elements, and the physical and chemical properties

of the three most important radioelements in the crust, are discussed. Taking into consideration the age of the Earth and half-lives of the radionuclides produced by the supernova event that preceded the formation of the Earth, most can now be said to be extinct or in quantities not measurable with the present instrumentation. However, the presence of these nuclides can be inferred from the abundances of the stable daughters, which were produced. It appears that they were very significant in generating heat to drive the chemical differentiation mechanisms operating in the early history of the earth (Durrance, 1986). Today most heat for these mechanisms comes from the three major radioelements. An excellent review of the nuclear properties of the elements has been made by Hyde et al. (1971).

2.2 Naturally Occurring Radioelements

There are over twenty naturally occurring radioelements in the Earth's Crust. All of these contribute to the natural radiation environment, so that for very detailed analysis and interpretation of radiometric data their effect has to be taken into account. However, most of these elements have radioactive isotopes which are rare, have very weak radioactivities, or both (Table 2.1). Therefore, for exploration purposes, they are not considered important. For example, the abundance of ^{130}Te in the crust is only about 0.017ppm, a concentration much below the limit of detection

Table: 2.1 Average crustal abundance of natural radioelements.

Nuclide	Decay mode	$t_{1/2}$ years	Isotopic abundance (%)	Crustal abundance (ppm)
^{238}U	α	$4.47.10^{8}$	99.28	4
^{235}U	α	$7.13.10^{8}$	0.72	0.03
^{232}Th	α	$1.39.10^{10}$	100	14
^{40}K	β^- and KC	$1.30.10^{7}$	3.8	25900
^{209}Bi	α	$2.7.10^{17}$	0.2	0.2
^{187}Re	β^-	4.10^{12}	<0.01	0.001
^{176}Lu	β^- and KC	$2.2.10^{10}$	0.02	0.08
^{150}Nd	β^-	2.10^{15}	1.34	24
^{147}Sm	α	$6.7.10^{11}$	1.06	7
^{138}La	β^- and KC	$1.1.10^{11}$	0.02	18
^{130}Te	β^-	10^{18}	<0.017	0.002
^{129}I	β^-	$1.72.10^{7}$	-	<0.01
^{123}Sb	β^-	$>10^{13}$	0.01	0.2
^{115}In	β^-	6.10^{14}	0.10	0.1
^{87}Rb	β^-	$6.15.10^{14}$	33.42	120
^{58}Ni		$>10^{19}$	54.21	80
^{50}V	β^- and KC	$>10^{16}$	0.41	110
^{48}Ca		10^{14}	67.16	36300

Crustal abundances based on average concentration of elements in the Earth's Crust by Mason (1960).

of most of the analytical instruments currently available. Only the ^{232}Th, ^{238}U and ^{235}U decay series and ^{40}K are of importance in exploration.

In addition, some transuranic elements also may be naturally present in the Crust, but this is not certain. The possibilities include ^{239}Pu, ^{244}Pu, ^{237}Np and ^{247}Cm. The chance of natural ^{239}Pu is slim, to say the least, but Levine and Seaborg (1951) claimed to have found ^{239}Pu in some U ores. They attributed the formation of this nuclide to neutron capture by ^{238}U. But this alone will not give the ^{239}Pu abundance reported, other reactions of the heavier elements may also be involved, or its original amount is much more than is thought to be the case. In most of the ores in which it was reported higher values than neutron capture reactions by ^{238}U would account for. Cherdyntsev et al. (1965; 1967) also reported ^{239}Pu in groundwaters and volcanic rocks and estimates by Diamond and Barnes (1956) showed that some ^{244}Pu may still be present. Intensive search for these nuclides with the modern analytical techniques and instruments may show some natural existence of these elements, but this is very unlikely to be on a major scale. However, the important thing to understand is that even if these nuclides are extinct, their effect is still very much around, and may in some way affect the accuracy of measurements of the natural radiation environment. For example, ^{239}Pu and ^{247}Cm decay to ^{235}U and if present in uraniferous ores at the time the ores were formed, will have produced an anomalous ^{235}U: ^{238}U ratio. In alpha-particle

studies also, the presence of ^{247}Cm, which has been suggested to have been present in very old Rare Earth Elements (REE) minerals (Hyde et al., 1971), would produce apparently strange activity ratios.

Other radionuclides are continuously produced in nature. These include those formed by the decay of naturally fissionable nuclides such as ^{238}U and ^{235}U, and those resulting from cosmic-ray induced reactions. The latter are mainly produced in the high atmosphere by spallation reactions with atmospheric Ar (Adams and Gasparini, 1970). They include ^{22}Na ($t_{1/2}$=2.62yrs), ^{24}Na ($t_{1/2}$= 14.96h), ^{38}Cl ($t_{1/2}$ = 37.29min.), ^{39}Cl ($t_{1/2}$ = 55.5min.), ^{38}S ($t_{1/2}$=2.87h), ^{34}Cl ($t_{1/2}$=31.99min.), ^{7}Be ($t_{1/2}$=53.6d) and ^{26}Al ($t_{1/2}$=7.4.105yrs) with their half-lives $t_{1/2}$ as shown in the brackets. Occurrences of these nuclides in rain water have been reported by Perkins et al. (1965).

2.3 Primordial Element Abundance and Distribution

The concensus view about the formation of the planets is the cold accretion nebula theory. In this the material making up the Earth is believed to have existed in a cloud of gas and small particles called the Primitive Solar Nebula. The Earth came into being as a result of the accretion of some of the particles in this nebula. The composition of these particles (planetesimals) is believed to be given approximately by that of the carbonaceous

chondrites, as noted previously. This is because this class of meteorite shows no sign of chemical differentiation, apart from loss of very light volatile elements, and has a chemical composition which corresponds closely with that of the Sun's outer atmosphere (the Sun also having formed by accretion from the Primitive solar Nebula) .(Brown and Mussett, 1981). Elements in the Primitive Nebula up to ^{56}Fe are believed to have been formed by fusion reactions in stars much larger than the Sun. But beyond ^{56}Fe, the heavier elements must have formed only when large amounts of energy were available - during a Supernova event. In this process the synthesis of the heavy elements would have been less likely as atomic weight increased. The age of meteorites is in the order of 4600Ma, which is taken to be the age of the Earth.

Chemical fractionation and the redistribution of the elements may have started even during the accretion of the Earth. Kohman(1961) thought the earliest separation of the elements was the differentiation of the volatiles from the non-volatiles when the Earth came into being as a planet. This is the hetrogeneous model for the formation of the Earth. In contrast, Urey (1968) believed that the Earth was initially homogeneous and that it has been differentiated entirely since its formation. This is the homogeneous model for the formation of the Earth. The concensus currently favours the latter model, but which is correct is largely immaterial to the formation of the Crust - both models suggest that the Crust formed by differentiation of the earth after it had developed a Core and Mantle.

2.4 Origin of Granites

Patterson et al. (1955) have shown that U is mainly concentrated in the top few kilometres of the Earth's Crust. Within this zone it is believed that at least 90% of the Earth's U is located. It is no coincidence that this part of the Crust is predominantly granitic (Mason, 1958; Adams, 1962; Paldevart, 1955). The fact that a large proportion of the U in granites becomes mobilised during alteration leads to the formation of U ore bodies. Therefore, it is impossible to overemphasise the importance of the U in granites in any discussion of the geochemistry of U. Clearly, also it is very important to consider how granites are formed.

Below the Earth's crust, the Core and Mantle make up about 90% of the Earth by volume. Whether separation of the core and the Mantle occurred after accretion of the earth as a whole, is immaterial to this discussion, but it is clear that this process predated the origin of the Crust - today we can see the evidence of new Crustal rocks forming from the Mantle below active mid-ocean ridges. Hargraves (1976) postulated that in the first billion years of formation, the Earth segregated the bulk of the Crust and hydrosphere. The Archaen appears to have been characterised by small, vigorous convection cells in the Mantle, but from the Protozoic a system of convection and plate movement similar to that

of the present-day, has been operating.

Two ideas for the origin of granites have been proposed: the magmatic origin, in which granites result from the differentiation of a more basic magma, and the non-magmatic origin, in which granites result from the transformation of the host rocks by partial melting. It is now generally accepted that the origin of granites can be either of these processes: it is a matter of investigating the total geological setting to determine the origin of a particular granitic mass. Essentially then we are dealing either with granites derived by fractional crystallization of basic magmas originating in the Mantle, or by melting of pre-existing Crustal rocks. Because of these different origins it is very difficult to discuss, in general terms, the occurrence of U in granites. However, it has been largely established that the Mantle is generally deficient in U relative to the Crust which, therefore, means that granites which are derived directly from the mantle will be deficient in U relative to granites derived from the Crust. Nevertheless, even for granites originating in the Mantle, the fractionation and consolidation which occurs during ascent of the magma means that U should be enriched in the late differentiates. Thus there will be a decrease of U with depth in these granites. For granites whose origin is by melting of Crustal rocks, the U abundance will depend both on the U content of the parent rock and the mode of crystallization.

The two types of granites have been labelled by Chappel and

White (1974) as I-type (for those derived from mantle material) and S-type (for those derived from crustal material). It has been observed by Pitcher (1979) that Sn mineralisation is associated with S-type granites, while porhyry Cu mineralisation is associated with I-type granites.

It must be emphasised, however, that the origin of a particular granite may not be easy to ascertain due to the interaction between the Mantle and the Crust. Of importance here is Crustal contamination of mantle-derived magmas during their ascent. Fyfe (1978) concluded that most granitic rocks are the result of reworking of the Crust and extensive dilution by mantle-derived material (which is itself often contaminated by subducted Crustal components). Thus for any discussion of the distribution of the elements in granites to be meaningful, each granitic body has to be considered individually.

KASHIM IBRAHIM LIBRARY
AHMADU BELLO UNIVERSITY
ARIA, NIGERIA.

2.5 Abundance and Distribution of U, Th and K in the Crust

The importance of U, Th and K in contributing to the total heat budget of the Earth is generally recognised. Indeed, the heat engine of plate tectonics is thought to be mainly fuelled by energy supplied from the decay of these elements. Knowledge of the distribution of U, Th and K in the Earth is thus important for more than just exploration purposes. Moreover, the fact that these elements are a source of heat means that both direct and indirect

methods can be employed for the determination of the abundance of the radioelements within the Earth's Crust. For example, gamma-ray spectrometric determinations on the Earth's surface, and borehole samples, have been used to determine their abundance and distribution, while heat flow studies have been used in some cases to develop composition/depth models for the heat-producing elements. Clark and Turekian (1979) used heat flow data to show that a layer which permits transfer of heat, but not the transfer of the heat-producing elements, exists in the mantle.

Average crustal abundances for U, Th, and K have been reported. Methods of determination were essentially based on two approaches: straight averages derived from analysis of samples from the continental crust and the weighted values based on geochemical models of the evolution of the Crust, Mantle and the Core. One in the latter category is the recent andesite model of Jaupart (1985). In the straight averages category, the methods of computation used by different workers can significantly vary. In the earlier methods, for example that used by Washington (1924), values were obtained by taking averages of analytical data from common rocks. Vogt (1931), on the other hand, derived the average abundance of the elements in igneous rocks by using published average values, and weighting them in proportion to their relative abundance in the Crust. This approach at least took into account the effect of the abundance of the crustal rocks on the averages, which was not considered in the earlier study. Subsequently, average crustal

abundances were obtained by taking averages of a mixture of granite and basalt Vinogradov (1962) used a ratio of 2:1 for granites and, but Taylor (1964) used a ratio of 1:2. These authors obtained values of 3ppm, 8ppm and 2.50% for U, Th and K, and 2.7ppm, 9.6ppm and 2.09%, repectively. The idea of considering only granite and basalt for the composition of the Crust was based on the reasoning that other materials (sedimentary and metamorphic rocks) were derived ultimately from igneous rocks. In the andesite model, Jaupart (1985) considered that andesites, believed to be derived from the mantle subduction zones, provide the best average composition of crustal rocks prior to internal differentiation. He reported values of 1.25ppm, 4.80ppm and 1.25% for average abundance of U, Th and K in the Earth's Crust based on this approach.

Another geochemical method is the Crust/Mantle model for which the process of evolution of the continental Crust from the Mantle forms the basis. In this approach, it was envisaged that the continental Crust grows at the expense of the Mantle, which becomes depleted in those elements preferentially located in the continental Crust (Jaupart, 1985). Using an initial Mantle composition obtained from meteorite studies, together with a depleted Mantle composition obtained from direct analyses, the evolution of the Crust and the Mantle were then modelled to give a crustal composition of 1.30ppm U, 6.10ppm Th and 1.70%K.

It is clear from the values quoted above that a wide variation exists in the average crustal abundances obtained from

the different methods. If other elements are considered it is found that this variation is especially true for the trace elements in general (including the REE). Average abundances must, therefore, only be used for general discussion of the overall amount of the radioelements in the Crust, rather than as a guide to their true concentrations. Moreover, the proportion of the Crust made up of the individual rock types are merely estimates which crustal model was used greatly affecting such estimates. Ranges of values, rather than overall crustal averages for the different rock types, may be more useful in any consideration of element abundances. In Table 2.2 are given average values for U, Th and K in various rock types. It can be seen from this Table that both U and Th are concentrated in igneous rocks. Thus U in common crustal rocks ranges from 0.001ppm to 7.15, Th from 0.004ppm to 13ppm and K from 0.83% to 4.5%.

Many studies of the depth distributions of the radioelements in the Crust have been carried out, but there seems to be no common view of the nature of these distributions. Thus, while Lambert and Heier (1967) reported a downward decrease of radioactivity with depth in the Australian Shield, Jaupart (1985) suggested an increase with depth. Divergent as these views may be, it is generally agreed that U has its greatest abundance in the upper part of continental Crust (Rankama and Sahama, 1949; Patterson et al. 1955).

Table 2.2: Average crustal abundance of U, Th and K

Rock type	U(ppm)	Th(ppm)	K(%)	Reference
Ultrabasic	0.001	0.004	0.0004	TW
Basalt	0.83	5.0	-	RS
	1	4	0.83	TW
Intermediate	2.61	9.97	-	RS
	3	13	4.8	TW
Acidic	-	13.00	2.59	RS
	3	12.75	3.36	TW
Igneous	4	11.5	2.7	RS
	2.6	13	3.36	G
Sedimentary	7.15	-	-	RS
	1.91	5.6	1.35	TW

note:

RS: Rankama and Sahama (1949)

TW: Turekian and Wedepohl (1961)

G : Green (1959)

: Averages for sedimentary rocks by TW were obtained by average concentrations in slates, sandstones, carbonates and clays.

2.6 Geochemical Controls on the Abundance and Distribution of U, Th and K.

2.6.1 Radioactive Properties

2.6.1.1 Systematics of Nuclear Decay

In addition to the naturally occurring radioactive elements, other known elements normally stable undergo change from natural nuclear interactions in the Earth. Radioactive decay is the transformation of an element into a new product by the emission of a particle, either a beta-particle or an alpha-particle, which may be accompanied by emission of electromagnetic radiation. The potential for such decay of an element is determined by its nuclear structure. In this Section the concept of nuclear stability, and the various decay modes in radioactivity, are discussed.

The basic unit carrying the identity of an element is the atomic nucleus. The nucleus is made up of neutrons and protons (nucleons) bound together by a very strong short-range force (the strong nuclear force). A nucleus is characterised by its charge number Z, which is the number of protons it contains, and the mass number A, which is the sum of the number of neutrons and

the protons. The binding energy B, of the nucleus is defined as the energy required to break the nucleus into its component nucleons. This is related to the difference between the mass of the nucleus and the sum of the masses of the constituent nucleons Δm, by:

$$B = \Delta mc^2,$$

where c is the velocity of light. Plots of the average binding energy, D/A (referred to as the binding fraction), against the mass number A, show clear features which are related to the energies in the radioactive decay processes (Evans, 1955). In the lighter elements, where A<28, variations are observed, such that nuclei where A is a multiple of four have higher binding energies than where A is not a multiple of four. This reflects the stability of the alpha-particle (which has a mass number of four). For A>28, the binding energy/mass number relationship follows a generally smooth curve.

The process of radioactive decay is a consequence of the instability of a nucleus. Each decay process is determined by the energy involved in the emission of a particular particle. This energy, referred to as the separation energy S_b, is defined as the energy required to separate the particle from the nucleus. S_b for a particle is given by:

$$S_b = [M_b + M_r - M(N,Z)]c^2$$

where M_r is the mass of the residual nucleus after separation of the particle of mass M_b (Eisenbud et al., 1967).

Among the lighter elements, the stability of the nuclei in

their ground state is exclusively dependent upon the process of beta decay. This process involves the emission of either a negative or a positive beta-particle from the nucleus, or the capture of an orbital electron by the nucleus. These changes alter the atomic number Z by +1. For the conservation of energy, momentum and angular momentum of the residual nucleus, the process is believed to be accompanied by the emission of particles called neutrinos. A neutrino has zero rest mass and is chargless. It possesses only an angular momentum. These processes are represented by:

$$X(A,Z) \longrightarrow X(A,Z-1) + \beta^{-} + \nu,$$

$$X(A,Z) \longrightarrow X(A,Z+1) + \beta^{+} + \nu ,$$

and $$X(A,Z) \longrightarrow X(A,Z+1) + \nu,$$

respectively. The process of beta emission determines the stability limits for nuclei throughout the periodic table (Ivanovich, 1982). Beta decay lifetimes are a sensitive function of spin and parity changes between the initial and final states of the nuclei. They also depend on the available energy. For a large spin change and low energy, the half-life becomes so long that the nucleus appears to be stable to beta decay.

In beta stable elements, more especially those among the heavy elements, other modes of decay decay operate which are independent of the beta decay process. Important among these decay modes is alpha emission, the ejection from the nucleus of two neutrons and two protons bound together as a ^{4}He nucleus. Theoretically, alpha emission is possible for any nuclei in which

the sum of the binding energies of the weakest two protons and two neutrons is less than the binding energy of an alpha-particle. Alpha-particle emission process is, infact, possible for all nuclei with A above 90. But, because of the potential barrier that must be overcome, the rate is usually very slow. Alpha emission only becomes significant when a positive binding energy difference of several MeV is present. Based on alpha decay theory, Hyde et al. (1971) estimated the minimum detectable alpha activity to be a transition with a half-life of 10^{18} years.

The relationship between alpha decay energy and atomic number reveals certain regular trends. It is found that the alpha decay energy of beta stable elements increases as Z increases towards Z=92 (U), and this trend reverses as Z becomes large (Z>92) (Burcham, 1963). Generally, the alpha decay energy increases with Z at constant A for all nuclei. Similarly, for constant Z, the alpha energy decreases with an increase in A. However, irregularities are observed in some regions. For example, for elements with A<128 the alpha decay energy increases with an increase in A. Also, at Z=84 the decay energies become much lower than expected. These variations are associated with the closure of a neutron shell at N=126 and a proton shell at Z=82, respectively.

Alpha decay half-lives are pronoucedly dependent on the alpha decay energy. The lifetimes increase with decreasing decay energy, thus ^{232}Th, for example, with an alpha energy of 4MeV has a half-life of 10^{10} years, while ^{212}Po with an alpha energy at 9MeV

has a half-life of 3.10^{-7} seconds. For individual nuclides, the half-life - energy relationship shows regular behaviour. Such relationships are usually more pronounced for even number-even number nuclear transitions.

The ejection of an alpha-particle may leave the residual nucleus in any one of the several excited states. Each of these states is characterised by different energies and a different probability of occurrence. De-excitation to the groundstate occurs by gamma-ray emission. In some cases this may be accompanied by beta-particle emission decay. An example of alpha emission is given by:

$$^{228}_{Th} \Rightarrow {}^{224}_{Ra} + \alpha$$

The alpha energy and the excited states of the $^{224}_{Ra}$ are shown in Table 2.3. As can be seen, alpha decay processes may be accompanied by the release of more than one energy of alpha particle. Thus there can be a fine structure in the alpha-energy spectrum. Usually in reporting alpha energies, the energy of the alpha decay with the highest intensity is quoted.

The second type of structure exhibited by alpha energy spectra is associated with long range alpha-particles. These are a group or groups of alpha-particles of considerably longer range than the main group of particles which occur in certain alpha transformations. They are believed to be produced by disintegration of the excited state of the initial nucleus rather than the

Table 2.3: Fine structure alpha-particle emission in the transition $^{232}Th \longrightarrow ^{228}Ra$.

Group	Alpha energy (MeV)	Abundance (%)	Excitation energy (MeV)
α_1	6.084	27	0
α_0	6.044	70	0.040
α_2	5.762	1.8	0.328
α_4	5.620	0.1	0.472
α_3	5.601	1.0	0.492

After Burcham (1963).

daughter nucleus, as is the case for the fine structure. The process is often associated with a population of highly excited nuclei and beta decay processes. The decay of excited states to the groundstate proceed by alpha emission in addition to gamma emission. Such mechanism are fully discussed for the nuclide ^{212}Bi by Evans (1955).

After the emission of beta and alpha particles during radioactive decay the daughter nucleus may be left in an excited state. The excited nucleus gives up this energy in a variety of ways, and returns to the groundstate. This transition commonly involves the emission of electromagnetic radiation in the form of gamma-rays. The emission of gamma-rays follows, in most cases, shortly after the primary radioactive decay. However, delays of up to an hour in gamma emission are known to occur in certain nuclei. Those nuclides which exhibit this phenomenon are referred to as nuclear isomers, for example, ^{137m}Ba, where the letter m following the mass number indicate an isomeric nuclide (Adams and Gasparini, 1970). Nuclear isomers represent unstable excited states of the atoms involved, but they have similar chemical properties to those of unexcited atoms. Measurements have shown that the half-lives involved in the emission of gamma-rays are much shorter than those for the emission of either beta or alpha particles. Indeed, many gamma half-lives are only in the order of 10^{-13} seconds (Halliday, 1950). These half-lives are a function of the transition energy, the nuclear spin charge and the atomic mass of the nuclei

undergoing the transition: half-life increasing with a decrease in the spin charge.

Although most excited nuclei return to the groundstate by gamma-ray emission, examples occur where both beta and alpha emission compete with gamma emission to the extent that de-excitation is dominated by particle emission. The emission of long range alpha-particles in the decay of ^{212}Po and ^{214}Po well illustrate the process.

In addition to the decay modes discussed above, another type of instability exists in the heavy nuclei. In this, decay occurs by spontaneous fission, the nucleus dividing into two or more fragments. This is accompanied by the release of a considerable amount of energy. For the heaviest nuclei, an excitation of the nucleus by a few MeV can produce fission. However, the potential barrier impeding fission is high, so that the probability of occurrence in nature is very small.

2.6.1.2 Radioactive Decay Series

All the naturally occurring isotopes of U and Th exhibit the emissions described above. ^{238}U and ^{235}U are the naturally occurring U isotopes and each form a decay series ending in a stable Pb isotope, ^{206}Pb and ^{207}Pb, respectively. ^{238}U gives rise

to the longest decay series, involving twenty daughters of ten different elements, with eleven alpha-emitting and eleven beta-emitting nuclides. It forms the main constituent of natural U, with an abundance of 99.27%. The decay of ^{235}U involves fifteen daughters, consisting of eleven different elements. Eleven of the nuclides are alpha emitters and seven beta emitters. The ^{232}Th decay series supports eleven daughters of nine different elements, with six which are alpha-emitters and five beta emitters.

In the ^{238}U decay scheme, ^{238}U decay to ^{234}Th by alpha emission with an energy of 4.196MeV (Durrance, 1986). This forms the energy of the main group with an abundance of 77%. Other alpha energies associated with this transition are 4.147MeV and 4.038MeV with abundances of of 23% and 0.23%, respectively. The transition has an alpha half-life of $4.51.10^{9}$ years corresponding to a specific activity of 738.6 disintegrations per minute per milligram. The transition is also accompanied by the emission of gamma-rays with an energy of 0.048MeV (Hyde et al., 1971). The decay series is shown in Figure 2.1.

The daughter nucleus, ^{234}Th, decay by beta emission with a half-life of 24.1 days (Knight and Machlin, 1948). The beta decay is accompanied by gamma-rays of energy 0.03 to 0.09 MeV. ^{234}Th decays principally to ^{234}Pa, but 0.14% of its disintegration produces an isomeric form ^{234m}Pa. 98% of the ^{234}Pa decays directly to groundstate ^{234}U. This transition is characterised by a continuous beta spectrum with a high end-point energy of 2.3MeV

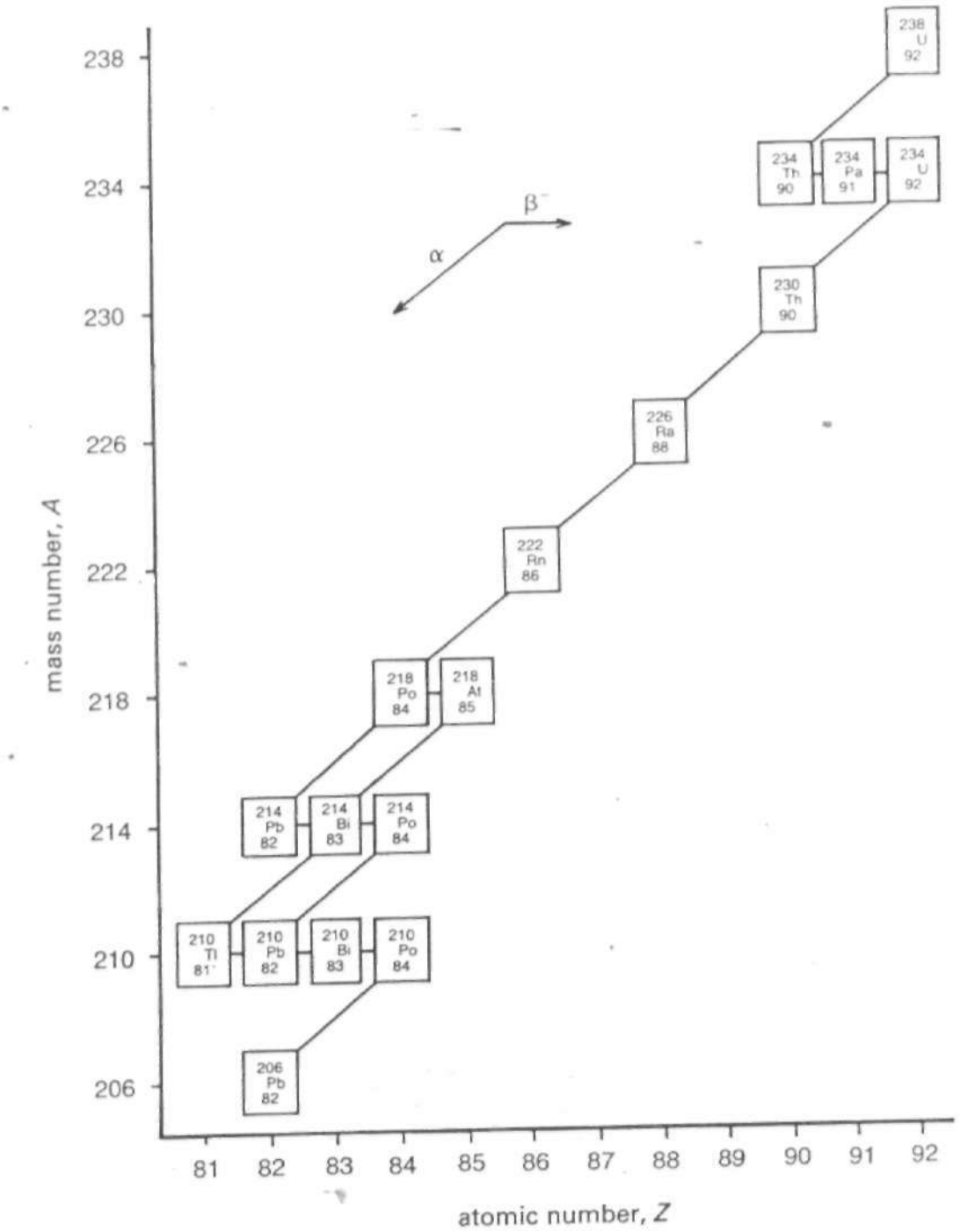


FIGURE 2.1 The ^{238}U decay series (After evans, 1955)

(Hyde et al., 1971). The transition of the isomer, ^{234m}Pa, is characterised by a complex spectrum of beta, gamma and electron conversion energies, which make study of the transition extremely difficult. The various decay schemes for this transition have been reviewed by Hyde et al. (1971). Of importance is the fact that the transition involves the emission of gamma radiation in the range 0.044 to 1.85MeV, which is within the range of measurement of gamma-ray spectrometers used in environmental studies. Also, because these are all short-lived nuclides (^{234}Pa, $t_{1/2}$=6.7 hours, ^{234m}Pa, $t_{1/2}$=1.18 minutes), they take only about three months to achieve secular equilibrium with ^{238}U.

^{234}U, the fourth member in the series is a beta stable nuclide. It decays by alpha emission with a half-life of $2.48.10^5$ years. The main group of alpha-particles (72%) have an energy of 4.774MeV. The second group, with an energy of 4.717MeV, makes up 28%. Baranov et al. (1960) reported another group with an abundance of 0.37%. Gamma-ray groups of 53keV and 118keV have also been reported. Its long half-life and alpha emission energy make ^{234}U an important and useful nuclide in ^{238}U series disequilibrium investigations. Fractionation of the ^{234}U from ^{238}U in nature, is widely reported (Chapter 7).

The immediate daughter of ^{234}U is ^{230}Th, another alpha-emitter in the series with a half-life of $8.0.10^4$ years. Its decay scheme is largely well established, with four alpha groups clearly identified with energies and intensities of 4.682MeV (76%),

4.615MeV (24%), 4.476 (0.12%), and 4.437MeV (0.03%) (Ivanovich, 1982). Its decay is accompanied by low-intensity gamma-rays. ^{230}Th decays to ^{226}Ra. Its alpha decay scheme is summarized in Figure 2.2 (Hyde et al., 1971). As can be seen, the energy of the main alpha group, with an abundance of 94.5%, has been determined as 4.781MeV. The transition involve four groups of alpha-particles at 4.781MeV, 4.59MeV, 4.340MeV and 4.191MeV, with intensities of 94.45%, 5.55%, 7.10^{-3}% and 10^{-3}%, respectively. The transition with an alpha energy of 4.598MeV involves gamma-rays of 186keV. These form the most prominent gamma radiation, but other low intensity gamma-rays were reported by Stephens et al. (1957). ^{226}Ra decays to a gaseous daughter, ^{222}Rn, with a half-life of 1622 years.

^{234}U, ^{230}Th and ^{226}Ra are the longest-lived nuclides, apart from ^{238}U, in the ^{238}U decay series, and so take a considerable time to approach secular equilibrium. The time needed for ^{234}U, the longest-lived daughter, to reach equilibrium with ^{238}U determines the secular equilibrium time for the ^{238}U decay series, as a whole, which is $1.66.10^{6}$ and $1.08.10^{6}$ years for 99% and 95% equilibrium, respectively.

^{222}Rn decays by alpha emission with a half-life of 3.825 days. The predominant group with an approximately 100% abundance, has an energy of 5.486MeV. Another group with an energy of 4.983MeV at approximately $8.0.10^{-2}$% has also been observed. This is associated with a gamma-ray deexcitation emission of 512keV (Madansky and Rasetti, 1956). ^{222}Rn's small half-life means that it

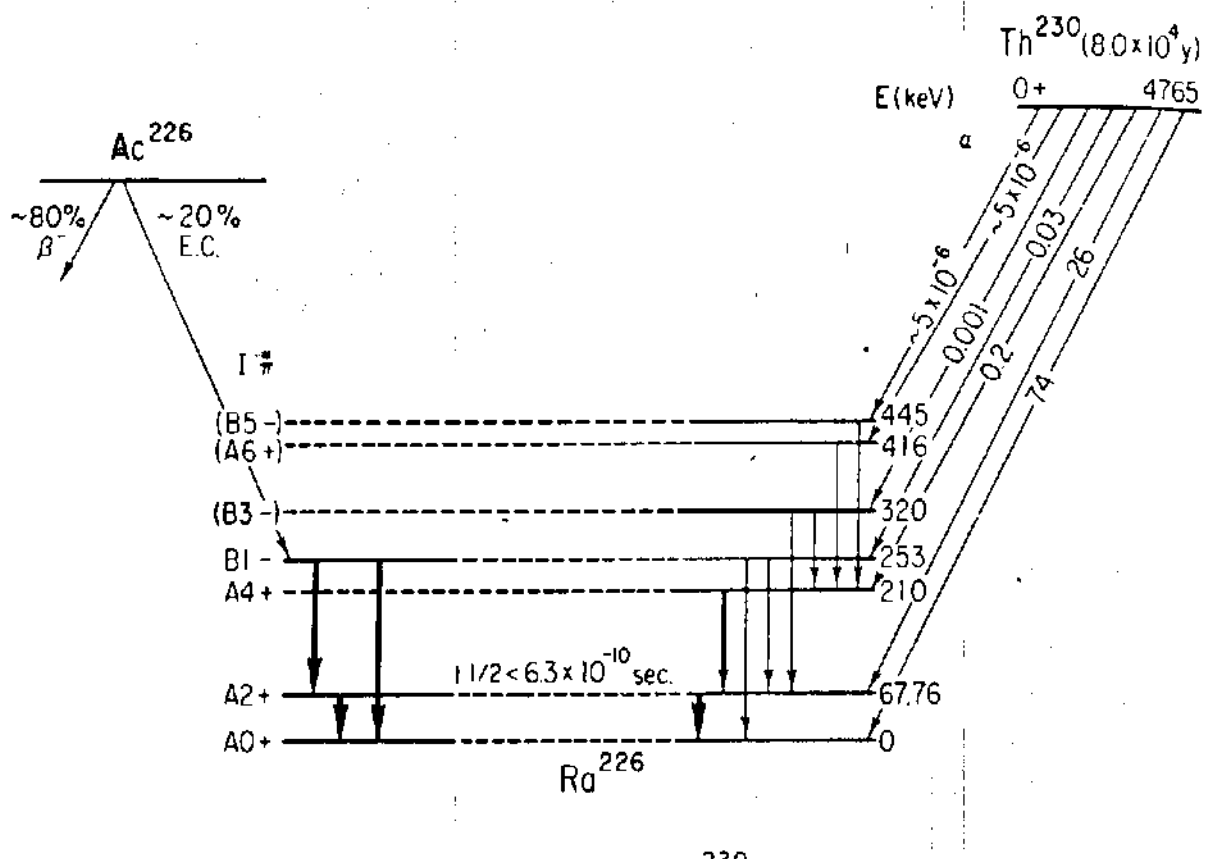


FIGURE 2.2 Alpha decay scheme of ^{230}Th (vertical arrows represent relative intensities of observed gamma transitions) (After Hyde et al., 1971)

takes a relatively short time to reach equilibrium with its immediate parent, ^{226}Ra.

^{222}Rn decays to a short lived daughter, ^{218}Po. This, in turn, mainly decays by alpha emission to ^{214}Pb. The alpha energy is 6.11MeV and a half-life of 3.05 minutes. However, ^{218}Po has a branched decay, so that 0.02% decays by beta emission to ^{218}At ($t_{1/2}$=2 seconds), which then decays by alpha emission to ^{214}Bi. ^{214}Pb decays by emission of beta-particles to ^{214}Po with successive beta emission to ^{214}Bi.

^{214}Bi decays largely by beta emission with an end-point energy of 3.26MeV. It is also associated with a low intensity alpha emission (0.04%). The beta transition involves numerous energetic beta-particles and de-excitation gamma-rays. Sixty gamma-ray energies, with more than forty above 1Mev, have been reported (Hyde et al., 1971). Gamma-ray spectrometric determinations of U employ measurement of one of these high energy gamma-rays, the 1.76MeV peak. Its beta decay daughter, ^{214}Po, decays by alpha emission to ^{210}Pb, with the very short half-life of only $1.64.10^{-4}$ seconds. Its other decay daughter, ^{210}Tl, also decays to this nuclide, ^{210}Pb, by beta emission.

^{210}Pb is a beta-emitter with a half-life of approximately 22 years. Branching with an alpha decay mode has been reported by Nurmia et al. (1961). The alpha decay mode with an abundance of $1.8.10^{-8}$% involves an alpha particle with energy of approximately 3.7MeV. The alpha decay daughter is ^{206}Hg, which is a beta-

emitter.

^{210}Bi, the beta decay daughter of ^{210}Pb, is a beta-emitter. Approximately 100% decays in this mode with a half-life of 5.02 days. However, an alpha decay mode was reported by Broda and Feather (1947). In this branch, it decays to ^{206}Tl, the same daughter as produced by ^{206}Hg. Isomerism in ^{210}Bi has also been reported. This is discussed in detail by Hyde et al. (1971).

^{210}Po, the daughter of ^{210}Bi, is beta stable. Its decay is characterised by a single alpha group with a half-life of 138.4 days. It decays to the stable Pb isotope, ^{206}Pb.

The ^{238}U decay series can thus be conviniently subdivided into group of nuclides, where successive members rapidly come into equilibrium with their parents. The nuclides derived from ^{238}U down to ^{234}Pa form a group in this division, where ^{234}Th and ^{234}Pa rapidly attain equilibrium values. ^{234}U, ^{230}Th and ^{226}Ra are in groups of their own, because of their long half-lives. The nuclides derived from ^{226}Ra down to ^{210}Tl are all short-lived and can form a group on their own division, with the daughters rapidly coming into equilibrium with the parent ^{226}Ra. The next group comprises the nuclides from ^{210}Pb to ^{210}Bi, and ^{210}Po. As will be discussed later, disequilibrium arises within the series because natural processes separate the different chemical and physical properties of the nuclides.

The other important natural decay series are due to ^{232}Th and ^{235}U. The ^{232}Th is summarized in Figure 2.3, and Table 2.4

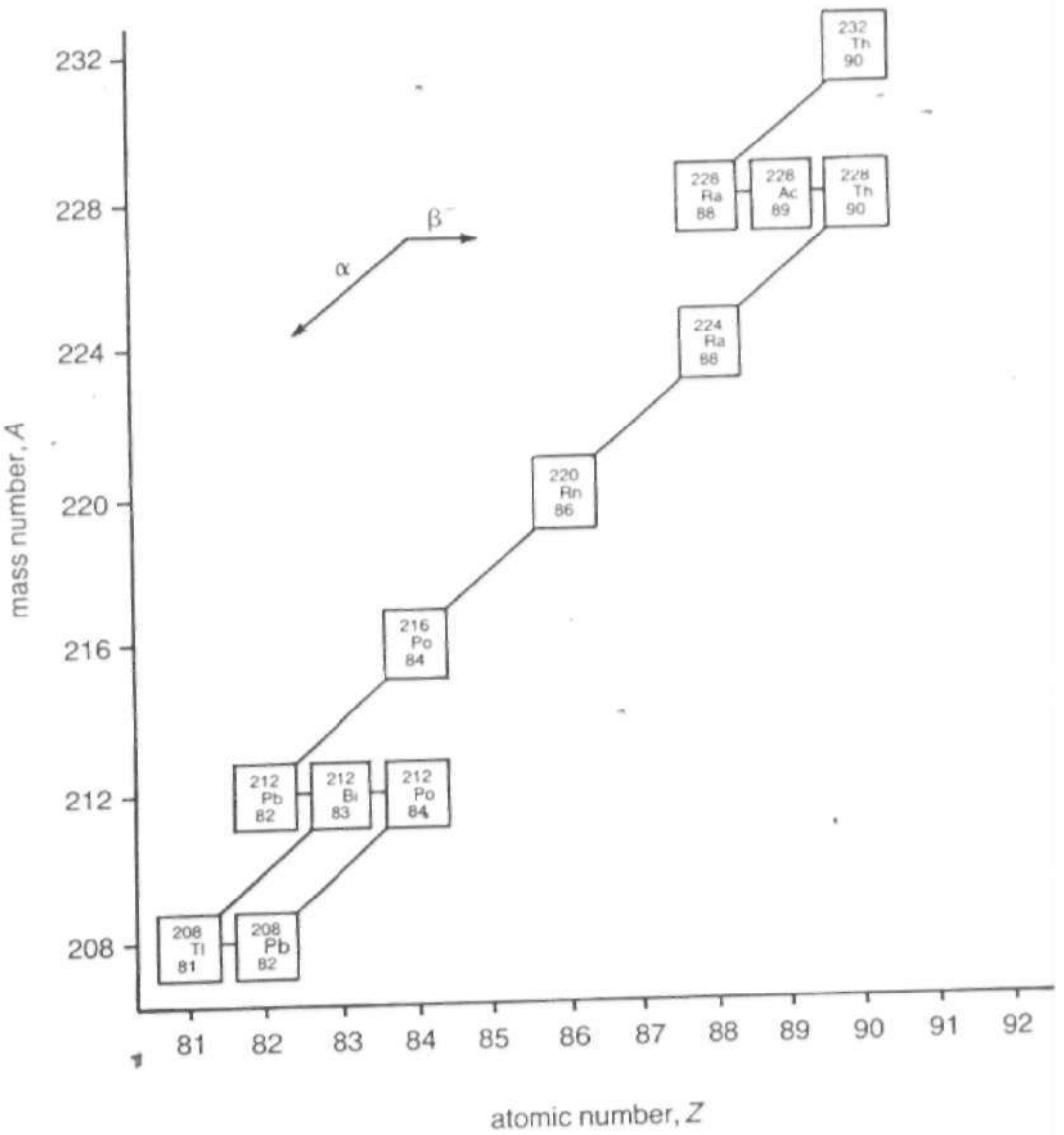


FIGURE 2.3 The ^{232}Th decay series (After Evans, 1955)

Table 2.4: ^{232}Th decay series.

Nuclide	Symbol	half-life	Radiation energy (MeV)	Alpha-particle abundance (%)	beta-particle energy (keV)	beta-particle abundance (%)
Thorium	^{232}Th	$1.39.10^{10}y$	4.007	76		
			3.952	24		
			3.882	0.2		
Radium	^{228}Ra	5.75y			55	100
Actinium	^{228}Ac	6.13h			2110	100
Thorium	^{228}Th	1.913y	5.421	71		
			5.338	28		
			5.208	0.4		
			5.173	0.2		
			5.137	0.03		
Radium	^{224}Ra	3.64d	5.684	94.5		
			5.447	5.5		
Radon	^{220}Rn	55.6s	6.296	100		
			5.761	0.3		
Polonium	^{216}Po	0.145s	6.777	100		
Lead	^{212}Pb	10.64h			580	comp
Bismuth	^{212}Bi	60.5m	6.09	30	2250	100
			6.05	70		
Polonium	^{212}Po	$3.04.10^{-7}s$	8.780	100		
Thallium	^{208}Tl	3.1m			1800	100
Lead	^{208}Pb	-	stable			

From Ivanovich and Harmon (982).

while the ^{235}U series is summarized in Figure 2.4, and Table 2.5. These decay schemes are fully discussed by Evans (1955), Lederer et al. (1967), Lederer and Shirley (1978), Hyde et al. (1971) and Ivanovich (1982). Important features of the ^{232}Th series are the prominent, high-energy gamma-rays produced by the decay of ^{208}Tl. This is used for the gamma-spectrometric determination of ^{232}Th. Except where natural fission reactions have occurred ^{235}U occurs in constant proportion with ^{238}U in natural U. Because of its low abundance, 0.72% of natural U, and low specific activity, it is the less important isotope in most investigations of natural U.

Another naturally occurring nuclide of importance in the natural radiation environment is ^{40}K. ^{40}K forms 0.0118% of naturally occurring K. It decays to ^{40}Ar by electron capture with a half-life of $1.30.10^{10}$ years (Adams and Gasparini, 1970). It also has a branched decay, with beta emission to ^{40}Ca, with an intensity of 89%. The electron capture transition leaves the ^{40}Ar in an excited state which de-excites to ground state by gamma-ray emission with an energy of 1.46MeV. This is used in the determination of K in gamma-ray spectrometry. The decay scheme is shown in Figure 2.5.

KASHIM IBRAHIM LIBRARY
AHMADU BELLO UNIVERSITY
ZARIA, NIGERIA.

2.7 Chemical Properties of U

U is a member of the actinide group of elements, the heaviest naturally-occurring elements in the cosmosphere. All U

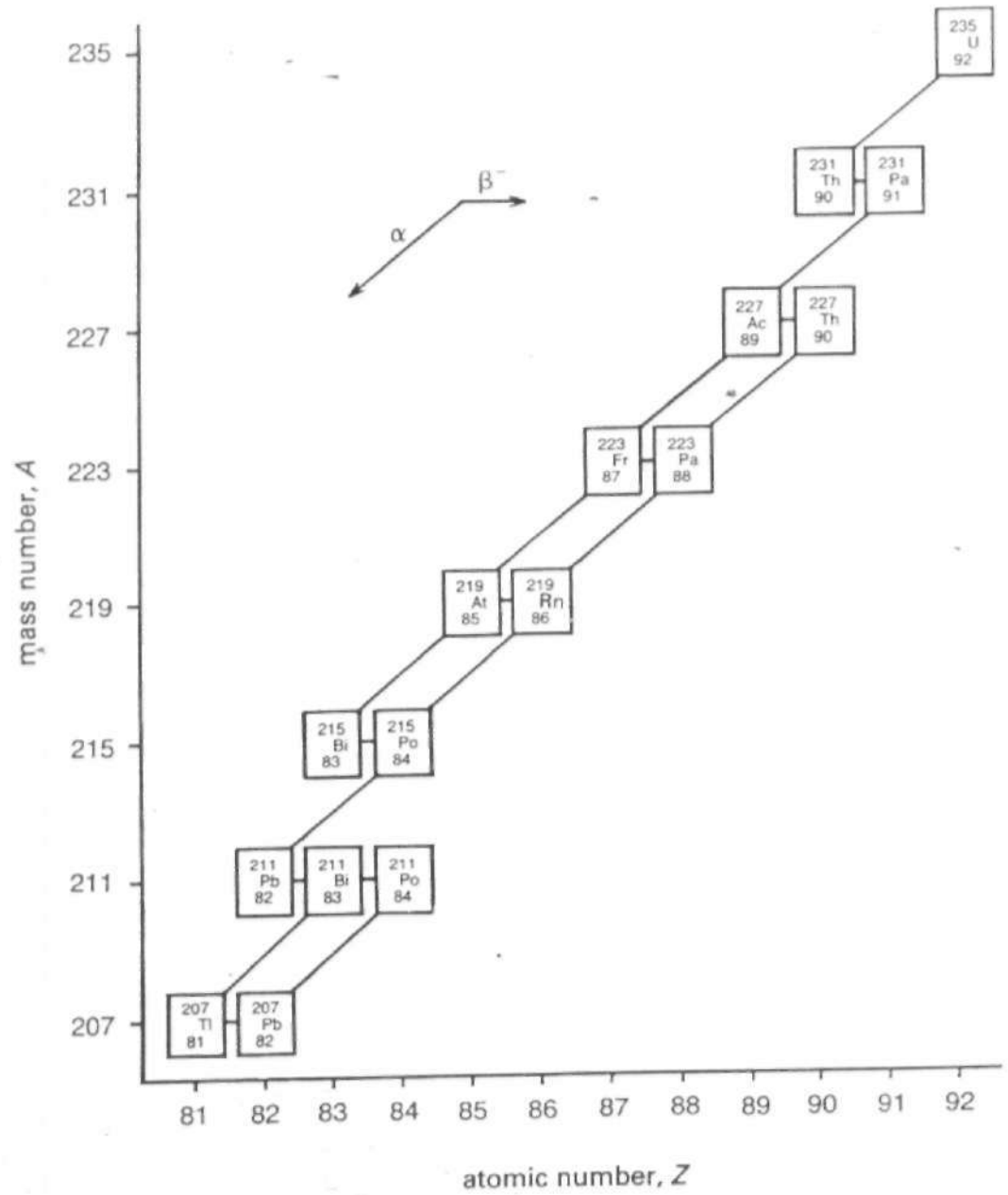


FIGURE 2.4 The ^{235}U decay series (After Evans, 1955)

Table-2.5: ^{235}U decay series.

Nuclide	symbol	half-life	Radiation	Alpha-particle energy (MeV)	Alpha-particle abund. (%)	beta-particle energy (keV)	beta-particle abund. (%)
Uranium	^{235}U	$7.13.10^{8}$y		4.391 4.361 4.1-4.6	57 18 25		
Thorium	^{231}Th	25.64h				300	100
Protact.	^{231}Pa	$3.43.10^{4}$y		5.050 5.016 4.999 4.938	11.0 <20 25.4 22.8		
Actinium	^{227}Ac	22y		4.724 4.949 4.937 4.866 4.849	8.4 48.7 36.1 6.9 5.5	46	100
Thorium	^{227}Th	18.17d		6.036 5.976 5.755 5.340	23 24 21 5.20^{-3}	1150	100
Francium	^{223}Fr	21m		5.745 5.714 5.605 5.538 6.28	9.1 53.7 26.0 9.1 100,	energy	
Radium	^{223}Ra	11.68d		6.813 6.547 6.419	81 11 8	unknown	
Astatine	^{219}At	0.9m				energy	
Radon	^{219}Rn	3.92s		7.384	100	unknown	
Bismuth	^{215}Bi	8m				1355 951 525 251	92.4 1.4 5.5 0.7
Polonium	^{215}Po	$1.83.10^{-3}$s		6.617 6.273	83 17	energy	unkno
Lead	^{211}Pb	36.1m		7.434 6.895	99 0.5		
Bismuth	^{211}Bi	2.16m				1440	100
Polonium	^{211}Po	0.52s					
Thallium	^{207}Tl	4.79m					
Lead	^{207}Pb	stable					

From Ivanovich and Harmon (1982).

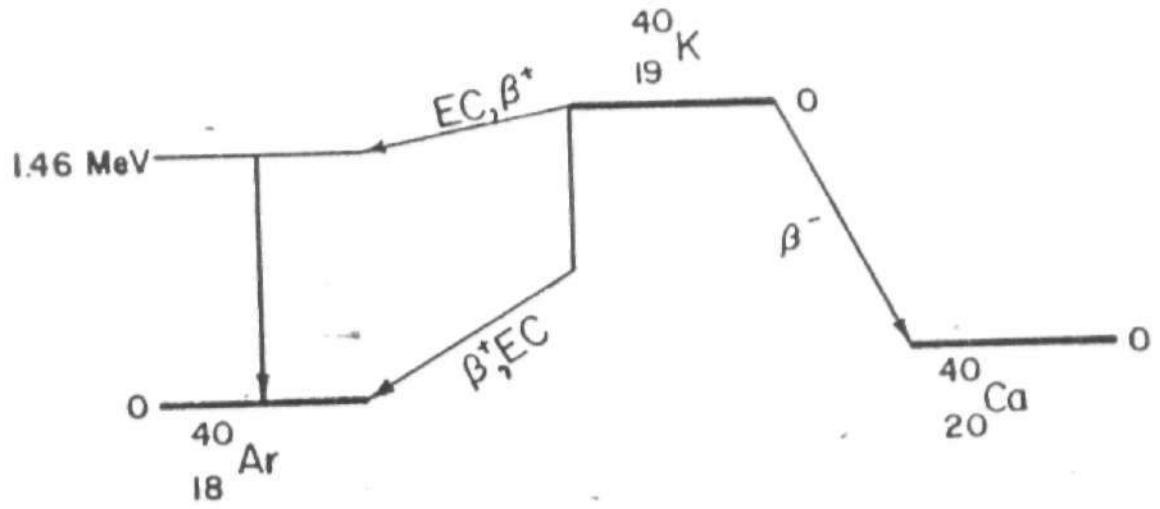
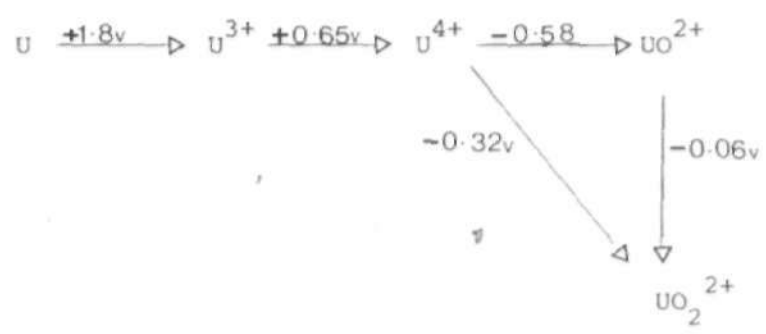


FIGURE 2.5 $^{40}_{K}$ decay scheme (After Adams and Gasparini, 1970)

isotopes are derived from the parent nuclides ^{238}U, and ^{235}U which are sufficiently long-lived to have survived since the formation of the Earth. Both are electropositive and tend to form strong ionic bonds, but a number of compounds in which they form covalent and semi-metallic bonds, are known. Both can exist in the +2, +3, +4, +5 and +6 oxidation states, but the most important of geochemical interest are the +4 and +6 states. The four oxidation states of U are represented as $5f^3$, $5f^2$, $5f^1$ and $5f^0$, with ionic radii of $1.03.10^{-10}$m, $0.93.10^{-10}$m, $0.89.10^{-10}$m and 0.83^{-10}, respectively.

U in aqueous solutions is determined to a great extent by the redox potential of the environment:



(Latimer, 1952). In solution, the four oxidation states occur as:

+3	U^{3+}
+4	U^{4+}
+5	UO^{2+}
+6	UO_2^{2+}

with red (U^{3+}), green (U^{4+}) and yellow (UO^{2+}) colours (Cordfunke,

1969). Both the 3+ and UO^{2+} are unstable in solution, with the former able to reduce water and librate H_2, according to the equation:

$$2U^{3+} + 2H_2O \longrightarrow 2U^{4+} + H_2 + 2OH^-$$

The latter is only stable within a very narrow acidity range around pH2 (Katz and Seaborg, 1957). The U^{6+} in solution readily combines with two oxygens to form the uranyl ion (UO_2^{2+}).

In geochemical processes, the behaviour of U is largely determined by the +4 and +6 valence states. The uranous and the uranyl ions are the most stable in aqueous solutions. The uranous ion, U^{4+}, is readily oxidised to the uranyl ion in the presence of oxidising agents. Garrels (1955) found that this reaction is greatly increased in the presence of metallic ions such as Fe^{2+} and Cu^{2+}, which probably explain the association of U with Fe in hydrothermal deposits. The +3 state occurs in a large number of soluble hydroxides. Its high charge and small radius enable it to combine in a number of complexes. These complexes are pH-dependent. It forms both cationic and anionic complexes. In alkaline media, uranyl di-carbonate and uranyl tri-carbornate are readily produced. Other complexes include uranyl sulphates, phosphates, chlorides, fluorides, nitrates, vanadates, arsenates and molybdates. It also forms organic complexes with C and gives rise to a number of soluble hydroxides.

The geochemical behaviour of U is governed to a great extent by the ability of the lower valence states to be oxidised to the uranyl ion, which is a very mobile ion in a variety of natural environments. For example in weakly acid solutions it is very mobile, but it is also mobile in both alkaline and neutral media in the presence of carbonate ions.

During magmatic processes, U in the +4 state subsitutes for Th, and both elements are involved in substitution reactions with the REE during the crystallization of igneous rocks. These substitutions also extend to some of the major elements, such as the substitution of Ca by U, and to some extent Th, in apatite and fluorite (Altschuler et al., 1958). However, in the late stages of the evolution of magmas, when oxidative processes become dominant, U^{4+} becomes oxidised to the U^{6+}, thereby increasing the solubility of U. This results in fractionation of U and Th.

The solution chemistry of U, as described above, determines its behaviour in weathering and other low temperature alteration processes within the Earth's Crust. Primary U minerals, mostly precipitated in the hexavalent state, are easily oxidised by surface and groundwaters, especially in the presence of complexing ligands. Thus the mobile uranyl ion is produced which is easily removed in solution. Thus rocks become leached of their U during weathering. The released U can then be precipitated in the hexavalent state when conditions become reducing, or fixed as adsorbed ions onto Fe, Mn or Al oxides, organic matter or clay.

These precipitative processes provide rich local concentrations which may form secondary U deposits. Secondary U minerals, such as gummite, schoeeckingerite, tobernite, carnotite, autunite, zippeite, tyuyamunite and uranophane, contain U in its hexavalent state (Boyle, 1982).

2.8 Interpretation

The discussion given above highlights some aspects of the complex behaviour of U in the natural environment, and the processes which could affect its abundance. Although the time of formation of the elements may not have direct relevance to element abundances in the Crust, the segregation of the Crust from the Mantle is, clearly, very significant. For U this process led to an enrichment in the Crust relative to the Mantle. The segregation process was also such that U will be more abundant in the continental Crust which lies close to the surface of the Earth. Average values for the crustal abundance of U should, therefore, take into consideration these variations. At present, average values are more likely to be averages for a limited layer of the Crust rather than the average for the entire Crust.

The radioactive and chemical properties of U give rise to great mobility of U in the environment. For example, its radioactivity produces heat which can drive hydrothermal convective circulation cells that oxidise and mobilise the U, or the

radioactivity can destroy the crystalline structure of minerals, thereby making them more easily leachable by solutions circulating in the environment. Radioactive decay can also lead to the loss by recoil of individual atoms. Moreover, the daughters of U produced by radioactive decay may have different chemical properties. If fractionation of these daughters takes place a great deal can be discovered about active processes in the environment. Finally, the large ionic size of U means that it is difficult to be incorporated into the major rock-forming minerals of the Earth's Crust. Thus it is present either in its own minerals, which are rare because of its low concentration, or it becomes concentrated, by diadochic substitution of the REE in accessory minerals. The significance of these aspects of the geochemistry of U are discussed in the following Chapters.

CHAPTER THREE: ALTERATION OF GRANITE - HYDROTHERMAL AND WEATHERING PROCESSES

3.1 Introduction

Apart from the biosphere, the crust is the most active part of the Earth. Here heat from deep in the earth, groundwater solutions and the weather are all operative. Earthquakes, both natural and manmade, open fractures and aid vigorous interaction between rocks and groundwaters. Also, Man acts to affect the crust in many ways, but especially in removing some components and replacing these with materials that can be out of chemical equilibrium with their surroundings.

Granites, being the largest constituent of the continental crust, are greatly affected by the processes of change experienced by the crust. On exposure, or in the shallow subsurface, they become prone to the hazards of this environment. Hard and impermeable as they may appear to be, they are altered with time. In some cases they are changed beyond recognition; in others they retain their texture and appearance, but develop a new mineralogy, as in the kaolinised granites of South-West England. Alteration may be local, but in some instances a whole pluton may be affected. There is also abundant evidence that changes at great depth also occur in granitic bodies. In particular, hydrothermal ore bodies

can be formed throughout the post-magmatic history of granites, depending on the thermal evolution of the area in which they are emplaced.

Granites alter to different end-products depending on the alteration agency involved and its duration, as well as the actual character of the granite itself. This Chapter discusses the alteration of granite with particular reference to hydrothermal and weathering processes. The most important agent in such alterations is water.

3.2 Hydrothermal Alteration

3.2.1 Introduction

The action of hydrothermal fluids in granites has been well documented. Especially, hydrothermal movement has been found to be responsible for the concentration of a great number of minerals in economic quantities in ore deposits. There are many hypothesis regarding the action of thermal fluids in granites, particularly those with a non-magmatic origin. These fluids derive their constituent elements by leaching of either the host rocks of the granites or the granites themselves. Numerous ore deposits of hydrothermal origin are known. Most are believed to have been formed by convective circulation systems. In the granitic batholith of South-West England, Moore (1982) proposed that polymetallic

veins associated with post-magmatic hydrothermal events were deposited by several generations of single-pass convection systems. He noted that the vein systems are similar in shape and size to the individual convective cells in modern thermal fields.

Recent studies indicate the development of active Hydrothermal convective cells in radiothermal plutons as means of explaining certain aspects of the distribution of radioelements and heat flow in plutonic environments. For example, Fehn et al. (1978), Heath (1982), and Durrance et al. (1982).

Although knowledge of the detailed chemistry of solutions involved in hydrothermal activity is still hazy, studies over the last few years have shown that the most important sources of these solutions are: (1) waters from a consolidating magma, (2) connate water, and (3) meteoric water. Either separately or mixed together, these could have been heated by the cooling of a pluton, by thermal activity in the mantle, or by heat due to the decay of radioelements in the rocks.

In any discussion of the operation of hydrothermal systems in granite it is important to consider the source of the solution, it's movement through the granite, and the physico-chemical conditions which control the changes it brings about.

3.2.2 Sources of Hydrothermal Solutions

As noted previously, there are basically two sources of

hydrothermal solutions: waters from the consolidation of a magma and groundwaters in the surrounding crust. The latter waters may be connate or meteoric. The source of such solutions, for any particular area where hydrothermal activity is found to have operated, may be obtained from oxygen and hydrogen isotopic studies of the fluid inclusions in the minerals produced by the activity. Identification of the source helps elucidate the nature of the solution/mineralisation processes which have acted and the dynamics of the system.

Hydrothermal solutions of magmatic origin are thought to be mostly the result of the expulsion of excess water during the cooling and crystallization of magma in the upper crust. Other sources of magmatic solutions which are more remote, such as the lower crust and the mantle, have also been invoked by some workers (Evans, 1980). Both the quantity of the solution which is available, and its chemistry, must necessarily depend on the nature of the source. In very acid and very alkaline igneous rocks, which originate from magmas rich in water (Hatch et al., 1972), for example, the quantity of water that is released by crystallization is much greater than that released during the crystallization of intermediate rock types. These waters will also be rich in K^+. The influence of the hydrothermal water will also depend on how far it travels from its source. In cases where precipitation from these solutions takes place in the immediate environment of the source, the products are likely to be quite different to those which form

far into the host rock. This is because interaction between the solutions and the host rocks will progressively change the chemistry of the solutions. Concomitantly, the nature of the host rock alteration which occurs, will also change.

Previously, because of the close association of hydrothermal activity with igneous bodies, magmatic fluids were believed to be the only important source of hydrothermal solutions. However, with new evidence of hydrothermal activity much younger than the period of intrusion, and isotopic data, other sources have to be invoked. Among these is connate water, which is water trapped in sedimentary host rocks at the time of deposition. This water may be driven out of the rocks by a rise in temperature (Armstead, 1978). The amount of such water available for alteration/mineralisation will depend on how much water has been trapped during sedimentation. Because most connate water is lost during compaction of the sediments, connate water as an important source of hydrothermal fluids is restricted to a limited depth range.

Today, meteoric water is considered to be the most important source of hydrothermal solutions. The driving force for convective circulation can be any thermal event: either a nearby igneous body, enhanced mantle heat flow, or heat from the decay of radioelements in upper crustal rocks. Clearly, the vigour of the driving force depends, in part, on the amount of heat available. However, convective circulation also depends on the properties of rocks through which the water passes - particularly its fracture

permeability. Also, the chemical conditions prevalent in the environment will determine the nature of the solution/mineralisation process. Rain water, for example, percolating through soils rich in organic matter will have great complexing capacity, and will be able to carry along with it a great quantity of ions.

In the tropics, the amount of water percolation may be very small, but extend well below the surface. This is due to evaporation and the fact that the water table will probably be at great depth. Therefore, waters finally reaching the circulation system below the water table will probably carry great amount of dissolved ions. Conversely, in humid climatic regions large volumes of water from the surface percolate through the subsurface, to join the circulation system in a shallow water table. In these conditions there will be much less concentration of dissolved ions. Therefore, once the solutions become part of the circulation system, these properties become important in determining the nature of the alteration/mineralisation produced.

For any one alteration/mineralisation event, it is often very difficult to abscribe a particular source for the hydrothermal fluids. To a large extent there is mixing between waters of magmatic origin and those with a connate or meteoric source, and between connate and meteoric waters. However, in other cases the origin can be be traced to a particular source. The granites of South-West England, for example, are generally believed to

originate from a magma with a limited water content (Stone, 1975) and, therefore, any large-scale hydrothermal alteration/ mineralisation must have had a water source other than magmatic. The fluids responsible for the large kaolin deposits, which are believed to be largely of hydrothermal origin, must have been meteoric. Indeed, Sheppard (1977) recognised meteoric water as being responsible for most of the metalliferous deposits of South-West England. Durrance (1983) also concluded that although all sources of groundwater have had their influence at different periods in the hydrothermal circulation and mineralisation observed in the granites of South-West England, meteoric water is involved in modern hydrothermal convective circulation systems.

3.2.3 Hydrothermal Convective Circulation Systems in Granites

Fluid movement in granite can occur in a variety of ways. Surface water, for instance, percolate through pores and along grain boundaries in granites to join groundwaters at depth. Conversely, groundwater from depth can rise to the surface via fissures and fractures in the granites. However, to explain certain aspects of hydrothermal activity, mass movement of fluid, mainly water, has to be invoked. The hydrothermal movement of fluid in granite can be viewed as mass flow which might have been developed

over a considerable period of time. In this Section, the transport of hydrothermal solutions through a granitic medium will be briefly discussed, but it must always be borne in mind that the most important constraints are the permeability of the medium and the physico-chemical properties of the fluid. Indeed, it has been observed that for convective hydrothermal circulation, the most important limiting factor in groundwater flow is the permeability of the rock (Durrance, 1983). A possible mechanism by which movement takes place in a hydrothermal system in a granite with limited permeability, is advanced below.

3.2.4 Permeability and Fluid Movement in Hydrothermal Systems

A hydrothermal system is made up of two components, namely the fluid and medium through which the fluid moves, and both impose their constraints on the system as a whole. The ability of a rock to allow the movement of fluid through it is expressed as its permeability, a property which is dependent on the void spaces and their interconnections in the rock matrix. Therefore, any discussion of the flow of a mass of fluid, such as is encountered in a hydrothermal system, must take into account this property. In fact, it is regarded as essential in all free-convection models describing hydrothermal systems (Fehn et al., 1978; Durrance, 1983; Heath, 1982). To consider the different aspects involved in hydrothermal activity, the systems, could be approximated to either

a pipe or set of pipes, or as diffuse flow in an extensive medium (Elder, 1981). Each of these approximations can be used to explain the behaviour of certain hydrothermal phenomena. For example, the pipe approximation can explain the great majority of hydrothermal mineralisations and wall rock alterations, while flow in an extensive medium may explain the vast areas of kaolin deposits which are encounted in South-West England. However, in both cases the flow of fluid is governed by Darcy's Law which, in it's simplest form, can be written as:

$$q = -(k/m).(dp/ds)$$

where dp/ds is the pressure gradient, k the permeability of the medium, m the viscosity of the fluid, and q is the average rate of flow.

The general process involved in hydrothermal systems is the heating of water at depth, which then causes an upward flow due to buoyancy. A model, such as is shown in Figure 3.1, can be used to discuss the flow of fluid in an extensive medium. Here the variables are, permeability (k), conductivity (k_m), saturated water water density (ρ), coefficient of expansion (γ), specific heat capacity (C), and viscosity (ν). The whole system is subject to an acceleration due to gravity (g). These properties are sufficient to describe any aspect of the system (Elder, 1981). To explain the development of convective fluid movement, consider a mass of

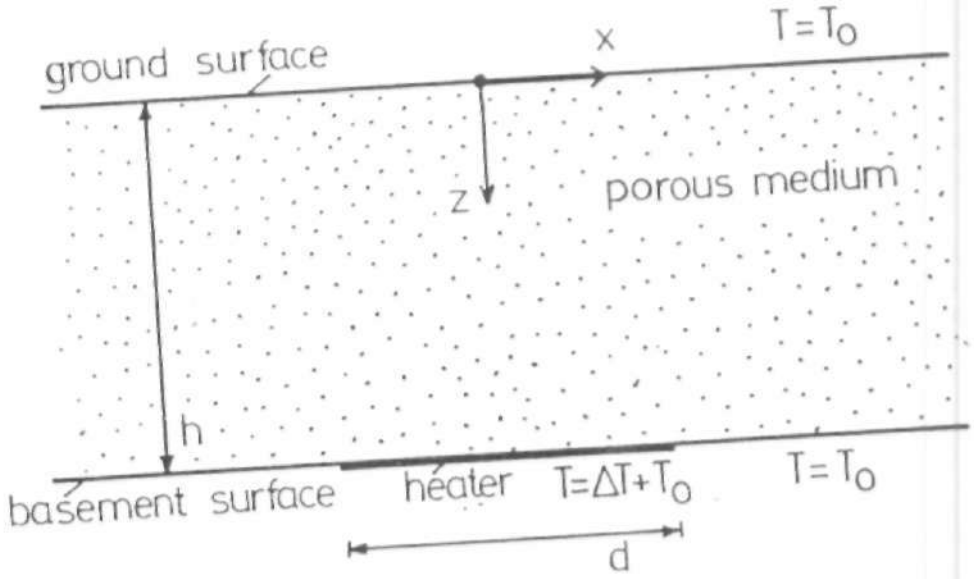


FIGURE 3.1 Arrangement for study of free convection in hydrothermal systems in a porous medium (After Elder, 1981)

relatively cold water incident on the heater; this becomes heated and rises by buoyancy, thus producing a vertical jet of rapidly moving fluid. As this plume or jet rises it spreads only a little. However, as it reaches the upper surface, it spreads out over the surface and therefore cools. The theoretical temperature distribution in such a model has been computed by Elder (1981), and is shown in Figure 3.2.

At the surface, provided it is permeable and recharge can occur to keep the system flowing, discharge will occur if the pressure over part of the surface is lowered. The consequent flow is thus made up of flow due to the discharge and the flow due to the free convection in the medium. Hydrothermal discharge systems manifest themselves on the surface as hot springs and geysers. The character of the discharged fluid is greatly modified in the surface zone (which extends to depths in the order of 100m), because of interaction with the surrounding rocks. Where discharge is not possible, free convection may persist until the heater becomes cold, but if discharge occurs then flow becomes dominated by the pressure difference. Taking the effect of discharge alone, the volumetric discharge, Q, is proportional to the pressure change dP, in a volume V of the confined fluid (Elder, 1981), such that;

$$Q \propto (kV^{1/3}).(dP/\mu)$$

where V is the volume of the confined fluid inside which the

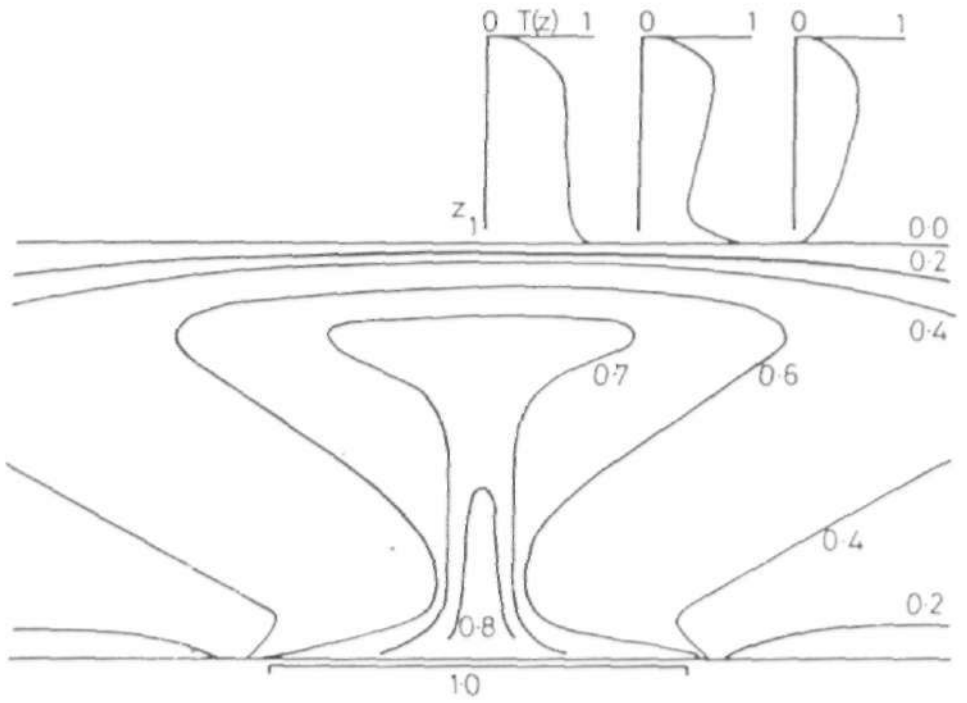


FIGURE 3.2 Temperature distribution in free convection model

(After Elder, 1981)

pressure change takes place. In this case, for a system in which the discharge is produced by lowering the pressure, discharge is conducted to the surface through a pipe (Figure 3.3). The effect of these flows on the shape of the bulbous volume of hot water above the heater, called the mushroom, for different power input (F) and power output (F_1) are shown in Figure 3.3. The most important effect is the progressive collapse of the mushroom until the system approaches that of the pipe flow model (fracture controlled flow), which ignores the details of heat entering the system and considers only forced convection (Durrance, 1983).

The simplest model for describing hydrothermal systems is the pipe model in which the bulk of the rising hot fluid passes once through the system. Figure 3.4 shows a model due to Donaldson (1968). In this model the pipe which acts as conduit for the fluid is a channelway of porous medium of uniform permeability between blocks of impermeable mass. The reservoirs are maintained at a uniform temperature (T_o). Cold water seeping down the vertical channelways is heated at depth in the horizontal channel which connects the vertical channels. This hot water rises by buoyancy and flows through the channel between the impermeable blocks. The mean mass flow rates are then a function of the permeability, the dimensions of the vertical channels, and the densities of the fluid in the hot and the cold channels. Thus assuming there is no secondary convective circultaion in any of the channels, the mean

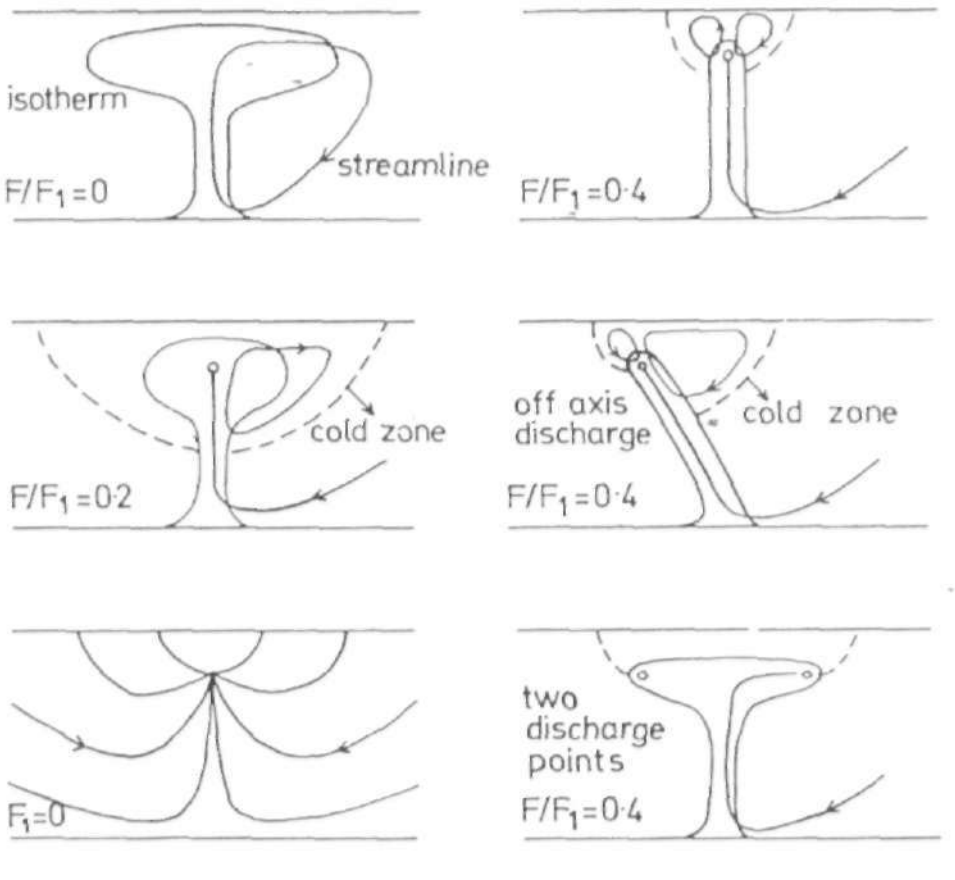


FIGURE 3.3 Effects of discharge on the temperature and velocity distribution in a free convection model for various power input F and power output F_1

(After Elder, 1981)

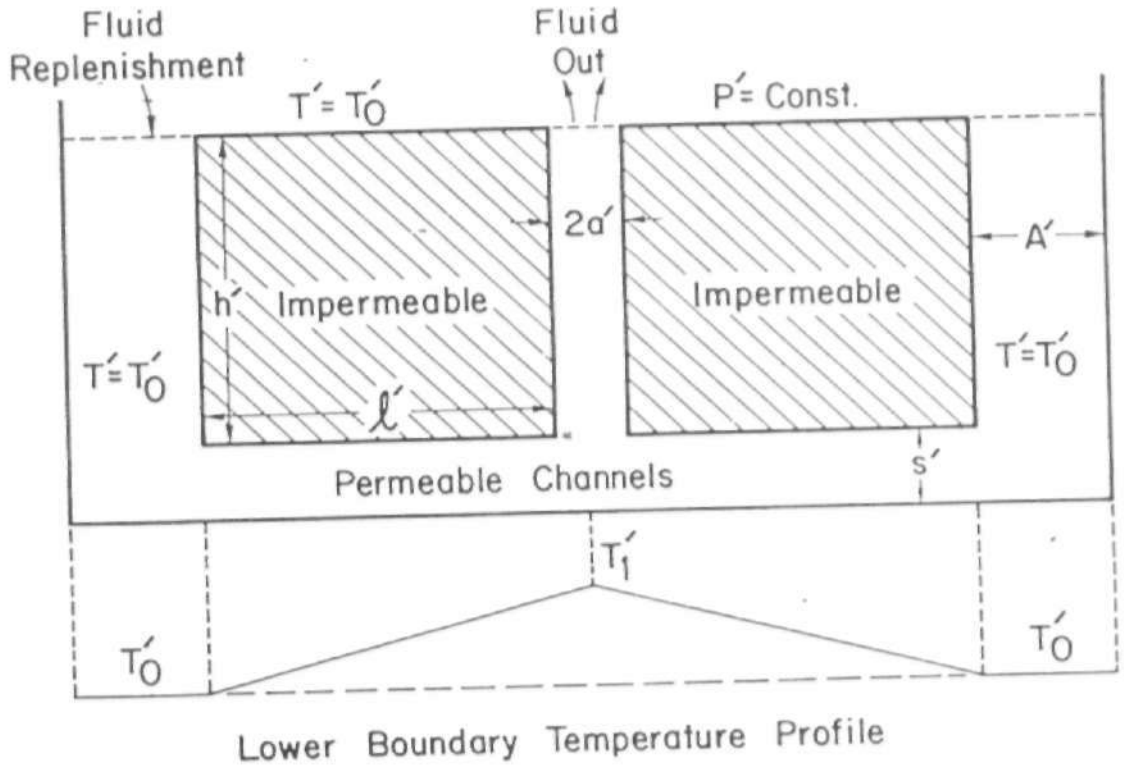


FIGURE 3.4 Pipe discharge in a model for hydrothermal systems

(After Donaldson, 1968)

upflow rate will be:

$$Q(\text{mean}) = \rho k B g (T_m - T_o)/Ld$$

where

ρ = the density of the fluid

d = 1+al/sh+A/h

T_m = mean temperature of hot vertical column

B = coeff. of expansion of fluid

L = viscosity of fluid

k = fluid permeablity

g = accelaration of gravity

and s,a, h and A are as defined in the Figure.

In this model, an increase in a increases the amount of fluid output.

Temperature variation across such a system has been studied by Donaldson (1968). He noted a marked difference in temperature between the conduit channel and the impermeable zones, and an increased heat conduction through the upper layers of the impermeable strata in the neighbourhood of the central channel. Therefore, temperature gradients in the field may indicate a much larger area for the hot channel than is really the case. The mass

of fluid discharged is largely determined by the head of recharge water, the flow being proportional to the pressure difference. For a typical discharge at Wairakei, at a temperature of 250^{o}C with a vertical column 5km deep, Elder (1981) has calculated that a head difference in the order of 1km is produced. The nature of the fluid discharge depends on the energy available for heating the water. With high energy input, the discharge may be gaseous.

Clearly, from the foregoing discussion, permeability is the most important property of the medium for convective transport in hydrothermal systems. On macroscopic scale, the flow in such systems are represented by Darcy's relation, but Elder (1981) has shown that permeability is only definable provided the mass of the fluid involved in the flow has a length scale which is large compared with the scale of the structure (the joints or fractures) in the medium in which the system occurs. However, the matrix permeability of unfractured granites is of the order of 10^{-3}mD, and permeabilities in the order of 100mD are required to maintain hydrothermal systems (Elder, 1981; Fehn et al., 1978) . Moreover, the permeability of rock systems decreases with depth due to compression, yet most hydrothermal systems are embedded at depth. In the study of a hydrothermal model of width 24km at a depth of 10km, Garg and Kassoy (1981) showed that an intergranular permeability of 10^{-3}mD is required for convective heat transfer to be significant, otherwise heat transfer will mainly be conductive, and there will be no transport of matter. In addition, the

permeability necessary to maintain a system depends on the extent of the system. In large systems, the permeability of the whole zone is dominated by the permeability due to the existence of joints and fractures. Indeed, fracture-induced permeability is usually much greater than intergranular permeability. Fracture permeabilities are anisotropic and much more sensitive to fluid pressure and rock stresses (Garg and Kassoy, 1981).

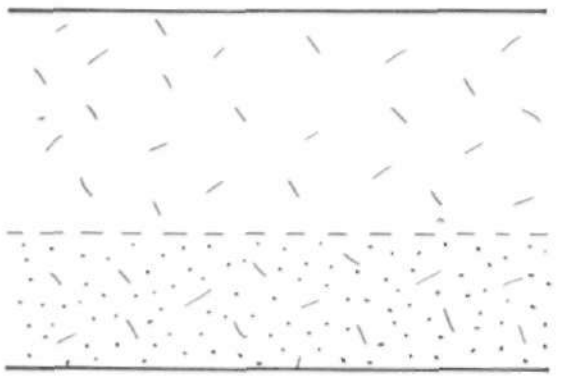
Thus, although the intergranular or matrix permeabilities in most of the media in which hydrothermal systems operate are much smaller than required to maintain such systems, it is not very difficult to see how fractures allow them to develop. Furthermore, any process that increases the number and/or size of fractures in the rock mass greatly increases the permeability. Presently available data have shown that most hydrothermal systems are located in seismically active zones. High heat production in granites can also enhance the overall permeability by inducing fractures and cracks. Durrance (1985) noted the opening of fractures in the granites of South-West England as being responsible for modern hydrothermal convection cells in the region. The permeability of the rocks, therefore, controls the amount of fluid, the rate of transport of such fluids and, to some extent, the fluid reactions with the host rocks.

Another mechanism that could be used to explain the movement of fluids in granites of very low permeability is saturation-dissolution, helped by osmosis. This can be visualised by

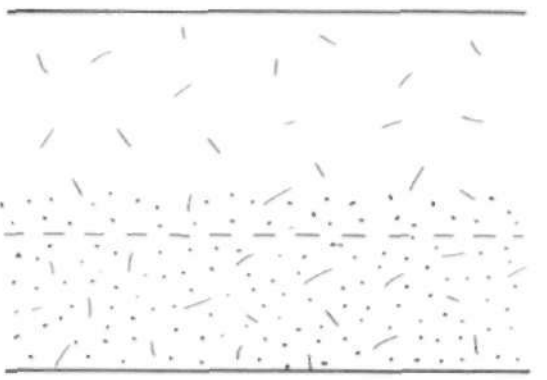
considering water trapped in a homogeneous impermeable igneous mass (Figure 3.5). When the water is induced to move by a change in one or more of it's properties, for example temperature or pressure (but more by temperature in hydrothermal systems), it starts dissolving the minerals in rock, and thus moves along grain boundaries. When a layer of the medium is saturated with this solution, the water left behind has a lower ionic concentration, hence osmosis sets in and the fresher water moves in to dilute the rather more concentrated solution. This keeps the solution in motion, and will continue until the solution discharges as run-off. This may be either in the near-surface zone or another reservoir. If it meets a medium of different physical properties, it may change direction and cause a convective cell to develop. Thus the first driving force in this model is the change in the physical state of the water in the reservoir, and the direction of motion of the solution is largely determined by osmotic pressure, rather than by buoyancy. That the dissolving power of the water is increased by a rise in temperature is well established. Water movement along grain boundaries in igneous rocks is also a common phenomena. Zonation and layering in some of the rock-forming minerals may also enhance solution movement in the rocks.

3.2.5 Recharge and Alteration

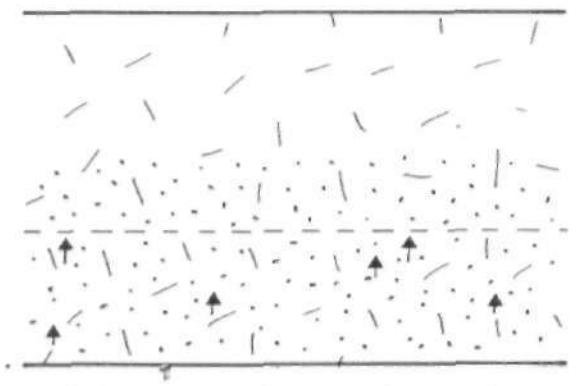
General ideas regarding the operation of hydrothermal



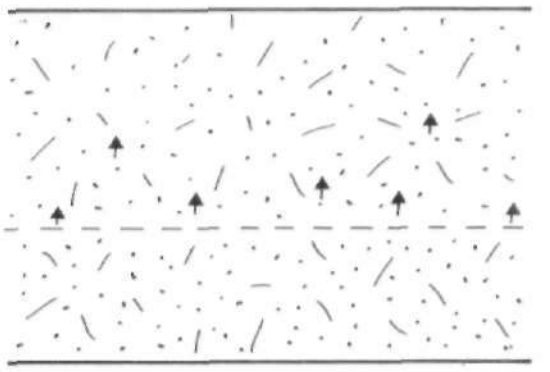
a) Water trapped in an impervious rock



b) Temperature of water rises thus increasing its reactive power. It starts dissolving easily dissolvable minerals and moves along grain boundaries.



c) A saturated water layer is formed at the top of the reservoir. This layer is more concentrated than the one below because of the dissolved ionic species.



d) Because of the difference in ionic concentration between the two water layers, the water at bottom moves up by osmosis. Hence the direction of water flow is set up.

FIGURE 3.5 Solution movement through non-porous rocks in hydrothermal systems

systems have been outlined above. This Section applies these ideas to explain the changes in granites caused by hydrothermal processes.

Where they are operative, hydrothermal systems usually manifest themselves on the surface as discharges. These can be hot water in hot springs or gases in geysers. However, enhanced surface heat flow is another sure indicator. All of these surface signatures are very important in the study of hydrothermal systems and processes. In the surface and the near-surface zone, water flows along the most permeable paths, and the direction of flow is modified by local topography. For example, spring-type discharges will only occur where the water table cuts the ground surface. Where the water table is below the surface, the discharge is trapped as hot aquifers, to give fumaroles or steaming ground. In convective hydrothermal circulation systems, the surface signature may only be in the form of enhanced heat flow. In such systems, the rising hot water is taken back to the source or reservoir through a different path, and the solution is recirculated such that relatively cold water is always taken back to the source. The circulation can be likened to the cooling system of a refrigerator. In such systems different effects are produced by the the rising (hot) and the descending (cold) fluids. In the modern hydrothermal circulation systems operative in south Devon, Durrance (1983) suggested that kaolinised areas are associated with the sites of drawdown, while upwelling sites produced U and other mineral

deposits.

The interaction of the fluids with the rock which they traverse is such that the rock is enriched or depleted in certain minerals. Many ore deposits show evidence of being produced by hydrothermal processes. In the circulation of hydrothermal solutions, both the upward and the downward moving fluids are effective in concentrating minerals in ore deposits. Mineralisation produced by the former are referred to as hypogene, while the latter produce supergene deposits. Because of the high temperature of hydrothermal solutions, they are capable of dissolving a great variety of mineral species (Meyer and Hemley, 1967), and transporting these until suitable conditions for releasing them are encounted. The most important reactions are hydration and ion-exchange reactions. Notable among the interactions between hydrothermal solutions and the rock medium is wall-rock alteration. Many types of wall-rock alteration have been identified, and have been discussed in detail elsewhere (Meyer and Hemley, 1967). The most prevalent of these alterations in acidic rocks such as granites, include serecitization, argillization, silicification and pyritization.

Hydrothermal solutions are generally acidic to start with (Evans, 1980), but subsequently may become neutral or basic due to mixing with groundwater in the surface zone, or due to reaction with the rock medium at depth where the solutions are at high temperature. Therefore, the type and rate of reaction will be

determined by position along the fluid path. In areas immediately near the source of the fluids, reactions may be pervasive both because of the relatively high temperature and the acidic nature of the fluids. Hydrogen-ion reactions may be dominant in this zone. Conversely, in the surface zone, where temperatures are low and solutions dilute, the reacting capacity of the solution may bé greatly reduced. At the temperatures and pressures typical of hydrothermal systems at depth, the solutions are capable of dissolving a wide range of elements. Consequently, most rock-forming minerals are vulnerable to attack. Also, of course, it follows that high temperature alteration products are more likely to occur near the source of the solutions. However, the distinction may not be that easy. Firstly, some of hydrothermal processes are more active than others, such that the initial temperature of a certain system may just be the near-surface temperature of another. Secondly, the reactions also depend on the chemistry, petrography and texture of the rock medium. But these not withstanding, documented studies of hydrothermal alteration show that the extent of base leaching increases upward over a certain distance travelled by the solutions on their way to the surface (Meyer and Hemley, 1967).

For wall rock alteration, and indeed hydrothermal processes in general, leading to the formation of ore deposits, the most

important aspect of the process is the source of the metals. However, mechanisms of transportation and the physico-chemical conditions for precipitation, are also significant. Although water at the temperature and pressure typical of hydrothermal systems is a strong solvent, studies show that solubility alone can not explain the transportation of metals in hydrothermal solutions. It is now generally believed that the most important mechanism of transport of metals in ore-forming solutions is through the formation of complex ions. Several complexes have been suggested as important in the transportation of certain metals. For example, Barnes and Zamansky (1967) showed that in the formation of ZnS deposits, transportation by bisulphide complexes is most likely. In Chapter 8, hydrothermal circulation in the granites of South-West England in relation to kaolinization will be considered, while in the next Section the formation of hydrothermal U deposits will be discussed.

3.2.6 Deposition of U in Hydrothermal Systems

There are three important considerations in discussing hydrothermal U deposits. These are the source of the U in the hydrothermal solution, the mechanism of transportation, and the conditions for deposition. In the foregoing discussion, we have seen that metals in hydrothermal systems are mostly transported as complexes. U can exist in two oxidation states, and form a variety

of complexes. However, it is most susceptible to leaching when in its tetravalent state. In being accessed by oxygenated waters and oxidised to the hexavalent state, U becomes highly mobile. Granites with their usually enriched levels of U are believed to be the source of most of the U in hydrothermal solutions. This is also due, in part, to the close association of hydrothermal U deposits with granites, but the fact must also be noted that most hydrothermal activity, in general, is associated with granites. Brown et al. (1953) found that up to 40% of radioactive elements in granites could be removed by a cold acid leach, while Pliler and Adams (1962) reported the removal of 90% of Th and 60% U in a hot acid leach. A report of the leaching of U and Th from Dartmoor granite by Heath (1982), in both cold and hot acid, showed that hot acid is twice as effective in leaching U than cold acid. Nevertheless, even in cold acid, as much as 96% U and 72% Th can be removed from the granite. These findings show that U is much more easily leached in hydrothermal processes than in weathering, simply by considering the hot and the cold acid leach experiments as simulations of hydrothermal and weathering processes, respectively. However, at whatever temperature, surface water which has equilibrated with oxygen and is percolating through granitic rocks, is able to leach and transport large quantities of U to groundwaters.

There are many sources of acidic and oxidising solutions in the natural environment. Surface waters which have equilibrated

with atmospheric oxygen have just been mentioned, but subsurface waters which have equilibrated with highly oxidised rocks have also been suggested to be an important source (Rich et al., 1977) . As noted above, U in such solutions is transported in it's hexavalent state. In acid solutions, the major species of U in aqueous solution are $UO_2(OH)^+$ and UO_2^{+2}, while $UO_2(OH)_2^0$, $UO_2CO_3^0$, $UO_2(CO_3)_2^{-2}$, and $UO_2(CO_3)^{-2}$ are important in near-neutral and alkaline solutions (Rich et al., 1977).

U transported in hydrothermal solutions is deposited when conditions become reducing and U^{+6} is reduced to the U^{+4} state. This process is believed to be the mechanism for the deposition of U from hydrothermal ore solutions. It was suggested by (Rich et al., 1977) that reductants in the crust, such as biotite, hornblende, pyrite, graphite, and hydrocarbon compounds, are adequate to reduce the hydrothermal solutions and lead to the formation of U ore deposits. Hydrothermal U deposits have often been found spatially associated with hematite. In a study of 41 hydrothermal U deposits, Rich et al. (1977) reported that most of the deposits show hematization, but this may simply mean Fe^{2+} was mobilised as well. Other major wall-rock alterations associated with hydrothermal U deposits are argillization, carbonatization, silicification, and chloritization (Boyle, 1970).

3.3 Weathering Processes

3.3.1 Introduction

Weathering is the breakdown of surface and near-surface rocks by physical and/or chemical processes. Physical weathering involves the mechanical fragmentation of rocks by such agents as temperature change, water, ice, plant roots and some fracturing due to movement of the Earth's crust. These take place without marked chemical changes. Also, rocks may weather to fragments of different sizes depending on the agency involved and the period over which it operates. Chemical weathering, on the other hand, involves chemical changes. Loughnan (1969) defined chemical weathering as the processes by which atmospheric, hydrospheric and biologic agents act upon and react with the mineral constituents of rocks within the zone of influence of the atmosphere, producing relatively stable, new mineral phases. Strictly, weathering is a combination of both physical and chemical processes, but available studies on rock weathering suggest that in most cases the chemical aspect plays the more important role in decomposing rock masses. Generally, physical processes are restricted to within a few metres of the rock surface. They become more important only in extreme conditions, for example in dry regions with very high temperatures, and in rugged terranes. Moisture, CO_2, O_2 and temperature are the most important agents in weathering, and any process that controls

these factors is bound to affect the rate of weathering. Environmental conditions such as the climate, topography, and parent material of the rock, all influence the weathering process. The climate controls the amount of rainfall, thus controlling the amount of water that comes into contact with rock surfaces. A combination of high temperature and high rainfall greatly increases the degree of weathering. Rocks in moist tropical climates are much more affected by weathering than those in temperate regions. In contrast to both of these environments, in arid regions with scanty rainfall, only the topmost part of the rocks may be affected by weathering. Topography also influences weathering in that it controls the amount of run-off and, therefore, the amount of water that percolates into the rock mass. Because the agents involved in weathering react differently with the different rock-forming minerals, the rate and degree of weathering, and the weathering products, may be different for different rock types under the same atmospheric conditions. This gives rise to the formation of different soil types in the same geographic locations.

3.3.2 Processes in Granite Weathering

Water percolating through the fractures and microfractures in granitic rocks interacts and dissolves the soluble constituents. As more water passes through along these pathways, a large proportion of the more soluble constituents is removed from the

zone influenced by the weathering environment, leaving behind the less soluble constituents. These insoluble residues may then be transformed into a new mineral assemblage which is stable under the prevailing conditions. The mechanism of the breakdown of mineral structures and/or their transformation into other phases has been studied by Loughnan (1969). He concluded that:

a) Hydrogen ions produced by the hydrolising action of water on mineral surfaces play an important role in the breakdown of silicate structures. These ions penetrate into crystal lattices and, because of their high charge to radius ratio, have a marked disrupting effect on the charge balance within the lattice.

b) The persistance of Al in tetrahedral coordination, and the retention of highly mobile cations in secondary mineral products, indicate that much of the parent mineral structure is inherited by the secondary product.

Jenny (1950) gave a clear picture of the mechanism involved in such reactions. He believed that exposed atoms and ions at free surfaces possess unsaturated valancies, so that when these come into contact with water, the water dipoles are attracted to these surfaces, and hydration ensues. He proposed that attraction of the dipole may be great enough to cause the dissociation of the water molecules into hydrogen and hydroxyl ions. The hydroxyl ions are then able to bond to the exposed cations and the hydrogen ions to oxygen and other anions. Simultaneously, the hydrogen ions may replace anions at the mineral surfaces causing the latter to be

released.

The hydrated fragments from weathering may pass into an aqueous phase. These then form a product whose removal depends on the amount and composition of the water, and the time it takes to pass through the rock. To a large extent these factors determine the nature of the product, and thus the extent of the weathering process. The mechanisms of mineral breakdown and the subsequent processes that follow are, therefore, influenced by many factors. Environmental conditions in particular, affect the mobilities of the common metallic ions. As noted above, studies of the effect of climate on weathering suggest that moist tropical climatic conditions promote weathering more than any other climate. Of the individual climatic factors, the most important are rainfall and temperature. Rainfall influences the amount of moisture in the weathering zone. In arid regions, for example, where rainfall is scant, the breakdown of rock-forming minerals is greatly impeded, while; in humid regions, with high rainfall, there is constant supply of water to the zone of weathering, and as the rocks are more in contact with this water the breakdown of the minerals is enhanced. In such areas, the soluble products of weathering are constantly being removed from the environment where they were formed, thus exposing more surfaces for attack by incoming solutions. Temperature, to some extent also influences the rate of reactions involved in weathering processes, and determines the amount of moisture that is lost through evaporation. Thus

temperature has a two-edged effect on weathering, but data collected by Loughnan (1969) showed an increase in the clay content in soils derived from basic igneous rocks, with increasing mean annual temperature. Clearly, this suggests that higher temperatures give rise to greater weathering, provided sufficient water is present. Crowther (1930) gave an empirical relationship showing the influence of temperature and rainfall on weathering. This he termed the leaching factor (LF). It is defined by:

$$LF = R-3.3T,$$

where R is the mean annual rainfall (cm) and T the temperature (^{o}C) The effect of climate on weathering is graphically illustrated in Figure 3.6.

Another important environmental factor is topography. In rugged terranes the low-lying, flat areas are usually the reservoirs of surface run-off, thus experiencing much more water infiltration than the steep slopes of higher areas, where any rain is largely lost as surface run-off. Other topographic influences include such effects as modification of the temperature of the surroundings, and control on the water table. In higher ground, such as on plateau tops, water collecting in small fractures may at some time of the day freeze, thus enhancing the effects of physical weathering.

In addition to these environmental factors, the nature of

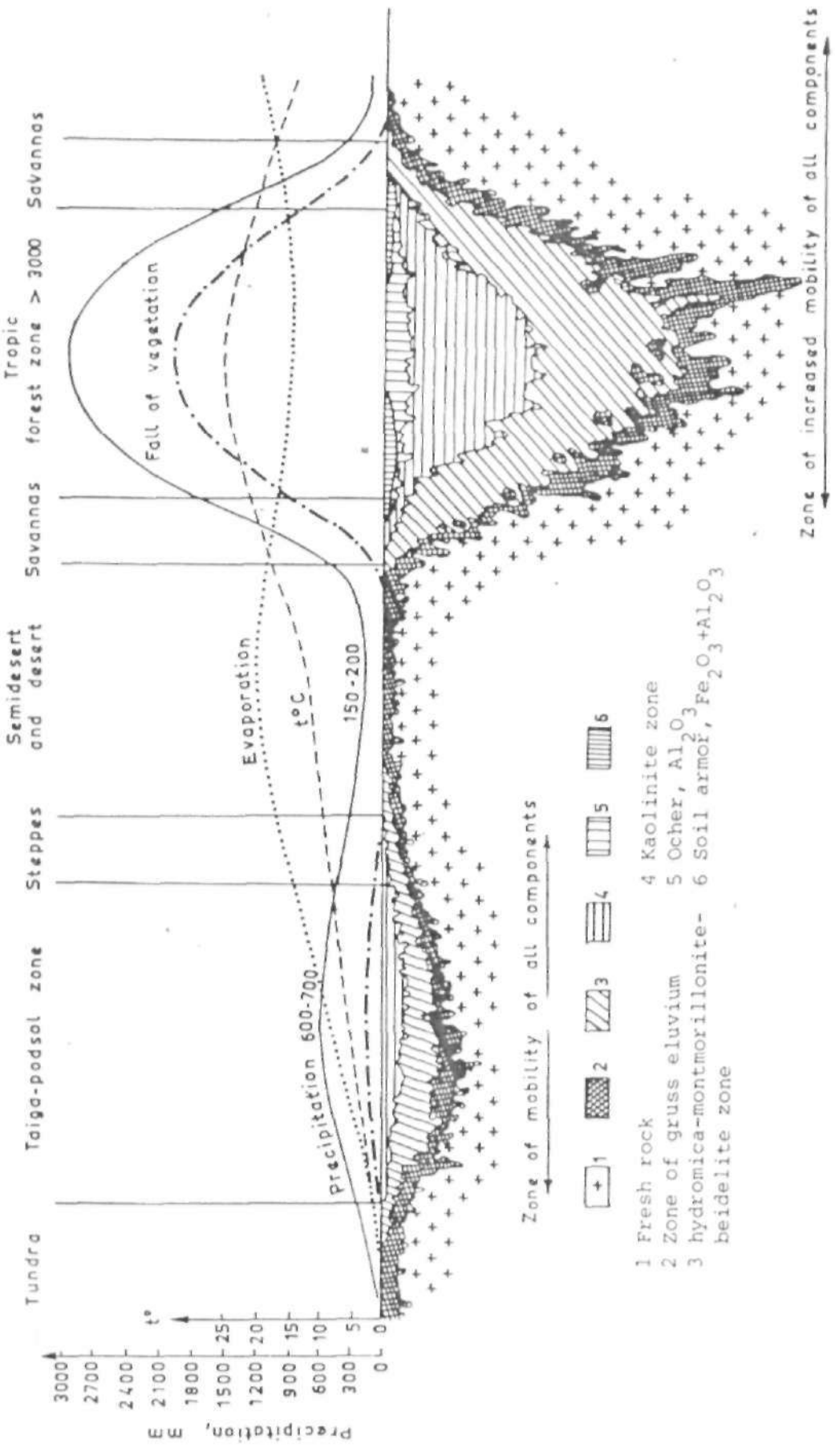


FIGURE 3.6 Cross section of weathering mantle showing the effects of climatic zones on the degree of weathering
(From Loughnan, 1969)

the rock is also important in weathering. Such properties as the texture, composition and the structure of the rock are significant. While texture and structure may influence the permeability of the rock matrix, and hence the amount of water permeating through it, composition determines the ease with which the water reacts with the rock. Crystalline rocks which have a high content of the more stable silicates, such as quartz, may require intense weathering, and /or a greater time interval, to be broken down compared to more Fe/Mg-rich rocks.

Other important factors are those which control the mobilities of the common metallic ions in the weathering environment. It is one thing to remove ions from the minerals in which they occur, and quite another to take them out of the weathering environment. Such factors as the pH of the percolating solutions, the Eh of the environment, fixation and complexing, and to some extent the atomic structure of the metallic ions themselves, have been found to exact a great influence on ionic mobility during weathering.

pH exerts a major influence on the solubility of ions. Solubility data for the major oxides and hydroxides occurring in rock-forming minerals compiled by Loughnan (1969) show that in the normal pH range of groundwaters, Ca(OH), Mg(OH), and the alkalies are completely soluble, while TiO_2, $Fe(OH)_3$ and Al_2O_3 are relatively insoluble. The solubility of $Ti(OH)_4$, $CaCO_3$ and $Fe(OH)_2$ is variable within this range. Therefore, differences in the pH of

the groundwater will affect the mobility of Ti, Ca, and Fe. Solubility alone can not account for the concentration of metallic ions in groundwaters, and it has already been pointed out that some ions are carried in solution as complexes. Mostly these are complexes with organic compounds derived from organic matter in the soil through which the solutions drain. Solutions passing through soils rich in organic matter, therefore, will have an increased potential for carrying metals in solution.

The Eh of the environment reflect the oxidation-reduction capacity. Hence, for metals such as Fe and Ti, which can exist in more than one valency state, their solubility or precipitation is greatly influenced by the prevailing Eh of the environment. In solutions with a low pH, for example, ferric hydroxides are precipitated, they remain in solution under normal weathering conditions. Conversely, ferrous hydroxides require a much higher pH for precipitation. Therefore, in reducing conditions and where the pH is low, much of the Fe may be leached from the weathering zone, but it remains in the insoluble ferric state in oxidising conditions.

Some cations may react with weathering products and become fixed in the immediate subsurface. It is generally believed that K is concentrated in weathering products through this process. It has been established that expandable clay minerals are responsible for this phenomenon in soils. Barshad (1954) believed that K-fixation by clay minerals depends on the layer charge of the clay minerals. Similarly, fixation may account for the concentration of otherwise

Similarly, fixation may account for the concentration of otherwise mobile elements, such as U and the alkaline earths, in weathering environments.

Because of the fact that all minerals do not weather with the same ease under the same conditions, it is generally believed that the structure of the minerals plays an important role in determining their stability in the weathering environment. That is why these factors are taken into account when assessing the weatherability of minerals.

A necessary condition for effective weathering is that the solution product must be effectively removed from the weathering environment, so that fresh surfaces are always in contact with the hydrolising solution. This is achieved by continuous flow of water through the weathering zone. The products are taken in solution through the subsurface drainage to such outlets as lakes, rivers, streams, and oceans, while some are deposited en route. The removal rate of the products clearly also depends on those factors which influence the mobilities of the common metallic ions.

In conclusion, therefore, we see that the loss or gain of elements in the weathering of rocks depends on many complex factors which are themselves interrelated. Mass balance relationships can be determined with some accuracy for each reaction only by considering individual environment, but always the most important

factor controlling the decomposition of any rock type is the rate of water movement, other factors only determining the rate of weathering and type of product formed.

3.3.3 Geochemistry of Granite Weathering

Weathering processes either enrich or deplete the weathering environment of certain elements. A soil which develops may have a composition completely different from that of the original rock material from which it is produced, although they are related. Some elements may be enriched, others depleted, while still others remain unchanged. Apart from the importance of the environment, and the physico-chemical conditions prevalent at the time of the weathering process, the geochemical properties of each element must be considered. Although a full discussion of the geochemical changes in weathering of a granite encounted within this study will be given in Chapter 9, a brief discussion of the general features is outlined here.

The redistribution of elements during weathering is essentially a measure of the mobility of the elements in different rock-water interaction regimes. Usually Al and Ti remain fairly constant during weathering and they are often used as base lines against which losses and gains of other elements are referred (Ruxton, 1968; Nesbitt et al., 1980).

Granites are generally associated with high abundances of

potash-rich and soda-rich feldspars, quartz, and lesser amounts of amphiboles and micas, while other components occur as accessory minerals. The minerals in abundance in granitic rocks rank among the most stable in the weathering environment, and require intense weathering activity for their complete breakdown. In the weathering of feldspars, clay minerals are the common end-products, with kaolinite and halloysite being the common minerals. Such reactions are represented by:

$$2NaAlSi_3O_8 + 9H_2O \longrightarrow \underset{\text{halloysite}}{Al_2Si_2O_5(OH)_4 2H_2O} + 2H_2SiO_3 + 2NaOH$$

$$3KAlSi_3O_8 + 8H_2O \longrightarrow \underset{\text{illite}}{KAl_2(AlSi_3)O_{10}(OH)_2} + 6H_2SiO_3 + 2KOH$$

$$2KAl_2(AlSi_3)O_{10}(OH)_2 + 5H_2O \rightarrow \underset{\textit{kaolinite}}{3Al_2Si_2O_5(OH)_4} + 2KOH$$

Studies of clay in soils have shown that minerals other than kaolinite are obtained from the weathering of feldspars. Sand (1956) found that in the formation of kaolinite, illite is first produced as an intermediary (as shown in the second equation above).

The reactions which occur in the weathering of the feldspars essentially involve their dissolution through hydrolysis, and

produce silica and alumina in solution. Such reactions have been extensively studied. Wollast (1967) observed that the first stage of hydrolysis is a reversible cation-exchange process, whereby cations are exchanged for H^+. In an experiment he found that K^+ was readily lost from crushed potash-feldspar, and H^+ taken up. In a study of mass transfer during the hydrolysis of potash feldspar and albite, Helgeson et al. (1969) showed that gibbsite, kaolinite, K-mica and gibbsite, and kaolinite and montmorillonite, were produced.

Quartz, which is another abundant mineral in granitic rocks, has been found to be relatively stable under weathering conditions. It can survive many cycles of weathering, and has been found in sediments where rounding of grains is the only visible effect of erosion and weathering. Unlike the other silicates, it does not alter to other minerals, but usually is slowly taken into solution during weathering. Interpretation of thermochemical data by Siever (1957) showed that quartz should have a solubility in the range of 7-14ppm at ambient temperatures.

The next most abundant minerals in granites are the amphiboles and the micas. Amphiboles have two well-developed cleavages parallel to the length of the chains of the hydroxyl groups, and these places are usually the target of attack by percolating groundwater. Common among the amphiboles in granites is hornblende $[(Ca,Na)_2(Mg,Fe,Al)_5(Al,Si)_8O_{22}(OH)_2]$, which on alteration yields chlorite as a major product. With more leaching

213884

the chlorite may be transformed to vermiculite. Stephen (1952) reported the alteration of hornblende to chlorite, with some sphene, hematite, and epidote, as the initial products. The common micas in granite are muscovite [$KAl_2(AlSi_3)O_{10}(OH)_2$], biotite [$K(Mg,Fe)_3(AlSi_3)O_{10}$] and, to some extent, phlogopite [$KMg_3(AlSi_3)O_{10}(OH)_2$]. It has been found that muscovite is relatively more resistant to weathering than the biotite/phlogopite group. Although the mechanism of weathering of the micas has been attributed to the solution of K in the K-O bond (Loughnan, 1969), and the introduction of water molecules, the reason for the disparity of dissolution between the two groups is not well understood. In contrast, the weathering of biotite has been extensively studied, and Walker (1949), Barshad (1954), Mortland (1958) and Basset (1960), have shown that vermiculite is the weathering product. Recently Bouda (1985) observed that biotite in the weathering of the granite of Dartmoor in South-West England is affected by hydrolysis, such that the dissolution is much more extensive within the structure than on the mineral surfaces. This leads to the oxidation of Fe, interlayer K exchange for hydroxyl ions, expansion of the layers, and exfoliation. Correns (1961) believed that the weathering of muscovite produces a mica which he called dioctahedral illite. The presence of vermiculite in the weathering of muscovite has also been reported, for example, by Rich and Obenshain (1955), and Brown (1953).

The accessory components in granite include such minerals as

zircon, apatite, and magnetite, with their importance varying from one rock to another. Zircon has been extensively studied, mainly because of it's U and Th content. It has been found to be stable under normal weathering conditions, but under intense weathering some zircons are found to be altered. Corrosion of zircon has been observed, and Carroll (1953) suggested the importance of both acid and alkaline solutions in such corrosion processes. Bouda (1985) found some evidence of the dissolution of zircon crystals in the A horizon soils developed on Dartmoor. Magnetite has also been found concentrated in sedimentary rocks thus showing its degree of resistance to weathering.

Efforts have been made to determine the order of stability of these minerals under weathering conditions. Goldich (1938), in a study of the weathering of a granite gneiss in Minnesota, obtained the order of stability of the minerals under the present-day weathering conditions as: zircon, quartz, microcline and orthoclase to be the most stable, while ilmenite/magnetite and biotite are relatively stable, and plagioclase, epidote, hornblende and apatite are the most unstable. Harriss and Adams (1966) also reported plagioclase feldspar, biotite, potash feldspar, and quartz to have increasing stability in the weathering of granite rocks. This order was observed regardless of climatic and/ or local physico-chemical variations. Ollier (1969) reported what he called a weathering series, in which the minerals were arranged according to their weatherability, as anatase, muscovite, rutile, zircon, tourmaline,

monazite, garnet, biotite, apatite, ilmenite, magnetite, staurolite, kyanite, epidote, hornblende, andalusite, topaz, sphene, zoisite, augite, sillimanite, hypersthene, diopside, actinolite and olivine; the weatherability decreasing in that order.

In the process of mineral destruction and the creation of new minerals in the weathering environment, some elements are lost from the weathering zone. The total amount of the element which is lost will depend largely on it's abundance in the rock being weathered, but also upon how it is held in the minerals which make up that rock, and its mobility. Generally, in the weathering of granites, there should be a decrease in Ca, Na, Al, K, Si, O_2, and H_2 due to the breakdown of feldspars, and a decrease in Mg and Fe from the breakdown of the micas and magnetite. But, because of the production of kaolinite and halloysite as products of the degradation of feldspar, some elements (more especially K, Th and U and some of the large ion REE) are retained in the environment. These may show some increase in abundance or no variation during weathering of granite rocks. Any U lost due to the possible alteration of zircon, for example, may be made up by the U that can be held on clay minerals. Similarly, the overall silica content may increase or show no sign of depletion, because of the concentration of such resistate minerals as zircon and quartz. If

the amount of an element lost during the weathering of a particular mineral could be determined, then it is possible to make an estimate of the gross element loss during the weathering of a particular rock type. Unfortunately no investigation of such a nature has been carried out. The nearest is the work of White et al. (1963) who reported analyses of drainage waters associated with different rock types. The data given in Table 3.1, show that waters from granitic rocks lie on the acid side of the pH scale, and there is associated a comparatively high Al loss. The results also show the close correlation of the values with the composition of the parent rock types. The acidic rocks yield solutions which are rich in silica, with corresponding low pH values. Very low alumina and Fe concentrations in these analyses are in agreement with the general observation of the mobility of these elements during weathering.

Bulk compositional changes in the weathering of different rock types have, however, been studied. These studies have shown that most loss of the common metallic elements occurs for Na and Ca (Smyth, 1913; Anderson and Hawkes, 1958; Feth et al. 1964; and Harriss and Adams, 1966). The behaviour of other elements is, however, also determined by the nature of the weathering environment. Butler (1953) reported the depletion of Sr, Ba, Ga, V, Sn, Li, Co, Mn, Y, LA, Pb, Cs, F, and B, and enrichment of Ti, Al, total Fe, Mg, P, Cr, Ni, Sr, Ba, Tl, and Zr, during the weathering of the Carnmenellis granite in South-West England. Crammer and

Table 3.1 Table showing major elements in ground waters draining through different rock types.

	pH	SiO_2	Al	Fe	Mg	Na	K	Ca
Granite	6.6	39	0.9	1.6	6.2	9.5	1.4	27
Rhyolite	6.6	37	0.1	0.2	0.8	3.9	2.3	3.6
Basalt	7.7	44	0.1	0.0	20	51	7.2	54
Gabbro	6.7	39	0.0	5.1	2.3	6.2	3.2	5.1
Andesite	7.2	31	0.2	0.2	5.6	9.6	0.4	14
Syenite	7.6	19	0.0	0.1	2.3	2.8	0.6	9.5
Sandstone	7.4	12	0.2	0.1	6.0	2.4	3.0	50
Shale	8.1	17	0.1	8.2	29	447	8.4	48
Limestone	8.2	11	0.1	0.0	34	9	1.1	61
Dolomite	7.4	14	0.2	4.2	86	76	3.5	178
Schist	6.3	14	0.0	0.2	1.2	3.3	0.8	3.1
Glacial deposit	7.4	14	0.8	0.3	49	122	6.2	120

Data taken from White et al.(1963).

Nesbitt (1980) found that Sc, Nb, Th, Y, La, V, and U were enriched during the weathering of granodiorite, and Sr, and P depleted, while, Cs, Zr, Hf and Ta remained relatively unchanged. Thus while Butler found the depletion of V, Y and La, Crammer and Nesbitt found the same elements being enriched. This well illustrates the complexities of the weathering environment.

3.3.4 Measures of Weathering

Weathering is a part of a cycle of mass movement in the Earth's crust. Knowledge of the degree of alteration in any weathering process is important for a better understanding of the geochemical behaviour of the elements during such processes. As important as it is, a weathering index of global application is yet to be formulated. To understand the behaviour of an element, or the changes produced by weathering, a comparison of the original rock mass with its weathered product can be adequate, but for a situation where there is a complex sequence of processes inbetween, such as in weathering, clearly some gauge has to be determined. A large number of weathering indices have been proposed in the past, but with increasing understanding of the mechanisms involved few have proved to be valid. As mentioned above, it has been thought that the amount of change produced in weathering was obtained by assuming alumina constant, and the degree of weathering assessed by the losses of the mobile oxides (Goldich, 1938; Merrill, 1906). For

example, Reiche (1943) proposed a weathering potential index (WPI) and weathering direction or product index (PI) as:

$$WPI = \frac{100.(K_2O+Na_2O+MgO+CaO-H_2O)}{TiO_2+SiO_2+Al_2O_3+Fe_2O_3+CaO+MgO+K_2O}$$

and

$$PI = \frac{100.SiO_2}{SiO_2+TiO_2+Fe_2O_3+FeO+Al_2O_3}$$

where the WPI decreases as the mobile oxides are lost, and an increase in hydroxyl ions occurs. The PI decreases with loss of silica. The water of hydration in Reiche's WPI is used as a weighting factor to correct for the energy content of the material. In both equations, the oxides are taken as their molar ratios.

These weathering indices either suppose that SiO_2, Fe and Al_2O_3 remain fairly constant during weathering, or that SiO_2 is lost. Ruxton (1968) compared the correlations between various indices of weathering and observed a high correlation between the SiO_2 to Al_2O_3 ratio and total element loss. He suggested the SiO_2 to Al_2O_3 molar ratio as an index of weathering for free-draining acid weathering environments in humid climates, where kandites are the initial end-products of weathering. However, the applicability of his index is restricted because of a number of limitations. The most important of these include the requirement

that the sesquioxides remain fairly constant during weathering, and the restriction that the initial products of weathering be free of smectite and vermiculites. Parker (1970) proposed an index for all rock types which is independent of the initial end-products. He considered that in humid climatic regions, the important weathering process is hydrolysis, and that this generally involves the exchange of Na, Ca, K, and Mg for H^+ in the mineral structures. To overcome the difference in susceptibility to weathering of the elements he suggested an index given by:

$$WI = Ca/Ca\text{-}O + Na/ Na\text{-}O + Mg/Mg\text{-}O + K/K\text{-}O$$

where the denominators in the ratios indicate the bond strength of the particular element, and both O_2 and the elements are represented by their atomic proportions.

These indices are basically a measure of the potential susceptibility to weathering, rather than an index of weathering. Modifications to some of these equations have been proposed and used in a number of studies. For example, Short (1961) proposed that the WPI of Reiche be scaled from one to zero for fresh and thoroughly weathered rocks, respectively, in order to provide a relative weathering index. Heath (1982) also used a local weathering index to take into account oxidation, in addition to hydrolysis, in his study of weathering of the Dartmoor granite. However, it must be emphasised that all these indices assume either

the loss of some constituents and/or that some constituents remain constant during weathering. As can be seen from the above discussions on the geochemistry of granite weathering, K may be lost from feldspars, micas or amphiboles, but fixed onto clay minerals. This situation would, to some extent, invalidate the use of these indices, although employing a number of elements may reduce these effects. It would, therefore, be advisable to take account of the different physico-chemical conditions of the weathering environment in the interpretation of such indices.

3.4 Conclusions

The foregoing discussion highlights the importance of the two major low-temperature alteration processes operative in the Earth's crust which affect granitic regimes. Hydrothermal circulation, and redistribution of elements which this causes, can produce concentration of elements in economic quantities. The two processes also complement each other. For example, a proportion of the elements leached out by percolating water in weathering environments is taken into the groundwater, and in the process of convective circulation these elements may be concentrated and precipitated as hydrothermal deposits. Similarly, elements precipitated during hydrothermal activity may be affected and redistributed by weathering. U deposits of both hydrothermal and weathering origins have been recorded. A part of this study is

concerned with the effect of these processes in the redistribution of U. Chapters 8 and 9 considered this in more detail.

CHAPTER FOUR: GEOCHEMICAL BEHAVIOUR OF U IN THE NIGERIAN YOUNGER GRANITES

4.1 *Introduction*

Geochemical techniques have been used in exploration programmes for many years. In mineral exploration the use of chemical analysis of samples, collected as dictated by the need of a survey, are now routine both as a means of delineating areas of interest in terms of mineral ore potential and value of reserves, or as a follow-up to surveys by other techniques. In the case of U exploration, geochemical techniques have found application mainly in advanced stages of exploration simply because gamma-ray techniques are faster and cheaper. The basic principles of geochemical investigations in the Earth Sciences concern the determination of the relative abundances of elements and then relating such abundances to the physico-chemical conditions in the immediate environment of investigation. In recent years, considerably improved detection limits for most of the elements have increased the reliability of chemical analysis, and hence the application of geochemical techniques. U in geological samples, for example, can now be detected within the part per billion (ppb) range. Gamma-ray surveys which comprise the main method of U explorations, especially in granitic terranes, have limitations.

Often only qualitative interpretation is possible from such determinations. This is partly because the measurements are based on one of the daughters in the decay series, and the U decay series frequently is not in radioactive equilibrium. Also, even a thin foreign overburden can absorb the gamma-rays from the decay of radioelements in the underlying rock, so that deposits may not be detected during routine surveys. Therefore, it is inevitably the case that at a certain stage in an exploration programme the need to use geochemical investigations becomes necessary.

This Chapter discusses the abundance of U and its geochemical associations in the Nigerian Younger Granites. Element concentrations were determined using X-ray fluorescence (XRF) techniques. In Chapter 6, U abundances as determined by gamma-ray measurements are compared with determinations given in this Chapter. The granites are known to be associated with occurrences of high radioelement abundance, so the results of these determinations are also important when discussing the origin of U mineralisation associated with the granite.

4.2 Analytical Methods in Geochemistry

A wide range of analytical methods are available for the determination of U and Th. The most important are delayed neutron activation analysis (DNAA) and XRF. Simplicity of analysis and improved detection capabilities have made XRF a major method for

the determination of element abundances in environmental studies. In this Chapter, the discussion that follows is based on analyses obtained using a Philips PW1400 fully automatic X-ray spectrometer.

Determination of element concentrations using this method is based on the electromagnetic radiation emitted by an atomic nucleus of an element when exposed to a beam of X-rays. In it's simplest mode of operation, an XRF unit consists of an X-ray source, an analysing crystal, and an X-ray detector. A beam of X-rays of sufficient energy to cause fluorescence in atoms of the elements of interest is directed at the target under investigation; this then produces a spectrum of energies for each element. Although these characteristic spectra are superimposed on a continuous spectrum, it is the measurement of their intensity which forms the basis of the XRF technique. The total energy of the spectrum produced is dependent on the type of element irradiated. This energy is related to the atomic number, Z, of the element (Durrance, 1986) by the relationship:

$$E = 1.1.10^{-9} ZV,$$

where V is the potential applied to the X-ray source. Because the whole spectrum is not used, selective filtering is applied to the spectrum. The radiation is then passed on to a dispersion crystal, which isolate the wavelengths of interest from what is considered the background. The dispersed radiation is then fed through a

collimator, to a detector and counted.

Various anode materials have been used for the X-ray source tubes; the choice of material being dependent on the elements the spectrometer is used for. W, Au, Pt, Cr, Al and Cu are used as anode materials in the manufacture of X-ray tubes. Because of the wide range of the spectra received, a variety of dispersive materials are also used. These include mica, gypsum, quartz, LiF, and LiCl. With a suitable choice of anode, window, and dispersive crystals, the detection limits of a spectrometer are very good. Detection limits down to 0.01% and 1ppm for the major and minor elements, respectively, can be achieved with a conventional laboratory XRF system. Wavelengths of $0.956.10^{-10}$ and $0.968.10^{-10}$m and 0.911 and and $0.923.10^{-10}$m are used for the analysis of Th and U, respectively (Durrance, 1986).

The increased importance of geochemical studies in mineral exploration has now also led to the development of portable XRF units that can be used in the field. In these instruments, radioactive elements are used as the source of the exciting radiation. Wollenberg et al. (1971) have described portable fluorescence equipment suitable for in situ analysis in the field. Such equipment has, however, not been used in this study.

4.3 Sample Description

The Younger Granites of the Jos Plateau are made up of rock

types which display a range of textural variations. Such textural varieties are well expressed in the Jos - Bukuru complex, where almost all the rock types of the Younger Granite intrusions are represented. Much of the north-eastern part of the complex is composed of biotite granite with migmatite, hornblende-fayalite and hornblende-biotite porphyries. The dominant rock types are a coarse-grained granite represented by Jos-type granite, and medium-grained to coarse-grained varieties known as N'gell-type granite. Other minor intrusions of microgranites occur, such as at Rafin Sanyi, and there are pegmatites, quartz veins, and felsic and basic dykes. Felsic and basic xenoliths are also present in the granites. The history of the igneous activity of the complex has been divided into two cycles, an outer (early) granitic cycle and a central (later) granitic cycle (Macleod and Berridge, 1971). In this sequence, the N'gell medium-grained type is intruded into the Jos' coarse-grained type. Because of the complexity of the intrusions and the general lack of exposure of the contacts, most of the boundaries have been delineated from mapping soil type. In the early cycle, most of the granite porphyry and coarse-grained granite, and some of the the medium-grained type, were emplaced. The later cycle saw the intrusion of the medium-grained, the fine-grained, and microgranite phases. Each of these intrusive phase was followed by the formation of quartz veins, felsic and basic dykes and, more rarely, tin lodes.

The Jos granite is mainly biotite granite and hornblende-

biotite granite, with some occurrence of hornblende-fayalite granite, notably at Shen. Hornblende-fayalite porphyries, biotite-aegerine granite, fayalite granite, riebeckite granite, riebeckite-aegerine granite, and riebeckite-biotite granite, are mostly restricted to the eastern part of the complex, notably at Shere and the Kigom hills.

The biotite granites are peraluminous, with an average 34.3% perthite (perthitic orthoclase and plagioclase) . The other major rock-forming minerals are quartz, perthite, albite, and biotite. There is also abundant fluorite. In the biotite granites, quartz grains usually occur in aggregates with feldspar. They range in size from about 1mm in the fine-grained and medium-grained granites to about 1cm in the coarse-grained types. The feldspars are generally perthitic orthoclase. They may attain a grain size of 2cm in the coarse-grained granites. Columbite and cassiterite occur as important accessory minerals, reaching economic quantities throughout the different phases of the biotite granites. Other accessory minerals are thorite, monazite, xenotime, zircon, ilmenite and magnetite (Buchanan et al., 1971).

The hornblende-biotite granites, contain much lower amounts of quartz than the biotite granites, ranging from about 20% to 30%, but have a high percentage of perthite, mostly orthoclase microperthite (Buchanan et al., 1971). The accessory minerals

include allanite, sphene, zircon, and fergusonite, with abundant ilmenite and fluorite.

The riebeckite granites have pyrochlore as an important accessory mineral. This sometimes attains the proportion of a major mineral in the rock. The occurrences have been fully described by Beer (1952). Detailed petrographic descriptions of the rocks of the Nigerian Younger Granite complexes have been given elsewhere, for example by Macleod et al. (1971) and Buchanan et al. (1971) for the whole area, and Ike (1979) for the Tibchi complex.

4.4 Geochemical Controls of U in Granitic Rocks

In any discussion of geochemistry of U in granitic rocks it is first important to consider it's mineralogical distribution. Although most of the U in granitic rocks is held in accessory minerals, it has been established by many workers, such as Basham et al. (1982b) and Silver et al. (1982), that where the abundance of the element is especially great, the accessory minerals could not alone account for the observed concentrations. In fact, in igneous rocks U can occur in both primary and secondary minerals, but occurrences of secondary minerals are largely controlled by alteration, fissure infillings, minor intrusions, and mineralised lodes.

Most reported occurrences of large concentrations of U in granitic rocks are found to be concerned with post-magmatic bodies (Bowie, 1972), but magmatic occurrences are also common where the

U is concentrated in refractory minerals. The only instance of large concentrations of U in the main rock mass is in an albite-riebeckite granite. In this occurrence, U is found in the mineral pyrochlore which, as noted above, forms a major accessory. Indeed, sometimes pyrochlore attains the proportion of a major rock-forming mineral in the other albite-riebeckite granites of Nigeria (Beer, 1952). Although the exploitation of U from such occurrences has not been reported, it is believed that it forms a major, low-grade deposit of strategic importance. Other hosts for large concentrations of U are either late-stage intrusions, or were formed as the result of post-magmatic alteration processes.

The association of high U with late differentiates in the magmatic suite has already been noted, and it follows that the frequency of occurrence of U-bearing bodies produced by alteration processes will increase with the greater abundance of dispersed U in the rock. Therefore, recognising granites with high U concentrations may usefully indicate the occurrence of associated U ore bodies.

The type of U mineralisation will also influence the result of supergene processes which mobilise U. In vein and related occurrences, U is mainly held in minerals such as uraninite and pitchblende, with betafite, fergusonite, uranophane and allanite as accessories. In such minerals, U is easily leachable and supergene processes will have a profound effect in near-surface environments. On the other hand, where U occurs in refractory minerals, these processes will have minimal effect on its mobilisation.

4.5 Sample Collection and Preparation

Samples were collected from rock outcrops in the area. This was carried out so that most of the rock types recognised in the complex were sampled. At each collection site, a large piece of rock was broken off from the exposure with a sledge-hammer. To obtain fresh samples, such pieces had to be broken into smaller pieces and the freshest selected. For each sample about 3-4kg of rock material was obtained. The samples were then divided into two, one part for laboratory gamma-ray spectrometry, as described in Chapter 6, and the other for chemical analysis and making thin sections. The latter part was trimmed and reduced to about 1 kg for transportation. At some exposures, more especially on the coarse-grained rock types, it was difficult to obtain samples devoid of some signs of weathering. Such samples show some discoloration and/or iron staining associated with percolating water. Sampling points are as shown in Figure 4.1. In addition to rocks, samples of the soils developed on the various rock types were also collected and studied for the effect of weathering on the granite, as reported in Chapter 9.

The discussion which follows is based on the chemical analysis of 46 granite samples collected as reported.

The samples were prepared for XRF analysis by producing pellets and fusion beads. In such preparations, the samples were first further trimmed to remove any signs of weathering and then a

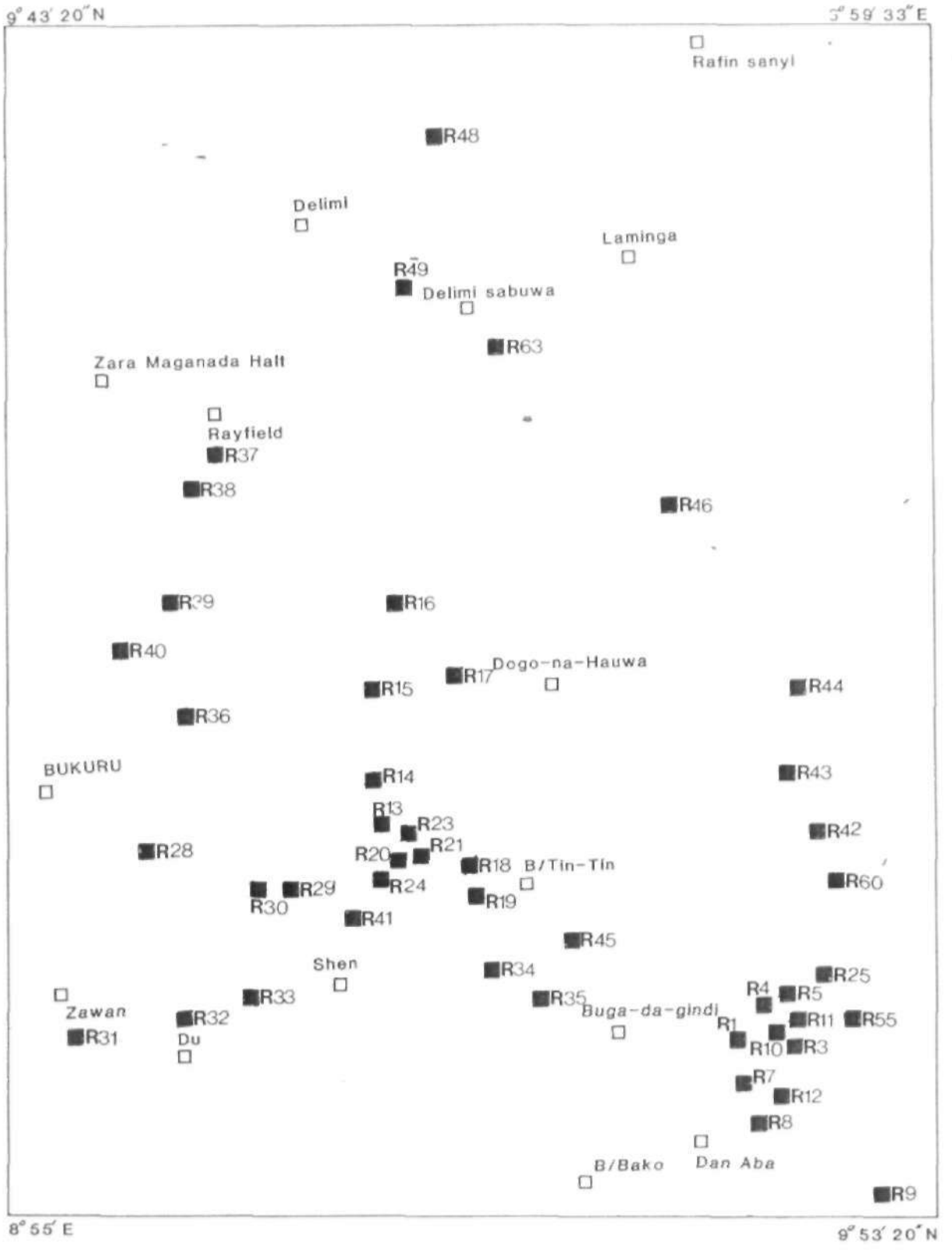


FIGURE 4.1 Granite sampling points(■R9)

piece broken off using the hydraulic rock splitter. This piece was crushed to gravel size with a jaw crusher. The crushed sample was then transfered to a Tungsten ball mill, and ground to a fine powder. For pellet making, 4gm of the powder was taken and mixed with 4 drops of a 2% solution of polyvinyl pyrrolidone (PVP) to bind the powder together. The mixture was then transfered to a pressure cup fitted with a spacer. The space produced after removing the spacer was filled with boric acid powder, the column made up to about 4/5 full, and a pressure of about 4 tonnes applied to a plunger placed on top of the column. This provided a cylinderical shaped pellet in a frame backing of boric acid. the pellets had flat homogeneous sample surfaces of about 2.0cm diameter and were about 1cm thick. The surfaces of the pellets formed the targets for the primary X-rays from the spectrometer of the analyser. These pellets were used for the analysis of trace elements.

Fusion beads were prepared based on the technique of Harvey et al. (1973). This was done by adding 0.45gm of the sample to 2.45gm of specpureflux (a mixture of lithium tetraborate, lithium carbonate and lanthanum oxide) and mixed thoroughly. The mixture was then fused in a Pt crucible in a furnace at 1000^{O}C for about one minute. The melt was then moulded in shape by pressing with a plunger in an Al disc and allowed to set on a hot plate at 200^{O}C. These beads were used for major element analysis.

Analysis was carried out using a Philips PW1400 fully automated X-ray wavelength dispersive spectrometer connected to a PDP 11/23 digital computer. The spectrometer had been calibrated both for major and trace elements using 170 international standards based on values from the 1984 compilations as described by Govingaratu (1984). The detection limits of the spectrometer for the elements on routine determination are given on Appendix 4.2. Details of the spectrometer are given elsewhere, for example, Leake et al. (1969) and the Philips PW1400 Instruction Manual (1984).

4.6 Discussion of Results

4.6.1 General Geochemical Features

Results of the analysis of the granite samples are shown in Table 4.1. Correlation coefficient data of these analyses are given in Table 4.2. In Table 4.3 are shown data comparing the average abundances of the elements in the granites to those of a granite of average composition.

From Table 4.1 it can be seen that the Younger Granites are anomalously enriched (> 5 times average concentration) in the elements Sn, Nb, and W; enriched in Ni, Zn, Ga, As, Th, U, Rb, Y, Zr, Cr, La, and Ce; and depleted in Sr, Mn, Ba, V, Ti, Mg, Cu and, P. They contain close to the average amounts of Si, Al, Fe, Na, K, Ca, Pb and Cs. Thus the average Younger Granites are enriched in the Large Ion Lithophile (LIL) elements and contain low abundances

Table 4.1: Chemical analyses of the Nigerian Younger Granite.

Samp. No.	SiO_2	Al_2O_3	TiO_2	Fe_2O_3	MgO	CaO
R1	74.84	12.72	0.18	2.17	0.05	0.68
R3	75.77	12.29	0.12	1.54	-	0.70
R4	71.77	13.39	0.47	3.95	0.26	1.28
R5	76.05	12.46	0.22	2.26	0.04	0.24
R7	74.18	12.73	0.21	2.33	0.04	0.70
R8	74.88	13.09	0.21	2.47	0.04	0.72
R9	67.58	15.41	0.71	3.94	1.38	1.80
R10	75.07	12.76	0.14	1.58	0.02	0.93
R11	74.99	12.41	0.22	2.24	0.02	0.67
R12	74.94	12.78	0.20	2.28	0.03	0.62
R13	76.85	13.24	0.06	1.24	-	0.07
R14	72.28	13.11	0.29	3.40	0.03	1.02
R15	77.06	12.62	0.12	1.53	-	0.04
R16	75.52	12.67	0.20	2.25	0.04	0.78
R17	75.79	12.81	0.12	1.51	0.03	0.42
R18	75.04	12.40	0.19	2.13	0.01	0.69
R19	76.87	12.05	0.16	1.86	0.03	0.61
R20	75.16	12.35	0.19	2.24	0.05	0.65
R21	74.48	12.29	0.20	2.02	0.07	0.67
R23	72.99	13.02	0.28	3.37	0.04	0.86
R24	76.87	12.56	0.09	1.15	0.03	0.42
R25	75.08	13.43	0.19	2.14	0.09	0.77
R28	75.73	12.43	0.15	1.91	0.05	0.65
R29	78.32	11.19	0.11	1.17	0.03	0.51
R30	75.81	12.40	0.16	1.93	0.01	0.62
R31	78.56	13.12	0.12	1.42	0.13	0.11
R32	77.28	11.50	0.11	1.62	0.01	0.61
R33	76.31	12.52	0.15	2.02	0.01	0.22
R34	69.49	15.79	0.13	2.12	0.02	1.03
R35	73.55	13.17	0.29	2.78	0.06	0.98
R36	78.29	11.32	0.09	1.21	-	0.37
R37	78.58	11.58	0.10	1.52	0.02	0.29
R38	77.56	11.94	0.10	1.37	0.05	0.47
R39	78.15	12.07	0.09	1.51	-	0.06
R40	77.27	12.27	0.10	1.45	0.01	0.26
R41	76.35	12.15	0.14	1.91	0.02	0.23
R42	76.56	11.99	0.17	1.92	0.02	0.64
R43	76.08	11.70	0.13	1.43	-	0.56
R44	73.92	12.93	0.21	2.38	0.06	0.71
R45	75.63	12.35	0.17	1.87	0.02	0.73
R46	73.18	13.24	0.25	2.90	0.07	0.70
R48	74.50	12.70	0.21	2.58	0.03	0.47
R49	76.04	12.55	0.10	1.66	-	0.47
R55	75.45	12.15	0.13	1.66	-	0.74
R60	73.84	13.62	0.13	1.60	-	0.68
R63	77.36	12.42	0.09	1.40	-	0.45

Continued.....

Table 4.1, Continued.

Sample	Na_2O	K_2O	P_2O_5	MnO	LOI
R1	3.87	5.21	-	0.03	0.33
R3	3.60	5.23	-	0.01	0.31
R4	3.56	4.79	0.06	0.07	0.82
R5	3.75	5.08	0.01	0.02	0.56
R7	3.64	5.23	-	0.03	0.49
R8	4.01	4.80	-	0.07	0.42
R9	4.32	4.19	0.22	0.07	0.44
R10	3.67	5.28	-	0.01	1.09
R11	3.75	4.99	-	0.03	0.98
R12	3.90	5.07	-	0.03	0.69
R13	4.30	4.45	-	0.02	0.31
R14	3.89	5.40	0.01	0.07	0.38
R15	3.38	4.78	-	0.02	0.42
R16	3.66	5.06	0.01	0.02	0.87
R17	3.87	5.11	0.02	0.01	0.16
R18	3.53	5.13	-	0.01	0.38
R19	3.50	4.78	-	0.02	1.82
R20	3.69	5.18	-	0.01	0.33
R21	3.54	5.15	-	0.02	1.11
R23	3.72	5.41	0.01	0.08	0.42
R24	4.18	4.69	-	0.01	0.64
R25	4.02	5.41	-	0.02	0.69
R28	3.83	4.67	-	0.02	0.00
R29	3.38	4.26	-	0.01	0.31
R30	3.75	4.96	-	0.03	0.36
R31	3.32	3.91	-	0.01	2.22
R32	3.69	4.34	-	0.02	0.00
R33	3.84	4.81	-	0.02	0.71
R34	4.86	5.87	-	0.05	0.44
R35	3.96	4.78	0.03	0.04	0.00
R36	3.68	4.15	-	0.02	0.44
R37	3.88	4.32	-	0.02	0.67
R38	3.93	4.43	-	0.02	0.00
R39	3.89	4.49	-	0.02	0.00
R40	3.99	4.51	-	0.02	0.00
R41	3.44	4.93	-	0.01	0.00
R42	3.45	5.10	-	0.03	0.00
R43	3.34	4.68	-	0.02	0.00
R44	3.85	5.35	-	0.03	0.04
R45	3.67	5.11	-	0.02	0.09
R46	4.13	5.21	0.02	0.05	0.53
R48	3.63	5.36	-	0.02	0.67
R49	3.89	4.72	-	0.02	0.02
R55	3.32	5.31	-	0.01	0.93
R60	4.20	5.53	-	0.01	0.71
R63	4.10	4.56	-	0.02	0.96

Continued.....

Table 4.1, Continued

Sample	Ni	Cu	Zn	Ga	As	W	Pb	Th	U	Rb	Sr
R1	8	6	54	34	2	245	17	24	8	320	22
R3	7	5	73	36	2	304	27	39	12	359	7
R4	11	9	121	32	5	236	12	19	5	161	99
R5	8	5	60	35	3	200	15	27	5	325	25
R7	7	5	119	34	4	138	13	25	9	250	32
R8	8	4	107	33	6	274	7	22	9	276	27
R9	10	10	90	20	3	131	21	17	-	163	355
R10	7	6	55	39	3	78	16	34	4	349	15
R11	7	5	49	34	5	101	14	27	6	309	30
R12	6	6	81	35	5	103	10	18	6	290	26
R13	10	5	66	59	7	127	-	30	7	937	3
R14	7	8	161	33	7	173	18	18	5	245	48
R15	7	6	93	45	4	266	16	37	9	545	4
R16	10	5	85	35	2	215	25	63	16	746	17
R17	9	10	75	36	4	311	16	73	20	790	14
R18	7	6	170	36	3	273	20	28	10	275	12
R19	8	10	156	37	5	297	33	26	11	308	7
R20	8	8	296	35	6	392	25	28	9	267	17
R21	11	5	204	35	-	155	27	30	11	276	18
R23	7	8	215	35	-	229	40	25	9	232	46
R24	7	5	76	47	3	286	18	24	8	402	3
R25	13	5	57	34	4	354	14	27	11	305	29
R28	8	5	77	39	4	249	17	34	11	493	17
R29	10	4	67	39	4	422	11	48	13	527	5
R30	8	5	99	39	1	168	33	34	15	430	12
R31	9	5	28	47	8	344	-	33	20	604	4
R32	9	3	104	38	5	375	15	33	12	492	16
R33	7	4	108	42	1	212	28	34	16	489	12
R34	7	6	93	50	3	167	18	22	5	166	118
R35	7	8	104	36	4	249	19	26	7	223	74
R36	8	4	75	41	6	346	7	40	12	573	2
R37	8	5	118	43	4	28	13	35	9	616	4
R38	15	1	94	40	2	251	25	36	24	615	11
R39	7	6	89	47	6	280	6	44	11	657	3
R40	8	5	75	45	3	229	20	38	10	656	7
R41	8	19	205	43	-	301	44	36	13	505	7
R42	8	5	47	32	3	221	17	30	17	272	17
R43	9	4	64	34	2	300	23	31	14	327	7
R44	8	5	99	35	2	253	18	27	10	294	30
R45	7	5	81	31	2	219	31	32	10	357	24
R46	7	6	106	35	3	149	17	23	8	341	50
R48	7	6	87	34	4	169	19	42	17	445	14
R49	9	5	54	38	4	287	16	40	9	482	8
R55	8	5	51	35	3	250	21	37	10	386	14
R60	9	6	62	35	3	288	19	22	8	318	34
R63	8	7	68	40	3	204	23	44	16	578	3

Continued....

Table 4.1, Continued

Sample	Y	Zr	Nb	Cr	Mn	Ba	La	Ce	Cs	Sn	V
R1	121	378	96	20	206	204	111	179	5	14	-
R3	133	145	152	14	78	68	132	175	-	18	-
R4	99	452	86	11	490	543	114	210	4	10	-
R5	89	360	118	11	163	212	101	171	5	15	-
R7	136	355	95	13	213	255	125	207	2	11	-
R8	146	342	104	11	529	205	79	125	2	16	-
R9	29	228	13	12	475	927	74	145	2	10	34
R10	86	109	135	14	71	99	161	219	2	14	-
R11	117	276	94	15	190	218	159	228	-	8	-
R12	102	300	105	14	249	195	57	130	3	18	-
R13	29	130	145	14	148	-	-	18	5	12	-
R14	118	515	112	11	519	380	153	258	4	16	-
R15	29	245	204	13	155	74	44	75	4	25	-
R16	197	278	200	12	125	175	147	218	6	11	-
R17	111	197	119	14	89	162	88	131	6	19	-
R18	151	384	159	12	82	135	102	211	4	16	-
R19	170	305	179	13	101	68	91	192	-	12	-
R20	170	387	148	12	68	169	172	277	5	38	-
R21	330	422	189	13	100	252	453	598	6	21	-
R23	133	519	122	12	535	334	156	299	4	23	-
R24	83	122	137	14	93	42	60	75	5	21	-
R25	150	317	129	10	126	257	87	168	2	18	-
R28	159	269	141	13	133	135	84	167	5	19	-
R29	163	144	251	14	81	75	94	128	6	52	-
R30	153	278	118	13	190	198	107	308	4	21	-
R31	114	201	203	13	57	50	58	91	5	22	-
R32	190	230	215	13	115	77	76	128	5	17	-
R33	69	284	215	13	220	139	72	104	8	29	-
R34	72	277	73	14	352	496	102	202	-	9	-
R35	99	392	111	10	332	452	105	194	-	14	-
R36	124	199	217	14	111	41	59	83	5	27	-
R37	105	233	225	14	168	69	90	101	9	27	-
R38	530	229	206	13	117	104	173	250	12	18	-
R39	42	189	184	13	164	48	41	53	7	14	-
R40	100	194	174	14	169	59	99	220	10	27	-
R41	67	278	228	13	83	112	65	106	5	27	-
R42	143	479	155	14	174	176	110	170	6	21	-
R43	184	233	175	13	152	53	194	181	4	15	-
R44	141	349	107	11	163	259	95	172	7	11	-
R45	43	279	91	13	152	182	94	174	4	16	-
R46	123	369	102	13	434	418	144	241	5	11	-
R48	93	384	124	12	212	212	114	235	7	12	-
R49	121	180	135	14	134	90	56	96	8	20	-
R55	133	170	117	13	68	74	113	176	3	19	-
R60	112	204	76	13	65	253	75	128	2	11	-
R63	149	140	118	13	101	33	44	94	5	14	-

Note: Major elements as oxides in %, others in ppm
: All sample numbers are prefixed JP.

Table 4.2: Correlation coefficient data for elements in the Nigerian Younger Granites

	SiO_2	Al_2O_3	TiO_2	Fe_2O_3	MgO	CaO	Na_2O	K_2O
Al_2O_3	-0.828							
TiO_2	-0.784	0.555						
Fe_2O_3	-0.809	0.547	0.893					
MgO	-0.592	0.564	0.837	0.520				
CaO	-0.844	0.565	0.791	0.730	0.654			
Na_2O	-0.445	0.671	0.121	0.142	0.273	0.234		
K_2O	-0.510	0.355	0.064	0.319	-0.330	0.323	0.154	
P_2O_5	-0.851	0.967	0.916	0.547	0.995	0.810	0.633	-0.887
MnO	-0.690	0.535	0.698	0.823	0.400	0.617	0.330	0.150
Ni	0.062	0.009	0.073	-0.060	0.215	0.090	0.053	-0.233
Cu	-0.287	0.240	0.311	0.337	0.217	0.146	-0.021	0.146
Zn	-0.206	-0.034	0.203	0.359	-0.050	0.138	-0.119	0.211
Ga	0.503	-0.103	-0.683	-0.620	-0.541	-0.692	0.212	-0.282
As	0.106	0.048	-0.009	0.058	-0.008	-0.158	-0.015	-0.301
W	0.339	-0.303	-0.262	-0.303	-0.151	-0.205	-0.313	-0.207
Pb	-0.068	-0.019	0.025	0.074	-0.023	0.026	-0.200	0.212
Th	0.500	-0.405	-0.443	-0.492	-0.249	-0.423	-0.257	-0.197
U	0.497	-0.373	-0.354	-0.375	-0.072	-0.365	-0.316	-0.353
Rb	0.676	-0.377	-0.574	-0.631	-0.269	-0.700	-0.029	-0.508
Sr	-0.803	0.729	0.866	0.666	0.926	0.761	0.417	-0.022
Y	0.184	-0.328	-0.157	-0.147	-0.201	0.027	-0.170	-0.058
Zr	-0.445	0.156	0.472	0.727	-0.082	0.356	-0.128	0.453
Nb	0.774	-0.710	-0.576	-0.585	-0.442	-0.651	-0.501	-0.487
Cr	0.231	-0.159	-0.358	-0.417	-0.138	-0.221	0.053	-0.053
Mn	-0.674	0.532	0.673	0.820	0.355	0.552	0.351	0.162
Ba	-0.919	0.796	0.899	0.855	0.745	0.816	0.468	0.236
La	-0.196	-0.073	0.113	0.152	-0.087	0.226	-0.190	0.287
Ce	-0.347	0.032	0.257	0.356	-0.077	0.377	-0.154	0.428
Cs	0.487	-0.451	-0.370	-0.333	-0.274	-0.466	0.028	-0.342
Sn	0.472	-0.495	-0.304	-0.353	-0.194	-0.357	-0.351	-0.326

Continued.....

Table 4.2, Continued.

	P_2O_5	MnO	Ni	Cu	Zn	Ga	As	W
MnO	0.366							
Ni	0.409	-0.062						
Cu	0.528	0.158	-0.171					
Zn	-0.189	0.216	-0.054	0.457				
Ga	-0.968	-0.370	-0.045	-0.078	-0.122			
As	-0.156	0.155	0.002	0.204	0.198	0.294		
W	-0.471	-0.309	0.232	0.025	0.081	0.039	0.099	
Pb	-0.091	-0.047	0.017	0.482	0.481	-0.042	-0.587	0.032
Th	-0.328	-0.511	0.164	-0.024	-0.195	0.207	-0.099	0.263
U	-0.253	-0.363	0.441	-0.124	-0.126	0.018	-0.172	0.337
Rb	-0.378	-0.501	0.240	-0.115	-0.281	0.632	0.175	0.106
Sr	0.989	0.597	0.099	0.259	0.038	-0.462	-0.047	-0.255
Y	-0.743	-0.112	0.638	-0.354	0.178	-0.139	-0.190	0.161
Zr	-0.414	0.584	-0.077	0.188	0.524	-0.475	0.059	-0.135
Nb	-0.813	-0.520	0.162	-0.108	0.125	0.471	0.118	0.378
Cr	-0.005	-0.282	-0.146	-0.088	-0.318	0.225	-0.183	-0.144
Mn	0.312	0.975	-0.149	0.162	0.202	-0.332	0.146	-0.338
Ba	0.902	0.742	0.097	0.286	0.155	-0.557	-0.010	-0.349
La	-0.623	0.063	0.276	-0.124	0.391	-0.261	-0.197	-0.231
Ce	-0.464	0.207	0.166	-0.033	0.478	-0.389	-0.306	-0.224
Cs	-0.789	-0.262	0.269	-0.263	-0.029	0.357	-0.156	0.033
Sn	-0.450	-0.315	0.005	-0.000	0.262	0.192	0.055	0.459

	Pb	Th	U	Rb	Sr	Y	Zr	Nb
Th	0.031							
U	0.277	0.621						
Rb	-0.053	0.735	0.486					
Sr	-0.020	-0.389	-0.467	-0.447				
Y	0.155	0.111	0.496	0.024	-0.218			
Zr	0.157	-0.427	-0.173	-0.587	0.150	0.115		
Nb	0.108	0.471	0.478	0.559	-0.587	0.301	-0.248	
Cr	-0.074	0.141	0.016	0.223	-0.197	-0.039	-0.322	0.061
Mn	-0.086	-0.495	-0.384	-0.469	0.564	-0.192	0.571	-0.504
Ba	-0.003	-0.486	-0.443	-0.613	0.900	-0.193	0.455	-0.685
La	0.257	-0.082	-0.009	-0.268	-0.027	0.551	0.362	0.043
Ce	0.361	-0.155	-0.024	-0.429	0.069	0.517	0.542	-0.119
Cs	0.060	0.432	0.501	0.518	-0.318	0.403	-0.135	0.540
Sn	0.088	0.276	0.218	0.229	-0.301	0.088	-0.143	0.620

	Cr	Mn	Ba	La	Ce	Cs
Mn	-0.299					
Ba	-0.296	0.727				
La	-0.010	0.018	0.126			
Ce	-0.136	0.155	0.265	0.911		
Cs	0.140	-0.233	-0.368	0.059	0.007	
Sn	0.063	-0.287	-0.395	-0.030	-0.053	0.285

Table 4.3: Average element abundance in the Nigerian Younger Granite compared with abundances in average granite.

Elements & oxides	Ref1	Ref2	NYG	CGG	MGG	HFG
SiO_2	69.10	74.66	75.388	74.766	77.077	74.382
Al_2O3	14.55	13.60	12.645	12.734	12.191	13.065
TiO_2	0.38	0.20	0.178	0.202	0.117	0.179
Fe_2O_3	3.86	2.03	2.020	2.194	1.563	2.209
MgO	0.27	0.27	0.081	0.059	0.030	0.033
CaO	2.21	0.71	0.606	0.725	0.382	0.624
Na_2O	3.73	3.48	3.791	3.761	3.574	3.840
K_2O	4.02	5.06	4.908	5.120	4.566	5.121
P_2O_5	0.16	0.14	0.043	0.030	-	0.010
MnO	-	-	0.027	0.029	0.018	0.036
Ni	0.5	4.5	8	8	8	8
Cu	10	10	6	5	6	7
Zn	40	39	98	77	87	144
Ga	18	17	38	34	42	41
As	1.5	1.5	4	3	4	5
W	-	-	.236	220	281	211
Pb	20	19	20	17	19	25
Th	17	20	32	27	39	27
U	4.5	4.7	11	9	13	8
Rb	150	110	413	303	555	373
Sr	285	100	29	31	8	32
Y	40	41	130	120	11 7	129
Zr	180	175	282	306	213	350
Nb	20	21	144	114	176	148
Cr	4	4	13	13	13	13
Mn	400	390	190	214	129	249
Ba	600	840	195	229	91	248
La	40	55	110	114	74	157
Ce	-	57	176	180	137	232
Cs	5	4	5	4	6	4
Sn	3	3	18	14	23	17
V	20	44	-	-	-	-
LOI	-	-	0.50	0.50	0.43	0.63

Note: Oxides in % and others in ppm
ref1: Taylor (1964)
ref2: Turekian (1977).
NYG : Nigerian Younger granite (this study)
CGG : Coarse-grained granite
MGG : medium-grained granite
HFG : Hornblende-fayalite granite.

of the transition metals. As noted by Kinnaird et al. (1985) these granites fit the A-type granite designation of Loiselle and Wones (1979). Granites in this classification have been intruded either late in the magmatic cycle or have intruded basements that have previously undergone partial melting Collins et al.(1982). The peraluminous character of the granites is seen from the ratio (Ca + K + Na)/Aĩ in Table 4.4, although the normál diagonistic peraluminous minerals such as garnet, muscovite and andalusite (Clarke, 1981) are not recorded. Skreckeisen modal plots (Kinnaird et al., 1985) show that the biotite granites plot in the regions defined as aluminous granitoids from an alkaline granite province.

Average values for the different textural types (Table 4.3) show that the coarse~grained granites contain more Al, Ti, Fe, Mg, K, P, Mn, Ni, Cu, Pb, Sr, Y, Cr, Ba, La, and Ce than the medium-grained granites.

4.6.2 Major Element Variation

Plots of the major element concentrations in the Nigerian Younger Granites are shown in as Harker variation diagrams in Figure 4.2. These diagrams show that Al, Ti, Fe, Ca, and K decrease with increasing SiO_2 content. Na and Mg are relatively constant with increase in SiO_2 while data for P show a slight decrease with increase in SiO_2. Presentation of major element variationin this fashion helps to elucidate changes in the composition of the magma during emplacement. The constant sum effect, where the SiO_2 forms

Table 4.4: Some element ratios in the Nigerian Younger Granites.

Sample	Alkali:Al	K:Rb	Rb:Sr	DI	Th:U
R1	0.77	163	14.34	29.43	2.9
R3	0.78	146	51.41	-	3.4
R4	0.72	297	1.64	27.17	3.4
R5	0.73	156	13.09	30.15	5.0
R7	0.75	209	7.73	29.22	2.8
R8	0.73	174	10.04	29.00	2.5
R9	0.67	258	0.46	23.54	-
R10	0.77	152	23.52	29.35	7.5
R11	0.76	161	10.23	29.30	4.2
R12	0.75	175	11.06	29.40	3.1
R13	0.67	=48	300	-	4.5
R14	0.79	221	5.11	28.44	3.4
R15	0.65	88	200	-	4.0
R16	0.75	68	43.77	29.41	3.9
R17	0.73	65	57.77	29.92	3.7
R18	0.75	186	23.22	29.44	2.8
R19	0.74	155	44.87	29.76	2.5
R20	0.77	194	15.50	29.53	3.1
R21	0.76	187	15.30	29.24	2.7
R23	0.77	233	5.05	28.84	2.8
R24	0.74	117	200	29.86	2.8
R25	0.76	177	10.51	29.58	2.6
R28	0.74	95	29.62	29.21	3.0
R29	0.73	81	97.53	29.83	3.8
R30	0.75	115	36.47	29.60	2.4
R31	0.56	65	2E+02	29.86	1.6
R32	0.75	88	30.23	29.48	2.7
R33	0.71	98	40.81	30.02	2.1
R34	0.74	353	1.41	27.98	4.7
R35	0.74	215	2.99	28.26	3.9
R36	0.72	72	200	-	3.4
R37	0.73	70	200	30.2	4.0
R38	0.74	72	56.81	29.76	1.5
R39	0.70	68	200	-	4.0
R40	0.71	69	98.83	30.00	3.9
R41	0.71	98	77.03	30.13	2.8
R42	0.77	187	15.78	29.96	1.7
R43	0.73	143	44.17	-	2.3
R44	0.77	182	9.72	29.22	2.7
R45	0.77	143	14.61	29.57	3.0
R46	0.76	153	6.78	28.83	3.0
R48	0.74	120	31.76	29.69	2.5
R49	0.72	98	58.11	-	4.4
R55	0.77	137	27.45	-	3.5
R60	0.76	174	9.38	-	2.7
R63	0.73	79	200	-	2.8

DI: Differentiation Index of Nockolds and Allen (1953).
: All sample numbers are prefixed JP.

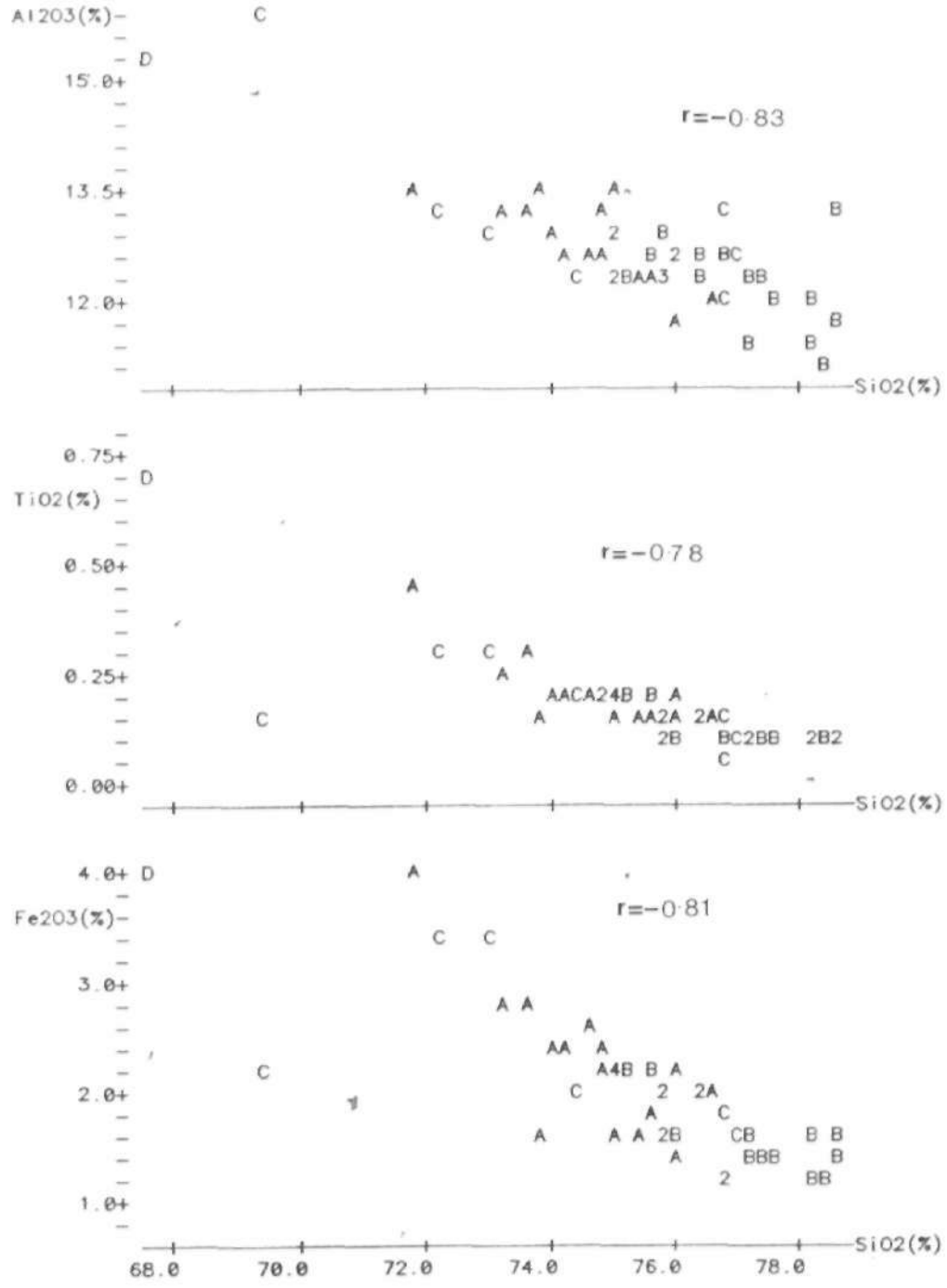


FIGURE 4.2 Major element variations

Note: For this Figure and subsequent Figures in the Chapter,
A: Coarse-grained granite
B: Medium-grained granite
C: Hornblende-fayalite granite
D: Undifferentiated migmatite

: Numbers in these plots and subsequent ones in the Chapter represent number of points sharing the same coordinates

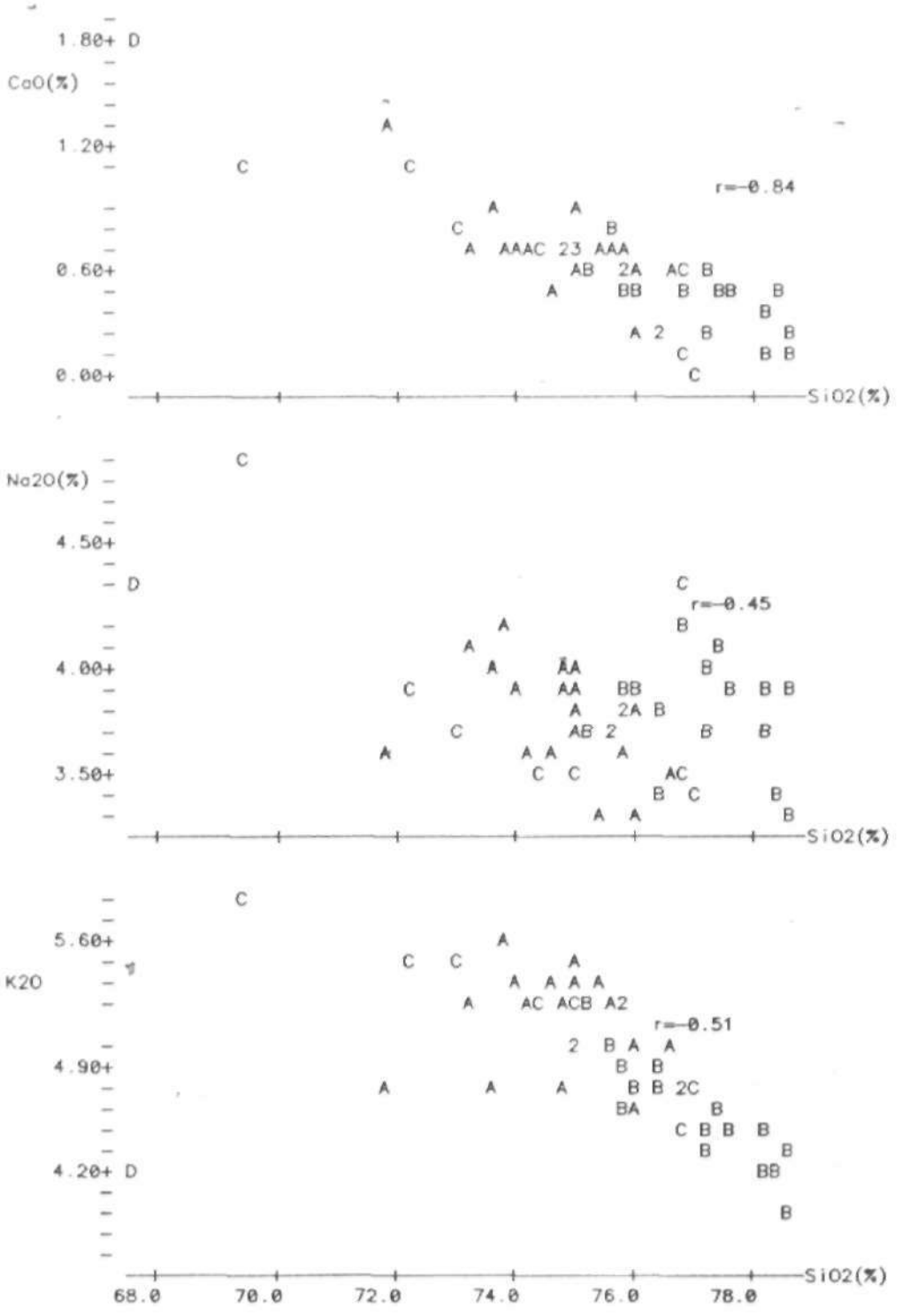


FIGURE 4.2 Major element variations

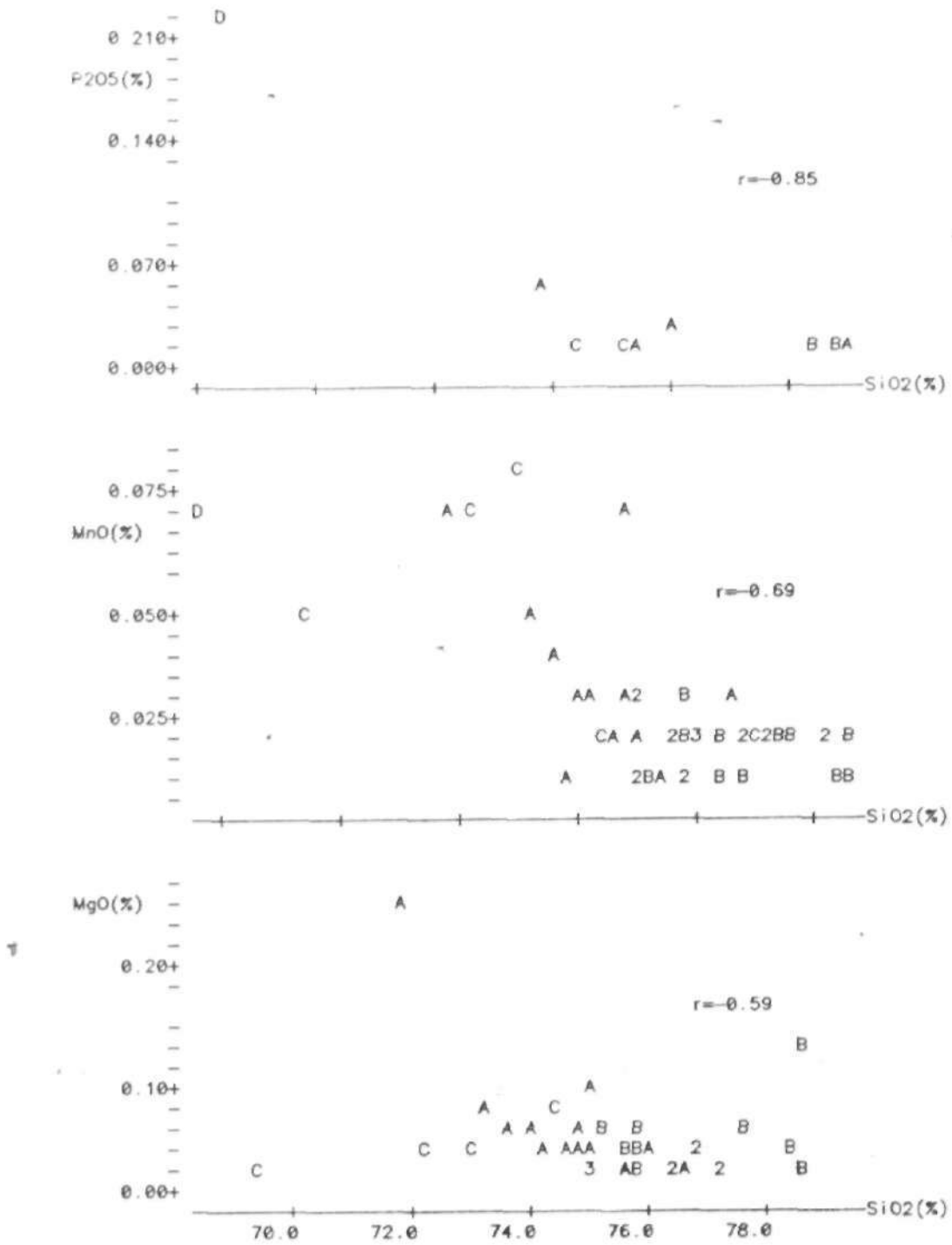


FIGURE 4.2 Major element variations

the largest proportion of the major oxides and, therefore, the the rock, was pointed out by Chayes (1964) as a limitation to the presentation of data in this way. However, Cox et al. (1979) have discussed limitations in the use of the Harker diagram, and shown that such limitations are most critical in basic rocks. They considered that the method could be useful for the interpretation of acid and intermediate rocks. Consequently, these diagrams are here considered to be valid.

The plots shown in Figure 4.2 suggest that the rock types are genetically related, belonging to the same fractionation trend. This agrees with the suggestion of Macleod and Berridge (1971) that four superimposed cycles of granitic intrusion are responsible for the emplacement of the Jos - Bukuru complex. The intimate relationship between the hornblende-fayalite granite and the coarse-grained biotite granite in these plots, suggests that the parent magmas might have been emplaced during a single cycle. This is despite the fact that the former belongs to the later central intrusive cycle, while the latter belongs to the early cycle in Macleod and Berridge's sequence of emplacement. Such features clearly reflect the complicated nature of the intrusive events.

The variation in average composition between the textural types already cited reflects the fractionation of the magma during the emplacement of the granites. The more felsic medium-grained granites, which form the later part of the intrusion, are less aluminous and contain less total alkali than the coarse-grained granites. During fractionation, the interplay of both ionic size

and ionic charge tend to concentrate incompatible trace elements and the Rare Earths Elements (REE) in the residual magmatic fluids. These elements are, therefore, usually abundant in late differentiates such as pegmatites. Examples of such an effect are seen in the variation of K and Rb during late magmatic stages in the evolution of a magma. The close association between K and Rb in igneous rocks has, therefore, been used in petrogenetic studies by workers such as Butler et al. (1962) and Henderson (1982). Being an incompatible element Rb becomes enriched in the magma during fractionation, thus altering the K:Rb ratio. From detailed statistical analysis of K-Rb relationships in 21 suites of igneous rocks, Shaw (1968) showed that K and Rb plot in three clear trends, with ratios in the range 1000-3000, 150-300, and 20-50, each representing different magmatic stages. These he referred to as the oceanic-tholeiitic trend, the main trend, and the pegmatitic-hydrothermal trends, respectively.

Plots of K_2O against Rb given in Figure 4.3 show the highly differentiated nature of the Nigerian Younger Granites. The difference between the various textural types is apparent in this plot, with the medium-grained granites having lower K:Rb ratios. Although the general trend is a decrease of K with increasing Rb content, the various textural types show different variations, with the coarse-grained granites plotting in different fields from those of the medium-grained granites. Clearly, the hornblende-fayalite granites show a decrease in K with increasing Rb content, a feature observed by Shaw (1968) exhibited by rocks of pegmatitic-

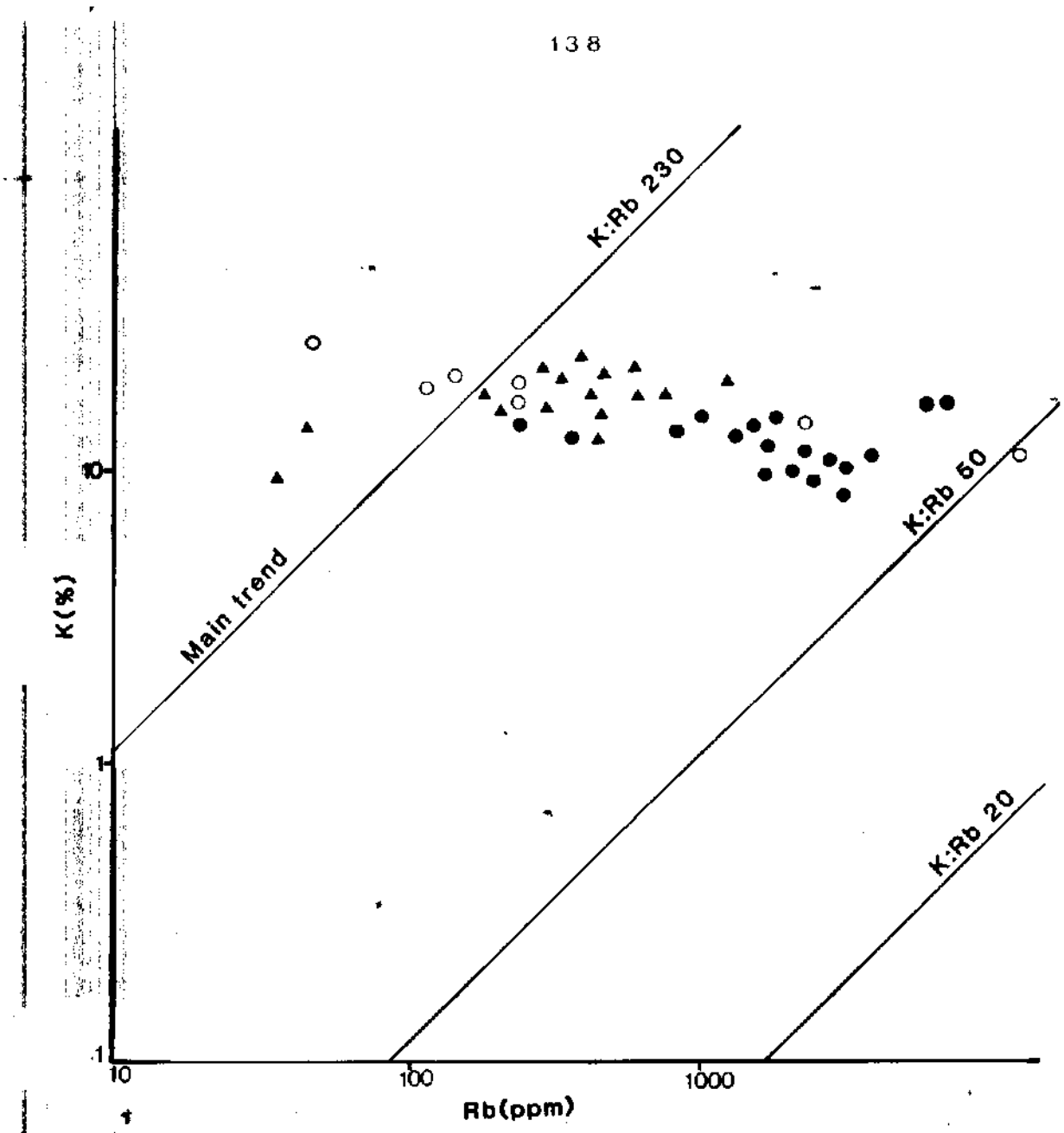


FIGURE 4.3 Plot of K_2O against Rb

hydrothermal events. Both the coarse-grained and the medium-grained granites plot well below the 230 line magmatic field of Shaw (1968), the latter plotting in the region between the main trend and the pegmatitic-hydrothermal fields showing the extreme fractionation of the granites. Fractionation is also shown in the ternary plot of total Fe as (Fe_2O_3), alkali and Mg (Figure 4.4), where the deficiency of Mg in the melt from which the granites crystallized is clearly shown. Here it can also be seen that with increasing fractionation, the granites become more alkaline.

Most of the trace elements are highly enriched in the granites, the exceptions being Sr, Ba, V and Cu, which are elements usually found highly enriched in early crystallizing phases. However, Sr, Ba and V are enriched in sample JPR 7, the only sample where V was detected. This sample was collected for the rock type identified as undifferentiated migmatite (Sheet 168: Naraguta). The REE are particularly highly enriched, with concentrations in excess of three times the abundance in average granite. Ba and Sr are thought to subtitute for K in early crystallizing potash feldspar (Rankama and Sahama, 1949), and their low abundances further suggest the highly differentiated nature of the Nigerian Younger Granites. Variation diagrams of the trace elements with SiO_2 in the granites show that Th, Rb, U, Pb, Y, Ga, Ni, W, Nb, Cs and Sn generally increase with increase in the SiO_2 content (Table 4.2) while Zr, Sr, Ba, Zn, As, Cu, and the cerium

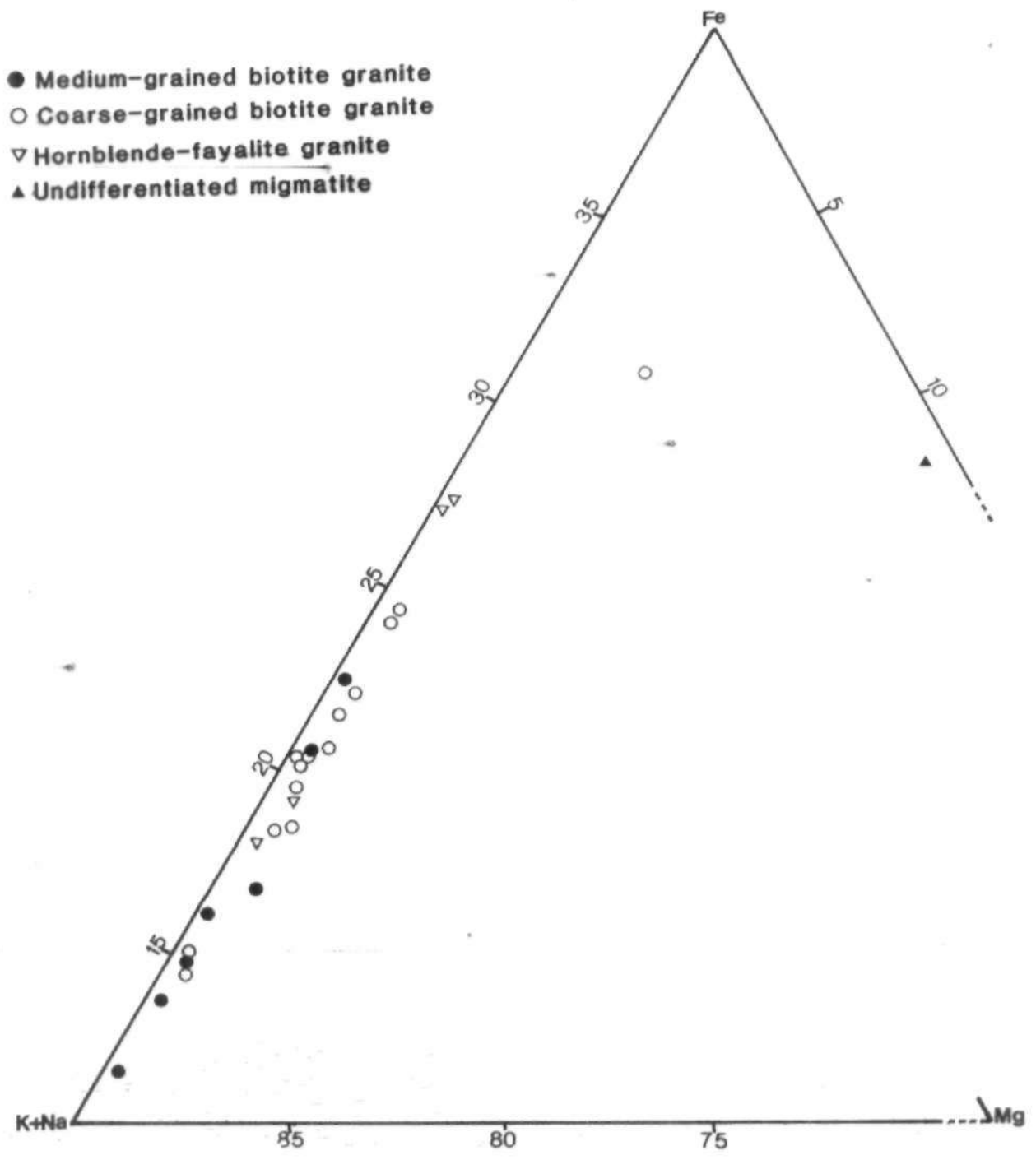


FIGURE 4.4 Ternary plot of Fe, Mg and K+Na

earths (Ce and La) show a decrease. Although most of the variations could be explained by fractionation, the behaviour of others can not be correlated with this effect. Late- stage post-magmatic process could have greatly - modified element abundances in the granite. The possibility of magma contamination might also have contributed to these variations. The difficulty of explaining trace element variation in alkaline granites by crystal-liquid fractionation, was also recognised by Taylor et al. (1961), who stressed the importance of alkali metasomatism.

The large abundance of K relative to Na in the granites can be seen from the averages of these elements in both textural types. Also, this is visible in the plot of K_2O against Na_2O shown in Figure 4.5. The dominance of potash metasomatism over soda metasomatism during the alkali metasomatism stage of Taylor et al. (1961) can thus be seen. The main mineral reactions can be described as K-silicate alteration. These reactions are believed to be sequential, with intense soda metasomatism followed by potash metasomatism. In some centres, this sequence is related to the composition of the residual fluids (Bowden, 1985). The reactions are also believed to be responsible for some of the mineralisation in these granites.

4.7 Geochemical Behaviour of U in the Nigerian Younger Granites

4.7.1 Abundance and Distribution

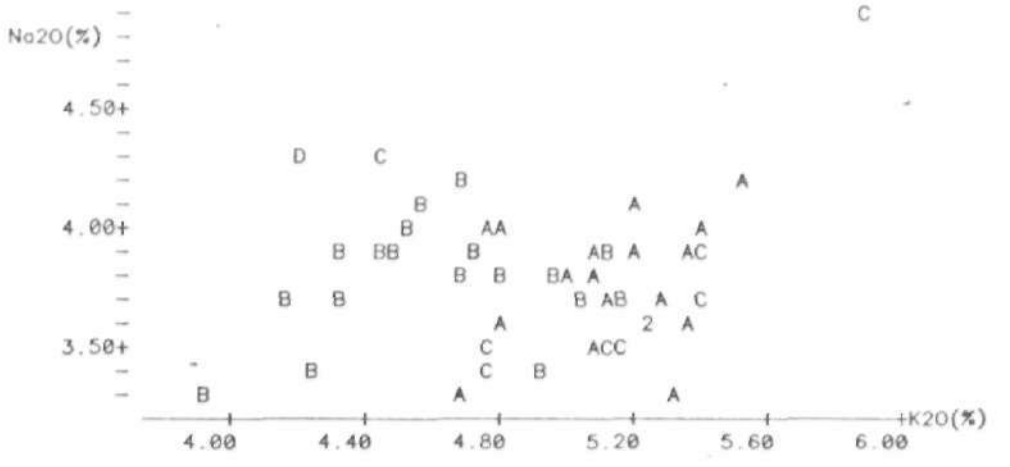


FIGURE 4.5 Correlation of Na with K in the Nigerian Younger Granite

Granites contain U with an average abundance of 4ppm, and the concentration is believed to increase with a decrease in the age of the intrusion. The average U content in the Jos-Bukuru complex is shown in Table 4.5, where it is compared with the abundance in a granite of average concentration and granites enriched in U. Abundance data from determinations on other complexes in the Younger Granites are also included. The data indicate that both U and Th are enriched in the Jos-Bukuru granites relative to an average granite. Comparison of the average U content of the different textural types of granite also indicates a relative enrichment of U especially in the medium-grained granites compared to other rock types in the region. Other highly U-enriched rock types in the complex include the biotite granites, albite-riebeckite granites, the riebeckite-aegerine granites and aegerine-albite granites. Figure 4.6 shows the geographical distribution of U in the Jos - Bukuru complex.

Ahrens (1954) studied the distribution of elements in igneous rocks and recognised a characteristic lognormal distribution of elements in certain igneous suites. In a study of the distribution of U and Th in the Conway granite, Rogers and Adams (1963) also observed that both elements are lognormally distributed. However, the frequency plots of U and Th for the Younger Granites shown in Figure 4.7, have a normal distribution.

Table 4.5: Showing average U content of the Nigerian Younger Granites compared to granites of enriched U levels.

Location	Rock-type	U(ppm)		Th(ppm)		Ref.
		mean	range	mean	range	
Dartmoor	biotite granite	11.33	4.20-11.4	21.4		1
Conway		15		57		2
NYG	biotite	11	9-15	33	17-74	4
	hornblende-fayalite	8		27		4
	arfvedsonite-aegerine	9.9	3.9-17.0	64	12-124	3
	arfvedsonite-albite	102	60-145	182	44-350	3
	biotite-albite	77		64		3
	albite	39		88		3
	zinwaldite	105		190		3
	microcline wall-rock	11.5	10.2-12.8	40.3	38.8-41.7	3

NYG: Nigerian Younger Granite

References:

1 Tammamegi and Smith (1975)

2 Fehn et al. (1978)

3 Kinnaird et al. (1985)

4 This study

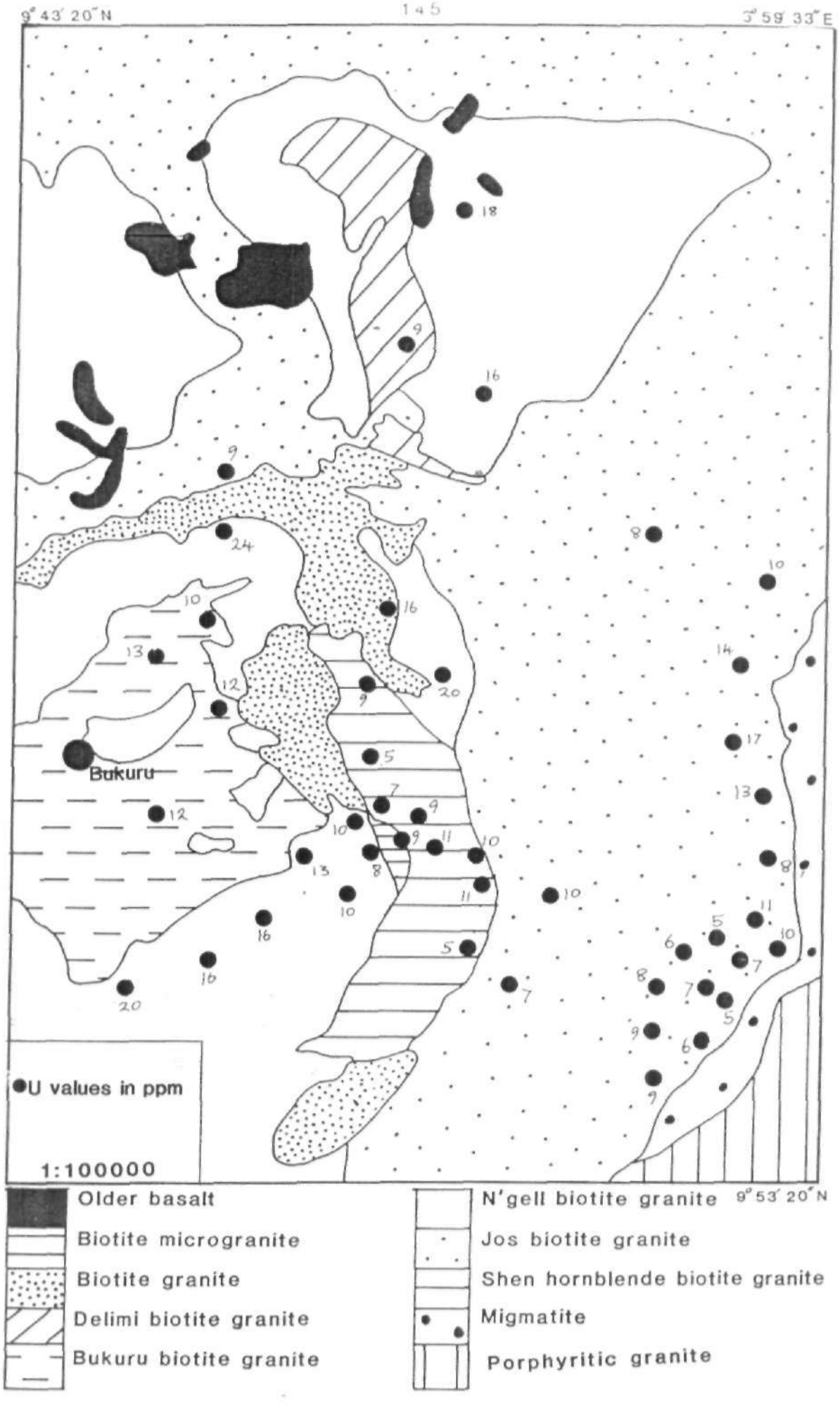


FIGURE 4.6 U in the Nigerian Younger Granites, Jos- Bukuru complex

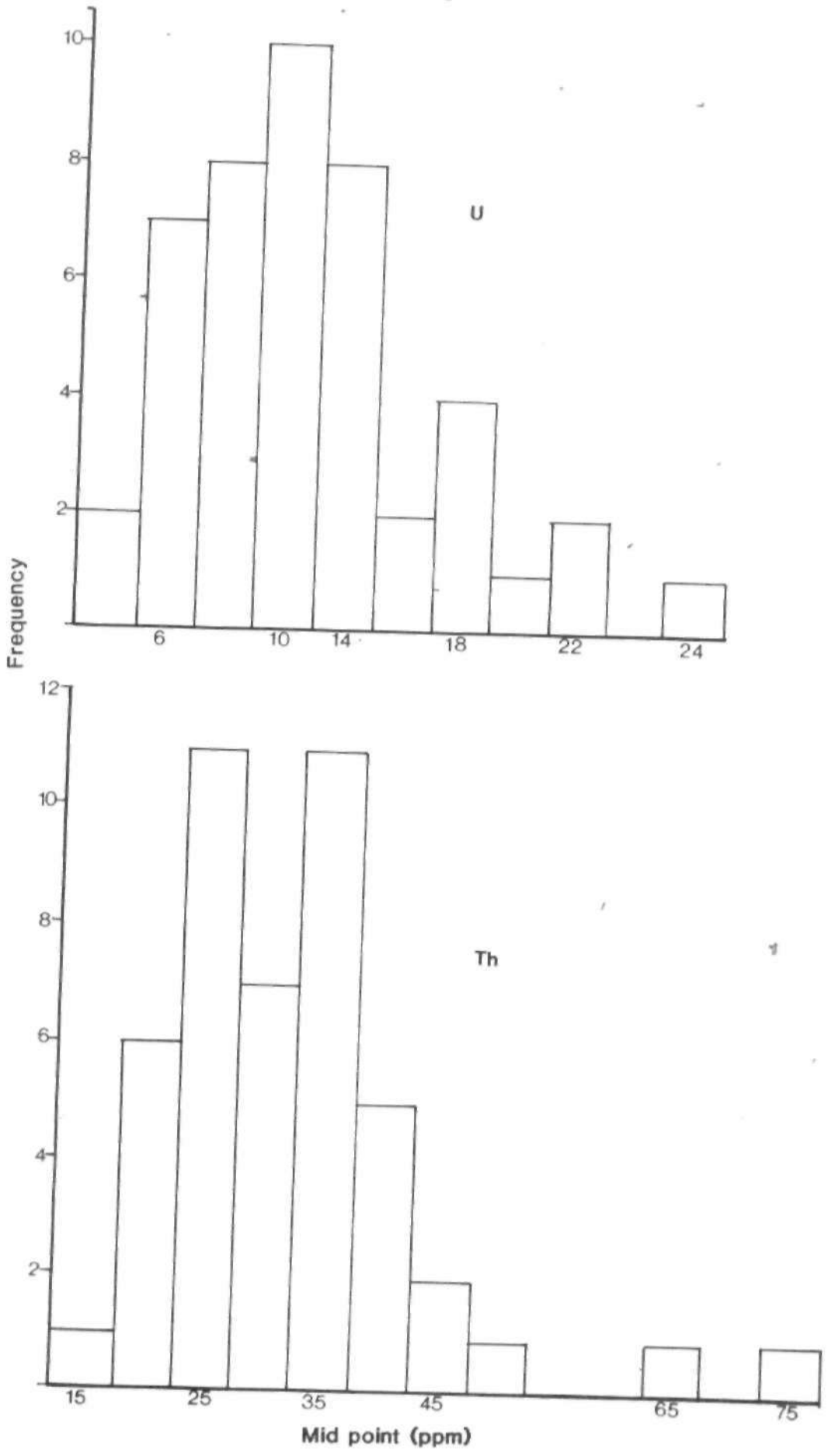


FIGURE 4.7 Frequency distribution of U and Th in the Nigerian Younger granites

4.7.2 Element Associations and Variation

The geochemistry of U and Th during magmatic processes and post-magmatic fluid-rock interactions, is fairly well known. Both are incompatible elements and tend to be associated in igneous rocks with a more-or-less fairly constant ratio of 3-4. Their relatively large ionic radii ($1.05.10^{-10}$m for U and $1.10.10^{-10}$m for Th) and high charge values (+4/+6 for U and +4 for Th) make them difficult to be taken into the crystal structures of the major rock-forming minerals. The result is that they become concentrated in the late magmatic fluid phases. Therefore U and Th are usually concentrated in the highly differentiated phases of intrusions. Fluid-rock intractions at the end of a cycle of magmatic activity are also capable of affecting the mineralisation of igneous rock suites.

The geochemistry given above reveals the highly differentiated nature of the Younger Granites of the Jos - Bukuru complex and, indeed, the Younger Granites intrusion in general. It also supports the view that late alkali metasomatism influenced the general geochemistry of the granite. To further investigate changes in U and Th abundance and the process of mineralisation, plots of these elements against various indicators of the degree of differentiation of the rock suite have been made.

Plots of U and Th against SiO_2 (Figure 4.8) show that both increase with increasing SiO_2 content. These trends are shown by the different textural types and clearly indicate the high concentrations of these elements in the medium-grained granite

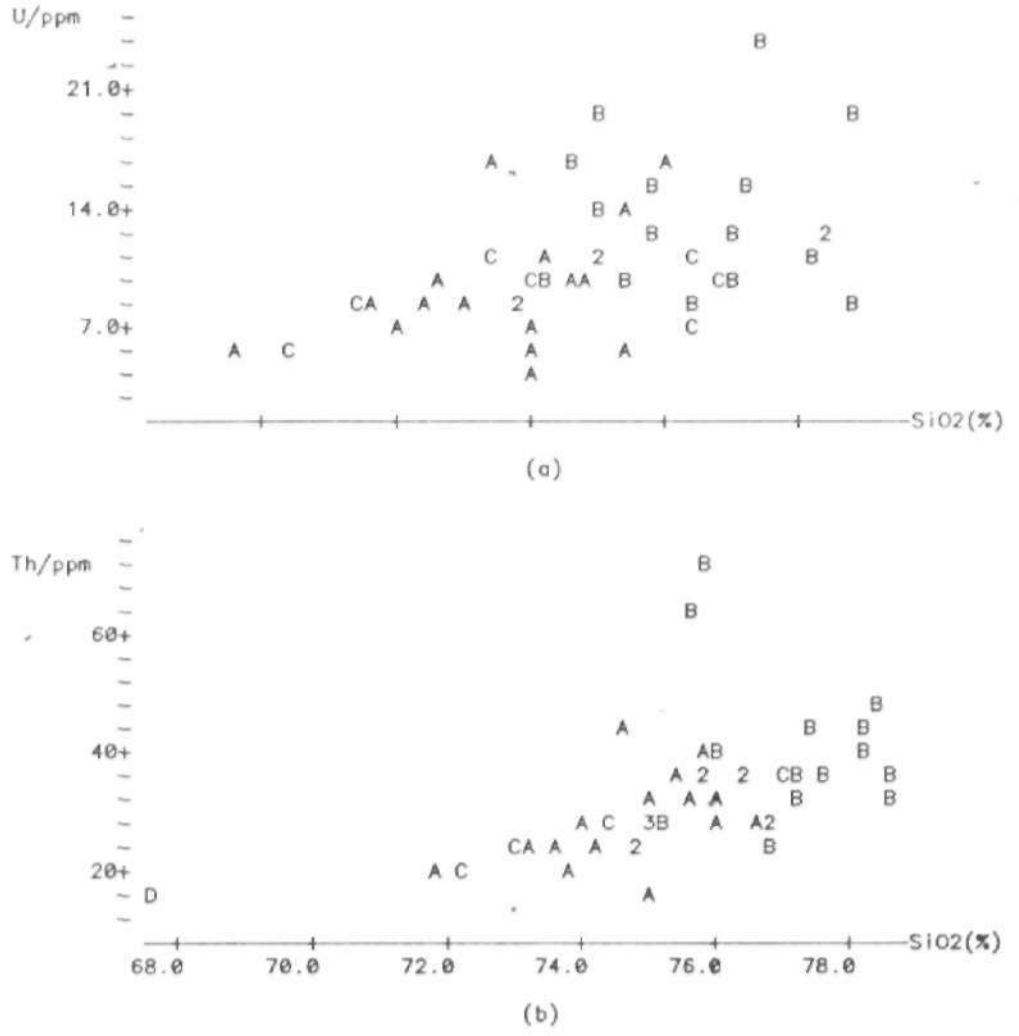


FIGURE 4.8 Plot of U (a) and Th (b) against SiO2

relative to the coarse-grained types. Both U and Th show an increase with increase in the differentiation index (DI) of Nockolds and Allen (1953) (Figure 4.9). Plots of both SiO_2 and Rb against the DI also have very good correlations.

The plots of U and Th against Rb (Figure 4.10) clearly show an increase with increasing Rb, a trend displayed by both main textural types. However, the hornblende-fayalite granites show some decrease in U and Th at higher Rb concentrations. Similar plots of U and Th against K:Rb ratio (Figure 4.11) indicate that both elements decrease with increase in the ratio. Here, again, both main textural types show this trend. The correlation is higher with Th than with U which shows a much wider scatter.

Both U and Th also show the same trend in their plots against the Rb:Sr ratio (Figure 4.12), but here the trend is different for the different textural types. While both elements increase with an increase in the ratio in the coarse-grained granites, they show a decrease in the medium-grained granites. The trend shown by the hornblende granites is an initial increase then a decrease at higher ratios.

In general, therefore, both U and Th vary systematically with SiO_2, DI, Rb, and the K:Rb ratio. The general increase of both U and Th with SiO_2, DI, and Rb, and their decrease with the K:Rb suggest that they are concentrated in the Younger Granites by fractionation processes. The higher correlation of Th relative to U in these plots may indicate the redistribution of U during late- and post-magmatic processes, or fractionation of the two elements

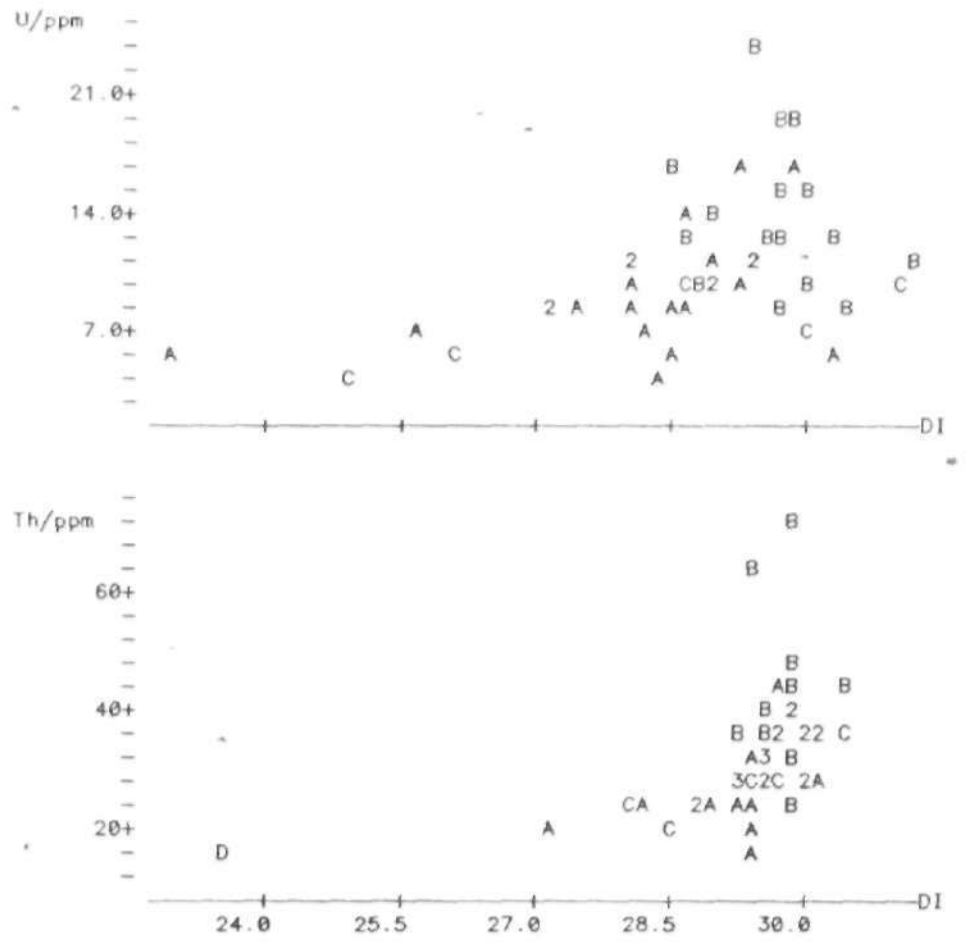


FIGURE 4.9 Plot of U (a) and Th (b) against differentiation index (DI)

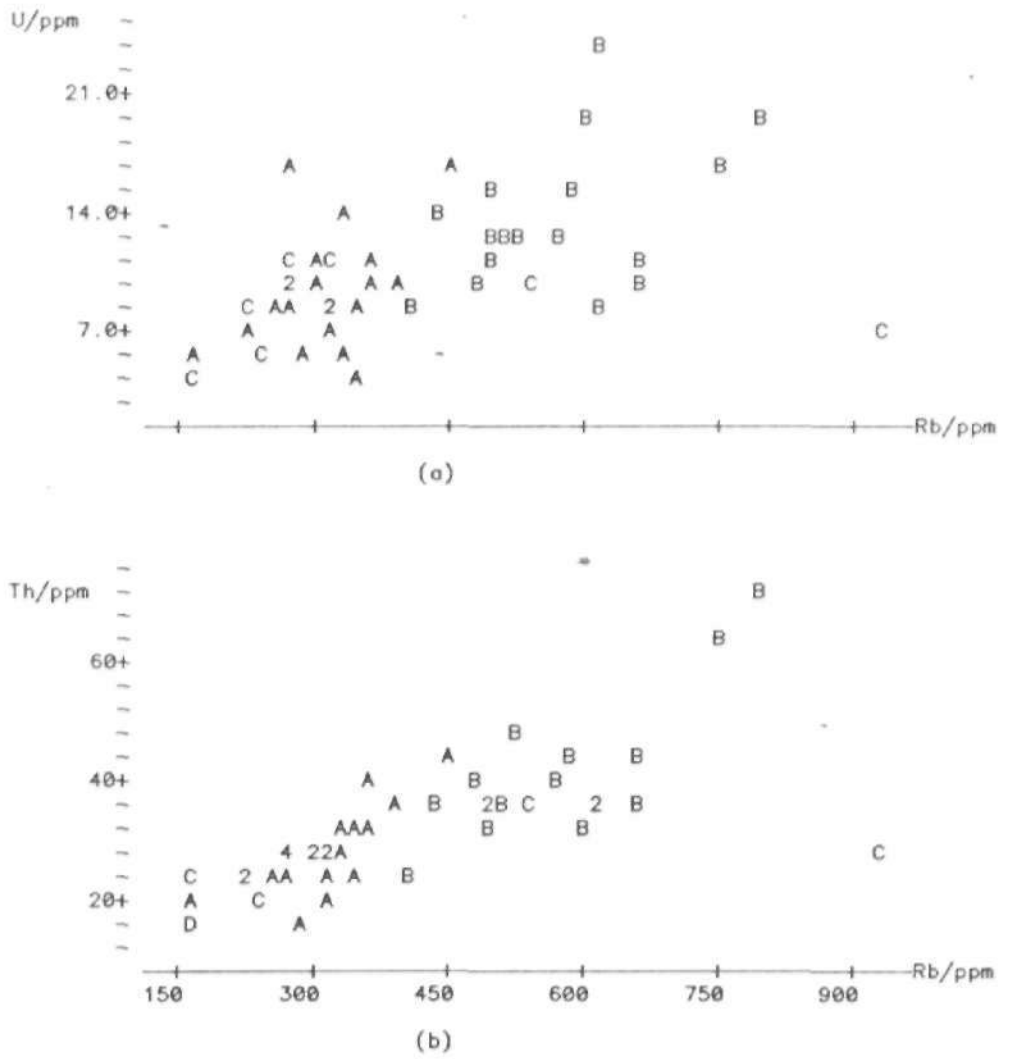


FIGURE 4.10 Plot of U (a) and Th (b) against Rb

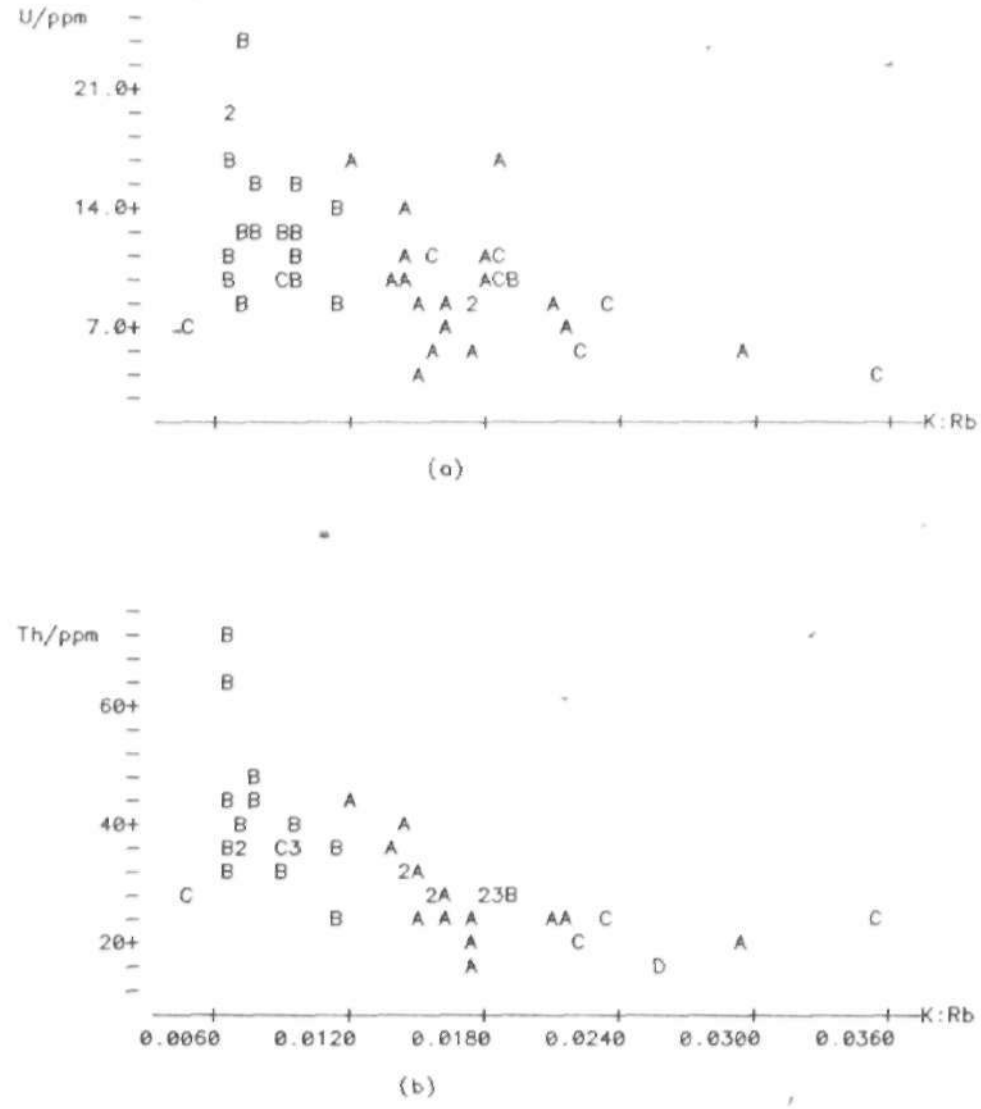


FIGURE 4.11 Plot of U (a) and Th (b) against K:Rb

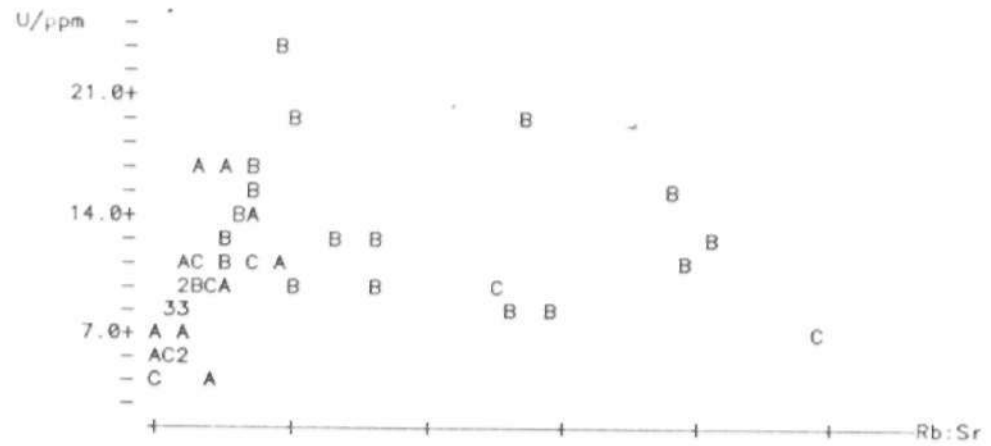


FIGURE 4.12 Plot of U (a) and Th (b) against Rb:Sr

during magmatic differentiation, although the former appears more likely.

The removal of U during late-stage differentiation has been proposed as a possible mechanism to explain the large variations of U and Th in highly fractionated igneous suites (Rogers and Ragland, 1961). U shows a wider scatter during the evolution of these rocks. The oxidation of the uranyl ion in late magmatic activity is thought to fractionate U and Th by taking U out of the system in volatile phases (Whitefield et al., 1959). The higher correlation of Th with Rb, relative to U, might be indicative of such a phenomenon in the Jos - Bukuru complex. The importance of alkali metasomatism as a late-stage process in the history of the complex has already been pointed out. It was also shown that, because of the high K content, potash-metasomatism might have been the latest in the sequence of metasomatic processes. Moreover, fluid inclusion studies by Kinnaird (1985), and the occurrence of fluorite in the granite, additionally indicate the importance of F-rich fluids in these processes. F-rich fluids could also have influenced the removal of U by forming U-F complexes, and hence caused the fractionation of U and Th. Plots of U and Th against K_2O show a closer correlation of K with U than with Th (Figure 4.13). Post-magmatic processes which could have led to the fractionation of U and Th are considered in detail in Chapters 8 and 9, but here it is worth mentioning that a number of hydrothermal alteration processes related to mineralisation have been identified in these granites. Important of these are soda and potash metasomatism. Soda

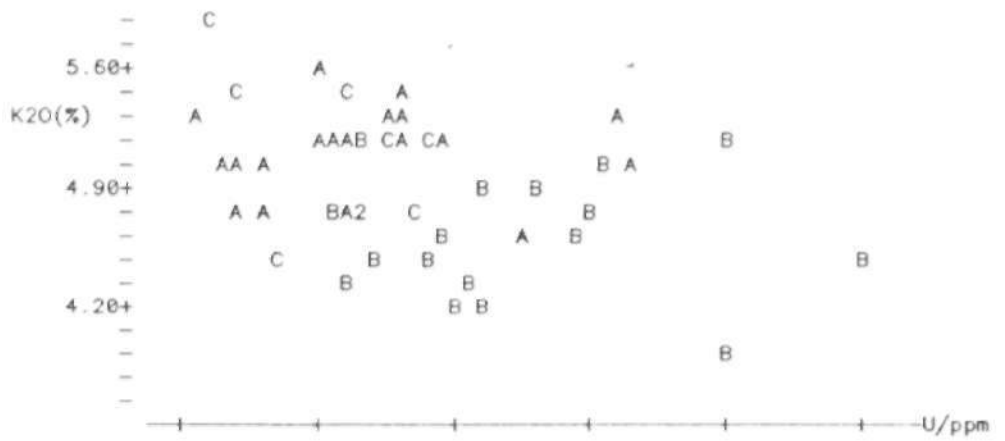


FIGURE 4.13 Plot of K2O against U (a) and Th (b)

metasomatism in particular was responsible for the introduction of Nb-bearing ore minerals such as columbite, pyrochlore, fergusonite and uraninite in the granites (Bowden and Kinnaird, 1984). The process is responsible for the alteration of potash feldspar to albite and enrichment of trace REE in the granites.

The variation of U as a function of Th in the granites is shown in Figure 4.14, from which a linear positive correlation can be seen. The close correlation again suggests that, overall, they must have been concentrated by the same fractionation process. Although U and Th variation in igneous rocks shows systematic trends, generally increasing with increasing fractionation of the magma, the Th:U ratio usually shows contrasting variations in different rock suites. Thus while Whitefield et al.(1959) and Heier and Rogers (1963) reported an increase in the Th:U ratio with differentiation, Larsen and Gottfried (1960) noticed no variation in the ratio as a function of differentiation. Plots of Th:U ratio against SiO_2, Rb, and DI (Figure 4.15-4.17) show that, in general, there is a slight increase in the ratio with fractionation. The coarse-grained granites show the widest scatter, thus further indicating the intimate relationship of the elements in the more silicious, and generally highly differentiated, phases of the granite.

In summary, therefore, the distribution of both U and Th in the Nigerian Younger Granites suggests that these elements were concentrated by fractionation processes during the evolution of the granites. The general erratic variation of U in the

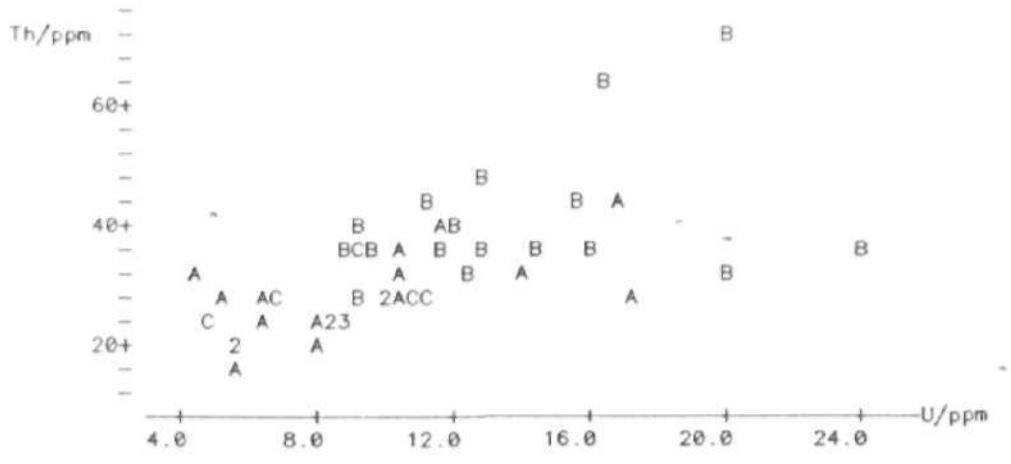


FIGURE 4.14 Plot of Th against U

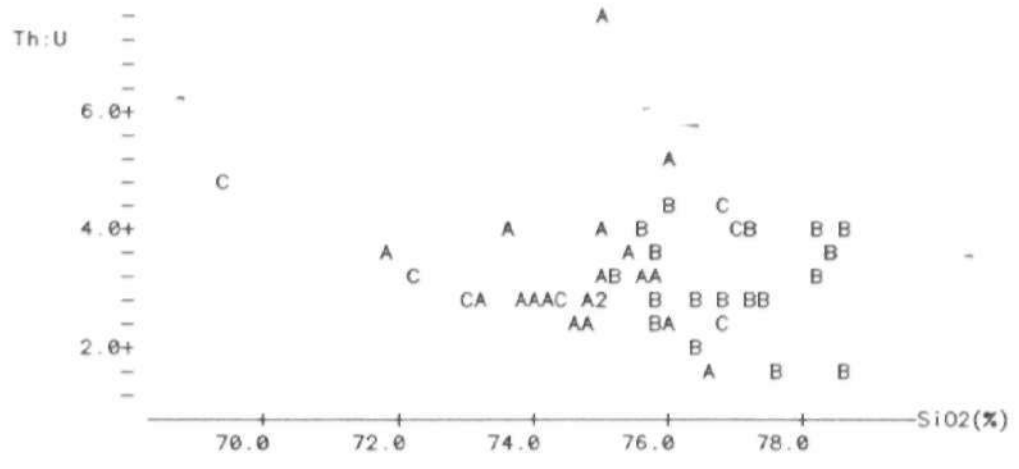


FIGURE 4.15 Plot of Th:U against SiO2

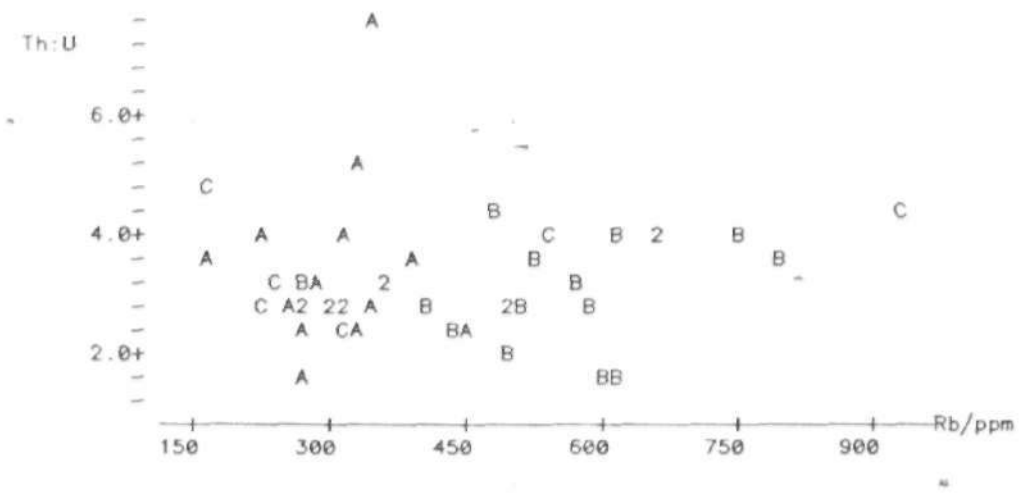


FIGURE 4.16 Plot of Th:U against Rb

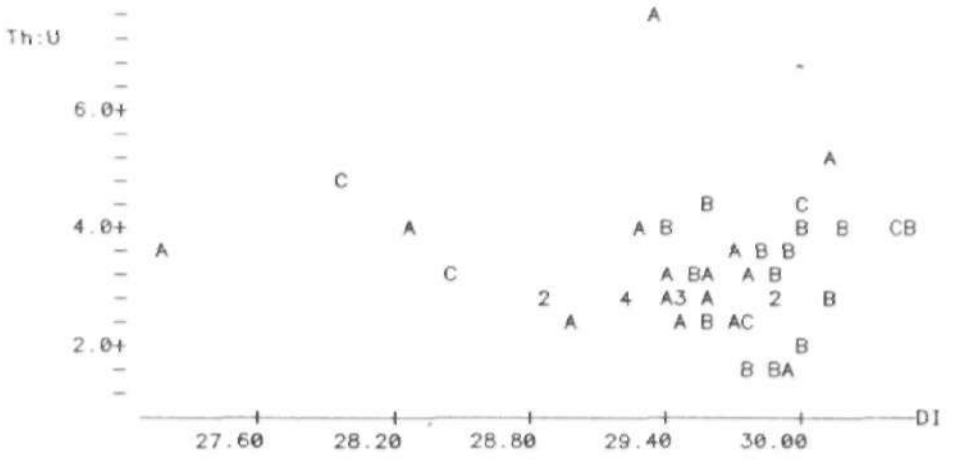


FIGURE 4.17 Plot of Th:U against DI

evolutionary trend could be explained by late magmatic or post-magmatic fluid-rock interactions. The replacement of Na by K in these processes also involved the depletion of U, with an attendant increase in the Th:U ratio.

Although the main geochemical associations of U in these rocks show the importance of magmatic processes, the influence of surface processes in modifying this picture is also apparent. Even if other influences are excluded, because these samples were collected from outcrop, they are likely to have been affected by weathering. That surface samples elsewhere in the Younger Granites were affected by weathering is shown by the data of Bowden et al. (1982), where both U and Th show a large increase with increase in the depth from which the samples were obtained.

4.7.3 U Mineralisation in the Granite

The geochemistry of granitic rocks can be used to specify a granite body in terms of its ore-forming potential. This is because it is commonly observed that mineral deposits are usually associated with local geochemical anomalies in the surrounding rocks. Covet (1983) reached this conclusion from whole-rock geochemical data of Sn-bearing and Sn-barren granites, and suggested that potential Sn-bearing granites could be identified on the basis of their K:Rb, Mg:Li, and Ba:Rb ratios. Similarly, Simpson et al. (1976) have shown the importance of whole-rock

geochemistry in the identification of vein-type U mineralisation in primary U provinces. The enrichment of the trace elements, more especially the radioelements, and their variable concentrations in the granites, together with the association of the granites with high heat production, are indicative that the Nigerian Younger Granites are the host of U mineralisation.

Disseminated, lode and vein-controlled Sn deposits in the Jos Plateau are associated with magmatic processes (Pastor and Turaki, 1985). Figures 4.18 and 4.19 show the association of Nb and Sn, and Nb and U, in the granite. The high correlation between Nb and Sn suggests that the Sn mineralisation observed in the granites occurs with Sn in cassiterite. The close association of U and Nb then further suggests the spatial association of cassiterite mineralisation with that of U in the granites. Thus the same processes which produced Sn mineralisation are also of importance in controlling the U mineralisation. For example, importance of fractionation in the enrichment of U in the granite has already been discussed. A plot of Th versus U (Figure 4.8) shows the preferential enrichment of U to Th in the granite, with most points falling below the 3-4 average Th:U ratio of granitic rocks. This suggests that fractionation processes favour the concentration of U. Also, fluid inclusion studies of the Jos Plateau granites (Kinnaird et al., 1985) show the enrichment of F and Cl in the volatile phase during the evolution of the magma. The enrichment of U might then have been brought about by these volatile phases, especially as U has the ability to form complexes with F and Cl.

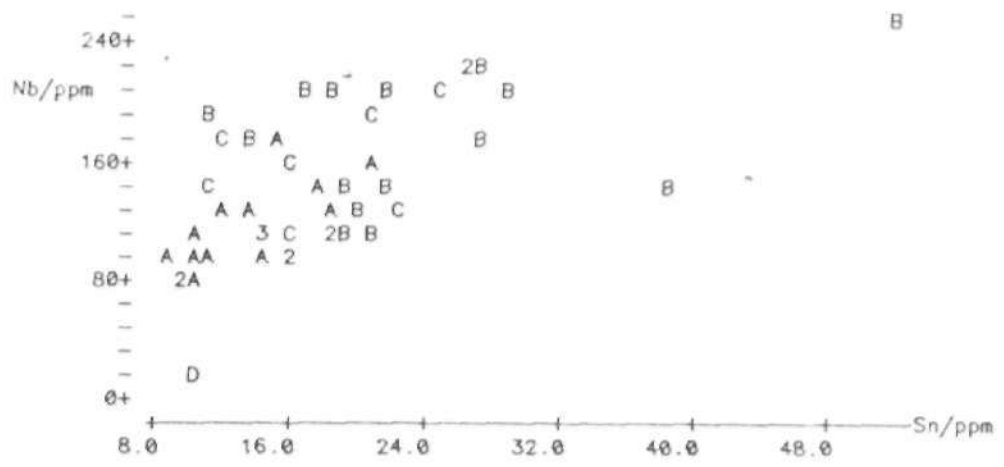


FIGURE 4.18 Plot of Nb against Sn

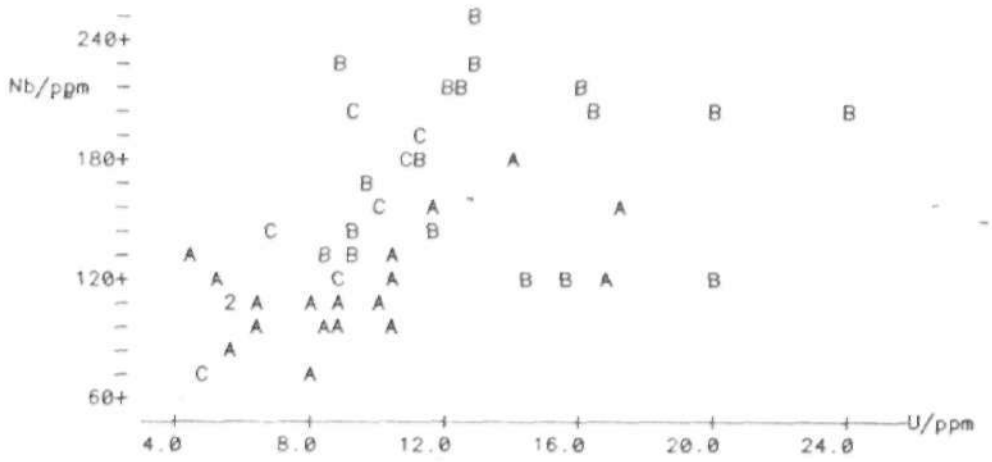


FIGURE 4.19 Plot of Nb against U

Late-stage magmatic processes associated with the volatile phase, such as the alkali metasomatism which is associated with the granites, could also produce U mineralisation, and pegmatites containing uraninite and other U minerals have also been recognised as a style of U mineralisation associated with the granites (Kinnaird, 1985). Even albitization leads to the concentration of U in pyrochlore in albite-riebeckite granites. These observations suggest that the enrichment of U occurred in the later crystallizing fluids.

In the Nigerian Younger Granites, more especially in the Jos - Bukuru complex, U is thus mostly concentrated in accessory primary minerals such as thorite, xenotime, sphene, and zircon. Interestingly, these minerals present some problems in Sn mining operations and thorite, in particular, has been extracted in substantial amounts as a by-product of such operations. However, the possibility that vein-controlled U mineralisation was formed by post-magmatic hydrothermal activity in the granites, is highly likely. The evidence for this is the reported occurrence of extensive vein deposits of U in uraninite associated with the granites. Kinnaird et al. (1985) observed that where hydrothermal processes have been extensive, disseminated and vein deposits of Sn, Zn, W, and Nb, with U, Cu, Fe, Bi, and REE are developed. These veins have been observed to extend to great distances into the country rocks.

4.8 Conclusions

The geochemistry of the Jos-Bukuru complex has been discussed on the basis of chemical analysis of 46 granite samples. The results of the investigation reveal the peraluminous character of the Nigerian Younger Granites. The granites are highly enriched in W, Sn, Nb, Ni, Zn, Ga, As, Th, U, Rb, Y, Zr, Cr, La, and Ce, and depleted in Ti, Mg, Mn, P, Cu, V, Ba, and Sr. In particular, W, Nb and Sn are anomalously enriched to an order of magnitude greater than their concentration in an average granite. The variation of the elements with SiO_2 show that Al, Ti, Fe, Ca and K decrease with increase in SiO_2, while Na and Mg remain fairly constant. Data in this study also indicate the highly differentiated nature of the granites, with low K:Rb ratios. K values for these ratios were obtained from k_2O analyses. The average K:Rb ratio for the biotite granites is 118 and for the coarse-grained and medium-grained types 169 and 82, respectively. Plots of K_2O against Rb show that the granites lie within the pegmatitic-hydrothermal field of Shaw (1968). The investigation also revealed the importance of magmatic fractionation in the concentration of the elements. Potash metasomatism forms one of the most important late-stage magmatic processes that have influenced the mineralisation in the area. Studies of the K:Rb ratio, the high K concentration relative to Na, and the dominance of microcline perthite in the feldspar, indicate the importance of potash metasomatism. The variation between the different textural types of granite show that the medium-grained

biotite granites are more acidic; less aluminous, and more enriched in the trace elements, than the coarse-grained granites. The hornblende-fayalite granites exhibit the same characteristic as the coarse-grained types, which suggests that they might have been emplaced during the same igneous cycle.

Geochemical investigations of U in the granite show that large abundances of the element occur, more especially in the medium-grained granites. The high U abundance of the granites is shown in the overall average in the granite types, which is much higher than in an average granite. Plots of U against various indicators of differentiation suggest that the observed mineralisation in the granites was largely controlled by primary magmatic activity. Evidence also exists which suggests that the mineralisations in the granite have been affected by metasomatic processes. The effect of K-metasomatism in the granite was a depletion in U.

Evidence from this study suggests the importance of vein-controlled U mineralisation produced by hydrothermal activity in the Jos-Bukuru complex, in addition to dispersed U-Sn mineralisations. There is the possibility of the granites being the source rock for some economic U mineralisation.

CHAPTER FIVE: DISTRIBUTION OF U IN THE NIGERIAN YOUNGER GRANITES AND THE KAOLINISED GRANITES OF SOUTH-WEST ENGLAND

5.1 Introduction

High levels of U and Th in the Nigerian Younger Granites has been established in Chapter 4. Because of the large proportion of U in the granites which appears to have been precipitated during post-magmatic hydrothermal circulation, it was suggested that some of the U could have been partitioned into primary U-bearing minerals, such as uraninite or pyrochlore. Both these minerals are present in sufficient quantities to constitute a significant U resource. In addition, a large amount of monazite concentrate has also been recovered as a by-product of tin mining in the region. However, the relative importance of these minerals as U hosts is unclear. This Chapter describes the techniques used to determine the location of the mineralogical sites of U and Th in the Nigerian granites and also the kaolinised granites of South-West England. In particular, alpha autoradiography was used to pin-point the sites of alpha emitters which are mainly found in the U and Th decay series.

A solid state nuclear track detector, CR 39 Lexan, was employed in the investigation. Small rock surfaces from standard thin sections were studied. Because samples from the kaolinised

granites are highly altered and friable, some had to be impregnated with resin. Because of the small surface area of the samples, a large number of thin sections were examined. Interpretation of the results also took into account the fact that the granite samples were collected close to the ground surface and that some of the U could have been mobilised as a result of weathering processes. In all 58 thin sections were analysed in this investigation.

5.2 Principles of Autoradiography

All of the three types of radiation (alpha, beta and gamma) emitted during radioactive decay affect photographic emulsions to varying degrees. This phenomenon forms the basis of the autoradiographic techniques used in the study of radioactive materials. The interaction of the emitted particles with the material in the photographic emulsion exposes the films, which may then be developed. Because of differences in ionisation potential, each of the three particles produces different effects.

The basic arrangement used in the autoradiographic technique involves a configuration where the source of the particles and the detecting material are positioned so that particles emitted from the source impinge directly onto the detecting film. To see how this works, consider a slab of material containing some radioactive elements placed onto a photographic plate, as shown in Figure 5.1. Radiation from the decaying atoms is emitted in all directions and

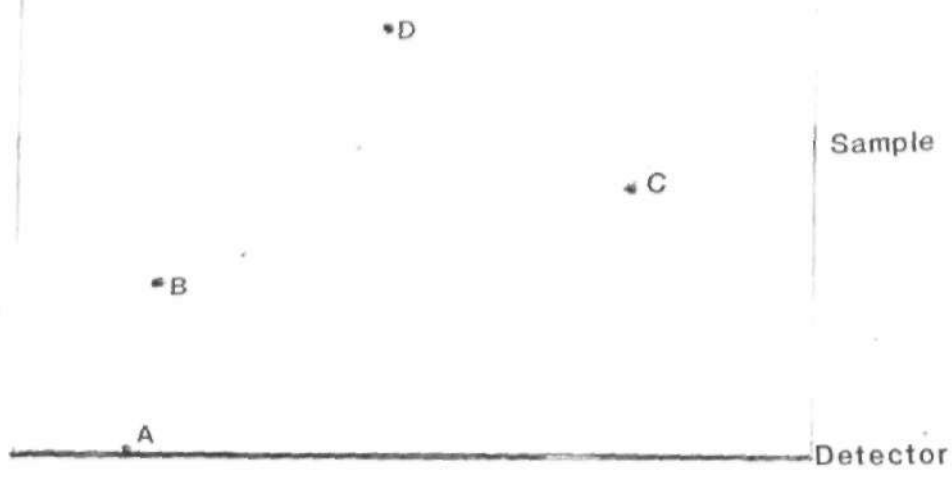


FIGURE 5.1 Source-detector arrangement in autoradiography

travels different distances in the material before being absorbed. For an atom directly at the surface in contact with the emulsion, such as point A, all types of radiation reach the emulsion with their full energy, since they have not passed through any part of the material. Alpha-particles, having a very low range, will expend all their energy in the emulsion and cause damage in their path through the emulsion. On being developed, the film will show a sharply defined image of the track around this point. In comparison, the more penetrative beta-particles and gamma-rays produce a diffuse image of their tracks. For an atom at points such as B and C, at a distance greater than the range of the alpha-particles away from the emulsion, only the very diffuse images produced by beta- particles and gamma-rays are found. These may just result in a general fogging of the developed film. Gamma-rays from an atom as far as point D, beyond the range of beta-particles, may also be registered on some emulsions. Both the track diameter and its depth within the emulsion depend on the energy of impact and the distance of the decaying atom away from the emulsion. All of these parameters are taken into account in present-day autoradiographic investigations of point sources, but in geological materials we are not dealing with such idealised circumstances, and only semi-quantitative or qualitative studies are possible. Nevertheless, it is feasible to adopt certain practices which make this approach less restricting than might first appear to be the case.

To obtain autoradiographs due only to a particular particle the effect due to others can be removed. In the first, early applications, ordinary photographic emulsions were employed. This necessitated the use of filters to screen the emulsion from visible light. For alpha-particle autoradiography, the emulsion had to be screened from both beta and gamma radiations as well. A Problem with such screens, which were usually just pieces of black paper interposed between the emulsion and the source of the alpha radiation, was the fact that because of the short range of the particles, most were absorbed by the screens themselves. This and other problems led to development of emulsions which were sensitive only to alpha-particles (Yagoda, 1946). Emulsions in the form of standard photographic plates were produced for such studies. In practice, a film slightly thicker than the range of the most penetrating alpha-particles in the source to be investigated was made of fine-grained silver halide (desensitized to light and beta and gamma radiations) coated onto glass plates. To absorb alpha-particles of high energy, a 50μm-thick layer of the emulsion was used. However, after developing, alpha particle images from these emulsions were found difficult to match with their sources in the samples (Poole and Bremmer, 1949). In a technique developed by Ford (1951), Ilford C2 emulsions were applied in gel form directly to the source material, and the film developed without separating it from the sample. This method was found to give good results, and the tracks could be matched directly to their sources in the

sample. Unfortunately, the emulsion obscured the sample for later microscopic examinations, as noted by Bowie (1954), Hee et al. (1954), and Ragland (1964).

In recent years most of the problems mentioned above have been overcome. Solid state nuclear track detectors made for detecting ionising particles have been developed. Now, alpha-sensitive plastic films desensitized to beta and gamma radiation and ordinary light have replaced the alpha autoradiographic emulsions. These plastic films are produced in flexible sheet form and come in varying sizes. They are made so that after exposure to the specimen they are removed and then processed separately, leaving the samples intact. The alpha-particle tracks in the plastic are made visible by etching in caustic solutions. In the early production of these films, Kodak made two types of film of different thickness: 12μm and 100μm. These were fully described by Basham and Easterbrook (1977). The thinner of the films when exposed to alpha-particles was found to be perforated, because it had a thickness less than most alpha-particle ranges. These perforations could be easily counted against the dark background of the film to give a numerical value for alpha-particle activity. However, for the 100 μm films, alpha-particles did not completely pass through; each traversing a distance proportional to its range in the material. Measuring the distances could then be used to estimate the energies of the particles. This approach has been employed to estimate the relative amounts of U and Th in an alpha-

ource (Henshaw, et al. 1982; Fews, 1986).

oda (1946) has studied the effect of environmental
emulsions and the conditions under which high quality
be obtained from them. Similarly, the influence of
al factors on solid state nuclear track detectors and
m operating conditions have been reported by Frank et
and Heins and Enge (1986). These have shown that the
hese detectors are greatly improved when they are
eated with anti-oxidants during their production. Best
obtained by etching in concentrated caustic solutions
res of between 60°C to 80°C. Most recent
y studies utilise the track detector commercially
an exceptionally sensitive themorset polymer. The
this film have been extensively investigated by
Shirk (1977) and Henshaw et al. (1986). Using this
es of alpha-emitters in many different types of
irly easily located. In rock samples with
lements, the major alpha-emitters are the
cay of ^{40}K does not involve alpha-
e only other important alpha-emitter
v and requires prolonged exposure
ore, alpha autoradiographic
is essentially a method of
stituent minerals.
een developed and used

in the study of beta-emitting nuclides. Bowie (1954) used one of these, a beta-sensitive Kodak NT-4 emulsion, to distinguish K-bearing minerals from U and Th minerals in ores. However, he recognised the difficulty of matching the beta tracks to their sources because of their high penetrating power. These emulsions are mainly used in the investigation of biological samples, particularly for locating artificial beta-emitting nuclides used as tracers in plant and animal tissues. They have not yet found any real use in geological studies.

5.3 Methods and Techniques in Alpha Autoradiography

Fairly standard methods have now been developed for autoradiographic techniques in the study of both natural and artificial radioactivity. Using plastic nuclear track detectors, the presence of alpha-emitters can easily be determined and much information can be obtained from analysis of the data acquired. More specifically, the sites of alpha-emitting nuclides in geological samples can be located fairly accurately using these detectors. The minerals in which the alpha emitters are hosted can then be identified using a petrological microscope or other techniques.

With the improvement of detecting materials, the autoradiographic method has often been used for quantitative assessment of the U and Th content of minerals. The pioneering work

in this direction can be attributed to Yagoda (1946). These applications, basically involve counting the number of alpha tracks, which is proportional to the number of the alpha-particles escaping from the mineral surface, and comparing this to the number of alpha-particles released by the decay of the U and Th series in equilibrium. Yagoda (1946) has shown that the relationship is given by:

$$P = \psi(30.1U+13.7Th),$$

where P is the number of alpha-particles which escape per second from $1cm^2$ of a polished mineral surface, U and Th are the weight of U and Th per gram of the mineral, and ψ is the permeability of the mineral. A plot of P against the photographic density of the alpha-particles D, defined as D= log(incident light/transmitted light), was found to be linear, but different minerals plot in different fields. When calibrated, these plots can be used to identify specific U and Th minerals. Singh et al. (1986) using a CR-39 (doped) plastic detector also developed a relationship, based on the method of Coppens (1977), from which the U and Th content of a sample could be estimated from alpha autoradiographic determinations. The relationship was found to be:

$$10^6 N = (6.77U+1.60Th).k$$

where N is the alpha track rate and k is the absorption

coefficient. U and Th are concentrations in ppm.

The difference in the range of the alpha-particles from the U and Th decay series can also be used as a means of estimating their relative proportions from alpha autoradiographic investigations. For example, the most energetic alpha-particles in the U decay series have a range of 8.57cm in air, while those in the Th decay series have a range of 6.91cm. As a means of distinguishing the contributions due to the U and Th decay series in a sample, Bowie (1954) suggested the use of a screen between the sample and the detector material - in his case photographic film. In this system, the sample was exposed to the film first without a screen, then with a suitable screen to stop all alpha-particles with energies less than the range of the most penetrating of the two decay series. But this proved to have many limitations, firstly because of the problems associated with finding a screen with the required properties, and secondly, any screen with a stopping power of 7.5cm, as used by Bowie, may not be reliable. This is because a large proportion of even the high-range alpha-particles will be absorbed, thus putting a severe restriction on the exposure period. Moreover, without the screen, alpha-particles originating from ^{214}Po sources within the specimen may reach the surface with reduced energies and be detected, but with the screen on they will not be detected. Thus the resulting tracks may be incorrectly assigned to lower energy alpha-particles. Therefore, the analysis will not give the true U concentration of

the sample. For these reasons, such determinations may only have qualitative applications.

An alternative method of using autoradiography for estimating U and Th is based on the number of tracks produced within a certain period of time, which is dependent on the relative half-lives of the alpha-emitters in the U and Th decay series. The theoretical considerations discussed by Senftle et al. (1954) showed that within a period of 72.72hours, as many as five tracks and three tracks observed are due to Th and U, respectively. Therefore, the ratio of 'five-track stars' to 'single and three-track stars' is directly proportional to the Th to U ratio. This method was used by Piccioto and Wilgain (1954) to measure Th isotopes in deep-sea sediments. These authors noted the problem of achieving ideal geometry and the lack of a large alpha track population in very weakly radioactive minerals meant poor counting statistics.

Another powerful technique in autoradiography is the fission track method. In this approach, fission fragments from ^{235}U, ^{238}U and ^{232}Th are used to identify these nuclides. The method involves exposing samples to a track detector and then the whole package is irradiated with neutrons capable of causing fission in these nuclides. Price and Walker (1963) described an early application of the method where muscovite was used as the detector. The tracks in the mica were made visible by being etched in HF. However, there were traces of U and Th in the mica which interfered with the

results. Present applications use plastic detectors. The problems of long exposure periods associated with samples of low Th or U concentrations are overcome by this method. With proper application working limits with U concentrations as low as 1ppb can be realised.

The length of the tracks in the detector can also be used as a diagonistic technique for identifying the source element of the alpha-particle: knowing the energy-range relationship in the detector, the track length can be converted to energy. These techniques can now be applied with great accuracy due to the availability of high quality track-scanning techniques. From such scans both the track number and other track parameters, such as track length and track diameter, can be obtained with ease. Both semi-automatic and fully automatic track scanning have now been developed, so that a large area of detector can be scanned within a relatively short time. Fews (1986) has described a fully automatic scan technique using an ordinary optical microscope coupled to a computer. Mohanty et al.(1986) also described techniques of enlarging tracks in nuclear track plastics which facilitate their study by such scanning software. However, the problem still arises in geological materials that the sources are irregularly distributed in depth below the surface of the sample. Thus a high-energy track from a particle originating at depth gives the same appearance as a low energy caused by a particle from an atom track at the sample surface.

It must be emphasised that all quantitative estimates of U and Th content from autoradiography rely on the assumption of secular equilibrium in the U and Th decay series. Nevertheless, problems of deteriotion of films, and the fading of latent images encounted with the use of nuclear emulsions, have been largely removed with the development of the recent nuclear track plastics. Moreover, Frank et al. (1986) have shown that doping CR-39 films with anti-oxidants greatly improves their stability and the stability of the latent tracks. At the rate autoradiographic techniques are progressing, it may be possible for them to be employed in routine U exploration in the near future.

5.4 Location of U in Granite

U in granite may occur either in the primary rock-forming minerals, in accessory minerals, usually in association with the Rare Earth Elements (REE), or in secondary alteration products. Six sites commonly occupied by U, and its common associate Th, in igneous rocks, which have been recognised by Neuerburg (1955), Larsen and Phair (1954), and Basham et al. (1986a), are:

1) In primary U minerals such as uraninite and thorite.
2) In complex Nb, Ta, Ti, Y and REE minerals such as pyrochlore, fergusonite, samarskite, betafite and euxenite.
3) In common accessory minerals such as monazite, xenotime, zircon, apatite, allanite, sphene and rutile.

4) In primary rock-forming minerals such as micas, feldspars and amphiboles.

5) In alteration products of rock-forming silicates such as kaolinite and leucoxene, where they are usually as adsorbed ions.

6) In small fractures in the rock-forming minerals and along grain boundaries usually as interstial material derived from late magmatic, deutric or hydrothermal solutions.

The importance of each of these to the overall U in an environment varies from one locality to another. In highly enriched granites, for example, most of the U occurs in Type 1 and 2 locations given above. U distribution studies have shown that most U and Th in granites are concentrated in the accessory minerals such as zircon, sphene, apatite, xenotime and allanite. But the importance of these minerals as hosts for U is, in fact, largely restricted to granites with average or below-average U abundances. In highly radioactive granites they contribute only a small percentage to the whole-rock U concentration. For example, in studies of granites with above-average U concentrations, Basham et al. (1982a) and Silver et al.(1982) found that the U and Th in accessory minerals could not account for the observed whole-rock abundances of these elements. Basham and his coworkers suggested that over 70% of the U in highly U-rich granites may be contained in uraninite, although this may be missed in normal routine investigations. Richardson

(1963) also found that 58% of the U and about 19% of the Th in New Hampshire granite could not be accounted for by the accessory minerals observed in the granite.

Variations in the radioelement content of various accessory minerals have also been observed, both within a mineral species and in the same mineral in different locations within the same rock. Hayase (1953), for example, found that zircon inclusions in biotite are more radioactive than zircon inclusions in quartz in the same rock. The rare accessories allanite, xenotime and monazite, were also found to be more radioactive than the zircon.

Among many studies of the distribution of U in the granites of South-West England, it is generally believed that most of the U is held in accessory minerals such as zircon, monazite, xenotime, sphene, apatite, allanite, epidote and opaque iron oxides (Zaghloul, 1958; Hamilton, 1958; Simpson et al., 1976). Recent investigations on fresh samples, however, suggest the importance of such minerals to the whole-rock U content has been overestimated. The former investigations were carried out on samples collected from surface exposures where minerals such as uraninite, although found by Basham et al. (1982b), would have been largely destroyed by weathering. Uraninite occurring as subhedral grains associated with the common rock-forming minerals is now believed to account for 60% to 90% of the U in these granites (Basham et al., 1982b). Because uraninite may not be homogeneously distributed in the

granites, studies based on small samples and thin sections may be unrepresentative. This suggests that for detailed distribution studies, large samples are needed. Basham et al. (1982a) proposed the use of samples about 200cm by 500cm in size for detailed investigations of U distribution. However, this involves the examination of a large number of alpha track clusters, which may prove tedious and difficult.

5.5 *Localization of U and Th in the Nigerian Younger Granites and* Kaolinised Granites from South-West England

Ordinary 32hour rising-temperature cured CR-39 nuclear track plastic supplied by Pershore Mouldings was used to investigate the location of alpha-emitters in the granites of the Nigerian Younger Granite complex and the kaolinised granites of South-West England. Plastic sheets of 1000 μm thickness were obtained in rectangles of 10cm by 8cm. The properties of the plastic as a detector have been fully investigated by Fews (1982). Preliminary studies showed that etching in 6.25M NaOH solution for six hours produced satisfactory results. Although desensitized to beta and gamma radiations, and ordinary light, the plastic is very sensitive to mechanical pressure. Care was therefore taken in handling the sheets, especially prior to etching. The sheets were separated from each other using layers of polythene, and stored in a freezer prior to use.

5.6 Track Registration and Developing Films

The sheets were cut into rectangular pieces a little bigger than the glass slides supporting the rock sections. This was achieved by placing the plastic sheets between sheets of paper and using a very sharp saw. Care was taken in removing the dust and fragments produced by cutting because it was observed that brushing-off, even with soft tissue paper, produced developable images. The thin sections were then mounted on the plastic sheets and outlines scored of the edges of the rocks on the plastic sheets. The thin sections were held in place with masking tape. The plastic sheets were then marked with the appropriate thin section sample number for proper correlation after they had been processed. Therefore, the precise position of each section on the plastic sheet could be located after it had been processed. The assembly of taped section and plastic was placed on a layer of hardboard lined with soft tissue paper, plastic down, and covered with another layer of soft tissue paper. Another hardboard layer was then placed on top of the assembly. The section was then pressed onto the plastic sheet under the weight of a piece of flat glass (about 800g) placed on the upper board, and the whole assembly left in a cupboard for the period of exposure. Preliminary investigations showed that an exposure period of six weeks was sufficient for the kaolinised granite samples, while a period of three weeks was

adequate for the granite samples from the Jos Plateau. Sections were exposed in batches of eighteen.

The plastic was found to be so sensitive that, even with great care being taken, scratches were observed after developing. These were probably produced by the movement of the sections against the film when separating the film for processing.

At the expiration of the exposure period the sections were removed and the plastic sheets etched in 6.25M NaOH solution. For developing, the sheets were held in a clip and suspended by wire in the developing tank. The developing tank consisted of a rectangular plastic trough containing the NaOH solution. The temperature of the solution was taken to 75^{o}C before dipping the plastic and this temperature was maintained to within $\pm 2^{o}C$ using a water bath. The tank was occasionally shaken to drive off any bubbles that may have formed and which would prevent contact of the sheets with the etching solution. The tank was kept closed throughout the etching period to keep evaporation of the etchant to a minimum so that there would not be large concentration changes. The sheets were kept in the tank for six hours, which meant that all tracks were fully developed. Each batch of sheets was etched in a fresh solutions so as to avoid contamination. Although different etching conditions, concentration of etchant, temperature of etching, and time of etching, have been used on CR-39, Beth et al. (1986) found that etching CR-39 at concentrations of 4-6M at 40-60^{o}C had no effect on the response of the detector. Therefore, slight

concentration changes in the etchant may be ignored.

After etching, the films were washed in cold water for 30 minutes to remove the etchant. For this, the films were immersed in a container, similar to the developing tank, and a jet of cold water directed into the container. After washing, the films were left to dry in air before examination.

5.7 Track Examination and Mineral Identification

The developed detector sheets were examined together with the thin sections to identify the mineral hosts of the alpha-emitters that had been registered. In this procedure, for proper correlation of the tracks and their sources in the section, a holder was designed so that after locating an area of interest in a detector, the sheet could be removed without moving the thin section. This was achieved by making a rectangular slot, big enough to fit a standard thin section, in a metal sheet. The metal sheet provided a base onto which the detector was taped, so that the detector could be flipped over whenever the thin section was to be examined. With the thin section in the slot, the detector sheet was adjusted until the thin section fitted the scored outline on the plastic. The sheet was then taped to the slab. With this arrangement, the thin section could be removed, and the sheet examined, without any interference from the thin section. To locate an area on the sheet, it was simply moved in the field of view of a

microscope. To ensure that the whole detector sheet was examined, the sheet was viewed in a series of traverses.

Initially, clusters of interest in the plastic together with their corresponding source in the thin section, were photographed. To achieve this, after locating an area of interest, the assembly of detector and the holder was taped to the stage of a microscope fitted with a camera. The detector sheet was then turned over and the thin section inserted and photographed. A magnification of 3.5 was used and 9-10 traverses were found to be sufficient to cover the length of the section of the plastic which had been exposed. The procedure outlined below was found to produce satisfactory photographic results.

1 Select area

2 focus using the microscope

3 set light meter on light box at 8

4 set light to camera position

5 check fine focus in camera and refocus if necessary

6 set aperture iris at 6

7 take photograph

All areas of interest were then examined using a petrological microscope for identification of the minerals. Minerals that could not be identified were recorded and later examined by a scanning electron microscope, as described in the next Section.

5.8 Discussion of Result

The purpose of the investigations described in this Chapter was to identify the minerals hosting U and Th in the granites. The alpha track numbers obtained were very high and clusters very common, especially in the Nigerian Younger Granite sections. This, therefore, necessitated the selection of specific clusters for examination. Areas with fairly high numbers of alpha tracks, about 30 tracks on the average, were examined to characterise the source minerals. Table 5.1 gives a summary of the results obtained, and pictorial representations of the areas examined are given in Figures 5.2 - 5.8.

From the results, the importance of the accessory minerals in the distribution of U and Th in the granite can be recognised. Among the accessory hosts, zircon and sphene crystals account for most of the clusters. In fact, almost all the clusters examined from the kaolinised granites are associated either with zircon crystals or secondary alteration products.

Zircon: Was found in almost all the sections examined. In the Nigerian granites it occurs as fairly large tabular crystals sometimes prismatic and triangular. Usually the crystals are colourless, but a fairly large number are smoky grey or brown with some degree of shattering. Although it occurs in association with most of the rock-

forming minerals, it is usually as inclusions in biotite, sometimes causing discoloration in the biotite. In quartz it typically occurs along grain boundaries and is normally fairly large.

Sphene: Just like zircon, this has been recorded in almost all sections examined. It mostly occurs as euhedral crystal inclusions in biotite. Sphene usually occurs together with zircon in biotite. Except in few occasions, tracks associated with sphene were not intense, suggesting only a low U and Th content.

Allanite: The common occurrence of allanite has also been found in the granites. It usually occurs in large euhedral crystals. Zircons with allanite rims are also common. Most occurrences show some alteration of the mineral, usually accompanied by staining of the surrounding minerals.

Apatite: This is usually found as small crystals associated with biotite. Occurrences are generally limited. The crystals have a fairly high radioactivity.

Monazite: This is only very rarely present in the sections examined, but one occurrence identified is as a large

Table 5.1: Summary of radioactive accessory minerals in Nigerian Younger Granites.

Samp.	No. of Clusters examined	Associated minerals Zirc.	Allan.	Sph.	Apt.	Urano.	Other
R1	4	2	1				
R3	18	14			1	2	
R4	6	3			1		
R5	9	7				1	in biotite
R8	9	6		2	2	2	in biotite
R9	8	4	1			6	
R10	7	3					stains
R11	4	4					
R12	5	4				1	
R13	5	5					
R15	6	5				2	grain boundary
R16	5	4	1				grain boundary
R17	15	13				4	grain boundary
R18	1	1					stains and biot.
R19	3					3	
R20	7	2				3	ilm.
R23	10	8		1	1	1	ilm.
R24	9	8				2	
R25	9	7		2			in biotite
R28	7	6		1			in biotite
R29	4	4					
R30	12	11					biot./ilm.
R31	3	3					
R32	5	4					ilm.
R33	3	2			1	1	ilm.
R34	8	2				6	ilm.
R35	4	1				4	epidote
R36	4	1				1	monazite
R37	4	2		1			epidote
R38	12	12		1			in biotite
R39	11	10				3	
R40	11	9		1			
R41	8	4				2	
R43	4	2					
R44	4	4		1		2	
R45	9	8		3		1	
R46	2	1		1		1	
R48	8	6				3	epidote
R49	6	3				1	ilm.
R55	7	5					in biotite
R60	3	3					
R63	10	6			1	4	grain boundary

All sample numbers are prefixed JP.

crystal which was found to be highly radioactive.

In addition to these minerals, epidote, ilmenite, thorite, uranothorite, and other Rare Earth accessory minerals, were also identified. Clusters of tracks have also been observed occurring in association with some of the rock-forming minerals. Frequently these occur along grain boundaries or along cracks that have secondary infillings. Many clusters have been found to be associated with biotite, but usually in such cases, the tracks are diffuse and the biotite shows some evidence of being oxidised. Of more importance are clusters associated with uranothorite. This mineral occurs in massive patches, dark brown or red brown in colour, fading to bright red brown to orange at the edges. It usually occurs with biotite, often enclosing tiny grains of zircon. The abundance of this phase in the granite is high, it being recorded in all but a few of the sections examined. Also of importance are metamict phases which occur as inclusions in a number of minerals, but usually in biotite. Unfortunately, identification of the original minerals with the petrological microscope has not been possible in these cases, but they might once have been uraninite. From sections from the kaolinised granites, tracks are typically found in association with sericite and other secondary alteration products.

To help identify those phases which could not be recognised by the use of the petrological microscope, specific studies were carried out with a scanning electron microscope connected to an

energy dispersive analyser, in the hope that major element abundances could be used to characterise the minerals.

Representative occurrences of the minerals, with their associated alpha tracks are shown in Figures 5.2 to 5.8. Figure 5.2 shows zircon crystals and quartz (a) zircon along grain boundaries and (b) zircon as inclusions in a crystal of quartz. Most of the zircons identified are associated with high-density alpha tracks, suggesting that they contain appreciable amounts of alpha emitters. This is especially the case with occurrences in association with quartz. Frequently the zircons appear to be altered and are usually covered with a brownish stain. In (a) the trail of tracks along the fracture seems to emanate from the zircon crystal. In (b) the zoning characteristic of most large zircons in the granite, can be seen. As already noted, occasionally the zircons are rimmed with allanite, and these usually produce higher track densities. Such an occurrence is shown in Figure 5.2 (c), while (d) is a zircon covered in some brownish stain as mentioned above. Figure 5.3 (a) and (b) shows grains of zircon in biotite. Although the zircon crystals appear to be rich in alpha emitters, no case of metamictization was observed.

Figure 5.3 (c) and (d) shows sphene crystals in biotite and in quartz. Although the crystals shown here have produced high alpha track densities, usually sphene only records low track densities. Figure 5.4 shows allanite crystals. The fairly high radioelement content of the allanites in the granite can be seen

FIGURE 5.2 Alpha autoradiograph of granite showing:-

a) zircon along grain boundary in quartz (X50),

b) zircon inclusion in quartz (X50),

c) zircon rimmed with allanite (X100),

d) zircon covered in brown stain (X50),

in the Nigerian Younger Granites.

Exposure period: three weeks

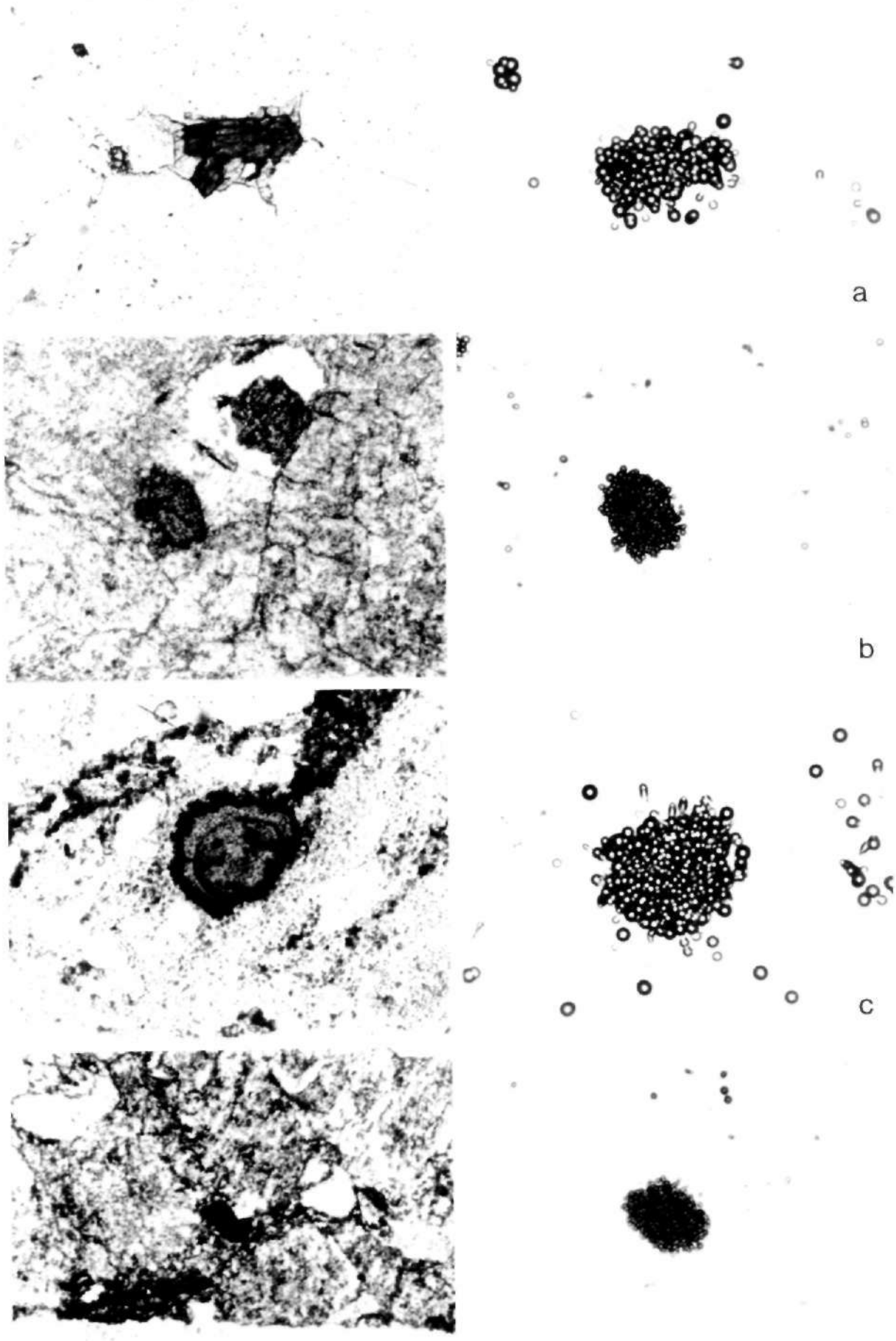

a
b
c
d

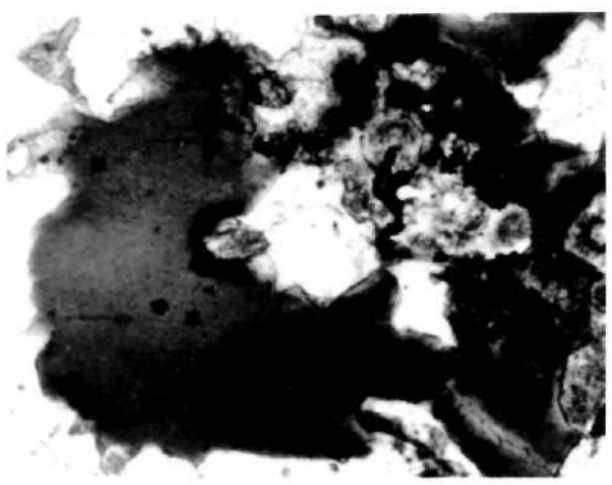
FIGURE 5.3 Alpha autoradiograph of granite showing:-

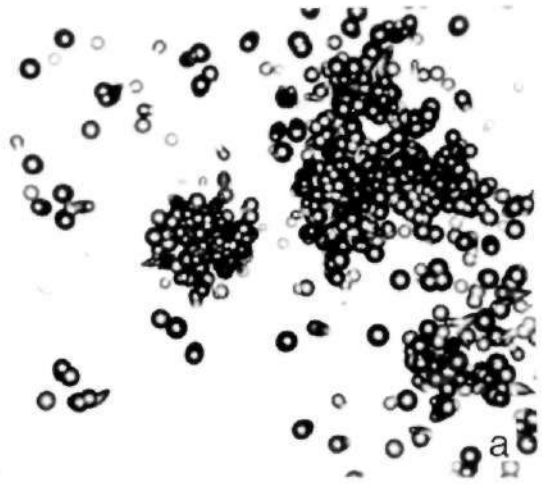
a) and (b) zircon in biotite (X50),

c) and (d) Sphene in biotite (X50),

in Nigerian Younger Granites.

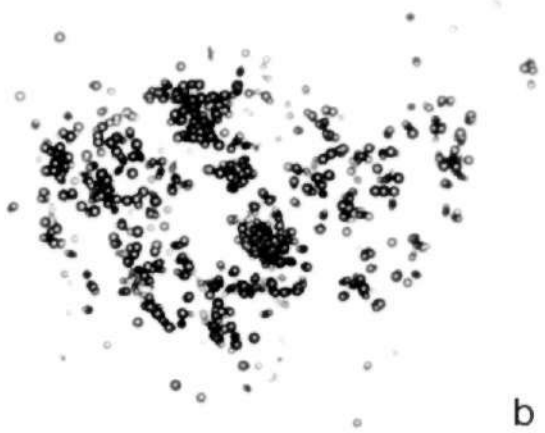
Exposure period: three weeks



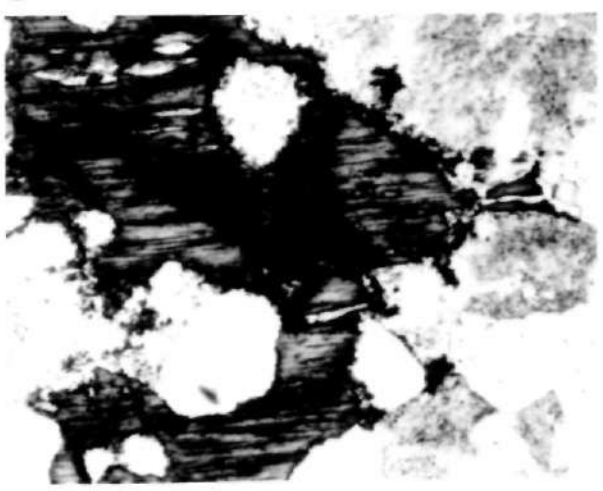


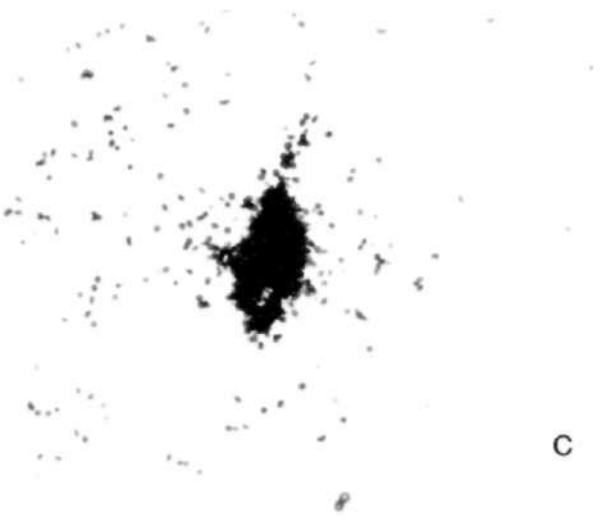
a





b





c

FIGURE 5.4 Alpha autoradiograph of granite showing allanite:-

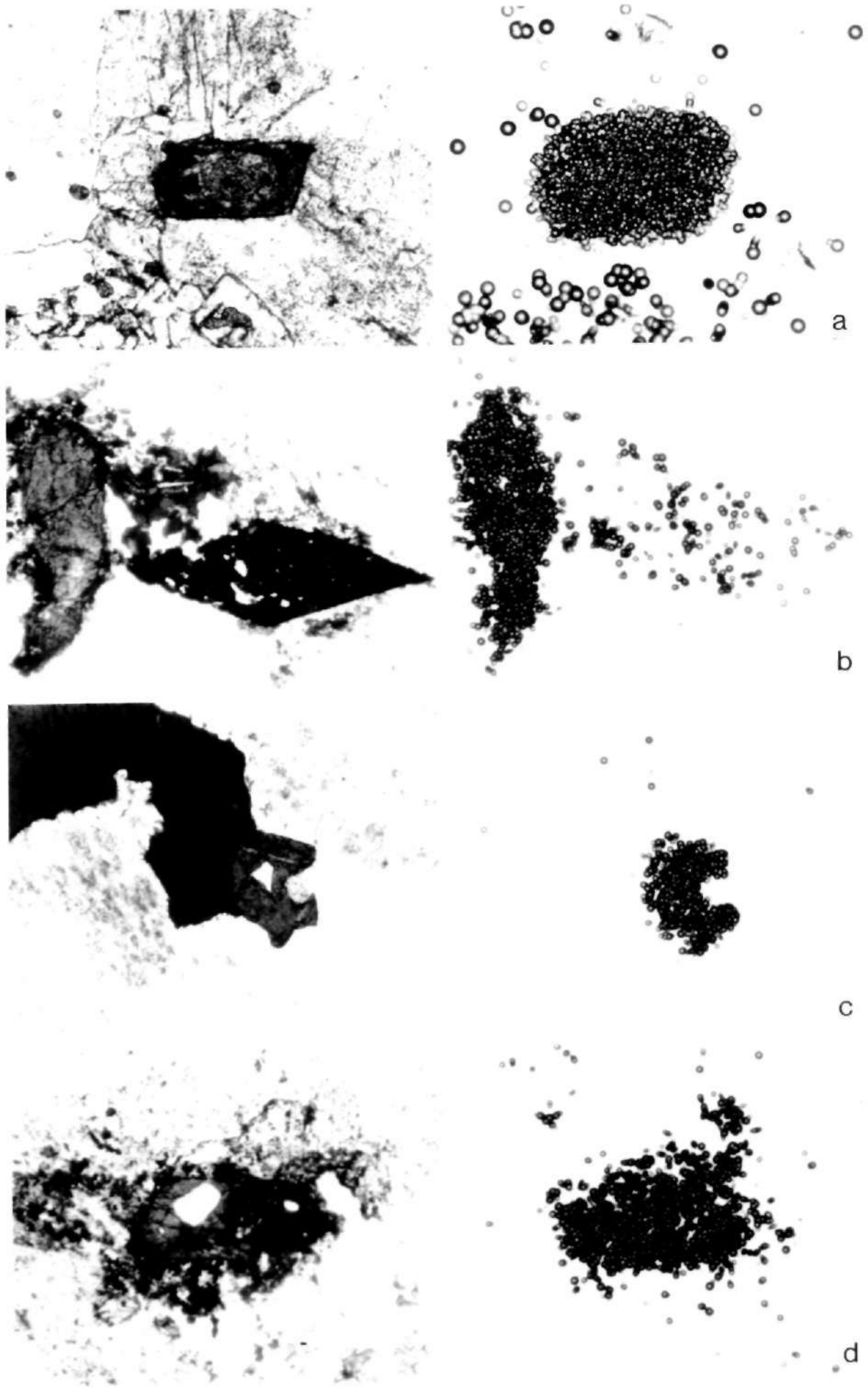
a) diffuse radiation caused by solution of allanite (X100),

b) the diamond-shaped black mineral is sphene demonstrating the high alpha activity of allanite compared to sphene (X50),

c) and (d) typical cystal size and alpha activity allanite (X50),

in the Nigerian Younger Granites.

Exposure period: three weeks


a
b
c
d

from the high density of alpha tracks in this presentation. In (a), the diffuse tracks around the main cluster is caused by a brown stain apparently originating from the allanite crystal. In (b), the higher radioactivity associated with allanite relative to sphene is demonstrated. The diamond-shaped black structure is a fairly large sphene crystal associated with what appears to be ilmenite. Figures 5.4 (c) and (d) show a fairly large allanite crystal associated with hornblende, and an allanite crystal with inclusions of small grains of zircon, respectively. Figures 5.5 (a) and (b) shows apatite crystals, and the high density alpha tracks associated with apatite in the granite.

In Figure 5.5 (c) is shown a large monazite crustal in microcline perthite. The fairly high density of alpha tracks associated with the monazite is also seen in this section. Figures 5.5 (d) and Figure 5.6 (a) show the occurrence of alpha tracks associated with biotite in the granite. Such occurrences are abundant, and usually associated with oxidised alteration of the biotite. In Figure 5.6 (b) is shown alpha tracks associated with epidote. In Figures 5.6 (c) and (d) are tracks associated with ilmenite, demonstrating the fairly high density of tracks in clusters in most of such occurrences.

Figure 5.7 (a) shows a small crystal of rutile surrounded by a pleochroic halo. Figure 5.7 (b) shows a thorite crystal with its associated alpha tracks while Figure 5.7 (c) illustrates a uranothorite with its associated alpha tracks. This uranothorite

FIGURE 5.5 Alpha autoradiograph of granite showing:-

a) and (b) apatite cystals with typical high alpha activity (X200),

c) is large monazite crystal (X50),

d) alpha actvity associated with biotite (X50),

in the Nigerian Younger Granites.

Exposure period: three weeks

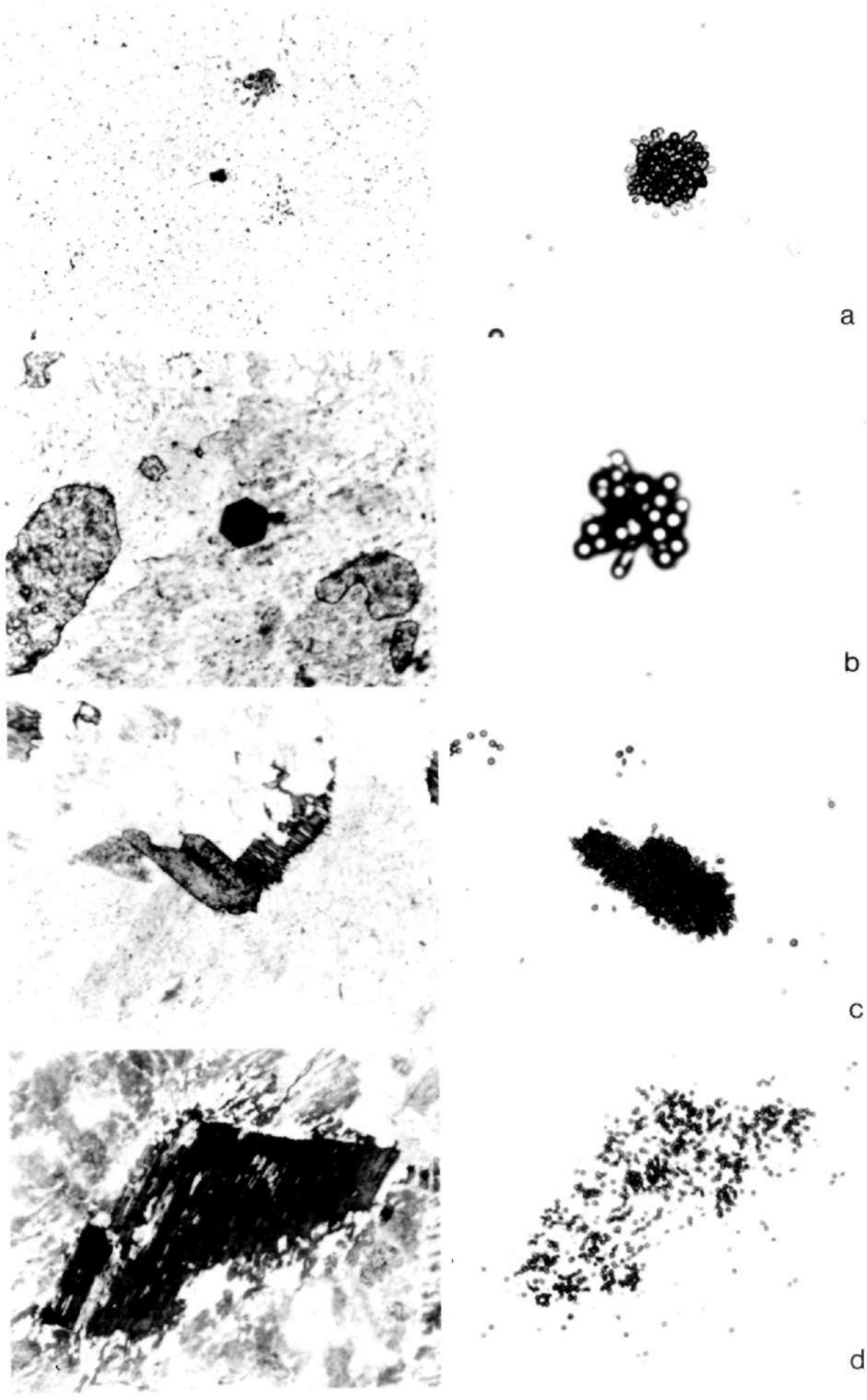

a
b
c
d

FIGURE 5.6 Alpha autoradiograph of granite showing alpha activity associated with some alteration products,

a) oxidised biotite (X35),

b) epidote (X50),

c) and (d) alpha-emitters in ilmenite (X50),

in the Nigerian Younger Granites.

Exposure period: three weeks

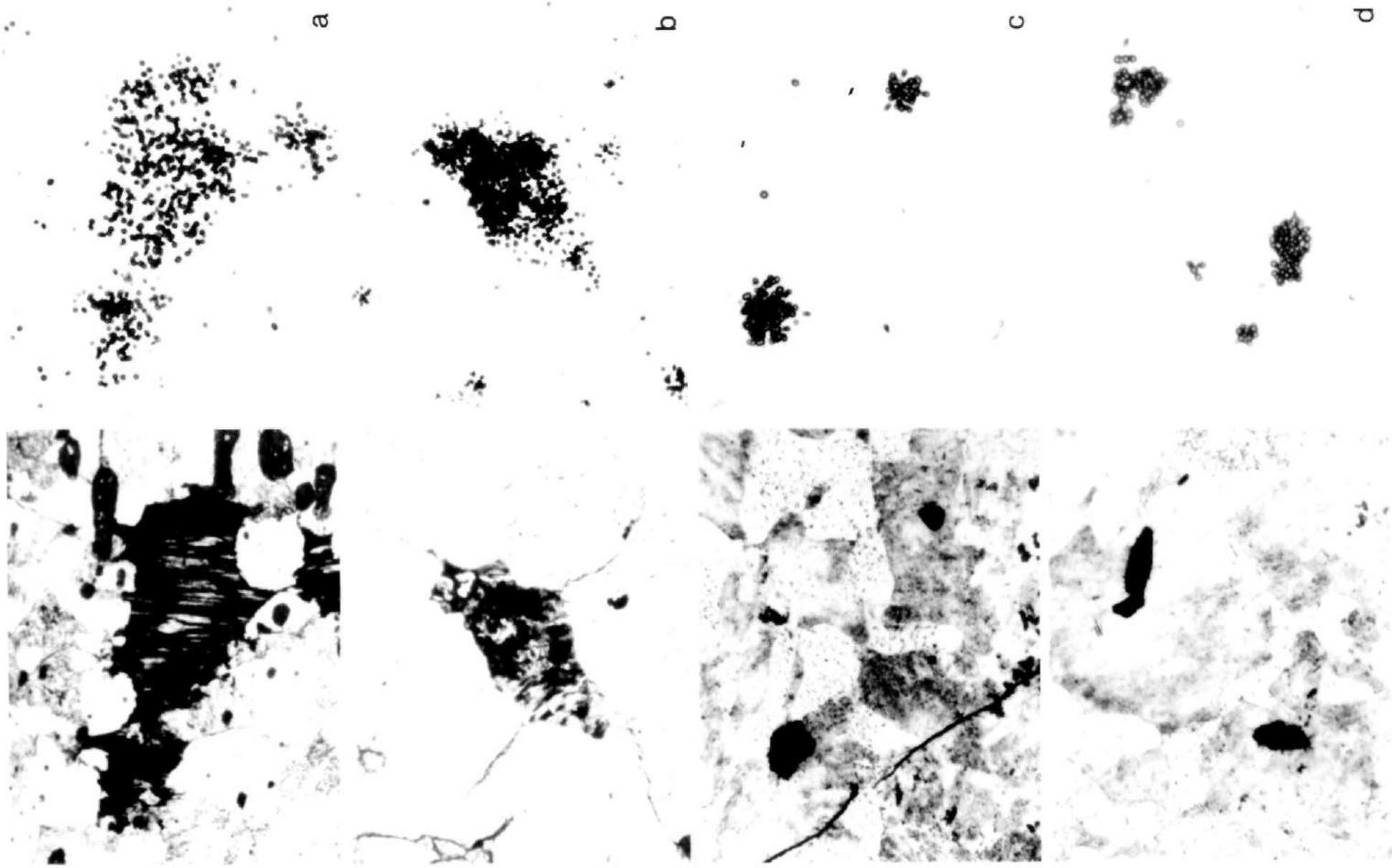

a
b
c
d

FIGURE 5.7 Alpha autoradiograph of granite showing:-

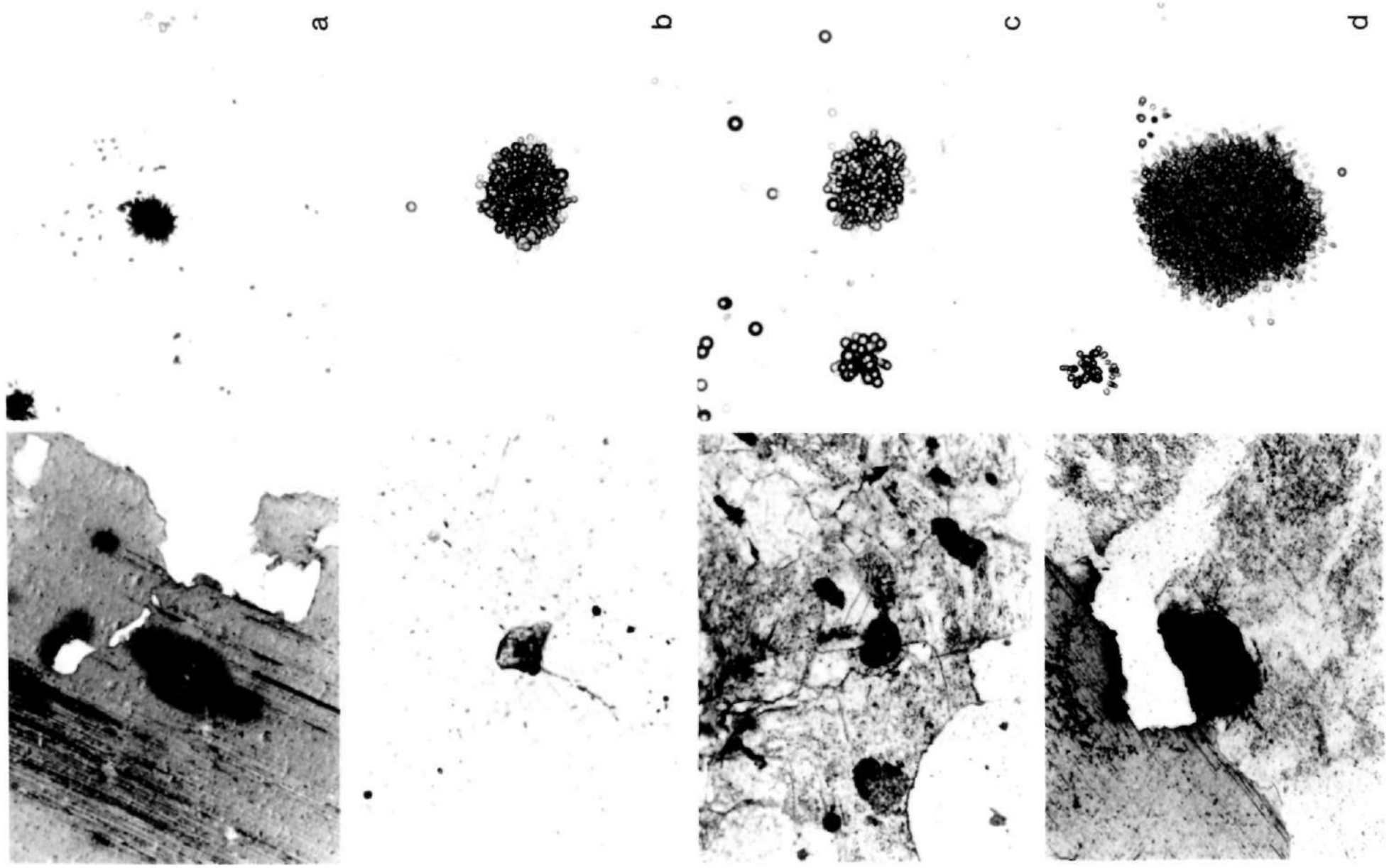
a) a crystal of rutile with its associated alpha tracks (X100),

b) a tiny thorite crystal (X200),

c) and (d) uranothorite (X100),

in the Nigerian Younger Granites.

Exposure period: three weeks


a
b
c
d

KASDI MERBAH UNIVERSITY
ARCHIVE - SCIENCE LIBRARY
ZARIA, ALGERIA.

occurs as a dark brown, bean-shaped mass in quartz. Major element peaks in the mineral are shown in Figure 5.8. A representative mineral of other dark brown masses which can thus be identified as uranothorite, are shown in Figure 5.7 (d) with its associated alpha tracks. In Figure 5.9 (a) and (b) are shown some of the Rare Earth minerals with their alpha track registrations. The mineral in Figure 5.9 (a) contains Ce and La as the abundant elements with some F, Si, Th and Sn (in decreasing order). It causes a pleochroic halo where it occurs. It is possibly fluocerite (composition in Figure 5.10). The mineral in Figure 5.9 (b) contains Y as an essential element, with Ca and some Si, Th and U (composition in Figure 5.11). In Figures 5.9 (c) and (d) are shown metamict phases (c) in biotite and (d) associated with biotite. Microprobe investigation of a section in (d) revealed U and Th as the main elements, with appreciable amounts of Si, Fe, Ti and Ce.

The foregoing account indicates the importance of the accessory minerals zircon, allanite and sphene in hosting a substantial amount of the U and Th in the granite. However, in order not to overemphasise the importance of these minerals, or underestimate the importance of other known U-hosting minerals, (especially in the light of the abundant occurrence of highly radioactive phases which have not been identified), it is important to assess the contribution of these minerals to the whole-rock U content of the granite. It must also be realised that in accessory minerals, such as the ones identified here, the occurrence of both

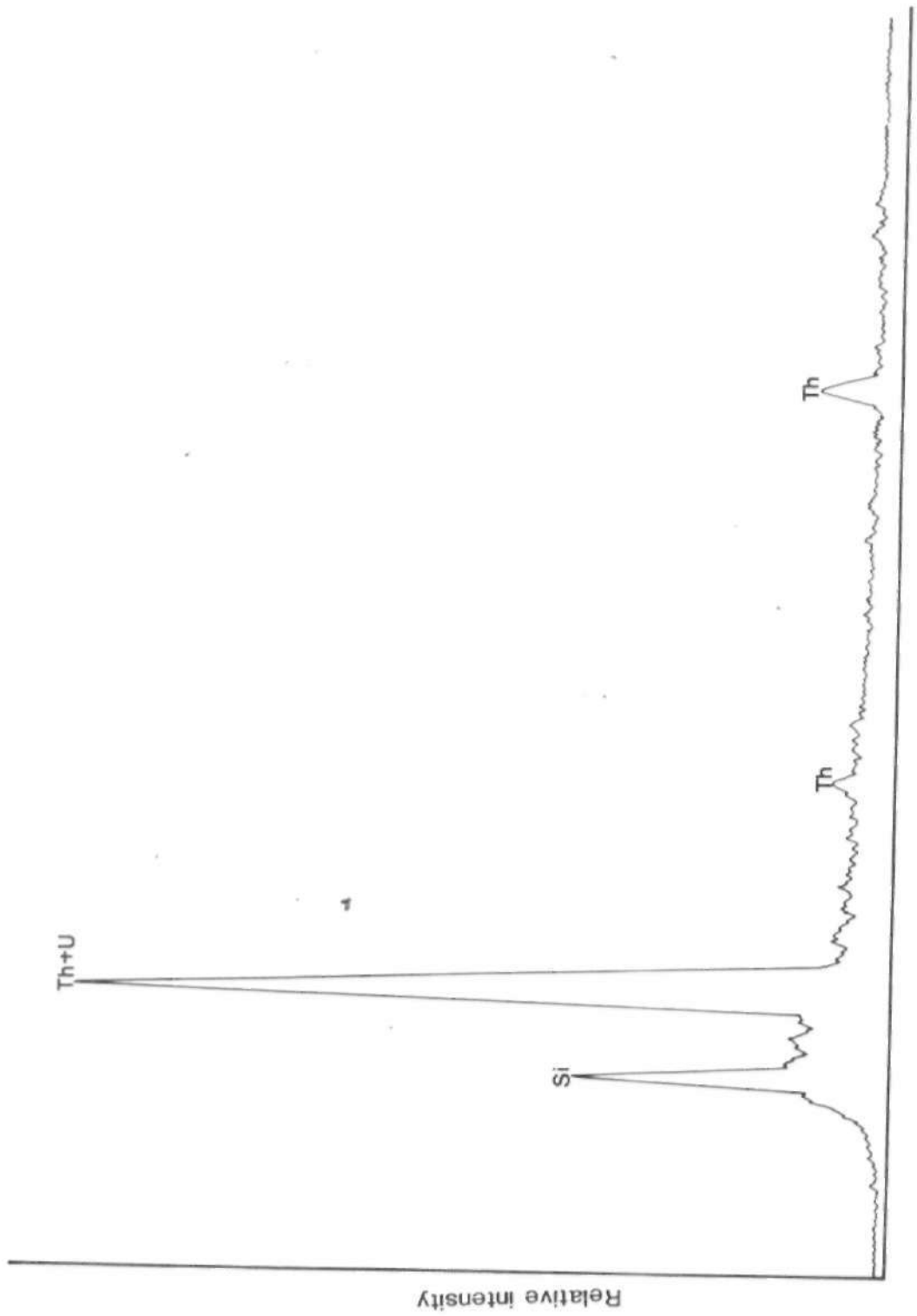


Figure 5.8 X-ray emission spectrum of a radioactive mineral (uranothorite, see text).

FIGURE 5.9 Alpha autoradigraphs of granite showing some Rare Earth minerals and highly radioactive phases

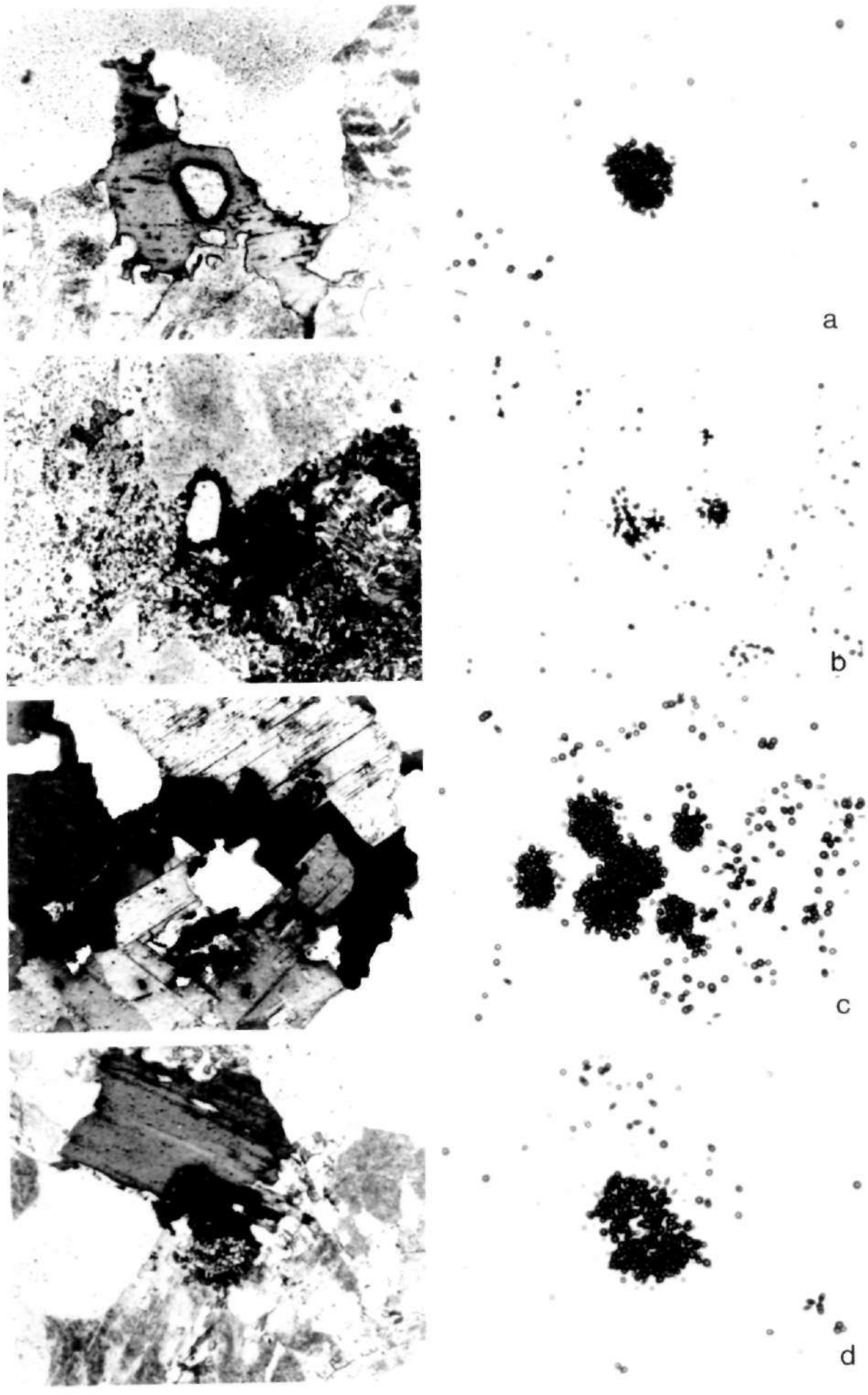
a) ? fluocerite (see Figure 5.10) (X100),

b) a Rare Earth mineral mainly composed of Y (Figure 5.11) (X50),

c) and (d) are metamict phases, former sites of highly radioactive minerals (X50),

in the Nigerian Younger Granites.

Exposure period: three weeks


a
b
c
d

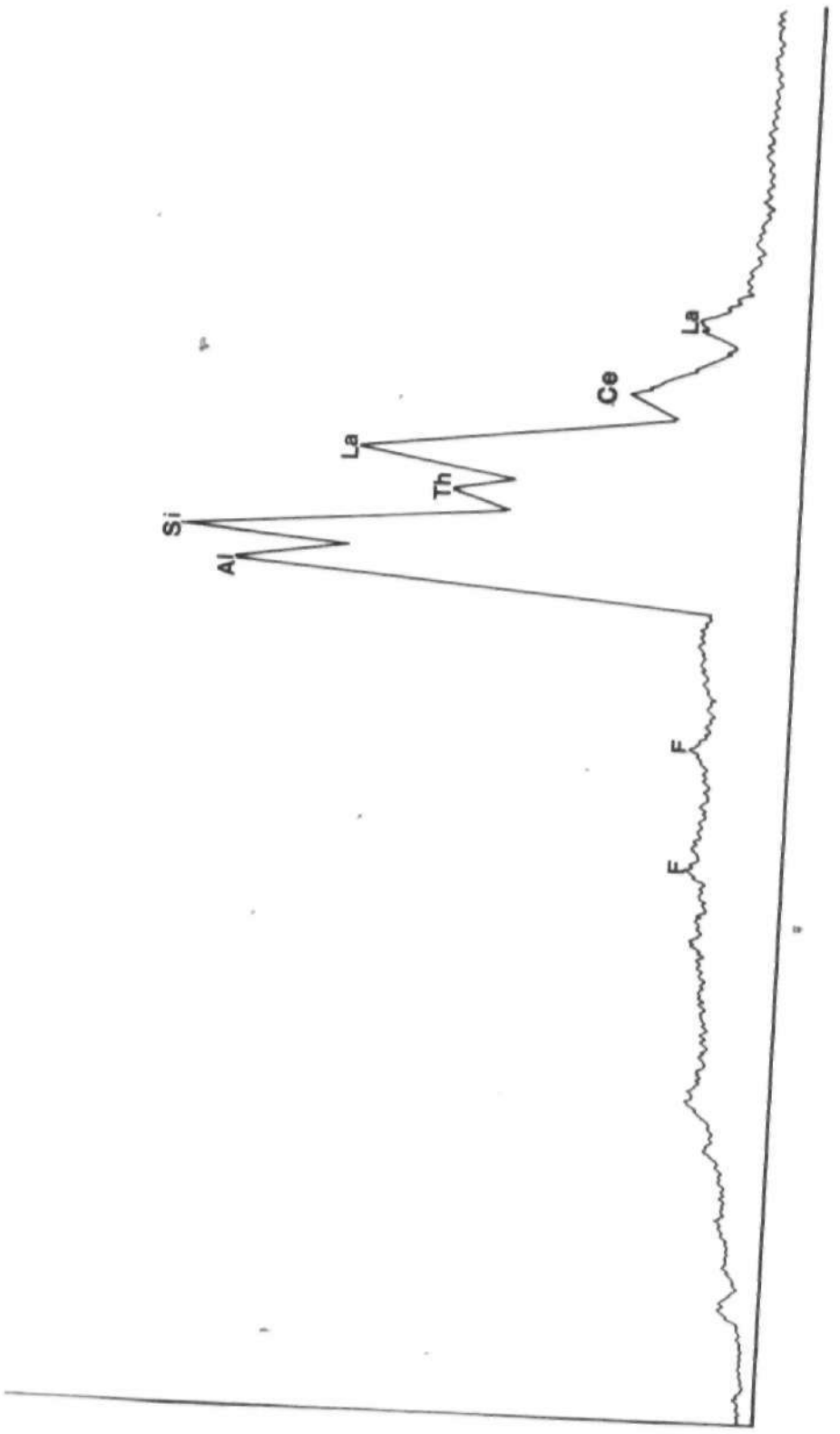


Figure 5.10 X-ray emission spectrum of a Rare Earth mineral
(? fluocerite, see text).

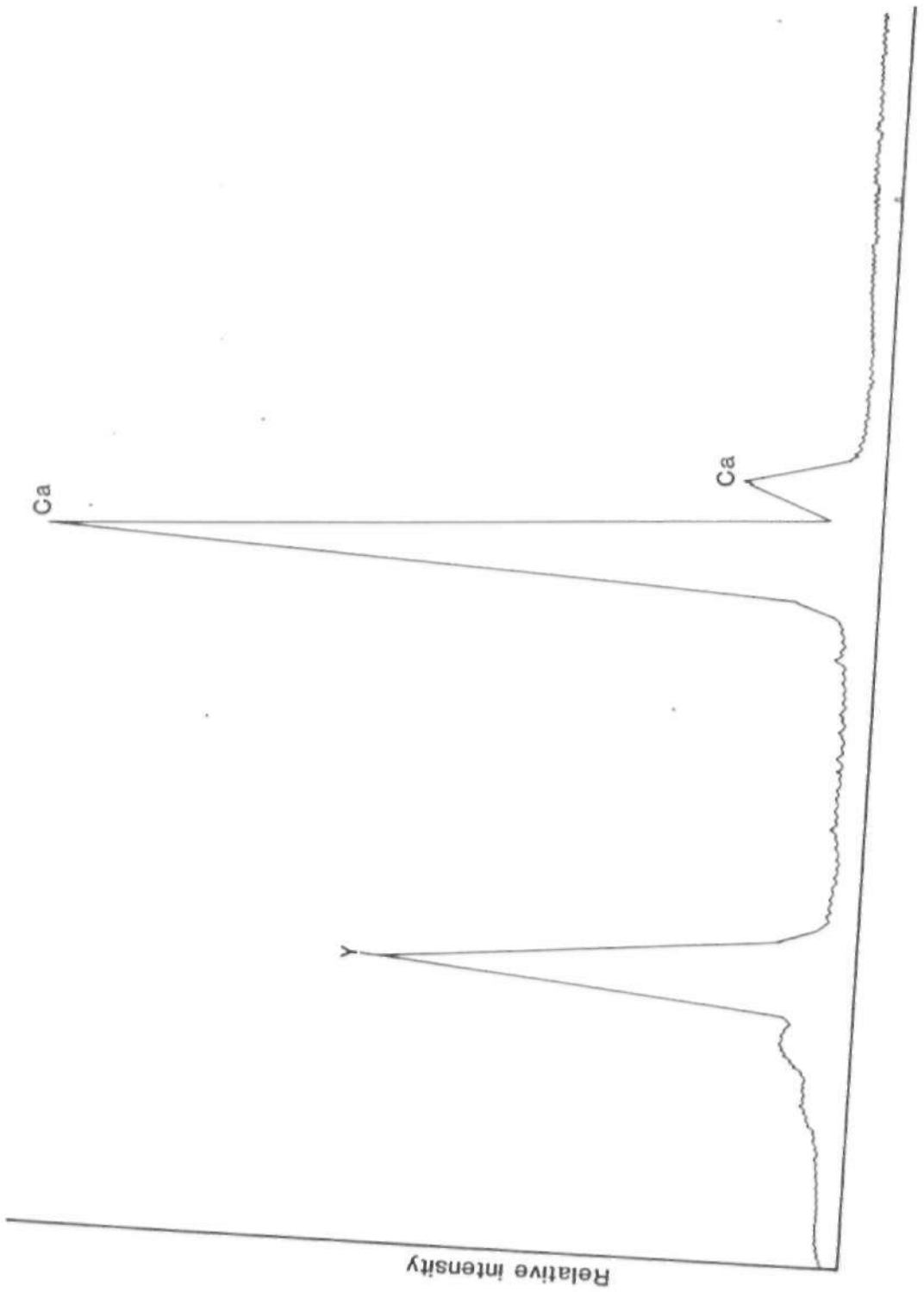


Figure 5.11 X-ray emission spectrum of a Rare Earth mineral

U and Th is highly controlled by diadochic substitutions. These substitutions favour Th replacing REE (Sahama and Rankama, 1949; Henderson, 1984). The similar ionic size of Th with the REE makes it possible to be present in lanthanide minerals. These substitutions are controlled by factors such as the amount of the Th and/or U in the system during crystallization of the minerals, and the mineral's structure in relation to the ionic size and charge. Because of these factors, the amount of U and Th a mineral can contain is necessarily restricted, as shown by the many chemical analyses of these minerals. Common accessory minerals, and their approximate chemical formulae, showing the possible sites of U and/or Th substitution, are given in Table 5.2

The amount of U and Th in accessory minerals has been extensively studied in recent years. Hurley and Fairbairn (1957) reported the distribution of U and Th in zircon, sphene, apatite, and monazite in granitic rocks, and showed wide variations are possible in the range to which they are concentrated in these minerals. U and Th concentrations in the common accessory minerals are shown in Table 5.3. Basham et al. (1982a; 1982c) have shown that quantitative estimates of U and Th in the accessory minerals can be obtained from mass-balance relations, and these estimates can prove useful in constraining the concentration of U in the minerals in relation to the whole-rock U content. These authors determined the amount of the U and Th contributions of various minerals to the whole-rock abundances in a granitic suite using

Table 5.2: Common radioactive accessory minerals in granite.

Mineral	Chemical formula
Zircon	$ZrSiO_4$
Sphene	$CaTiSiO_5$
Epidote	$Ca_2(Al,Fe)_3(OH)(SiO_4)_3$
Allanite	$(Ca,Fe^{2+})_2(Al,Ce,Fe^{3+})_3(OH)(SiO_4)_3$
Monazite	$(Ce,LA,Nd,Pr)PO_4$
Appatite	$3Ca_3(PO_4)_2CaF_2$
Xenotime	YPO_4

Table 5.3: U and Th content of some common radioactive accessory minerals in granite.

Mineral	U(ppm or %)	Th(ppm or %)
Allanite	30-3000	1-3%
Zircon	100-3000	75-2100
Sphene	10-1400 (generally <500)	20-3150(generally<500)
Epidote	<200	65-600
Appatite	10-250	5-400
Monazite	500-5000	2.6-7.5%
Xenotime	300-4000(generally in lower range)	2-3%
Rutile	<100	
Thorite	1%	48-71%
Uraninite	80%	
uranothorite	1-10%	

U values from Basham et al. (1982a)

Th values from Hurley and Fairbairn (1957).

chemical analyses of other trace elements. In this study, zircon in the granite was determined by mineral separation. The amount of zircon in these samples, together with their REE, U, Th, Y and P_2O_5 concentrations, are given in Table 5.4. Before making estimates of the U and Th contributions of the accessory minerals, it is worthwhile to consider their association with the common elements which are present in these minerals. In Figures 5.12 to 5.15 are plots of U and Th against Zr, Ce, La and Y. These plots show a negative correlation between both U and Th, and Zr, Ce and La, and a positive correlation with Y. In particular, the negative correlation with Zr may indicate that the concentrations of these elements are not attributable to zircon. Similarly, their relationship with Ce (which may be assigned to monazite and allanite) and La, seem to suggest that the contributions of these minerals to the whole-rock U and Th abundances also may not be very significant. In view of the paucity of monazite in the granites, most of the REE could be concentrated in allanite and zircon, and possibly other Rare Earth minerals. The high positive correlation of U and Y may indicate the importance of multiple oxides of the REE, and possibly also xenotime (even though it has not been recorded).

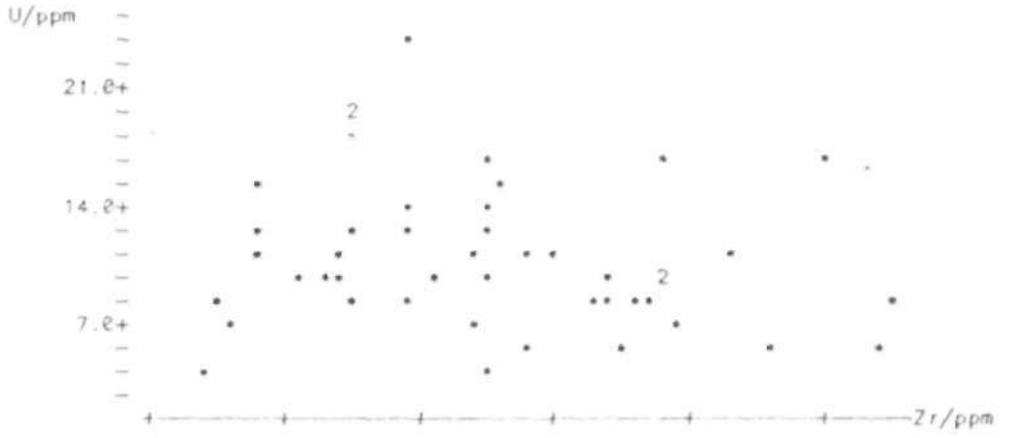
Estimates of the contributions of the accessory minerals to the whole-rock U content of the granites are shown in Table 5.5. Although such mass balance calculations are limited, values obtained can be used to constrain the amount of U attributable to

Table 5.4: Zircon and some selected elements analyses in Nigerian Younger Granite.

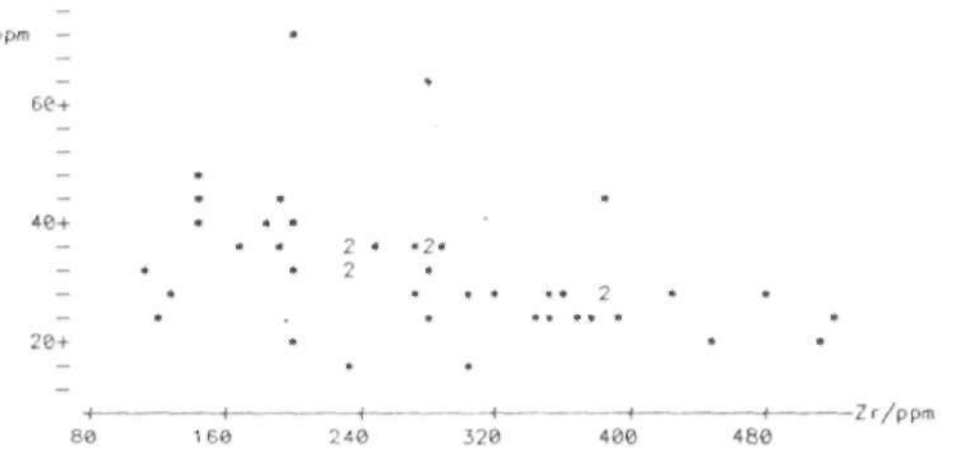
Samp.	Zir.	U	Th	Ce	La	P_2O_5	Y
R3	1.64	11.51	38.62	174.95	132.16	-	133.05
R16	2.68	16.33	62.88	218.05	146.67	0.01	197.17
R17	0.93	20.21	73.50	130.66	87.56	0.02	110.90
R30	0.78	14.54	34.44	308.06	106.51	-	152.84
R42	6.16	17.23	29.54	170.43	110.43	-	143.37
R45	0.35	13.87	31.30	180.65	193.60	-	184.42

Note: Zircon in g (1g of zircon in 104g of sample)

: U, Th, Ce, La and Y in pmm, and P_2O_5 in %.



(a)



(b)

FIGURE 5.12 Plot of U (a) and Th (b) against Zr

Note: In this and subsequent plots, numbers in the plot represent number of points having the same coordinates

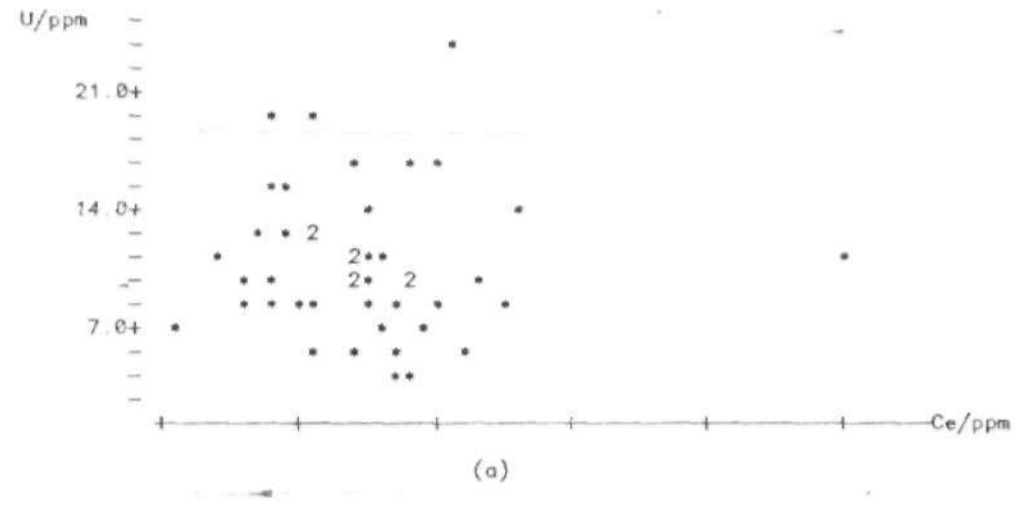


FIGURE 5.13 Plot of U (a) and Th (b) against Ce

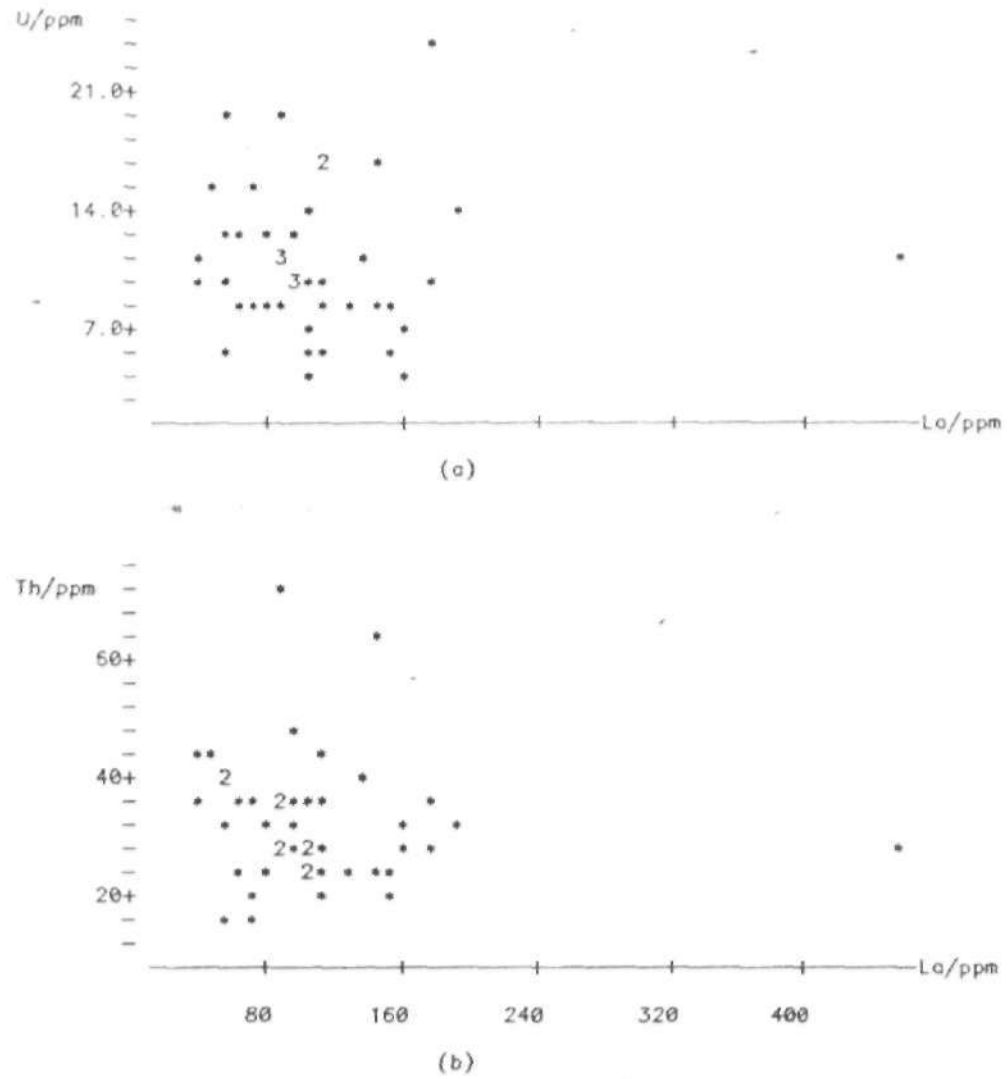


FIGURE 5.14 Plot of U (a) and Th (b) against La

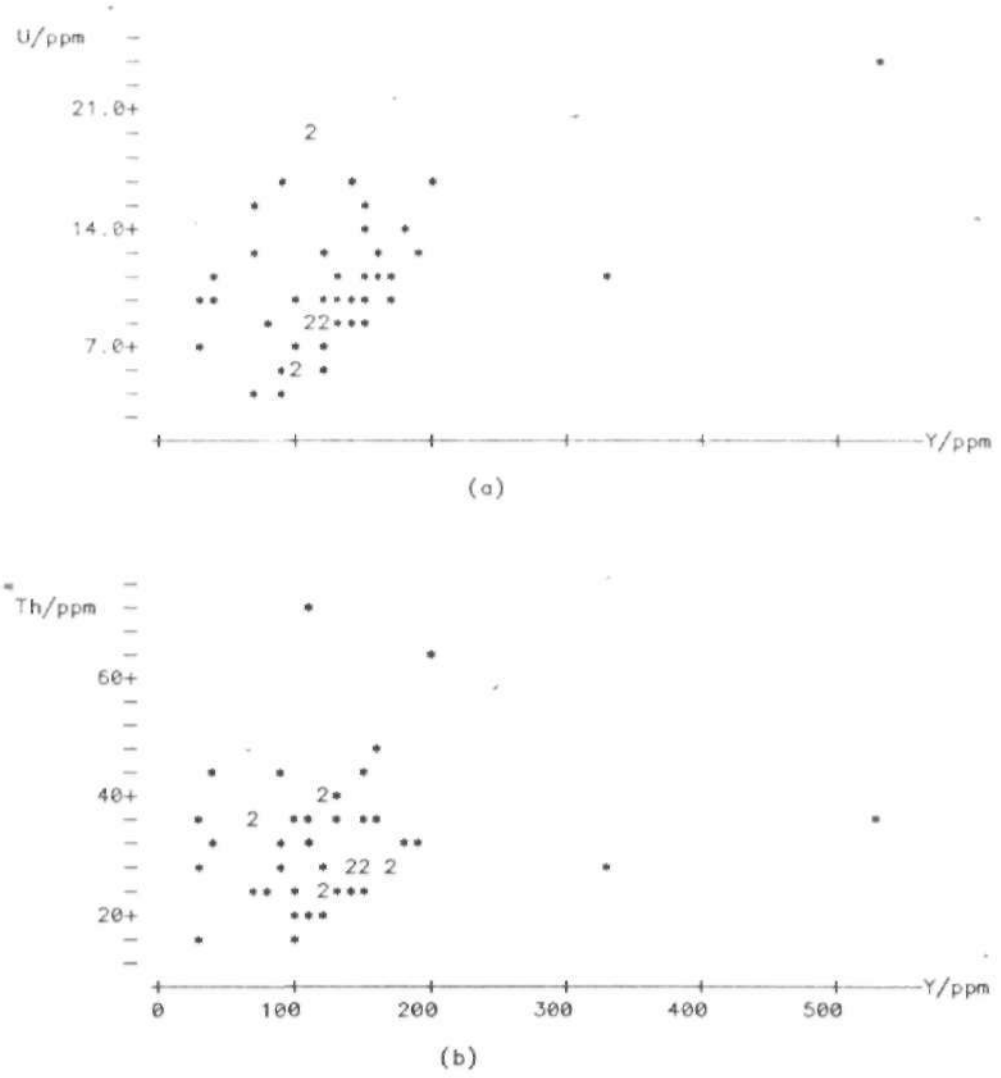


FIGURE 5.15 Plot of U (a) and Th (b) against Y

Table 5.5: Accessory mineral contributions to whole-rock U in Nigerian Younger Granites.

Sample	Amount of mineral in wt%[1]				
	Zircon	Allanite	Apatite	Monazite	Uranothorite
JPR3	0.016	0.029	-	0.51	$3.63.10^{-3}$
JPR16	0.027	0.035	0.012	0.061	$5.90.10^{-3}$
JPR17	0.009	0.021	0.023	0.036	$6.90.10^{-3}$
JpR30	0.008	0.039	-	0.069	$3.23.10^{-3}$
JPR42	0.062	0.027	-	0.047	$2.77.10^{-3}$
JpR43	0.004	0.036	-	0.073	$2.94.10^{-3}$

Sample	Attributable U in ppm[2]								
	Zirc.	All.	Ap.	Mon.	Tot.	Tot(%)	Uranoth.	Tot.	Tot(%)
JPR3	0.16	0.19	-	1.53	1.88	16	3.63	5.51	48
JPR16	0.27	0.23	0.03	1.83	2.36	15	5.90	8.26	51
JPR17	0.09	0.14	0.06	1.08	1.37	7	6.90	8.27	41
JPR30	0.08	0.25	-	2.07	2.40	17	3.23	5.63	39
JPR42	0.62	0.18	-	1.41	2.21	13	2.77	4.98	29
JPR43	0.04	0.23	-	1.87	2.14	15	2.94	5.07	37
Ave.	0.21	0.20	0.04	1.63	2.06	14	4.23	6.29	41

Notes:

1: Except for zircon normative mineral amount calculated from chemical analyses as follows:-

a) 74% P_2O_5 assigned to apatite

b) 95% RE_2O_3 assigned to monazite and alanite in the ratio 86% 14% respectively.

c) 94.5% Th assigned to uranothorite (5.5% being assigned to monazite zircon and allanite).

2: Amount of U calculated based on:- monazite 3000ppm U
Ziron 1000ppm U
Apatite 25ppm U
Uranothorite 10% U

the different minerals in the granites. Despite the fact that the calculations are on the high side, for example only one monazite crystal was recorded in the samples examined, the results clearly show the relatively small overall contributions from these minerals. Monazite, zircon, allanite and apatite together contribute only about 1.5 to 2.5ppm U, amounting to about 1% to 15% of the whole-rock value. High percentages by even small amounts of U-rich minerals is demonstrated by the contribution due to uranothorite in the granites. However, even taken together with the accessory minerals, they still contribute only about 40% to 50% of the whole-rock U. Thus a fairly large amount of U still remains to be accounted for. The low radioactivity of sphene in the granites has already been mentioned, so sphene is not the answer. Indeed, Staatz et al. (1977) have found that the amount of REE and Th (and U) partitioned into sphene during crystallization is generally low in granites with abundant allanite and zircon. Other minerals that may make some contribution to the U abundance are secondary alteration minerals such as epidote (even though only one occurrence was recorded), and the materials associated with Fe oxides. Even so, the contribution of these sources is not likely to amount to anything in excess of 10%. Therefore, the remainder of about 50% of the U must be the occurrences within major minerals

and along grain boundaries plus unidentified highly radioactive phases which have been observed. These, more especially the metamict phases and the grain boundary coatings, may be the sites of primary U minerals such as uraninite. Basham et al. (1982a) have shown the importance of uraninite in accounting for most of the U in such granites and the difficulties involved in determining its full occurrence even in granites where it has been identified. Although modally uraninite occurs less frequently than either zircon or monazite, it can account for several times their combined contribution of U. Indeed uraninite is now generally believed to host most of the U in U-rich granites with enhanced levels of radioelements. Basham and his coworkers observed that about one uraninite grain may occur in about 5 - 10 average thin sections of such granites.

From the kaolinised granites, most of the alpha track clusters occur in association with the resistate accessory mineral zircon, and secondary alteration products like sericite, Fe-stained patches, and the surfaces of clay minerals. Generally the zircons are small, usually not exceeding 30μm across. Figure 5.16 (a) shows a grain of zircon in biotite with its associated alpha tracks. Figure 5.16 (b) shows alpha tracks associated with sericite and (c) Fe-staining. Figure 5.16 (d) shows alpha emitters adsorbed on clay minerals, in this case kaolinite. The generally smaller alpha track diameters in this section contrast with those recorded from the Jos

FIGURE 5.16 Alpha autoradiograph of kaolinised granite showing:-

a) Zircon in biotite (X50),

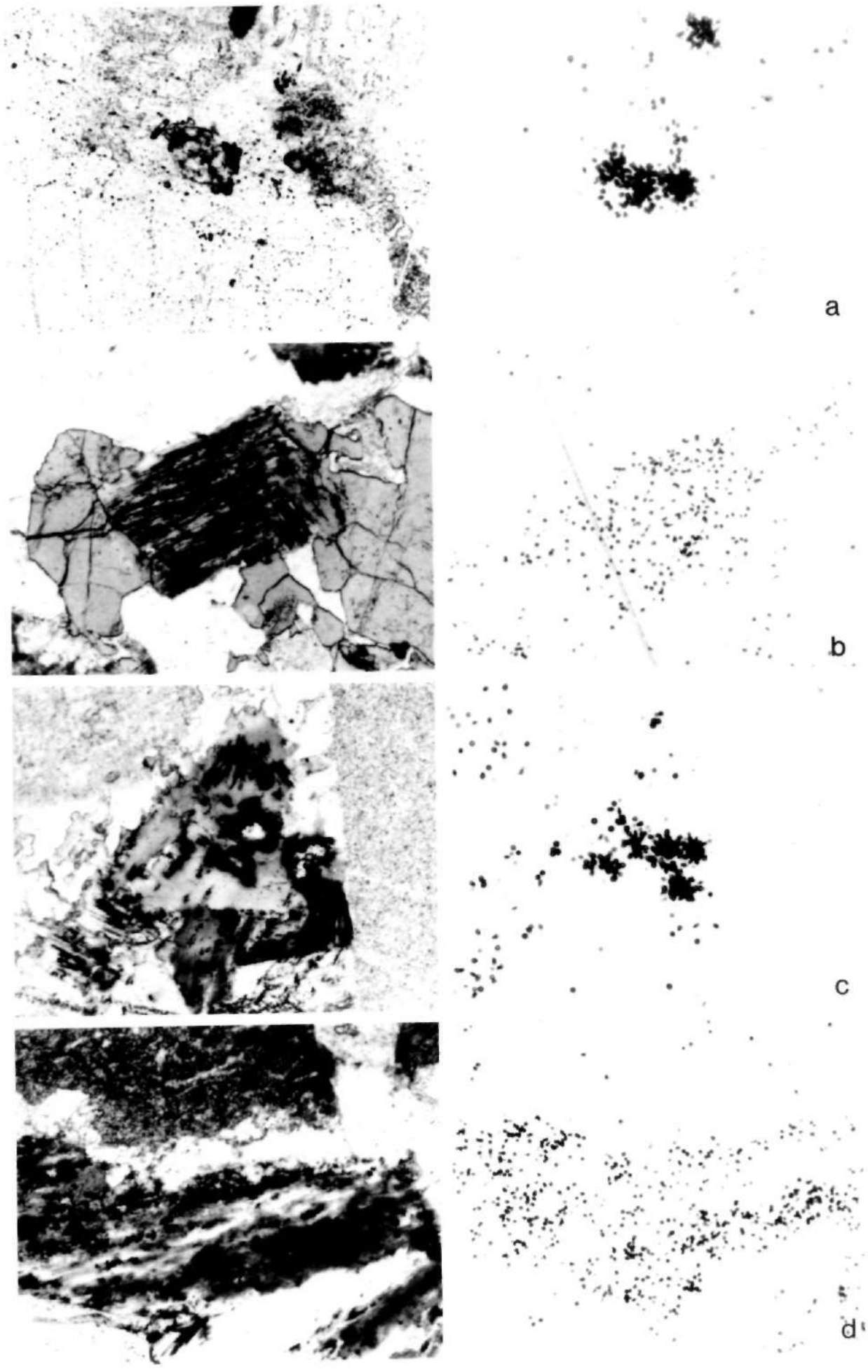
b) radioactivity associated with sericite (X35),

c) Fe-stained phases (X100),

d) alpha-emitters adsorbed onto clay (X35),

in granites of South-West England.

Exposure period: six weeks


a
b
c
d

Plateau samples. This suggests a lower energy for the alpha particles in the kaolinised granites and thus their origin high in the U decay series. Also, these track registrations were obtained over a longer period (6 weeks) than those from the Jos Plateau. Although, it may appear that the Jos Plateau granites are more radioactive than the kaolinised granites, chemical analyses (Chapters 4 and 8) indicate that, on the average, they contain the same amount of U. The implication is that the kaolinised granites have lost most of the alpha-emitters in the lower part of U decay series. The significance of this in terms of the 1Ma period needed for the U decay series to approach equilibrium is discussed in Chapter 7.

5.9 Conclusions

Alpha autoradiographic investigations using plastic nuclear track detectors show the efficiency of the technique in locating U and Th sites in geological minerals. In the study presented in this Chapter, 44 granite samples from the Jos - Bukuru Younger Granite complex and 14 kaolinised granite samples from Bodmin Moor were examined. Exposure periods of 3 weeks for the Nigerian Younger Granite samples and 6 weeks, for the Bodmin more kaolinised granite samples were employed in the investigations, and found sufficient to produce sufficient alpha tracks to be used for the identification of the location of the alpha emitters in the

samples. The technique proved to be a simple and inexpensive method of obtaining excellent images of alpha-particle activity.

The investigations indicated the importance of the accessory minerals zircon, allanite and sphene in hosting sources of alpha activity in the Nigerian Younger Granites. In particular zircon, sphene, and allanite have been found in large amounts in the granites. Allanite and zircon appear to contain substantial amounts of U and Th, as shown by the high density of alpha track clusters associated with their occurrences. Sphene, although occurring in abundance, is comparatively much less radioactive. Other accessory minerals such as apatite, rutile, monazite, thorite and minerals of the REE were also found, but are very minor components of the samples examined. Monazite, rutile and thorite give rise to high density clusters of alpha tracks, suggesting that they contain appreciable amounts of alpha emitters. In addition to these, major constributors to the alpha activity in the rocks are associated with uranothorite and some highly radioactive metamict phases.

Mass balance calculations indicate that the accessory minerals zircon, apatite, monazite and allanite contribute only about 10% to 15% of the whole-rock U budget, while uranothorite may account for up to twice that amount. An average of about 50% to 60% of the U in the granite is, therefore, unaccounted. This, in addition to the occurrence of the minute, highly radioactive phases, suggests the presence of uraninite and/or other U-rich minerals in the granite. As most of the samples were collected

close to the ground surface, and had suffered the effects of weathering, other examples of such minerals could have been destroyed and the U remobilised. The absence of monazite, a relatively stable mineral during weathering which has been recorded as an important accessory of these granites, seems to support this idea. Evidence of labile U in the granite is also shown by intense alpha activity associated with Fe-stained phases along cracks and fractures. Diffuse concentrations of alpha tracks unrelated to any radioactive mineral may also be caused by U released during weathering processes and adsorbed onto other minerals. This may account for a significant amount of the U in the surface samples.

In the kaolinised granites, most of the alpha activity is found to be associated with zircon, secondary alteration products such as sericite, and adsorbed onto clay minerals. Although zircon was found to be the source for most of the clusters in these samples, a major contribution to the alpha activity appears to be adsorbed alpha emitters, and this may even account for most of the U in the granites. These locations can usually be identified by clusters of alpha tracks associated with opaque Fe oxide coatings or diffuse tracks associated with kaolinite and oxidised biotite. The absence of other accessory minerals, such as monazite and apatite, suggests that they could have been removed during kaolinisation.

KASHIM IBRAHIM LIBRARY
ZARIA, NIGERIA.

CHAPTER SIX: GAMMA-RAY SPECTROMETRY OF GRANITE AND GRANITE-RELATED MATERIALS

6.1 Introduction

Four-channel gamma-ray spectrometry is a widely used method that has seen many applications in natural environmental studies. Despite having a number of limitations, the method has been one of the main techniques used in U exploration programmes. It is also extensively used in the broader study of all radioactive minerals. In U exploration, the method forms the major component of many reconnaissance surveys and, to date, it has been responsible for the discovery of most of the major U deposits in the world. The main advantages of the method are that it is cheap and fast, so that a large area can be covered in a relatively short time, and the simplicity of data reduction. Gamma-ray spectrometry depends on one of the physical properties of most radionuclides, namely the emission of gamma-rays, when they decay. The principles of the method have been fully described by Adams and Gasparini (1970), and Durrance (1986). An account of it's different applications has been given by Bowie (1972). Field gamma-ray spectrometric surveys can be carried out on foot, by car or aeroplane. Most reconnaissance surveys are carried out using aeroplanes, where a large amount of data can be obtained in a relatively short time. The use of aircraft for radioactive surveys

has been discussed by Darnley et al. (1969), Darnley (1970), and Darnley (1972).

The main drawback of the method in U exploration is the fact that determinations of radioelement concentrations, more especially U, are not reliable because of disequilibrium in the U decay series. To a lesser extent this also applies to the Th decay series. Without a more complete record of the gamma-ray energy spectrum than that given by a four-channel spectrometer, disequilibrium can not be recognised. However, various prospecting techniques using these methods have been described by Miller and Loosemore (1972) and, where justified by reconnaissance surveys, detailed follow-up studies have yielded U concentrations. Dodd and Eschleman (1972) have discussed also the use of gamma-ray bore-hole logging in U exploration, and Ostrihansky (1976) has reported using gamma-ray spectrometry in U series disequilibrium investigations.

In this study, the use of four-channel gamma-ray spectrometry has been assessed for the exploration of U in granites, more especially to typify areas affected by kaolinisation and lateritization alteration processes. Both field and laboratory techniques were adopted for this study. The work also aimed at determining the relationship between radioactive equilibrium in the U and Th decay series, and the recorded gamma-ray activity.

To date, the use of the method for quantitative determinations of the radioelements is based on the assumption that

radioactive equilibrium exists in the U and Th decay series. Any progress in our understanding which will reduce or eliminate the necessity of this assumption is, therefore, of paramount importance for the success of the method in U exploration.

6.2 Properties of Gamma-Rays

Gamma-rays are high energy, penetrative electromagnetic radiation. They have an energy range between 40keV and 4MeV and are emitted by de-excitation of the products from the decay of unstable nuclei. Gamma-rays are best differentiated from X-rays on the basis of their source. The former originate from within atomic nuclei while the latter originate from the electron cloud around nuclei (Adams and Gasparini, 1970). However, it is also possible to separate them in terms of energy, when 40keV is used as the arbitrary upper limit of X-rays.

Environmental gamma-radiation is mostly produced by the decay of the radionuclides concentrated in the Earth's crust. The most abundant of these are isotopes of U, Th and K, and the daughter products of the U and Th decay series. Gamma-rays in the energy range between 0.03MeV and 2.43MeV and between 0.03MeV and 2.62MeV, are produced in the decay of ^{238}U and ^{232}Th, respectively, to their stable daughters. 1.46MeV gamma-rays are produced by the decay of ^{40}K. Gamma-rays, like all other ionising radiations (alpha-particles and beta-particles) which originate from

radioactive decay, interact with any medium through which they pass, and become absorbed. This absorption is a severe restriction on the applicability of gamma-ray spectrometry. Absorption of gamma-rays occurs primarily through three main processes, these are:

i) Compton scattering, in which the photons in a beam of gamma-rays give up part of their energy to an electron in the material, and become deflected at an angle away from the beam direction,

ii) the photoelectric effect, in which gamma-ray photon transfers all its energy to an electron, which is then ejected from the atom of the medium, and

iii) pair production, in which gamma-ray photons interact with the electron field of the nucleus to produce a positron-electron pair.

Which of these effects is dominant depends on the energy of the gamma-rays. The photoelectric effect predominates in the region of lower-energy gamma-rays, that is energies of less than 0.2MeV, Compton scattering predominates in the energy range 1MeV to 5MeV, while pair production takes place when the gamma-rays have an energy greater than 1MeV (Fano, 1953). Thus, in environmental gamma-ray spectrometry, Compton scattering and the photoelectric effect are the most important processes.

The intensity of a beam of gamma-rays at a distance x away

from their source is given by:

$$I = I_0 e^{-\mu x} \qquad \text{.....6.1}$$

where μ is the absorption coefficient of the medium in which they are travelling, and I_0 is the initial intensity of the gamma-rays. The absorption coefficient expresses the probability of an absorption process occurring per unit thickness/distance travelled. The total absorption coefficient due to the three absorption processes is:

$$\mu = \mu_{pc} + \mu_{cs} + \mu_{pp} \qquad \text{.....6.2}$$

where μ_{pc} is the absorption coefficient for photoelectric interactions, μ_{cs} is the absorption coefficient due to Compton scattering, and μ_{pp} is the absorption coefficient due to pair production. From Equation 6.1 it can be seen that the absorption coefficient has the unit of m^{-1}.

Clearly, the absorption coefficient depends on the composition or quantity of the medium, and this quantity is defined as the thickness traversed by the beam multiplied by its density. This gives the absorber thickness. The absorption coefficient is then referred to as the mass absorption coefficient, denoted by $m\mu$ and has the units of $cm^2 g^{-1}$. The value of the mass absorption coefficient for any material depends on the constituent elements

making up the material, and is given by the combination of the separate mass absorption coefficients of these elements (Siegbahn, 1965). Thus:

$$(m\mu)\text{material} = m\mu_1 a_1 + m\mu_2 a_2 + \ldots\ldots\ldots\ldots + m\mu_n a_n \quad \ldots\ldots 6.3$$

where $m\mu_1 \ldots\ldots m\mu_n$ are the mass absorption coefficient of the constituent elements and $a_1 \ldots\ldots a_n$ are the atomic proportions of the elements in the material. The probability of a given process taking place is a function of the target area, known as the cross-section, presented by a particle to the incident photon beam. This target area is usually measured in barns ($10^{-24} cm^2$). The atomic absorption coefficient μa, expressed in barns per atom, is related to the mass absorption coefficient $m\mu$ by:

$$m\mu = (N_a/A)\mu a \qquad \ldots\ldots\ldots\ldots\ldots\ldots 6.4$$

where N_a is the Avogadro's number ($6.0228.10^{23}$), and A is the atomic weight of the element.

Another important property of the medium for gamma-ray absorption, is the half-thickness. This is defined as the thickness of the material which reduces the intensity of the rays passing through it to half the intensity on entering the material. From

Equation 6.1, this is given by:

$$x_{1/2} = \ln(2)/\mu$$
$$= 0.693/\mu \qquad \ldots\ldots\ldots\ldots\ldots\ldots 6.5$$

Davisson and Evans (1952) listed the atomic absorption coefficients of some elements for gamma-rays with energies between 0.01MeV and 6MeV. Thus, knowing the major element composition of a rock for which gamma-ray spectrometry measurements were undertaken, the parameters in Equations 6.3 and 6.5 can be determined. The results for the sites investigated in this study are given in Section 6.4.

6.3 Principles of Gamma-Ray Spectrometry

The detection of radionuclides by gamma-ray spectrometry depends on the interaction of the gamma-rays with the detecting material. The interaction is such that the energy of the gamma-ray photon is transferred to the electrons of the detecting material. For efficient coversion of the gamma-ray energies, detector materials with the characteristic of extracting most of this incident energy are used. Typically, materials with scintillation properties are used. In these, the energies of gamma-ray photons are converted to lower energy photons, which are then emitted. These lower energy photons are converted into electrical pulses via a photomultiplier. The intensity of each pulse is proportional to the quantity of the nuclide characterised by the particular

gamma-ray energy. Still the most commonly used scintillation material in four-channel gamma-ray spectrometers is high density Tl-activated sodium iodide, NaI(Tl). This has the advantage of possessing a high atomic number, which increases the cross-section of the interaction processes and in turn, increases the conversion efficiency of the detection. A detailed discussion of detectors in gamma-ray spectrometry has been given by Adams and Gasparini (1970).

The spectra of the ^{238}U, ^{232}Th decay series and ^{40}K, are shown in Figures 6.1, 6.2, and 6.3. Threshold spectrometers used in four-channel gamma-ray spectrometry discriminate between the energy peaks shown in these spectra, thus enbaling the identification of the different radionuclides. The spectral analysis for the energy discrimination required to identify and quantify the radionuclides is achieved in two ways. One is by recording the whole spectrum from a predetermined low position up to and including the energy peak of interest (integral spectrometry); the second is by obtaining information on the energy peaks with an 'energy window', E, set about the peak (differential spectrometry). Most of the instruments designed for field use incorporate both types. Differential spectrometry is employed in three channels: K is determined from the 1.46MeV energy peak, while the 1.76MeV and 2.62MeV energy peaks are used for determinig U and Th, respectivly. A fourth channel is used for integral spectrometry.

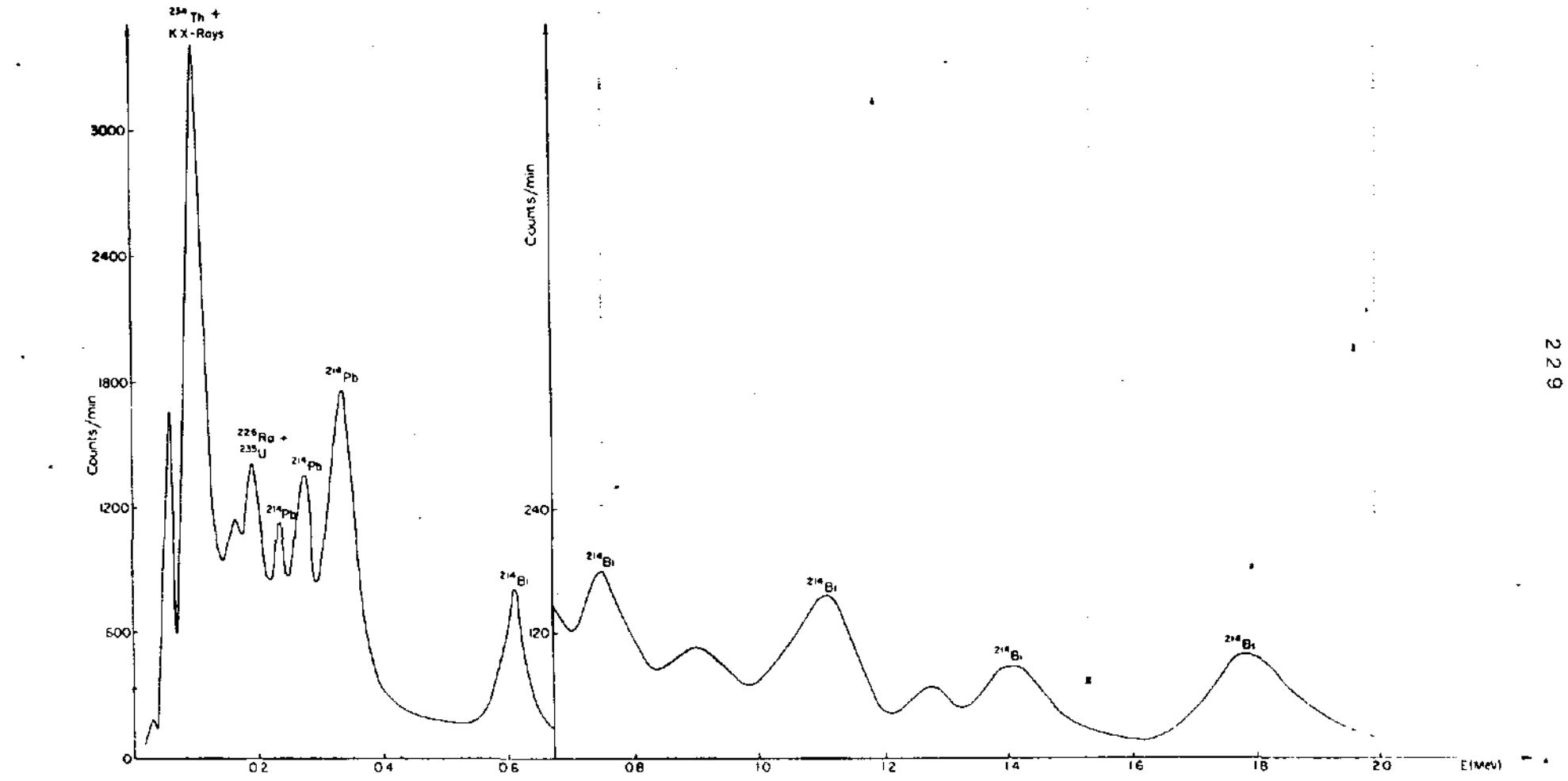


FIGURE 6.1 Gamma-ray spectrum of ^{238}U in secular equilibrium (After Adams and Gasparini, 1970)

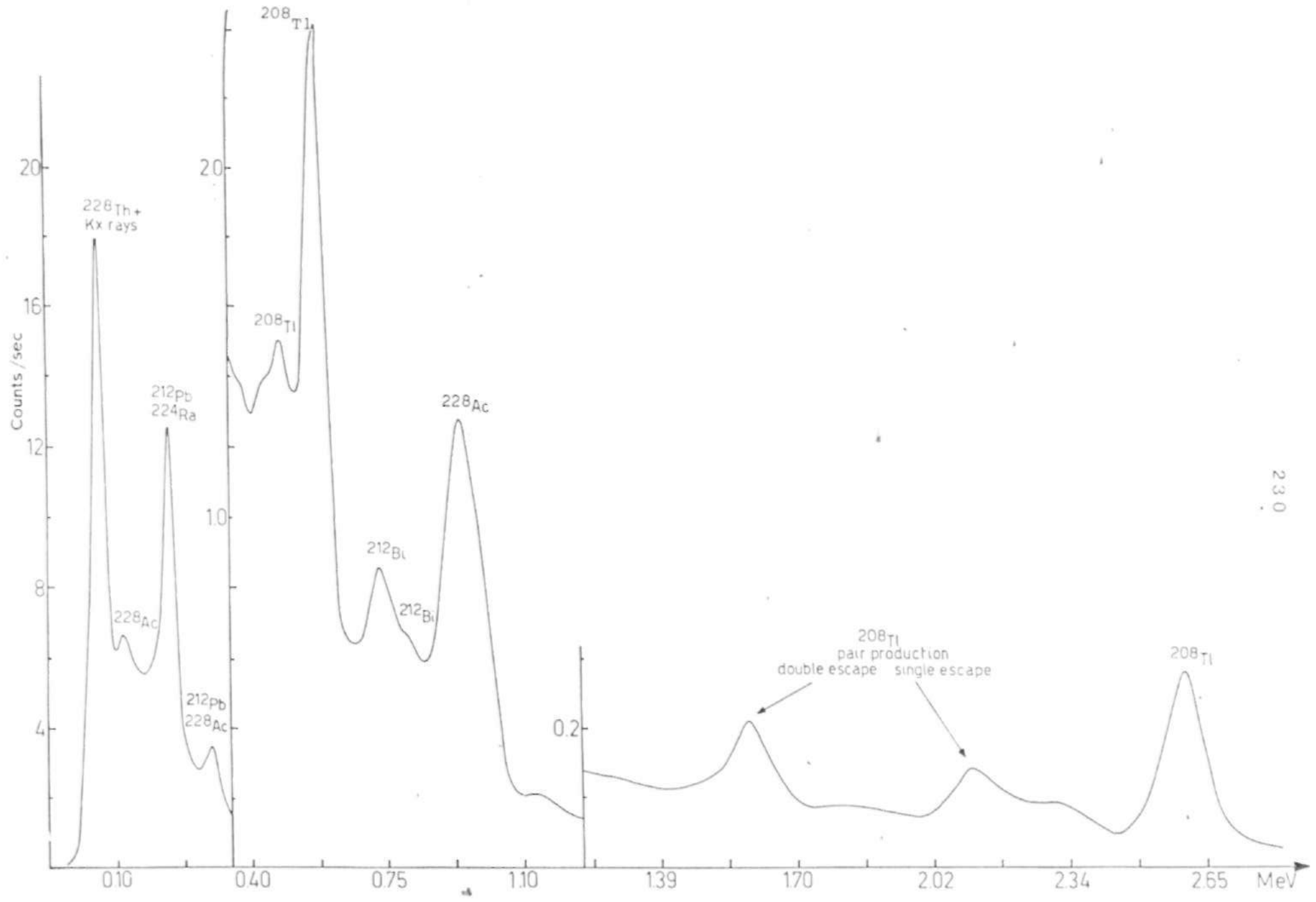


FIGURE 6.2 Gamma-ray spectrum of ^{232}Th in secular equilibrium
(After Adams and Gasparini, 1970)

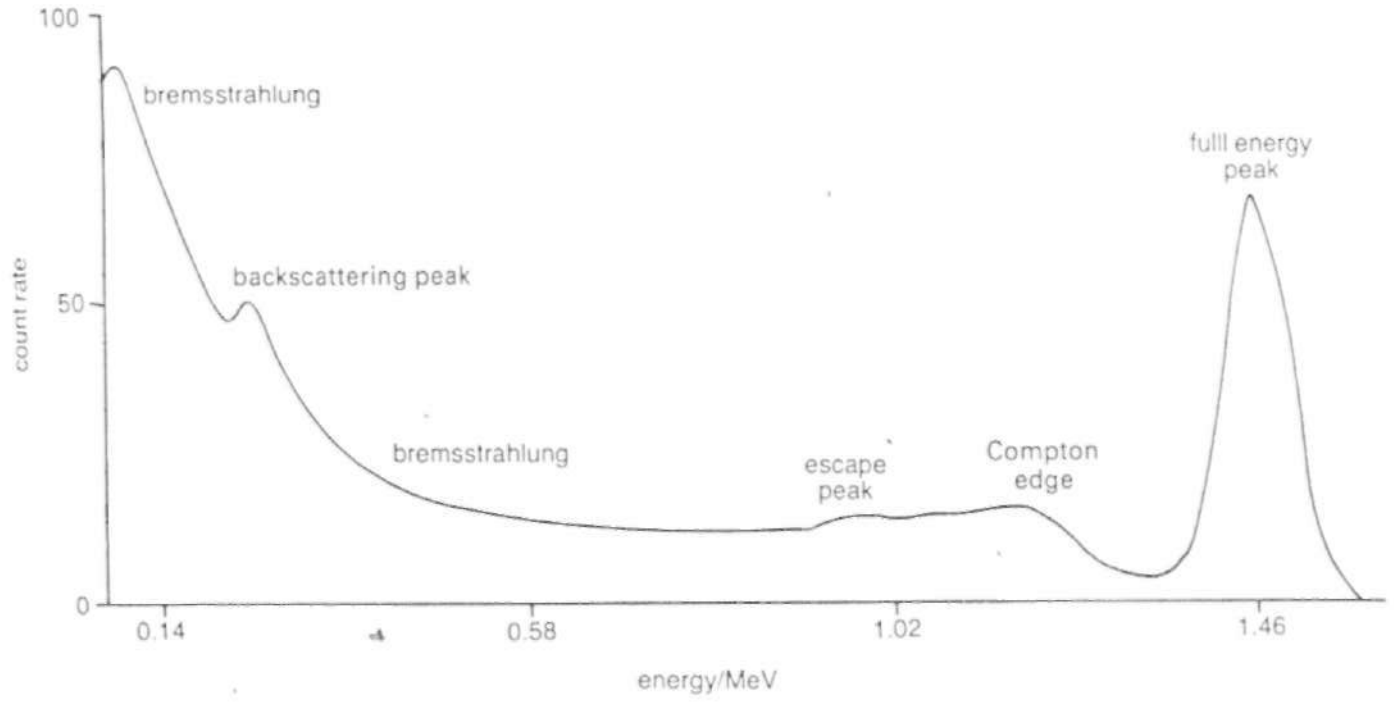


FIGURE 6.3 Gamma-ray spectrum of ^{40}K
(After Adams and Gasparini, 1970)

6.4 Gamma-Ray Spectrometry and U-Series Disequilibrium

As shown in Section 6.3, quantitative determinations of the concentrations of U and Th in four-channel gamma-ray spectrometry is based on the 1.76MeV energy peak in the ^{238}U decay series. This peak is due to ^{214}Bi. In the ^{232}Th decay series the 2.62MeV peak is used, which is due to ^{208}Tl. Table 6.1 gives gamma-ray details of the ^{238}U decay series from which it can be seen that ^{214}Bi is a long way down the decay chain from their parent nuclides. Similarly, ^{208}Tl from ^{232}Th. Therefore, analysis of U and Th by four-channel gamma-ray spectrometry is based on the assumption that secular equilibrium exists in these decay series.

The decay of ^{238}U to ^{206}Pb, and ^{232}Th to ^{207}Pb, involves nineteen and eleven daughters, respectively. If none of these daughters is removed out of the series, sometimes after the formation of a U or Th-bearing crystal, a state of equilibrium is reached, whereby the loss of a daughter due to its decay is made up by the decay of the preceding parent. This occurs where the half-life of the parent is much larger than the half-life of the daughter. If one of the daughters is taken out of the system, however, disequilibrium is established, and the nuclides above the one which has been lost become proportionally more enriched in the series. Similarly, the nuclides developed from the decay of the lost daughter are depleted in the series. If the nuclide which has

Table 6.1: Energies and proportions of gamma-rays from the ^{238}U decay series.

Nuclide	Energies(MeV)	Proportions(%)
^{238}U	0.048	23
^{234}Th	0.0935; 0.0639	7
	0.0931; 0.0632	12
	0.0698	81
^{234}Pa	0.0435	1
^{234}U	0.0535	28
^{230}Th	0.0678	24
^{226}Ra	0.1857	-
^{214}Pb	0.534; 0.489; 0.275	2
	0.3520	47
	0.2952; 0.2419	44
^{214}Bi	0.45-2.43	-
^{210}Pb	0.0465	81

been lost has a short half-life, then equilibrium is restored within a short time. On the other hand, the loss of nuclide with a long half-life will mean that the series takes a long time to regain equilibrium. Due to the exponential character of radioactive decay, nuclides in a decay sries approach their equilibrium values assymptotically, so that 100% equilibrium is never achieved. In a decay series containing nuclides of varying half-lives, and where the series are headed by parents of long half-lives, disequilibrium between the daughters and their parents is better described by secular equilibrium. In this case, the daughters can attain 99% equilibrium with their parents, and equilibrium are usually quoted for 95% or 99% equilbrium. The ^{238}U decay series contains a number of daughters with very long half-lives. ^{234}U, ^{230}Th, and ^{226}Ra, which are members in this series, have half-lives of $4.5.10^5$ years, 8.10^4 years and 1622 years, respectively, so that it will take approximately 1 million (10^6) years for the ^{238}U series to attain secular equilibrium. Thus, a loss of ^{234}U from the series means that a period not less than 10^6 years will be required before 99% equilibrium between the members in the series is restored. In the ^{232}Th decay series, however, the longest-lived daughter, ^{228}Ra, has a half-life of just 6.7 years, so that equilibrium is restored within a relatively short period of time should a member be lost from the decay series. This makes the assumption of secular equilibrium in the ^{232}Th decay series safer than for the ^{238}U series.

The need to assume secular equilibrium in four-channel gamma-ray spectrometry is a most important drawback in the use of the method for U exploration. This is because many factors may cause disequilibrium to occur, especially in the U decay series. The development of secular equilibrium in the decay series is further complicated due to the difference in geochemical behaviour of the various daughters in each series. Moreover, physical properties are also important because of the presence of gaseous daughters, ^{222}Rn and ^{220}Rn in the ^{238}U and ^{232}Th decay series, respectively. The question of disequilibrium is discussed more fully in Chapter 7

Procedures to determine whether or not equilibrium exists in the U decay series from gamma-spectrometric data and chemical analyses, have been suggested. Comparison of the results of chemical analysis and the determination of equivalent uranium (eU) from gamma-spectrometry, is one such method. However, any conclusion reached from such methods must be treated with caution because of the possible complexity of the disequilibrium which may occur in the U decay series. For example, such comparisons may be found to show a linear relationship between chemically determined uranium (cU) and eU in samples where ^{214}Bi is not in equilibrium with U. This can be due to escape of ^{222}Rn, but may also be due to leaching of ^{226}Ra. Onstrihansky (1976) studied disequilibrium in the ^{238}U series using a gamma-ray spectrometry system that measured both the low energy section of the spectrum

(40keV-100keV) and the high energy section. The low energy section was measured using a Ge(Li) detector and the high energy section by a NaI(Tl) detector. A standard was used in which the concentration of the U was known, and determinations from other samples were compared with this spectrum. His method was used to investigate the ^{232}Th decay series as well as the ^{238}U series.

These methods, as can be seen, require chemical determinations. With such data available there may be no need of gamma-ray determinations which involve the long and tedious exercise of counting, and which may be difficult to interpret. However, Durrance (1983) has proposed a method in which the data obtained from four-channel gamma-spectrometric determinations are used to investigate disequilibrium directly. In this method a term called the Disequilibrium Factor is determined from each of the four individual readings of the gamma-ray spectrometer. Constants C_K, C_U and C_{Th} are determined such that the equation:

$$C_K K(\%) + C_U.U(ppm) + C_{Th}.Th(ppm) = C_T$$

is satisfied;

where K(%) is the equivalent K concentration in $\%K_2O$

U(ppm) is the equivalent U concentration in ppm

Th(ppm) is the equivalent Th concentration in ppm, and

C_T is the count in the Total Count channel of the

spectrometer. The constants C_K, C_U and C_{Th} are, respectively, associated with the contribution of ^{40}K, and the ^{238}U and ^{232}Th decay series to the total gamma-ray activity.

These constants were determined for samples where the decay series of U and Th were in secular equilibrium but the author argued that even if disequilibrium was present, that will only produce a systematic error and not invalidate comparative studies elsewhere. Using the same spectrometer in subsequent measurements, the sum $C_K K(\%) + C_U U(ppm) + C_{Th} Th(ppm)$ was compared to the readings in the Total Count channel. For samples in equilibrium, the sum was equal to the reading in the Total Count channel, so where this sum was less than the Total Count, disequilibrium occurs due to recent removal of ^{238}U. Conversely, where the sum was greater than the Total Count, disequilibrium was caused by recent addition of ^{238}U. Disequilibrium effects in the ^{232}Th decay series were considered negligible compared to those in the ^{238}U series.

However, a problem with any method which compares the readings from the U, Th and K channels with those of the Total Count window is the fact that there is disproportionate increase in the Total Count window with a very small increase in the concentration of either U or Th. An increase in U even in a sample in secular equilibrium will only increase the readings in the U window by a comparatively very small amount, because this channel only responds to the ^{214}Bi in the series. But such an increase will produce a tremendous increase in the Total Count window due to the increase

in ^{234}Th which contributes significantly to the lower energy part of the total count. Therefore, small changes in the ^{214}Bi window due to the recent addition or subtraction of U are accompanied by large changes in the Total Count channel. For this reason Durrance (1983) used Total Count values/100 for comparative purposes and found no correlation between eU given by ^{214}Bi and the magnitude or sign of the Disequilibrium Factor. An application of this approach has been used by Jefferies (1988) to define recent U movement.

6.5 Gamma-Ray Spectrometric Procedures

Both in-situ and laboratory gamma-ray spectrometry have been employed for the analysis of samples in this study. Two spectrometers, a DISA 400 and a GR-410, in each case manufactured by EXPLORANIUM, were used. These are fitted with NaI(Tl) scintillation detectors of 7.6cm in diameter and 7.6cm thick, thus giving the detectors an absorber thickness of 27.89gcm^{-2}. They are both conventional four-channel systems and operate on the differential window and integral Total Count modes. The detectors are connected to high gain photomultiplier tubes which amplify the signals sent by the detected gamma-rays. Counts accumulated during the operation of the spectrometers are displayed in the four channels, each channel with the specifications shown in Table 6.2.

A typical gamma-ray spectra with the normal window settings for the DISA 400 is shown in Figure 6.4. From this the overlap in the energy windows can be seen. Temperature changes in the environment causes a relative shift in these window settings and this has to be monitored at intervals during the course of counting. For its calibration the DISA 400 is provided with a ^{137}Cs source. The 0.662MeV energy peak of the source is used to centre the energy windows. A maximum response is obtained from the spectrometer when this peak is centred in the calibration window. In the GR 410, the calibration procedure uses a ^{133}Ba source with an energy peak at 356keV. The ^{133}Ba source is included in the detector assembly so that the position of the windows is continuosly monitored. This prevents the instrument being used for disequilibrium studies of the type employed by Durrance (1983).

In the in-situ determinations, exposed granite surfaces on the Jos Plateau were analysed. The procedure involved placing the detector on a flat surface of the granite free of overburden or any inhomogeneity in the 'field' of the detector. The detector-sample geometry when the spectrometer is used in this way is shown in Figure 6.5. The gamma-rays which are received by the detector come from the region bounded by a 2 surface - the 'effective

Table 6.2 Window data for DISA 400 and GR410 portable gamma-ray spectrometers.

Element	Energy peak used (MeV)	Window width ΔE(MeV) DISA400	GR410[1]
^{40}K	1.46	200	176
U	1.76	200	210
Th	2.62	400	320
Total count	0.1<E<3		

1 Window width variable.

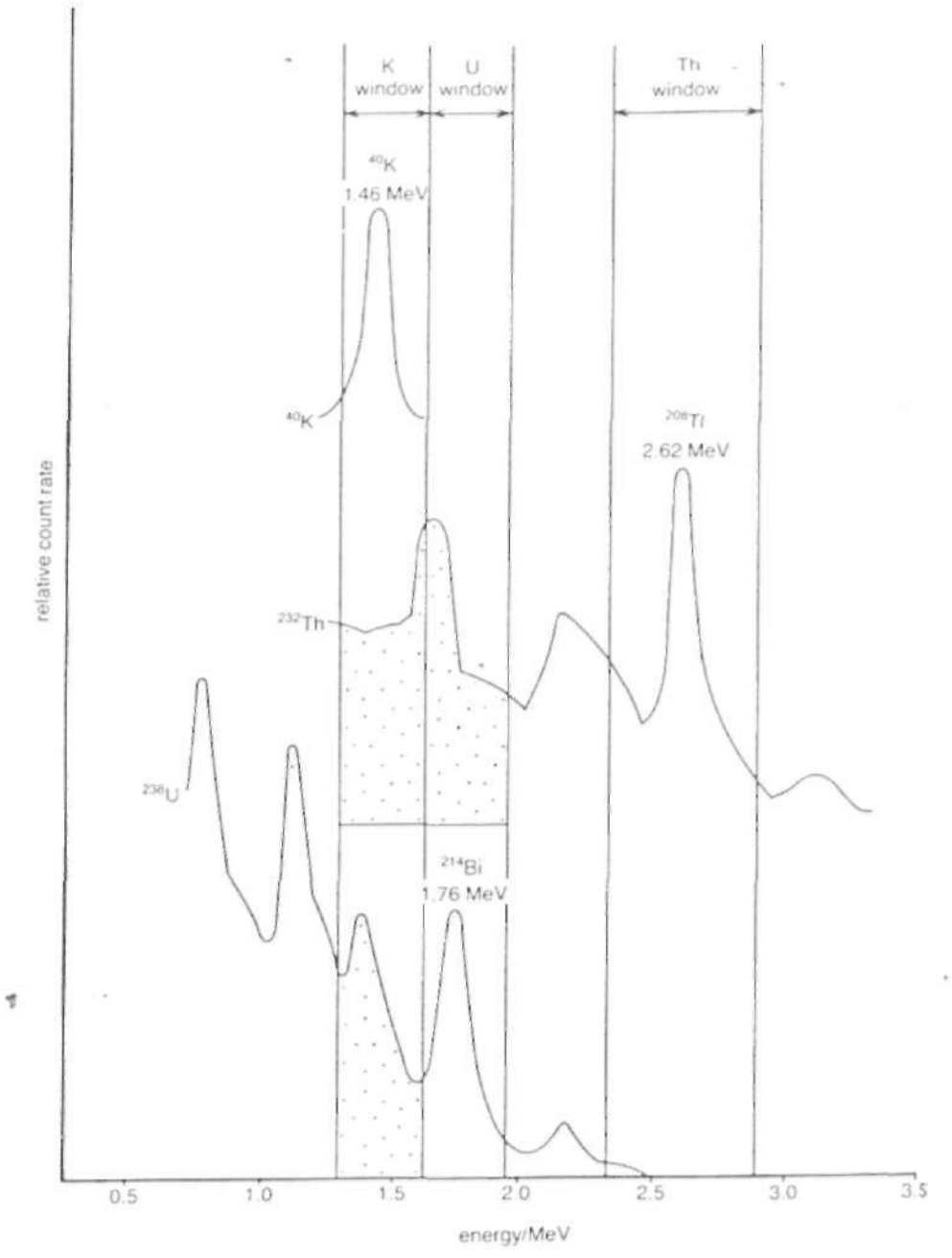


FIGURE 6.4 Gamma energy window setting for the DISA 400 spectrometer

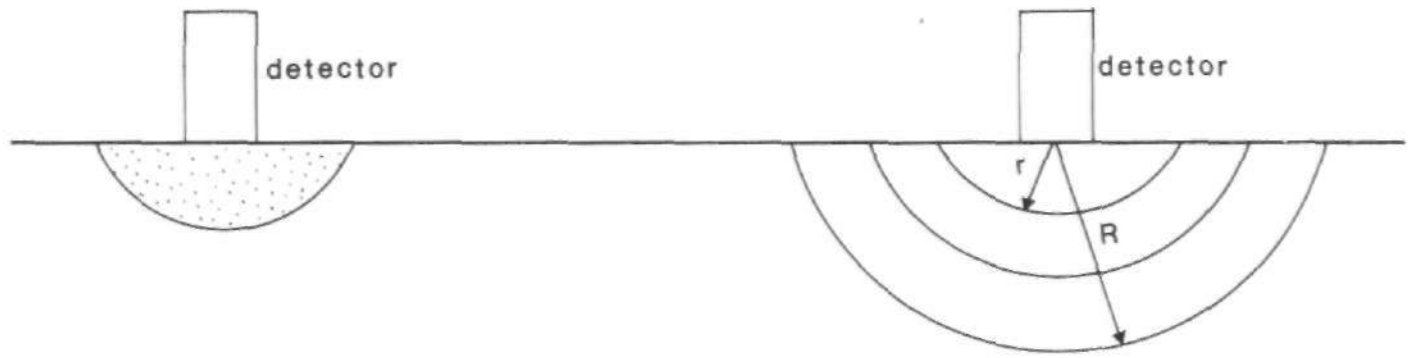


FIGURE 6.5 Detector-sample geometry in gamma-ray spectrometry

(a) 2 geometry

(b) area sampled by detector

R = Maximum distance from which gamma-rays reach the detector

$r = x_{1/2}$

sample'. They obey the relationship $I = I_o \exp(-\mu x)$, where I_o is the initial intensity of the gamma rays, and I is the intensity after travelling distance x through a material with an absorption coefficient μ. Hence 50% of the rays whose source is within the hemisphere of radius $x_{1/2}$ will be received at the detector. Similarly, 25% of the rays originating from a region bounded by the surfaces $X_{1/2}$ and $2x_{1/2}$ will be registered at the detector. Thus if concentric spherical surfaces of radius $nx_{1/2}$ are drawn, the contribution of each zone of the 'effective sample' to the total gamma-ray activity received at the detector, can be evaluated. Clearly, the contribution decreases the further the zone lies away from the detector. But, as the distance increases so does the volume of the zone and, therefore, the intensity of the gamma-rays. Thus the proportion of the rays contributed by a zone further away from the detector also increases. However, beyond a certain distance, absorption will dominate and the contribution decrease towards zero. Theoretical calculations of the contribution by each zone to the total gamma-ray activity at the detector in this geometry, show that the proportion increases from the first zone and then starts to decrease from a distance of about $9x_{1/2}$. Figure 6.6 shows such a distribution. From this it can be seen that about 99% of the gamma-rays reaching the detector originate within a distance of about $12x_{1/2}$. However, in practice this may not be the

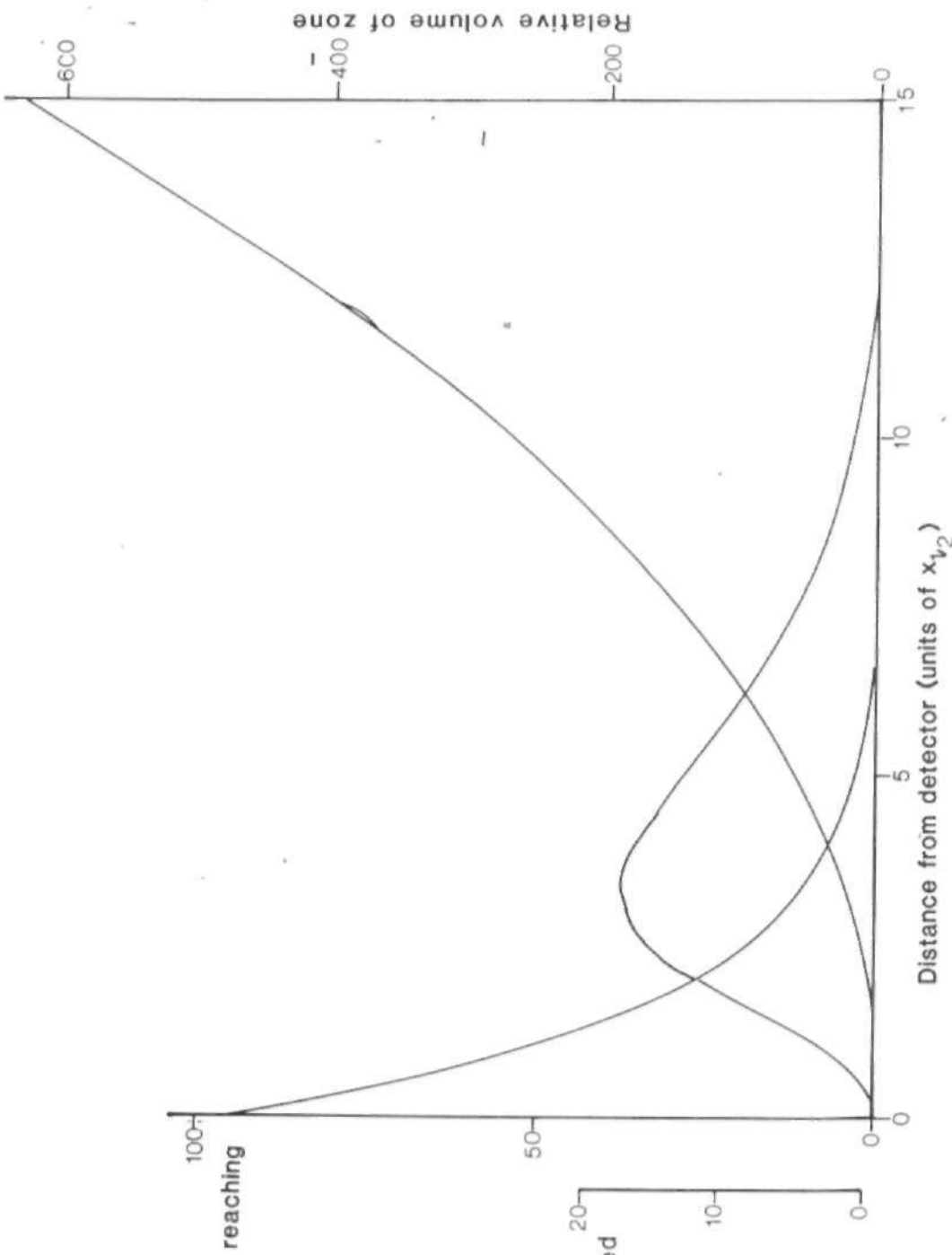


FIGURE 6.6 Gamma-ray source profile in gamma-ray spectrometry
(After Heath, 1982)

case. Because of the self-absorption of gamma-rays in passing through the source, more than 50% of the rays received at the detector come from within the first zone. This is discussed in more detail in Section 6.6.

The mass absorption coefficients of some elements for energies of the gamma-rays used in the detection of U, Th and K have been calculated using Equation 6.3. These are given in Table 6.3. In Table 6.4 the average composition of the Jos Plateau granite, where in-situ investigation were carried out, is given, together with the atomic proportions of the elements in this composition. The mass absorption coefficient of each element is shown in Table 6.5. From these values, the gamma-ray linear absorption coefficient and the half-thickness for the energies used were calculated. Both are also given in Table 6.5.

From Table 6.3 it can be seen that on the Younger Granite, for the most energetic gamma-rays from the Th decay series to contribute to the count, the spectrometer must be surrounded by a rock surface to a distance of 84cm. The equivalent distances for U and K are 69cm and 63cm, respectively. Therefore, on such granite, gamma-spectrometric determinations are best obtained when the spectrometer is placed on a flat surface with a minimum radius of about 1m about the detector. However, since the air-sample boundary is not a closed surface for gamma-rays, rays from the sample are recorded which originate from surfaces other than the surface in contact with the detector. In practice, the actual

Table 6.3 : Mass absorption coefficient of some elements at the energies used in gamma-ray spectrometry.

Element		1.46MeV		1.76MeV		2.62MeV	
	At. wt.	a_μ	$m\mu$	a_μ	$m\mu$	a_μ	$m\mu$
Si	28.09	2.450	0.0523065	2.220	0.04759920	1.822	0.03906552
Al	26.98	2.254	0.05031650	2.120	0.04732519	1.729	0.03859682
Ti	47.90	3.857	0.04872307	3.520	0.04425941	2.908	0.03656431
Fe	55.85	4.579	0.04937941	4.162	0.04488253	3.515	0.03790537
Mg	24.31	2.100	0.05202748	1.902	0.04712203	1.550	0.03840123
Ca	40.08	3.505	0.05202748	3.192	0.04796601	2.650	0.03982141
Na	22.99	1.925	0.05043014	1.740	0.04558361	1.420	0.03720042
K	39.10	3.330	0.05129392	3.042	0.04685769	2.510	0.03866299
P	30.97	2.630	0.05114615	2.385	0.04638159	1.951	0.03794150
O	16.00	1.389	0.05228543	1.260	0.04729550	1.020	0.03839535
Mn	59.94	4.447	0.04875026	3.660	0.04012277	3.364	0.03687787

Table 6.4: Atomic proportions of the major constituents of an average granite of the Jos Plateau.

Element	Composition (% oxide)	Atomic proportion
Si	75.38	35.24
Al	12.65	6.69
Ti	0.18	0.11
Fe	2.02	1.41
Mg	0.08	0.05
Ca	0.61	0.43
Na	3.72	2.81
K	4.91	4.08
P	0.04	0.02
Mn	0.03	0.01
O		48.82
Total	99.62	99.68

Table 6.5: Gamma-ray absorption coefficients and depth of investigation data for an average Nigerian Youger Granite.

Element	Atomic proportion $m\mu$ at:		
	1.46MeV	1.76MeV	2.62MeV
Si	$1.84328.10^{-2}$	$1.67740.10^{-2}$	$1.37667.10^{-2}$
Al	$3.47184.10^{-3}$	$3.28435.10^{-3}$	$2.66318.10^{-3}$
Ti	$5.35954.10^{-5}$	$4.86854.10^{-5}$	$4.02207.10^{-5}$
Fe	$6.96250.10^{-4}$	$6.32844.10^{-4}$	$5.34466.10^{-4}$
Mg	$2.60137.10^{-5}$	$2.35610.10^{-5}$	$1.92006.10^{-5}$
Ca	$2.26479.10^{-4}$	$1.96010.10^{-4}$	$1.71232.10^{-4}$
Na	$1.41709.10^{-3}$	$1.31670.10^{-3}$	$1.04533.10^{-3}$
K	$2.09279.10^{-3}$	$1.89237.10^{-3}$	$1.57745.10^{-3}$
P	$1.02292.10^{-5}$	$9.27632.10^{-6}$	$7.58830.10^{-6}$
O	$2.34343.10^{-2}$	$2.11978.10^{-2}$	$1.72088.10^{-2}$
Mn	$9.75005.10^{-6}$	$8.02455.10^{-6}$	$7.37557.10^{-6}$
Total	$= 4.55829.10^{-2}$	$3.8708.10^{-2}$	$3.15821.10^{-2}$
$\mu\rho$	$= 0.0456 cm^2 g^{-1}$	$0.0387 cm^2 g^{-1}$	$0.0316 cm^2 g^{-1}$
ρ	$= 2.67 g cm^{-3}$	$2.67 g cm^{-3}$	$2.67 g cm^{-3}$
μ	$= 0.1218 cm^{-1}$	$0.1033 cm^{-1}$	$0.0844 cm^{-1}$
$x_{1/2}$	$= 5.21 cm$	$5.72 cm$	$7.01 cm$
$12x_{1/2}$	$= 76.44 cm$	$84.00 cm$	$102.96 cm$

geometry presented to the detector is as shown in Figure 6.8. Other radiation reaching the detector constitutes the background radiation.

To reduce the effect of these sources, sampling sites were chosen such that lateral contributions from vertical surfaces were avoided. Where such structures occurred, the sampling site had to be chosen so that the distance to the detector was about twice the half-thickness of the most energetic gamma-ray in air which is about 150m.

For laboratory analysis, crushed samples of rock were taken in a 1000ml plastic beaker to provide a sample depth of 11.5cm. Blocks of Pb of 1.5cm thickness were used for shielding the beaker, both from lateral contributions of gamma-rays and those coming from beneath the beaker. The arrangement is shown in Figure 6.9. The average chemical composition of the kaolinised samples from Bodmin Moor, together with the atomic proportions of the elements, are given in Table 6.6. The gamma-ray absorption coefficients of these samples, based on their composition, and the depth of investigation are given in Table 6.7. An average density of 2.67gcm^{-3} (Dewu et al., 1984) for the fresh Jos plateau Younger Granite was used in the computation. The average density of the kaolinised granite from Bodmin Moor was determined by laboratory measurements of 60 samples. The density of soil was estimated using the method of Harrison and Bocock (1981). The gamma-ray mass absorption and depth of investigation data for the soil samples,

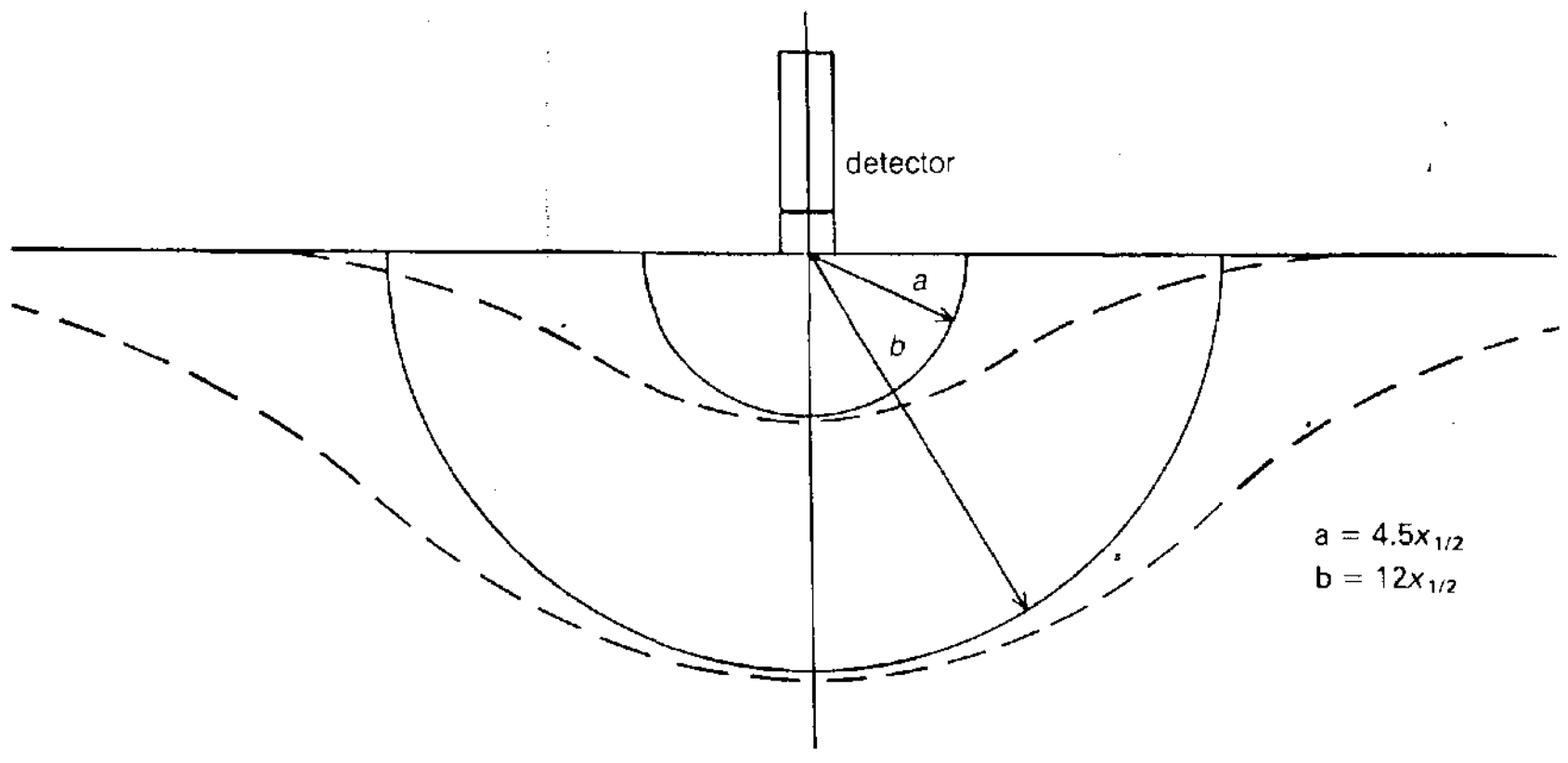


FIGURE 6.7 Actual detector-sample geometry in gamma-ray spectrometry

(after Durrance, 1986)

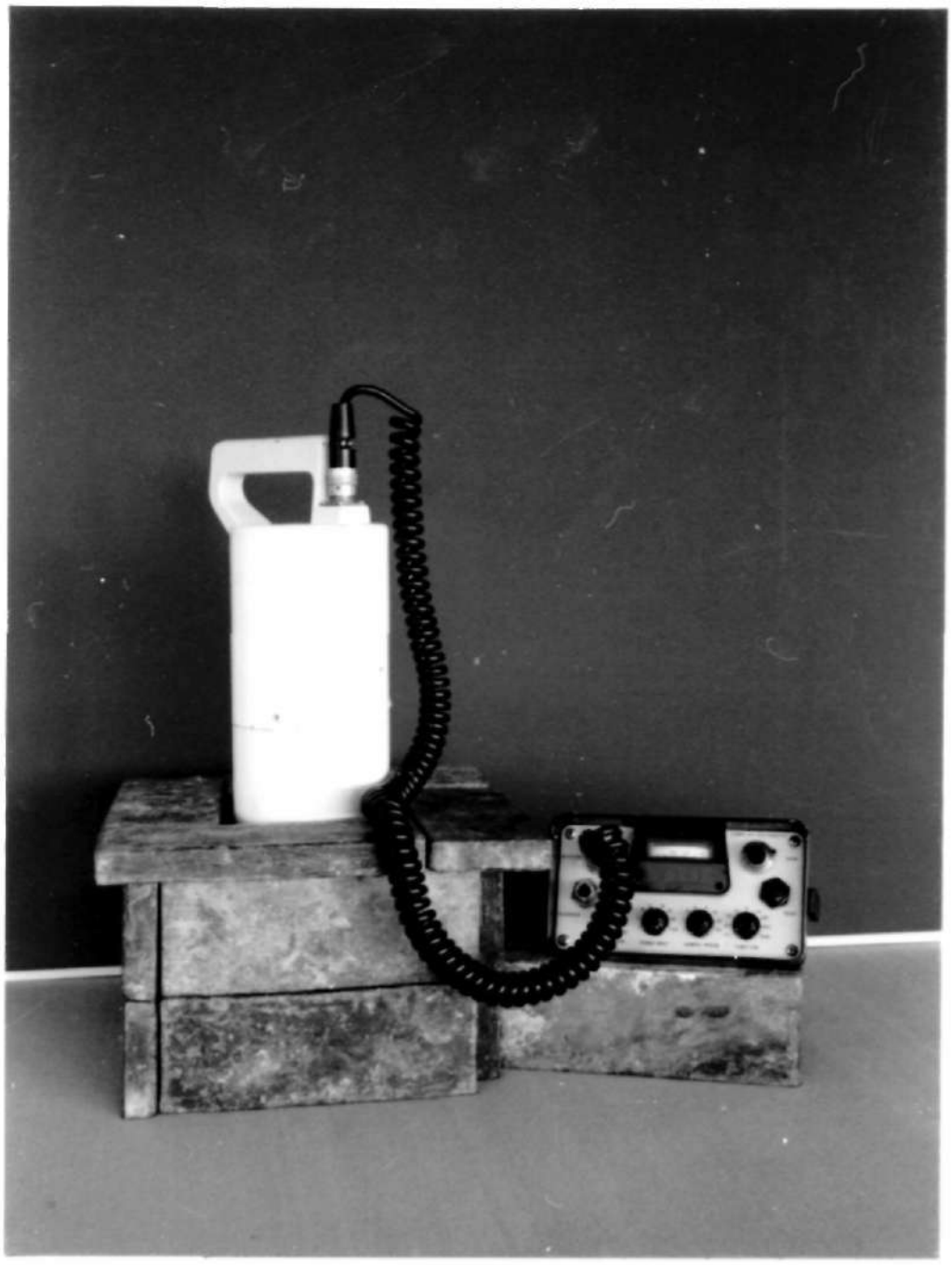


FIGURE 6.8 Laboratory arrangement for gamma-ray spectrometry

Table 6.6: Average composition of kaolinised granite and the atomic proportions of the elements.

Element	Composition(% Oxide)	Atomic proportion
Si	72.01	33.66
Al	17.96	9.50
Ti	0.15	0.09
Fe	1.15	0.80
Mg	0.18	0.11
Ca	0.13	0.10
Na	1.13	0.84
K	5.57	4.63
P	0.11	0.05
Mn	0.04	0.03
O		48.81
Total	98.43	98.62

Table 6.7: Gamma-ray mass absorption coefficients and depth of investigation data for kaolinised granite from Bodmin Moor.

Element	Atomic proportion($m\mu$) at:		
	1.46MeV	1.76MeV	2.62MeV
Si	$1{:}76064.10^{-2}$	$1.60219.10^{-2}$	$1.31495.10^{-2}$
Al	$4.78007.10^{-3}$	$4.49589.10^{-3}$	$3.66670.10^{-3}$
Ti	$4.38508.10^{-5}$	$3.98333.10^{-5}$	$3.29079.10^{-5}$
Fe	$3.95035.10^{-4}$	$3.59060.10^{-4}$	$3.03243.10^{-4}$
Mg	$5.72032.10^{-5}$	$5.18342.10^{-5}$	$4.22414.10^{-5}$
Ca	$5.26695.10^{-5}$	$4.79660.10^{-5}$	$3.98214.10^{-5}$
Na	$4.23613.10^{-4}$	$3.82902.10^{-4}$	$3.12484.10^{-4}$
K	$2.37491.10^{-3}$	$2.16951.10^{-3}$	$1.79010.10^{-3}$
P	$2.55731.10^{-5}$	$2.31908.10^{-5}$	$1.89708.10^{-5}$
O	$2.55205.10^{-2}$	$2.30890.10^{-2}$	$1.87408.10^{-2}$
Mn	$1.46251.10^{-5}$	$1.20368.10^{-5}$	$1.10634.10^{-5}$
Total =	$5.12945.10^{-2}$	$4.66931.10^{-2}$	$3.81078.10^{-2}$
μ/ρ =	$0.0513cm^{2}g^{-1}$	$0.0467cm^{2}g^{-1}$	$0.0381cm^{2}g^{-1}$
ρ =	$2.12gcm^{-3}$	$2.12gcm^{-3}$	$2.12gcm^{-3}$
μ =	$0.1087cm^{-1}$	$0.0990cm^{-1}$	$0.0808cm^{-1}$
$x_{1/2}$ =	6.37cm	7.00cm	8.58cm
$12x_{1/2}$ =	76.44cm	84.00cm	102.96cm

is given in Table 6.8 and 6.9, respectively. The half-thicknesses computed from these data show that high energy gamma-rays emitted by the decay of ^{232}Th are received from a depth of 8.58cm, and the depths for the U series and K are 7.00cm and 6.37cm, respectively.

6.6 Data Reduction

The counts obtained from gamma-spectrometric measurements have to be converted to element concentrations to be meaningful. This can be achieved if the spectrometer is standardised, such that counts recorded from each channel can be related to the concentration of the radioelement in the sample analysed. Where the background is zero the concentration of the element is proportional to the counts recorded from the respective channels: Therefore:

$$Th(ppm) = Th(cpm).k_1$$

$$U(ppm) = U(cpm).k_2$$

and

$$K(\%) = K(cpm).k_3,$$

where k_1, k_2 and k_3 are the sensitivity constant of the spectrometer for the Th, U and K channels, respectively. However, Where background are not zero the Th(cpm), U(cpm) and K(cpm) must

Table 6.8: Average composition of Jos plateau soil and the atomic proportions of the elements.

Element	Composition (% oxide)	Atomic proportion
Si	69.96	32.70
Al	14.55	7.70
Ti	0.53	0.32
Fe	6.45	4.52
Mg	0.13	0.08
Ca	0.08	0.05
Na	0.26	0.19
K	1.72	1.43
P	0.03	0.01
Mn	0.02	0.02
O		46.71
Total	93.73	93.73

Table 6.9: Gamma-ray mass absorption coefficients and depth of investigation data for an average Jos Plateau soil.

Element	Atomic proportion ($m\mu$) at:		
	1.46MeV	1.76MeV	2.62MeV
Si	$1.71042.10^{-2}$	$1.55649.10^{-2}$	$1.27744.10^{-2}$
Al	$3.87347.10^{-3}$	$3.64404.10^{-3}$	$2.97196.10^{-3}$
Ti	$1.55914.10^{-4}$	$1.41630.10^{-4}$	$1.17006.10^{-4}$
Fe	$2.23195.10^{-3}$	$2.02870.10^{-3}$	$1.71332.10^{-3}$
Mg	$4.16220.10^{-5}$	$3.76976.10^{-5}$	$3.07210.10^{-5}$
Ca	$2.63347.10^{-5}$	$2.39830.10^{-5}$	$1.99107.10^{-5}$
Na	$9.58173.10^{-4}$	$8.66089.10^{-4}$	$7.06808.10^{-4}$
K	$7.33503.10^{-4}$	$6.70065.10^{-4}$	$5.52881.10^{-4}$
P	$5.11462.10^{-6}$	$4.63816.10^{-6}$	$3.79415.10^{-6}$
O	$2.44225.10^{-2}$	$2.20917.10^{-2}$	$1.71157.10^{-2}$
Mn	$9.75005.10^{-6}$	$8.02455.10^{-6}$	$7.75574.10^{-6}$
Total =	$4.95634.10^{-2}$	$4.50815.10^{-2}$	$3.61242.10^{-2}$
μ/ρ =	$0.496 cm^2 g^{-1}$	$0.0451 cm^2 g^{-1}$	$0.0361 cm^2 g^{-1}$
ρ =	$1.03 gcm^{-3}$	$1.03 gcm^{-3}$	$1.03 gcm^{-3}$
μ =	$0.0511 cm^{-1}$	$0.0463 cm^{-1}$	$0.0372 cm^{-1}$
$x_{1/2}$ =	13.58cm	14.96cm	18.63cm
$12x_{1/2}$ =	162.90cm	174.46cm	223.50cm

where background are not zero the Th(cpm), U(cpm) and K(cpm) must be corrected values. Also, as can be seen from Figure 6.4, there is an overlap in the spectra of U and K at the energies used for their measurements. Both U and the Th series contribute to counts in the K window, while the Th series contributes to the counts in the U window. Therefore, these interferences must be taken into account in converting the raw data to element concentrations. Stripping constants (s_1, s_2, s_3) are introduced such that the count rate-concentration conversion equations become:

$$Th(ppm) = Th(cpm).k_1$$

$$U(ppm) = [U(cpm)-s_1.Th(cpm)].k_2$$

$$K(\%) = [K(cpm)-s_2.(U(cpm)-s_3.Th(cpm))].k_3$$

For the determination of these constants, sites with known U, Th and K concentrations, and where the U and Th decay series are in equilibrium, are required. As pointed out previously, such sample sites must have an areal radius of about 1m and extend to a depth of about 10cm. The instruments manufacturers' use calibration pads for the determination of these constants. However, as the electronic components in the instrument age these constants change and need to be checked regularly. Values of the constants as determined by the manufacturer and others are given in

Table 6.10. The constant k_3, for the ^{40}K channel is not provided by the manufacturers, but the spectrometer fitted with a GPX-21 detector shows a very large error in the constant. In this study, the constant was determined by comparing chemical determinations of K_2O by XRF analysis with determinations from the spectrometer using the stripping constants as supplied by the manufacturer.

It must be emphasised that the constants were determined without applying any initial corrections to the data. In practice, the measurement of the background in each window is very difficult because, as pointed out previously, gamma-rays are received from all areas within a radius of approximately 100cm about the detector. Therefore, to accurately measure the background, an area of the same radius must be shielded. However, the value of the background can be estimated by comparing the results of gamma-ray spectrometric determinations with the chemically analysed compositions. The results of the in-situ gamma-ray spectrometric determinations on the Jos Plateau and the laboratory determinations on samples from the Jos Plateau and the kaolinised granite from Bodmin Moor, are shown in Tables 6.11 to 6.14.

6.7 Discussion of Results

Before the results are discussed in detail, a few points need to be considered. Firstly, whenever possible the DISA 400 was used in the collection of gamma-ray spectrometry data but on some

Table 6.10: Calibration and stripping constants for the DISA 400 portable gamma-ray spectrometer.

Constant	Manufacturer	Cassidy	Used in this study
k_1	0.1205	0.1190	0.1205
k_2	0.0556	0.0512	0.0556
k_3	-	0.0047	0.0060
s_1	0.62	0.49	0.62
s_2	0.79	0.99	0.79
s_3	1.23	1.11	1.23

Cassidy (1972).

occasions, equipment failure meant that the GR-410 had to be used. To utilise both sets of results it was necessary to convert readings from the GR-410 into a form similar to those from the DISA 400 by finding a correlation factor between the two spectrometers. Secondly, wherever possible the samples for chemical analysis were collected from rock outcrops where gamma-ray spectrometric determinations were obtained, so as to directly compare the results from both methods. However, at many sites this was not possible and the samples had to be collected from loose surface material. Soil samples showing the texture of the rock surface investigated by gamma-ray spectrometry were taken as near enough to the outcrops as possible.

The equivalent radioelement concentrations, eX and their concentrations determined chemically by XRF methods, cX, for the samples analysed in-situ and those analysed in the laboratory, are given in Tables 6.11 to 6.14. Comparison of the chemical determinations with the count rates from the spectrometer windows are used to estimate the background radiation in the counting environment. Figures 6.9 - 6.14 show such comparisons. These give the background levels as 122, 182, and 91 counts per minute for the K, U and Th channels, respectively, for the measurements on the Jos Plateau, and 552, 602 and 228 counts per minute for the laboratory determinations. The greater background values for the laboratory measurements reflect the greater sources of extraneous gamma-rays in the laboratory environment. However, even the background for

Table 6.11: Results of in-situ gamma-spectrometric determinations for Nigerian Younger Granites.

Sample	TC	K	U	Th	eK	eU	eTh	cU	cTh
R3	28678	1698	982	467	4.18	33.78	62.27	12	39
R14	18452	1682	379	310	7.58	9.11	41.33	5	18
R16	32303	1708	889	655	3.64	23.56	87.33	16	63
R20	18776	1568	443	348	6.35	11.08	46.40	9	28
R21	18698	1493	435	323	6.03	11.45	43.07	11	30
R28	24351	1766	654	463	6.09	17.90	61.73	11	34
R43	16927	1249	377	228	5.22	11.49	30.40	14	31
R44	16769	1416	388	308	5.82	9.61	41.07	10	27
R45	17762	1481	441	340	5.84	11.23	45.33	10	32
R46	18425	1598	416	322	6.81	10.55	42.93	8	23
R48	26817	1997	676	468	7.46	18.82	62.40	17	42
R49	22772	1594	600	447	5.30	15.75	59.60	9	40

Notes: TC, K, U and Th are the counts in cpm in total count, K, U and Th windows, eK, eU, and eTh are % equivalent K, ppm U, and ppm Th, and

cU and cTh are chemical U and Th in ppm.

: All sample numbers are prefixed JP.

Table 6.12: Results of laboratory gamma-spectrometric determination on crushed Younger Granite rocks.

Sample	TC	K	U	Th	eK	eU	eTh	cK	cU	cTh
R1	16837	1181	466	214	3.29	18.53	25.77	5.21	8	24
R3	17475	1230	580	238	2.86	24.05	28.71	5.23	12	39
R4	17518	1254	586	238	2.98	24.37	28.72	4.79	5	19
R5	17275	1230	853	231	1.62	39.44	27.88	5.08	5	27
R7	17475	1254	615	235	2.87	26.09	28.32	5.23	9	25
R8	17356	1238	612	235	2.79	25.93	28.29	4.80	9	22
R9	17279	1230	638	239	2.59	27.24	28.74	4.19	-	17
R10	17786	1261	645	250	2.66	27.24	30.09	5.28	4	34
R11	17477	1214	645	238	2.47	27.65	28.64	4.99	6	27
R12	13639	1252	636	241	2.72	27.07	29.03	5.07	6	18
R13	17648	1270	660	253	2.62	27.98	30.45	4.45	7	30
R14	17573	1261	638	241	2.76	27.18	29.02	5.40	5	18
R15	16277	1214	829	210	1.79	38.85	25.36	4.78	9	37
R16	18074	1273	657	253	2.65	27.83	30.46	5.06	16	63
R17	17088	1277	835	231	1.99	38.45	27.85	5.11	20	73
R18	17359	1253	595	250	2.85	24.46	30.07	5.13	10	28
R19	17245	1245	581	244	2.90	23.88	29.46	4.78	11	26
R20	16909	1268	556	238	3.21	22.74	28.63	5.18	9	28
R21	19258	1151	779	190	1.81	36.79	22.88	5.15	11	30
R23	17103	1245	553	238	3.09	22.56	28.66	5.41	9	25
R24	17065	1229	556	237	2.98	22.72	28.61	4.69	8	24
R25	17109	1221	523	234	3.11	20.98	28.24	5.41	11	27
R28	17474	1237	552	229	3.11	22.80	27.61	4.67	11	34
R29	17512	1244	548	234	3.14	22.36	28.23	4.26	13	48
R30	16141	1197	498	204	3.32	20.67	24.52	4.96	15	34
R31	17610	1214	515	220	3.21	21.00	26.56	3.91	20	33
R32	17592	1236	569	234	2.99	23.53	28.23	4.34	12	33
R33	18149	1297	678	256	2.67	28.86	30.89	4.81	16	34
R34	13830	2069	390	244	8.76	13.23	29.46	5.87	5	22
R35	19779	1669	656	139	5.88	31.70	16.71	4.78	7	26
R36	17995	1269	655	250	2.67	27.79	30.07	4.15	12	40
R37	17631	1244	614	243	2.76	25.79	29.25	4.32	9	35
R38	17765	1221	603	244	2.66	25.10	29.44	4.43	24	36
R39	18112	1261	686	256	2.41	29.33	30.89	4.49	11	44
R41	18191	1280	697	260	2.45	29.82	31.30	4.93	13	36
R42	18033	1265	647	253	2.65	27.23	30.47	5.10	17	30
R43	17997	1261	687	256	2.42	29.34	30.87	4.68	14	31
R44	18771	1092	797	184	1.41	37.97	22.22	5.35	10	27
R45	18035	1277	672	253	2.60	28.65	30.50	5.11	10	32
R46	20516	1410	884	281	2.19	39.46	33.81	5.21	8	23
R48	20926	1430	889	289	2.23	39.48	34.78	5.36	17	42
R49	20243	1359	858	277	2.03	38.17	33.39	4.72	9	40
R55	12688	2211	301	286	9.72	6.88	34.40	5.31	10	37
R60	20127	1394	583	282	3.52	22.67	33.96	5.53	8	22
R63	20321	1410	856	292	2.24	37.49	35.22	4.56	16	44

Note: TC, K, U and Th are counts for the total count window and the K, Th and U windows in cpm,
eK, eU, and eTh are equilvalent K, U nd Th concentrations in % (for K) and ppm (for U and Th) and
cK, cU, and cTh are concentrations of K, U, and Th determined by XRF analysis.
: All sample numbers are prefixed JP.

Table 6.13: Results of gamma-ray spectrometric determinations on kaolinised granites.

Sample	TC	K	U	Th	eK	eU	eTh	cK	cU	cTh
P1	2507	260	54	33	1.05	1.87	4.03	5.81	7	13
P2	2432	245	54	28	1.00	2.02	3.37	4.96	10	7
P3	2379	242	55	27	0.98	2.12	3.29	5.35	8	5
P4	2317	202	47	18	0.85	1.99	2.22	5.21	10	4
P5	2343	226	48	23	0.96	1.86	2.74	5.57	8	5
P7	2654	267	60	35	1.06	2.12	4.16	6.47	8	13
P8	2747	248	55	30	1.00	1.99	3.66	5.38	5	10
P9	2561	260	59	31	1.05	2.22	3.68	5.44	9	13
P10	2537	267	56	28	1.12	2.15	3.43	6.37	8	6
P11	2797	262	75	27	1.01	3.25	3.20	4.98	12	6
P12	2440	253	51	28	1.06	1.87	3.38	5.48	10	7
P13	2437	250	50	23	1.09	1.98	2.76	6.62	8	6
P14	2113	212	53	25	0.84	2.07	2.97	4.69	7	6
P15	2364	219	48	19	0.94	2.02	2.31	5.32	7	6
P16	2408	258	53	26	1.10	2.02	3.17	5.21	7	4
P17	2486	253	55	31	1.02	1.97	3.76	6.01	6	10
P18	2437	244	53	28	1.01	1.97	3.34	5.90	10	7
P19	2623	264	64	32	1.04	2.46	3.83	6.09	11	10
P20	2486	570	57	24	2.98	2.33	2.86	6.11	10	7
P21	2205	179	55	26	0.61	2.15	3.18	6.71	9	10
P22	2471	264	55	27	1.12	2.13	3.21	1.36	9	8
P23	2139	486	48	21	2.53	1.93	2.48	5.64	10	5
P24	2332	511	52	23	2.65	2.09	2.74	5.18	7	5
P25	2321	238	50	26	0.99	1.87	3.15	5.49	6	6
P26	2132	240	54	29	0.96	2.02	3.49	5.78	9	10
P27	2802	600	71	27	3.06	3.03	3.24	6.90	20	8
P28	2282	212	54	26	0.82	2.10	3.11	4.70	8	9
P29	2540	260	61	28	1.06	2.42	3.39	6.14	11	7
P30	2313	174	41	17	0.71	1.70	2.10	5.09	9	8
P31	6042	277	59	31	1.15	2.18	3.76	6.24	9	12
P32	2304	206	45	20	0.87	1.79	2.46	5.58	7	5
P33	2386	242	52	29	0.99	1.87	3.45	5.06	8	7
P34	2476	257	55	28	1.07	2.09	3.40	5.48	10	8
P35	2748	568	68	23	2.91	2.94	2.81	5.40	17	6
P36	2875	574	74	26	2.90	3.19	3.13	5.11	24	7
P37	2442	260	52	30	1.09	1.87	3.61	6.01	7	11
P38	2394	252	54	29	1.04	1.99	3.52	4.89	8	6
P39	2322	225	47	23	0.95	1.84	2.75	5.45	8	5
P40	2409	256	54	25	1.09	2.16	2.96	5.98	7	8
P41	2437	253	58	27	1.04	2.31	3.27	6.01	10	8
P42	2195	206	45	24	0.84	1.68	2.86	6.31	8	6
P43	2255	214	52	27	0.83	1.95	3.31	3.63	7	9
P44	2452	240	54	27	0.98	2.08	3.23	5.37	9	7
P45	2443	256	50	30	1.07	1.76	3.60	5.92	6	11
P46	2357	232	50	27	0.95	1.84	3.24	4.72	8	7
P47	2602	243	60	26	0.97	2.45	3.11	5.17	16	7
P48	2307	175	45	20	0.69	1.82	2.40	4.78	6	8
P49	2483	190	49	20	0.75	2.04	2.40	5.71	10	13
P50	2650	258	54	26	1.09	2.11	3.15	8.05	12	14

Continued...

Table 6.13, Continued.

P51	2656	291	61	28	1.25	2.43	3.31	5.29	8	14
P52	2565	121	-49	21	0.33	2.01	2.56	7.51	11	10
P53	2690	273	65	27	1.12	2.69	3.25	5.48	9	10
P54	2676	236	65	24	0.92	2.78	2.89	6.16	11	10
P55	2617	253	61	33	0.98	2.26	4.02	6.07	17	13
P56	2387	211	43	18	0.93	1.78	2.17	6.48	18	9
P57	2579	244	60	25	0.99	2.47	2.99	6.23	14	10
P58	2544	265	62	25	1.11	2.55	3.03	6.72	8	12
P59	2080	177	48	23	0.66	1.86	2.82	5.47	23	8
P60	2295	205	50	18	0.86	2.13	2.16	5.08	7	7
P61	2222	236	60	26	0.93	2.44	3.15	5.27	12	8
P62	2738	244	55	28	1.00	2.11	3.31	5.24	10	10
P63	2223	186	53	24	0.69	2.11	2.84	2.03	7	7
P64	2571	255	60	28	1.03	2.33	3.42	6.41	10	9
P65	2612	466	60	25	2.32	2.45	3.01	6.38	11	20
P66	2518	261	54	31	1.08	1.95	3.70	5.73	8	10
P67	2466	256	55	28	1.07	2.07	3.36	5.32	6	5
P68	2431	237	50	22	1.02	2.01	2.69	5.95	11	11
P69	2453	234	50	27	0.96	1.82	3.26	5.59	6	10
P70	2458	241	52	31	0.96	1.83	3.75	5.59	8	13

Note: TC, K, U and Th are counts for the total count window and the K, Th and U windows in cpm,
eK, eU, and eTh are equilvalent K, U nd Th concentrations in % (for K) and ppm (for U and Th) and
cK, cU, and cTh are concentrations of K, U, and Th determined by XRF analysis.

Table 6.14: Results of gamma-spectrometric determinations on soil of the Nigerian Younger Granites.

Sample	TC	K	U	Th	eK	eU	eTh	cK	cU	cTh
JPS2	19818	1367	836	288	2.10	36.54	34.75	4.58	13	32
JPS7	19158	1311	1095	267	0.71	51.65	32.15	3.25	8	24
JPS8	20213	1420	858	290	2.31	37.70	34.93	3.38	7	22
JPS9	19421	1333	809	280	2.10	35.33	33.71	2.69	4	18
JPS13	20158	1397	837	285	2.30	36.74	34.31	1.07	6	21
JPS14	19476	1322	813	273	2.06	35.81	32.87	0.24	12	31
JPS15	19980	1350	829	284	2.07	36.29	34.18	0.68	13	28
JPS16	20216	1369	815	295	2.17	35.13	35.55	0.37	8	25
JPS17	19528	1345	793	277	2.26	34.50	33.42	0.18	23	32
JPS20	19584	1333	805	285	2.08	34.91	34.29	1.30	10	23
JPS23	19711	1345	797	295	2.11	34.13	35.53	0.73	10	28
JPS24	20275	1362	833	280	2.15	36.66	33.72	0.97	11	28
JPS28	19987	1356	812	280	2.22	35.53	33.69	1.62	9	25
JPS29	20104	1329	813	285	2.01	35.35	34.34	0.30	16	37
JPS31	19423	1334	809	280	2.10	35.32	33.69	2.61	8	24
JPS33	20677	1362	825	288	2.13	35.94	34.65	2.33	12	33
JPS35	18950	1918	815	250	5.79	36.70	30.15	1.13	7	21
JPS36	20446	1373	837	280	2.20	36.91	33.70	1.27	5	14
JPS39	19701	1333	789	275	2.23	34.36	33.11	0.79	10	29
JPS41	20104	1362	829	280	2.17	36.46	33.69	0.21	12	42
JPS42	19356	1306	796	280	1.99	34.62	33.73	0.60	7	20
JPS43	20047	1356	801	295	2.16	34.34	35.53	4.12	6	23
JPS44	19586	1317	801	275	2.08	35.05	33.10	3.78	7	28
JPS45	18306	1345	715	235	2.94	31.62	28.33	3.07	9	31
JPS46	19931	1373	837	285	2.16	36.73	34.32	3.45	7	25
JPS48	20107	1380	841	290	2.15	36.80	34.90	1.53	9	27
JPS49	19535	1317	837	285	1.82	36.71	34.37	0.50	19	30
JPS50	19416	1372	806	285	2.30	35.00	34.36	0.32	13	22
JPS52	20158	1362	829	280	2.17	36.44	33.72	2.03	12	19
JPS53	20734	1397	833	295	2.25	36.16	35.50	1.57	8	20
JPS54	20212	1374	817	278	2.32	35.85	33.44	1.02	8	25
JPS55	19817	1328	825	285	1.95	36.04	34.33	2.79	8	19
JPS56	19476	1362	809	280	2.27	35.31	33.74	2.79	6	17
JPS57	19757	1373	784	275	2.48	34.12	33.16	3.75	8	24
JPS58	19360	1329	792	275	2.18	34.58	33.11	0.44	7	24
JPS59	20443	1342	815	262	2.25	36.30	31.54	0.26	8	26
JPS60	19474	1351	1235	280	0.18	58.98	33.76	0.64	11	23
JPS61	19589	1329	829	275	2.01	36.62	33.13	5.19	9	28
JPS62	19593	1341	805	280	2.16	35.08	33.75	4.52	7	20
JPS65	19991	1345	833	280	2.05	36.65	33.75	0.19	5	21
JPS66	19358	1356	825	275	2.20	36.37	33.09	0.37	12	24
JPS67	19905	1385	858	280	2.17	38.04	33.74	1.08	7	26
JPS68	19073	1282	767	272	2.04	33.27	32.82	0.09	8	42

Note: TC, K, U and Th are counts for the total count window and the K, Th and U windows in cpm,
eK, eU, and eTh are equilvalent K, U nd Th concentrations in % (for K) and ppm (for U and Th) and
cK, cU, and cTh are concentrations of K, U, and Th determined by XRF analysis.

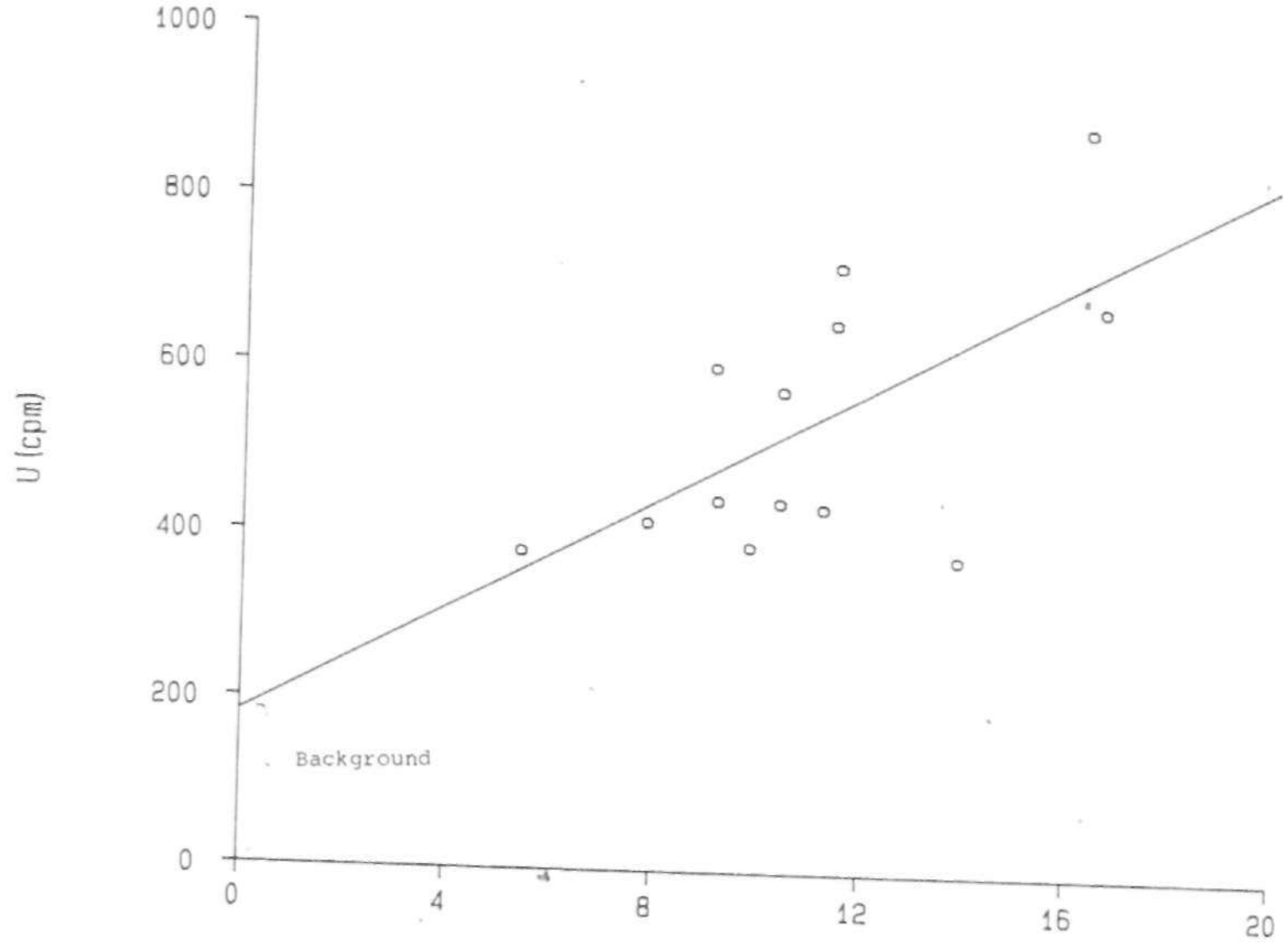


FIGURE 6.9 Correlation of U(ppm) with U(cpm) for Nigerian Younger Granite (for in-situ determinations)

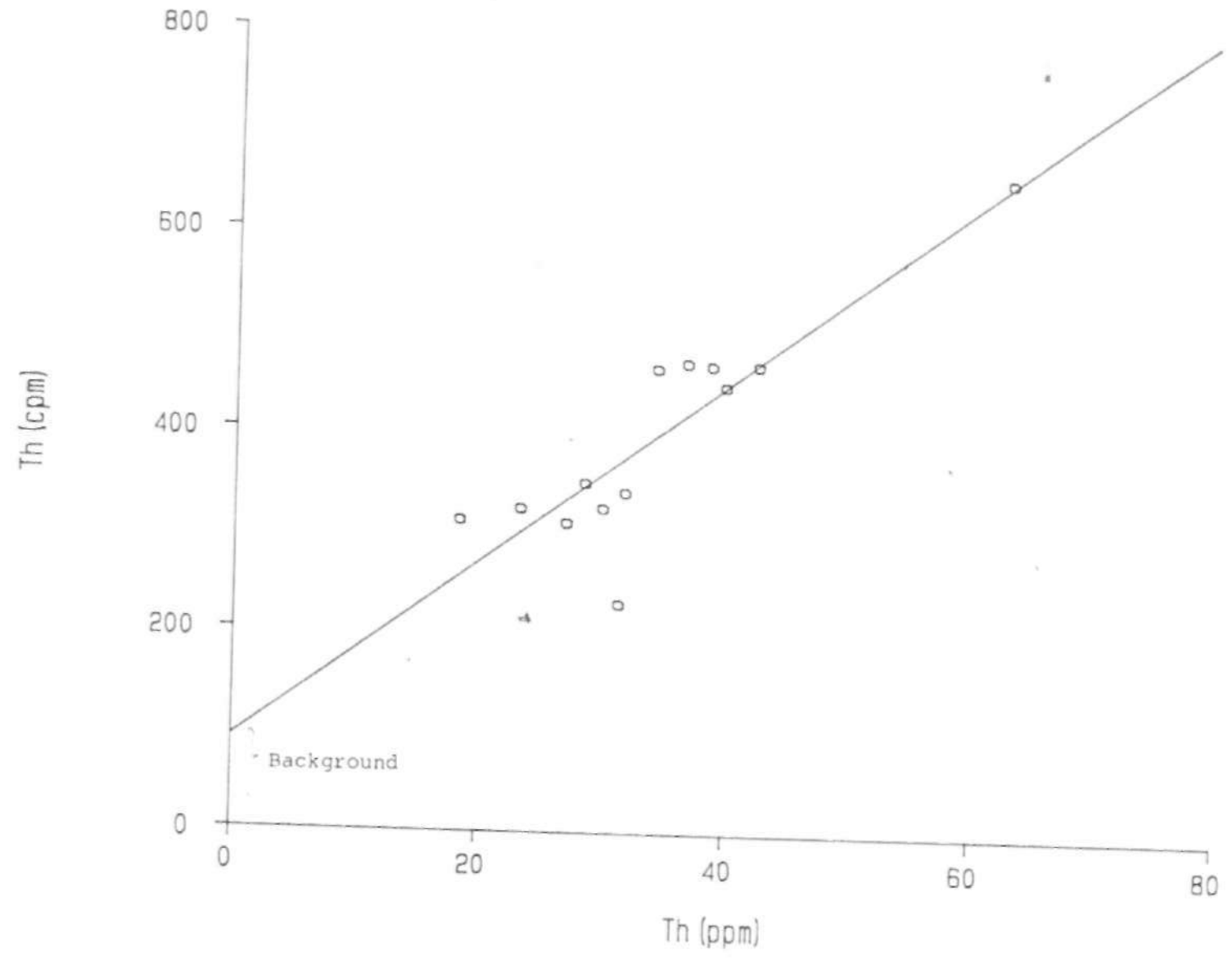


FIGURE 6.10 Correlation of Th (ppm) with Th (cpm) for Nigerian Younger Granite (for in-situ determinations)

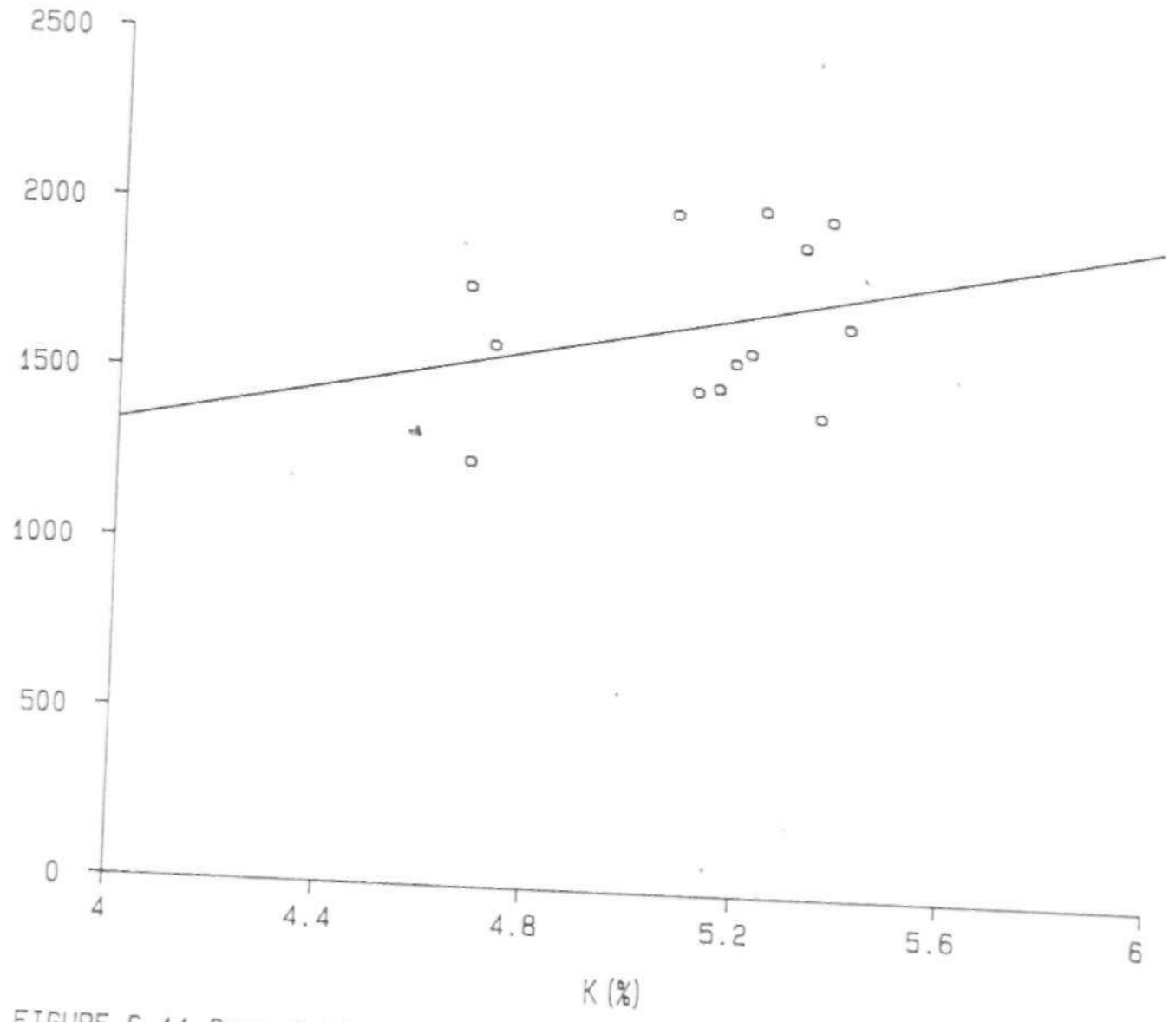


FIGURE 6.11 Correlation of K(%) with K(cpm) for Nigerian Younger Granite (for in-situ determinations)

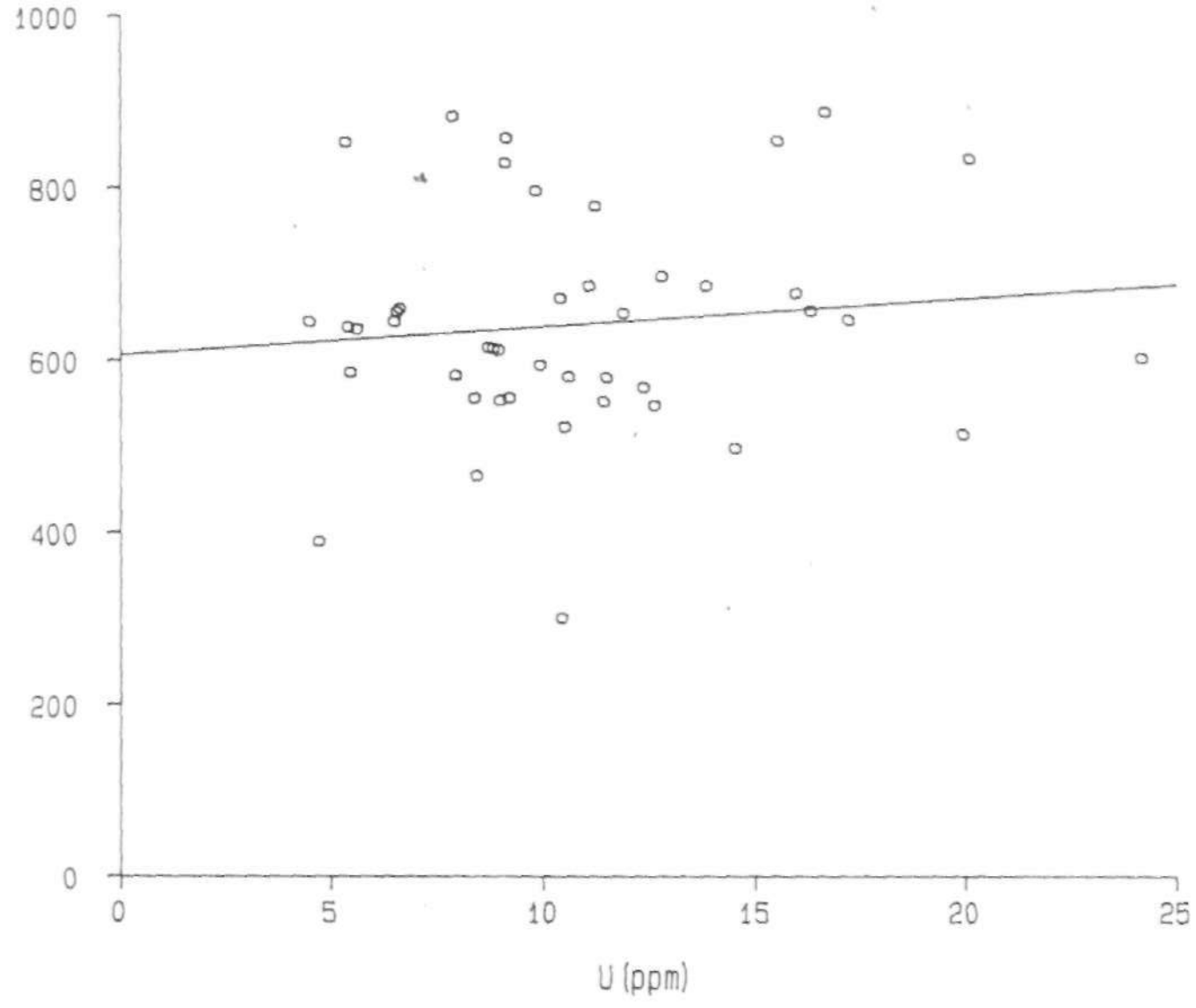


FIGURE 6.12 Correlation of U(ppm) with U(cpm) for Nigerian Younger Granite (for laboratory determinations)

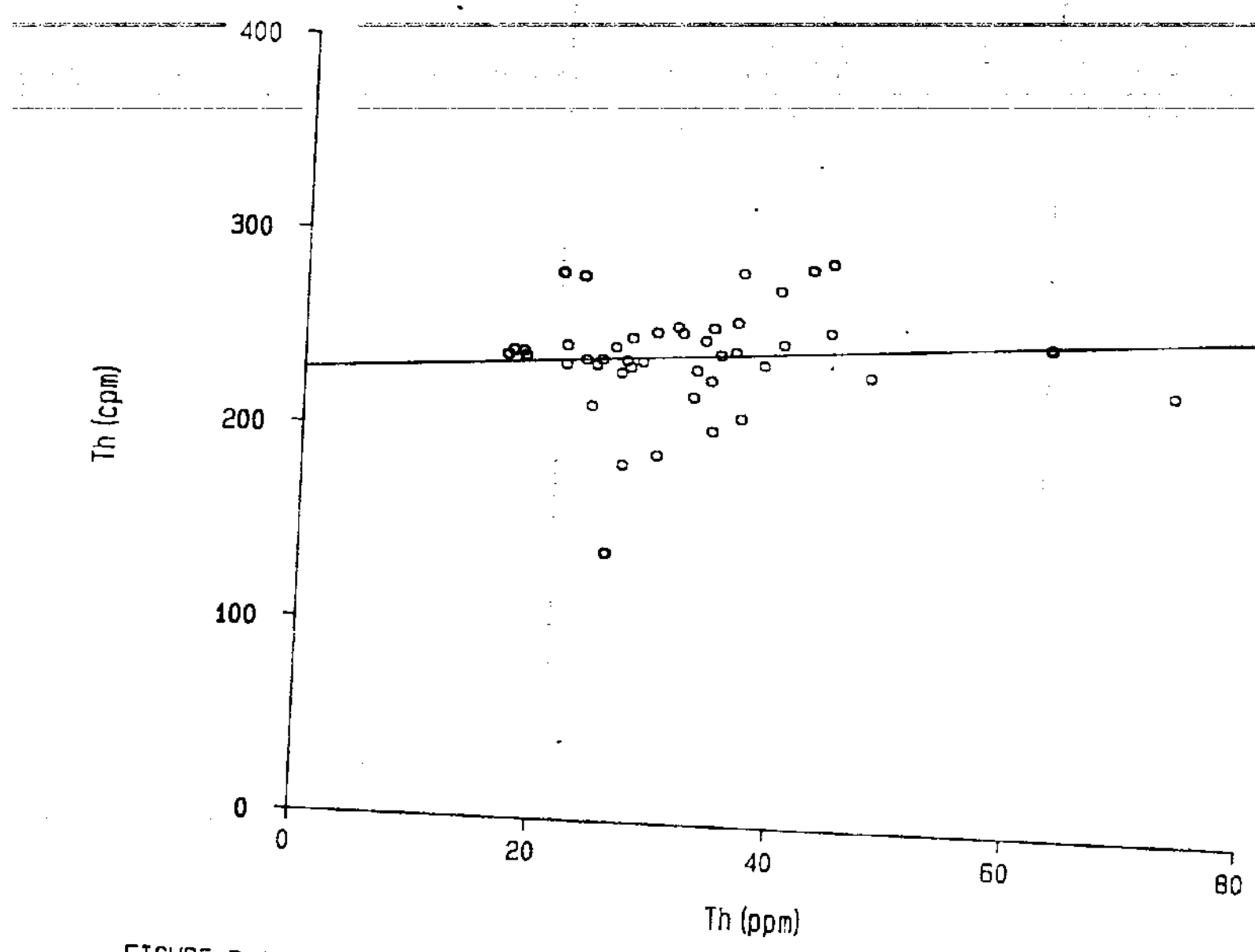


FIGURE 6.13 Correlation of Th (ppm) with Th (cpm) for Nigerian Younger Granite (for laboratory determinations)

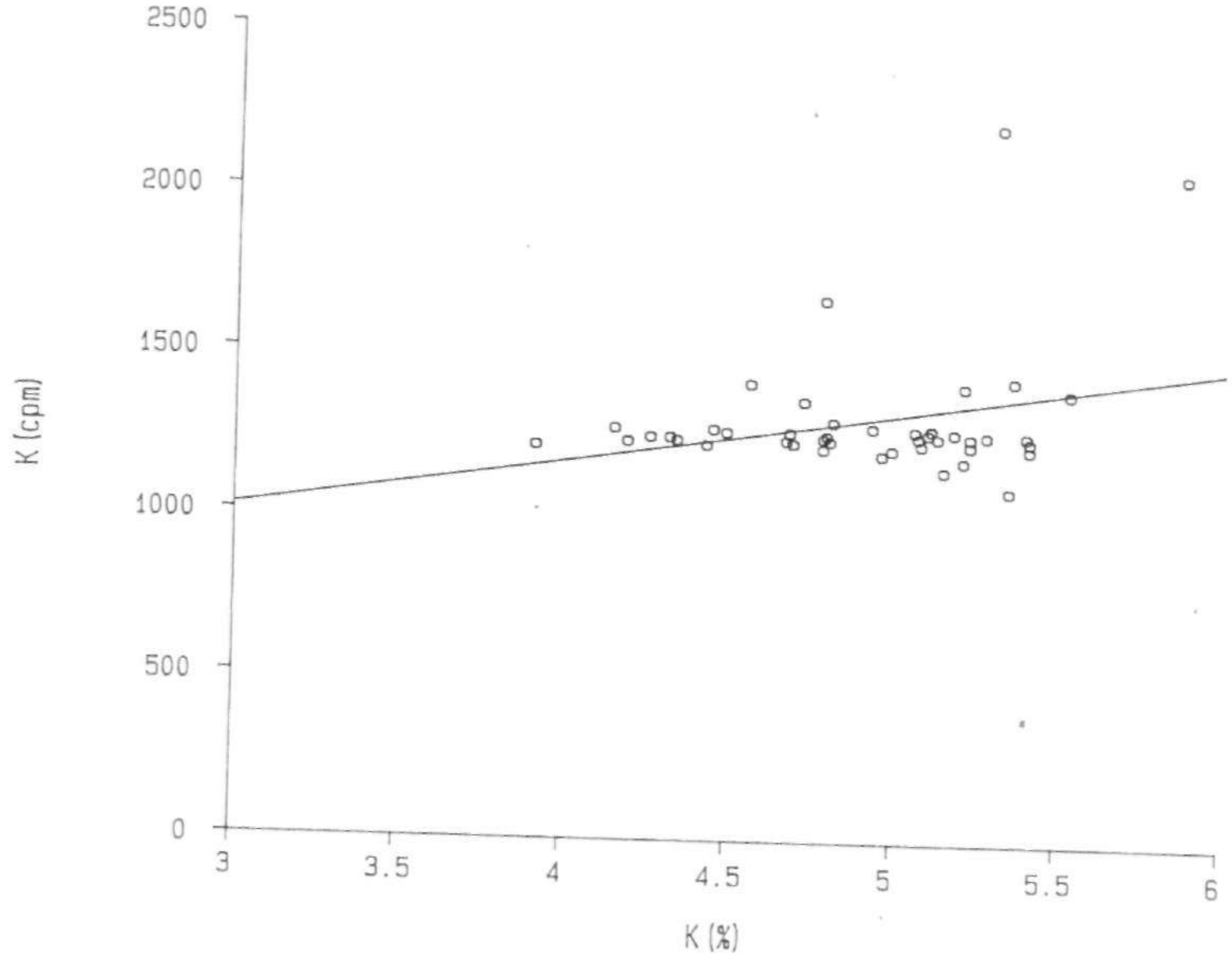


FIGURE 6.14 Correlation of K(%) with K(cpm) for Nigerian Younger Granite (for laboratory determinations)

gamma-radiation on the Jos Plateau is very high. This was recognised by Dewu (1986), and might be from cosmic-ray contributions, because of the high altitude of the Plateau. The spectrometer used in the laboratory determinations on samples collected from the Jos Plateau could not be properly calibrated, so that readings taken on the same spot were not reproduceble. The results obtained from these readings may, therefore,, not be reliable and they will not be discussed further.

As described above, in the measurements of the kaolinised samples, the sample container was placed on Pb blocks thick enough to absorb any gamma-ray contributions from beneath the beaker. Similarly, lateral contributions were also removed by the blocks of Pb erected around the beaker (Figure 6.8). Therefore, the only possible background contributions that may reach the detector are from gamma-rays in the air in the space within the Pb casing, which are negligible. Therefore, background in these measurements have been eliminated for all practical purpose, so no attempt was made at quantitative estimation.

In all the gamma-spectrometric determinations, a counting time of 35 minutes was used. Counts greater than 400 and 22 per minute were obtained on the Th window for the in-situ and the laboratory determinations, respectively. The granite samples for laboratory counting were crushed with a jaw crusher. Most of the kaolinised samples were, however, so friable that after drying, crushing was achieved by simply squeezing with the hand. Only

occasionally, where the samples were hard, was the jaw crusher used. Comparisons of the results obtained from in-situ and laboratory determinations show that the laboratory determinations yield results which are much lower than those determined in-situ. This is probably due to the smaller volume of the sample analysed in the laboratory, and the difficulty of correcting exactly for the differences in effective sample geometry. However, an approximate correction can be found. Thus, in the case of the samples in the laboratory the half-thickness values are 8.58cm, 7.0cm and 18.63cm for the kaolinised granite, the fresh granite samples and the soil samples, respectively, whereas the depth of sample used in the laboratory determinations is 11.5cm. This means that the detected gamma-rays come only from approximately a $2x_{1/2}$ zone in the 2π sample-detector geometry. Therefore, only about 75% of the gamma-rays are detected. Furthermore, the lateral extent of the sample is such that it is the same as the detector, thereby further reducing the sampling area. The ratio of the volume sampled to the total volume in a 2π geometry (that is the volume of the sample contributing 99% of the gamma-rays) is found to be about 1:8. Hence, to a rough approximation, only about 15% of the emitted gamma-rays were recorded. In other words, recorded count rates are only 15% of their potential level. In fact in these experiments, the ratio was found to be only 1:1.8. This difference cannot be explained just by an error in the estimation of the correction factor. It clearly shows that the Jos Plateau Younger Granite is

enriched with U and Th, with a high Th:U ratio. The ratio ranges from 2 to 4. In the kaolinised granite, the Th:U ranges from 1 to 2. These ratios compare well with the ratios obtained from the chemical determinations. Results obtained from the gamma-ray spectrometric determinations give average values of 17.51ppm U, 47.00ppm Th and 4.11% K for the Younger granites. The same values for the kaolinised granites are, 2.12ppm, 3.14ppm and 0.97%, respectively.

Figures 6.15 to 6.20 show plots of equivalent element concentrations (eX) against chemically determined concentrations (cX), where gamma-ray spectrometry and XRF techniques have been used, respectively. The plots of both U and Th show that there is a good correlation between such analyses for both the in-situ and the laboratory determinations. In such plots the scatter of points about a regression line passing through the points can be used to determine the error in the correlation. The error (SE) in the gamma-ray spectrometric determinations can be calculated using the standard statistical formula:

$$SE = \mathrm{sqrt}(((eX-\bar{eX})^{2})/n-2)$$

where $\bar{eX}$ is the fit on the value of eX, by regressing a line through the plots of eX against cX.

In this plot, the error may not be the only cause

for the scatter of the points. Radioactive disequilibrium in the U or Th decay series will also be a contributing factor. Where error is the cause, for statistically significant measurements (N>30; Spiegel, 1961), 68% of the points should lie within +/-SE. Two lines each 2SE apart about the regression lines for U and Th are shown as broken lines for the in-situ determinations (Figures 6.15, 6.16). They show that more than 80% of the points lie within ±1 SE limit, which indicates both series are largely in equilibrium. The few points which plot outside these lines may be caused by sampling error, inhomogeneity in the samples and effects of geometry (Killeen and Carmichael, 1970), or because the U and/or Th decay series in these samples are not in equilibrium. Similar plots the the in-situ determinations are shown in Figures 6.18 to 6.20. These also suggest that the U and Th decay series are in equilibrium.

As noted above, disequilibrium in the U decay series can also be investigated by comparing readings from the Total Count channel with those due to ^{214}Bi in the 1.76MeV channel. Since ^{40}K has no intermediary daughters, there is no disequilibrium problem associated with it's measurement. Therefore, any increase in K concentration, indicated by an increase in counts from the 1.46 MeV channel, will show a corresponding increase in the Total Count window. Similarly, we have seen that the ^{232}Th decay series only takes about 50 years to reach secular equilibrium. Thus the Th series in geological environments is likely to be in equilibrium unless recent major activity, involving Th mobilisation, has

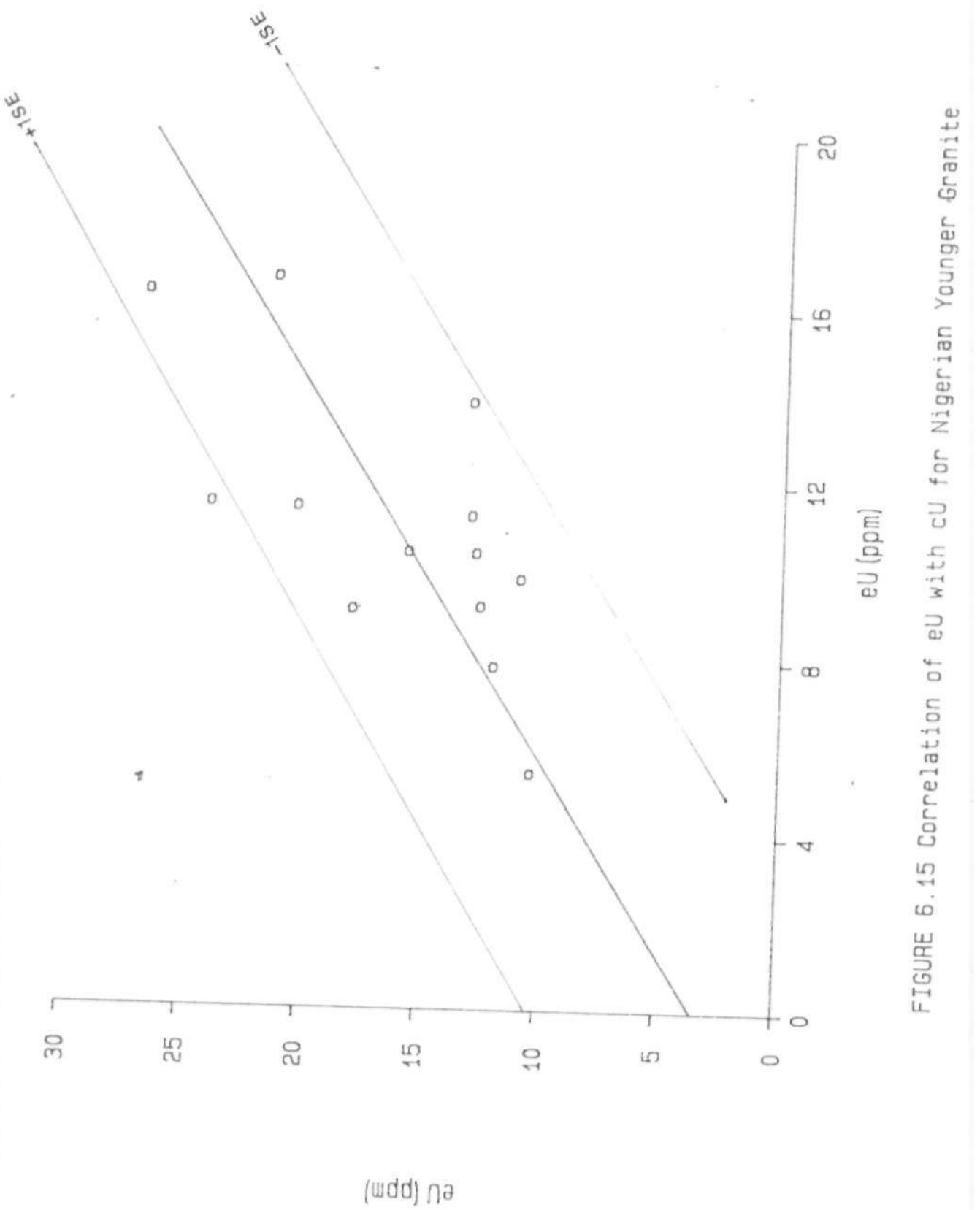


FIGURE 6.15 Correlation of eU with eU for Nigerian Younger Granite

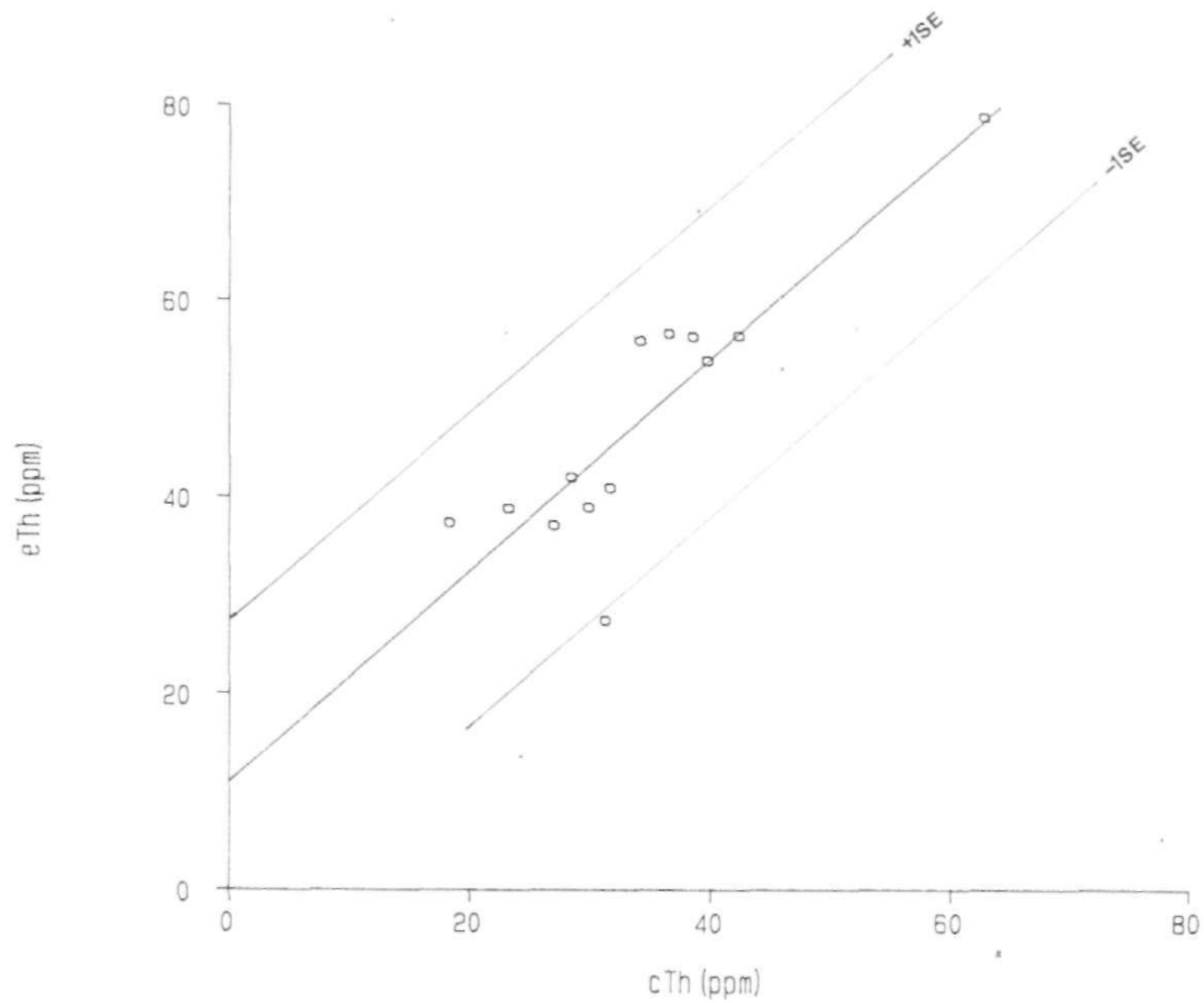


FIGURE 6.16 Correlation of eTh with cTh in for Nigerian Younger Granites.

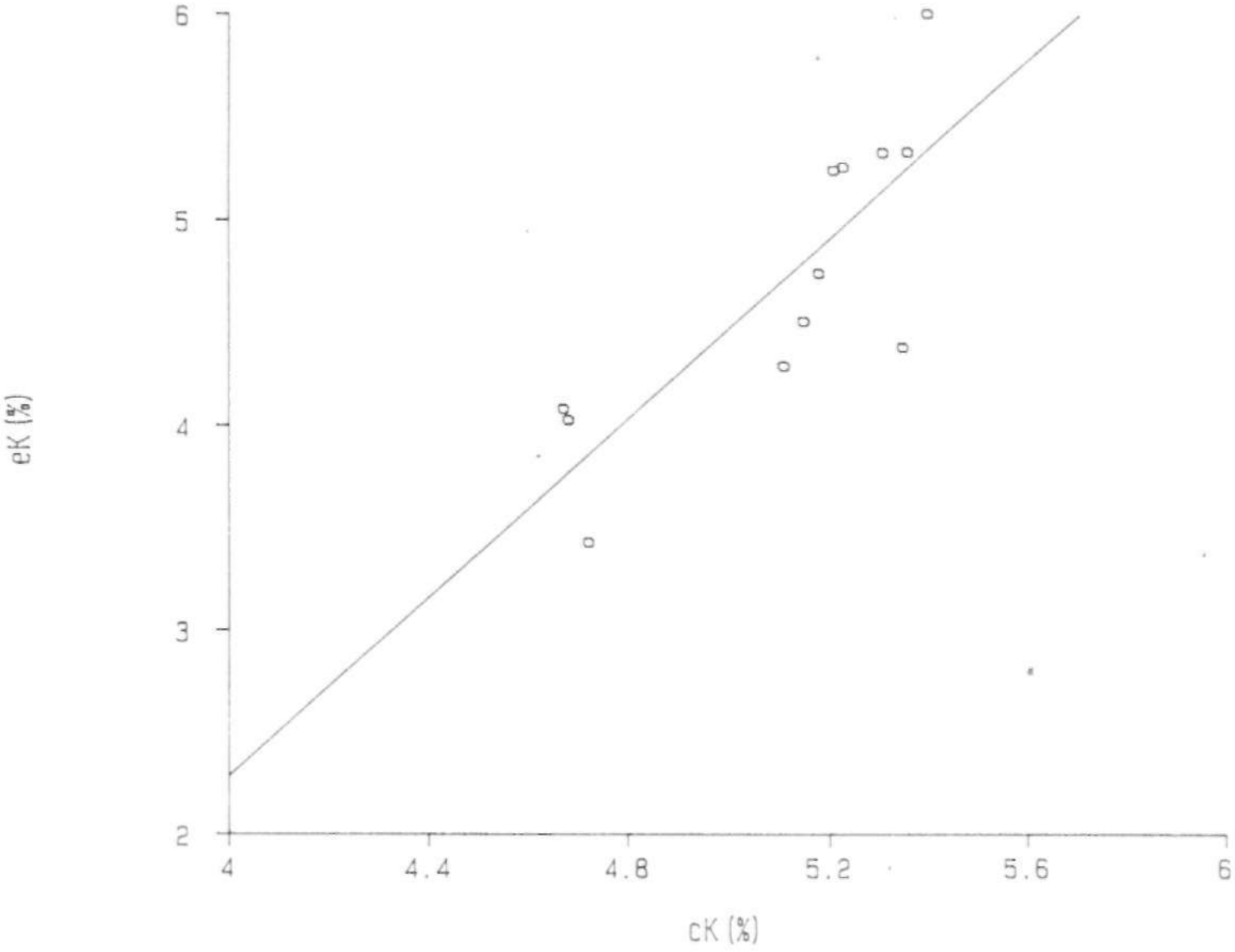


FIGURE 6.17 Correlation of eK with cK for Nigerian Younger Granites

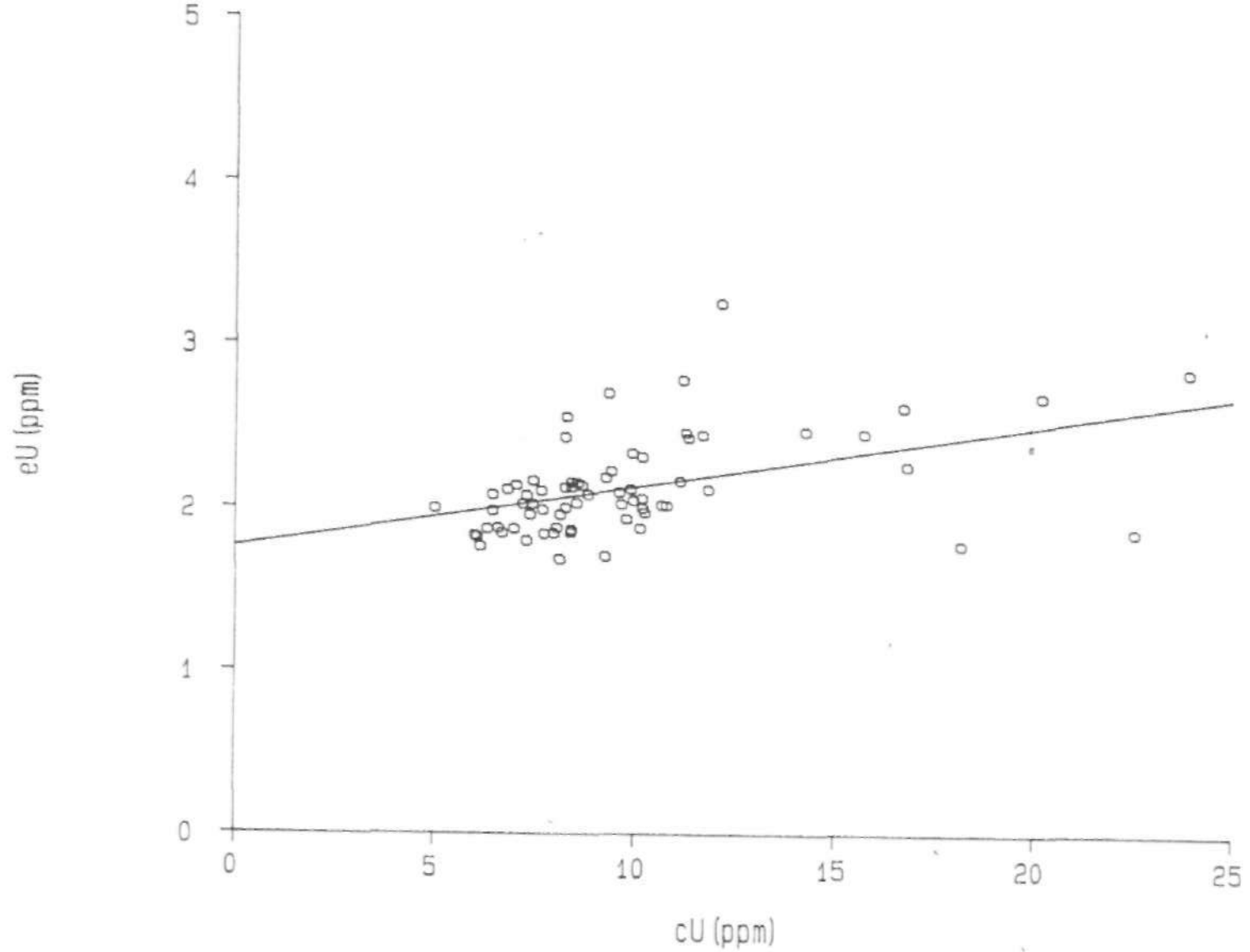


FIGURE 6.18 Correlation of eU with cU for kaolinised granites.

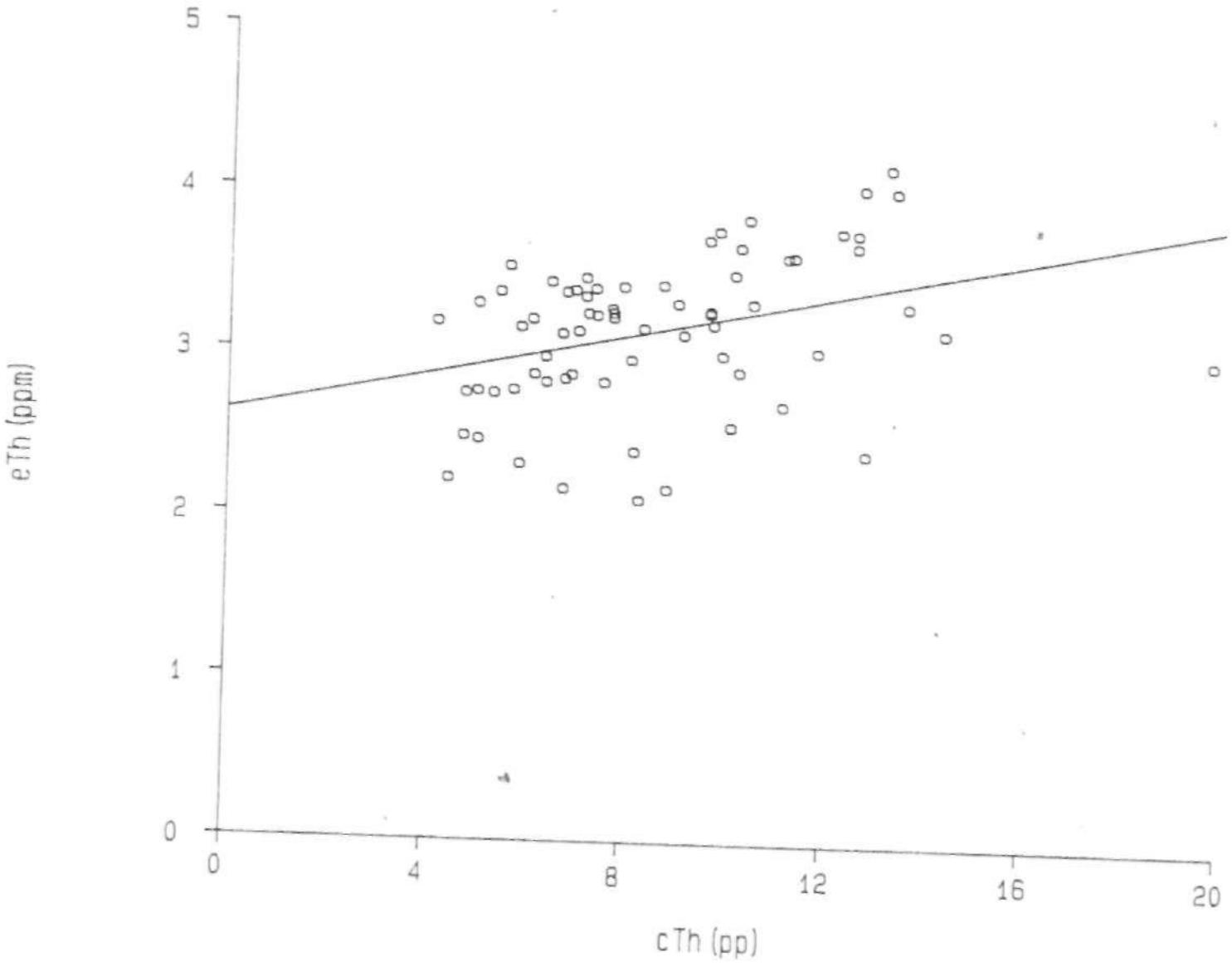


FIGURE 6.19 Correlation of eTh with cTh forkaolinised granites

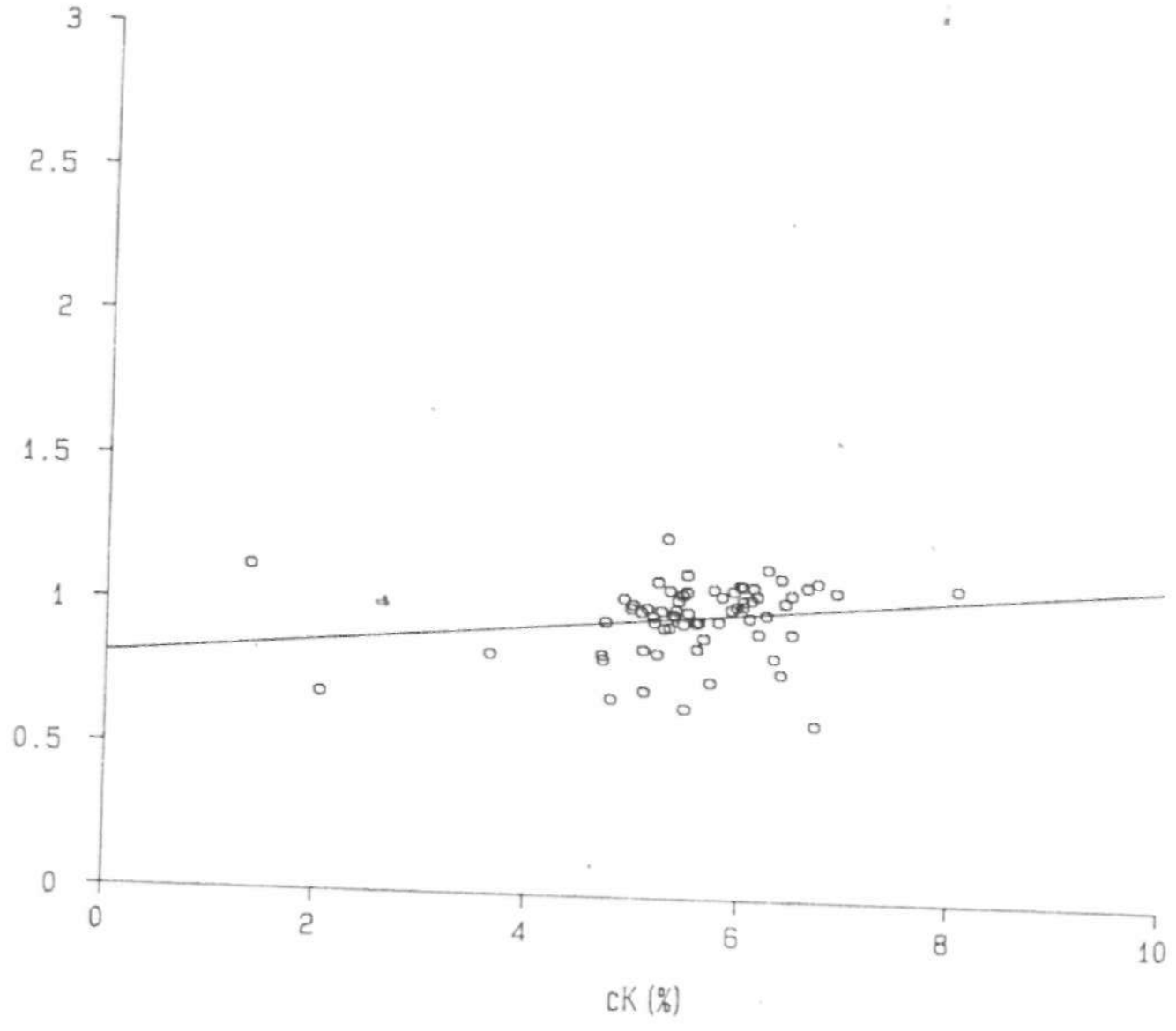


FIGURE 6.20 Correlation of eK with cK for kaolinised granites.

occurred. Consequently, any increase in the 2.62MeV channel will also produce a corresponding increase in the Total Count channel. In the case of the U decay series, however, this relationship is possible only if the ^{234}Th group is in equilibrium with ^{214}Bi. Therefore, a plot of the count rate from measurements made of ^{214}Bi against Total Count would be linear for samples where the decay series is in radioactive equilibrium. Departure from a linear relationship in such a plot may indicate disequilibrium in the decay chain. If the relationship is such that the Total Count increases while the count from ^{214}Bi decreases, then excess activities from the ^{234}Th group exist. This would be most likely due to addition of ^{234}U. Conversely, where an increase in the count from ^{214}Bi is not accompanied by an increase in the Total Count, the cause of disequilibrium is probably the loss of ^{234}U out of the system. To test this method, plots of the count rates on the ^{40}K and ^{208}Tl channels need to be made and examined to see if there is any increase as the count rate in the Total Count channel increase. Plots of the Total count against count in the U channel for the in-situ field determinations and for determinations on the kaolinised samples are shown in Figure 6.21 and 6.22, respectively. These also suggests that the U decay series is in equilibrium.

However, it is important to note that the results from this method should be treated with care. This is because of the problems associated with such comparisons which have already been discussed. Killeen and Carmichael (1970) found that where there is a large

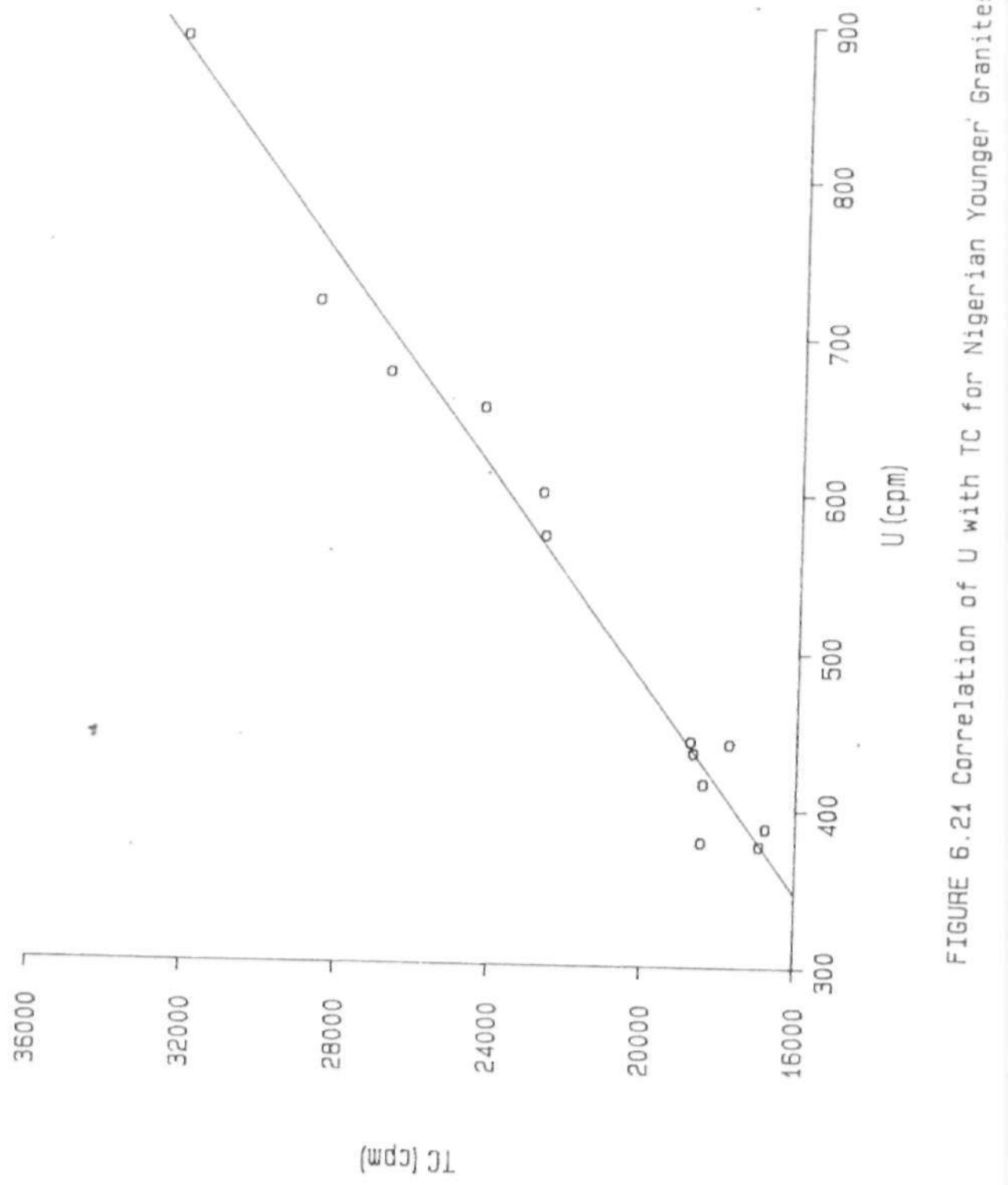


FIGURE 6.21 Correlation of U with TC for Nigerian Younger Granites

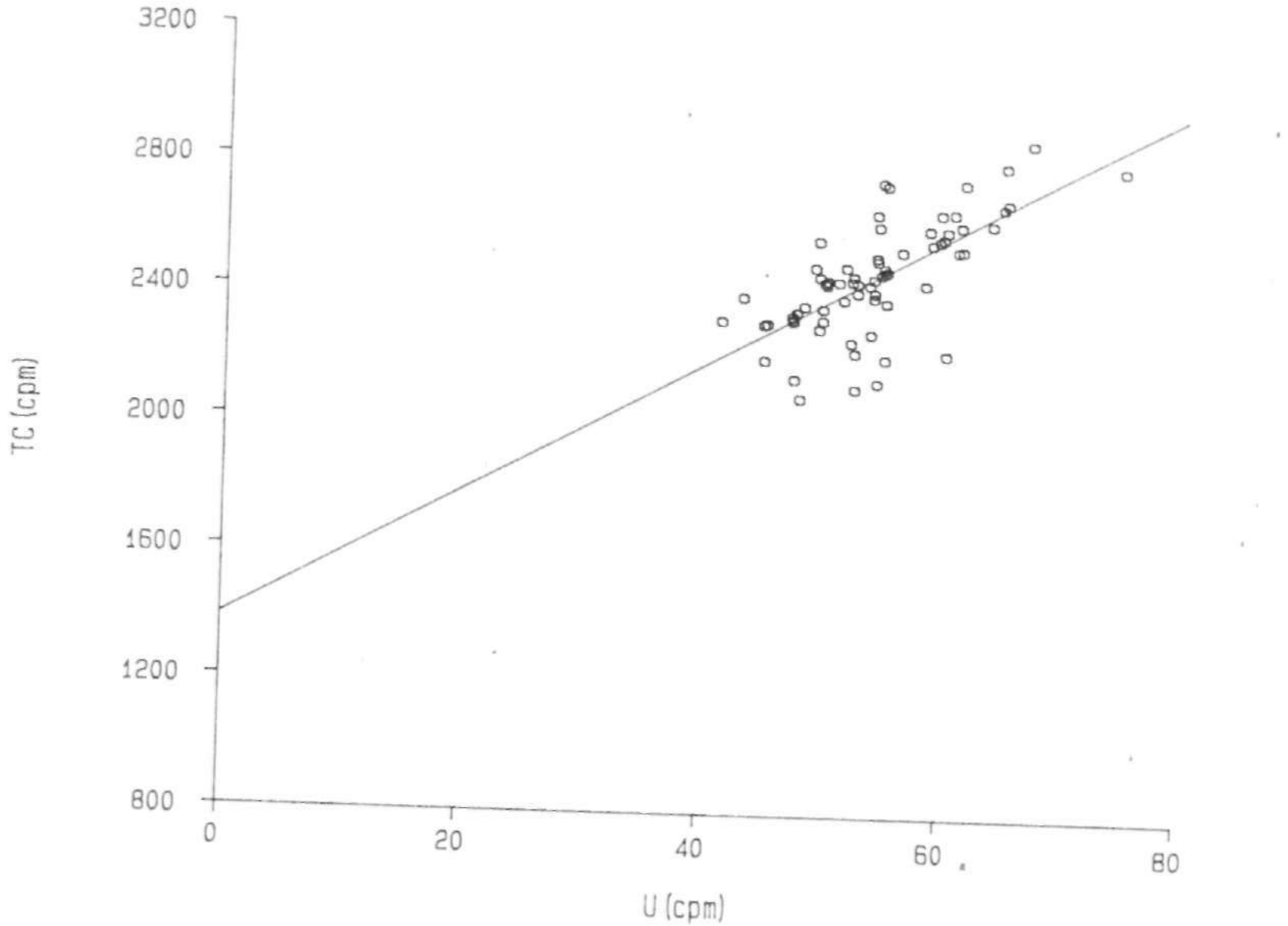


FIGURE 6.22 Correlation of U with TC for kaolinised granites.

range in the count rates, the relationship is not linear, due to the finite resolution of the instruments (Doig, 1968). For the determination of calibration constants of the instruments in such cases, they suggested dividing the samples into two groups: the high count rate group and the low count rate group, and treating each separately.

Total Count readings, together with the Disequilibrium Factor values obtained obtained for the kaolinised granites, as outlined above, are given in Appendix 6.1. The positive values of the Disequilibrium Factor suggest that U-series disequilibrium exists, and is caused by recent addition of U. Although the previous analysis given above indicate the U decay series to be in equilibrium, the high U content, but relatively low gamma-ray activity of the samples, are indicative of some recent addition of U to the environment. These results are also in agreement with the airborne gamma-ray activity map of Cornwall as shown in Figure 8.1. This clearly demonstrates that the kaolinised granites show much lower activity than the surrounding unkaolinised granites, although depletion of U rather than addition would appear more likely in this case, because of the leaching of U during kaolinisation. Because of their high U-content, it appears likely that leached U was adsorbed onto clay minerals while other members of the decay series were removed in solution during the alteration process. The very important implication of this is that the process of kaolinisation is still taking place.

6.8 Conclusions

Using a portable four-channel instrument both in-situ and laboratory gamma-ray spectrometric techniques were used to determine the concentrations of U, Th and K in granite, and granite-related material. The results obtained show that laboratory technique gave consistently low concentration values. This is largely due to the small volume of sample analysed, and difficulty in correcting for sample geometry from the normal 1m, 2π configuration used in the field. Therefore, radionuclide abundances obtained by using this approach, must be corrected by application of a suitable conversion factor. Correlations can then be made with in-situ field determinations. In this study a theoretical conversion factor of 1.8 was obtained, but the results usually still show that the gamma-spectrometric determinations giving lower concentrations than chemical determinations, a phenomenon also noted by Heath (1982). Overall, it would appear that the instrumental calibration and stripping factors are not correct. The errors in the gamma-ray spectrometric determinations obtained was 8.51ppm and 6.09ppm for U and Th in the laboratory determinations, and 6.99ppm and 16.24ppm for the in-situ, field determinations.

The results of disequilibrium studies shows that for the kaolinised samples analysed, the Th decay series is largely in equilibrium. The possibility of disequilibrium in the U decay

series is highly likely as indicated by the positive values of the Disequilibrium Factor. The adsorption of U onto clay minerals may explain recent addition of U in this environment. This possibility is discussed further in Chapter 8, in connection with U mobility studies in the kaolinised granites. From the Jos Plateau samples, although the reliable data obtained is not statistically significant, the results indicate that both the U and Th decay series are in equilibrium. This is significant because the samples analysed were collected from outcrops which have been affected by surface processes. This result confirms that these elements, more especially U, are held in resistate minerals. The location of U and Th in the granite have been fully discussed in Chapter 5.

It is important that up to now no standard techniques have been developed for estimating the equilibrium position of U and Th in field gamma spectrometry. The importance of such methods in U exploration cannot be over emphasised, and lack of such a technique to check the validity of the assumption of secular equilibrium necessarily reduces its power as a tool in such applications. Simple and rapid methods of obtaining information regarding equilibrium in the U decay series have been proposed in this study, but problems still exists. Before coming to any conclusions about the validity of the methods it is necessary to apply them to a much wider range of samples of different radionuclide concentrations where the U and Th decay series are known to be in equilibrium.

This particularly need to be done for samples with high U and or Th.

Generally, therefore, the results in this study suggest that gamma-ray spectrometry can be successfully used in exploration for U in granite terranes. With proper management of results, the reliability of the method in such operations can be greatly improved. For the exploration of low-grade U in such 'difficult environments' the cost of exploration can be greatly reduced if the reliability of the field spectrometric method is improved. This necessarily means developing a method to overcome the assumption of secular equilibrium, an assumption which is always very difficult to justify especially since surveys always involve material greatly affected by surface processes.

CHAPTER SEVEN: INVESTIGATION OF U SERIES DISEQUILIBRIUM IN GRANITE AND GRANITE-RELATED MATERIALS

7.1 Introduction

The most commonly used methods for U and Th determinations in field studies are based on the assumption that secular equilibrium exists in the decay series of these elements. For example, in simple gamma-ray spectrometry of the type described in Chapter 6, U and Th analyses are obtained by gamma-ray counts of their daughters, ^{214}Bi and ^{208}Tl, respectively, and then calculations based on the relationship between the parents and these daughters. However, as the parent elements and their daughters behave differently in different environments, serious doubts are raised about the validity of the assumption of secular equilibrium.

In Chapter 6, gamma-spectrometric investigations on the Nigerian Younger Granites and the kaolinised granites from South-West England were reported. It was found that samples from both areas showed some disequilibrium in the U decay series, especially the kaolinised samples, where it was suggested that most of the U is young and held adsorbed onto clay minerals. In connection with alpha autoradiographic investigations, it was found that some of the U in the samples of the Nigerian Younger Granites could also

have been recently mobilised as a result of weathering. In this Chapter, secular equilibrium in the U decay series is investigated, the possible causes of disequilibrium, where such exists, is discussed.

7.2 Secular Equilibrium

In a radioactive decay series, a radionuclide designated the parent decays to produce another nuclide referred to as the daughter, which may itself decay to produce its own daughter. The decay of a nuclide to its immediate daughter is represented by the Decay Law:

$$dn/dt = -\lambda N \quad \ldots\ldots\ldots\ldots\ldots 7.1$$

where N is the number of atoms of the nuclide that decay and λ the decay constant measured in s^{-1}. The number of atoms of the nuclide remaining after a time, t, can be obtained by integration of the above equation. This is given by:

$$N = N_o e^{-\lambda t} \quad \ldots\ldots\ldots\ldots 7.2$$

where N_o is the number of atoms of the nuclide at some initial time, t=0. The time required for a nuclide to decay to half its original number of atoms, called its half-life, can be calculated from equation 7.2. Subtituting N by $N_o/2$ and t by $t_{1/2}$, the half-life becomes:

$$t_{1/2} = \ln 2/\lambda$$

$$= 0.693/\lambda \quad \ldots\ldots\ldots\ldots 7.3$$

Thus the half-life is a function of the decay constant.

As it is produced, each nuclide in a series decays to its immediate daughter at a rate dependent on its half-life. A state of secular equilibrium is said to be established when the number of atoms of a nuclide that are produced, is equal to the number that decay. For the whole decay series to be in secular equilibrium, this relationship must exist for all unstable members of the decay series. Clearly, this will take a long time to establish in a series containing nuclides with long half-lives. This can be demonstrated as follows.

For any two successive members in a decay series, the decay rate of the daughter can be written as:

$$dN_2/dt = \lambda_1 N_1 - \lambda_2 N_2 \quad \ldots\ldots\ldots\ldots 7.4$$

where N_2 and λ_2 are the number of atoms of the daughter nuclide and its decay constant, and N_1 and λ_1 those of the parent, respectively. Now subtituting N_1 from equation 7.2, 7.4 becomes,

$$dN_2/dt = N_o \lambda_1 e^{-\lambda_1 t} - \lambda_2 N_2,$$

This is a first order linear differential equation which can be solved by assuming a solution of the form, $N_2 = Ae^{-\lambda_1 t} + Be^{-\lambda_2 t}$. With the condition that, when $t = 0$, $N_2 = 0$, the solutions is given by:

$$N_2 = N_o \lambda_1 / \lambda_2 - \lambda_1 (e^{-\lambda_1 t} - e^{-\lambda_2 t}) \quad \ldots\ldots\ldots 7.5.$$

Therefore, at equilibrium, the activity of both the daughter and parent are equal, that is, $N_1 \lambda_1 = N_2 \lambda_2$. From equations 7.5 and

7.2, the ratio of the amount of parent and daughter at any given time can be obtained. This, from equation 7.5, is:

$$N_2/N_1 = N_o\lambda_1/\ \lambda_2-\lambda_1\ (e^{-\lambda_1 t} - e^{-\lambda_2 t}).1/N_o e^{\lambda_1 t}$$
$$=\lambda_1/\lambda_2-\lambda_1(\ 1-e^{(\lambda_1-\lambda_2)t})$$

The time taken to reach equilibrium, t_{eq}, is then given by:

$$t_{eq} = 1/\lambda_2-\lambda_1.\ln(\lambda_2/\lambda_1).$$

This state of equilibrium is an ideal condition. Because of its exponential character, it can not be fully realised. Once it is approached, it can only be maintained where the half-lives of the nuclides are similar and, therefore, it is only a transient condition which represents the time when the daughter attains its maximum activity. Equilibrium times are thus usually given for 99% or 95% equilibrium. These can calculated as shown in the following.

Where the half-life of the parent is much longer than the half-life of the daughter, the number of atoms decaying exceeds that produced by the decay of the parent. In this case, their activities (= $N\lambda$), are related by:

$$N_2\lambda_2 = N_1\lambda_1\ (1-e^{\lambda_2 t}) \quad .....7.7$$

and the two nuclides are said to be in equilibrium. Thus the activity of the daughter at any time t, is dependent on λ_2 (or its half-life). This can be seen more clearly by determining the time needed for the two nuclides to attain equilibrium. From equation 7.6,

$$1-e^{-\lambda_2 t} = 1 - N_2\lambda_2/N_1\lambda_1$$

$$= (N_1\lambda_1 - N_2\lambda_2)/N_1\lambda_1$$

and $$\lambda_2 t = -\ln((N_1\lambda_1 - N_2\lambda_2)/N_1\lambda_1)$$

$$= \ln(N_1\lambda_1/(N_1\lambda_1 - N_2\lambda_2))$$

rearranging the terms under the log, and expressing λ_2 in terms of half-life ($\lambda = \ln(2)/t_{1/2}$), we get

$$t = \ln[1/(1-N_2\lambda_2/N_1\lambda_1)]/\ln 2.(t_{1/2}) \quad \ldots\ldots 7.8$$

where $t_{1/2}$ is the half-life of the daughter.

An activity ratio of 0.5 between two successive nuclides means that they are 50% in secular equilibrium and the time to attain this, from equation 7.8 is:

$$t_{0.5} = \ln(1/(1-0.5))/0.693.(t_{1/2})$$

$$= t_{1/2};$$

that is 50% secular equilibrium is attained after a period equal to the half-life of the daughter. Similarly for 95% and 99% equilibrium, the times are given by:

$$t_{0.95} = \ln(1/1-0.95)/0.693.(t_{1/2})$$

$$= 4.323.t_{1/2} \quad \ldots\ldots\ldots 7.9$$

and

$$t_{0.99} = \ln(1/1-0.99)/0.693.(t_{1/2})$$

$$= 6.645.t_{1/2} \quad \ldots\ldots\ldots 7.10$$

Equilibrium times for 95% and 99% equilibrium for the nuclides in the ^{238}U, ^{232}Th and ^{235}U series computed using equations 7.7 and 7.8 are given in Table 7.1

Table 7.1: Time required to reach 99% and 95% secular equilibrium for nuclides in the ^{238}U, ^{232}Th and ^{235}U decay series

Nuclide	$t_{1/2}$	$t_{0.99}$	$t_{0.95}$
^{238}U	$4.468.10^{9}$ y	-	-
^{234}Th	24.1d	160.15d	104.18d
^{234}Pa	1.18m	7.84m	5.10m
^{234m}Pa	6.7h	44.52h	28.96h
^{234}U	$2.48.10^{5}$y	$2.313.10^{6}$y	$1.072.10^{6}$y
^{230}Th	$7.52.10^{4}$ y	$4.997.10^{5}$y	$3.251.10^{5}$y
^{226}Ra	1602y	$1.065.10^{4}$ y	$6.926.10^{4}$ y
^{222}Rn	3.825d	25.42d	16.54d
^{218}Po	3.05m	20.27m	13.19m
^{214}Pb	26.8m	178.09m	115.86m
^{218}At	2s	13s	8.65s
^{214}Bi	19.7m	130.91m	85.16m
^{214}Po	$1.64.10^{-4}$s	$1.09.10^{-3}$s	$7.09.10^{-4}$s
^{210}Tl	1.32m	8.77m	5.71m
^{210}Pb	22y	146y	95.11y
^{210}Bi	5.02d	33.36d	21.70d
^{206}Hg	8.6m	57.15m	37.18m
^{210}Po	138.3d	919d	597.87d
^{206}Tl	4.19m	27.84m	18.11m
^{206}Pb	-		
^{232}Th	$1.39.10^{10}$ y	-	
^{228}Ra	5.75y	38.21y	24.86y
^{228}Ac	6.13h	40.70h	26.50h
^{228}Th	1.913y	12.712y	8.270y
^{224}Ra	3.64d	24.19d	15.74d
^{220}Rn	55.6s	369.5s	240.4s
^{216}Po	0.145s	0.964s	0.627s
^{212}Pb	10.64h	70.70h	46.00h
^{212}Bi	60.5m	402.0m	261.5m
^{212}Po	$3.04.10^{-7}$s	$2.02.10^{-5}$s	$1.31.10^{-6}$s
^{208}Tl	3.1m	20.6m	13.4m
^{208}Pb	-		

Continued.....

Table 7.1, Continued.

^{235}U	$7.13.10^{8}$ y	-	-
^{231}Th	25.64h	170.38h	110.84h
^{231}Pa	$3.43.10^{4}$ y	$2.28.10^{5}$ y	$1.48.10^{5}$ y
^{227}Ac	22y	146y	95y
^{227}Th	18.17d	120.74d	78.55d
^{223}Fr	21m	140m	91m
^{223}Ra	11.68d	77.61d	50.49d
^{219}At	0.9m	6.0m	3.9m
^{219}Rn	3.92s	26.05s	16.95s
^{215}Bi	8m	53m	35m
^{215}Po	$1.83.10^{-3}$ s	$1.22.10^{-2}$ s	$7.91.10^{-3}$ s
^{211}Pb	36.1m	239.9m	156.1m
^{211}Bi	2.16m	14.35m	9.34m
^{211}Po	0.52s	3.46s	2.25s
^{207}Tl	4.79m	31.83m	20.71m
^{207}Pb	-		

Note: y years
d days
h hours
m minutes
s seconds.

7.3 Secular Disequilibrium

In the above discussion we have seen that a state of equilibrium will be established in a decay series where the members are all present in the environment. When U and Th are deposited, each daughter will reach equilibrium with its parent source, ^{238}U or ^{232}Th, in the time as given in Table 7.1. Daughters with short half-lives will reach equilibrium with their parent nuclides first, so that by the time the longest-lived daughter reaches equilibrium, all the other daughters must have reached equilibrium as well. Therefore, the time required for the whole series to reach equilibrium is determined by the equilibrium time of the daughter with the longest half-life. These are ^{234}U and ^{228}Ra for the ^{238}U and ^{232}Th decay series, respectively. Where any one or more of the members of the decay series is physically removed by a process other than radioactive decay, then a state of non-equilibrium is established. In this condition, the activity of the nuclides in the series is no longer proportional. Where the nuclides removed from a series have very long half-lives, it takes a long time for equilibrium to be regained. However, if the nuclide removed has a short half-life, then equilibrium can be regained within a relatively short period of time. From Table 7.1 it can be seen that in the ^{232}Th decay series, equilibrium can be quickly regained (within a period of about 45 years) even if the daughter with the longest half-life is removed. In the ^{238}U decay series, however, nuclides with very long half-lives exist, and following a loss of

any of these it will take the series an extremely long time to regain equilibrium. The loss of ^{234}U, for example, will mean a period of $2.3.10^{6}$ years is required before 99% equilibrium is established with its parent.

Disequilibrium is a serious problem in the use of simple gamma-ray spectrometers for U and Th determinations because both analyses are based on daughters which are far down the decay series. To obtain correct abundances requires the existence of equilibrium between the daughters and parents: ^{214}Bi with ^{238}U and ^{208}Tl with ^{232}Th. In the ^{232}Th decay series, this requirement is, however, largely met in natural environments because of the relatively short half-lives of the members in the series, the longest being ^{228}Ra ($t_{1/2}$=6.7 years), which attains 99% equilibrium in less than 45 years. In addition, its gaseous daughter ^{220}Rn ($t_{1/2}$=54.5sec) is short-lived, and can all decay before it ever gets the chance to escape from its parents. The ^{238}U series, however, contains a number of very long-lived daughters (^{234}U, ^{230}Th, ^{226}Ra), and loss of any one of these will mean a much longer period is needed for reestablishment of equilibrium. Of serious concern also is the half-life of its gaseous daughter, ^{222}Rn ($t_{1/2}$=3.825d), which is sufficiently long for it to survive to be transported considerable distances away from its parent.

Disequilibrium in the ^{238}U decay series has been recognised for quite some time. Instances where ^{238}U was found separated from its daughter products have been reported, as has fractionation

between ^{234}U and ^{238}U (Cherdyntsev, 1955; Hurley, 1956; Thurber, 1962). For example, Cherdyntsev (1955) reported a $^{234}U/^{238}U$ activity ratio much greater than unity in the secondary mineral schroeckingerite, and in solutions leached from U-bearing minerals. In natural waters, Osmond and Cowart (1967) found $^{234}U/^{238}U$ activity ratios in the range of 0.5 to 20. Three possible explanations have been advanced for the observed $^{234}U/^{238}U$ variations in nature (Gascoyne, 1982). These are: (1)leaching from radiation damaged sites, where ^{234}U having been displaced from its original site in the atom due to recoil is more accessible and easier to remove by filtrating fluids; (2) oxidation, where it is thought that there is a possibility of oxidation of U^{+4} to U^{6+}, which is more soluble, aided by decay from ^{238}U to ^{234}U; and (3) alpha recoil into solution, in which decay of ^{238}U near water surfaces release ^{234}Th by recoil into the water. The last mentioned mechanism has been used to explain the higher ^{234}U activity than ^{238}U activity in ocean waters by many investigators, for example Kigoshi (1971) and Kronfield (1974).

Apart from ^{238}U and ^{234}U fractionation, ^{238}U has also been found separated from its other daughters in natural environments. Of importance in disequilibrium studies are the relationship with and between ^{226}Ra, ^{231}Pa, ^{222}Rn, ^{210}Pb and ^{210}Po. Whereas fractionation between ^{234}U and ^{238}U may be due to physical

processes such as alpha recoil, fractionation between ^{238}U and its other daughters is better explained by the difference in chemical properties. Ra, in particular, has been found to be more soluble in water than either U or Th, and can thus be removed by moving water from the sites of its production. Titayeva et al. (1977) reported excess ^{226}Ra over ^{230}Th and ^{238}U in soils and sediments. This was attributed to either the deposition of ^{226}Ra as adsorbed ions onto clay minerals and organic matter, or preferential leaching of ^{238}U. ^{226}Ra is also associated with oil field brines and deposits from hot springs.

Chemical fractionation preferentially enriching ^{231}Pa relative to ^{230}Th in Mn nodules has also been reported by Gascoyne (1981). High ^{231}Pa in high grade black U minerals was reported by Rosholt (1959).

Rn isotopes, being gases, are easily removed from other members in the decay series, and may be the most important cause of disequilibrium in the ^{238}U decay series in environments favourable to Rn diffusion. Rn is also soluble in water and can, therefore, be transported in aqueous solution. In natural waters, Rn has often been found unsupported by its parent ^{226}Ra, which was at one time thought to be the source of Rn in solutions (Rogers, 1958; Rose and Korner, 1979; Heath, 1982). Finally Rn loss can lead to disequilibrium during sample preparation for U analysis. Durrance et al. (1980) found that as much as 50% disequilibrium between ^{226}Ra and ^{214}Pb in the U-bearing nodules in East Devon is caused by

artificial Rn degassing during sample preparation.

Fractionation between ^{210}Pb and ^{210}Po has been found in ocean waters. Bacon et al. (1976) reported excess ^{210}Po, which was attributed to the recycling of Po from particulate matter onto which it had been adsorbed, whereas ^{210}Pb remained with the particulate matter.

The foregoing discussion has shown that disequilibrium in the ^{238}U and ^{232}Th decay series can be caused by a variety of factors. Previous disequilibrium studies have been reviewed by Rosholt (1959) who proposed a classification of disequilibrium patterns in the decay series of ^{238}U, ^{232}Th and ^{235}U. This classification is shown in Figure 7.1. In the classification each group is headed by a nuclide with a long half-life which is believed to be always in equilibrium with the other nuclides in that group. Thus ^{238}U, ^{230}Th and ^{226}Ra are in a group of their own, while ^{222}Rn and ^{210}Pb form separate groups, ^{222}Rn supporting ^{218}Po, ^{214}Pb, ^{214}Bi, and ^{210}Pb supporting ^{214}Po, and ^{210}Bi, ^{210}Po and ^{206}Pb. The U group comprises ^{238}U, ^{235}U, ^{234}U and ^{234}Th, and also ^{234}Pa, as Rosholt assumed ^{235}U and ^{234}U to have a constant abundance relative to ^{238}U. The important disequilibrium patterns in this classification are as follows.

1: Daughter-product deficiency

Here ^{231}Pa, ^{230}Th and ^{226}Ra are depleted relative to U. This may result from recent U deposition, in which case U has not

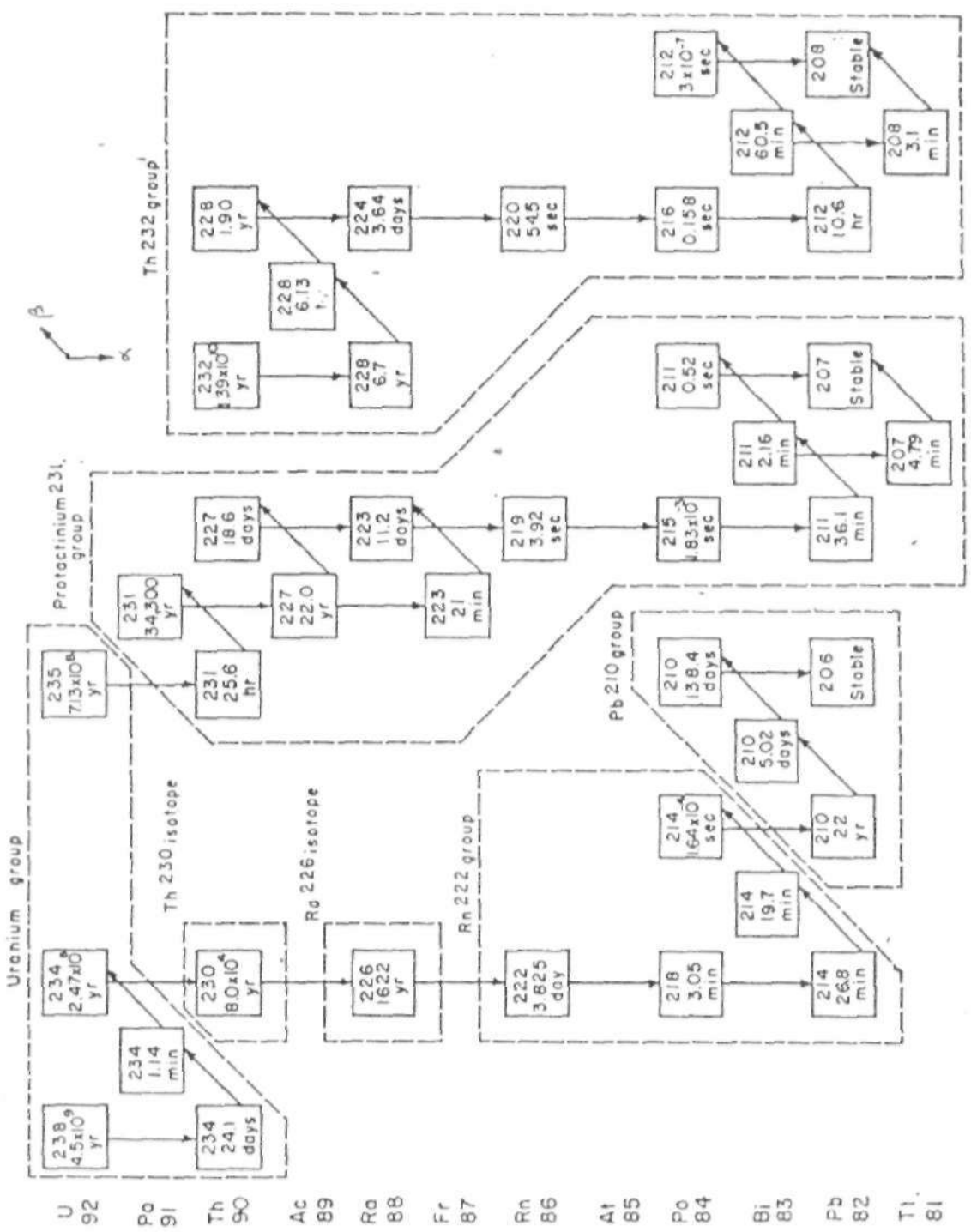


FIGURE 7.1 Disequilibrium patterns in the ^{238}U, ^{232}Th and ^{235}U decay series (After Rosholt, 1959)

reached equilibrium with its daughters, or from the differential leaching of the daughters. Both types of situation are found in a variety of natural environments. Examples are the recent U deposition in secondary minerals such as carnotite and tyuyamunite, and the precipitation of U onto secondary minerals such as clays, or Fe, Al and Mn oxides. Conversely, in old U deposits this type of disequilibrium may be due to the leaching of daughters. In gamma-ray spectrometric determinations, this situation will be indicated by low gamma-ray activity in the U channel with possible disproportionate high total count readings, due to contributions from ^{234}Th.

2: Time-related daughter product deficiency

Here all daughters are depleted relative to U and the relationship, $^{231}Pa/U > {}^{230}Th/U > {}^{226}Ra/U$ holds. The growth of each of these daughter nuclides from pure U requires the same time interval. This is believed to be caused by the recent addition of U. In such situations, gamma-spectrometric assays will also record lower U than is actually the case.

3: ^{230}Th deficiency

In this type of disequilibrium, ^{230}Th is highly deficient. Samples in this category are generally found to have a $^{231}Pa/U$ ratio greater than or close to unity, indicating that ^{231}Pa is in equilibrium with U. Rosholt suggested that this may be caused by

recent U deposition, accompanied by contamination by daughter products in which the solution do not contain the insoluble Th isotopes. U and its other daughters are often found deposited together with SiO_2 and various salts. Apparently this type of disequilibrium may also be found in environments where there is preferential leaching of Th, so that daughters not related to the decay of ^{230}Th are unaffected, but daughters such as ^{226}Ra are reduced due to ^{230}Th loss. The effect on gamma-spectrometric determinations is the same as for type-2 disequilibrium.

4: Daughter-product excess

This is represented by low U but with the long-lived daughters in equilibrium. This may result from preferential leaching of the U group of nuclides. Rosholt found that samples with this type of disequilibrium occurred in oxidised environments. High radioactivity was also present, most certainly due to ^{234}Th. Generally samples in this category have a high ^{231}Pa content, with equilibrium values of ^{230}Th, U and ^{226}Ra. This Rosholt attributed to the ability of Pa to be hydrolysed and separated from the solutions responsible for leaching U.

5: ^{226}Ra excess

This is characterised by high ^{226}Ra activity in the samples due to Ra enrichment. In addition to low U abundance, both ^{231}Pa and ^{230}Th are well below their equilibrium values. This situation

is widely reported in pyritic ores or ore dumps where ^{226}Ra is thought to be retained in sulphates.

6: Ra isotopes exclusively

This is characterised by Ra isotopes and their immediate decay products forming the bulk of the radionuclides, with very little or no U, ^{230}Th, ^{231}Pa or ^{232}Th. ^{228}Ra from ^{232}Th is commonly an associate of ^{226}Ra in these conditions. This type of disequilibrium is generally found in oil and gas field brines. Also, in deposits of radioactive hot springs, Ra is frequently found coprecipitated with Ba sulphate, Sr sulphate and occasionally Fe hydroxide. Waters draining U-rich zones are believed to be responsible for such deposits. Materials with significant ^{228}Ra unsupported by ^{232}Th, are believed to be of very recent origin. This is confirmed by low ^{210}Pb in such environments.

The types of disequilibrium discussed above are special conditions of two main disequilibrium patterns: either U-deficiency or U-enrichment. Both are capable of producing misleading U results in gamma-spectrometric determinations. The first three conditions, where U is in excess of its daughters, will generally give rise to a low U count in gamma-spectrometric determinations coupled with a high total count. The other three disequilibrium types, where U is depleted relative to its daughters, produce a high total count possibly coupled with a high count in the U channel, depending on whether or not the ^{226}Ra group of nuclides is in equilibrium with

its daughters. This is particularly important in environments where ^{222}Rn is continuosly removed. In these circumstances the same response is produced as for the first three types of disequilibrium with a particularly low U count occurring with a high total count. This state of affairs is fully discussed in Chapter 6.

7.4 Methods in Disequilibrium Studies

Investigations of disequilibrium in the ^{238}U and ^{232}Th decay series have been carried out by a number of methods. These utilise both gamma-ray spectrometry and alpha-particle spectrometry, neutron activation analysis and fission track registration. Of these, the most widely used are the gamma-spectrometric and alpha-spectrometric methods. Gamma-ray spectrometry has been mostly used for the analysis of U ores, but where high accuracy and good resolution for all the nuclides are required, alpha-particle spectrometry gives better results. The use of gamma-ray spectrometry in U-series disequilibrium studies have been described by Mero (1960) and Ostrihansky (1976). Mero used measurements on the 0.190MeV and 0.240MeV energy peaks in the U spectrum to determine what he called the 'Equilibrium Factor', given by the ratio of the count in the 0.190MeV and the 0.240MeV channels. He found that for an Equilibrium Factor range of 1.0 to 1.3, the count on the 0.190MeV channel was proportional to the amount of U in the sample so that the U decay series can be considered essentially to

be in equilibrium. Conversely, high values, greater than 3.0, indicated U enrichment while ores with values less than unity indicated Ra enrichment.

Ostrihansky (1976) determined disequilibrium in the ^{238}U series in samples from the Elliot Lake U mining district by measuring the low energy parts of the gamma-ray spectrum. ^{234}Th, ^{226}Ra and ^{210}Pb were determined by measurements of the 63keV, 83.3keV and 46keV peaks, respectively, and comparing these with measurements on standard samples. Using this method he recognised three types of disequilibrium in the samples he studied, namely ^{238}U deficiency, ^{238}U excess, and excess ^{231}Pa.

In alpha-particle spectrometry, alpha activities in the ^{238}U and ^{232}Th decay series are determined by analysing the alpha-energy spectra. Provided great care is taken to produce an ultra-thin source and a high vacuum in the counting chamber, the alpha-particles emitted from the surface of a sample which are registered on a detector can produce spectra with sharply defined energy peaks (Figure 7.2). However, even in optimum conditions, because there are overlaps in the alpha-particle energies of some of the alpha-emitters in the ^{238}U and ^{232}Th decay series, for example ^{230}Th and ^{234}U (Table 7.2), some peaks will not be clearly resolved. Therefore, most investigations involve chemical separation of U and Th. Where conditions are less than optimum,

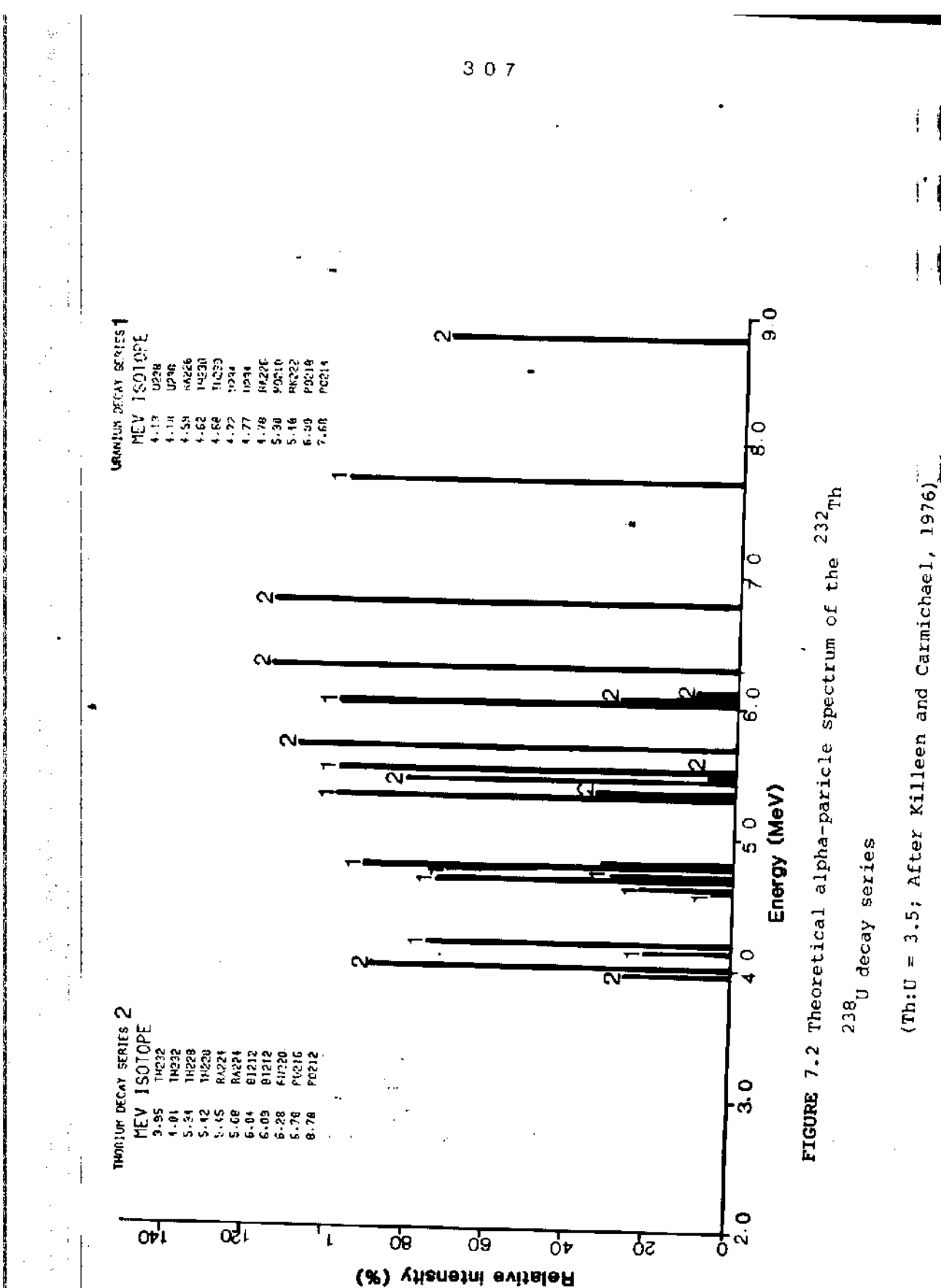


FIGURE 7.2 Theoretical alpha-paricle spectrum of the ^{232}Th ^{238}U decay series

(Th:U = 3.5; After Killeen and Carmichael, 1976)

Table 7.2: Alpha group energies of nuclides recovered after radiochemical separation U and Th.

Nuclide	Alpha energy(MeV)	Intensity (%)
^{238}U	4.195	77
	4.147	23
	4.038	0.23
^{234}U	4.768	72
	4.717	28
	4.600	0.3
^{232}Th	4.007	76
	3.952	24
	3.882	0.2
^{230}Th	4.682	76
	4.615	24
	4.476	0.12
	4.437	0.03
^{228}Th	5.421	71
	5.338	28
	5.208	0.4
	5.173	0.2
	5.137	0.03

for example a less-than-perfect vacuum, the alpha-particles may suffer absorption to give peaks with low-energy tails, thereby making it difficult for the peaks to be well resolved. In a technique described by Killeen and Carmichael (1976), theoretical alpha spectra of all the alpha-emitting nuclides in the two decay series in equilibrium were computer generated, so that the results of measurements made of the spectra from samples in disequilibrium could be compared to those standard spectra. In this case, there was no necessity to separate U and Th, and contributions due to the ^{232}Th decay series in the ^{238}U spectrum were removed by subtracting the computed ^{232}Th series spectrum from the spectra obtained from the samples.

The resolution and height of peaks mainly depend on the absorption suffered by the alpha-particles before detection. In practice the shape of a peak is not gaussian but skewed towards the low energy due to self-absorption within the sample. The interaction of alpha-particles with matter has been extensively studied. The Bragg-Kleeman relation

$$R_\rho = 0.32.10^{-3} W^{1/2} R_a$$

gives the range of alpha-particles in solids (Nogami and Hurley, 1948), where the range $R\rho$ is measured in g/cm^2,

R_a is the range (in cm) of alpha-particles in air,

W is the atomic weight of the material calculated on the atomic fraction basis, and ρ is the density of the medium in gcm^{-3}.

R_a is also related to the energy, E, of the alpha-particle. For

alpha-particles in the range 4MeV to 8MeV Glasstone (1967) gave:

$$R = 3.09E^{3/2}$$

Therefore, where the sources are significantly thicker than the alpha-particle range in the material, alpha-particles from within the sample are totally absorbed. In such cases, the number of alpha-particles, N_o, from the sample surface is given by:

$$N_o = NRA/4 \quad \ldots\ldots\ldots\ldots 7.11$$

where N is the number of disintegration per unit time, A is the surface area of the sample and R is the range of alpha-particles in the sample (Cherry, 1964). Where the thickness is greater than the range, the alpha-particles lose most of their energy before reaching the detector. For ultra-thin sources, in which sample thickness is less than the alpha particle range, the relationship is given by:

$$N_o = NRA/4(2t/R-(t/R)^2) \quad \ldots\ldots\ldots 7.10$$

where t is the thickness of the source. From this it can be seen that, for thin-source samples, the count rate is lower than for thick-source samples,so that long count times must be employed to obtain satisfactory counting statistics.

Apart from having higher count rates, thick sources are also much easier to prepare than ultra-thin sources and there is less risk of loss of nuclides during preparation. For these reasons, thick sources have frequently been used in alpha-particle spectrometry, both for disequilibrium studies and in the gross determination of alpha activity. Evans (1934), and Finney and Evans

(1935) described the use of thick sources for total alpha activity determinations. Killeen and Carmichael (1976) described a technique using thick-source alpha-particle spectrometry for determining disequilibrium in the ^{238}U series in a number of U ore samples. These authors found that a limiting U concentration in the order of 0.1% U_3O_8 was needed for good energy resolution with the detector-sample geometry they used. Thick-source alpha spectrometry was also used by Durrance (1983), to investigate disequilibrium in the ^{238}U decay series in radioactive nodules from South-East Devon. In this case the spectra were compared with that obtained from a uraninite sample in which the ^{238}U was in equilibrium.

However, where high resolution is required, thin sources offer very much better results. In this case most of the alpha-particles originating from the sample are able to reach the detector with little or no energy loss. The actual distribution of energies depends on the source thickness, so that, for ideal results, infinitely thin sources must be used. Because this is impractical only approaches to the ideal are possible.

Various techniques for the preparation of thin sources for alpha spectrometry have been described. These include vacuum sublimation, direct evaporation, electro-spraying, and electrodeposition from aqueous or organic solutions. The requirements are that for routine work, these methods must be simple to apply, reproducible and relatively quick (Lally, 1982). Vacuum sublimation produces excellent sources (Jackson, 1960), but

is not readily adaptable to routine laboratory working environments. Evaporation from aqueous solutions or organic solvents is widely used and gives excellent results (Ku, 1965), but it may also produce adherent deposits, as noticed by Miller and Brouns (1952). Electrodeposition is now widely used and is being almost universally adopted as a reliable technique for thin-source preparations. It involves deposition of the radionuclides onto a flat metallic surface from an electrolyte. A variety of electrolytes have been used for this purpose, but it has been found that although deposition from organic solvents is more rapid and reliable for a wider range of actinides than deposition from aqueous solutions, alpha spectra from sources prepared in this way may be observed to be degraded due to deposition of traces of Fe and Al (Lally, 1982). In aqueous electrolytes Fe and Al usually remain in solution during electrodeposition. Aqueous solutions are thus more suitable for alpha spectrometric source preparations. Solutions are generally made slightly alkaline or slightly acidic, by addition of suitable reagents, to improve their electrolytic properties.

High recovery rates from electrodeposition of aqueous solutions have been reported. Talvitie (1972), for example, noted a recovery rate of 98% U and 100% Th by electrodeposition from acid media in 1h and 2h, respectively. Lally and Eakins (1978) found that recovery rates were greatly improved and clean samples obtained by adding ethyldiamine tetra-acetic acid (EDTA) to the

electrolyte, which complexed any residual Fe present. They reported recovery rates of 100% for both U and Th by electrodeposition for 3 and 4 hours, respectively.

Radiochemical separation and alpha counting of ultra-thin sources produce accurate measurements of the U and Th decay series. The determinations allow the nature of any disequilibrium in these decay series to be precisely determined to the extent that U series disequilibrium results are also widely applied in age determinations on young geological samples.

7.5 Investigation of Disequilibrium in the U Series in the Nigerian Younger Granites, and their Associated Soils, and the Kaolinised Granites of South-West England

U disequilibrium in the Nigerian Younger Granites, and their associated soils, and the kaolinised granites of South-West England were investigated for this study using thin source alpha spectrometric methods. Sources were obtained by electrodeposition onto stainless steel planchets from solutions of pure U and Th following radiochemical separation. The procedure of U separation developed in the Radiochemical unit of the School of Chemistry, University of Bath, as described by Heath (1982) was used. This involved taking the samples into solution and adding a known quantity of tracer nuclide, known as the spike, then separation using ion-exchange columns. U and Th were finally deposited on

stainless steel planchets using a simple electrolysis procedure. The processes are briefly described below, and the stage by stage procedure is given in Appendix 7.1.

Two samples each of the fresh granite, soil and kaolinised granite were investigated by this technique. Soil samples with high and average U concentrations, and their corresponding fresh granite samples, were selected to determine the equilibrium state in each concentration range. Similarly, in the kaolinised granites, a sample in the high U range and another with an average U concentration were selected. Details of the samples selected and their U and Th concentrations are given in Table 7.3.

7.5.1 Preparation of Sample Solution

From each sample 0.4g was dissolved in acid by pressure digestion. For this, sample powders, were produced as described in Chapter 4, thoroughly dried, and 0.4g of this taken in a PTFE beaker. Concentrated HCl and HNO_3 were then added before being heated in an oven at $110^{o}C$ for 2 hours in a stainless steel digestion bomb. After cooling, the solution was evaporated, and the residue transfered to a volumetric flask by washing with deionised water and made up to 100ml. In a study of the Dartmoor granite by Heath (1982), only 0.1g of sample was used. Heath believed that this was responsible for the low counts he obtained, and the need for counting periods of about a week. For this reason it was

Table 7.3: U and Th concentrations for samples selected for alpha spectrometric investigation

sample	cU	eU	cTh	eTh	cTh/cU	eTh/eU
BMP33	8	3.37	7	3.45	1.85	0.42
BMP36	24	5.74	7	3.13	0.98	0.24
JPS17	23	-	32	-	1.39	-
JPS42	7	-	20	-	0.97	-
JPR17	20	-	74	-	3.70	-
JPR42	17	-	30	-	1.77	-

decided to use higher concentrations of 0.4g in this study, in the hope of reducing the counting periods. Indeed, it was originally discovered that the bomb capacity was such that only this amount could be effectively taken into solution. Even though larger amounts could be taken into solution, shortly after cooling a residue was formed.

7.5.2 Spiking with ^{236}U and ^{229}Th

For the determination of recovery rates and the efficiency of the separation procedure, tracers were used. To keep to a minimum interference by nuclides used as tracers, certain considerations have to be taken into account. Minimum quantities of spikes should be used, the tracers should not naturally occur in the sample to be analysed, their alpha-particle energies and those from its decay daughters must be sufficiently different from the nuclides in the sample, and there must be no chemical fractionation between tracers and the nuclide it is supposed to trace in the sample (Ivanovich, 1982).

In this determination, the nuclides ^{236}U and ^{229}Th were used as tracers for U and Th, respectively. The half-lives and alpha-particle energies of these nuclides is given in Table 7.4. They were prepared artificially by Harwell Laboratories, ^{229}Th by

Table 7.4: Alpha-particle energies and half-lives of the nuclides used as spikes (^{236}U and ^{229}Th).

Nuclide	$t_{1/2}$	Alpha energies (MeV)	Intensity (%)
^{236}U	$2.391.10^{7}$ yrs	4.499	73
		4.45	27
		4.337	0.5
^{229}Th	7340yrs	4.845	56.1
		4.901	10.6
		4.814	10.1
		4.906	5.7
		4.975	5.6
		5.797	2.0
		4.763	1.5
		4.695	0.4
		>5.070	<0.2
		4.608	0.05
		4.480	0.03

separation from ^{233}U which was produced by bombardment of Th with neutrons (Hyde et al., 1971). The decay of ^{229}Th to stable ^{209}Bi involves nine daughters, three of which are alpha-emitters with energies at 6.30MeV, 7.02MeV and 8.34MeV. ^{236}U was produced by neutron capture on ^{235}U and then purified by electromagnetic separation. Its decay to ^{232}Th may be thought a cause for concern, but, because of its long half-life, the amount of ^{232}Th produced is negligible. A solution containing 100dpm per mg of each of the spiking nuclides was used.

7.5.3 Column Preparation and Separation of U from Th

Separation was carried out using ion-exchange columns containing two resin types, one in chloride form (Amberlite) and the other in nitrate form (Dowex). The columns consisted of burettes of 1.2cm internal diameter, fitted with stoppers. Glass wool was plugged at the closed end, and resin added to a depth of 10.0cm. Another plug of glass wool was then inserted on top of the resin (Figure 7.3). The suspension of resin in the column was then washed with HCl prior to generation. The chloride column and the nitrate column were generated by eluting with 150ml of 9M HCl and 9M HNO_3, respectively.

After spiking, excess Fe was removed by solvent extraction before separation of U and Th was carried out. Th was separated in 9M HCl by transfering the residue into the column and carefully

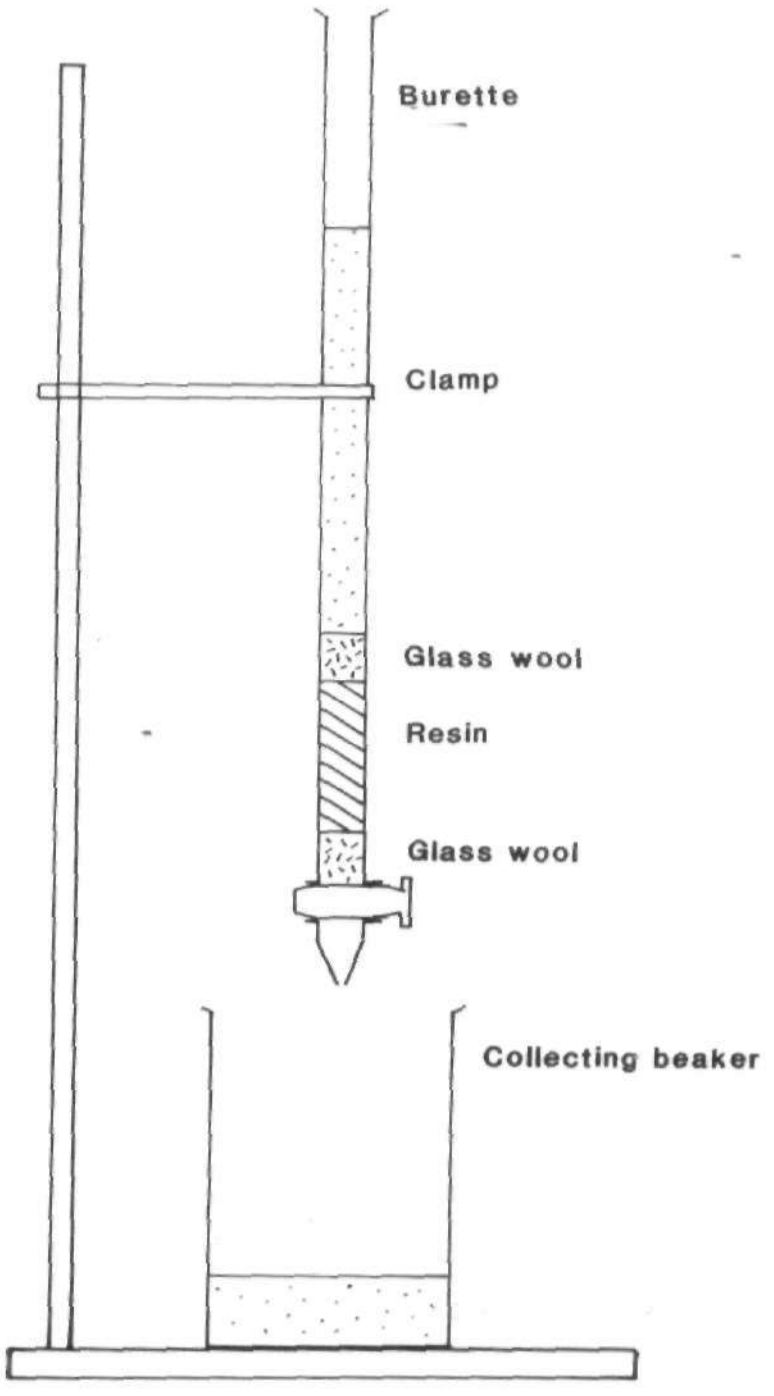


FIGURE 7.3 Ion exchange column

washing with 10ml 9M HCl. This was then followed with another 10ml of the 9M HCl, added 1-2ml at a time, and the percolating solution collected in a beaker. This solution contained Th and other cations, separated from U, which remained adsorbed onto the resin together with Pa and Fe^{3+}. The adsorbed U was then extracted using dilute HCl. To do this, the column was first eluted with 0.1M HCl until all the concentrated HCl had been removed. This was shown by a colour change in the resin to pale yellow-brown. When the 0.1M HCl had percolated down the column, U was flushed by the systematic addition of more 0.1M HCl.

Because the U and Th extracted in this way contained other cations, they were further purified by the nitrate column. Any Cl^- was removed by eluting with concentrated HNO_3 solution and then checking the absence of Cl^- by adding a few drops of $AgNO_3$ solution. If still present, Cl^- was indicated by the formation of a white precipitate. Each of the U and Th solutions was then evaporated to dryness and the residue dissolved in 7M HNO_3, before being transfered to the column. The same column was used for both U and Th purification by generating the column again after Th had been recovered, but different columns were used for each sample to avoid any possible contamination. The cations associated with the Th solution were flushed out using concentrated HNO_3, and the Th extracted with dilute HCl. Similarly, Fe^{3+} in the U solution was removed by concentrated HNO_3, and U (with Pa) extracted with dilute HCl. Any organic matter that might have been present in the

solutions was removed by adding drops of concentrated $HClO_4$. The solutions containing U (plus Pa), and Th were then evaporated to dryness and prepared for electrodeposition.

Although Pa is usually coprecipitated with U, only ^{231}Pa emits alpha-particles with an energy within the range of measurement, and this has a very low activity in normal samples. Therefore, separation of Pa and U is not necessary. Some ^{210}Bi may be coprecipitated with Th (Heath, 1982) and its daughter, ^{210}Po, is an alpha-emitter with an energy in the range of measurements. However, because its effect can be minimised if the source is counted soon after sample preparation, it is not separated from Th.

7.5.4 Electrodeposition

Ultra-thin sources were prepared by electrodeposition onto stainless steel planchets. The electrodeposition cell consisted of a screw-capped polythene bottle with the bottom removed. The planchet was held in the inverted bottle by support on the inside of a cap made of brass. The brass contained the planchet which acted as the cathode in the cell. The anode was a wire made of 1mm diameter Pt tubing which is suspended in the bottle (Figure 7.4).

The separated U and Th residues had first to be purged of any Cl^- that could have been carried over during the separation processes, as it tends to corrode the Pt anode. The residue was, therefore, first dissolved in 5-10 drops of 18M H_2SO_4 and then

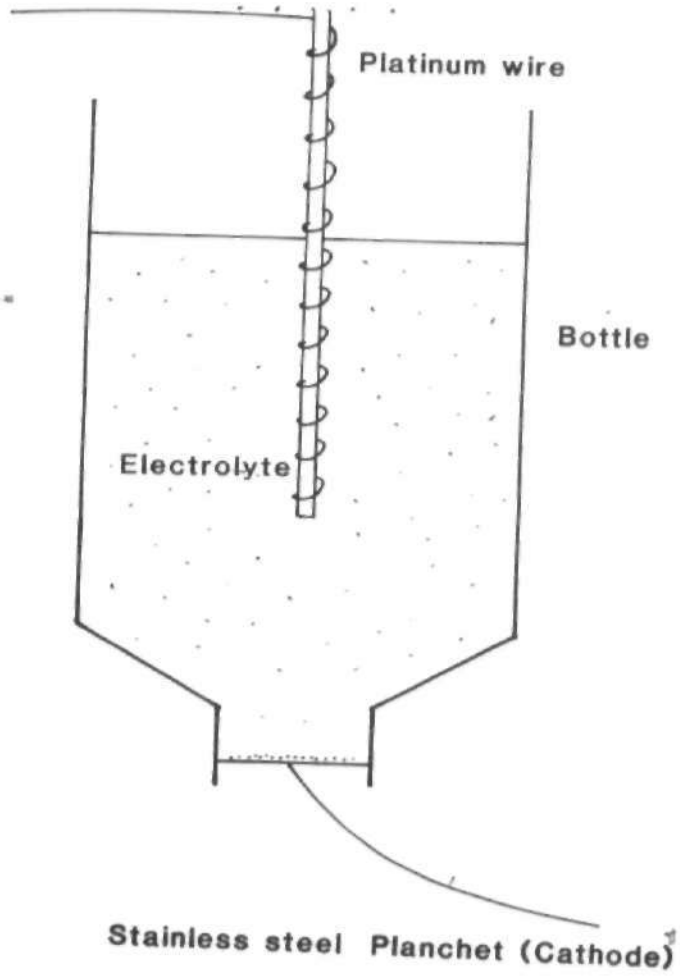


FIGURE 7.4 Electrodeposition cell

evaporated to dryness. This was then transfered to the electrodeposition cell in $(NH_4)_2SO_4$ solution. Deposition of the U and Th was effected by passing a current of 0.5A for 3 hours and 6 hours, respectively, through the U and Th solutions.

7.5.5 Alpha-Particle Counting and Analysis

The planchets were put into the detector chamber as soon as was practically possible after preparation, and the alpha-particles emitted counted for a preset period. However, because of time constraints and the number of samples involved, longer periods between preparation and counting were involved in the work reported here, than is usually the case, with up to a month elapsing after planchet preparation. The detector, a Canberra model 2004Dm silicon barrier detector, was housed in a Canberra vacuum chamber model 7400A. The counting efficiency for the detector-sample geometry used was between 60% and 90%. Alpha-energy spectrum analysis was carried out using a multichannel analyser connected to the detector assembly. The spectrometer was calibrated using the spike nuclides, such that channel numbers could be directly related to energy. Each sample was counted for a period of 200,000 seconds which was found sufficient to accumulate enough counts to identify the peaks of interest. The counts in each channel, together with the number were then recorded for analysis.

7.6 Results

As previously mentioned, it was decided to try and reduce the counting period used by Heath (1982), and although it was not possible to bring it down to a few hours, it was greatly improved to about 3 days. This meant that results for both U and Th counts could be obtained in about one week, including both separation and plating, using a single detector.

Unfortunately, the separation techniques were not 100% efficient, so that, invariably, spectra of U nuclides were formed from the Th planchets and vice versa. For example, in the spectra obtained from the Th planchets, peaks due to the ^{236}U spike plus ^{238}U and ^{234}U were often clearly seen. These effects were less pronounced in the results from the U planchets, suggesting that the problem had more to do with U being extracted along with Th during Th extraction than Th being extracted with U. This is probably due to U not being effectively adsorbed onto the resin. Such an effect may be caused by the amount of resin used, especially as the amount of U had been greatly increased in the 0.4g sample with no proportionate increase in resin. In these circumstances, the resin can only complex a limited amount of U while the rest would pass through. That this may be the case is shown by the fact that samples with high U concentrations produce greater interference in the results from the Th planchets than did samples with less U. The relatively poor separation meant that counts for U nuclides

recorded on both planchets had to be combined in order to obtain the true counts due to those nuclides. In addition to the poor separation causing difficulty, the amount of tracer used was found to be high, so that the low energy tail of the ^{229}Th peak tended to interfere with part of the energy range of interest and reduced resolution. These difficulties together meant that absolute nuclide concentrations could not be determined with high accuracy. Nevertheless, the results were sufficiently accurate to be employed for the investigation of disequilibrium in the samples, provided a cautious approach was taken in their interpretation.

The quantitative results obtained from this work are given in Table 7.5. Alpha spectra obtained are given in Figures 7.5 to 7.10. Details of radiochemical separation and counts obtained from each sample are given in Appendix 7.2. The results show substantial disequilibrium in the U decay series in both the kaolinised granites and the soil samples.

Of the kaolinised granites, in BMP33 the ^{234}U/^{238}U activity ratio showed that ^{234}U and ^{238}U are approximately in equilibrium, indicating that there was no isotopic fractionation of U in the kaolinised granites. In addition, the low ^{230}Th/^{234}U activity ratio suggests recent U deposition, within the last 40,000 years at most.

BMP36 also has ^{234}U and ^{238}U in equilibrium, as shown by the ^{234}U/^{238}U activity ratio. Disequilibrium does, however, exist between ^{230}Th and ^{238}U, and ^{230}Th and ^{234}U. The Th/U activity ratio indicates recent U deposition, not earlier than 110,000 years ago.

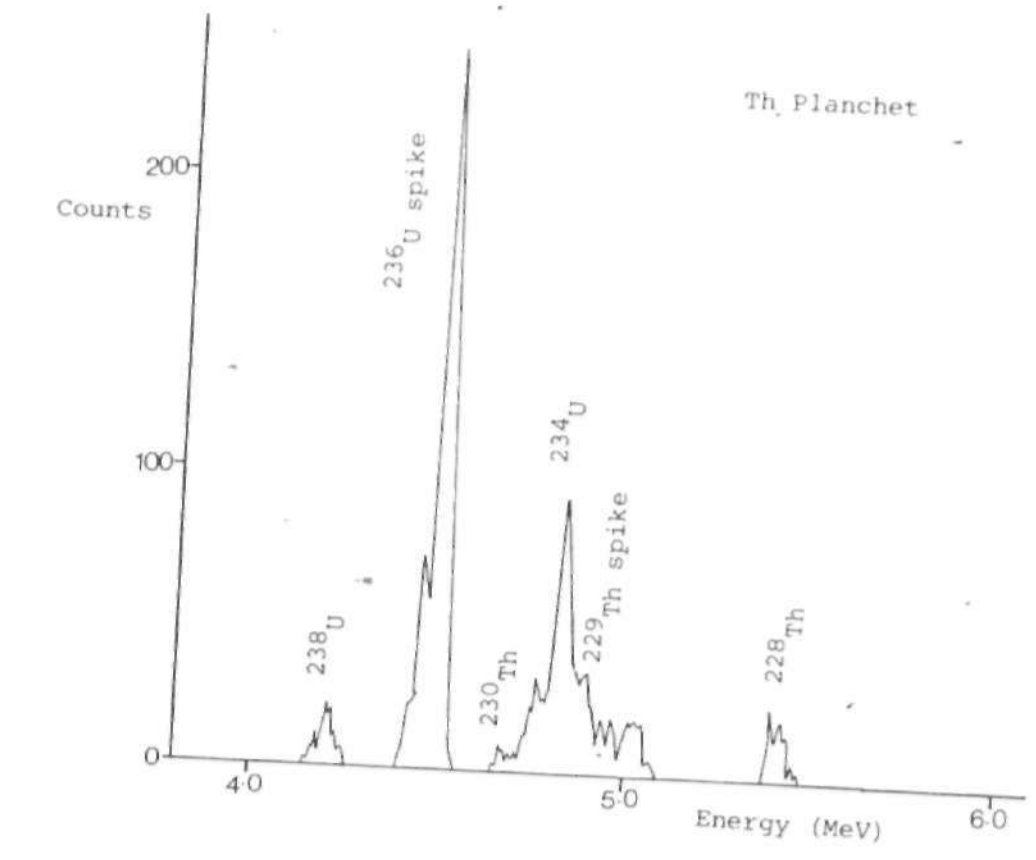
Table 7.5: Results of alpha spectrometric analysis

Sample[1]	$^{234}U/^{238}U$	$^{230}Th/^{238}U$	$^{230}Th/^{234}U$
BMP33	0.96	0.28	0.29
BMP36	0.99	0.62	0.62
JPS17	0.91	0.44	0.49
JPS42	1.28	0	0
JPR17	1.04	0.78	0.81
JPR42	1.69	1.00	0.59

1 BPM: Kaolinised granites

JPS: Soil samples

JPR: Rock samples



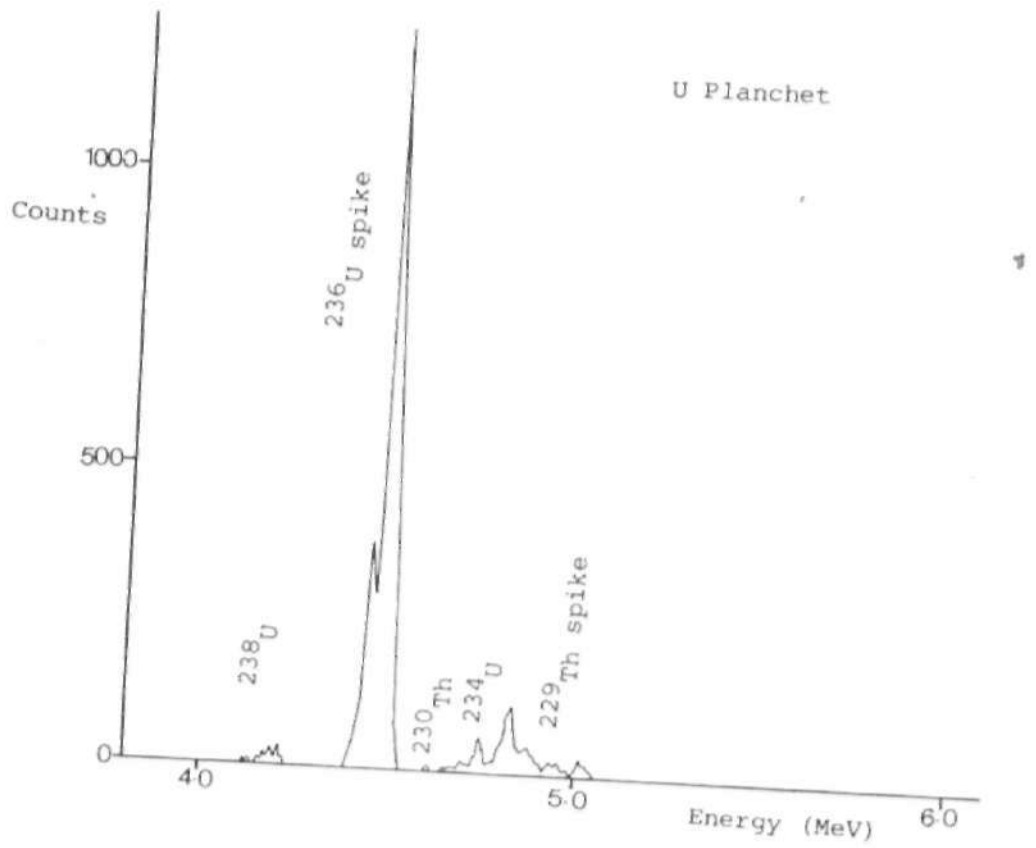


FIGURE 7.5 Th and U alpha-particle spectrum for kaolinised granites (BMP33)

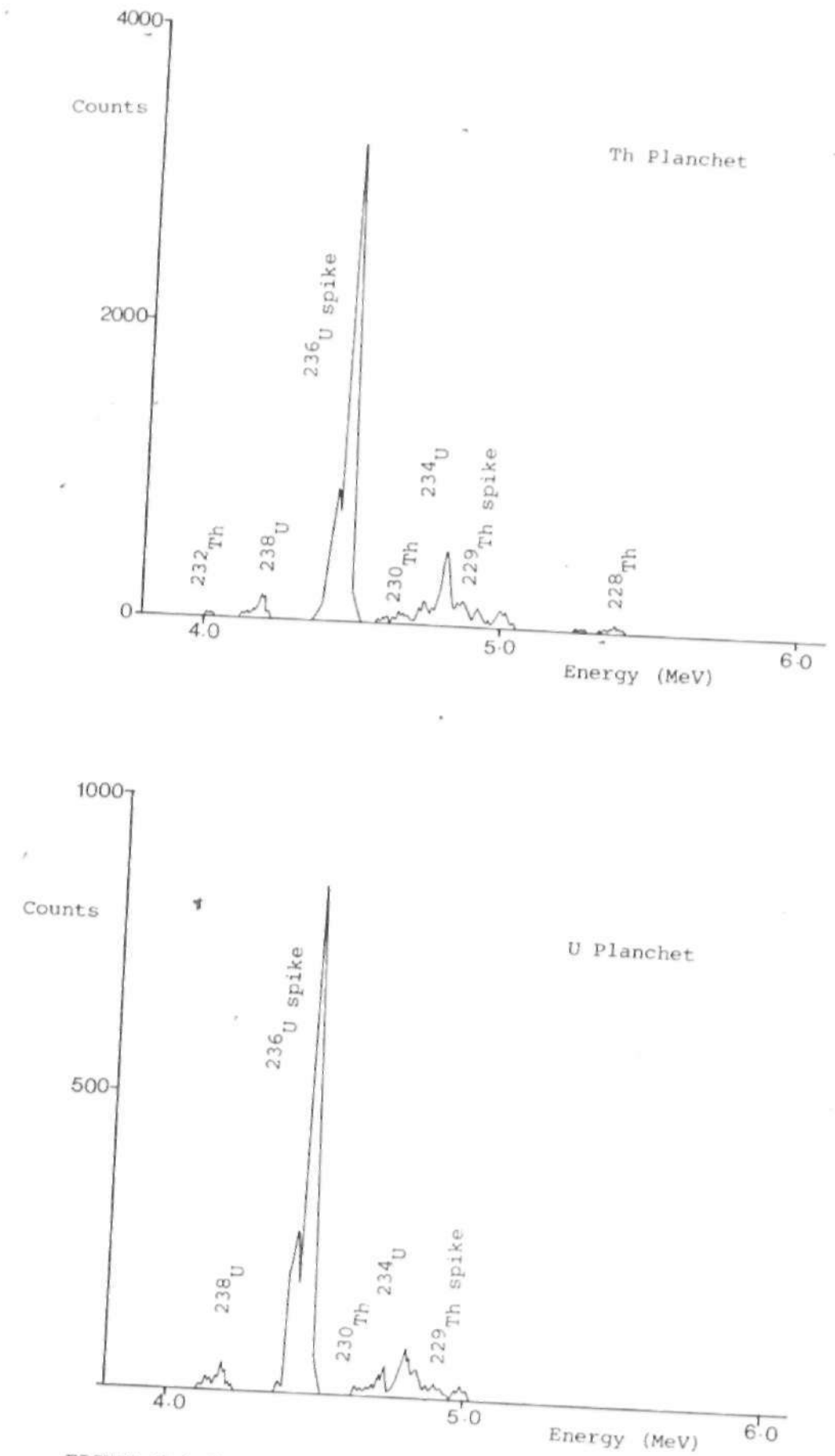
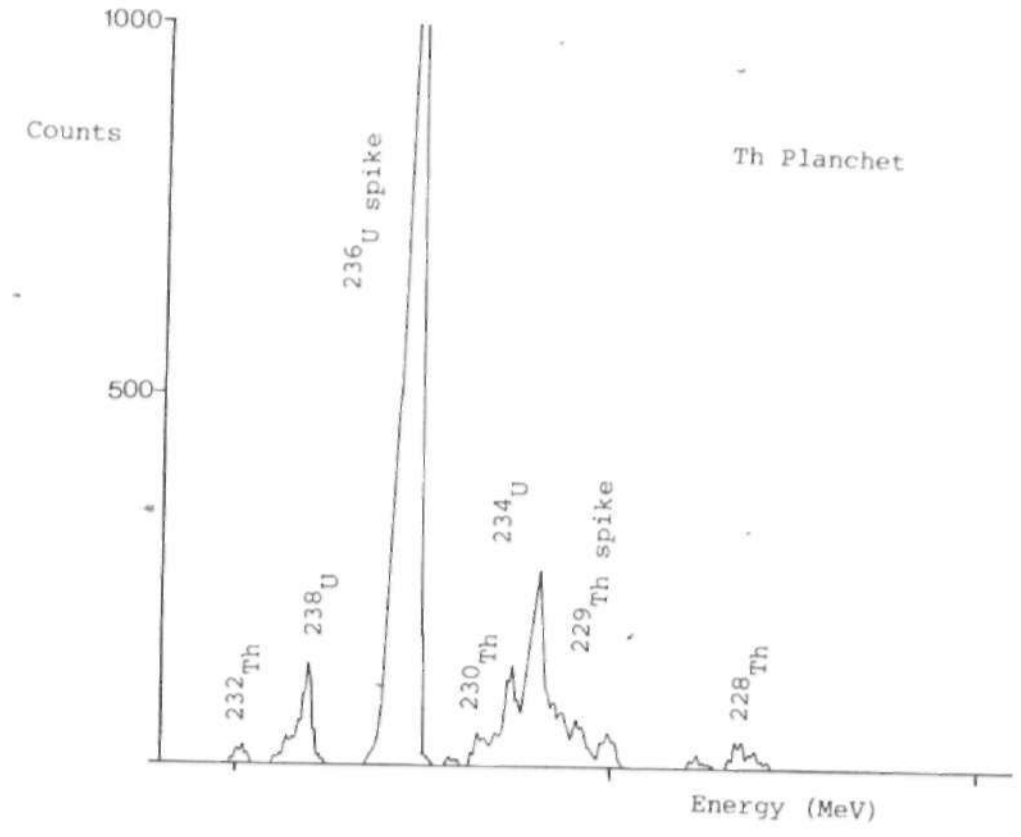


FIGURE 7.6 Th and U alpha-particle spectrum for kaolinised granites (BPM36)



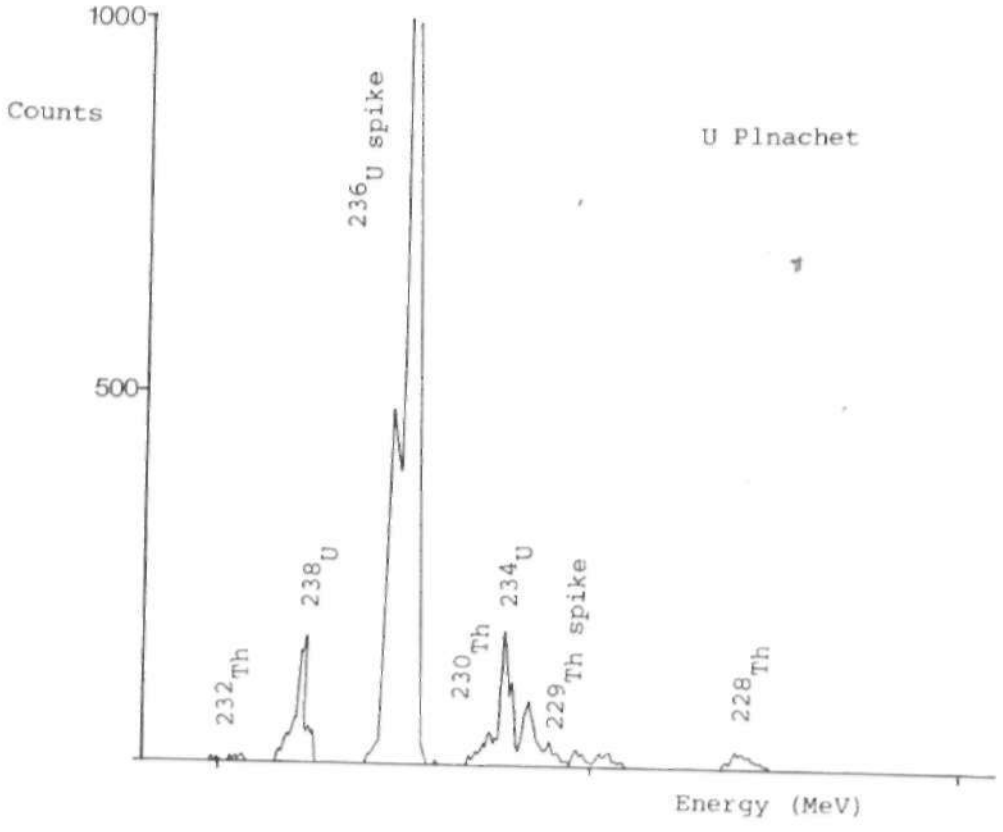
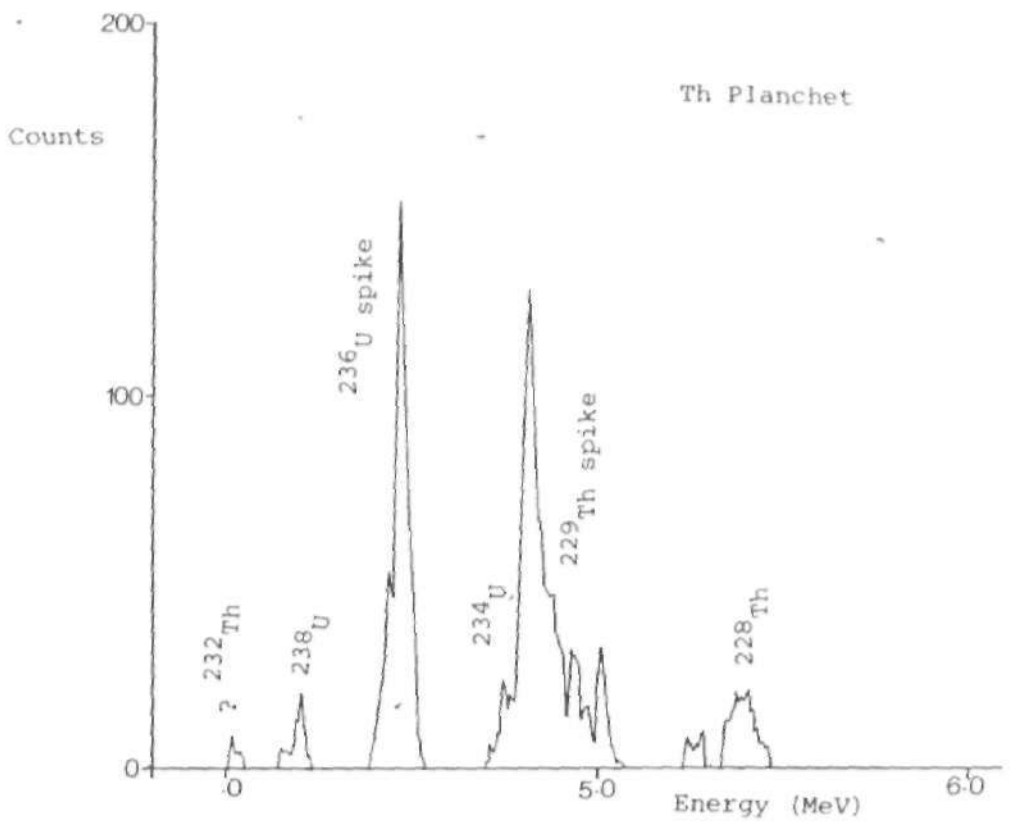


FIGURE 7.7 Th and U alpha-particle spectrum for soils, Jos Plateau (JPS17)



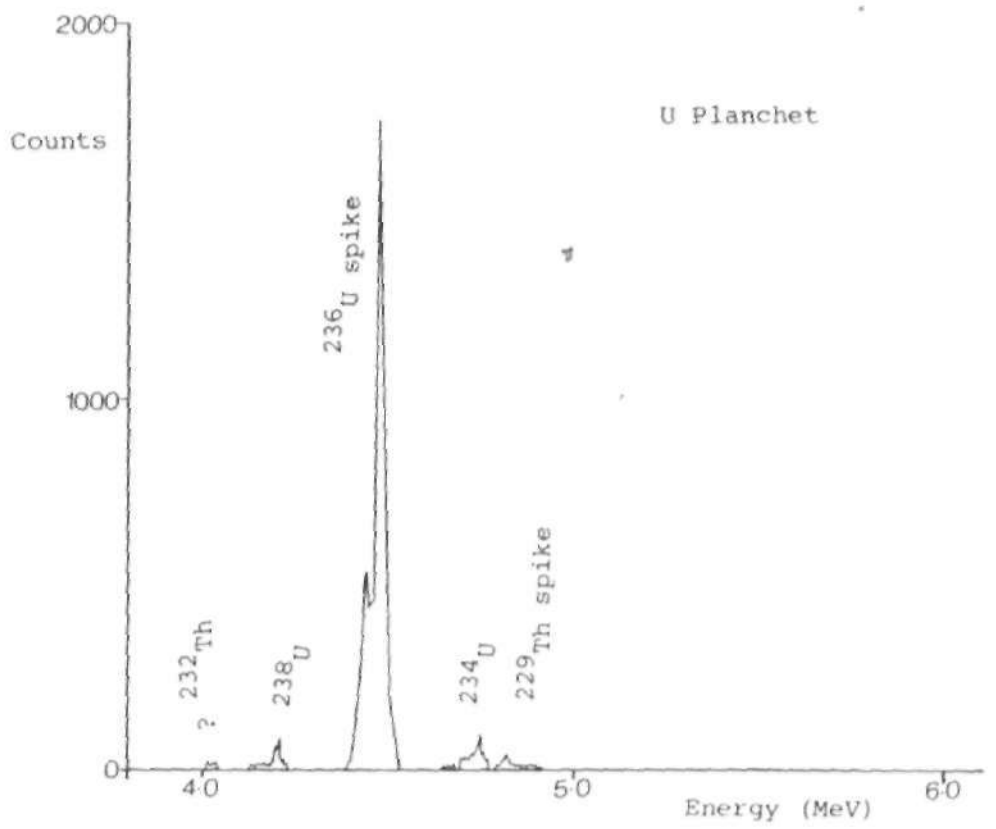
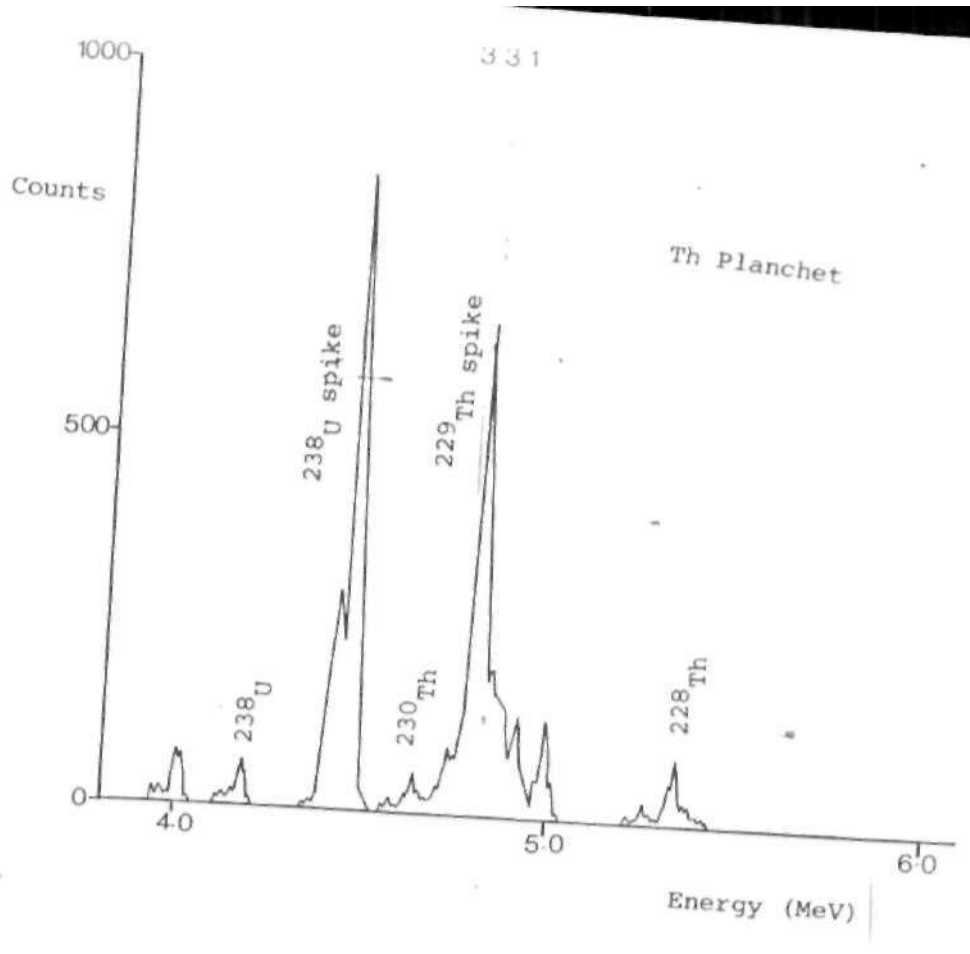


FIGURE 7.8 Th and U alpha-partcile spectrum for soils,

Jos Plateau (JPS42)



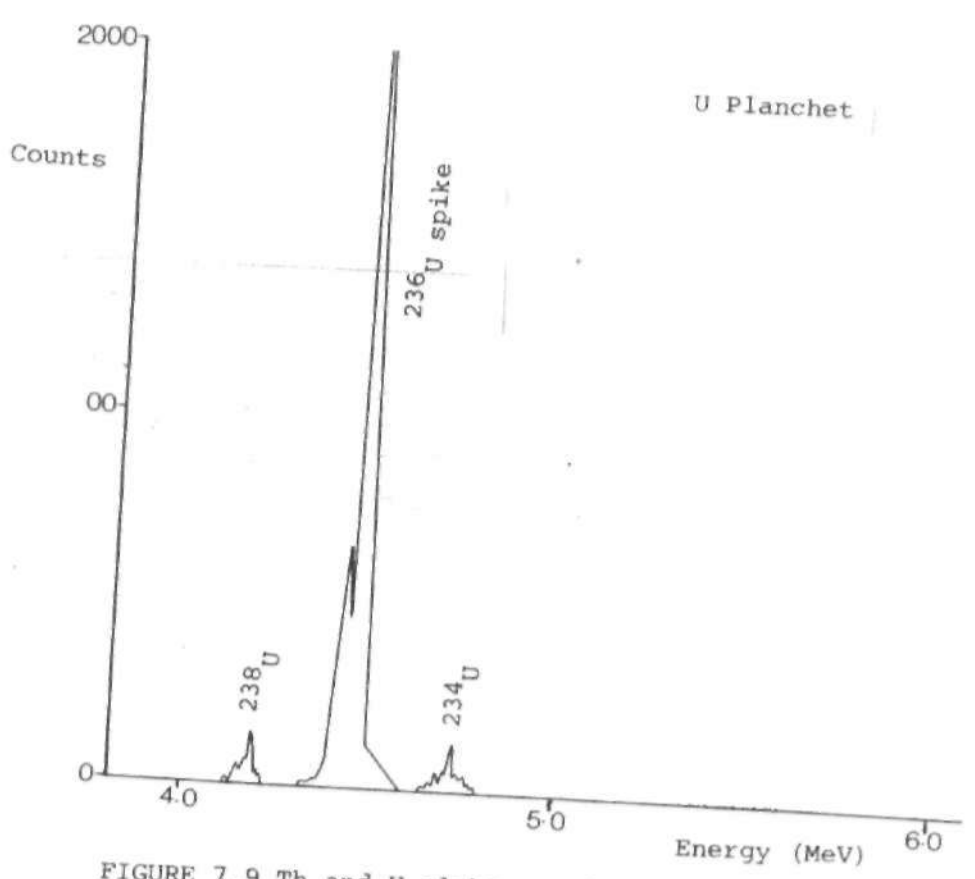
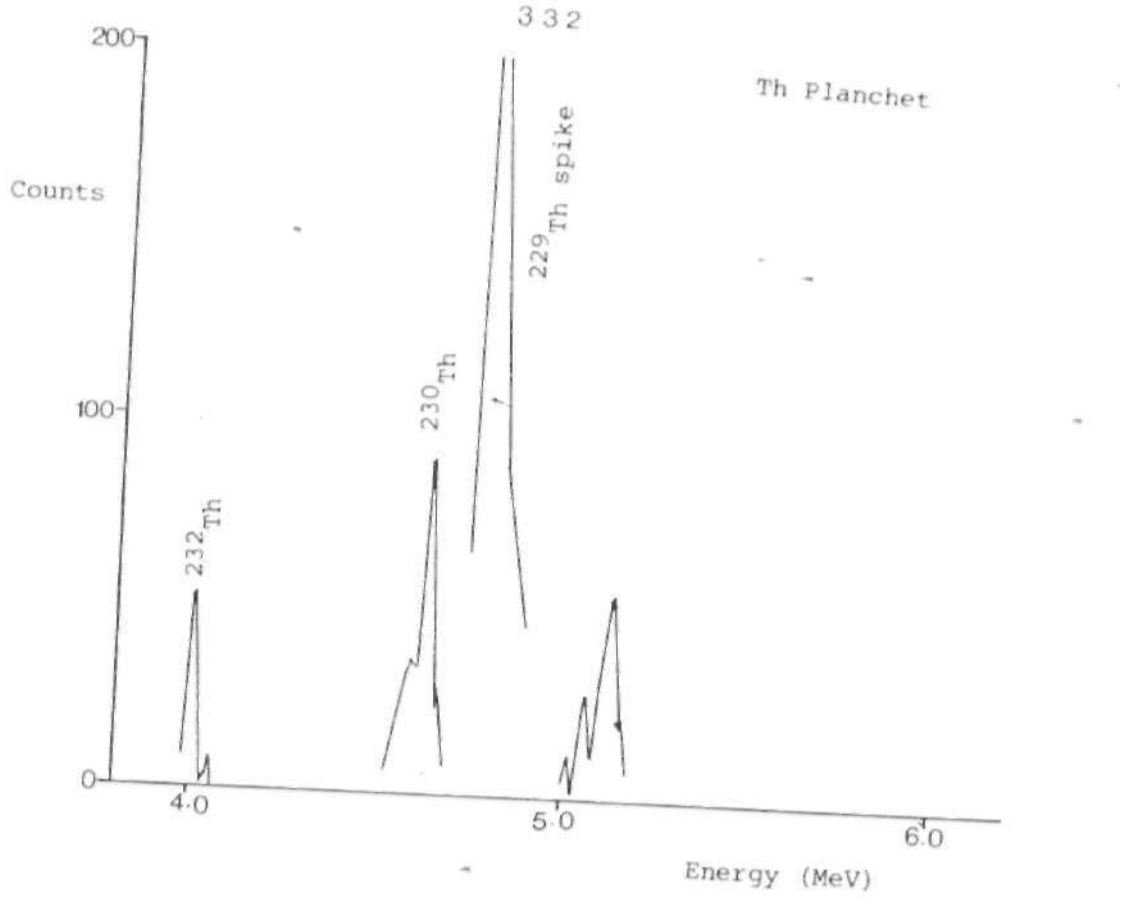


FIGURE 7.9 Th and U alpha-particle spectrum for granites, Nigerian Younger Granites (JPR17)



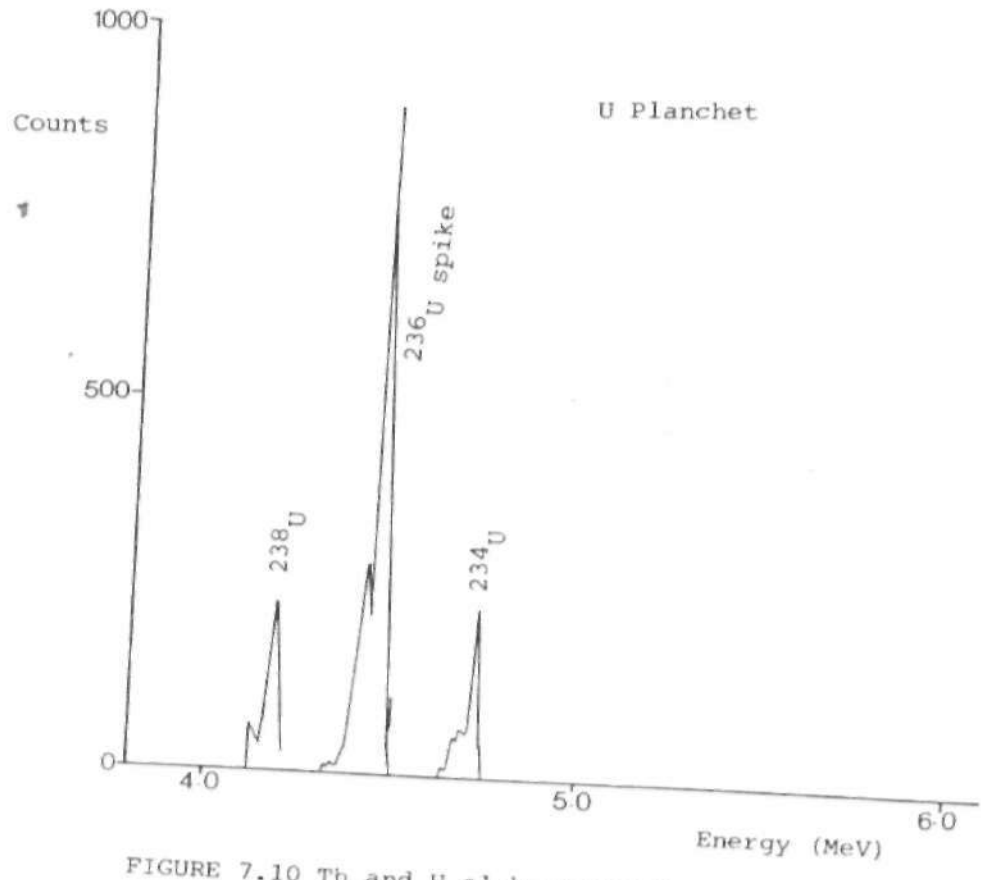


FIGURE 7.10 Th and U alpha-particle spectrum for granites, Nigerian Younger Granites (JPR42)

Results from sample JPS17 show that ^{234}U and ^{238}U are in approximate equilibrium, with some possible ^{238}U enrichment as shown by the $^{234}U/^{238}U$ activity ratio. ^{230}Th, however, is not in equilibrium with either ^{234}U or ^{238}U. The $^{230}Th/^{234}U$ activity ratio indicates recent U deposition, within the last 80,000 years.

The $^{234}U/^{238}U$ activity ratio indicates enrichment of ^{234}U in the sample JPS42. The absence of ^{230}Th suggests very recent deposition of U from ^{234}U-rich waters. At most, this deposition must have been within the last few thousand years. Enrichment of ^{226}Th suggests that the waters responsible for deposition were also charged with ^{226}Ra.

Results for JPR17 indicate that there was no fractionation between ^{234}U and ^{238}U. Both $^{230}Th/^{234}U$ and $^{230}Th/^{238}U$ activity ratios indicate some ^{230}Th deficiency suggesting remobilization of U in the granites. Equilibrium in the ^{238}U decay series was disturbed within the last 170,000 years as indicated by the $^{230}Th/^{234}U$ activity ratio.

The $^{234}U/^{238}U$ ratio in JPR42 indicates ^{234}U enrichment. Excess ^{234}U is also shown by $^{230}Th/^{234}U$ activity ratio. Generally, thus, ^{234}U had been introduced into the rock, within the last 70,000 years, at most.

Taken together, it can be seen that in kaolinized granites there is no U isotopic fractionation. These results contrast with

observations from weathered granite outcrops from the same region (Heath, 1982), where U isotopic fractionation was recorded in almost all the samples investigated. Differences between the processes involved in the kaolinisation of the granites and weathering have also been observed in the variation of elements associated with the two processes (Chapter 8). As previously mentioned, the kaolinised samples were representative of high and average U values in the environment. The sample representing average values (BMP33) showed more disequilibrium in the U series than the sample with high values. This also suggests that U deposition in the kaolinised granites is very recent. That samples with high values show U to be more in equilibrium may suggest that above-average U values in the kaolinised granites are due to a greater proportion of resistate accessory minerals.

The period of the main kaolinisation event is dated at 260Ma (Bristow and Exley, 1988), and the U deposition observed in the samples took place well after the kaolinisation of the granites, and is probably an ongoing process separate from the formation of the china clay deposits. However, the geological setting of the U in the deposits, discussed in Chapter 8, make any distinction between the processes of mobilisation and fixation very difficult to explain. That both relate to active hydrothermal circulation, as suggested by Durrance et al. (1980), is more reasonable, and differences in chemistry between the products of weathering and deep kaolinisation probably reflect the alteration

caused by the de-ferruginization phase of hydrothermal activity which occurred prior to kaolinization.

The results from the Nigerian Younger Granite samples indicate U remobilization during weathering. Equilibrium in the ^{238}U decay series was disturbed some 170,000 years ago. Weathering of the granites is characterized by fractionation between ^{234}U and ^{238}U, in which U is largely removed in solution as ^{234}U and redeposited elsewhere in the granites. Recent remobilization of U from the granites is best illustrated in the results for the soils associated with these granites.

Both soil samples from the Jos Plateau have significant disequilibrium in the ^{238}U decay series, but they have contrasting $^{234}U/^{238}U$ activity ratios. JPS17, with a high U concentration there is clear evidence of recent U deposition, with no fractionation between U isotopes. Similarly, JPS42, representing average U concentrations, also contains a very recent U deposition. The high $^{234}U/^{238}U$ activity ratio indicates precipitation from ^{234}U-enriched water, probably from leaching of U-rich minerals. The two important features shown by U series disequilibrium in the soils are, therefore, (1) very recent U deposition, and (2) the solutions responsible for U deposition are enriched in ^{234}U. This evidence indicates that most U in the soils is not contained within resistate accessory minerals which occur in the rocks from which these soils are derived. Instead, it supports the suggestion made in Chapter 5, that U has been precipitated or adsorbed onto

clay minerals, and Fe and Al oxides, or deposited in secondary U-rich minerals.

The high $^{234}U/^{238}U$ activity ratio of JPS42 may indicate a long residence time for water in contact with rock during lateritization: sufficient to have accumulated the ^{234}U displaced by recoil. Alternatively, Lally (1982) has shown that waters from U-enriched rocks in which disseminated mineralisation occurs are often characterised by high ^{234}U. In these environments, it is believed that ^{234}U loss due to recoil is greater than from rocks where U occurs in sporadically distributed coarse crystals where any displaced ^{234}U is easily accomodated in ^{238}U sites. Such disseminated U occurrences occur in the rocks associated with these soils.

It is interesting to compare the results of both the soil and rock samples; thus in the rock sample JPR17 and its associated soil JPS17, there is slight ^{230}Th deficiency with ^{234}U and ^{238}U in approximate secular equilibrium in both samples; in the rock sample JPR42 and its associated soil, JPS42, both are characterised by excess of ^{234}U. JPR42 is coarse-grained granite, and as noted (Chapter 4) these rocks are the most affected by weathering. This phenomenon may indicate a difference in the type of minerals that are important host of U in the various rock types. It is also an indication of the differential effects of weathering on the different rock types in the granites.

7.7 Conclusions

Investigations of U series disequilibrium were undertaken to determine the time frame and nature of U mobility in the kaolinised granites of South-West England and the lateritic soils associated with the Nigerian Younger Granites. Also of interest was the effect the equilibrium conditions have on gamma-ray activity in the two environments. It was hoped that in this way disequilibrium studies would help elucidate the nature of the processes involved in kaolinisation. In addition, experiments were carried out to reduce the count times normally used in alpha-particle spectrometry. A large measure of success was achieved in this direction by a fourfold increase in the size of sample. This allowed a reduction in the count time from two weeks to about three days for materials of similar character. However, the changes were not without new problems. Thus difficulties in separation of U from Th occurred because the amount of resin used in the ion-exchange columns designed for small samples was not sufficient for all the U to be absorbed while extracting Th. In future any work using large amounts of sample should include a new design of ion-exchange column with the ability to hold a large amount of resin yet still give efficient solution/resin exchange.

The results obtained from the two environments show large disequilibrium in both the kaolinised granites and the lateritic soils. In both cases, the patterns suggest very recent U

deposition, at most within the last 110,000 years and 80,000 years in the kaolinised granites and the soils, respectively. Indeed, in these environments U deposition is probably an active process. In the case of the kaolinised granites of South-West England, substantial U mobilisation long after the main kaolinisation process which liberated the U is very unlikely. The new evidence supports the view that active hydrothermal circulation believed to be responsible for the kaolinisation of the granites operates long after the kaolinisation of the granites. The young age of kaolinsation and U mobilisation, plus the fact that a good proportion of the U becomes adsorbed on the clay minerals in the zones of alteration, may also explain the failure to find large-scale U veins in the nearby areas - deposition of the limited U would be at greater depth than detectable by the survey methods used to date.

However, the isotopic evidence from the kaolinised granites contrasts with that obtained by Heath (1982) from weathered granite in the areas adjacent to the china clay deposits. This contrast was also noted in the general geochemistry described in Chapter 8. These differences probably reflect the fundamental changes suffered by the now deeply kaolinised zones in the precursor phase of de-ferruginisation alteration - deep kaolinisation has only developed where the descending limb of an active hydrothermal circulation coincides with a zone of de-ferruginisation.

Overall the type of disequilibrium which is present in the

kaolinised granites, with recent U precipitation, explains the generally low gamma-ray activity associated with above-average levels of U in these environments: gamma-ray spectrometric determinations give U abundances which are much lower than chemical U (Chapter 6).

Results from both the soil and rock samples from the Jos Plateau indicate relative ^{234}U enrichment, a feature which suggests either long residence times for the waters in contact with rocks from which the U was leached, or the importance of large-scale disseminated U mineralisation in the rocks. The latter explanation is the more likely. The age of U precipitation in the soil indicates that lateritization is young active process. In addition, the absence of ^{230}Th with excess ^{228}Ra in JPS42 reflects very recent movement of Ra from decay of ^{232}Th. This may be either a localised phenomenon, where solutions containing Ra evaporated before percolating to great depth, or there may be accumulation in association with U-bearing phases. It is also clear from these results that U is most affected in the coarse-grained members of the granites compared with the other varieties in the Younger Granites.

From the results of ^{234}U, ^{238}U and ^{230}Th activities, it is clear that secular equilibrium in the ^{238} decay series can not be assumed to exist for gamma-ray spectrometry on outcrops in the granites of the Jos Plateau. Evidence thus shows that the frequent association of high gamma-ray activity based on measurements on

^{214}Bi are likely to be the result of deposition of Ra or immediate ^{214}Bi parents during the deposition -of U in the secondary processes.

CHAPTER EIGHT: KAOLINISATION AND U MOBILITY

8.1 Introduction

Alteration processes in granites produce a redistribution of the elements: while some elements are lost in solution, others are concentrated in the residual material. Water-rock interactions during kaolinisation, are responsible for the removal of about 25% by weight of the rock mass in the affected parts of the granites of South-West England. Clearly, these processes, have greatly modified the chemistry of the granite in producing china clay, and it is important to note that the elements removed during kaolinisation would have been concentrated in the channel-ways through which the fluids moved out of the environment.

In the discussion in Chapter 6, on gamma-ray spectrometry, it was pointed out that disequilibrium can exist in the ^{238}U decay series. Moreover, studies of the South-West England granites have established that they contain a high radioelement content, with minerals such as uraninite being important. However, the results of the investigation of the radioactivity of the kaolinised granites, reported in Chapter 5, have shown that most of the alpha-particle emitters are concentrated in resistate minerals, particularly zircon, but that activity is also associated with surfaces of the clay minerals. This suggests the mobilisation of U during

alteration. Minerals like uraninite are, therefore, unstable during kaolinisation. Overall, there is a considerable loss of gamma-ray activity on kaolinisation. This is well shown by airborne surveys where areas of kaolinised granite have a very low gamma-ray activity (Figure 8.1).

This Chapter investigates the mobility of elements, particularly U, during kaolinisation. Clearly, in this study, the choice of a suitable indicator of kaolinisation is essential. Samples obtained from a borehole in the St. Austell granite were used in the preliminary investigations for determining suitable methods to be used. It was especially important to find a suitable index for the degree of kaolinisation. Two important implications of U mobility in kaolinised granites concern the location of U-mineralisation that would be associated with such granite areas, and the potential use of the clay material as a backfill in the isolation of radioactive waste. Backfill material must satisfy the requirement that ion species leaking from such wastes will be retarded by sorption. It was also hoped that the results of this study would further our understanding of the processes of kaolinisation.

8.2 Clays and Clay Minerals

Over the years the term clay has been defined in many ways, but all such definitions invoke the physical properties of the

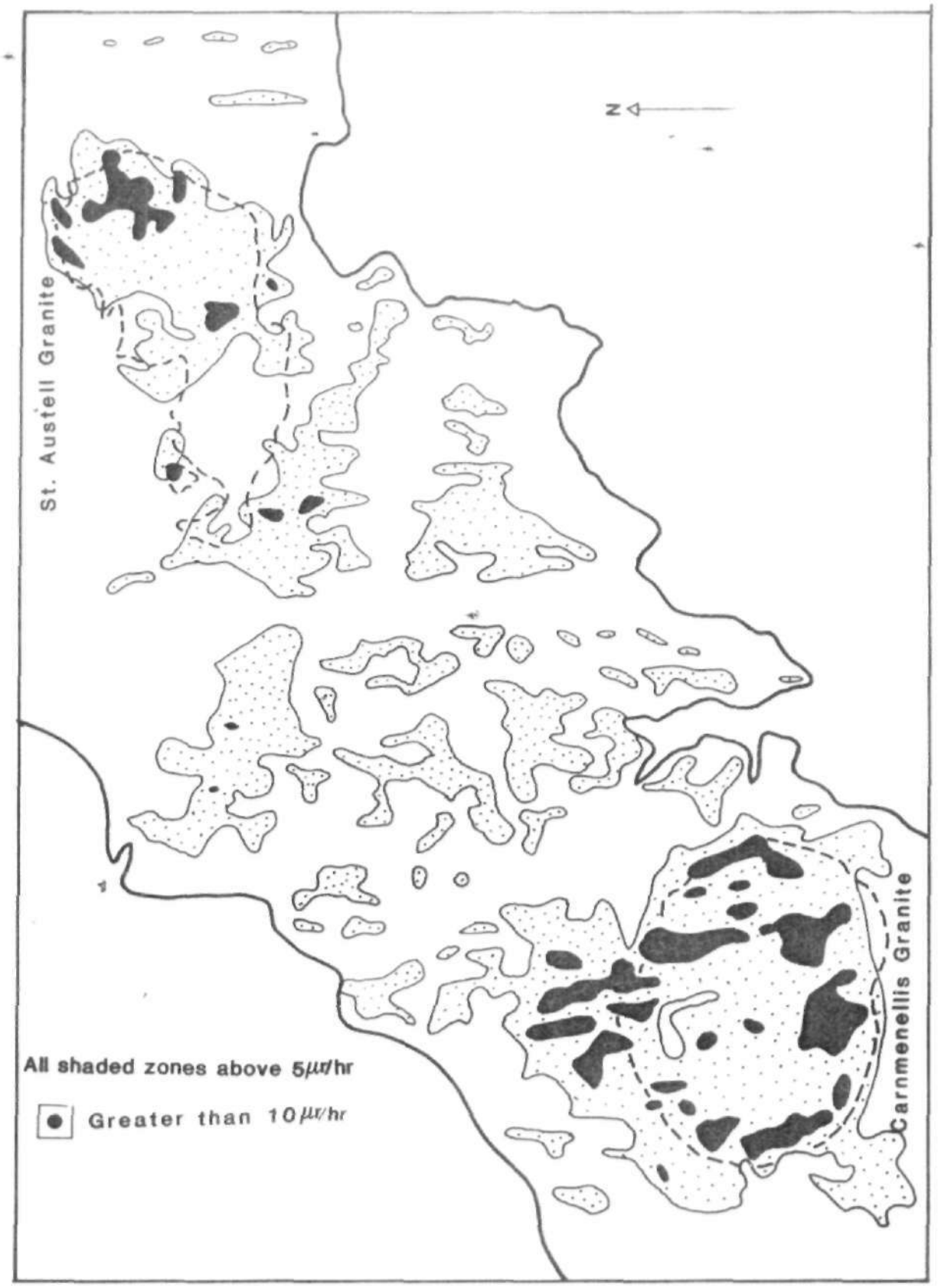


FIGURE 8.1 Airborne gamma activity showing low activities over kaolinised granites

substance. In some cases clays have been defined by the use of particle size, in others the plasticity when mixed with water. Recently, the definition of a fine-grained natural earthy argillaceous material has been used (Grim, 1962). Clays are generally composed of Al_2O_3, SiO_2 and water (Loughnan, 1969; Grim, 1953; Grim, 1962) with Fe, alkalies, and alkaline earths also sometimes present in various amounts. The small crystalline particles of a group of minerals which makes up a clay are referred to as the clay minerals. Many ideas have been put forward to explain how clay minerals are organised in clays. Hickling (1908), Grim (1953), Keller (1964) and Bristow (1977) have all given detailed accounts of the origin of clays. Clays and clay deposits occur in almost every environment of the Earth's crust, from within crystalline rocks to ocean beds. These deposits are formed mainly in two ways: hydrothermal and weathering. While it is sometimes possible to identify a single process as being mainly responsible for a specific deposit, in most cases this is very difficult. Usually, a combination of processes has to be invoked to explain their origins.

Clay minerals are usually subdivided into five groups: the kaolinite minerals, the mica minerals, the montmorillonite minerals, the chlorite-vermiculite minerals, and the fibrous clay minerals (Loughnan, 1969). Each group displays its own properties. These are shown in Table 8.1. Clay minerals possess certain properties which allow them to influence the mobility of ions in

Table 8.1: Classification of clay minerals.

Kaolinite group	
i) Dioctahedral series	
kaolinite	$Al_2Si_2O_5(OH)_4$
Disordered kaolinite	$Al_2Si_2O_5(OH)_4$
Nacrite	$Al_2Si_2O_5(OH)_4$
Dickite	$Al_2Si_2O_5(OH)_4$
Halloysite	$Al_2Si_2O_5(OH)_4.2H_2O$
Metahalloysite	$Al_2Si_2O_5(OH)_4$
ii) Trioctahedral series	
Antiggorite	$Mg_3Si_2O_5(OH)_4$
Chrysolite	
greenalite	$Fe^{2+}Si_2O_5(OH)_4$
Cronstedite	$(Fe^{2+}Fe^{3+})(Fe^{3+}Si)O_5(OH)_4$
Amesite	$Mg_2Al(AlSi)O_5(OH)_4$
Mica group	
i) Dioctahedral series	
IIlite (Three layer trigonal illite)	
Illite(Two layer monoclinic iilite)	$KAl_2(AlSi_3)O_{10}(OH)_2$ with
Illite (one layer monoclinic illite)	with K less unity and
Illite(One layer disordered monoclinic illite)	Mg^{2+} Fe^{2+} and Fe^{3+} partly replacing Al^{3+}
Glauconite	$K(Fe^{3+}Fe^{2+}AlMg)_2(AlSi_3)O_{10}(OH)_2$
ii) Trioctahedral series	
Illites rich in Mg and Ferrous iron	
Montmorillonite group	
i) dioctahedral series	
Beidelite	$Al_4(Si_{7.33}Al_{0.67})O_{20}(OH)_4\cdots M_{0.67}^{+}$
Montmorillonite	$(Al_{3.33}Mg_{0.67})Si_8O_{20}(OH)_4\cdots M_{0.67}^{+}$
Nontronite	$Fe^{3+}4(Si_{7.33}Al_{0.67})O_{20}(OH)_4\cdots M_{0.67}^{+}$
ii) Trioctahedral series	
Saponite	$Mg_6(Si_{7.33}Al_{0.67})O_{20}(OH)_4\cdots M_{0.67}^{+}$
Hectorite	$(Mg_{5.33}Li_{0.67})Si_8O_{20}(OH)_4\cdots M_{0.67}^{+}$
Chlorite-Vermiculite group	
i) Dioctahedral series	
Clay minerals with such structures have been identified but their structural formulae are unknown	
ii) trioctahedral	
These include clay minerals related to chlorite and	$(MgFe)_{6-x}(AlFe)_x(si_{4-x}Al_x)O_{10}(OH)_8$
vermiculite	$Mg_3(AlSi)_4O_{10}(OH)_2.Mg_{0.45}.4.5H_2O$
Fibrous clay group	
Palygorskite(attapulgite)	$(AlMgFe)_5(AlSi_7)O_{20}(OH)_2.4H_2O.4H_2O$
sepiolite	$Mg_9Si_{12}O_{30}(OH)_6.4H_2O.6H_2O$

(after Loughnan, 1969).

their environment. The most important of these are their ion-exchange capacity and their tendency to form complexes with organic compounds. Because of their fine structure, they may also influence the flow of fluid in their surroundings. These properties are controlled by certain factors of the clay mineral. The most important factors are the clay mineral composition, the composition of the associated minerals, the presence of organic material, the chemistry of exchangeable ions and soluble salts in the environment, and the clay texture (Grim, 1953).

8.3 Kaolinisation

This is the alteration of feldspars to the mineral kaolinite. Chemically, the process is represented by the equation:

$$2KAlSi_3O_8 + 3H_2O \Rightarrow Al_2Si_2O_5(OH)_4 + 4SiO_2 + 2KOH$$

The alteration was originally believed to be carried out in two stages. Exley (1959) showed that potash feldspar was first altered to secondary mica and then to kaolinite. In this process, all the potash must be removed or illite, and not kaolinite, will be the product (Loughnan, 1969). Bates (1952) also reported that montmorillonite is commonly formed when solutions are alkaline and leaching poor. Conditions favourable for kaolinite formation, therefore, should be indicated by the presence of low pH solutions,

with very good drainage to allow the soluble products of alteration to be removed. Thus the process is essentially the hydration of the Al-silicates and the removal of the alkalies. However, this mechanism does not take into account the presence of other minerals in the system. For example, occasionally Fe oxides are produced which tend to colour the kaolinite. This will mainly occur where the unaltered rock is rich in Fe-bearing minerals. Because the granites of South-West England are mostly quite rich in Fe (average value of 1.79%) and yet staining of the china clay deposit is not common, it has been suggested by Durrance et al. (1982) and Bristow (1986) that kaolinisation itself is preceded by a phase of de-ferruginisation. Kaolinisation, as such, only occurs in areas where de-ferruginisation has been profound. Current views on the mechanisms involved in kaolinisation itself are based on the observation that the formation of synthetic kaolinite is favoured by the migration of dissolved alumina, and subsequent reactions with either local or introduced silica. Nevertheless, whatever the mechanisms, the process involves the removal of a considerable amount of rock material.

In addition to the controversy on the origin of kaolinite, there is also controversy over the environment in which the process takes place, particularly whether hydrothermal or weathering agencies have been dominant in the formation of the South-West England deposits. In hydrothermal alteration processes, hot waters circulating through the upper crust are considered to be

responsible for the alteration of the feldspars, while in weathering, cold surface waters seeping through the parent rock are invoked. Possible sources for heating the water in hydrothermal processes which have been suggested are (1) magmatic heat from the emplacement of the granites, and (2) heat generated by the decay of the radioelements in the granites (Durrance and Bristow, 1986; Durrance, 1985).

8.4 Hydrothermal Activity and Kaolinisation in South-West England

Evidence abounds which indicates the operation of hydrothermal activity at various periods after emplacement of the granites of South-West England. This evidence will be discussed when considering the properties of the granites in the region.

For the operation of a hydrothermal circulation system, three essential requirements exist: (i) the rocks must be relatively permeable (a minimum permeability of 0.5mD has been suggested by Fehn et al., 1978), (ii) there must be some source of water, and (iii) a source of heat must be present. Both in-situ and laboratory permeability determinations have been carried out on the granites of the region. Black (1980) obtained an average permeability of 100μD and Batchelor (1980) obtained a range of between 0.001μD and 0.1μ D. However, these values are for intact-rock samples. Essentially, the in-situ permeability will be governed by the presence of fractures. Consequently, much higher

permeabilities have been obtained from interpretations of in-situ electrical resistivity data by Durrance et al. (1982). They even suggested that there might be some increase of permeability with depth in the granites. Moreover, available geological data suggest that the overall permeability of the plutons in South-West England is enough to support hydrothermal activity. Interpretation of the geological and topographical maps of Dartmoor by Heath (1982) showed many linear structures which he considers to be faults or fracture zones. These are enough to increase the overall permeability of the granite to many orders of magnitude greater than the intact-rock permeabilities. Many small-scale fractures are also present, and there is reactivation, even today, by movement on wrench faults as reported by Dearman (1963).

While some kaolinisation probably occurred as a result of hydrothermal activity driven by the magmatic heat of emplacement, the origin of the main kaolin deposits in this way is unlikely: typically such fluids have a K^+/H^+ ratio which is too high for kaolinisation. Moreover, the development of the main china clay deposits appears to be associated with a surface close to the present day landscape, suggesting an origin long after the granites had lost their magmatic heat. If a hydrothermal mechanism is proposed, it therefore follows that radiogenic heat is the likely source of energy.

The evidence for a source of radiogenic heat in the granites is overwhelming. High heat flow over the entire batholith

has been recorded by Wheildon et al. (1980), and they show the association of particularly high heat flow with the granite outcrops. Heat flow values as high as 132, 121 and 123mWm^{-2} occur on the Dartmoor, Bodmin Moor, and Carnmenellis granites, respectively (Figure 8.2). The detailed pattern of high flow from the plutons, where marginal high values occur as well as centrally-located highs, could either result from hydrothermal circulation or heat refraction at the granite-host rock boundaries. Wheildon et al. (1980) favoured the latter explanation, but Durrance et al. (1982) suggested that modern hydrothermal circulation is taking place, driven by the radiogenic heat.

Heat production values of up to 2.4hgu have been indicated by Wheildon et al. (1980) to occur in the South-West England plutons. Indeed, Tammemagi and Smith (1975) obtained an average heat production of 11.2hgu from the surface of the granites.

The presence of groundwater in the region is obvious because of the numerous springs. The region enjoys an average rainfall of 102-203cm per year, and with the soil cover and the vegetation obtained in the region, the surface water could easily percolate to great depth over the years. However, since the emplacement of the plutons in the late Carboniferous, the availability of water in the granites has varied greatly. Durrance et al. (1982) suggested that in the late Triassic or early Jurassic fresh water must have massively invaded the granite with the end of the arid conditions of the Permian and early Triassic. However, in the late Mesozoic,

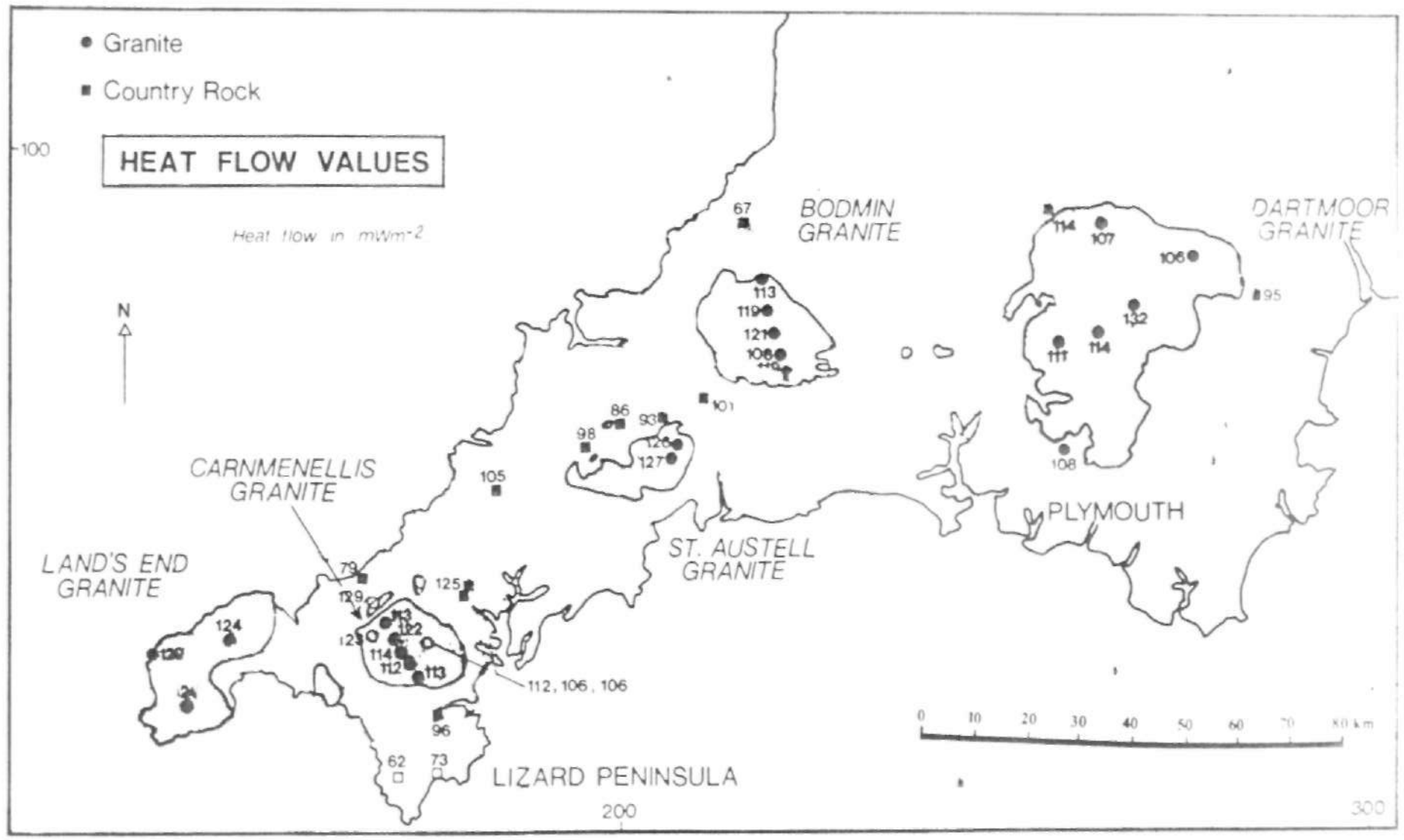


FIGURE 8.2 Heat flow values over granites in South-West England

(After Wheildon et al., 1980)

marine waters entered the area as a result of a global rise of sea level. Sheppard (1977) recognised the contribution of meteoric water in the formation of the hydrothermal metalliferous mineral deposits of the region.

Overall, therefore, the conditions required for hydrothermal circulation in the granites of South-West England are met. More especially, the plutons meet the requirements imposed by the model developed by Fehn et al. (1978) for the realisation of convective hydrothermal circulation in radiothermal plutons. Today there is evidence of hot springs discharging in mines at about 50^{o}C, so hydrothermal circulation in the form of convective cells is operative in the region. Thus although Wheildon and coworkers suggested that the distribution of high heat flows observed in the region could be explained without invoking the circulation of groundwater, the view of Durrance et al. (1982) is more likely to be correct. This view is substantiated by Bloomer et al. (1982), and Fehn (1985). In this system, upwelling limbs of convection cells are located at sites where there is especially high heat flow.

Before considering how modern hydrothermal convective circulation systems can help explain the origin of the china clay deposits of South-West England, it is necessary to explore the evidence which favours a hydrothermal mechanism in more detail. The most important lines of evidence for a hydrothermal origin, as opposed to a weathering origin, for the china clay deposits were

given by Bristow (1977) as:

1) The funnel-shaped form of the deposits which extend to depths greater than 250m,

2) The occurrence of kaolinised granite under layers of unaltered granite,

3) The association of kaolinisation with greisen-bordered quartz-tourmaline veins, and

4) Known instances of the crystallinity index of the kaolinite increasing towards major quartz-tourmaline veins.

Based on fluid inclusion studies of samples from kaolinised granite in the region, Bray (1980) has supported a hydrothermal origin for the deposits. Especially important is the fact that K-Ar age determinations on fine-grained mica, believed to be produced during the de-ferruginisation precursor phase to kaolinisation, yield a date some 7-13Ma younger than the emplacement of the granites. Temperatures in the range of 220-460^{O}C and salinities of 0.1-0.36 % wt. NaCl were obtained for the Goonbarrow deposits in the St. Austell granite.

China clay deposits are associated with almost all the granitic intrusions in the region. The St. Austell, Dartmoor, Bodmin Moor and Carnmenellis plutons all host some of the most important deposits of economic interest. Major producing areas are shown in Figure 8.3. As mentioned previously, the distribution of the deposits has been suggested to be controlled in part by the height of the plutons relative to the land surface (Bristow and

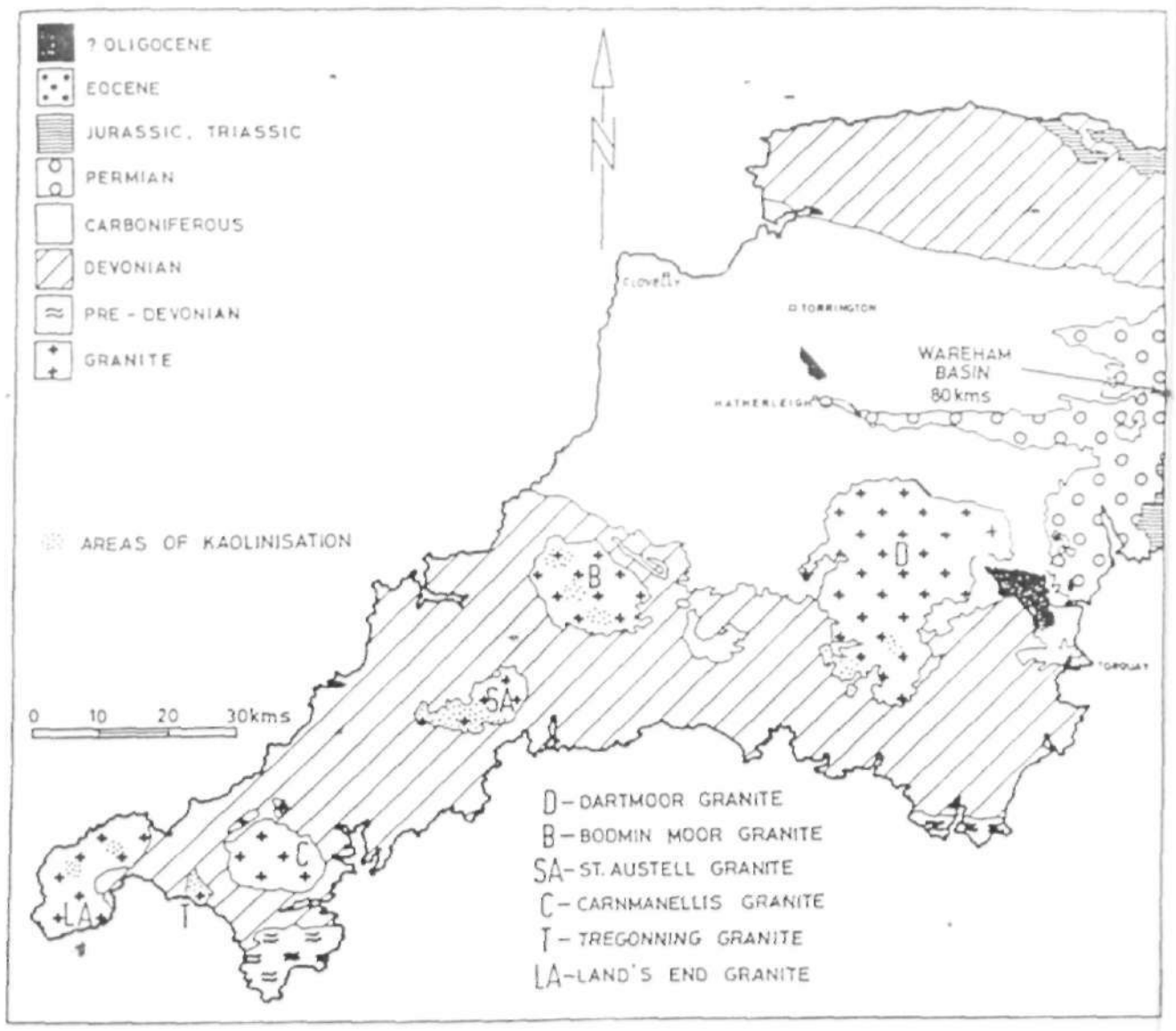


FIGURE 8.3 Major china clay producing areas in South-West England

Exley, 1988). The most important china clay deposit are in the St. Austell granite, but the most thoroughly altered zone is in the Lee Moor area of Dartmoor.

8.5 Kaolinisation Index

This study was undertaken to develop the methodology of the research program. In the investigation of U mobility during kaolinisation, it was found necessary to determine an index which was indicative of the degree of kaolinisation.

To determine which index was best, samples from a single bore hole from a kaolinised pit (St. Austell granite) were considered. The choice of a single bore hole was to avoid the possibility of confusion caused by variation in different rock type from one site to another. The hole was bored from the surface of a level that fresh granite was encountered, thus running through the whole depth of the kaolinised granite in the area. The samples were grouped into three series: (1) fresh, (2) slightly kaolinised, and (3) wholly kaolinised. Sample categories and other information are given in Table 8.2.

To divide the samples more finely, the most apparent physical parameter affected, their density, was determined. This was found to correlate well with the grouping of the samples. The method of density determinations is given in Appendix 8.1. However, density can only be related to the degree of kaolinisation if it can be related to the kaolinite content. So the clay content of the

Table 8.2: Chemical analyses, physical appearance and the depth for samples used to determine index of kaolinisation.

Sample	Depth/m	state
BB1	>17 < 24	Relatively fresh
BB2	> 17 < 24	Slightly kaolinised
BB3	12.00	Thoroughly kaolinised
BB4	>24	Fresh
BB5	>24 < 27	Slightly kaolinised
BB6	>27 < 30	Relatively fresh
BB7	>30 < 31	Thoroughly kaolinised
BB8	>31 < 33	Fresh
BB9	33	Relatively fresh
BB10	41	Slightly kaolinised
BB11	42	Thoroughly kaolinised
BB12	45	Thoroughly kaolinised

b: Chemical analyses

Sample	SiO_2	Al_2O_3	TiO_2	Fe_2O_3	MgO	CaO	Na_2O	K_2O	P_2O_5	MnO
BB1	72.28	16.44	0.22	1.23	0.21	0.07	0.60	5.05	0.06	0.03
BB2	75.13	13.15	0.18	1.94	0.17	0.07	0.31	5.93	0.01	0.37
BB3	79.43	11.59	0.15	1.23	0.08	0.09	0.40	6.41	0.04	0.03
BB4	73.43	14.18	0.19	3.16	0.17	0.07	0.31	5.16	0.02	0.30
BB5	74.60	12.74	0.17	1.59	0.09	0.07	0.35	7.69	0.06	0.15
BB6	74.38	13.58	0.20	2.02	0.15	0.08	0.53	6.56	0.03	0.17
BB7	75.50	13.85	0.20	1.24	0.14	0.06	0.22	3.84	0.05	0.03
BB8	74.56	13.63	0.19	2.71	0.13	0.05	0.50	5.19	0.02	0.17
BB9	78.89	11.36	0.18	1.68	0.20	0.08	0.37	4.78	0.01	0.06
BB10	72.95	15.81	0.20	1.07	0.16	0.08	0.37	4.49	0.06	0.02
BB11	73.75	16.05	0.21	0.95	0.17	0.07	0.43	4.78	0.06	0.02
BB12	73.38	15.51	0.24	0.76	0.16	0.11	0.23	5.39	0.04	0.01

Sample	Ni	Cu	Zn	Ga	As	W	Pb	Th	U	V	Cr	Ba
BB1	9	12	34	26	16	817	17	11	7	6	14	93
BB2	9	8	62	30	-	1208	14	8	5	3	14	91
BB3	9	11	41	14	23	1424	14	6	4	5	14	184
BB4	9	18	106	29	17	875	15	9	7	5	15	70
BB5	9	12	54	24	12	1242	22	10	10	5	14	108
BB6	10	10	74	28	14	1216	5	10	7	5	15	77
BB7	8	10	43	25	15	1741	13	11	7	4	14	62
BB8	8	10	98	31	8	1138	-	10	6	5	15	66
BB9	9	9	52	21	16	1741	9	7	5	5	15	174
BB10	8	10	32	24	59	959	22	9	6	5	14	82
BB11	8	9	29	24	52	934	19	9	7	5	13	108
BB12	6	9	20	21	27	736	7	11	5	4	14	73

Continue.....

Table 8.2, Continued.

Sample	La	Ce	Rb	Sr	Y	Zr	Nb	Cs	Sn
BB1	28	45	636	43	31	84	19	103	40
BB2	14	24	822	26	28	54	18	69	348
BB3	9	33	561	71	26	41	13	31	23
BB4	26	30	1020	10	35	55	17	111	410
Bb5	24	44	913	39	33	53	17	79	48
BB6	21	39	911	23	33	56	18	76	79
BB7	25	47	516	32	24	83	19	80	37
BB8	23	31	900	11	31	54	18	84	107
BB9	16	30	573	46	24	51	18	46	148
BB10	25	45	529	55	26	78	19	71	34
BB11	18	41	491	60	26	80	20	45	35
BB12	-	20	178	42	17	87	23	16	42

Major elements as oxides in %, others in ppm.

samples was also determined. The results obtained are shown in Table 8.3. There is remarkable agreement between the two sets of data. The procedure of clay determination which was used is outlined in Appendix 8.2. X-ray diffraction studies were carried out to check that the clay was indeed kaolinite in each sample. Therefore, density was found to be very valuable index of alteration in the kaolinisation process.

8.6 Geochemistry of Kaolinisation of Granites

8.6.1 Granite Textures

Detailed studies of the geochemistry of kaolinisation have been carried out on samples from the Park Pit on Bodmin Moor (SX219708). Petrological and textural descriptions of the granites of South-West England have been given by Brammal and Harwood (1934) Exley and Stone (1966), and Exley et al. (1983), but much of the variation given is irrelevant to the specific site of the Park Pit. Consequently, it follows that the review which follows is a simplified account largely drawn from the terminology of these publications.

Texturally the exposures on Bodmin Moor are largely made of the type-B classification of Exley and Stone (1966) and Exley et al. (1983), with some fine-grained varieties. The type-B granites are characterised by abundant large megacrysts which may attain

Table 8.3: Density values in relation to clay content in kaolinised granite.

Sample	Density gcm^{-3}	Clay cont. g/10g
BB1	1.93	1.68
BB5	2.51	0.84
BB7	2.41	1.16
BB9	2.54	0.69
BB10	1.90	1.80
BB11	1.97	1.50
BB12	1.96	1.58

sizes of 5-17cm across. They are much coarser than any of the other granite types in the region. Gosh (1927) recognised the composite nature of the coarse-grained phase and found it to be composed of two varieties which he classified as the Normal type and the Godaver type; with the latter intruding the former. The Godaver type is suggested to be medium-grained, and has fewer phenocrysts than the Normal type. The fine-grained type has less biotite and also contains few orthoclase phenocrysts, which sometimes are completely absent. It is believed that the intrusive history of the various textural types can be divided in to four separate cycles. First came the intrusion of the Normal type. This was followed by the Godaver type and then by the fine-grained type. Each of the intrusive phases was followed by the formation of quartz and quartz-tourmaline veins with occasional metalliferous lodes (Gosh, 1927). Intrusive bodies include pegmatites, and melanocratic veins and aplites in the Normal type.

The Bodmin Moor granite is hypidiomorphic in texture. The coarse-grained granite which makes up most of the pluton is a two-mica (biotite and muscovite) granite which contains a large proportion of quartz. The quartz occurs in large granular patches. Biotite and muscovite are present in almost equal proportions. The major rock-forming minerals; quartz, potash feldspar and plagioclase, constitute about 98% of the rock, with tourmaline occurring as an abundant accessory mineral. Other accessory

minerals include zircon, apatite, andalusite, magnetite, ilmenite, cassiterite, rutile, anatase, and corrundum (Gosh, 1927). Feldspar megacrysts 5-17cm in length, with a mean of about 2cm, are abundant in the coarse-grained phase (Exley et al., 1983).

8.6.2 Sample Collection

The discussion of the geochemistry of U mobilisation during kaolinisation which follows is based on samples collected from Park Pit, which is being worked for china clay by ECC International on the Bodmin Moor granite. The pit is located near the southern edge of the granite. It covers an area of about $1.7.10^4$ m^2, and is surrounded by farmland. In the vicinity of the pit there are no major rock outcrops of any extent, only small exposures and rock boulders, and these more especially around the water reservoir about a kilometre from the pit (Figure 8.5). The most important features identifiable in the pit include some greisen veins which have been kaolinised, and small quartz and tourmaline veins. In addition to these veins, dotted here and there, are small masses of granite which evaded alteration. These are generally Fe-stained, and this might have contributed to the poor quality of the china clay produced from Bodmin Moor, as noted by Bristow and Exley (1988). A panoramic view of the pit is shown in Figure 8.5.

Both unaltered granite samples and kaolinised granite samples were collected from the vicinity of the pit. Fresh samples were

obtained from small exposures to the north of the pit just across the stream shown in Figure 8.4, and some from the unkaolinised rock masses within the pit. From the kaolinised granite, samples were collected on traverses across the pit. To obtain 'fresh' kaolinised surfaces, the washed surfaces were scrapped with a scoop before sample collection. Samples were taken in labelled polythene bags for transportation to the Geology Department in Exeter for analysis. For each sample, about 2.5kg of the material was taken. Sampling points and some features of the pit are shown in Figure 8.4.

After collection, the samples were allowed to dry in air before being prepared using the methods described in Chapter 4 for XRF analysis. In addition, about 200g was taken from each sample for density measurements as described above, and other portions reserved for gamma-ray spectrometry as reported in Chapter 6. Overall, 70 samples were collected from the pit.

8.6.3 Results

8.6.3.1 Element Variation

The chemical analyses of the samples, together with the correlation coefficient values of the elements, are shown in Table 8.4. Table 8.5 gives the average concentrations of elements in the

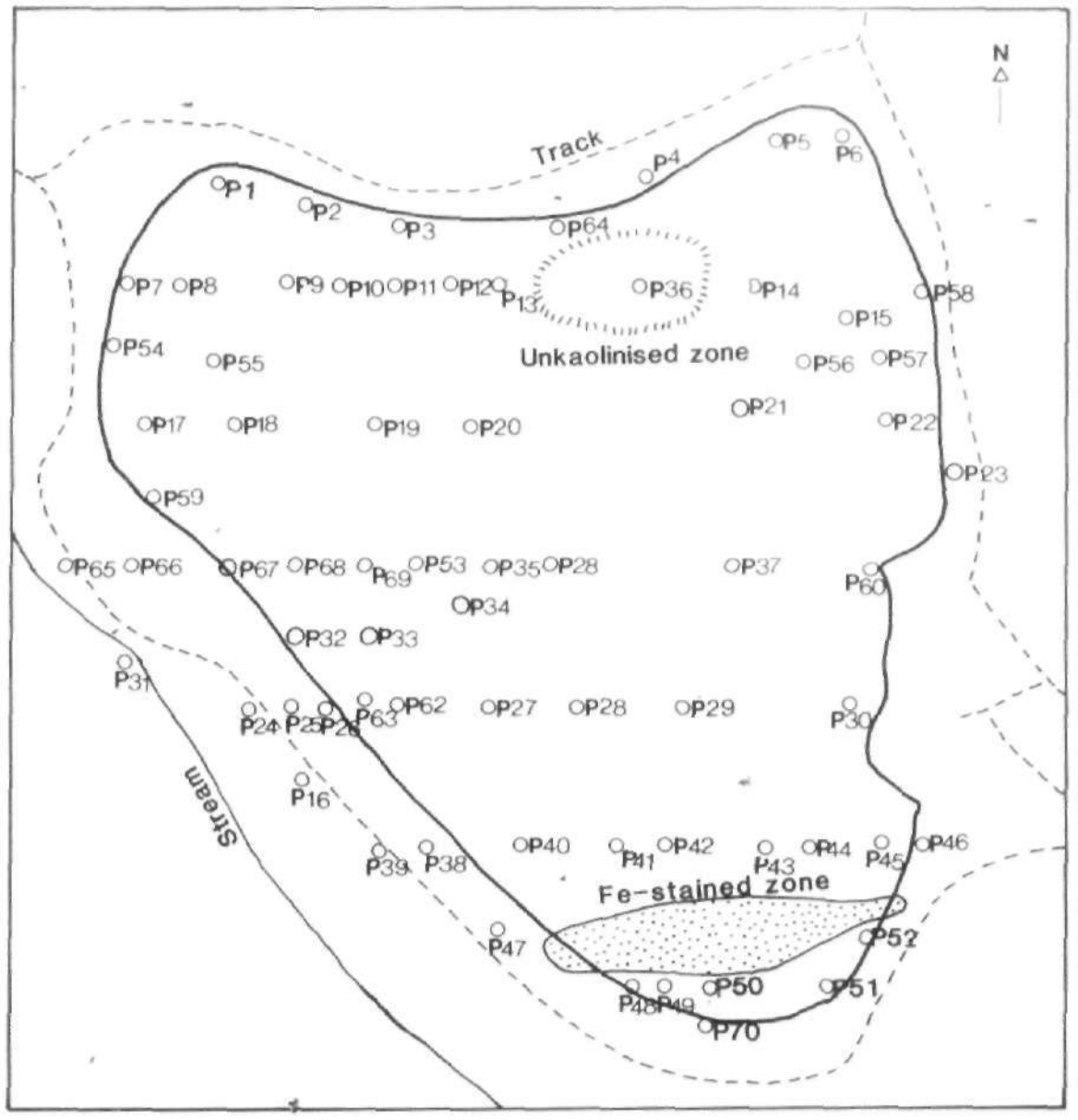


FIGURE 8.4 Sampling points (OP28) showing major features of the Park Pit

Table 8.4a: Chemical analyses[1] for kaolinised granites and their density

Samp. no.	Density	SiO_2	Al_2O_3	TiO_2	Fe_2O_3	MgO
P1	1.97	71.16	17.54	0.25	1.43	0.28
P2	2.39	72.61	17.46	0.13	1.10	0.17
P3	2.30	74.15	20.63	0.12	1.07	0.17
P4	2.45	73.75	18.00	0.10	0.93	0.13
P5	2.57	72.19	16.68	0.10	1.09	0.19
P6	2.45	72.26	16.77	0.09	1.12	0.15
P7	1.94	72.64	18.42	0.23	1.21	0.21
P8	2.00	70.17	19.05	0.18	1.40	0.27
P9	2.03	72.26	17.53	0.17	1.16	0.20
P10	2.27	72.11	17.08	0.13	1.17	0.16
P11	2.53	74.06	15.47	0.13	1.00	0.17
P12	2.20	70.74	18.31	0.14	1.13	0.14
P13	2.24	71.22	15.43	0.11	0.99	0.24
P14	2.18	72.92	19.59	0.14	1.06	0.20
P15	2.08	71.67	19.79	0.11	1.10	0.12
P16	2.57	73.18	18.11	0.11	1.06	0.12
P17	2.00	70.23	19.25	0.19	1.38	0.24
P18	2.52	73.44	16.71	0.16	0.93	0.19
P19	2.10	72.16	18.95	0.18	0.82	0.16
P20	2.26	70.65	16.53	0.11	0.83	0.09
P21	2.02	71.21	19.51	0.12	0.93	0.20
P22	1.92	68.65	21.18	0.13	1.28	0.13
P23	2.58	72.66	16.82	0.11	1.05	0.17
P24	2.38	72.78	18.31	0.10	1.12	0.13
P25	2.12	72.25	18.37	0.09	1.07	0.18
P26	2.07	71.73	19.10	0.18	1.12	0.21
P27	2.43	73.27	19.35	0.20	1.45	0.36
P28	2.17	75.26	16.28	0.14	0.90	0.14
P29	2.18	72.36	20.10	0.13	1.04	0.16
P30	2.50	72.26	15.30	0.12	1.01	0.11
P31	2.51	72.83	15.96	0.16	1.33	0.19
P32	2.26	70.90	19.99	0.19	1.31	0.17
P33	1.82	70.03	19.68	0.13	1.22	0.20
P34	2.04	69.95	20.67	0.14	1.19	0.17
P35	2.58	72.37	16.45	0.14	1.10	0.23
P36	2.54	72.33	17.56	0.14	1.12	0.17
P37	1.97	71.86	19.20	0.14	1.24	0.21
P38	2.51	72.92	16.42	0.12	1.07	0.18
P39	2.37	72.25	16.01	0.12	1.07	0.14
P40	2.11	70.59	19.42	0.16	1.20	0.16
P41	2.28	73.33	17.34	0.14	1.14	0.23
P42	2.29	73.19	18.77	0.14	1.10	0.15
P43	1.81	70.92	19.35	0.15	1.30	0.15
P44	2.08	71.80	19.42	0.13	1.23	0.16
P45	1.91	73.03	15.37	0.14	1.27	0.16
P46	1.88	68.93	19.95	0.15	1.31	0.18
P47	2.59	73.06	17.22	0.16	1.25	0.35
P48	2.01	71.83	18.31	0.20	1.06	0.15
P49	2.02	71.20	19.59	0.21	0.92	0.22
P50	2.34	72.79	14.25	0.25	0.89	0.21

Continue....

Table 8.4a, Continued.

P51	2.02	70.94	16.25	0.23	0.96	0.18
P52	2.38	71.76	18.58	0.16	1.13	0.21
P53	2.40	72.21	16.37	0.18	1.26	0.19
P54	2.19	72.45	18.80	0.18	1.12	0.20
P55	2.25	71.78	19.17	0.15	1.26	0.19
P56	2.36	75.83	15.08	0.14	1.95	0.16
P57	2.06	73.09	20.57	0.17	0.85	0.16
P58	2.47	74.07	14.96	0.11	0.86	0.09
P59	2.25	72.08	16.45	0.15	1.21	0.14
P60	2.12	72.76	16.74	0.13	1.05	0.15
P61	2.14	71.37	20.12	0.13	1.26	0.21
P62	2.17	72.74	20.24	0.13	1.35	0.15
P63	1.86	68.20	20.20	0.14	1.45	0.17
P64	2.28	70.29	19.34	0.13	1.32	0.13
P65	2.57	71.93	15.44	0.18	1.34	0.20
P66	2.46	72.60	17.07	0.17	1.19	0.22
P67	-	72.79	16.38	0.14	1.14	0.17
P68	2.26	70.48	18.54	0.13	1.16	0.16
P69	2.04	70.53	16.53	0.19	1.26	0.15
P70	1.87	71.90	17.55	0.21	1.05	0.16

Continue...

Table 8.4, Continued.

Sample	CaO	Na_2O	K_2O	P_2O_5	MnO	Rb
P1	0.05	0.49	5.81	0.06	0.02	611
P2	0.23	2.70	4.96	0.20	0.05	641
P3	0.25	2.52	5.35	0.17	0.05	591
P4	0.27	2.67	5.21	0.20	0.05	615
P5	0.16	2.23	5.57	0.13	0.06	675
P6	0.11	2.65	5.32	0.08	0.06	816
P7	0.04	0.20	6.47	0.07	0.02	647
P8	0.06	0.60	5.38	0.08	0.04	697
P9	0.06	0.53	5.44	0.08	0.03	663
P10	0.06	0.71	6.37	0.08	0.04	670
P11	0.48	2.89	4.98	0.18	0.05	540
P12	0.08	0.90	5.48	0.09	0.03	625
P13	0.07	0.83	6.62	0.07	0.04	629
P14	0.18	1.24	4.69	0.08	0.02	450
P15	0.05	1.16	5.32	0.06	0.06	671
P16	0.39	3.30	5.21	0.24	0.06	636
P17	0.04	0.27	6.01	0.08	0.05	758
P18	0.27	2.51	5.90	0.18	0.04	595
P19	0.04	0.35	6.09	0.06	0.02	605
P20	0.05	0.34	6.11	0.10	0.02	542
P21	0.06	0.29	6.71	0.07	0.02	548
P22	0.04	0.22	1.36	0.02	0.03	280
P23	0.25	2.71	5.64	0.21	0.05	574
P24	0.15	2.24	5.18	0.12	0.06	648
P25	0.10	1.10	5.49	0.08	0.04	599
P26	0.05	0.18	5.78	0.06	0.02	641
P27	0.42	3.01	6.90	0.26	0.04	609
P28	0.05	0.34	4.70	0.04	0.03	558
P29	0.13	0.39	6.14	0.08	0.03	618
P30	0.32	2.86	5.09	0.23	0.03	536
P31	0.31	2.03	6.24	0.23	0.05	631
P32	0.04	0.36	5.58	0.07	0.06	709
P33	0.04	0.14	5.06	0.05	0.05	647
P34	0.05	0.23	5.48	0.05	0.04	672
P35	0.21	2.68	5.40	0.12	0.04	624
P36	0.29	3.20	5.11	0.18	0.04	592
P37	0.06	0.64	6.01	0.06	0.04	670
P38	0.33	3.30	4.89	0.24	0.05	597
P39	0.31	2.74	5.45	0.19	0.04	557
P40	0.04	0.88	5.98	0.06	0.04	682
P41	0.07	0.67	6.01	0.06	0.04	640
P42	0.07	0.23	6.31	0.07	0.04	653
P43	0.05	0.11	3.63	0.03	0.03	491
P44	0.06	0.19	5.37	0.07	0.02	638
P45	0.06	0.35	5.92	0.09	0.03	638
P46	0.03	0.24	4.72	0.05	0.04	621
P47	0.59	3.42	5.17	0.27	0.05	587
P48	0.03	0.14	4.78	0.06	0.03	579
P49	0.05	0.25	5.71	0.10	0.02	573
P50	0.04	0.13	8.05	0.02	0.01	736

Continue.....

Table 8.4a, Continued.

P51	0.04	0.22	5.29	0.08	0.02	587
P52	0.05	0.32	7.51	0.06	0.03	637
P53	0.20	2.26	5.48	0.15	0.04	590
P54	0.05	0.21	6.16	0.07	0.03	665
P55	0.06	0.59	6.07	0.07	0.03	671
P56	0.05	0.68	6.48	0.10	0.03	616
P57	0.06	0.20	6.23	0.08	0.02	608
P58	0.08	0.28	6.72	0.07	0.02	522
P59	0.08	0.47	5.47	0.15	0.05	672
P60	0.04	0.31	5.08	0.05	0.03	532
P61	0.06	0.23	5.27	0.05	0.05	694
P62	0.03	0.14	5.24	0.04	0.05	715
P63	0.04	0.37	2.03	0.02	0.06	468
P64	0.07	0.33	6.41	0.03	0.05	869
P65	0.38	1.84	6.38	0.28	0.04	607
P66	0.33	2.22	5.73	0.21	0.04	590
P67	0.34	2.89	5.32	0.21	0.05	592
P68	0.05	0.26	5.95	0.14	0.03	643
P69	0.04	0.31	5.59	0.07	0.03	653
P70	0.03	0.29	5.59	0.04	0.02	616

Continue.....

Table 8.4a. Continued.

Sampl.	Sr	Y	Zr	Nb	Ni	Cu	Zn	Ga	As	W	Pb
P1	61	21	120	15	9	14	36	24	4	177	23
P2	44	20	55	19	8	13	39	23	7	301	18
P3	76	29	50	19	9	13	40	22	7	330	24
P4	49	19	48	19	8	9	35	22	8	308	18
P5	40	20	46	25	8	9	44	22	11	191	12
P6	24	25	44	26	8	8	42	24	5	372	11
P7	63	27	115	15	9	13	30	24	3	213	21
P8	55	26	98	21	8	13	40	27	5	207	25
P9	48	27	78	19	8	10	33	24	3	210	21
P10	38	25	60	19	8	8	39	24	3	260	18
P11	57	31	53	15	8	7	34	22	4	495	20
P12	40	29	64	18	8	9	43	25	4	226	24
P13	54	30	47	21	7	11	38	23	4	300	17
P14	36	29	61	16	7	13	40	23	6	276	19
P15	38	25	52	22	7	11	33	25	2	225	23
P16	52	26	48	21	8	8	35	23	5	198	17
P17	48	24	87	17	8	9	36	25	2	259	20
P18	72	28	67	15	8	10	36	22	7	228	21
P19	42	25	92	17	8	13	27	24	5	277	16
P20	46	24	49	31	7	17	28	25	2	228	29
P21	50	27	58	12	7	11	25	23	5	232	21
P22	31	26	65	23	5	12	32	29	-	158	37
P23	77	27	48	15	8	18	29	21	5	346	18
P24	31	21	40	27	8	8	42	26	3	385	18
P25	44	24	61	16	8	10	35	23	4	257	19
P26	52	22	88	15	8	20	36	24	5	253	21
P27	89	24	75	16	8	9	41	23	5	287	20
P28	41	19	57	20	8	16	26	22	3	346	15
P29	52	23	57	20	8	12	34	23	6	257	20
P30	57	27	52	15	7	9	28	22	840	317	15
P31	57	27	62	16	9	7	37	23	26	412	10
P32	37	21	55	23	8	17	36	27	6	235	13
P33	29	19	62	16	7	9	34	25	4	238	24
P34	35	25	69	19	8	9	32	26	2	161	24
P35	79	23	57	18	8	15	35	23	6	367	14
P36	85	29	60	14	8	10	37	23	7	329	17
P37	47	54	69	19	8	9	34	24	5	288	17
P38	43	22	48	19	8	7	33	22	7	349	11
P39	51	20	53	14	8	6	30	21	5	316	22
P40	33	26	72	22	8	11	32	26	3	214	19
P41	41	22	66	16	8	13	29	24	3	240	17
P42	56	20	61	17	8	16	32	23	15	285	19
P43	25	19	74	18	7	17	39	25	8	255	12
P44	53	25	54	20	8	9	33	26	5	229	15
P45	46	22	65	17	9	19	40	24	10	159	10
P46	49	19	75	20	8	12	40	25	7	235	17
P47	67	24	67	16	8	6	36	22	28	252	16
P48	47	26	95	22	8	8	27	26	4	392	19
P49	90	22	103	14	8	17	24	23	5	305	23
P50	71	27	122	13	8	10	12	22	10	246	-

Continue.....

Table 8.4a, Continued.

P51	67	23	114	21	8	14	22	26	4	276	19
P52	51	25	69	13	9	30	40	23	15	469	12
P53	74	24	80	17	9	15	52	24	6	464	19
P54	60	26	84	18	8	14	42	24	3	311	31
P55	48	23	75	18	8	15	38	25	5	335	18
P56	47	20	60	12	10	22	38	21	24	466	25
P57	46	24	85	20	9	13	22	25	4	339	21
P58	47	26	53	9	8	14	29	19	4	265	20
P59	127	62	64	21	10	15	39	25	16	350	22
P60	35	28	52	20	9	12	34	24	4	212	20
P61	38	32	59	19	7	12	36	26	6	159	13
P62	45	24	53	24	8	14	37	26	5	224	11
P63	14	23	76	31	6	11	39	30	4	162	11
P64	21	28	67	30	9	14	45	27	7	228	-
P65	53	22	78	16	9	8	42	24	65	611	6
P66	68	18	79	17	9	7	36	23	4	336	23
P67	52	20	60	17	8	8	39	22	5	118	24
P68	45	24	63	18	8	23	36	25	6	237	24
P69	49	21	82	19	8	10	38	25	5	235	16
P70	58	39	112	16	8	7	30	26	6	221	16

Continue....

Table 8.4a, Continued.

	Th	U	Cr	Mn	Ba	La	Ce	Cs	Sn	V	LOI
P1	13	7	16	204	223	32	53	67	30	-	3
P2	7	10	13	403	91	15	28	59	26	4	2
P3	5	8	19	370	220	12	25	49	34	-	1
P4	4	10	15	360	104	16	23	55	39	-	1
P5	5	8	13	503	97	14	20	71	27	-	2
P6	5	5	13	464	78	16	17	85	27	-	1
P7	13	8	22	203	248	40	64	95	37	-	4
P8	10	5	14	344	149	32	54	91	30	-	4
P9	13	9	15	246	161	22	40	61	28	-	3
P10	6	8	14	298	129	21	28	60	26	-	3
P11	6	12	13	362	132	14	28	39	25	-	2
P12	7	10	14	303	138	14	31	49	22	-	3
P13	6	8	17	359	113	16	26	68	49	-	2
P14	6	7	14	187	80	15	25	43	25	-	3
P15	6	7	16	443	92	17	28	86	36	-	3
P16	4	7	14	515	84	14	17	50	29	3	1
P17	10	6	16	279	167	26	47	90	34	-	3
P18	7	10	16	311	160	21	37	79	24	-	2
P19	10	11	14	154	189	21	40	55	25	7	4
P20	7	10	13	158	103	12	15	34	18	-	4
P21	10	9	14	166	130	16	29	43	60	-	3
P22	8	9	21	246	59	17	30	34	46	-	6
P23	5	10	14	423	114	16	26	89	30	1	2
P24	5	7	14	442	70	15	21	60	24	-	3
P25	6	6	15	315	102	19	35	54	22	-	3
P26	10	9	15	198	181	21	42	64	24	-	3
P27	8	20	14	310	220	26	45	105	26	-	0
P28	9	8	13	186	125	20	37	47	28	-	2
P29	7	11	14	248	136	16	22	52	27	-	3
P30	8	9	14	244	92	15	78	29	45	-	1
P31	12	9	14	378	144	21	44	46	26	1	2
P32	5	7	15	426	107	22	29	99	31	-	4
P33	7	8	16	384	113	23	31	106	37	2	4
P34	8	10	19	298	122	17	30	66	31	-	4
P35	6	17	20	344	245	16	27	56	23	-	2
P36	7	24	12	315	413	19	39	61	23	4	1
P37	11	7	16	288	146	19	34	48	23	-	3
P38	6	8	14	431	88	16	20	77	22	1	1
P39	5	8	15	332	108	15	28	69	18	-	2
P40	8	7	14	308	151	19	32	67	26	-	4
P41	8	10	13	275	122	21	36	63	21	-	3
P42	6	8	15	305	167	20	34	58	31	2	3
P43	9	7	15	242	90	18	28	42	25	-	5
P44	7	9	18	252	136	20	39	45	24	-	4
P45	11	6	17	271	160	20	36	52	31	-	3
P46	7	8	15	326	141	25	36	95	36	1	5
P47	7	16	14	336	143	25	36	91	23	1	2
P48	8	6	13	243	155	29	48	82	27	-	4
P49	13	10	15	126	239	54	92	69	26	-	4
P50	14	12	13	102	499	35	74	32	37	-	2

Continue.....

Table 8.4a, Continued.

P51	14	8	12	149	232	35	63	64	24	- 3
P52	10	11	14	194	292	18	36	61	22	3 2
P53	10	9	15	345	237	29	44	81	17	1 2
P54	10	11	13	261	213	29	46	76	28	- 3
P55	13	17	15	273	170	25	46	67	22	2 3
P56	9	18	14	253	216	19	40	54	38	4 1
P57	10	14	15	164	213	36	30	34	16	1 3
P58	12	8	16	160	158	13	24	44	27	- 2
P59	8	23	13	387	82	22	39	100	30	9 2
P60	7	7	13	265	88	20	23	45	28	- 3
P61	8	12	16	388	169	21	32	85	31	2 4
P62	10	10	14	420	132	17	21	87	39	- 4
P63	7	7	14	478	32	13	22	78	31	- 6
P64	9	10	16	432	101	19	29	68	39	- 3
P65	20	11	16	330	175	27	48	52	23	- 2
P66	10	8	14	354	187	30	42	86	25	2 1
P67	5	6	15	402	100	18	30	54	25	- 2
P68	11	11	17	285	120	29	43	79	29	- 4
P69	10	6	19	295	153	32	41	81	24	- 3
P70	13	8	17	182	243	31	55	68	32	- 3

1: Major elements as oxides in % and others in ppm.
: Fe2O3 is total Fe
: All sample numbers are prefixed BM
: LOI Loss On Ignition

Table 8.4b: Correlation coefficients of the elements in a kaolinised granite.

	SiO_2	Al_2O_3	TiO_2	Fe_2O3	MgO	CaO	Na2O	K2O
Al_2O_3	-0.469							
TiO_2	-0.135	0.012						
Fe_2O_3	-0.176	0.139	0.148					
MgO	-0.017	0.069	0.464	0.306				
CaO	0.418	0.340	0.179	0.047	0.258			
Na_2O	0.412	0.356	0.327	0.083	0.131	0.896		
K_2O	0.360	0.303	0.242	0.137	0.229	-0.032	-0.085	
P_2O_5	0.402	0.395	0.153	0.021	0.186	0.912	0.857	0.074
MnO	-0.015	0.083	0.486	0.263	-0.021	0.386	0.518	-0.277
Rb	0.007	0.009	0.095	0.173	0.123	-0.187	-0.088	0.563
Sr	0.296	0.279	0.352	0.106	0.338	0.335	0.274	0.309
Y	-0.006	0.008	0.003	0.062	-0.032	-0.067	-0.081	0.074
Zr	-0.249	0.056	0.921	0.081	0.384	-0.314	-0.433	0.170
Nb	-0.415	0.298	0.259	0.060	-0.302	-0.235	-0.114	-0.409
Ni	0.454	0.356	0.294	0.199	0.112	0.125	0.109	0.556
Cu	0.004	0.101	0.075	0.106	-0.082	-0.444	-0.426	0.180
Zn	-0.088	0.080	0.259	0.533	0.116	0.186	0.262	-0.143
Ga	-0.755	0.609	0.170	0.299	-0.094	-0.506	-0.508	-0.457
As	0.031	0.217	0.091	0.066	-0.165	0.203	0.203	-0.066
W	0.412	0.367	0.002	0.027	0.005	0.348	0.320	0.226
Pb	-0.137	0.232	0.088	0.063	-0.044	-0.174	-0.188	-0.087
Th	-0.084	0.130	0.654	0.121	0.207	-0.251	-0.441	0.333
U	0.261	0.094	0.073	0.133	0.220	0.278	0.208	0.200
Cr	-0.201	0.236	0.080	0.165	0.028	-0.156	-0.172	-0.083
Mn	-0.050	0.045	0.506	0.303	-0.062	0.378	0.527	-0.291
Ba	0.193	0.178	0.619	0.061	0.327	-0.047	-0.079	0.510
La	-0.129	0.042	0.793	0.040	0.400	-0.219	-0.331	0.250
Ce	-0.062	0.146	0.733	0.037	0.318	-0.108	-0.214	0.250
Cs	-0.256	0.207	0.211	0.372	0.405	-0.023	0.019	0.005
Sn	-0.186	0.131	0.102	0.099	-0.057	-0.216	-0.211	-0.052
V	0.115	0.202	0.123	0.047	-0.374	-0.240	-0.188	0.081

Continue.....

Table 8.4b, Continued.

	P_2O_5	MnO	Rb	Sr	Y	Zr	Nb	Ni
MnO	0.361							
Rb	-0.112	-0.291						
Sr	0.444	0.145	0.015					
Y	-0.045	0.012	0.095	0.383				
Zr	-0.302	0.561	0.070	0.241	0.025			
Nb	-0.240	0.411	0.172	0.407	0.020	-0.221		
Ni	0.262	0.018	0.481	0.446	0.173	0.202	-0.276	
Cu	-0.326	0.300	0.012	0.046	-0.097	0.061	-0.085	0.111
Zn	0.196	0.494	0.190	0.107	-0.002	-0.314	0.230	0.157
Ga	-0.520	0.083	0.078	0.402	0.072	0.250	0.649	-0.349
As	0.251	0.066	0.157	0.046	0.021	-0.103	-0.118	-0.090
W	0.398	0.061	0.017	0.278	0.037	-0.106	-0.230	0.394
Pb	-0.160	0.283	0.278	0.151	0.064	0.169	-0.067	-0.131
Th	-0.164	0.567	0.084	0.151	0.062	0.692	-0.307	0.248
U	0.301	0.055	0.011	0.573	0.269	-0.028	-0.233	0.301
Cr	-0.176	0.132	0.075	0.038	-0.006	0.100	-0.100	-0.129
Mn	0.370	0.946	0.290	0.149	-0.001	-0.562	0.441	0.005
Ba	-0.056	0.465	0.179	0.497	0.026	0.579	-0.485	0.380
La	-0.124	0.429	0.157	0.365	-0.055	0.806	-0.231	0.336
Ce	-0.013	0.502	0.053	0.448	0.040	0.748	-0.412	0.257
Cs	0.053	0.425	0.401	0.189	0.016	0.145	0.124	0.183
Sn	-0.223	0.016	0.010	0.100	0.054	-0.048	0.004	-0.242
V	-0.094	0.125	0.202	0.487	0.676	0.120	0.110	0.407

	Cu	Zn	Ga	As	W	Pb	Th	U
Zn	0.021							
Ga	0.018	0.163						
As	-0.084	0.109	0.147					
W	0.079	0.141	0.356	0.093				
Pb	0.070	0.173	0.097	0.129	-0.255			
Th	0.179	0.216	0.092	0.023	0.174	-0.098		
U	0.132	0.015	0.213	0.006	0.309	0.075	0.060	
Cr	0.039	0.064	0.193	0.043	-0.230	0.139	0.117	-0.136
Mn	-0.306	0.575	0.106	0.070	0.009	-0.287	-0.560	-0.070
Ba	0.169	0.286	0.242	0.095	0.205	0.034	0.485	0.407
La	0.071	0.274	0.142	0.106	0.020	0.148	0.609	0.039
Ce	0.073	0.346	0.015	0.360	0.090	0.100	0.649	0.107
Cs	-0.027	0.312	0.229	0.240	-0.090	-0.041	-0.092	0.066
Sn	-0.006	0.144	0.095	0.269	-0.255	0.147	-0.013	-0.132
V	0.189	0.022	0.098	0.083	0.061	0.272	-0.008	0.520

	Cr	Mn	Ba	La	Ce	Cs	Sn
Mn	-0.065						
Ba	0.024	0.482					
La	0.095	0.440	0.506				
Ce	0.058	0.527	0.556	0.788			
Cs	0.026	0.419	0.054	0.297	0.064		
Sn	0.245	0.020	0.099	0.089	0.081	0.023	
V	-0.562	0.155	0.013	0.257	0.171	0.007	0.154

Table 8.5: Average element abundance in a kaolinised granite (KG) compared to their abundance in partially kaolinised (PKG) and fresh granite (FG).

Elements & oxides	FG	PKG	KG
SiO_2	72.14	72.722	71.912
Al_2O_3	15.08	16.866	18.138
TiO_2	0.22	0.132	0.152
Fe_2O_3	1.79	1.134	1.152
MgO	0.36	0.193	0.177
CaO	0.70	0.318	0.102
Na_2O	2.75	2.738	0.857
K_2O	5.44	5.482	5.589
P_2O_5	0.21	0.210	0.090
MnO	-	0.05	0.036
Rb	440	614	621
Sr	82	60	50
Y	11	24	26
Zr	77	56	70
Nb	14	18	19
Ni	11	8	8
Cu	-	10	13
Zn	44	36	35
Ga	25	22	24
As	27	17	20
W	-	336	271
Pb	29	14	20
Th	13	8	9
U	8	12	9
Cr	-	15	15
Mn	341	394	289
Ba	171	161	153
La	30	18	22
Ce	58	30	37
Cs	44	65	65
Sn	12	27	29
V	14	2	3
LOI	-	1.5	3
Density	0.00	2.55	2.16

Fresh granite analysis from Exley (Unpublished data).

kaolinised granite compared to averages in the unkaolinised granite. From Table 8.5 it can be seen that there is a decrease in Si, Mg, Ca, Na, P, Mn, Ti, Fe, As, Pb, Th, V, Sr, Ni, Zn, W, U, Ce, Ba, and La and an increase in Al, K, Rb, Y, Zr, Nb, Cu, Ga, Cs, and Sn in the kaolinised granite relative to the unkaolinised granite. The remarkable decrease in density is also shown in these results. Ca, Na, P, and U are particularly depleted in the kaolinised granite. Conversely, Pb increases an order of magnitude relative to the unkaolinised and the partially kaolinised granites. It is worth noting that these elements are greatly affected even in the slightly altered granite.

Figure 8.6 shows plots of the major elements against the degree of kaolinisation (which is taken as 1/density multiplied by 10). These plots clearly show the variation of each elements during kaolinisation. Si, Ca and Na show a general decrease with increase in kaolinisation, while Al generally increases with an increase in kaolinisation. The trends for Ti, Fe, K, and Mg are no clear change with kaolinisation. The elements most affected in the process are Ca and Na, and their plots against density are shown in more detail in Figure 8.7. An interesting pattern emerges in these plots, showing distinct separation between the stages involved in the process. The possible separation of the kaolinisation processes in the South-West England granites into two phases, as proposed by Durrance and Bristow (1986), is supported.

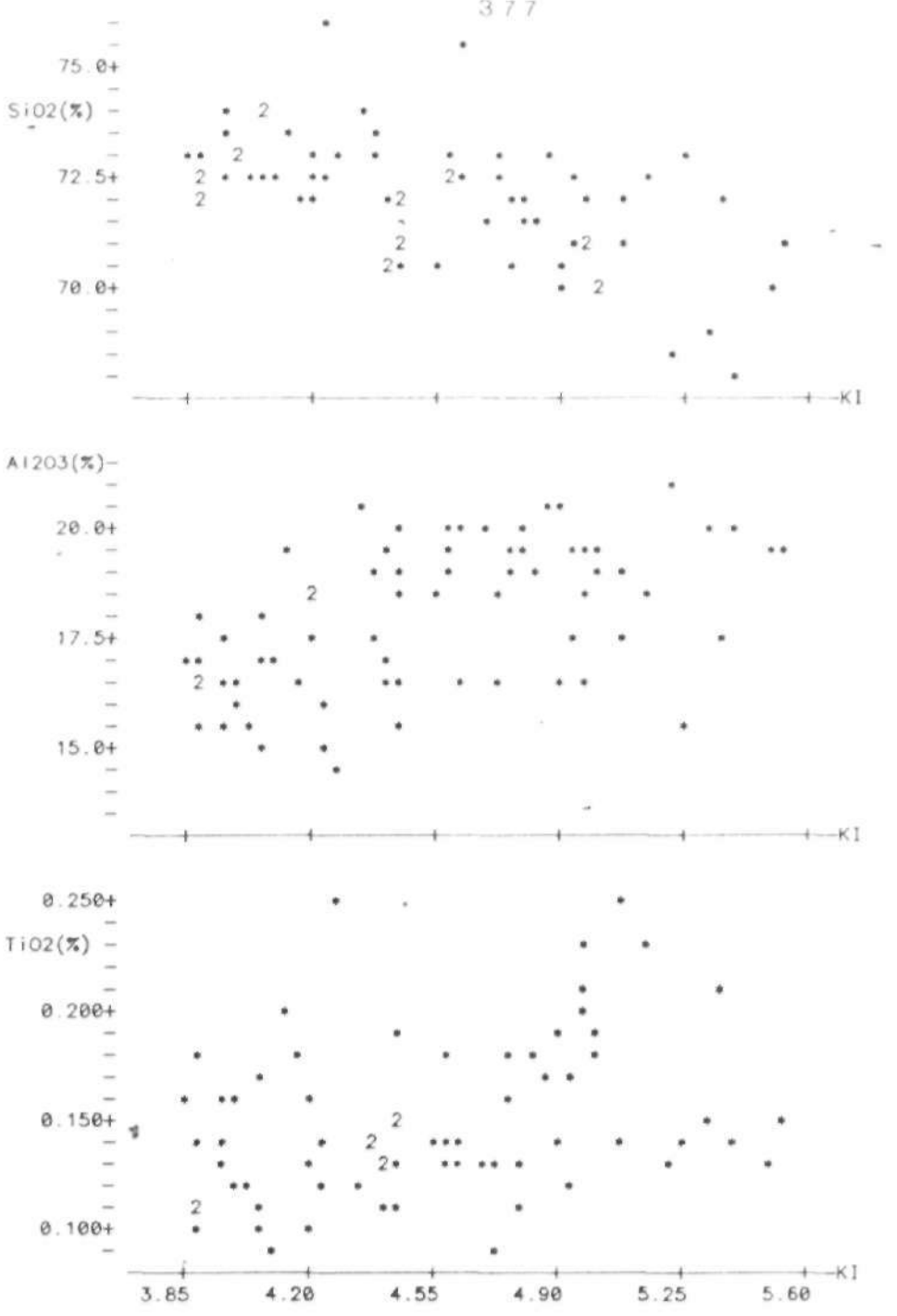


FIGURE 8.6 Major element variations with kaolinisation in kaolinised granites (See text for explanation of KI)

Note: Numbers in these plots and subsequent ones in the Chapter represent number of points sharing the same coordinates

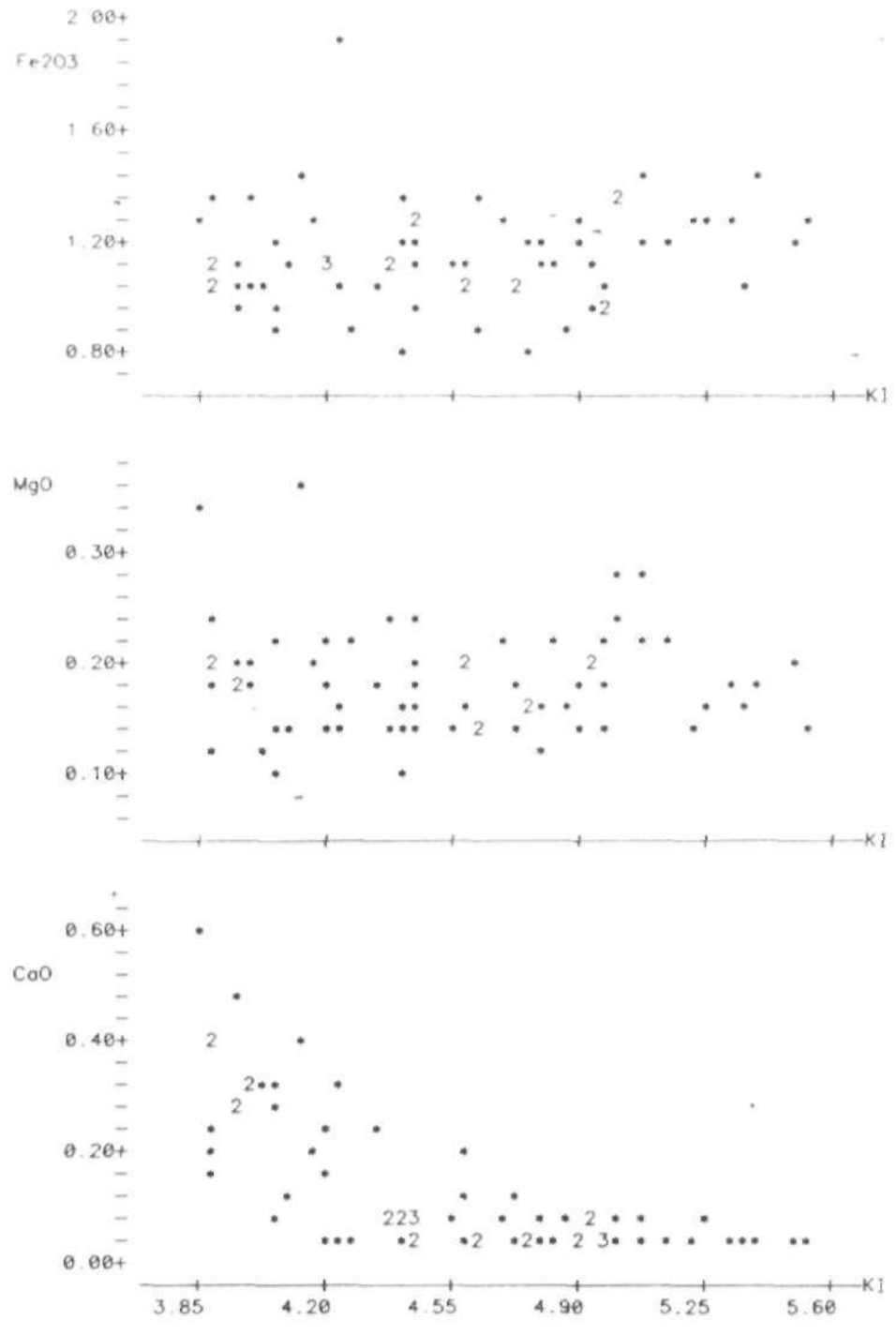


FIGURE 8.6 Major element variations with kaolinisation in kaolinised granites (See text for explanation of KI)

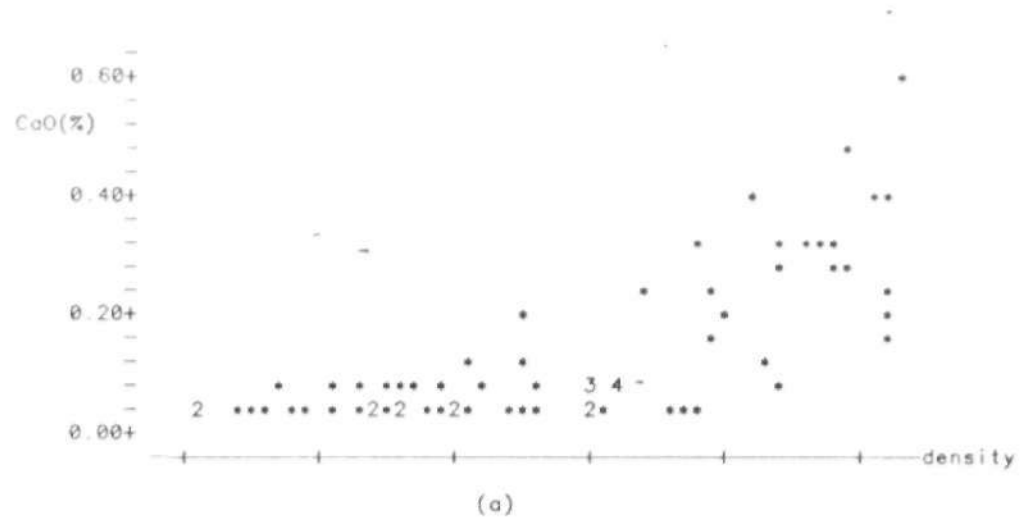


FIGURE 8.7 Plot of Ca (a) and Na (b) against density for kaolinised granites

The plots show an initial gradual decrease of the elements in the first stage of the process and then their complete instantaneous removal at a certain point. This shows that the operation of the kaolinisation process took place in two main phases. The two phases are diagrammatically illustrated in Figure 8.8. This sketch is based on the changes in Na_2O and CaO observed in this study. The first phase probably consisted of the opening-up of the solution pathways, and is represented by the faint sloping line making an angle with the average concentrations of the elements at the top of the figure. Durrance and Bristow (1986) believed that circulation during this stage was confined to open joints and ingress of water along grain boundaries. The process involve argillic alteration, a situation which led to a decrease in permeability as the clay minerals formed. This phase involved a reduction of the overall density of the granite mass as a whole from an average of about $2.65gcm^{-3}$ to an average of $2.55gcm^{-3}$. This density reduction could have led to isostatic readjustment in the rock mass, which Durrance and Bristow (1986) suggested will greatly increase the permeability and allow the continued operation of hydrothermal circulation systems. The results of this study confirm that the first stage process was mainly responsible for opening-up the pathways for the second stage, because only low-activity alteration accompanied the process. An interval of quiesence then ensued, as shown by the vertical line separating the two phases. This forms an important divide between the main processes. The second phase which followed this quiet

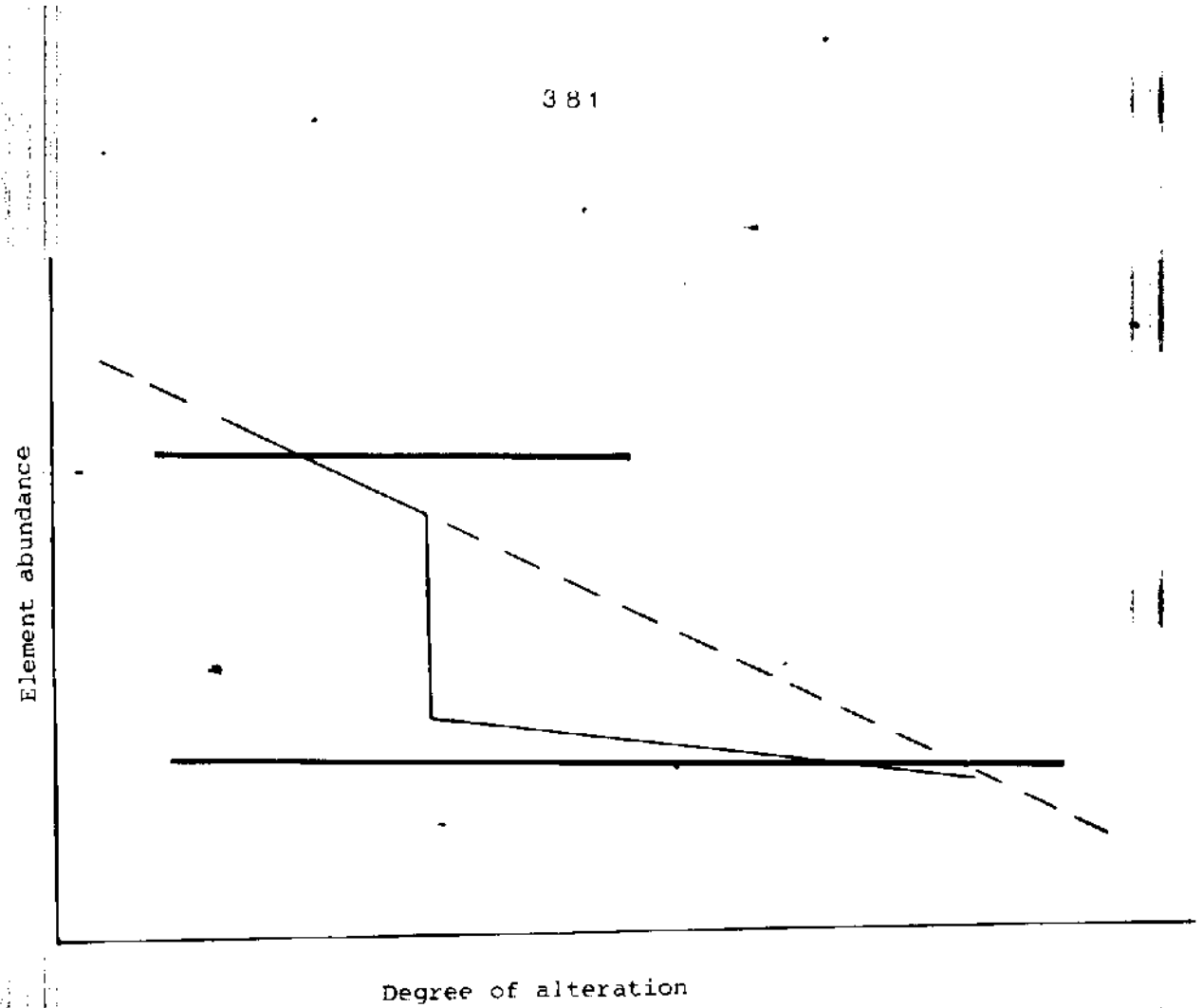


FIGURE 8.8 Major stages in kaolinisation process

a: Heavy lines represent average element concentration

b: Broken line represent change in element concentraion in single stage process

c: Faint full line represent observed stages in kaolinsation

period is characterised by a greatly increased pervasity of alteration, as shown by the small angle between the line representing the variation of element concentration and the average concentration. It must be noted, however, that the change in direction in the sketch is only relative, that is some elements show an increase during kaolinisation, as for example does Al.

The presence of these distinct phases is also shown in the plots of other components. Thus, while both Fe and Mg do not show any regular variation overall, they do show a general decrease with increase in kaolinisation in the second phase. Similarly, K shows a general increase in the first phase, but only a small decrease in the second phase.

The increase in Al and decrease in Si in these plots agrees with the general processes involved in kaolinisation. During the hydration of the feldspars, silica, the alkalies, and the alkaline earths were taken into solution and lost, thus increasing the overall, Al content even though no Al was added. The first stage may correspond to the first phase of argillic alteration in the granite which was associated with saline waters at temperatures of about 350^{o}C (Sheppard et al., 1985). In this phase Durrance and Bristow (1986) have shown that soda and potash feldspars were altered to smectite-illite and illite, respectively. K^{+} ions could have been sorbed onto the clay minerals produced, and thus show the initial increase of the first phase. Further fluid flushing through the environment as kaolinisation progressed helped to leach out some of the K. The relative stability of potash feldspar would also

have enabled it to resist alteration in the first, mild phase of alteration, until the commencement of the intense second phase. Oligoclase, the richest calcic mineral, is the most unstable among the feldspars. Thus the loss of Ca occurred even in the initial stages of alteration. The second phase, in which alkalies and alkaline earth elements were removed may have involved highly alkaline solutions, in which both Fe^{3+} and Ti^{2+} were not soluble. The lowered mobility of these species would then be explained. Some alteration of dark micas, especially biotite, in which Fe was oxidised, could have contributed to the observed variation of Fe in the second phase. Associated with these variations was loss of P, possibly from apatite and monazite, which form important accessories in these granites.

The characteristics of the second phase of alteration suggest that a large volume of rapid moving water must have been involved. The heavy lines in Figure 8.8 represent averages in the kaolinised and the unaltered granites. The small slope of this line in the second phase might be a result of the low mobility of Na and Ca sorbed onto clay, or held in minerals other than plagioclase. This suggests that dissolution in the second phase occurred very quickly, again supporting the view that hydrothermal activity was responsible. Moreover, it is possible that isostatic uplift, which allowed the fractures to open, occurred very rapidly - perhaps only when critical stress condition had been reached in the imbalance caused by the mass loss during the first stage of alteration.

Immediately prior to this uplift, the solutions must have been confined at very high pressure. The increased permeability produced on uplift would certainly have provided a pressure release which could have permitted forced convective circulation of the solutions.

Although hydrothermal activity must, therefore, have played a major role in the kaolinsation process, the role of weathering can not be completely dismissed. During the final phase of kaolinisation identified in the granites, South-West England had a wet climate capable of producing weathering mantles of kaolinite as described by Bristow (1988). Relics of this mantle associated with ball clays in Devon have been reported by Bristow (1968). However, weathering alone is unlikely to produce such effects, at depths of more than 200m unless the weathering environment is actively drawn down into the granite. For these reasons Durrance et al. (1982) proposed that the main china clay deposits occur at the drawdown sites of hydrothermal systems. That the china clay deposits are located on major faults agrees well with Fehn's (1985) model which shows drawdown sites locked onto major high permeability zones in radiothermal plutons. Nevertheless, because kaolinisation in the Bodmin Moor granite is only shallow, Bristow (pers. comm.) has suggested that weathering could have played an unaided role in the kaolinisation of this particular granite.

Another important feature of this model of kaolinisation is the period in which there is a break in activity, so that the

process was almost at a standstill. Determination of the length of this period would be helpful in furthering our understanding of the origin of kaolinisation.

Plots of trace element concentrations against degree of kaolinisation are shown in Figure 8.9. Some of the plots show the same break in activity between the two main phases. W, V, La,Cr, Ga, Th, Y, Sr, Cs, and Zr displa variation with kaolinisation, with Th, Ga, Cr, La, Cs, and Zr showing an increase, while, W, V, Y, and Sr show a decrease with increasing kaolinisation. Although no overall regular variation is shown in the plots of Nb, Ni, Cu, Ce, and Sn, some trends are present separately in the main phases. Ni and Cu show a general decrease with increasing kaolinsation in the second phase, and Ce and Sn show an increase. Ni, just as in the plot of K_2O, shows an increase in the partially altered granite. Zn, As, Ba, Rb, and Mn show no clear pattern. Such factors as adsorption onto clay minerals, and the relative resistance to alteration of the minerals in which these trace elements occur, could largely explain much of this irregular variation. For example, because the process of kaolinisation involves the removal of a large amount of material, elements concentrated in the resistate minerals increase due to the accumulation of these minerals in the alteration product. The important mineral in which Zr occurs is zircon, and this ranks among the most stable during alteration. Thus the increase of Zr with alteration, is easily explained. Similarly, substantial amounts of Cr and Ga in igneous rocks are held in the resistate

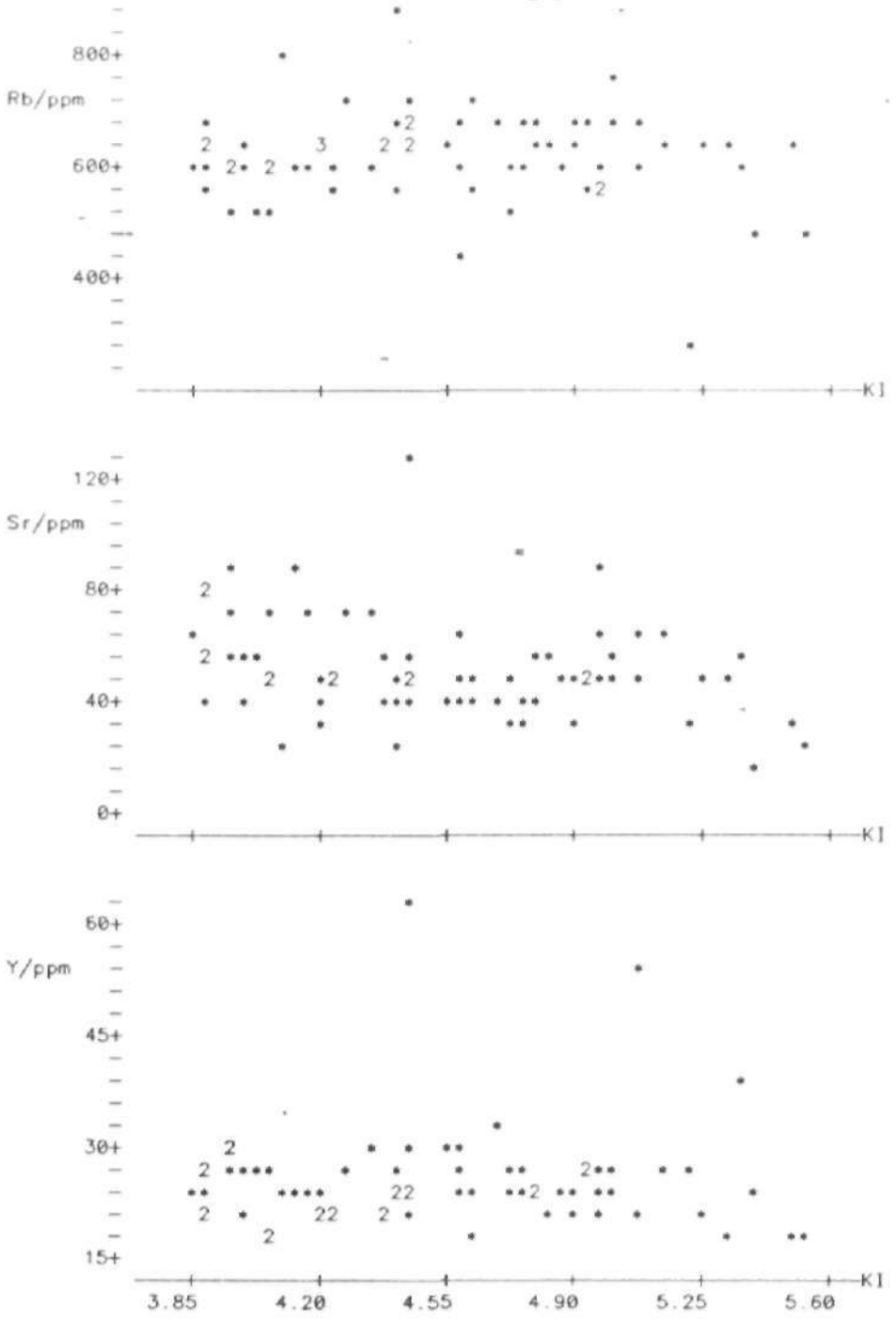


FIGURE 8.9 Variation of trace elements with kaolinisation index (KI) in kaolinised granites (See text for explanation of KI)

Note: Numbers in plots represent number of points with the same coordinates

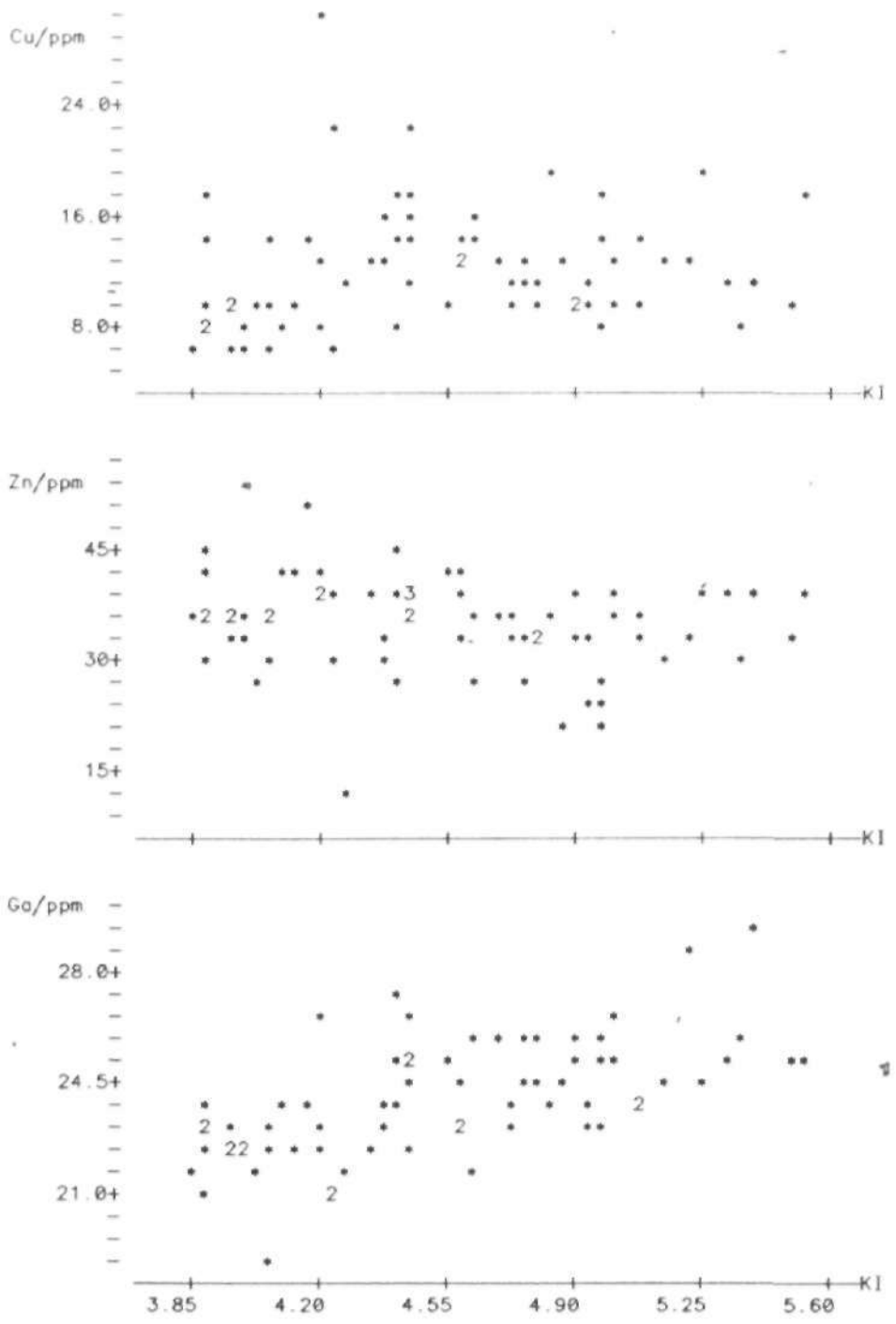


FIGURE 8.9 Variation of trace elements with kaolinsation index (KI) in kaolinised granites (See text for explanation of KI)

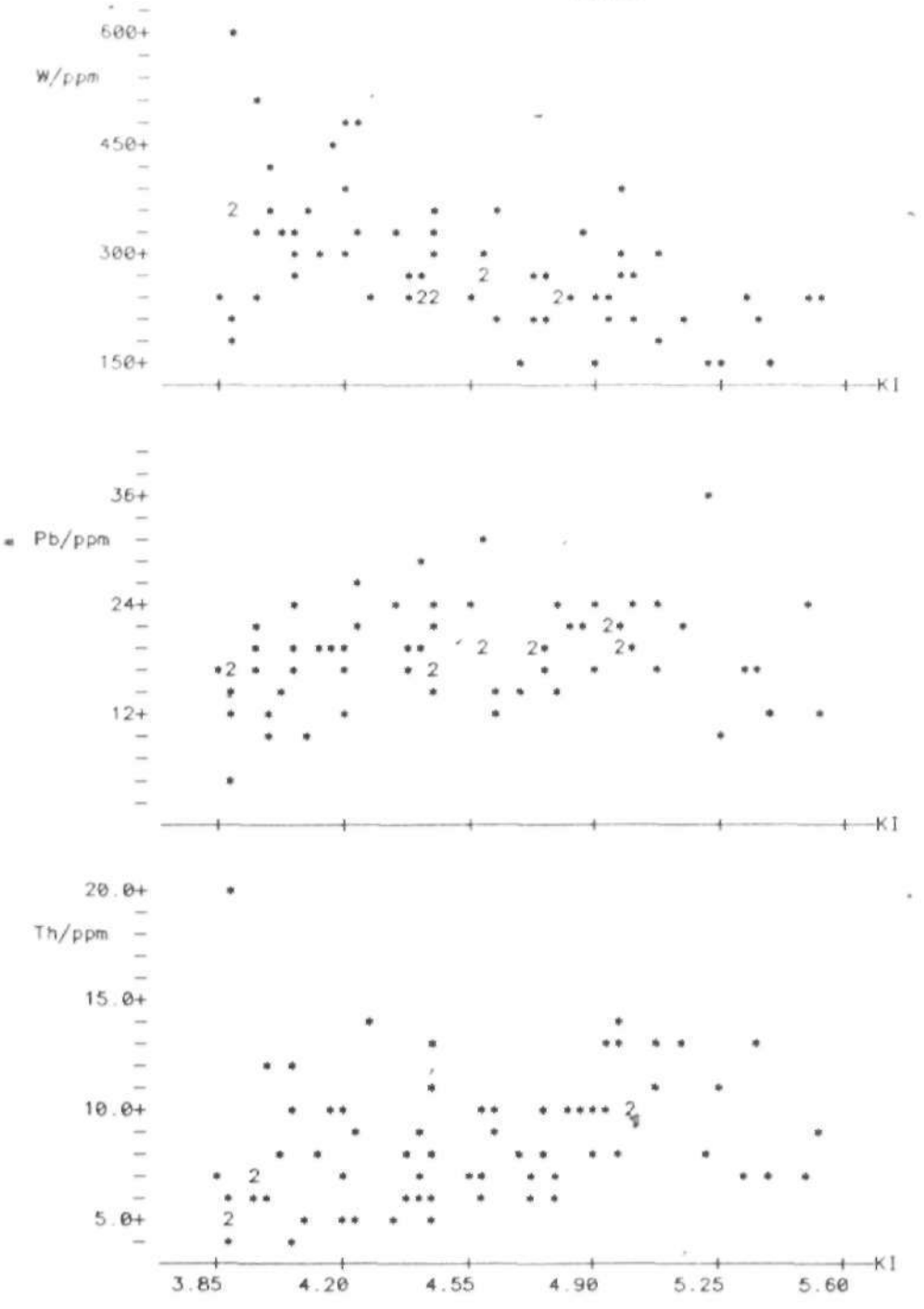


FIGURE 8.9 Variation of trace elements with kaolinisation index (KI) in kaolinised granites (See text for explanation of KI)

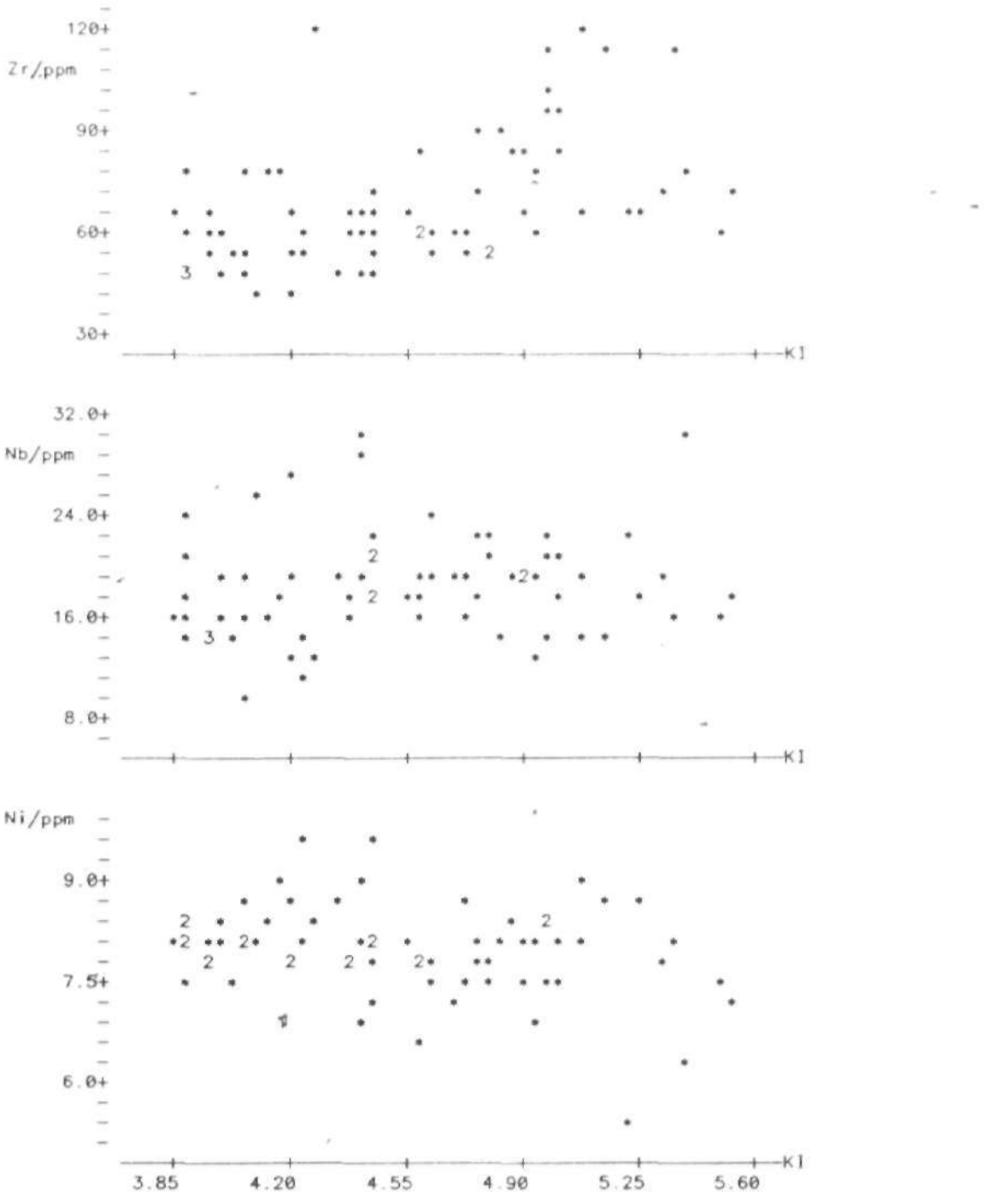


FIGURE 8.9 Variation of trace elements with kaolinisation index (KI) in kaolinised granites (See text for explanation of KI)

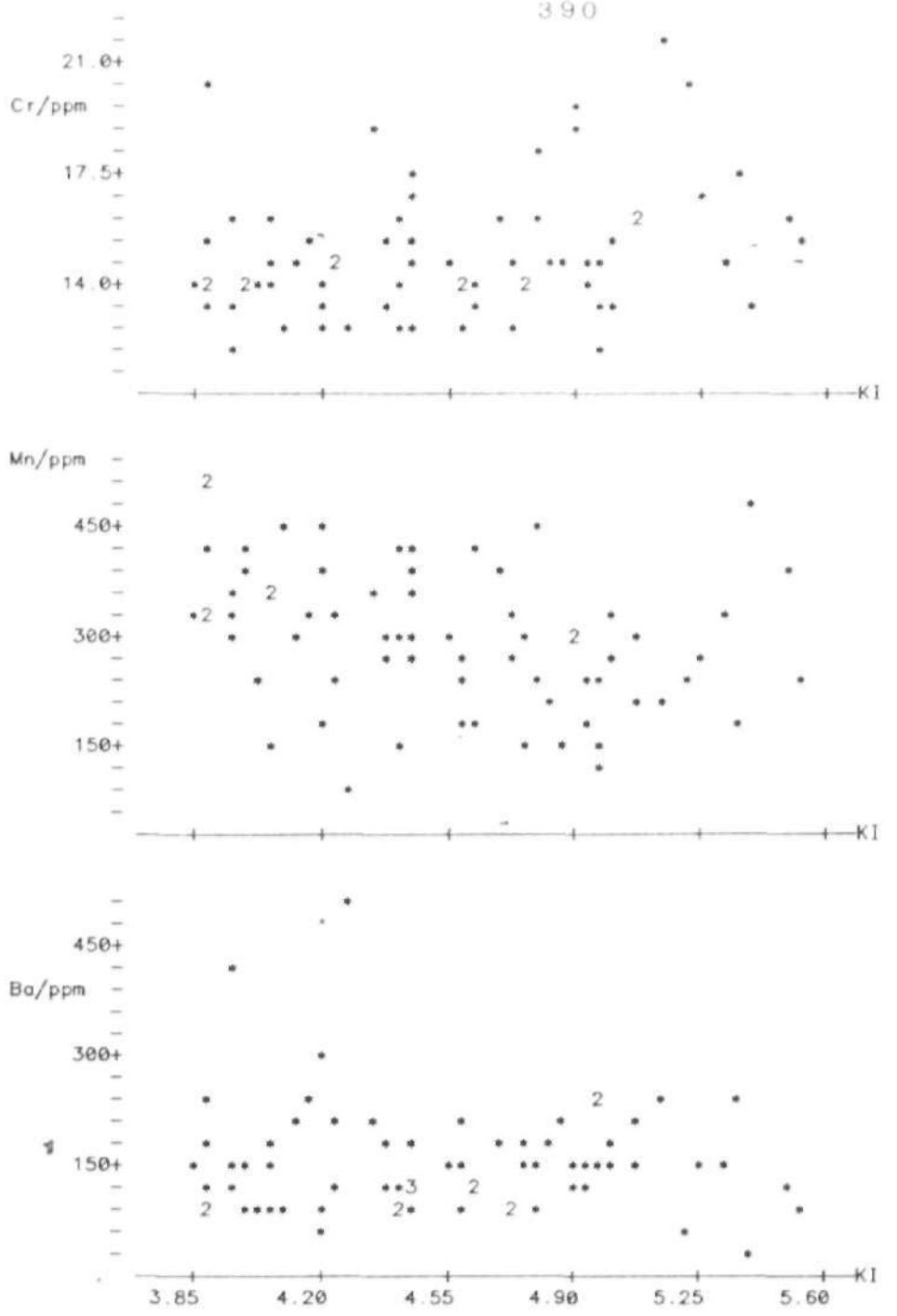


FIGURE 8.9 Variation of trace elements with kaolinisation index (KI) in kaolinised granites (See text for explanation of KI)

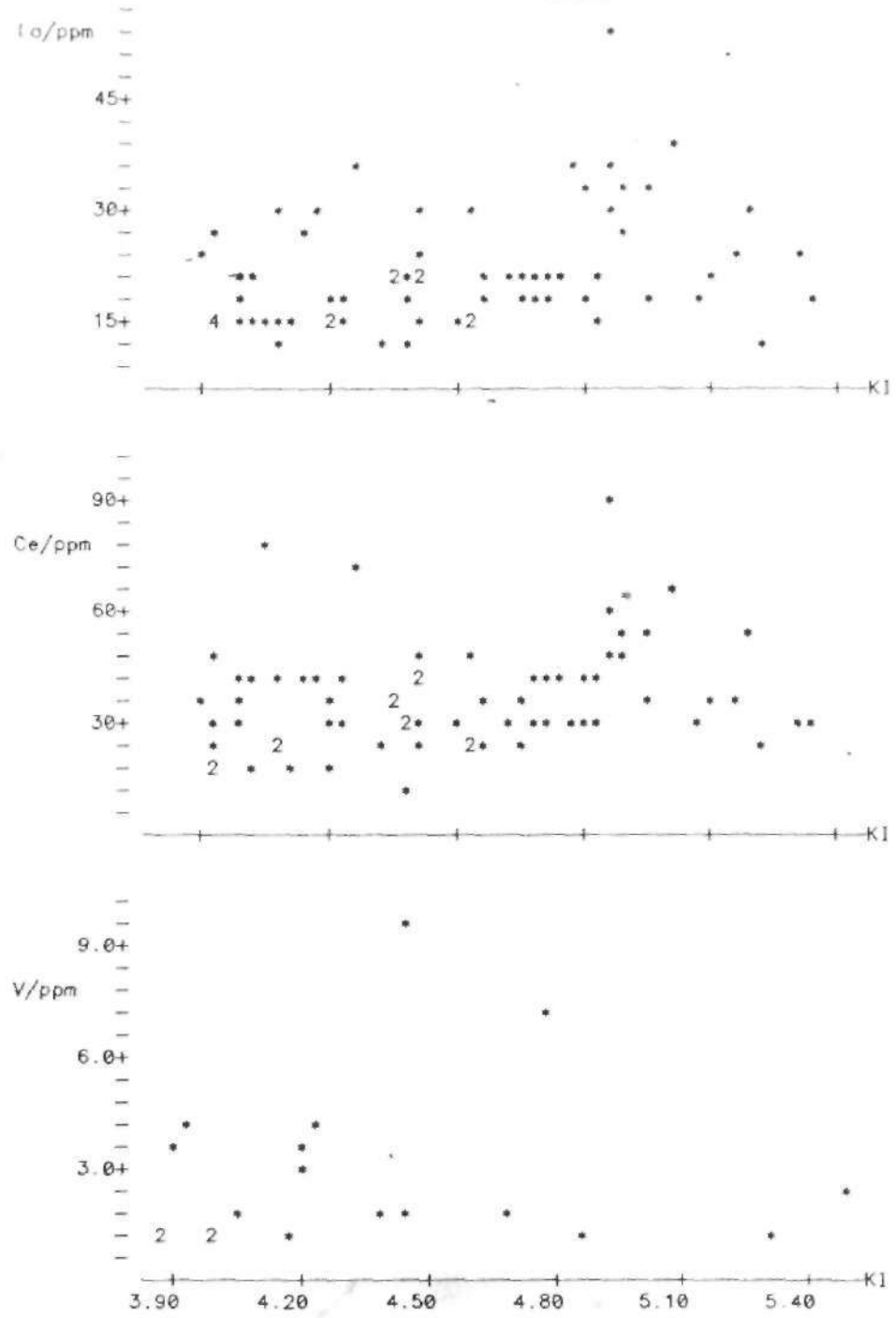


FIGURE 8.9 Variation of trace elements with kaolinisation index (KI) in kaolinised granites (See text for explanation of KI)

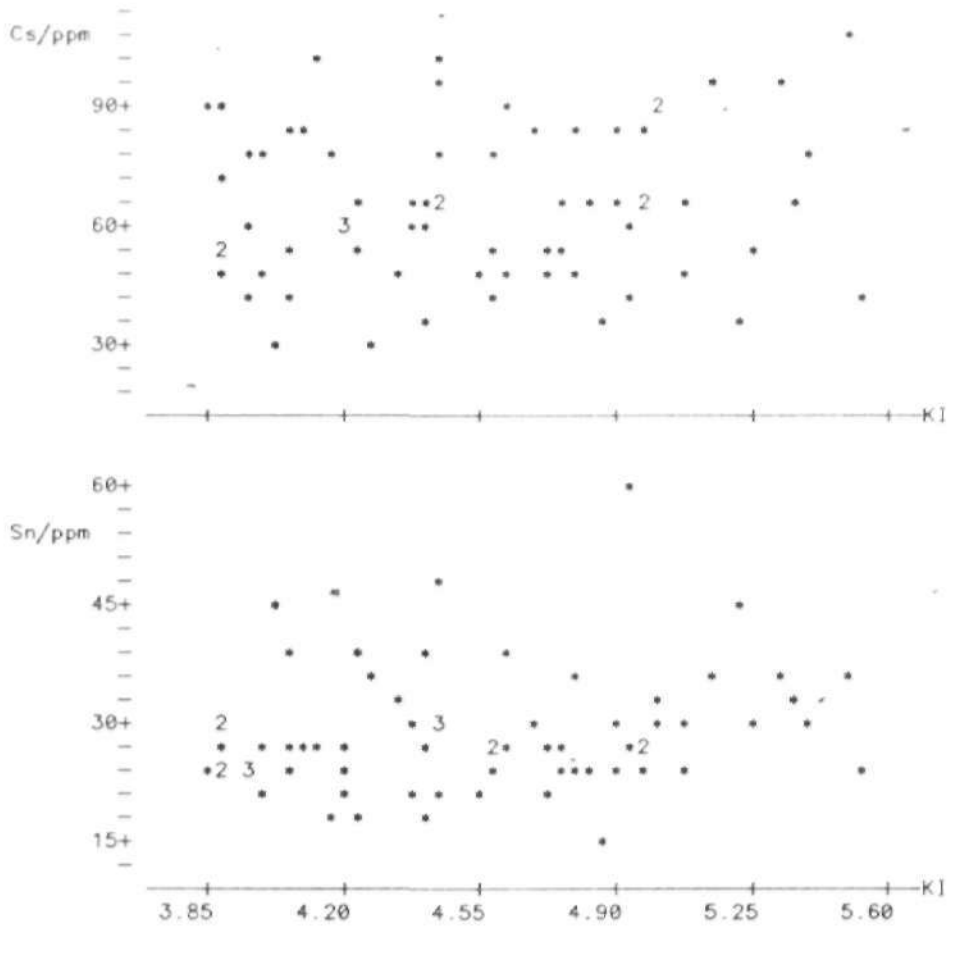


FIGURE 8.9 Variation of trace elements with kaolinisation index (KI) in kaolinised granites (See text for explanation of KI)

minerals chromite, magnetite and ilmenite. The accumulation of these minerals with increasing kaolinisation appears to be responsible for the observed variation of Cr and Ga. The variation of Th appears to be controlled by the increase in zircon already discussed.

The results of this geochemical study thus show clearly the separation of two main phases of alteration in the kaolinisation of the granite. Most of the elements do not show any clear trend in the first phase, but within the second phase the data are sufficiently clear that it is possible to speculate that irregularities in the variation plot may indicate more than one pulse of activity. At the very end of the kaolinisation process, general mobilisation of the elements must have operated, as shown by a decrease in abundance of most of the elements. This can only be associated with extreme hydration of the alteration product.

The effect of weathering on the granites of South-West England has been extensively studied. Butler(1953) published data on the weathering of the Carnmenellis granite. This granite is similar in composition to the Bodmin Moor granite. His study showed that in the weathering of the granite to clay, the elements Ti, Fe, Mg, Ca, P, Zr, Sr, Rb, Cr, Ba, Pb, and Ni, were enriched, while Si, Na, K, Mn, V, Ga, Sn, and Cs, were depleted. Comparison of these findings with the data from this study shows that there is a contrast between the geochemistry of the weathering process and

that of the processes which led to the kaolinisation of the granites. Thus while Ti, Mg, Fe, Ca, P, Sr, Ba, Pb, and Ni were depleted, and K, Y, Ga, Sn, and Cs enriched in the kaolinised granite, these two groups of elements were enriched and depleted, respectively, in the weathering product. Analyses of both the weathering product and the kaolinised granite are shown in Table 8.6. This evidence further supports the argument for hydrothermal processes being dominant in the formation of the china clay deposits in the granites of South-west England.

8.6.3.2 U Mobility During Kaolinisation

From the foregoing discussion, it is clear that the mobility of U during kaolinisation must be controlled, at least in part, by it's solubility in solutions which are apparently alkaline. The average U content of kaolinised granite, compared with relatively fresh granite, is markedly less, showing that mobilisation of U does occur during the kaolinisation processes. The values in Table 8.5 show that about 23% of U was removed in the interval between the initial kaolinisation process and the final stages of alteration. Plots of U against kaolinisation index (Figure 8.10) show the general loss of U with increasing alteration. Even in the initial phase of the alteration, which has been characterised as low-activity in terms of alteration, there is a general decrease of U. The points plotting high in this diagram,

Table 8.6: Chemical analyses of products of weathering and kaolinisation of granite

Elements & oxides	Granite	Silt	Clay	KG
SiO_2	72.15	48.45	33.59	71.912
Al_2O_3	14.84	26.56	26.29	18.138
TiO_2	0.18	0.86	0.94	0.152
Fe_2O_3	0.41	5.95	10.60	1.152
MgO	0.47	1.12	2.63	0.177
CaO	1.17	1.01	3.48	0.102
Na_2O	3.17	2.65	0.21	0.857
K_2O	5.14	2.71	2.48	5.589
P_2O_5	0.18	-	2.30	0.090
Rb	400	230	550	21
Sr	80	65	220	50
Y	15	25	15	26
Zr	150	280	180	70
Ni	15	45	90	8
Ga	20	15	15	24
Pb	40	15	45	20
Cr	15	45	120	15
Mn	400	900	260	89
Ba	110	180	500	53
La	40	40	40	22
Cs	50	50	50	65
Sn	45	15	15	29
V	15	10	15	3

Granite analyses from Gosh (1934)
Silt and clay analyses from Butler (1953)
KG- Kaolinised granite: this study

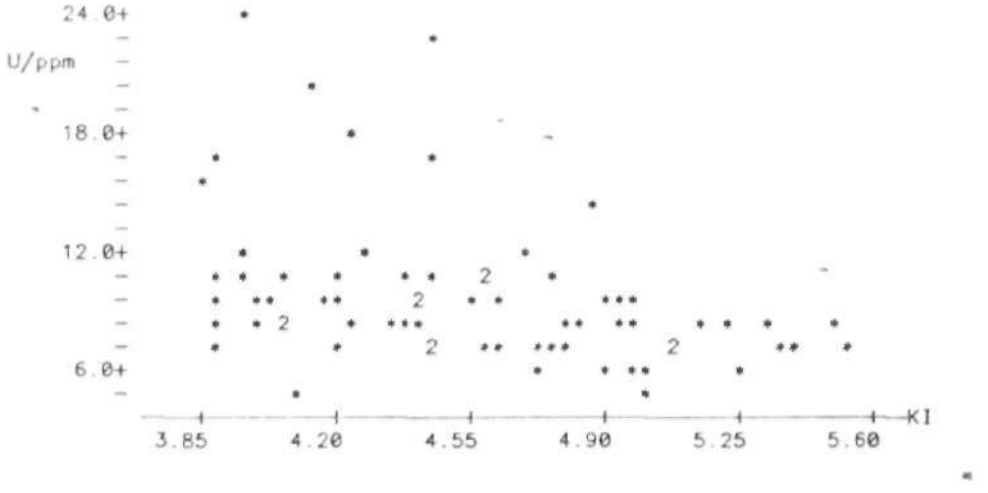


FIGURE 8.10 Plot of U against KI

indicating high U, may be represent U adsorbed onto the first-formed clays and Fe oxides and oxyhydroxieds. During the second phase, U was highly mobilised, with substantial loss of U from the environment. Even U adsorbed onto clays and Fe oxides/oxyhydroxides, was leached during the final phase of alteration.

A Th:U ratio of about 1.63 in the fresh granite was reduced to 0.63 and 0.93 in the partially altered and the wholly kaolinised granites, respectively. These changes plus the massive loss of U, indicate the importance of leachable U minerals as the primary hosts of U in the granites. The importance of the primary mineral uraninite in contributing to the total U content of the granites has already been discussed in Chapter 5. The dissolution of uraninite also controls the loss of U relative to Th in the kaolinised granite. An increase in Th coupled with a decrease in U would greatly increase the Th:U ratio. But, as previously shown, an increase in the Th:U ratio was only seen in the more thoroughly kaolinised granites and, on average, the ratio decreases through the alteration process. A plot of U against Th is given in Figure 8.11, where this trend is shown more clearly. There appear to be two likely explanations for this variation: either the original U content of the granite is higher than the quoted average, or the Th content is lower. That the former explanation is more likely to be the case is shown by the high average U content of the partially kaolinised granite, even though the U content

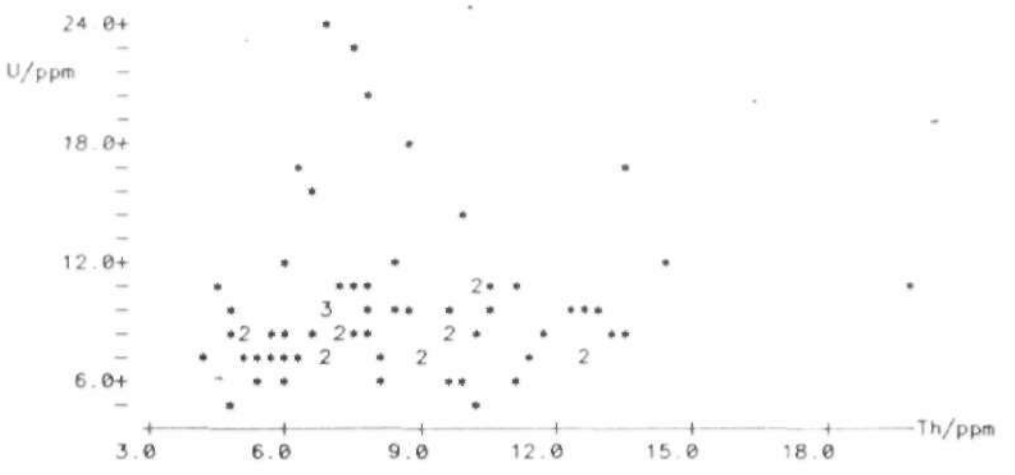


FIGURE 8.11 Plot of U against Th for kaolinised granites

Note: Numbers in plot represent points with the same coordinates

decreases in this phase of alteration. This means that the granite was enriched in U. Indeed, it is the decay of this U which could have contributed significantly to the radiothermal heat source of the granites, and the operation of forced convective circulation. Alpha-particle autoradiographic investigations, reported in Chapter 5, indicate the importance of the resistate mineral zircon as a host of most of the observed activity in the kaolinised granite. As shown in Figure 8.9, Zr increases with an increase in alteration, indicating increasing importance of zircon as a constituent of the alteration product. Plots of U and Th against Zr are shown in Figure 8.12. A positive correlation between Zr and Th can clearly be seen. Although the overall Zr concentration can not account for all the Th being present in zircon, at least this is demonstrated to be an important host.

Although U has been removed from the granites during kaolinisation, it is worth noting that there is still a relatively high concentration of U in the kaolinised granite. Since most of the U can not be correlated with the observed presence of resistate minerals in the altered granite, it shows the importance of adsorption of U on the clay minerals. Indeed it was shown that most of the U in the kaolinised granites is very young (Chapter 7) suggesting that most of this U was introduced sometime after the kaolinisation of the granites.

The implications of U mobilisation during kaolinisation can be appreciated most by considering the amount lost in the

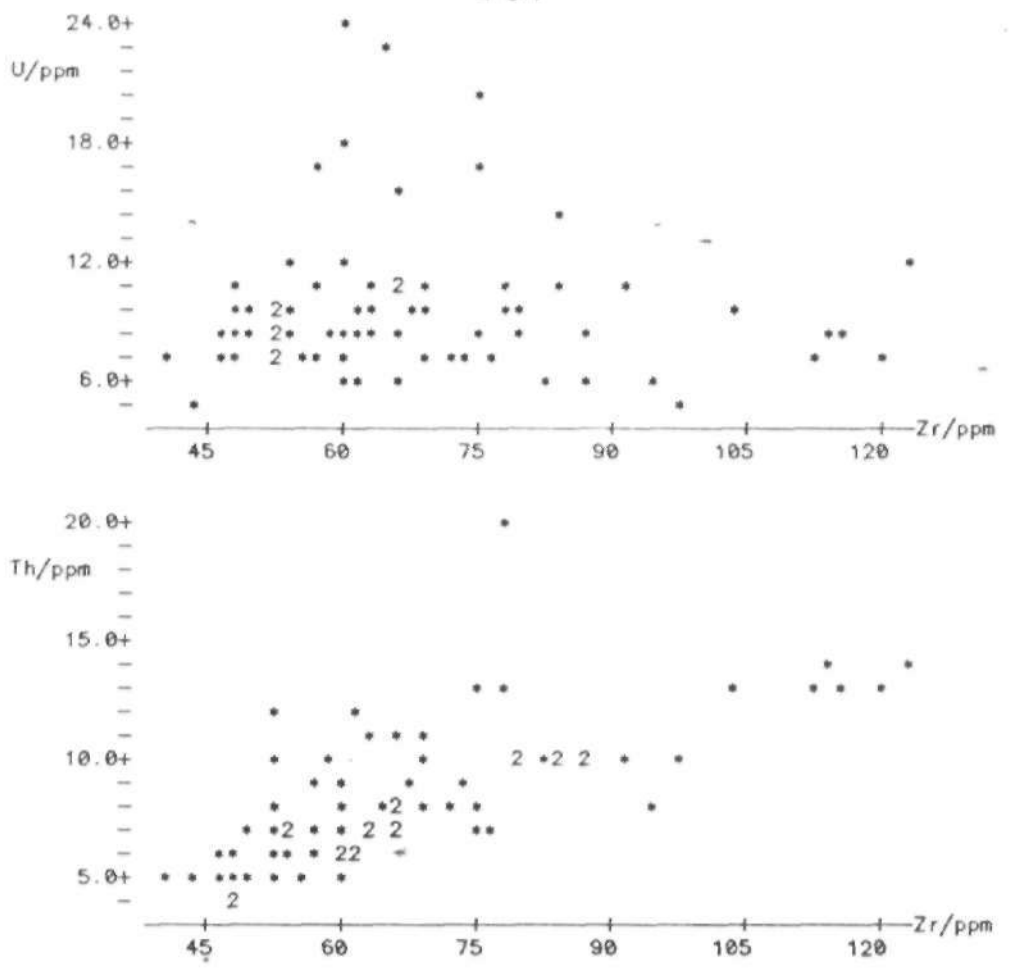


FIGURE 8.12 Plot of U (a) and Th (b) against Zr

kaolinsation of a granitic mass. In the case of the pit studied on Bodmin Moor, during the period between the first phase and the final part of the alteration processes, on average 2.75ppm U was lost. This constituted about 23% of the total U in the rock mass. With an average density of 2.65gcm^{-3}, and considering that kaolinisation has reached about 1 km deep, then assuming a rectangular block of the rock was kaolinised the original U content of this volume of 5.4.10^{5}kg, was reduced by about 1.3.10^{5}kg. This mass of U should have been deposited by the convective circulation system in the areas around the kaolinised zone, wherever favourable conditions for precipitation were encounted. This is a very sizeable amount of U ore, but the fact that important U ore bodies have not been found is something of a mystery. Possible answers to this mystery are: (1) the ore bodies are there, but have not been found because they are masked by non-radioactive rocks, (2) precipitation did not occur and the U was carried away in surface run-off into the sea, (3) precipitation did occur, but as many small veinlets in the rock mass rather, than as ore bodies of any significant size. Of these alternatives, the most likely to be the correct explanation is the last - certainly minor U-mineralisation is well documented in the vicinity of china clay pits (Dines, 1956; Bowie et al., 1973; Jackson, 1982). However, some element of the first and second explanations are also likely.

8.7 Conclusions

The mobility of the rock-forming elements in general, and U in particular, during alteration processes leading to the kaolinisation of granites has been investigated. The importance of changes in rock density resulting from these process was recognised, and found to be an effective indicator of the degree of kaolinisation. Two main processes leading to the kaolinisation of the South-West England granites have been identified as distinct phases. These phases were separated by a period of very low alteration activity. A model based on changes in Na and Ca during the kaolinisation process in the South-West England granites has been developed. In the first phase, the processes involved were mainly responsible for the opening-up of the pathways for the later processes, with some very mild alteration which led to a reduction in the density of the granite from about $2.65gcm^{-3}$ to about $2.55gcm^{-3}$. The second phase has been identified as being responsible for most of the chemical and mineralogical changes observed in the kaolinised granite, and believed to have caused a further reduction of density to about $2.17gcm^{-3}$. Evidence of chemical change presented in this study supports hydrothermal circulation as being the mechanism mainly responsible for kaolinisation of the granites.

The kaolinisation of the granites led to the mass

mobilisation of Na and Ca out of the environment, and the depletion of many other elements. On average, Si, Ti, Fe, Mg, P, Ni, Sr, Zn, W, Pb, As, Ba, La, Th, Ce, and V were depleted and in relative terms, Al, K, Rb, Y, Zr, Nb, Cu, Cr, Cs, and Sn were increased. Ga remained fairly unchanged relative to its average abundance in unaltered granite. Variations of the major elements with increased kaolinisation of the granites, indicate that, in general, both Si, Ca, Na, and P decrease with increasing kaolinisation, while Al, Ti, Fe, and Mg increase. The behaviour of K and Ti are not regular. In the second phase of the alteration K decreases, Ti increases. The behaviour of the trace elements is an increase with increasing kaolinisation for Th, Ga, Cr, La, Cs, and Zr, and a decrease with increase in kaolinisation for W, V, Y, and Sr. The effect of kaolinisation on U abundance is to produce a decrease with increasing intensity of alteration. On average, about 25% of the whole-rock U was removed in the process. Because of the young age of the U in the kaolinised granites, suggesting that most of the U was introduced after the kaolinisation of the granites, it is believed that the amount of U removed must have been much more than this. The investigation shows the importance of primary U-bearing minerals such as uraninite, as the host of most of the U in the granites.

Comparison of the effect of weathering on the elements in the South-West England granites, with the processes that led to kaolinisation, shows a strong contrast. This further suggests the

importance of hydrothermal action in the kaolinisation process. For example, while K, Y, Ga, Sn, and Cs are enriched by weathering, they are depleted during kaolinisation. Similarly, the elements Ti, Mg, Fe, Ca, P, Sr, Ba, Pb and Ni were depleted and enriched, by weathering and kaolinisation, respectively.

CHAPTER NINE: LATERITIZATION AND U MOBILITY

9.1 Introduction

Soils, being the end-product of alteration of rocks, may give clues as to the chemical changes which might have taken place in the process of their generation. The breakdown of rock in the formation of soil involves a redistribution of the elements. Such redistributions are controlled by a variety of complex, sometimes inter-related, factors which usually make studies of the system very complicated. In particular, the mobility of an element is not only affected by the relative ease with which it is librated from a mineral, but also by its tendency to be incorporated in the formation of new minerals. Generally, the study of the redistribution of elements during rock alteration involves a comparison between the composition of the product and the parent material. However, major limitations in such mass-balance relations include volume changes involved in the transition from rock to soil, and the fact that the weathering environment is essentially an open system.

The importance of obtaining knowledge of U mobility in overcoming these difficulties and understanding the weathering processes involved in the decomposition of granites, can not be overemphasised. Moreover, using gamma-ray spectrometry in

conjunction with mineralogical and geochemical studies of near-surface materials, the character of the U mobilisation can be easily found, so that knowledge is quite accessible.

In Chapter 4, the chemical composition of the Nigerian Younger Granites was studied in relation to U distribution. It was suggested that a significant proportion of the U occurs in primary U minerals. In Chapter 5, the detailed mineralogical distribution of U in the granites was discussed and phases which were formed during weathering processes were identified as important alpha-emitters. This suggested that mobilisation of U occurred during weathering of the granite. In this Chapter, chemical change accompanying the breakdown of the granite by what is believed to be deep lateritic weathering, is investigated in more detail, specifically with reference to the mobility of U. For this purpose, chemical analyses were carried out on 43 soil samples collected in close proximity to the points where fresh granite was sampled. In addition, a soil gas survey was undertaken to determine Rn activity and its association with the U content of the soil.

9.2 Processes in Soil Formation

Soils comprise one of the important steps in the rock cycle: they may form sediments in their own right or they may be transported and later be deposited. In pedogenic processes, two important stages are weathering and profile formation. Although in

most simple cases of soil development the former stage precedes the latter, often the two can not be separated and take place simultaneously. In general, however, soil-forming process first produce a regolith by the breakdown of the parent rock. The regolith then undergoes further changes in the profile development process. Such soils are termed primary soils, while soils developed from deposits of materials that have undergone more than one cycle of weathering are referred to as secondary soils.

Soil formation from crystalline rocks necessarily involves chemical and physical weathering. In the rocks undergoing weathering, a mantle of disaggregated material forms which continues to develop as weathering proceeds. The mechanisms involved in weathering of crystalline rocks have already been discussed in Chapter 3. Such factors as climate, rock type, topography, vegetation, and the period of time involved, determine the nature of the soil. These factors influence the speed of weathering and thus the processes of profile development. Of particular importance in weathering is the moisture content of the ground. Water in the regolith leaches out weatherable materials and affects the rate at which chemical reactions occur within the soil. Also, because of loss by evaporation and transpiration, the effectiveness of the moisture supply in soil forming processes varies considerably with local environmental conditions. Moisture content also controls microbiological growth and activity, which are other agents in the process of soil development.

Topographic influences on pedogenic processes are basically two-fold. These are the effects on climate and the rate of erosion. The climate of a region can be greatly modified by the relief relative to sea level. Generally, there is a decrease in temperature with altitude. Therefore, upland regions in an area usually have colder and wetter climates than the surrounding low-lying regions. The effect of topography on the rate of erosion is expressed most in areas of steep slopes, where heavy rain, especially in the tropical regions, washes down the soils. Other effects associated with topography are its influence on the height of the water table and on drainage conditions. For example, in areas of high relief, the water table is usually at a much lower level relative to the ground surface than in the adjoining lowlands, so that the overall moisture content of the soil may be quite small even though rainfall is greater.

Factors such as the vegetation cover and human interference also affect the processes of soil formation. Although the former is largely controlled by the climate, once a vegetative cover has been established it has a profound effect on the type of soil which is formed. For example, vegetation may prevent oxidation by forming a barrier between the soil and the atmosphere, while decay of roots and fallen leaves will increase the organic acid content of the soil. However, it has been observed by Robinson (1951) that grassland soils are appreciably richer in organic matter than soils of forest regions. This is because in forest regions, although

there are many trees, there is usually an absence of ground vegetation and, in fact, leaf-fall is not as significant a source of organic matter as vegetation of grassland or steppe environments. As organic matter increases, so does the reactive capacity of solutions seeping through the ground due to higher concentration of organic acids. Therefore, solutions draining through grassland areas are more effective in pedogenic processes than those in forested regions, and soil profiles are developed to a greater depth. Man may also influence the processes through agricultural and mining activities.

The above-mentioned factors operate to produce soils of different type and properties. These are best characterised by the nature of the soil profile. The top part of the full sequence is designated the O horizon, which is the zone of organic matter. The A horizon, the layer directly beneath the O horizon, is the zone of maximum leaching (Brady, 1974), while the underlying B horizon is where most of the leached species become precipitated. Finally, the C horizon is the layer just above the undisturbed bedrock, which is made up of disaggregated rock.

The production of the soil profile as a whole can be divided into two basic parts: the development of the organic component and mineralogical changes. However, these parts are often inter-related. Although the organic component of a soil may develop independently, it is usually associated with the formation of clay minerals, and the two together form a clay-humus complex (Robinson,

1951).

The leaching of the O horizon ensures the distribution of organic molecules among the various lower horizons of the soil. This is helped by the activity of microorganisms within the organic matter which is, in turn, determined by the moisture content of the ground (Jenny, 1941).

The development of stable mineral phases in the soil is also controlled by water movement within the soil profile. In humid climates, where rainfall exceeds evaporation, there is a constant supply of water to the soil. Regolith minerals are therefore, subjected to leaching, and the leached constituents may either be deposited in lower horizons of the soil, or carried out of the environment. In some cases, downward movement may be impeded, resulting in either lateral movement of the water where this is possible, or the water can become trapped. Where trapping occurs the soil may become permanently saturated and reducing conditions develop throughout the profile. These conditions result in the accumulation of silicious minerals which would otherwise have been removed by percolating water. Moreover, in water-logged soils where there is a constant flunctuation of the water table, pan formation may occur (Mohr and Van Baren, 1954; Maignien, 1966). Extreme examples of pan formation are the development of ferruginous and aluminous crusts in surface horizons of laterite soils. Under arid conditions, only a limited thickness of the regolith is affected by the rain and, even then, evaporation tends

to remove most of the soil moisture so there is no effective chemical loss from the system. Under other circumstances, molecular ratios such as SiO_2 to sesquioxides and SiO_2 to Al_2O_3, are often used to determine the degree of leaching in the soil. Because of the preferential leaching of SiO_2 relative to either Al_2O_3 or Fe, these ratios are believed to vary according to the degree of leaching suffered by a soil. Intensily leached soils are characterised by a SiO_2:Al_2O_3 ratio below 2.0 (Young, 1980), while the SiO_2 to sesquioxide ratio in such soils may be as low as 1.0.

9.3 Lateritization

Opinions vary as to the processes involved in lateritization and, indeed, even in the use of the term. For example, the name laterite has been applied to residual products, detrital sedimentary products, and volcanic materials (Maignien, 1966). In modern usage, however, lateritization is defined as the leaching and elimination of SiO_2, alkalis and the alkaline earths, and the concentration of hydrated Al_2O_3 and Fe (the former partly *combined with* SiO_2) *in the soil-forming process* (*Mohr and Van* Baren, 1954). The important factors controlling these changes appear to be climate and the duration of the pedogenic processes. They are usually associated with tropical climates and a prolonged period over which the mineral reactions occur.

The most important components in a laterite are Al

sesquioxides in the form of gibbsite and (sometimes) boehite, Fe sesquioxide in the form of hematite and goethite, the clay minerals, aluminous and ferruginous amorphous products, and residual materials in varying proportions. Typical profiles consist of four horizons. In ascending order these are the parent rock, the zone of primary weathering, the lateritic horizon, and a surface horizon of ferruginous incrustations (Robinson, 1951; Mohr and Van Baren, 1954). Typically laterite formations are found associated with Fe precipitation within zones of extensive leaching, but concentration of the lateritic components may occur either as a result of the removal of the soluble materials, or the addition of less-soluble materials after the first-stage of weathering. Opinions vary concerning the mechanisms of Fe enrichment. Three commonly advanced explanations are: (1) enrichment through leaching of top horizons, (2) enrichment by capillary rise of groundwater, and (3) enrichment through a seasonally flunctuating water table. The most popular of the explanations so far advanced is that enrichment occurs by changes in the chemical environment produced by a flunctuating water table. The idea is that in the rainy season the water table rises, and the soil profile becomes saturated. Both Fe and Al_2O_3 leached from the soil by hydrolysis of silicate minerals are then held in solution in ferrous and alkaline aluminate forms, respectively. On recession of the water table during the dry season, these materials are deposited in their oxidised form, and remain as solid phases during the next rise of

the water table. This process can affect a great depth range, and influence more than just the soil horizons. For example, where the zone of groundwater flunctuations are within the bed rock, ferruginised zones are produced (Mohr, 1952; Pendleton, 1953). Conversely, Mohr and Van Baren (1954) and Maignien (1966) showed that capillary rise can only affect a limited thickness and can not, therefore, explain the formation of lateritic horizons. Lateritic soils of considerable thickness must have evolved over longer periods than those required for normal soil profile development. Also, as pointed out by Robinson (1951), the requirement for O_2 during oxidation means that their formation must take place in aerated ground.

9.4 Lateritization on the Jos Plateau

In the tropics the most important factors in pedogenic processes are temperature and the amount of rainfall. With mean annual temperatures generally above 26°C, the rate at which chemical reactions occur in the tropics is greatly increased over cooler climates. However, because the Jos Plateau is at a height of about 1500m above the surrounding plains, much lower temperatures are recorded than in most other parts of northern Nigeria, and the mean annual temperature is only 22°C. The coldest months are December-February, marking the Harmattan period. Although receiving much more rainfall than the surrounding plains, there are still

clear dry and wet seasons on the Jos Plateau. The wet season starts earlier than other places in the region and ends later, with July-August being the wettest months (Table 9.1). Although as much as 90% of the rain falls within the period April-October, some precipitation even in the driest months is not uncommon.

Predominantly, the Plateau presents an undulating surface with scattered occurrences of mountain masses and hilly outcrops. De Swart (1956) has described the main erosion surfaces on the plateau. The highest points, referred to as the older erosion surfaces, are characterised by hard, ferruginous laterite cappings. These form a flat watershed, below which is a later surface largely developed on alluvial sediments. After emplacement of the Younger Granites, believed to be in the mid Jurassic, and the formation of the planation surfaces by erosion, a period of lateritization set in. This is believed to be of early Pliocene age, and is considered to be the main period of laterite formation on the Jos Plateau (Alford et al., 1979).

At present, most of the Plateau forms a vast area of grassland, with some shrubs and occasional trees, which provides pasture for animal grazing. Upland forest and woodland occur in the wetter areas of the Plateau. Most of the soils with hard ferruginous bands are scarcely farmed, although the grasses which dry out during the dry season may contribute some organic matter to the soil. The hard ferruginous bands with occasional large quartz crystals and large concretions, are detectable by surface

Table 9.1: Average rainfall in the Jos Plateau.

Month	Rainfall/mm
January	2
February	4
March	32
April	89
May	159
June	194
July	260
August	266
September	222
October	90
November	10
December	2
Annually	1331

Data from Odumodú (1983).

magnetic surveys (Dewu, 1986). In some places, the lateritic cover is thin while in others digging in excess of 6m (for example in laterite excavations around Rayfield) has not penetrated the base of the laterite.

9.5 Mobility of U in Low Temperature Alteration Processes

Supergene alteration processes involve the destruction of a large number of minerals with the subsequent release of elements into solution. The rate at which an element is mobilised in such processes is determined by the nature of the minerals in which it occurs, the chemistry of the water involved, and the properties of the environment, such as temperature. In the near-surface zone, rain water and soil water are mainly responsible for weathering, while at depth, groundwaters are involved. The compilations of Baas et al. (1960) showed that rain waters have a pH range of 3-9, with a fairly high concentration of dissolved O_2 (high Eh), while groundwaters have pH values in the range 5-9 and often have a low Eh. The stabilities of mineral phases in such environments are largely determined by the thermodynamic parameters of the reacting phases. Phase stability diagrams have been found helpful in identifying stable phases. Thermodynamic relations for the phase diagrams presented in this Section have been calculated by Langmuir (1978).

Figure 9.1 shows the phase equilibrium diagram of U species at low temperature and low U concentration. The diagram indicates the large stability field of crystalline U oxide. It is stable under most pH conditions encounted in surface and groundwaters. The hydrolysis of the oxide produces the uranyl ion UO_2^{2+} according to the equation:

$$U^{4+} + 2H_2O \Rightarrow UO_2^{2+} + 4H^+ + 2e^-$$

The diagram shows the stability of the uranous species with only small fields for UOH^{3+}, $U(O)_2^{2-}$, $U(OH)^{3+}$ and $U(OH)^{4+}$ under acid conditions. Therefore, in normal surface water conditions, U is only soluble in the hexavalent state. The uranyl ion predominates under oxidising conditions and forms the dominant species within the Eh-pH conditions of surface waters.

However, most water involved in weathering has undergone chemical exchange with various soil and rock formations and, as such, is potentially more reactive than surface water. This is depicted in the phase diagram in Figure 9.2. These waters carry along with them ions which readily form complexes with dissolved U species. Important among these are carbonate, vanadate, phosphate, fluorine, and organic matter. Studies of the stabilities of the uranyl and uranous complexes by Langmuir (1978) revealed that these complexes greatly increase the stability of U under a wide range of conditions prevalent in weathering environments. In particular, the

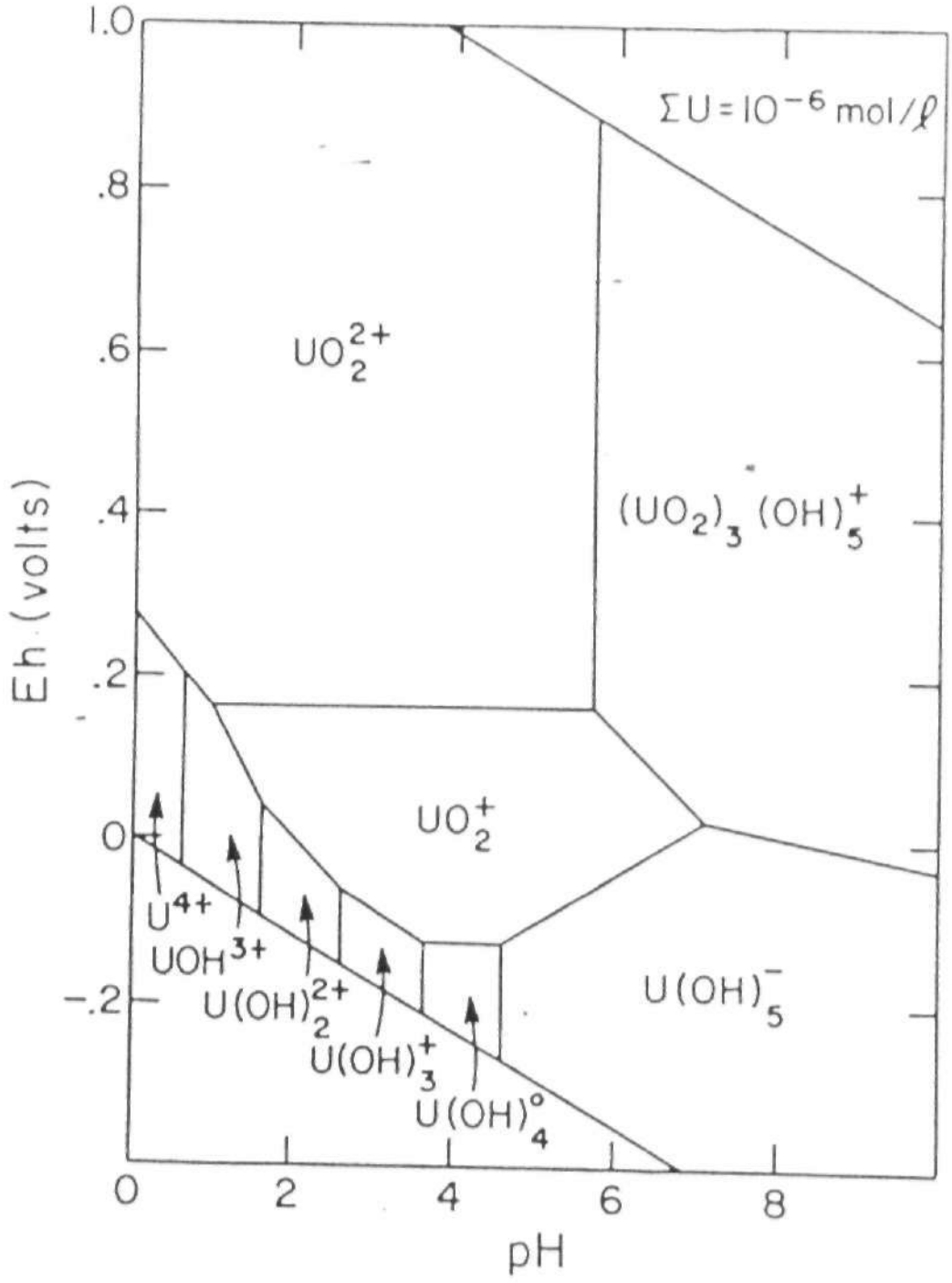


FIGURE 9.1 Phase stability diagram for U species at 25°C in an open system, at groundwater CO_2 partial pressure of 10^{-2} atm. and U concentration of 10^{-6}M (0.24ppm)

(After Langmuir, 1978)

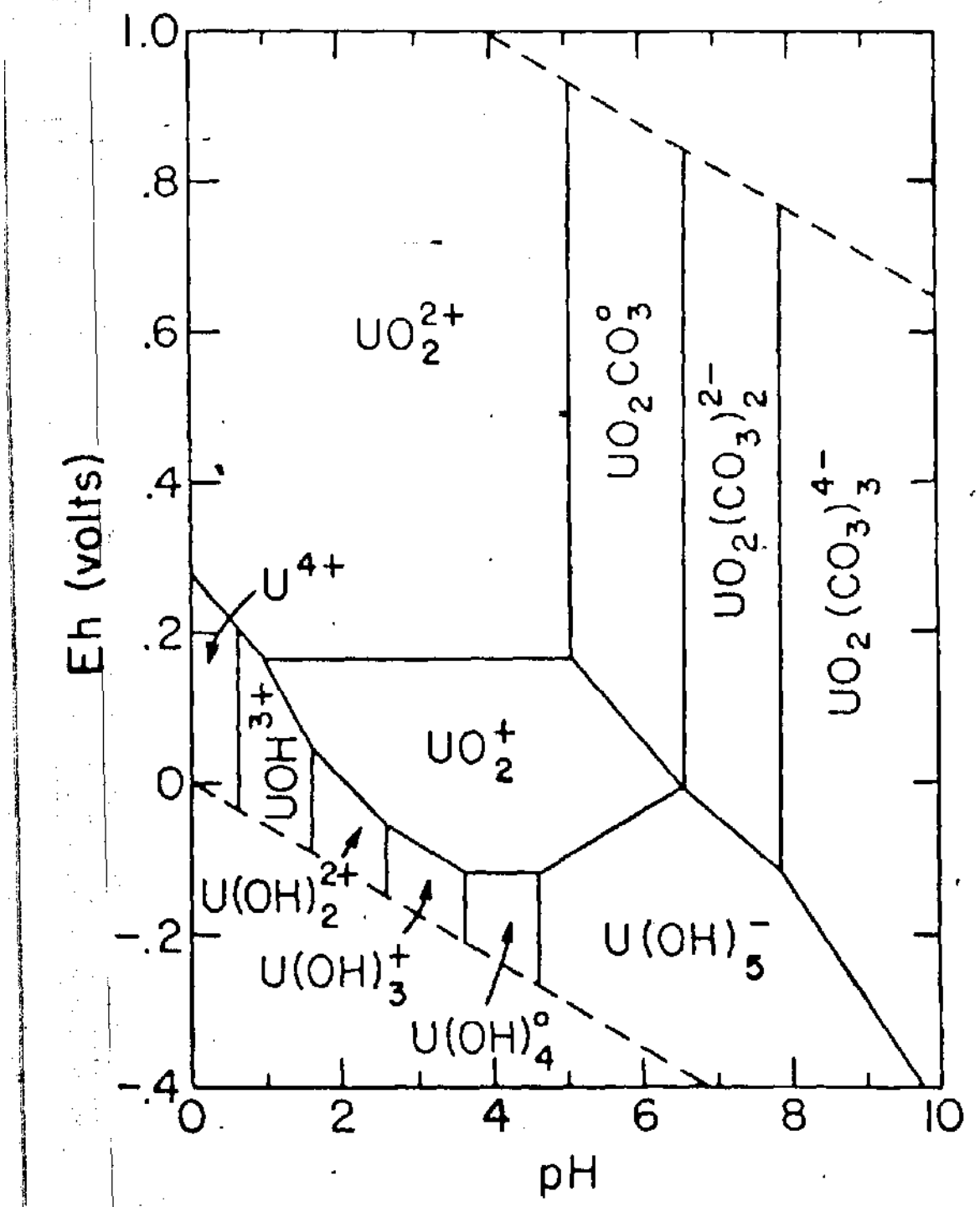


FIGURE 9.2 Phase stability diagram for U species at 25°C in a closed system at CO_2 partial pressure of 10^{-2} atm. and U concentration of 0.24ppm (After Langmuir, 1978)

complexing effect of CO_2 on U is very important. Hostetler and Garrels (1962) reported a range of 100-300ppm of dissolved CO_2 in groundwaters and found CO_2 partial pressures exerted a major control on the stability of U species under weathering conditions. Stability fields of U species in aqueous solutions involving CO_2 are shown in Figure 9.3. This Figure demonstrates the importance of the carbonate complexes, displacing most of the fields of the uranyl hydroxo species. The uranyl carbonate complexes thus give rise to a wide field of solubility under oxidising conditions for all pH values. Hostetler and Garrels (1962) identified the uranyl carbonate species as rutherfodine $[UO_2CO_3]$, uranyl di-carbonate $[UO_2(CO_3)_2.2H_2O]^{-2}$ and uranyl tri-carbonate $[UO_2(CO_3)_3]^{-4}$. From Figure 8.3 it can be seen that in acid oxidising conditions U is transported as UO_2^{2+} and $UO_2(OH)^+$, while in neutral and alkaline oxidising solutions, uranyl di-carbonate and uranyl tri-carbonate, respectively, predominate. The importance of these complexes is largely determined by the carbonate concentration.

As well as carbonates, the presence of phosphates and vanadates also influences the solubility of U, and the importance of carbonate complexes depends on the concentrations of these other ligands. In environments with relatively low carbonate concentrations, vanadates and phosphates are the carriers of the uranyl species. The vanadate minerals carnotite and tyuyamunite, and the phosphate autunite, are the important precipitates in such systems. However, Evans and Garrels (1958) suggested that carnotite

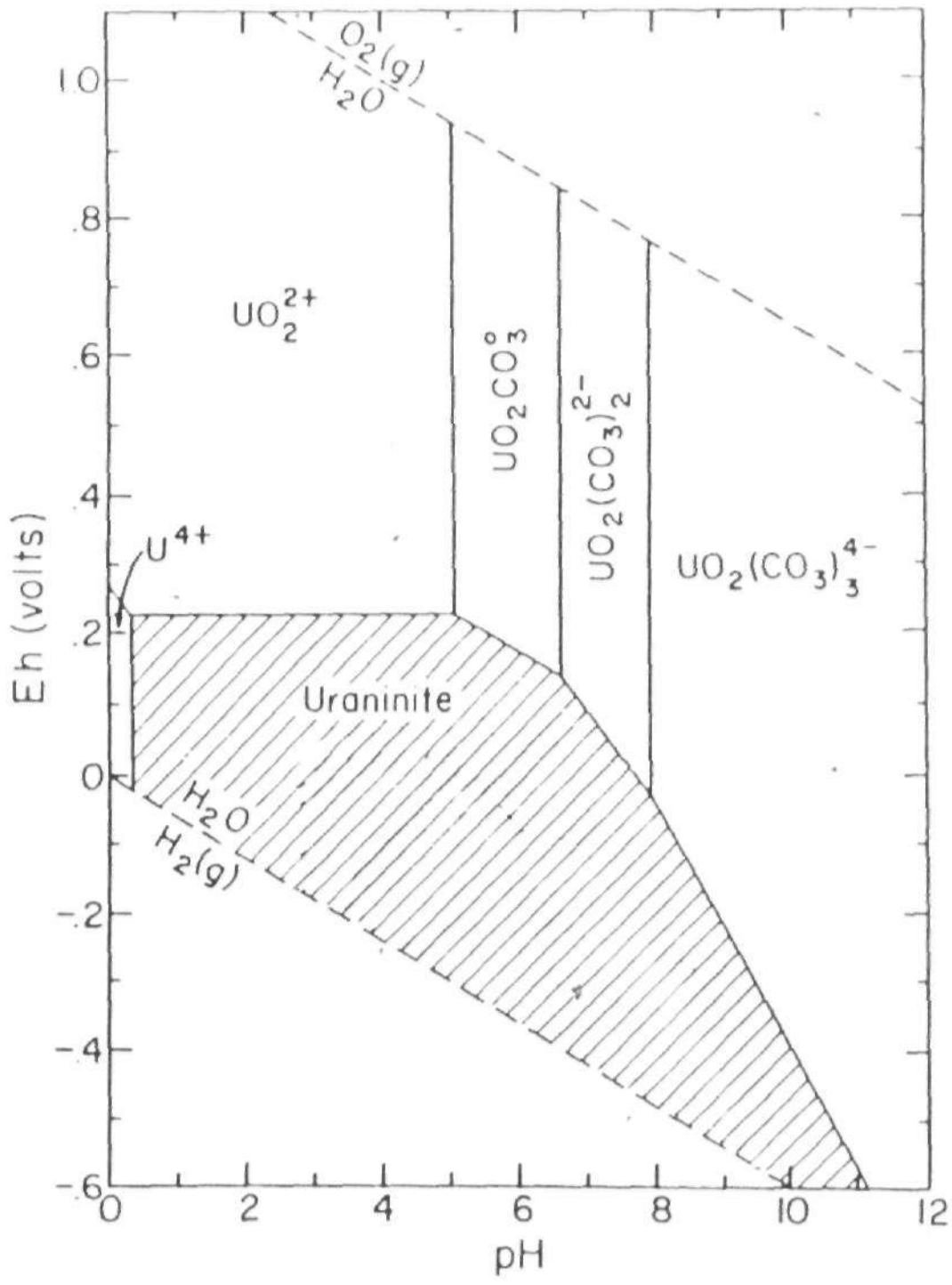


FIGURE 9.3 Stability field of U species in the system U-O_2-CO_2-H_2O with dissolved U of 0.24ppm (After Langmuir, 1978)

can be precipitated from groundwaters rich in CO_2.

The foregoing discussion shows the importance of surface water percolating through rocks in scavenging and transporting U in aqueous solutions. The significance of such processes in later precipitating U in economic quantities is well recognised (Barbier, 1974). The high concentration of U in the granites of the Nigerian Younger Granite province has already been discussed in Chapters 4 and 5. In connection with the mineralogical distribution of U in the granites, the importance of weathering solutions in leaching some U was also noted. In the highly oxidising environment involved in lateritization, considerable leaching, transportation and deposition of U can be expected to have occurred.

9.6 Soil Survey

9.6.1 Sample Collection and Analysis

As this study was concerned with the changes in U distribution in the granitic rocks of the Jos Plateau brought about by soil-forming processes, samples were collected only to investigate spatial variability in relation to the bed rock type; no attempt was made to sample the different soil horizons at each site, although sampling depths did cut across different horizons. Soil samples were thus collected close to sites where rock sample

had been obtained, so that the soil could be correlated with the rock type. In practice this meant the distance between sites sampled for soil and rocks ranged from about 10m to 50m. At each site where a soil sample was obtained a hole was bored, using a hand operated mechanical auger, to a depth between 27cm and 60cm. At most sites this extended to the disaggregated rock layer (C horizon). Samples of about 2kg were taken from each point. In addition to the lateritic soils, other soil samples of local occurrence were also collected for comparison. Soil sample points are shown in Figure 9.4. To minimize any possible artificial influence on the soil chemistry, farmed areas and ground disturbed by mining were avoided.

Samples were air dried and those for chemical analysis packaged in polythene bags for transportation. The remainder of each sample was used for gamma-ray spectrometric analysis as described in Chapter 6. Samples for XRF analysis were prepared as outlined in Section 4.5.

9.6.2 Sample Description

The soils collected show clear differences in their physical state, especially their colour. Three different colours were identified in samples collected from the near-surface, although superficially all show the same red-brown colour typical of lateritic soils. As well as differences between one locality and

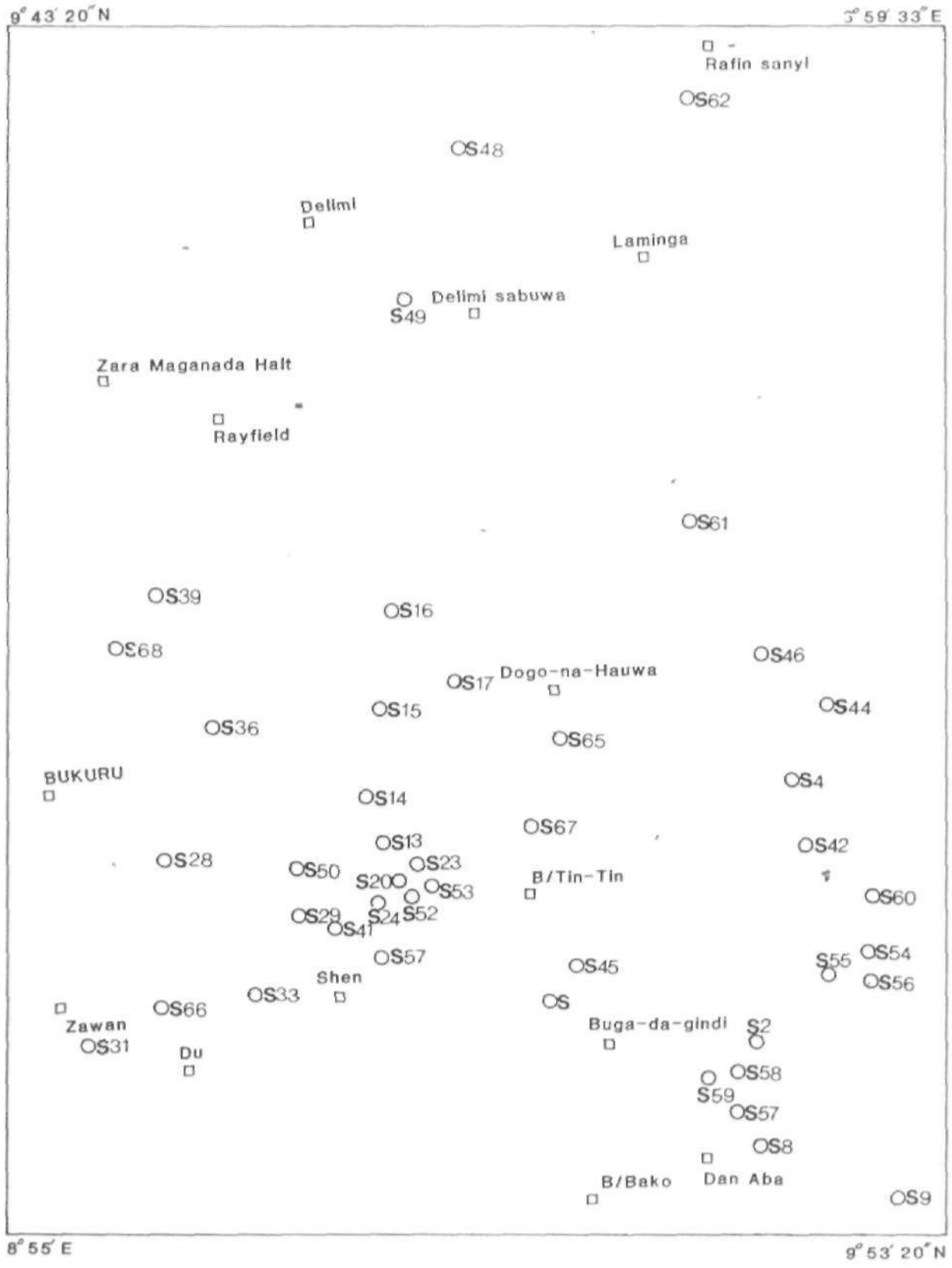


FIGURE 9.4 Soil sample collection points (OS28), Jos Plateau

another, colour changes were also observed with depth in most locations. Thus brown and yellowish-brown layers occur in addition to the red-brown. The red-brown and the light brown coloured soils usually contain many concretions of large size, usually enclosing darker minerals and, sometimes, cassiterite. The yellowish-brown soils contain abundant kaolinite concretions which are usually coated with Fe oxides. Descriptions of the different types together with the depth at which they were collected, are given in Table 9.2. In addition to these lateritic soils there is the development, especially under some vegetation, of dark grey soils and clay loams, around streams and rivers. The dark grey soils have a loose, sandy texture with abundant, large quartz grains. Generally they are coaser than the other soil types and easier to excavate.

Further to the collection of the soil samples, soil Rn measurements were made in the holes from which the soil samples were obtained. Soil Rn measurements were carried out using alpha track detector cards. These are fully discussed later in this Chapter.

9.6.3 Discussion of Results

Results of the analyses of the soils, together with correlation coefficient data for various elements are, given in Table 9.3. In Table 9.4 are given the average abundances of these

Table 9.2: Soil variants in lateritized soils of the Jos Plateau

Sample	Colour	depth/cm
JPS2	lb	43
JPS7	yb	46
JPS8	yb	60
JPS9	rb	41
JPS13	rb	47
JPS14	lb	40
JPS15	lb	44
JPS17	yb	44
JPS20	lb	44
JPS23	yb	38
JPS24	yb	30
JPS28	rb	44
JPS29	yb	39
JPS31	yb	40
JPS33	lb	46
JPS35	yb	49
JPS36	yb	50
JPS39	lb	39
JPS41	lb	47
JPS42	lb	59
JPS43	yb	53
JPS44	yb	48
JPS45	rb	35
JPS46	yb	46
JPS48	yb	53
JPS49	rb	45
JPS50	rb	40
JPS52	lb	30
JPS53	lb	27
JPS54	lb	44
JPS55	yb	53
JPS56	yb	44
JPS57	yb	35
JPS58	lb	48
JPS59	lb	48
JPS60	rb	52
JPS61	yb	50
JPS62	yb	44
JPS65	rb	51
JPS66	rb	46
JPS67	lb	32
JPS68	rb	37

Note: lb - light brown
rb - red brown
yb - yellow brown

Table 9.3a: Chemical analyses of soils of the Jos Plateau.

Sample	SiO_2	Al_2O_3	TiO_2	Fe_2O_3	FeO	MgO	CaO
JPS2	72.65	14.09	0.31	2.61	0.07	0.08	0.08
JPS7	75.72	12.67	0.49	3.58	n.a	0.15	0.06
JPS8	76.21	11.95	0.44	2.98	n.a	0.13	0.08
JPS9	60.16	21.13	0.94	6.66	n.a	0.54	0.23
JPS13	70.01	15.28	0.69	4.55	n.a	0.19	0.10
JPS14	38.37	24.58	0.60	22.95	0.13	0.12	0.05
JPS15	65.00	16.23	0.37	7.19	0.28	0.10	0.07
JPS16	85.08	6.59	0.26	4.20	0.17	0.05	0.04
JPS17	64.99	15.92	0.92	6.16	n.a	0.06	0.05
JPS20	69.84	16.33	0.72	4.48	n.a	0.20	0.07
JPS23	63.63	18.25	0.74	7.56	0.20	0.13	0.06
JPS24	72.32	15.04	0.48	4.01	n.a	0.15	0.05
JPS28	84.40	9.74	0.46	3.12	0.30	0.12	0.07
JPS29	66.15	16.95	0.55	8.01	n.a	0.12	0.06
JPS31	79.83	10.50	0.31	2.39	n.a	0.12	0.16
JPS33	71.55	15.29	0.41	3.46	n.a	0.19	0.09
JPS35	69.65	16.63	0.88	5.62	0.34	0.17	0.06
JPS36	88.86	5.56	0.42	1.61	n.a	0.06	0.05
JPS39	80.42	10.80	0.31	2.86	n.a	0.14	0.04
JPS41	70.97	16.71	0.28	4.46	n.a	0.03	0.04
JPS42	74.33	13.21	0.53	5.23	0.18	0.11	0.08
JPS43	72.15	14.15	0.36	3.57	0.25	0.14	0.08
JPS44	70.47	17.54	0.36	3.48	0.21	0.15	0.12
JPS45	73.04	13.38	0.30	4.35	n.a	0.08	0.04
JPS46	65.46	18.53	0.68	4.90	n.a	0.24	0.13
JPS48	71.60	15.07	0.82	4.32	n.a	0.16	0.13
JPS49	60.64	11.58	0.37	19.66	0.14	0.12	0.05
JPS50	61.70	14.13	0.47	15.50	0.17	0.12	0.05
JPS52	70.59	11.56	0.56	9.50	n.a	0.09	0.05
JPS53	73.40	12.89	0.73	4.88	0.15	0.15	0.06
JPS54	72.81	14.81	0.40	3.85	0.14	0.15	0.04
JPS55	82.76	8.64	0.45	1.82	n.a	0.08	0.07
JPS56	82.04	9.02	0.40	2.42	0.16	0.06	0.08
JPS57	72.63	14.75	0.30	2.73	0.15	0.09	0.07
JPS58	67.94	17.26	0.50	4.86	n.a	0.09	0.05
JPS59	69.86	15.50	0.64	6.09	n.a	0.11	0.07
JPS60	78.03	11.44	0.37	3.99	n.a	0.11	0.05
JPS61	69.02	15.34	0.33	3.31	n.a	0.07	0.13
JPS62	63.20	17.06	0.59	6.38	n.a	0.09	0.10
JPS65	68.51	14.41	0.58	8.65	0.13	0.14	0.04
JPS66	56.01	18.18	0.73	15.68	0.15	0.17	0.06
JPS67	63.52	19.52	1.04	5.81	0.22	0.28	0.15
JPS68	42.70	17.61	0.71	28.36	0.16	0.08	0.05

Continue.....

Table 9.3a, Continued.

Sample	Na_2O	K_2O	P_2O_5	MnO	LOI
JPS2	0.37	4.58	-	0.01	3.33
JPS7	0.19	3.25	0.01	0.02	4.56
JPS8	0.43	3.38	0.02	0.02	4.36
JPS9	0.23	2.69	0.02	0.07	8.64
JPS13	0.12	1.07	0.02	0.02	8.02
JPS14	0.01	0.24	0.13	0.02	13.02
JPS15	0.24	0.68	0.02	0.01	8.24
JPS16	0.09	0.37	0.02	0.01	3.38
JPS17	0.07	0.18	0.06	0.03	7.82
JPS20	0.13	1.30	0.02	0.02	6.84
JPS23	0.17	0.73	0.04	0.06	7.80
JPS24	0.18	0.97	0.02	0.02	5.96
JPS28	0.41	1.62	0.03	0.01	4.07
JPS29	0.05	0.30	0.02	0.01	7.24
JPS31	0.71	2.61	0.05	0.02	3.11
JPS33	0.81	2.33	0.02	0.02	6.04
JPS35	0.15	1.13	0.03	0.03	6.62
JPS36	0.40	1.27	0.01	0.01	2.38
JPS39	0.27	0.79	0.01	0.01	4.67
JPS41	0.03	0.21	0.01	0.01	7.36
JPS42	0.11	0.60	0.03	0.01	7.13
JPS43	0.58	4.12	0.01	0.02	4.96
JPS44	0.21	3.78	0.01	0.02	5.53
JPS45	0.32	3.07	0.01	0.02	5.51
JPS46	0.45	3.45	0.02	0.02	6.31
JPS48	0.25	1.53	0.03	0.02	6.58
JPS49	0.09	0.50	0.05	0.01	6.69
JPS50	0.11	0.32	0.06	0.01	7.33
JPS52	0.19	2.03	0.04	0.04	4.96
JPS53	0.06	1.57	0.01	0.03	5.00
JPS54	0.08	1.02	0.01	0.01	6.33
JPS55	0.36	2.79	0.01	0.01	2.78
JPS56	0.40	2.79	0.01	0.01	3.02
JPS57	0.25	3.75	0.01	0.01	5.62
JPS58	0.17	0.44	0.02	0.01	7.60
JPS59	0.06	0.26	0.03	0.02	7.24
JPS60	0.17	0.64	0.02	0.01	5.02
JPS61	1.24	5.19	0.01	0.02	4.18
JPS62	0.44	4.52	0.01	0.05	6.22
JPS65	0.10	0.19	0.04	0.01	7.49
JPS66	0.06	0.37	0.06	0.02	9.24
JPS67	0.09	1.08	0.04	0.02	9.27
JPS68	0.10	0.09	0.10	0.01	10.20

Continue...

Table 9.3a, Continued.

Sample	Ni	Cu	Zn	Ga	As	W	Pb	Th	U	Cr	Mn
JPS2	13	7	38	37	-	318	29	32	13	21	29
JPS7	19	11	50	27	5	223	16	24	8	29	150
JPS8	17	11	50	26	6	365	12	22	7	32	127
JPS9	41	26	55	26	3	119	25	18	4	50	446
JPS13	29	13	50	29	7	172	12	21	6	46	80
JPS14	32	27	58	43	22	51	43	31	12	195	78
JPS15	23	14	51	40	12	252	15	28	13	81	73
JPS16	11	10	25	13	7	394	9	25	8	38	27
JPS17	23	33	59	35	-	177	42	32	23	29	214
JPS20	27	15	82	32	5	173	25	23	10	42	77
JPS23	23	19	85	37	5	160	26	28	10	55	320
JPS24	25	12	61	37	6	499	18	28	11	38	90
JPS28	18	10	27	19	7	524	9	25	9	38	65
JPS29	28	15	36	37	7	181	18	37	16	63	61
JPS31	16	10	53	26	7	305	9	24	8	29	125
JPS33	22	11	64	39	5	249	23	33	12	38	112
JPS35	31	17	67	31	6	156	20	21	7	97	193
JPS36	12	7	17	11	5	582	7	14	5	29	67
JPS39	20	10	50	27	7	325	11	29	10	35	70
JPS41	15	11	46	47	8	188	11	42	12	34	43
JPS42	28	13	27	22	9	299	10	20	7	69	67
JPS43	18	8	79	34	3	259	21	23	6	27	138
JPS44	20	9	76	38	5	196	22	28	7	27	129
JPS45	19	15	-	33	-	244	85	31	9	25	111
JPS46	35	16	67	36	6	106	20	25	7	42	134
JPS48	25	13	38	27	5	220	19	27	9	39	123
JPS49	23	24	28	32	27	190	26	30	19	137	64
JPS50	24	18	29	29	20	179	24	22	13	140	50
JPS52	15	24	90	29	-	197	84	19	12	50	260
JPS53	23	17	87	27	1	211	32	20	8	40	169
JPS54	21	8	29	32	6	268	12	25	8	33	50
JPS55	15	9	18	16	5	611	11	19	8	30	76
JPS56	14	8	19	18	6	366	10	17	6	32	80
JPS57	18	8	27	33	4	286	15	24	8	27	48
JPS58	24	10	31	34	7	243	12	24	7	38	65
JPS59	29	16	31	30	5	115	28	26	8	75	103
JPS60	21	12	51	25	9	467	7	23	11	52	54
JPS61	13	7	95	38	3	304	26	28	9	19	141
JPS62	20	12	-	42	2	131	39	20	7	27	326
JPS65	30	16	18	20	13	169	13	21	5	173	46
JPS66	40	23	33	33	16	101	26	24	12	145	67
JPS67	42	17	39	30	5	109	23	26	7	68	150
JPS68	32	48	32	50	34	79	18	42	8	408	52

Continue...

Table 9.3a, Continued.

Sample	Ba	La	Ce	Rb	Sr	Y	Zr	Nb	Cs	Sn	V
JPS2	127	91	106	300	16	125	460	192	3	74	7
JPS7	236	73	158	203	22	83	593	109	3	10	15
JPS8	241	64	136	199	23	70	629	91	3	12	15
JPS9	791	51	148	156	105	31	533	23	5	27	65
JPS13	182	45	96	150	29	70	622	139	5	25	30
JPS14	132	47	79	36	15	33	544	86	4	22	230
JPS15	81	26	65	127	13	45	452	175	4	17	75
JPS16	65	33	65	61	7	24	366	90	-	36	31
JPS17	259	113	198	55	38	137	457	142	4	24	25
JPS20	183	61	133	138	26	91	833	137	6	28	29
JPS23	197	66	169	80	19	84	970	157	7	38	37
JPS24	128	45	98	170	17	61	570	191	5	17	25
JPS28	129	39	69	171	15	56	629	129	2	15	16
JPS29	99	35	76	64	12	60	553	194	4	23	67
JPS31	141	18	70	285	17	35	413	181	8	16	14
JPS33	138	46	109	310	18	77	541	236	4	21	18
JPS35	303	77	299	127	26	81	940	107	4	16	12
JPS36	121	15	46	144	15	30	615	140	2	39	6
JPS39	87	28	87	163	11	63	371	191	3	22	22
JPS41	49	26	67	75	7	31	383	255	3	26	17
JPS42	127	28	73	84	17	40	478	75	4	11	45
JPS43	230	71	131	246	23	100	457	110	4	14	7
JPS44	271	72	161	219	21	88	518	118	5	12	9
JPS45	184	57	122	236	16	65	441	121	5	22	8
JPS46	337	82	153	214	38	102	901	118	4	12	21
JPS48	195	63	113	179	27	64	862	95	4	12	18
JPS49	75	15	35	80	7	30	344	84	-	17	252
JPS50	93	19	37	52	12	31	444	118	2	14	195
JPS52	229	66	247	124	25	80	575	116	4	-	60
JPS53	251	105	208	131	30	146	724	131	3	40	23
JPS54	145	49	203	119	13	70	501	107	4	13	16
JPS55	219	36	77	192	25	62	591	97	9	19	14
JPS56	210	39	62	189	21	62	500	90	3	13	13
JPS57	219	60	128	240	18	75	428	112	7	19	11
JPS58	143	57	199	102	14	71	554	110	7	23	27
JPS59	126	51	141	51	18	58	741	192	4	29	53
JPS60	72	28	61	105	13	42	473	149	-	15	30
JPS61	328	89	200	248	26	127	615	112	4	12	-
JPS62	413	87	181	208	24	98	-	160	6	38	-
JPS65	83	29	64	25	12	27	472	46	-	17	100
JPS66	121	34	65	58	17	42	559	136	4	34	182
JPS67	277	91	145	129	43	87	895	80	7	22	44
JPS68	72	10	34	9	9	11	334	96	-	20	394

Note: Major elements as oxides in %, others in ppm.
: LOI - Loss On Ignition.

Table 9.3b: Correlation coefficient of elements in soil.

	SiO_2	Al_2O_3	TiO_2	Fe_2O_3	MgO	CaO	Na_2O	K_2O
Al_2O_3	-0.830							
TiO_2	-0.455	0.533						
Fe_2O_3	-0.837	0.419	0.251					
MgO	-0.235	0.456	0.560	-0.009				
CaO	-0.063	0.297	0.334	-0.215	0.696			
Na_2O	0.295	-0.217	-0.361	-0.381	-0.058	0.408		
K_2O	0.28	-0.086	-0.283	-0.444	0.070	0.46	0.711	
P_2O_5	-0.754	0.418	0.340	0.814	-0.030	-0.11	-0.308	-0.474
MnO	-0.263	0.401	0.537	0.000	0.540	0.466	0.039	0.211
LOI	-0.886	0.844	0.561	0.692	0.317	0.016	-0.506	-0.518
Ni	-0.649	0.714	0.765	0.450	0.679	0.317	-0.418	-0.382
Cu	-0.755	0.440	0.567	0.817	0.178	-0.051	-0.413	-0.438
Zn	-0.136	0.214	0.029	-0.079	-0.016	0.105	0.253	0.445
Ga	-0.706	0.732	0.080	0.423	-0.031	-0.011	-0.007	0.044
As	-0.635	0.170	-0.001	0.919	-0.184	-0.341	-0.340	-0.511
W	0.779	-0.777	-0.531	-0.532	-0.338	-0.187	0.315	0.162
Pb	-0.313	0.223	0.151	0.227	-0.032	-0.087	-0.038	0.160
Th	-0.426	0.369	-0.121	0.371	-0.234	-0.212	-0.097	-0.221
U	-0.271	0.091	-0.022	0.320	-0.297	-0.356	-0.200	-0.325
Cr	-0.707	0.320	0.256	0.901	-0.023	-0.219	-0.342	-0.464
Mn	-0.191	0.333	0.520	-0.067	0.533	0.526	0.123	0.291
Ba	-0.118	0.342	0.463	-0.196	0.699	0.734	0.235	0.515
La	-0.052	0.312	0.392	-0.318	0.150	0.251	0.161	0.489
Ce	-0.019	0.277	0.369	-0.285	0.182	0.146	0.095	0.309
Rb	0.436	-0.204	-0.363	-0.610	0.091	0.444	0.748	0.858
Sr	-0.139	0.356	0.595	-0.150	0.835	0.761	0.075	0.269
Y	0.110	0.127	0.189	-0.421	-0.008	0.135	0.303	0.526
Zr	-0.080	0.288	0.528	-0.170	0.217	0.277	0.076	0.226
Nb	0.166	-0.037	-0.315	-0.233	-0.341	-0.238	0.129	-0.067
Cs	-0.092	-0.200	0.143	-0.129	0.128	0.295	0.042	0.116
Sn	0.007	-0.123	0.033	0.078	-0.096	-0.117	-0.066	0.040
V	-0.771	0.318	0.170	0.977	-0.024	-0.181	-0.379	-0.457

Continue.....

Table 9.3b, Continued.

	P_2O_5	MnO	LOI	Ni	Cu	Zn	Ga	As
MnO	0.013							
LOI	0.675	0.205						
Ni	0.429	0.276	0.783					
Cu	0.763	0.288	0.667	0.545				
Zn	-0.178	0.521	-0.003	-0.086	-0.005			
Ga	0.308	0.157	0.567	0.242	0.376	0.369		
As	0.800	-0.319	0.522	0.274	0.758	-0.293	0.300	
W	-0.442	-0.381	-0.749	-0.641	-0.565	-0.243	-0.596	-0.298
Pb	0.204	0.413	0.171	0.025	0.355	0.601	0.284	0.132
Th	0.325	-0.222	0.372	0.051	0.345	-0.008	0.719	0.440
U	0.346	-0.117	0.206	-0.057	0.343	-0.047	0.354	0.468
Cr	0.774	-0.139	0.609	0.463	0.772	-0.211	0.319	0.889
Mn	-0.062	0.967	0.118	0.225	0.254	0.522	0.108	-0.374
Ba	-0.214	0.761	0.035	0.286	0.087	0.374	0.001	-0.434
La	-0.203	0.446	-0.037	0.040	-0.053	0.440	0.216	-0.587
Ce	-0.240	0.531	-0.016	0.048	-0.026	0.405	0.180	-0.547
Rb	-0.548	0.063	-0.595	-0.413	-0.584	0.314	-0.018	-0.593
Sr	-0.106	0.692	0.155	0.451	0.204	0.123	-0.085	-0.355
Y	-0.353	0.272	-0.228	-0.147	-0.201	0.393	0.200	-0.624
Zr	-0.149	0.534	0.082	0.247	-0.081	0.538	0.087	-0.428
Nb	-0.199	-0.135	-0.138	-0.285	-0.244	0.148	0.393	-0.181
Cs	-0.016	0.232	0.092	0.140	-0.016	0.167	0.083	-0.240
Sn	0.074	0.272	-0.102	-0.180	0.179	0.143	-0.022	-0.125
V	0.797	-0.098	0.606	0.409	0.776	-0.205	0.375	0.957

	W	Pb	Th	U	Cr	Mn	Ba	La
Pb	-0.366							
Th	-0.307	0.092						
U	-0.127	0.281	0.531					
Cr	-0.421	0.010	0.347	0.081				
Mn	-0.327	0.392	-0.262	-0.129	-0.191			
Ba	-0.235	0.208	-0.371	-0.339	-0.263	0.828		
La	-0.265	0.383	-0.079	0.024	-0.406	0.483	0.524	
Ce	-0.282	0.388	-0.199	-0.113	-0.343	0.573	0.527	0.782
Rb	0.324	0.035	-0.149	-0.253	-0.595	0.130	0.314	0.336
Sr	-0.237	0.137	-0.326	-0.251	-0.192	0.738	0.914	0.401
Y	-0.092	0.288	-0.059	0.114	-0.496	0.314	0.347	0.913
Zr	-0.236	0.128	-0.304	-0.264	-0.206	0.526	0.428	0.520
Nb	0.098	-0.031	0.471	0.379	-0.258	-0.189	-0.405	-0.061
Cs	-0.037	0.009	-0.082	-0.175	-0.152	0.213	0.202	0.078
Sn	-0.068	0.605	-0.158	0.129	-0.045	0.273	0.047	0.124
V	-0.438	0.108	0.356	0.267	0.930	-0.154	-0.231	-0.430

	Ce	Rb	Sr	Y	Zr	Nb	Cs	Sn
Rb	0.192							
Sr	0.361	0.167						
Y	0.692	0.455	0.222					
Zr	0.498	0.115	0.266	0.414				
Nb	-0.094	0.198	-0.396	0.147	0.004			
Cs	0.148	0.158	0.165	0.032	0.225	-0.116		
Sn	0.322	-0.039	0.039	0.107	0.018	0.016	-0.048	
V	-0.406	-0.582	-0.170	-0.504	-0.298	-0.245	-0.154	-0.000

Table 9.4: Average elements concentrations in soils and associated rocks.

Elements & oxides	Soil	Rock
SiO_2	66.78	75.39
Al_2O_3	15.93	12.64
TiO_2	0.57	0.18
Fe_2O_3	7.42	2.02
MgO	0.14	0.08
CaO	0.08	0.61
Na_2O	0.23	3.79
K_2O	1.69	4.91
P_2O_5	0.03	0.04
MnO	0.02	0.02
Ni	25	8
Cu	16	6
Zn	62	98
Ga	34	38
As	9	4
W	201	236
Pb	26	20
Th	27	32
U	10	11
Cr	72	413
Mn	125	29
Ba	201	130
La	57	282
Ce	131	144
Rb	140	13
Sr	23	190
Y	71	195
Zr	609	110
Nb	129	176
Cs	5	5
Sn	35	18
V	66	-

Note: Major elements as oxides in %, the rest in ppm.

elements in the soil compared to their average abundances in the fresh granite. Although a number of processes are involved in the transformation from rock to soil, the analyses should indicate the overall effect of weathering on chemical mobility. On average, Al, Ti, Fe, Mg, Ni, Cu, As, W, Pb, Cr, Zr, Sn, and V are enriched in the soils relative to the fresh granites, while Si, Ca, Na, K, P, Zn, Ga, Th, U, Ba, La, Ce, Rb, Sr, Y, Nb, and Cs are depleted.

Before any discussion of the enrichment or depletion of specific elements can be made, it must be understood that absolute changes are very difficult to determine directly from chemical analyses made on soils. This is because many properties are affected by the soil-forming processes. Important among these is the mass change that may accompany the transformation: elements may show an enrichment not necessarily because they have been enriched in the environment, but because of the relative change in mass. Where a 50% reduction by mass occurs, for example, an element which has not been affected by the process, will show a two-fold increase over its original abundance. If the degree of loss of the elements were to be uniform, then all the elements would be depleted in amounts proportional to the amount of material lost. But because of the complex nature of the processes involved, the different mobilities of the elements within particular environments, and the location of these elements in the rock minerals, these computations are not straight-forward. In soil chemical analyses, such as those given in Table 9.3, the number of

constituents is fixed at the number of elements analysed, and the proportion of each constituent is adjusted to produce a constant sum of 100% for each sample. Clearly, this procedure does not take into account the undetermined constituents and, therefore, the values are only relative.

The problem of mass change discussed above, and the irregular distribution of the elements within the different soil horizons, make it difficult to determine absolute changes in element abundances, but several methods have been proposed which minimize these effects.

The problem of relative gain or loss in a horizon can be removed by applying a correction factor, obtained by assuming that a particular element or oxide is immobile during weathering (Pettijohn, 1949; Short, 1961). The correction factor is then computed as the ratio of the amount of the assumed constant element, say Al_2O_3, in the parent rock to its amount in the soil horizon, that is:

$$Al_2O_3 \text{ in parent rock}/Al_2O_3 \text{ in soil.}$$

All other elements are then multiplied by this factor to remove the effects of the relative change which are not caused by weathering. The sum of all corrected concentrations when compared to the original 100% represents the apparent total gain or loss of all the constituents. The net change of any constituent in the soil

relative to the rock is then given by the ratio of the difference between its concentration in the soil and its concentration in the rock. This ratio multiplied by 100 gives the percent net gain or loss of the element. The percent net changes in soil in this study have been computed and are given in Table 9.5.

Connor et al. (1957) introduced the concept of a distribution index (DI) and a concentration index (CI) in determining relative element changes during soil formation. In their application the authors defined DI as the ratio of an element's abundance in the A horizon to its abundance in the C horizon, while CI was defined as the ratio of the element's abundance in the clay fraction from either the A or B horizon, to its abundance in the C horizon. These indices were modified by Short (1961) so that the DI was taken as the ratio of an element's concentration in the bulk soil to its concentration in the parent rock, and the CI as the ratio of an element's concentration in any size fraction in a specified horizon to its concentration in the bulk soil. The DI for the soils analysed in this study are also shown in Table 9.5.

The statistical presentations in Tables 9.3 and 9.5 both show the same trend in element concentrations when compared with the fresh rocks. Accompanying an increase in the concentration of Fe and Al, is a massive increase in Ti and Mg. It is believed that during decomposition of the rocks, SiO_2 is removed from silicate minerals as alkaline silicates in carbonated vadose water. Any Fe

Table 9.5: Percent net change and Distribution Index (DI) in soils.

Elements & oxides	net change(%)	DI
SiO_2	-23	1.0
Al_2O_3	0	1.2
TiO_2	190	2.7
Fe_2O_3	160	2.3
MgO	239	2.2
CaO	-71	0.1
Na_2O	-94	0
K_2O	-67	0.2
P_2O_5	130	0·4
MnO	-15	0.7
Ni	8	2.8
Cu	7	2.2
Zn	146	0.5
Ga	113	0.9
As	-37	1.5
W	-25	0.8
Pb	79	1
Th	-19	0.8
U	6	0.8
Cr	-26	0.3
Mn	-17	0.9
Ba	-87	0.6
La	812	1.9
Ce	143	0.9
Rb	-82	3.1
Sr	11	0.5
Y	1023	0.9
Zr	-88	0.5
Nb	-51	0.7
Cs	418	0.9
Sn	14	0.9
V	-14	-

also released goes into solution as ferrous carbonate. Both Ca and Mg are released in the same way. Mg follows Fe because its occurrence in silicate minerals is largely controlled by diodochic substitution for Fe (Rankama and Sahama, 1949). Similarly, Ti which occurs mainly in ilmenite and other titaniferous silicates such as sphene and augite, is taken into solution as SiO_2 is removed. The release of Ti from ilmenite in such processes would also be accompanied by the release of Fe.

Although most of the major elements are released by weathering, it is their concentration during lateritization that is important. The mechanisms of deposition of Fe in such processes are fairly well known. Hydrated ferric compounds are deposited upon oxidation of the Fe^{2+} in solution (Campbell, 1917; Mohr and Van Baren, 1954). The overwhelming abundance of Fe^{3+} in the soils under study is shown in Table 9.3, where over 95% of Fe is shown to be in ferric state.

Campbell (1917) believed that an amorphous hydroxide of Al is derived via the action of CO_2 on alkaline aluminate and crystalline Al hydrate (gibbsite) by the spontaneous decomposition of sodium aluminate. It is generally known that these minerals are produced under different pH conditions. An explanation attributed to Herbillion and Gastuche (1962) by Maignien (1966), for the mechanisms acting in the crystallization of gibbsite from precipitated Al gel, involves the elimination of extraneous ions which are present in the hydrated shell of the cations. At low pH,

the positively charged ions in the gel are surrounded by foreign anions. As these tend to be retained in the structure, they inhibit crystallization. As a result, a strongly hydrated, disordered gel is formed on drying. In this, a large proportion of the Al is in four-fold coordination. Conversely, at high pH values, the negatively charged ions in the gel repel the foreign anions. In these gels, the structure is such that Al is in six-fold coordination and a crystalline aluminium trihydrate forms on ageing.

Alteration of titaniferous silicates yields the mineral anatase, which has been observed in laterites (Eyles, 1952), and could account for a large part of the observed concentration of Ti. However, sphene has been recorded as an important accessory associated with alpha-particle emitters in the granites of the Jos Plateau (Chapter 5), and survives to form a component of the lateritic soils, while ilmenite also continues as a residual product of rock alteration. Both these resistate minerals will also contribute to the accumulation of Ti in the soils.

The processes of lateritization cause the massive loss of Na, Ca and K, so that Ca and Na are almost completely removed. This illustrates well the intense leaching associated with lateritic weathering. The fact that some K is retained while Na is lost could be a result of K being adsorbed onto clay minerals and colloidal hydroxides in the soils, or it may be retained within secondary minerals.

Amongst the trace elements, those most affected are V, Cr, Ni, Cu, Zr, As, La and Rb. V, Ni, Zr, As and Cr are particularly highly enriched. Although V was only detected in one rock sample, it attains an average of 66ppm in the lateritic soils, and Cr increases from an average of 13ppm in the fresh rock to 125ppm in the soil.

Zr, Cr and Ni occur in minerals which are resistant to alteration and tend to be concentrated in the solid products of chemical weathering. Zr, in particular, occurs in zircon which forms an important accessory in the granites from which these soils were derived. Similarly, magnetite and ilmenite are important hosts for Cr and are also resistant to weathering. Plots of these elements against the weathering potential index (WPI) of Parker (1960) are shown in Figure 9.5, where it can be seen that the highest concentrations occur in the most weathered soil samples. However, under high redox potentials, Cr^{3+} is oxidised to Cr^{6+} and follows V during alteration (Rankama and Sahama, 1949). This process could have contributed to the observed Cr abundances in these soils, especially because Cr and V are highly correlated.

V is one of the elements most affected by oxidation reactions in weathering zones. In solution it occurs mostly in the V^{3+} state, but is easily oxidised to V^{5+}. In the V^{3+} state it readily forms complexes. In addition, many V minerals of secondary origin are known. In oxidising environments in the presence of heavy metals, rich local concentrations of vanadates of such

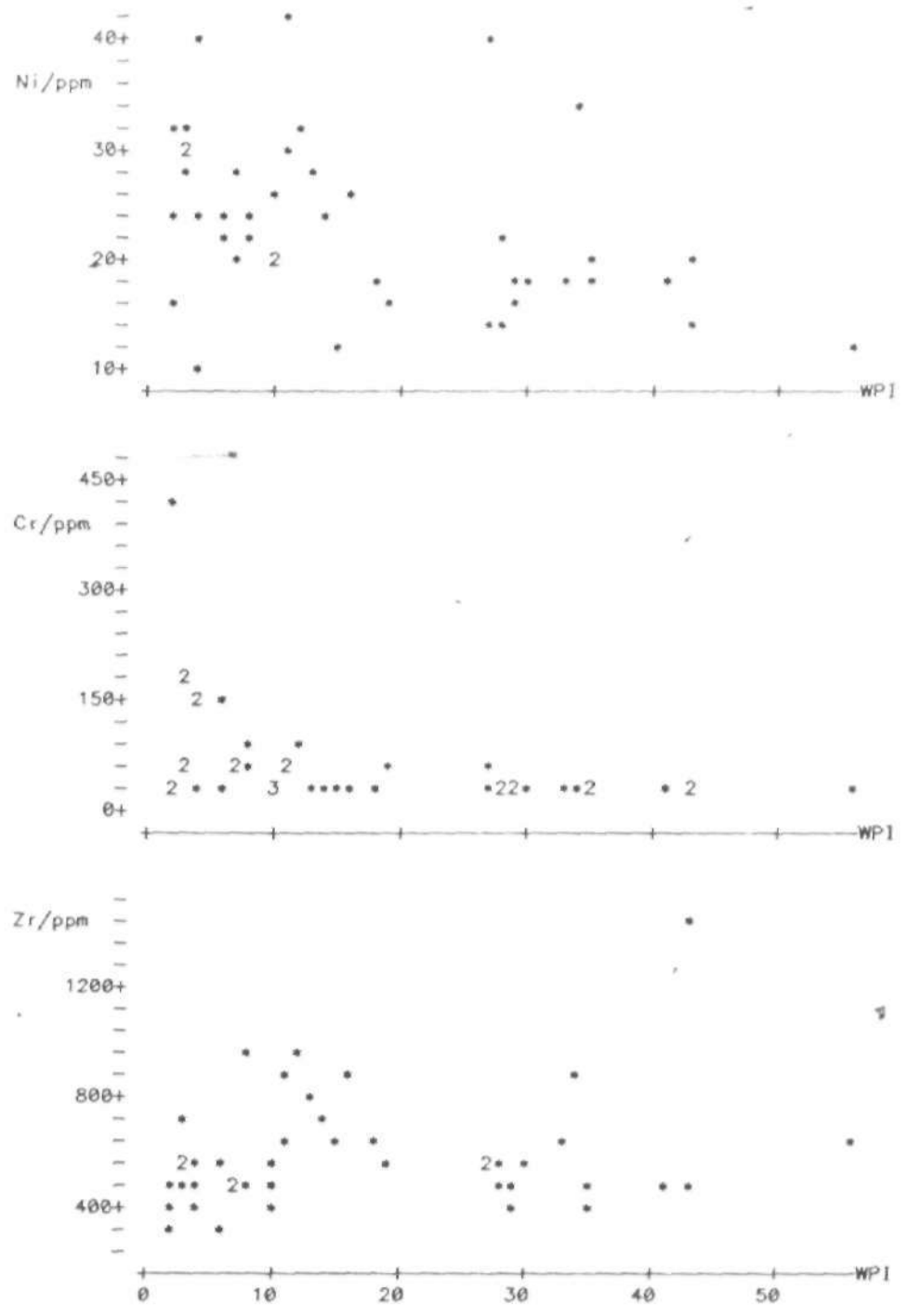


FIGURE 9.5 Correlation of Ni, Cr and Zr with WPI

Note: Numbers in these plots and subsequent ones in the Chapter represent number of points sharing the same coordinates

elements as U, Pb Cu and Zn are produced.

Cu can enter solution during weathering, but a large part may be trapped in hydrolyzates by sorption. This could explain its observed enrichment in these soils. Similarly, As is also known to be concentrated in this phase.

Although Rb, Cs, and La are taken into solution during weathering, Rb and Cs have a tendency to be adsorbed onto clay minerals, just like K. However, both Rb and Cs have been lost from these soils, the loss of Rb being very marked. That these elements have been lost suggests that adsorption of elements onto clay minerals might not have been important in the formation of the lateritic soils. The depletion of La relative to Al can be explained by the fact that its hydroxides are much stronger bases than those of Al and, therefore, remain in solution while Al is precipitated during the formation of the laterites.

Because of the different effects of the pedogenic processes at different levels in the soil profile, variations in element concentration across the profiles are observed. In the top horizon, which is the zone where leaching is most active, all elements are usually depleted. Conversely, in the B horizon, some precipitation takes place and enrichment of some elements may be observed. Chemical variation between different soil horizons has been extensively studied in the past and is not repeated here. However, because of the various depths of sampling, the results obtained from this work can be used to provide useful information about the

depth variation of the elements in the soils, as shown in Figure 9.6. These plots indicate that among the major elements, Fe, Si, Ti, and Na increase with increasing depth, while Al, Mg and K decrease. This pattern probably reflects secondary changes in the laterites due to the leaching of Fe. The trends for Ca and P are not very clear. Of the trace elements, Cr, Ce, W, Ni, As, and Zr show an increase with depth, while Zn, Ga, Pb, Th, U, La, Rb, Y, Nb, Cs, Sn, and Ba decrease. Al, Mg, Ti, Ca, P, Cr, Ba, As, La, Ce, Sr, and Y are highly depleted in the first 35cm of the soil, as a result of leaching, but Cu, Zn, Pb, and Th are enriched, probably because they are held in organo-metallic complexes.

Soils associated with the different rock types show some variation in their chemistry, probably reflecting the influence of lithology on the pedogenic processes. In particular, Si, Ca, Na, K, Pb, Th, U, Cr, Ce, Zn, Sn and V show these variations very clearly (Table 9.6). Although some of the variations correlate with the original composition of the parent rock (for example, Ca and K), others do not. Thus although the medium-grained granites have the highest SiO_2 content the soils associated with these rocks have the lowest SiO_2 concentration. Similarly, the medium-grained granites have the lowest Fe content while the associated soils have the highest Fe concentration. Of interest also are the U and V abundances. In the soils associated with the medium-grained granites, V concentrations are four and two-times as great as in the coarse-grained granites and the hornblende-fayalite granites,

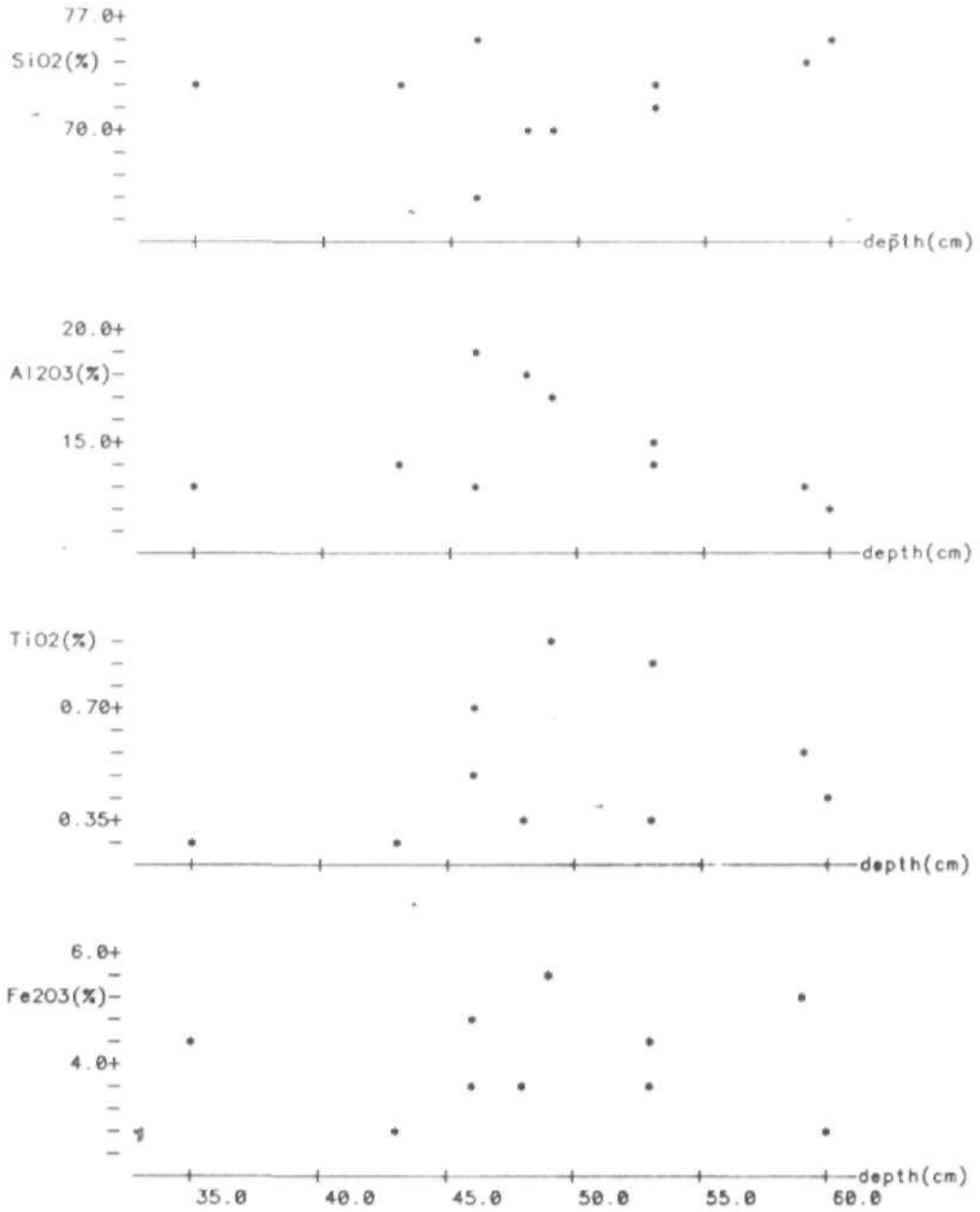


FIGURE 9.6 Depth variation of element concentrations in Jos Plateau soils

Note: Numbers in these plots and subsequent ones in the Chapter represent number of points sharing the same coordinates

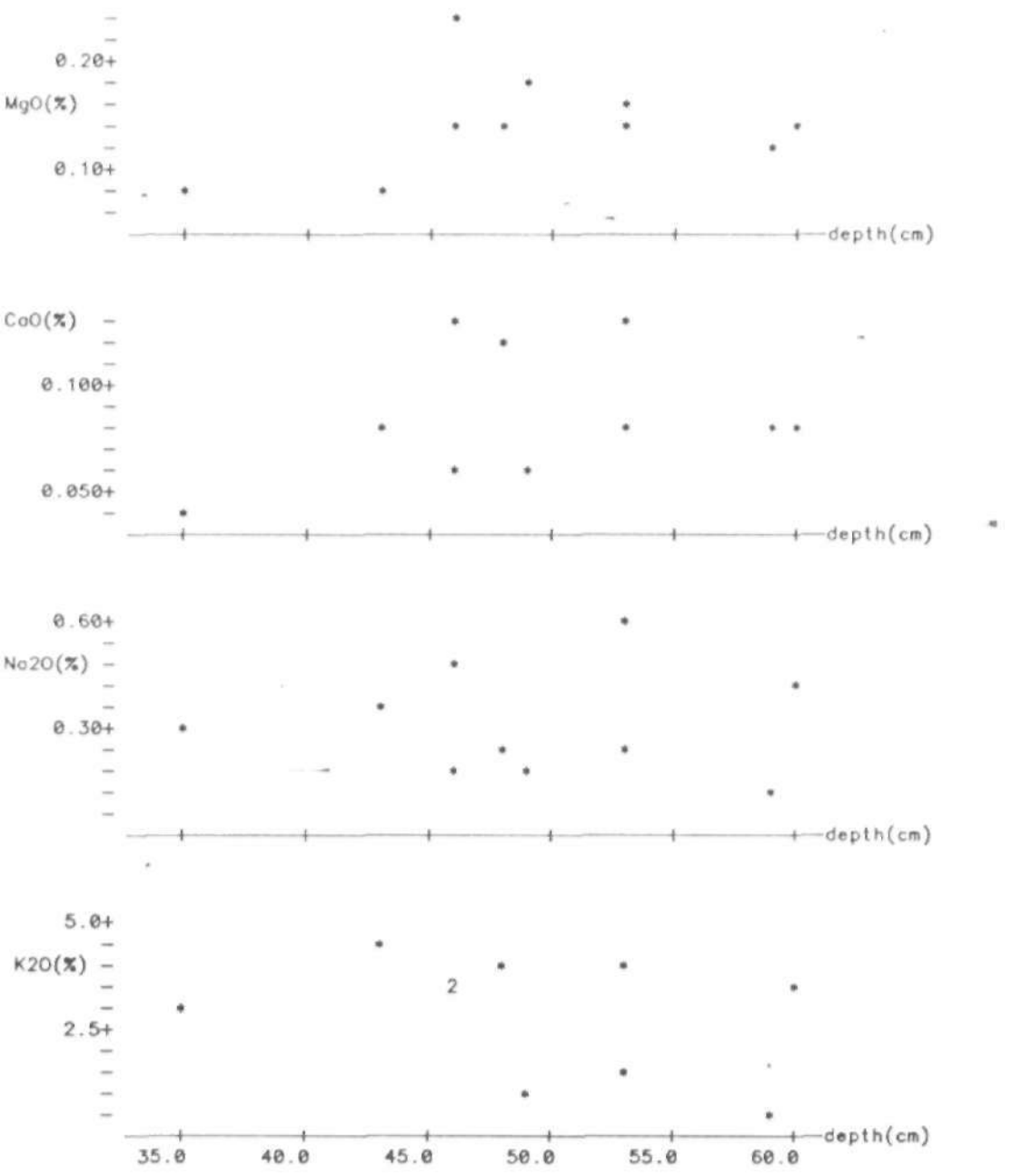


FIGURE 9.6 Depth variation of element concentrations in Jos Plateau soils

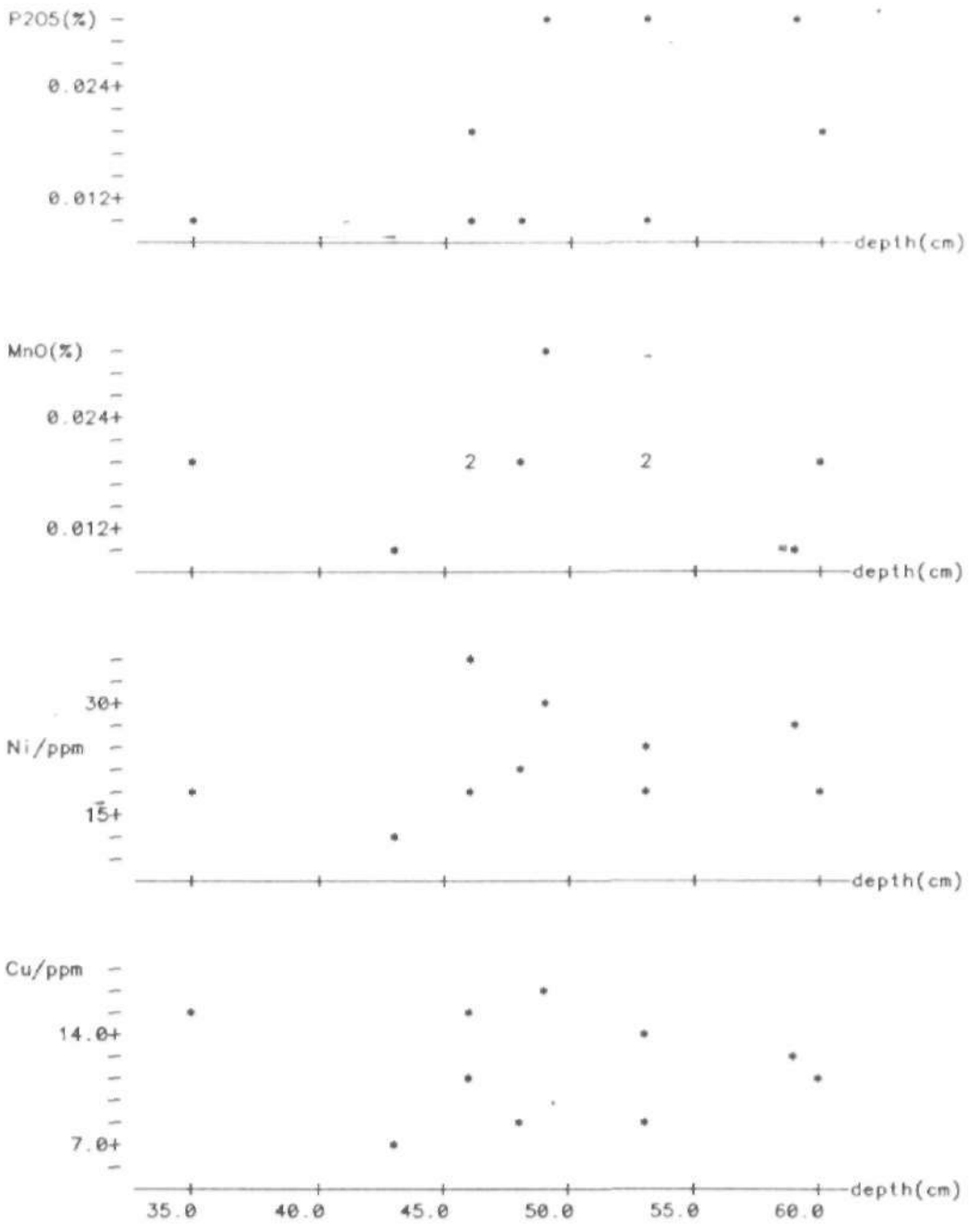


FIGURE 9.6 Depth variation of element concentrations in Jos Plateau soils

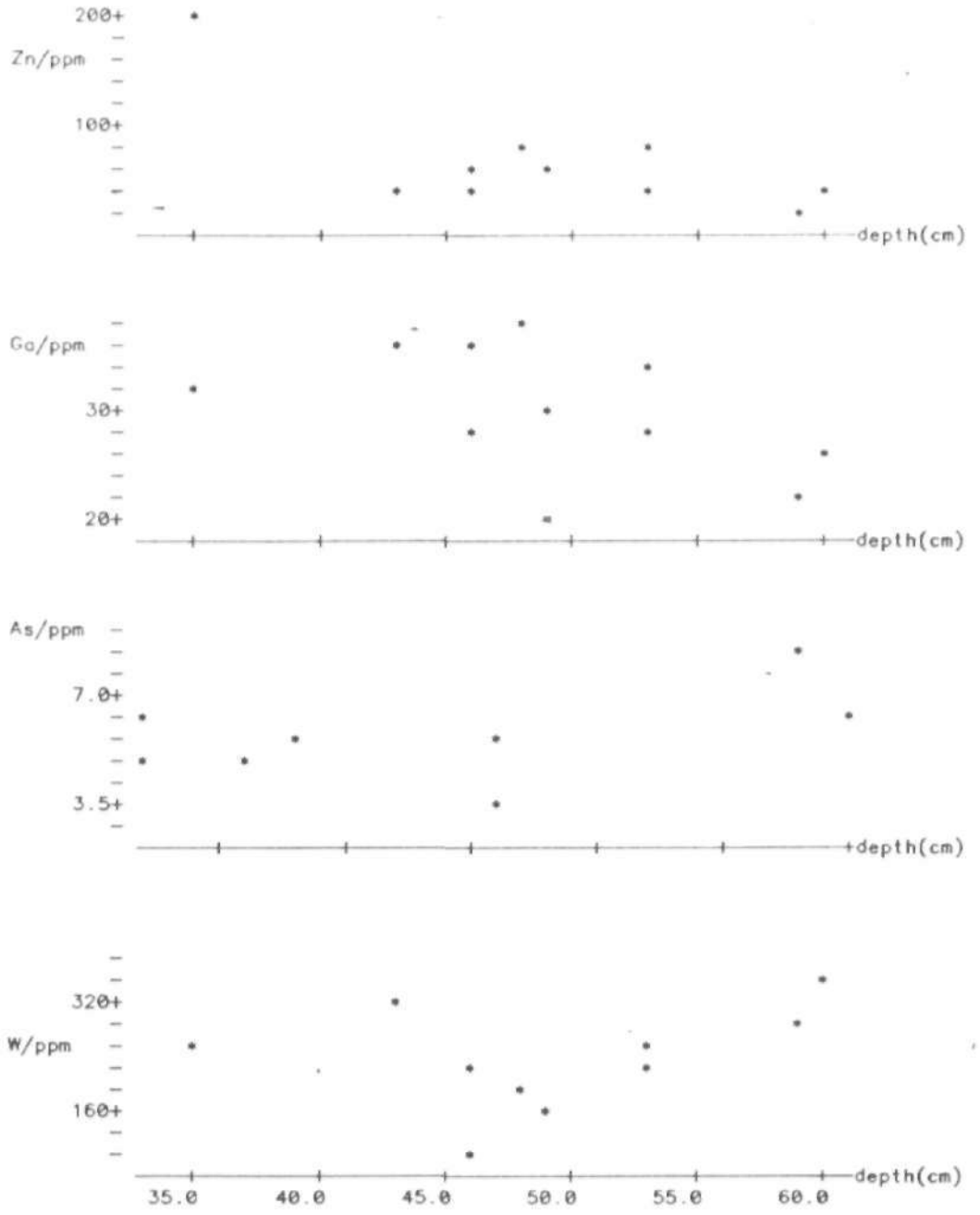


FIGURE 9.6 Depth variation of element concentrations in Jos Plateau soils

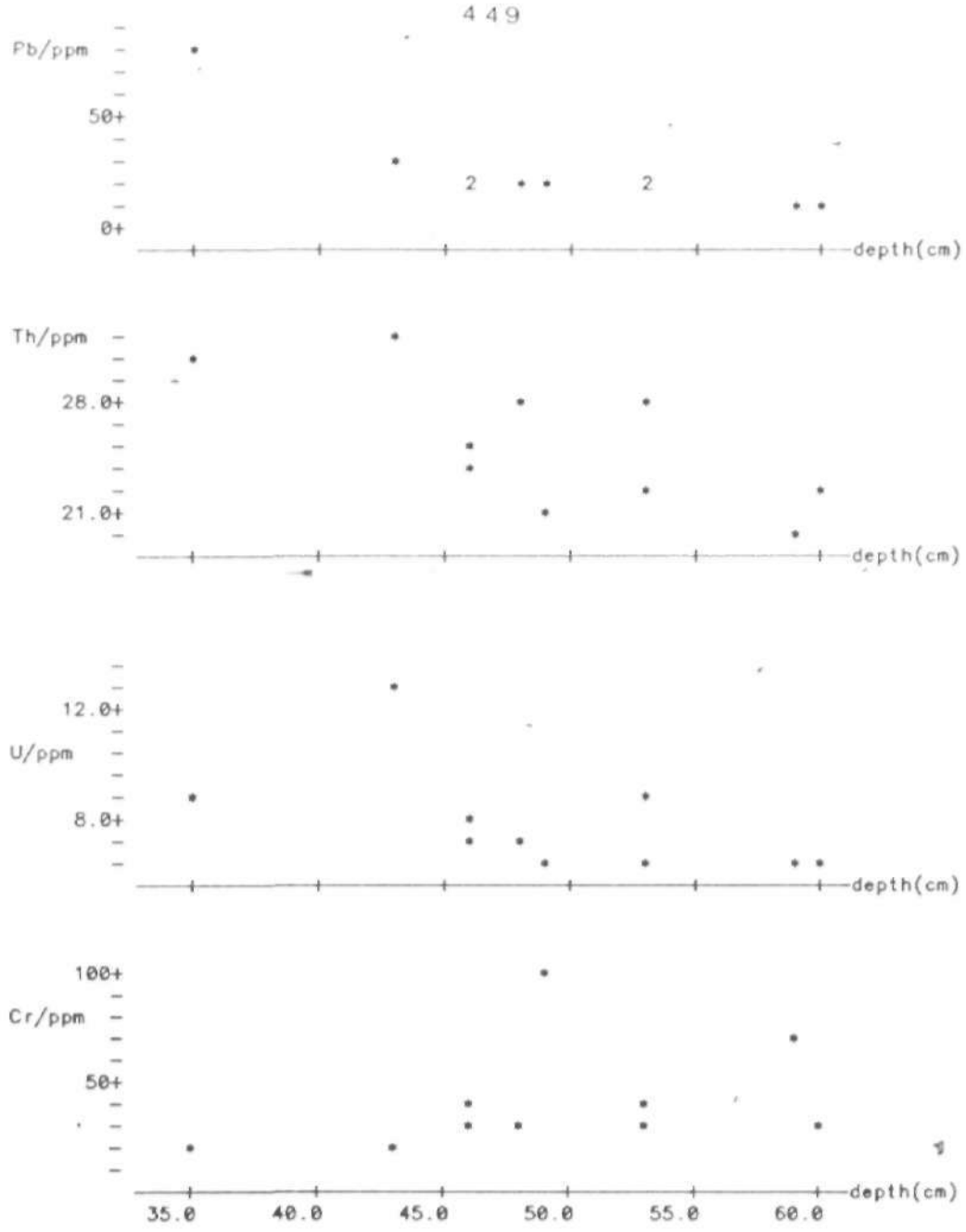


FIGURE 9.6 Depth variation of element concentrations in Jos Plateau soils

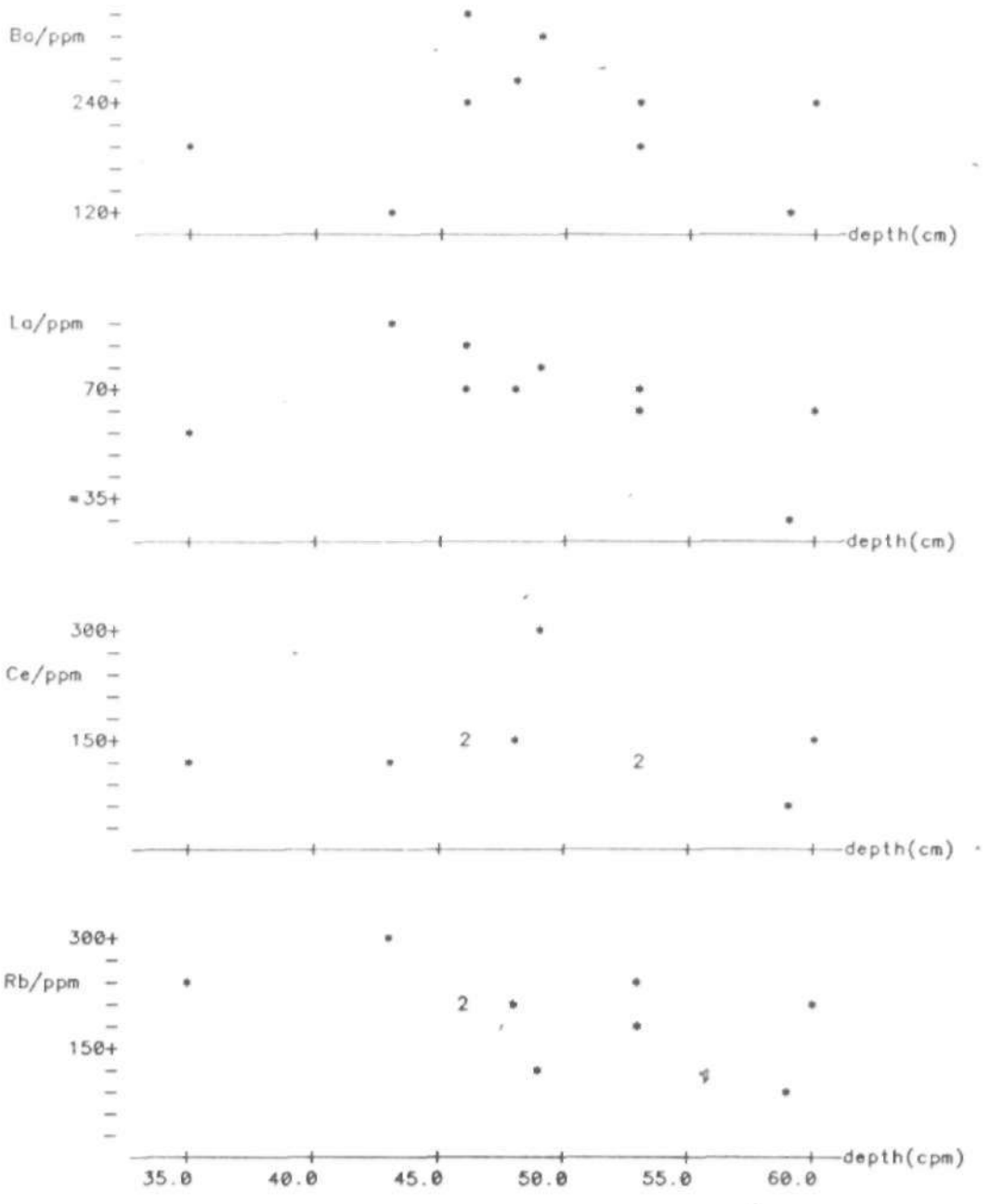


FIGURE 9.6 Depth variation of element concentrations in Jos Plateau soils

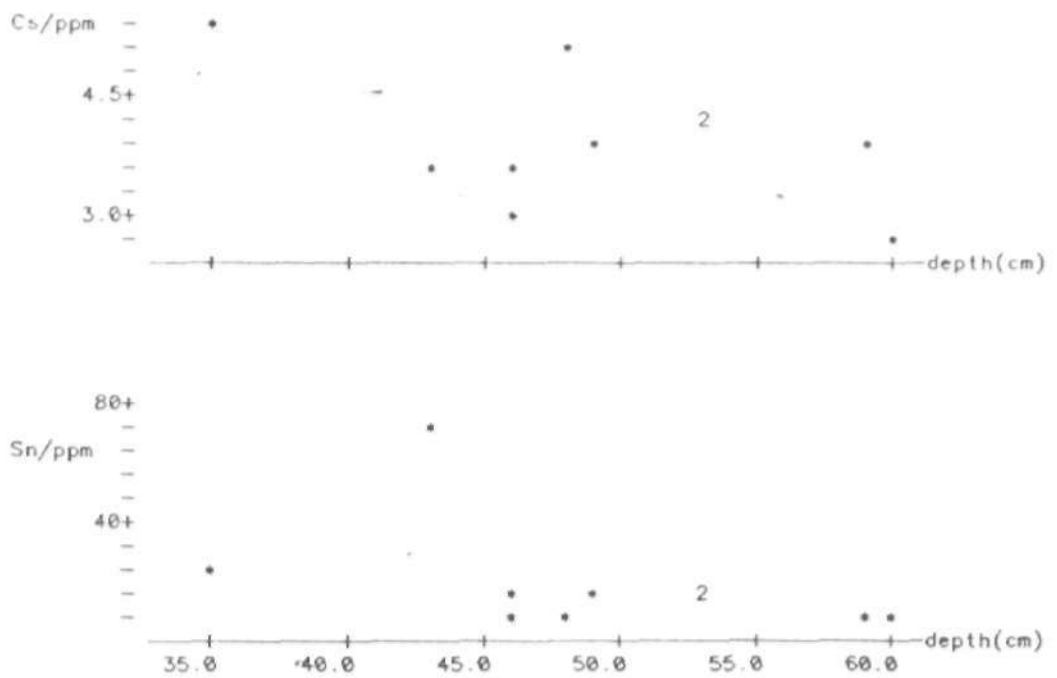


FIGURE 9.6 Depth variation of element concentrations in Jos Plateau soils

Table 9.6: Average elements concentrations in soils associated with various rock types.

Elements & oxides	CGBG	MGBG	HFG
SiO_2	70.45	66.48	64.80
Al_2O_3	15.47	15.00	16.22
TiO_2	0.55	0.54	0.57
Fe_2O_3	4.68	9.36	8.48
MgO	0.14	0.12	0.12
CaO	0.08	0.07	0.07
Na_2O	0.29	0.25	0.15
K_2O	2.25	1.18	1.44
P_2O_5	0.02	0.04	0.04
Ni	24	24	23
Cu	12	19	17
Zn	59	63	64
Ga	31	35	34
As	6	12	9
W	215	229	188
Pb	24	22	33
Th	25	29	24
U	8	12	10
Cr	52	90	71
Mn	108	103	147
Ba	208	146	185
La	65	42	60
Ce	151	90	142
Rb	165	129	127
Sr	22	17	21
Y	79	59	76
Zr	628	575	617
Nb	113	158	131
Cs	5	4	5
Sn	20	23	84
V	27	103	67

Notes: Major elements as oxides in % and others in ppm
: CGBG - coarse-grained biotite granite
: MGBG - Medium-grained biotite granite
: HFG - Hornblende-fayalite granite

respectively. U also shows an increase in the soils overlying the medium-grained granites. The possibility of precipitation of V as secondary vanadate minerals has already been mentioned. This is probably a good example of the result of such precipitation. The fact that the V is associated with enhanced U concentrations in the soils of the medium-grained granites probably indicates that V and U have been precipitated together in minerals such as carnotite and tyuyamunite. This is further discussed in the next Section.

9.6.4 Mobilisation of U During Lateritization

On average, U is depleted in the soil relative to its abundance in the underlying granites. This is in agreement with most studies on the weathering of granites (Pliler and Adams, 1962; Hanson and Stout, 1968; Tieh, et al., 1980). The ease with which U is mobilised during weathering depends on factors such as the mineral sites in which it occurs and the physico-chemical conditions prevalent during the pedogenic processes.

Analyses of the 43 soil samples in this study indicated concentrations of U in the range 4ppm to 23ppm, with an average of 10ppm; and Th concentrations in the range 18ppm to 42ppm, with an average of 27ppm. Th/U ratios in these samples range from 1.39 to 5.26, with an average of 2.7. Typically, about 10% and 18% U and Th, respectively, have been lost relative to the source rocks, during the lateritization processes. The fact that Th is greatly

depleted relative to U in the soils is noteworthy.

In Chapter 4 the relative abundances of U and Th in the Younger Granites was considered, and it was suggested that the high U content indicated the possibility of U being partitioned into primary U minerals. In connection with the investigation of the mineralogical distribution of U in the granites reported in Chapter 5, the importance of U derived from weathering was also recognised. Although the depletion of U in the soils is relatively small, an important consideration is whether the U present in the soil is in minerals of secondary origin or concentrated in resistate minerals. Knowing the partition of U between these phases could indicate the extent of mobilisation which takes place, and the geochemical conditions operating, during lateritization. For example, the precipitation of carnotite from solutions rich in U and V was discussed by Hostetler and Garrels (1962), who showed that such precipitation is largely controlled by the amount of U and V, but also by the presence of CO_2 in solution.

Plots of U and Th against their common associates in the accessory resistate hosts are shown in Figures 9.7 to 9.10. These clearly indicate that the presence of resistate accessory minerals can not account for the U and Th abundances in the soil. The only mineral that appears to be significant is apatite, as indicated by the positive correlation between P and U/Th. Even Y, which is significantly correlated with U in the parent rock (Chapter 5), has a negative correlation with U in the soil, suggesting that the Rare

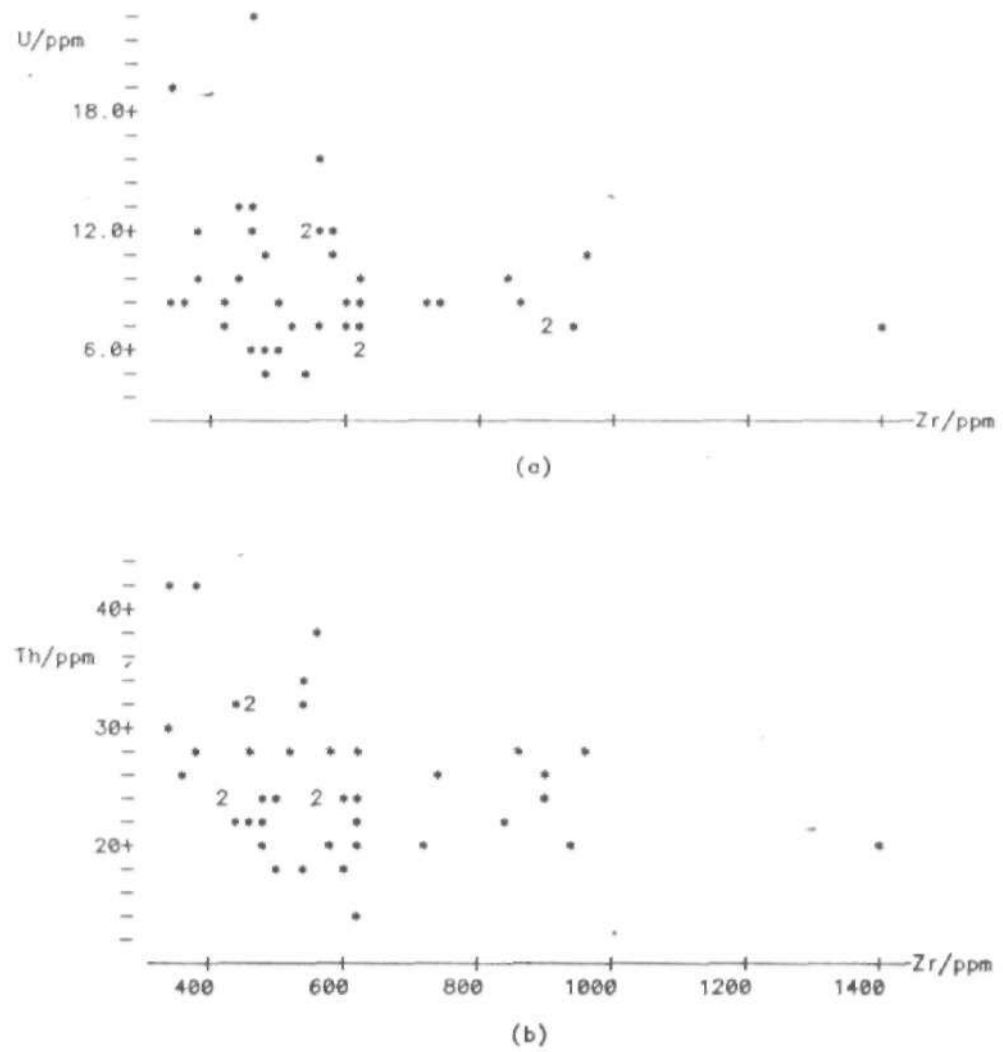


FIGURE 9.7 Correlation of U (a) and Th (b) with Zr

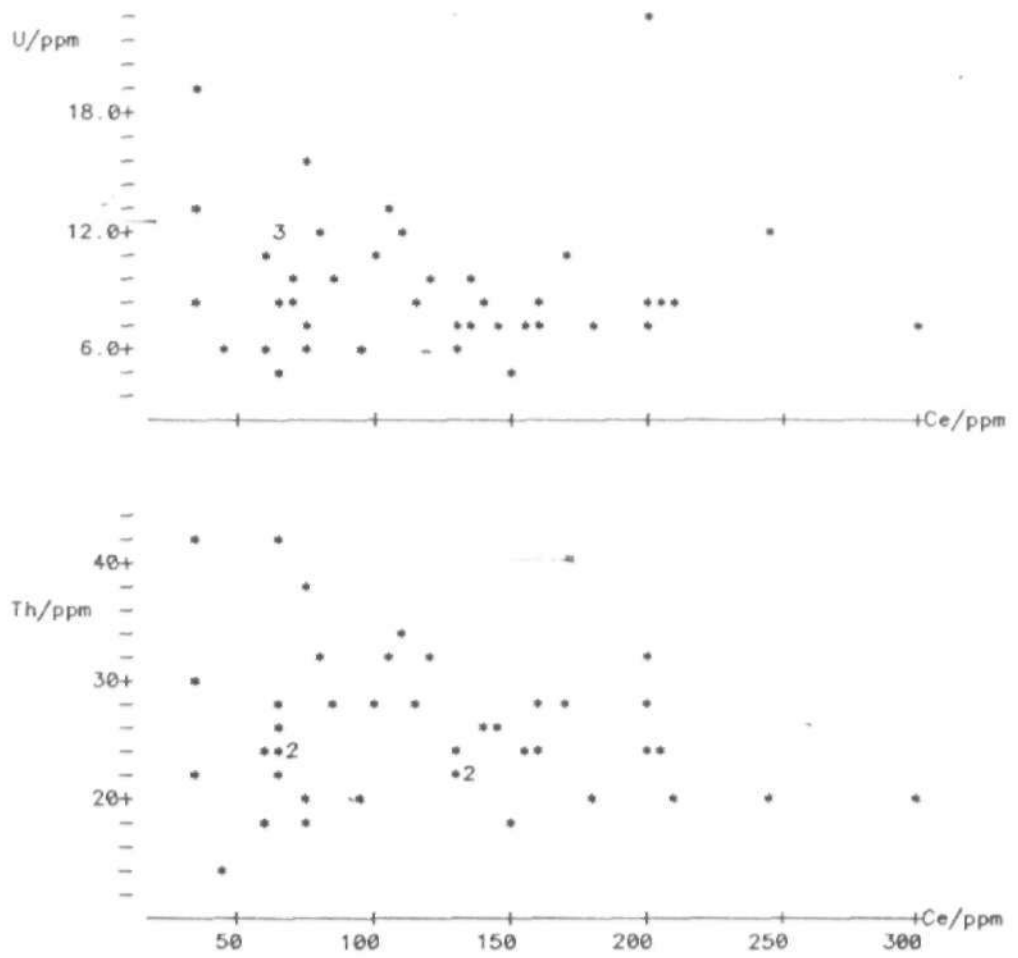


FIGURE 9.8 Correlation of U (a) and Th (b) with Ce

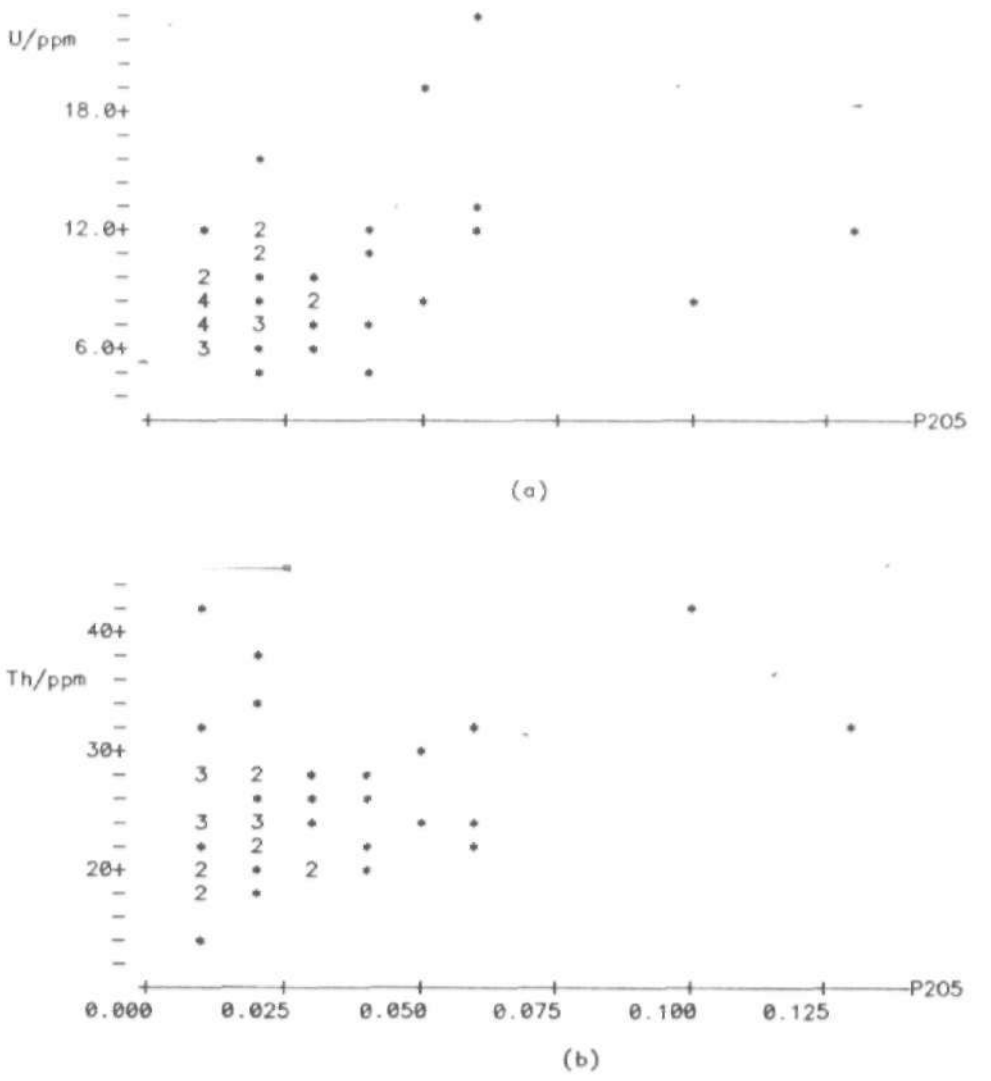


FIGURE 9.9 Correlation of U (a) and Th (b) with P

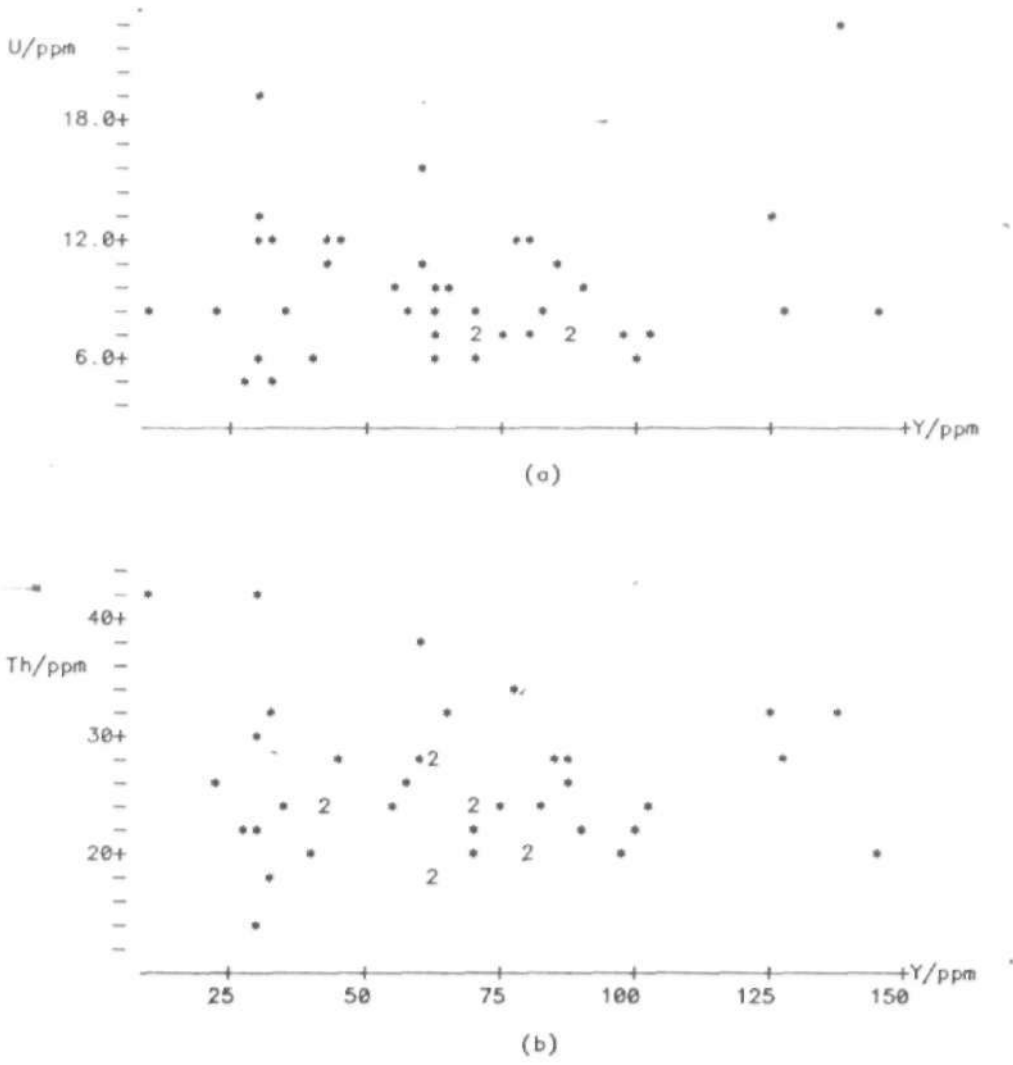


FIGURE 9.10 Correlation of U (a) and Th (b) with Y

Earth minerals were not stable under weathering conditions. Therefore, it appears likely that the U concentration in the soil is controlled by formation of secondary precipitates. Minerals containing high levels of U, such as uranothorite and possibly uraninite, and the radioactive Rare Earth minerals, would have been leached U during lateritization, the leached U then being precipitated during the oxidation of Fe. Either independent secondary minerals such as carnotite then formed, as discussed above, or the U became adsorbed onto the secondary Fe oxides. The association of U with Fe in the soil is shown in Figure 9.11. In addition to Fe, other elements showing significant positive correlations with U' are V, Ga, Cu, and As (Table 9.3b), which are also highly correlated with Fe (Figures 9.12 to 9.15). Most of these elements are held in soils as adsorbed compounds. It thus appears likely that most of the U in the soil occurs by adsorption on Fe oxides. Other minerals of secondary origin, as suggested above, may also contribute, but are a minor component. The association of the Jos Plateau soils with high a U content was also noted by Dewu (1986), more especially in clayey soils in areas of impeded drainage.

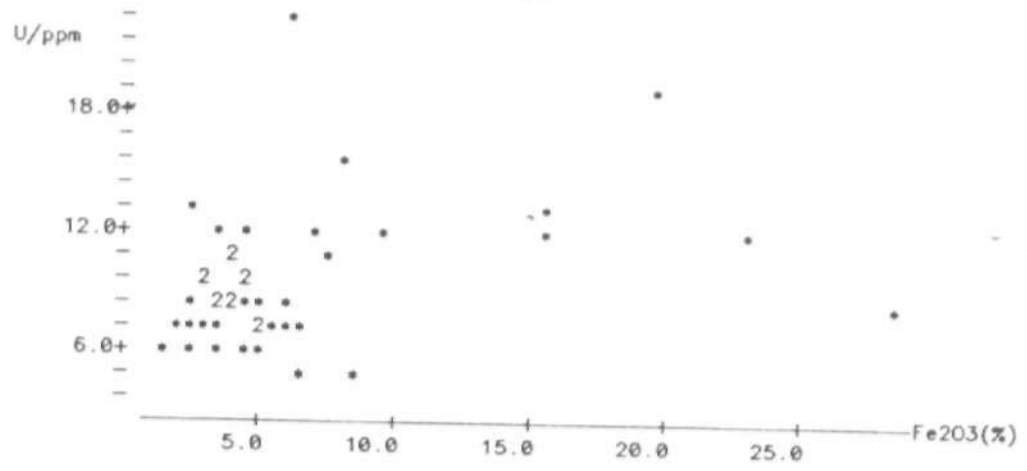


FIGURE 9.11 Correlation of U with Fe

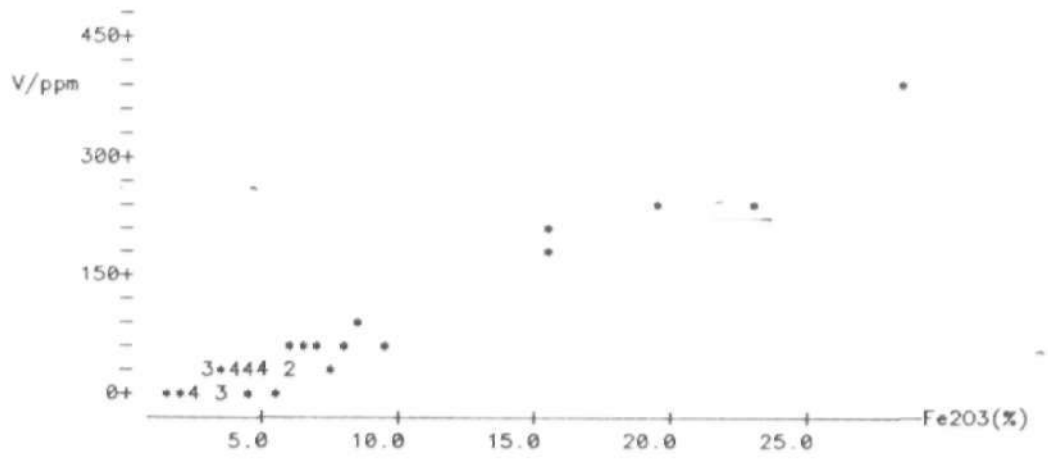


FIGURE 9.12 Correlation of V with Fe

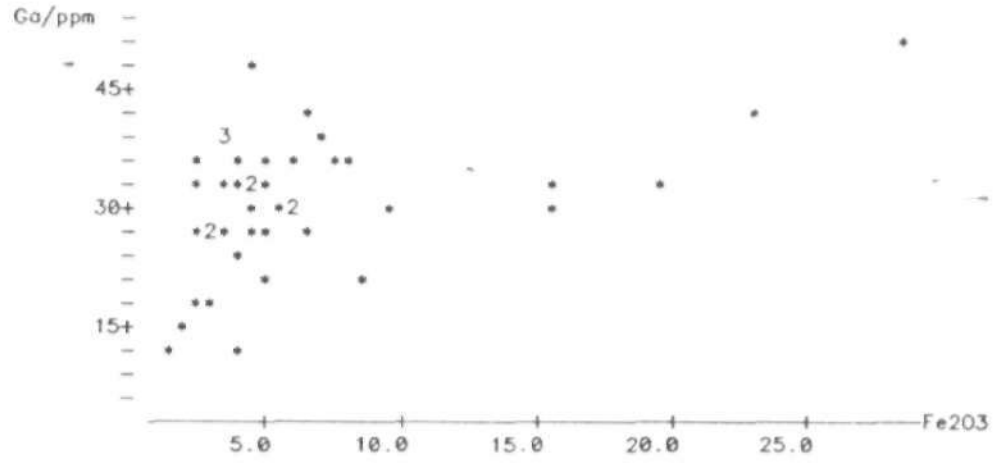


FIGURE 9.13 Correlation of Ga with Fe

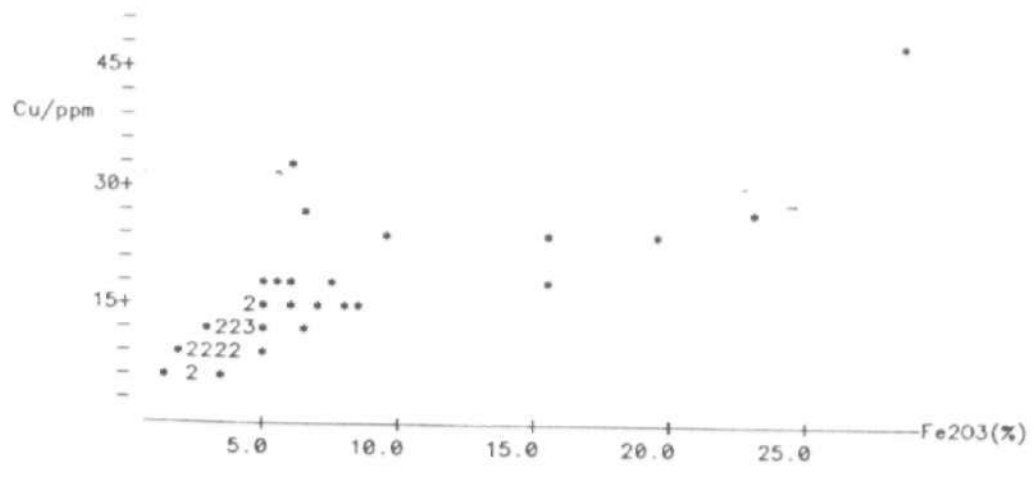


FIGURE 9.14 Correlation of Cu with Fe

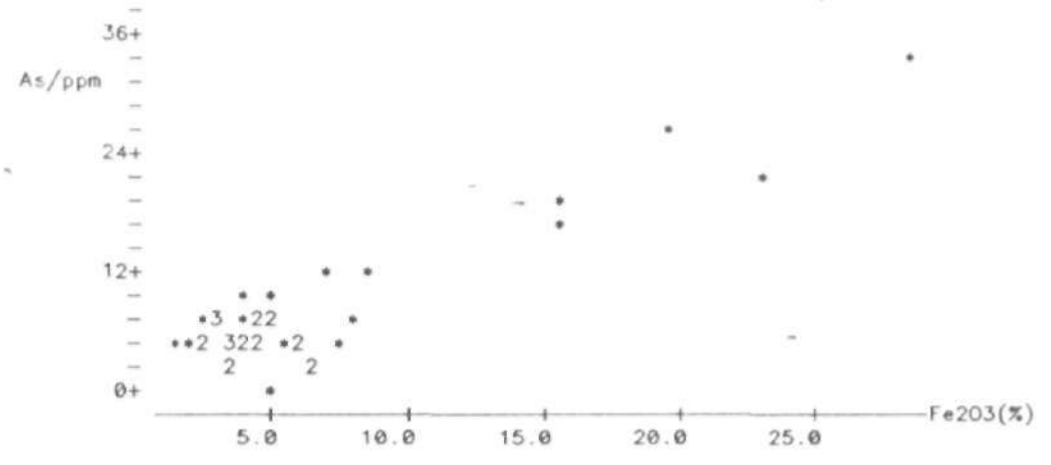


FIGURE 9.15 Correlation of As with Fe

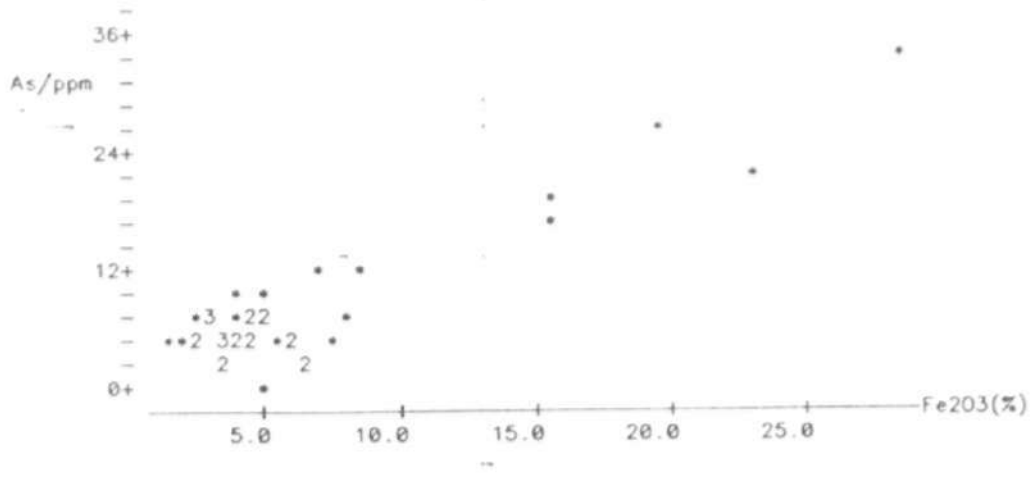


FIGURE 9.15 Correlation of As with Fe

9.7 SOIL RN INVESTIGATIONS

9.7.1 Rn in the Natural Environment

Rn is a chemically inert radioactive gas produced by the decay of Ra in the U and Th decay series. In the natural environment it occurs in three isotopes, radon (^{222}Rn), thoron (^{220}Rn) and actinium (^{219}Rn) due to ^{238}U, ^{232}Th and ^{235}U, respectively. In each series it undergoes radioactive decay into Po with the release of alpha-particles. These transmutations together with the half-life of the Rn isotopes are shown below:

$$^{226}\text{Ra} \Rightarrow {}^{222}\text{Rn} + {}^{4}\text{He}$$
$$^{222}\text{Rn} \Rightarrow {}^{218}\text{Po} + {}^{4}\text{He} \qquad 3.825 \text{ days}$$

$$^{223}\text{Ra} \Rightarrow {}^{219}\text{Rn} + {}^{4}\text{He}$$
$$^{219}\text{Rn} \Rightarrow {}^{215}\text{Po} + {}^{4}\text{He} \qquad 3.92 \text{ sec.}$$

$$^{224}\text{Ra} \Rightarrow {}^{220}\text{Rn} + {}^{4}\text{He}$$
$$^{220}\text{Rn} \Rightarrow {}^{216}\text{Po} + {}^{4}\text{He} \qquad 55.6 \text{ sec.}$$

Its gaseous property gives Rn the ability to escape into the atmosphere from lithospheric sources. In soils it is mostly supported in soil water or the pore spaces, while in streams and

other water channelways, it occurs in solution.

Of the three isotopes, the geochemically most important is ^{222}Rn, both because of its abundance and the relatively long half-life. In the atmosphere, ^{222}Rn concentrations have been estimated to be in the range $3.7.10^{8}$ to $1.67.10^{10}$ Bq/l (Dyck, 1972). Variations in these concentrations in air over land and oceans were noted by Gingrich (1984), who reported values of $5.55.10^{9}$ to $3.7.10^{10}$ Bq/l over land and $3.7.10^{8}$ Bq/l over oceans. These values indicate the importance of Rn migration from the lithosphere as an important contributor to its concentration in the atmosphere. In waters, determinations from Canadian lakes gave values of $3.7.10^{9}$ to $2.6.10^{10}$ Bq/l (Dyck and Cameron, 1975), while stream waters contain as much as $1.9.10^{12}$ Bq/l (Dyck and Smith, 1968), probably reflecting the variation of Rn in waters associated with different source rocks. Temperature has also been found to greatly affect the solubility of ^{222}Rn, so that waters at higher temperatures contain lower concentrations ^{222}Rn than waters at lower temperatures (Seidell, 1965; Morse, 1976).

The concentration of ^{222}Rn in soil has been found to be in the range $3.7.10^{11}$ to $3.7.10^{13}$ Bq/l Gingrich (1984), while rocks with an average U concentration of 2ppm produce $3.7.10^{12}$ Bq/l of ^{222}Rn (Alter, 1978). However, much of the ^{222}Rn in soil is dependent on sources within the soil itself, as contributions from underlying rocks may be limited except over faults and other fractures.

The release of Rn from U-bearing and Th-bearing minerals and its diffusion into the surrounding rocks, have been extensively studied by Andrews and Wood (1972). Its loss from its host minerals is largely controlled by the physical condition of the minerals and the nature of its immediate environment. Compact, well-crystalline materials experience less loss compared with loosely-held aggregate materials. Similarly, minerals surrounded by well-crystalline materials as, for example, minerals enclosed in quartz, usually suffer less Rn loss than minerals occurring in loose unconsolidated material such as soils and sedimentary formations. Where such minerals are in contact with flowing water, Rn may also be removed and transported in solution.

Three mechanisms identified by Tanner (1964) have been used to explain the process of Rn migration from its source minerals. These are:

1) Formation and recoil of the Rn atoms by the disintegration of the parent Ra isotope,
2) diffusion through mineral grains, and
3) diffusion and mass transport through permeable pathways in rocks and soils.

Recoil ranges for ^{222}Rn in various media have been reported. Heckter (1934) gave a range of about 64 m in air and Zimens (1943) had a value of 0.03 m in rocks of average density. Recent values for ^{222}Rn recoil in rocks are in the range 20 m to 70 m (Gingrich, 1984). This, therefore, suggests that only ^{222}Rn atoms produced in

a thin surface layer of the minerals are librated by recoil. Because of the small contribution that these make to the overall ^{222}Rn loss from a mineral, it is generally believed that loss through diffusion is more significant.

The ease of diffusive loss of ^{222}Rn from minerals and amorphous materials is typically expressed by the emanation coefficient. This is the fraction of the total ^{222}Rn produced which actually escapes. Emanation coefficients in the range 0.0006 to 0.166 for radioactive minerals were reported by Giletti and Kulp (1955). They noted that these coefficients increase with increasing temperature, but decrease with increasing pressure. These changes probably reflect the importance of internal fractures in controlling ^{222}Rn movement. ^{222}Rn loss from minerals in air, and when immersed in various liquids, was investigated by Prutkina and Shashkin (1966), who found that the emanation coefficient was higher in water than in kerosene, alcohol or air. They suggested that in dry samples ^{222}Rn might be absorbed onto the walls of capillary fractures, which when wetted by liquids de-sorbed the ^{222}Rn. These effects indicate the significance of surface processes in the release and build-up of ^{222}Rn in the environment. Barretto et al. (1973) summarized emanation coefficients of 0.03 to 0.17 for granites, 0.02 to 0.15 for gneissic rocks, 0.04 to 0.12 for sandstones, and 0.02 to 0.27 for conglomerates. The values for soils were 0.37 to 0.45 for granitic soils, 0.1 to 0.2 for sandy soils, 0.17 to 0.5 for alluvial soils and 0.18 to 0.55 for

calcareous soils. Thus the values of the emanation coefficients for soils are much greater than those for crystalline rocks. As shown by the investigations of Prutkina and Shashkin (1966), the presence of moisture in soils and rocks is likely to increase the emanation coefficient. Nielson et al.(1982) observed that an increase in soil moisture content of 5% increased the emanation coefficients by a factor of four.

From the foregoing discussion it can be seen that the amount of Rn in the environment is controlled by factors other than simply the abundance of the minerals from which it is derived. These factors make the interpretation of Rn surveys very difficult. For any meaningful conclusions to be drawn from such surveys, these controls have to be taken into account.

9.7.2 Soil ^{222}Rn in U Exploration

As one of the daughters in the main U decay series, ^{222}Rn determinations have been proposed as a method of U exploration, especially in areas where thick overburden prevents gamma-ray detection. Because of its relatively short half-life, its presence in soils has been considered to be associated with U-bearing minerals in the immediate environment, but this is not always the case.

Success in using the technique as a U exploration method has been reported in a number of investigations, particularly in

Canada. In the first application of the method, Ridland (1945) detected a vein of pitchblende about 18m below the surface. Dyck (1968) found a close correlation between ^{222}Rn determinations and gamma-ray activity in a determination of soil ^{222}Rn over a known U deposit in Bancroft. Development of instrumental techniques, largely pioneered by the Geological survey of Canada (Dyck, 1969), has led to wide application of the method in U exploration (Butt and Gole, 1985; Gregory, 1987). In areas lacking soil cover, such as in parts of Canada, ^{222}Rn surveys have concentrated on surface waters. For example, regional surface water surveys over the Bancroft and Elliot Lake areas by Smith and Dyck (1968) outlined zones of U enrichment. Similarly, ^{222}Rn anomalies related to U mineralisation were found from measurements of groundwaters from boreholes in areas of known U mineralisation (Dyck, 1975; Reimer et al., 1979).

Although successes have thus been reported for both soil and surface/groundwater surveys, the present position is that soil surveys have proved to be the more successful in indicating U mineralisation. For example, in an investigation of a U vein reported by Gregory (1987), both soil and stream ^{222}Rn determinations were carried out. The soil survey detected the vein quite clearly, but water ^{222}Rn values were barely above background even over the vein. Similarly, in a Rn survey in South-West England in an area known to contain nodular U mineralisation, stream water ^{222}Rn activity values failed to indicate this occurrence. Anomalous

Rn activity associated with fractures was, however, identified (Durrance, 1983). The ^{222}Rn distribution was interpreted as having been produced by groundwater discharge possibly, from deeper U sources.

Both soil and water ^{222}Rn detection and measurement are carried out by alpha-particle recording systems. These either employ integrating methods with measurement times of hours or longer, or are non-integrating, with count times usually no more than a few minutes. Both types have been fully described by Durrance (1986). In-situ measurements, and measurements involving transfer of the gas from the collection point to a remote detection system, are both employed in soil ^{222}Rn surveys. The former approach involves planting alpha-particle detectors in the soil. These are retrieved after a predetermined period of time and the Rn activity which has accumulated over that period is then determined. In one form of this method, the track-etch technique, thin sheets of cellulose nitrate are taped inside cups which are then inserted into the soil, open end down, and left undisturbed for a period of time (Gingrich and Fisher, 1976; Pedersen et al., 1980). After the period of Rn collection, the plastic sheets are etched, allowing the tracks produced by alpha-particles to be counted. Inserting a permeable barrier between the soil gas and the plastic detector allows partition of the tracks due to ^{222}Rn from those caused by ^{220}Rn. In the latter approach, Rn gas is usually pumped from the soil either directly into a detecting system or into a container

for transfer to the measuring instrument. Simply counting the activity over successive periods allows ^{222}Rn activity to be distinguished from ^{220}Rn activity. In water Rn measurements, dissolved Rn is librated from samples by degassing, and the ^{222}Rn and ^{220}Rn contents determined using scintillation counters. Alternatively, liquid scintillation techniques can be used to directly determine the activity of the dissolved ^{222}Rn and ^{220}Rn.

The Rn content of the soil gas at any particular locality is subject to changing atmospheric and soil conditions. Studies have shown that variations due to flunctuating weather conditions are particularly significant. Kovach (1944, 1945, 1946) carried out a series of observations of soil ^{222}Rn which show the correspondence on soil Rn with a combination of meteorological factors (Faul, 1954). In areas of cold climate, ground freezing and snow cover act to prevent the release of ^{222}Rn. Therefore, ^{222}Rn build-up may take place under such conditions. Where a windy, dry atmosphere prevails, the ^{222}Rn content of the soil may be depleted. The effect of high winds and turbulent air movement on soil ^{222}Rn was also reported by Kramer et al. (1964), who noted that a combination of these factors and atmospheric pressure could affect the concentration of ^{222}Rn to depths of up to 2.5cm in a weathered tuff. As shown by the influence of water on the emanation coefficient of ^{222}Rn, previously discussed, soil moisture content was also found to have a profound effect. Caneer and Saum (1974) observed that an increase in the moisture content tended to lower

the soil ^{222}Rn content.

Variations in the Rn content of surface waters as a function of various other parameters have also been reported. In an investigation of the distribution of ^{222}Rn in surface waters in the Beaverlodge area of Canada, Dyck (1972) concluded that the major factors affecting the ^{222}Rn content were depth of water, water temperature, and water alkalinity. He found that the further the sampling point at the water surface was away from the stream bed, and the lower the temperature, the lower was the ^{222}Rn content. However the association between alkalinity and the ^{222}Rn concentration was found to be specific to the region, and the presence of a U-rich calcite host for the U mineralisation in the area. Other variables which produced noticeble effects were the size of the water body, elevation above sea level, flow rate, water level and degree of turbulence.

The various environmental factors which control ^{222}Rn content, both in the soil and surface waters, put restrictions on the use of ^{222}Rn surveys in U exploration. Therefore, although the presence of U mineralisation may manifest itself by an increase in ^{222}Rn, other factors not related to mineralisation may also produce the same effect. Some problems associated with surface water ^{222}Rn surveys have already been noted above. In addition, Rose and Korner (1979) pointed out the problem of addition of ^{222}Rn to surface waters due to the influx of groundwater. The usefulness of the technique as an indicator of U mineralisation can also be affected

by ^{222}Rn degassing from the water within a short distance of the ^{222}Rn source. The fact that ^{222}Rn can also be supported by its immediate parent, ^{226}Ra, in solution, and thus be found any distance away from the U deposit from which it was derived, is a further limiting factor on the use of water ^{222}Rn surveys. For example, Morse (1970) found a direct correspondence between ^{226}Ra and the ^{222}Rn content of the waters in the streams of the Bancroft area. He suggested that the ^{226}Ra content was more than sufficient to account for the observed ^{222}Rn concentration in the surface waters. However, in many other cases ^{222}Rn concentrations far exceed those that can be explained by ^{226}Ra in solution (Durrance, 1986). In soils, the ^{222}Rn distribution tends to be largely controlled by the presence of fractures in the underlying rocks. Soil gas ^{222}Rn surveys may, therefore, be more useful in tracing fracture than locating U mineralisation. The direction of groundwater flow along fractures also influences the soil ^{222}Rn content (Durrance, 1986). Soils above ascending groundwater typically contain higher ^{222}Rn concentrations than those above descending flow.

Because of the complexity of the factors controlling ^{222}Rn release, transport and accumulation in the natural environment, ^{222}Rn surveys are often simply used to delineate areas of anomalous ^{222}Rn concentration. However, with proper control on the meteorological, geological, hydrogeological and geochemical setting, ^{222}Rn surveys can be made to yield valuable information

regarding U distribution, more especially at depth, as well as details of the major features capable of influencing gas transport and groundwater movement.

9.7.3 ^{222}Rn Distribution in the Soils of the Jos Plateau

9.7.3.1 ^{222}Rn Measurements

Rn activity was measured using an alpha card (integrated) detecting system. An alpha card is a thin aluminised mylar disc supported by a rectangular plastic frame. The whole system consists of a catridge of alpha cards and a card reader. Holes where soil samples were collected were used to expose the cards to Rn from the soil. The holes were made with a diameter of 15cm to 20cm, and the cards centrally suspended using a string supported on cross-sticks wedged between the sides of the hole. As the holes were of variable depths, different string lengths were used to provide a consistent depth of card burial of about 35cm. The holes were then covered with hard boards, usually cardboard sheets, with polythene sheets spread over the boards. The sheets were then covered by a layer of soil. The arrangement used is shown in Figure 9.16. The card number, station number and time the card was exposed were recorded at each site. Cards were exposed over-night and recovered for reading the following day, giving an exposure period of between 18 and 24 hours. A base station was set up to monitor daily variations

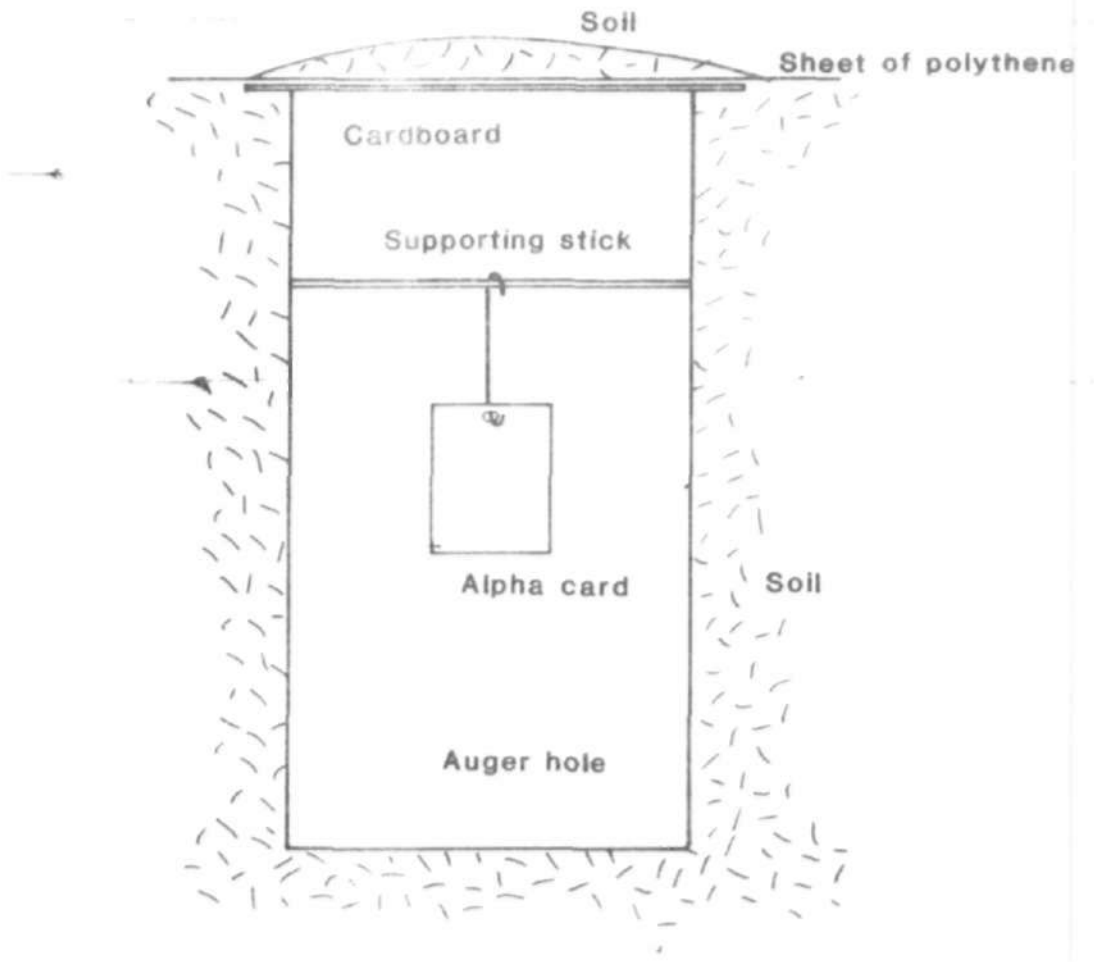


FIGURE 9.16 Arrangements for soil ^{222}Rn measurements (not to scale)

in the area.

To obtain the Rn concentration in the soil at any one location, the activity of the card was read using the card reader. At each station, the card was retrieved after intervals. The card reader, and the card immediately inserted into the card reader. As the strings had to be removed from the cards, and in some cases it was necessary also to wipe moisture from the cards, there was always some time lag between retrieval of the card and its insertion into the card reader. This delay would have had some effect on the reading for ^{220}Rn, but can be ignored for ^{222}Rn. However, data for ^{220}Rn have only been obtained from some sites. The whole Rn survey was carried out between 16/10/87 and 3/10/87.

The Rn instrument used for this work was based on the principle of Rn determination by alpha-particle counting. Rn decay products from the soil gas are collected onto the aluminised mylar discs during exposure in the hole. The cards are then analysed for alpha-particles due to Rn decay products: ^{218}Po and ^{214}Po from ^{222}Rn and ^{216}Po and ^{212}Bi from ^{220}Rn. The card reader employs two diffused-junction alpha radiation detectors, which detect the alpha-particles from the disc (alphaNUCLEAR, operators manual). The two detectors ensure that all the products are collected and counted over an almost perfect 4π geometry. The alpha-particle decays are counted over a five minute period and counts displayed in counts per minute.

Because the recorded activity is due to both ^{222}Rn and ^{220}Rn

daughters, an additional procedure is needed when separation of these isotopes of Rn is required. This procedure is based on the fact that ^{212}Bi has a relatively long-lived daughter, ^{212}Pb, with a half-life of 10.64hrs, while all the daughters of ^{222}Rn which decay by alpha-particle emission, are short lived. Thus if only ^{222}Rn daughters are collected on the card, a period of about 3 hours is sufficient for all the alpha activity on the card to decay to negligible levels, but if ^{220}Rn daughters are also collected, then significant activity can be recorded even when all activity due to ^{222}Rn daughters would be undetectable. For determination of the ^{220}Rn contribution, the instrument manufacturer has prepared a table based on a three 'cooling off' periods for ^{222}Rn daughters (Table 9.7). By taking second readings on the cards some time after the elapse of this 'cooling off' period, ^{220}Rn contributions are then computed as follows:

If the second reading 5 hours after the first reading be ycpm, then count due ^{220}Rn = y/0.742 cpm

This value is subtracted from the first reading to give the corrected ^{222}Rn count. These determinations are only possible if the cards are not exposed to any contamination after the first reading.

Table 9.7: Thoron (^{220}Rn) correction data.

Time/hours	Correction Factor
3	0.837
3.5	0.812
4	0.788
4.5	0.765
5	0.742
6	0.670
7	0.659
8	0.621
9	0.585
10	0.552
11	0.520
12	0.490
13	0.461
14	0.435
15	0.410
16	0.386
17	0.364
18	0.343
19	0.323
20	0.304

9.7.3.2 Results

The survey was carried out to investigate the distribution of Rn in the soil, and discover any relationship between Rn activity and U and Th content of both the soil and the underlying rocks. These objectives have been achieved. The results of the survey are given in Table 9.8. The survey was carried out towards the end of the rainy season in the region and, therefore, the soil was moist with a high rate of Rn diffusion expected. However, the rainfall which often occurs in the tropics has also been found to wash Rn down to lower soil horizons (Tanner, 1964), and this possibility needs to be considered in interpreting the data. Nevertheless, as the investigation was not concerned with Rn concentrations per se, this problem does not affect the broad conclusions which can be drawn from the results. ^{222}Rn isotopic abundances together with both soil and rock U and Th values for the sites at which Rn was determined, are given in Table 9.9.

From Table 9.8, it can be seen that there is a wide variation in the soil Rn activity. Activity values range from as low as 4cpm to 71cpm. The distribution of Rn in the area is shown in Figure 9.17, where areas of possible Rn importance are marked. The highest counts, with activities of 41 and 71cpm, are associated with soils of very high porosity, and indicate the importance of diffusion in controlling Rn activity. In Figure 9.18 are shown

Table 6.P: Results of [illegible] Mr obtained.

Sample	Card no.	t1	t2	Pr Activity/cpm
JPS2	2514	[illegible]	1130	28
JPS7	2183	[illegible]	1107	11
JPS8	2253	1331	0922	12
JPS9	2796	1335	0959	10
JPS13	2643	1317	0823	8
JPS14	2798	1345	0834	13
JPS15	2259	1736	1405	2
JPS16	2782	1706	1417	4
JPS17	2791	1447	0849	14
JPS20	2182	0917	0938	21
JPS23	2178	0936	1003	
JPS24	2258	1028	0928	
JPS28	2256	1200	0820	
JPS29	2792	1122	0856	
JPS32	2750	1045	0912	
JPS31	2646	1023	0926	
JPS33	2786	1105	1022	
JPS35	2188	1222	0947	
JPS36	2879	1220	1028	
JPS39	2884	1636	0959	
JPS40	2776	1332	1039	
JPS41	2645	1126	0925	
JPS42	2754	1147	0936	
JPS43	2753	1206	0943	
JPS44	2795	1125	1036	
JPS45	2787	1245	1012	
JPS46	2874	1401	1054	
JPS48	2784	1511	1120	
JPS49	2877	0850	0850	
JPS50	2751	0924	0946	
JPS52	2521	1014	0952	
JPS53	2881	1620	1120	
JPS54	2252	1716	1201	
JPS55	2885	1700	1151	
JPS56	2254	1152	0907	
JPS57	2878	1512	1049	
JPS58	2190	1529	1057	
JPS59	2780	1056	0910	
JPS60	2772	1225	1000	
JPS61	2517	1343	1039	
JPS62	2783	1500	0910	
JPS65	2296	1105	0839	
JPS66	2257	1553	0943	
JPS67	2779	1242	1000	
JPS68	2781	1659	0816	

Note: t1 and t2 are the times of exposing and [illegible]wading of cards, respectively.

Table 5. [illegible] isotopes activity compared with soil and rock U and Th content.

	^{222}Rn	^{220}Rn	U_s	Th_s	U_r	Th_r
JPR/JPS8	7.4	4.[illegible]	7	22	9	[illegible]
JPR/JPS9	7.0	[illegible]	[illegible]	18	-	[illegible]
JPR/JPS14	6.2	6.[illegible]	12	31	5	[illegible]
JPR/JPS15	5.2	9.[illegible]	[illegible]	28	9	[illegible]
JPR/JPS16	14.9	19.[illegible]	[illegible]	25	16	[illegible]
JPR/JPS17	10.8	3.[illegible]	[illegible]	28	20	[illegible]
JPR/JPS28	27.5	7.[illegible]	[illegible]	25	11	
JPR/JPS41	9.0	8.[illegible]	[illegible]	42	13	[illegible]
JPR/JPS42	11.9	5.[illegible]	[illegible]	20	17	
JPR/JPS43	9.6	6.[illegible]	[illegible]	23	14	
JPR/JPS44	4.0	8.[illegible]	[illegible]	28	10	
JPR/JPS46	7.6	6.[illegible]	[illegible]	25	-	
JPR/JPS48	7.4	7.6	9	27	9	40
JPR/JPS49	10.5	4.[illegible]	[illegible]	[illegible]	[illegible]	[illegible]
JPS61	12.9	4.[illegible]	[illegible]	28	-	[illegible]
JPS62	4.0	0	[illegible]	20	-	-
JPS65	2.4	7.[illegible]	[illegible]	21	-	-

Note: The subcripts s and r refer to soil and rock.

: Rn activity in cpm,

: U and Th in ppm.

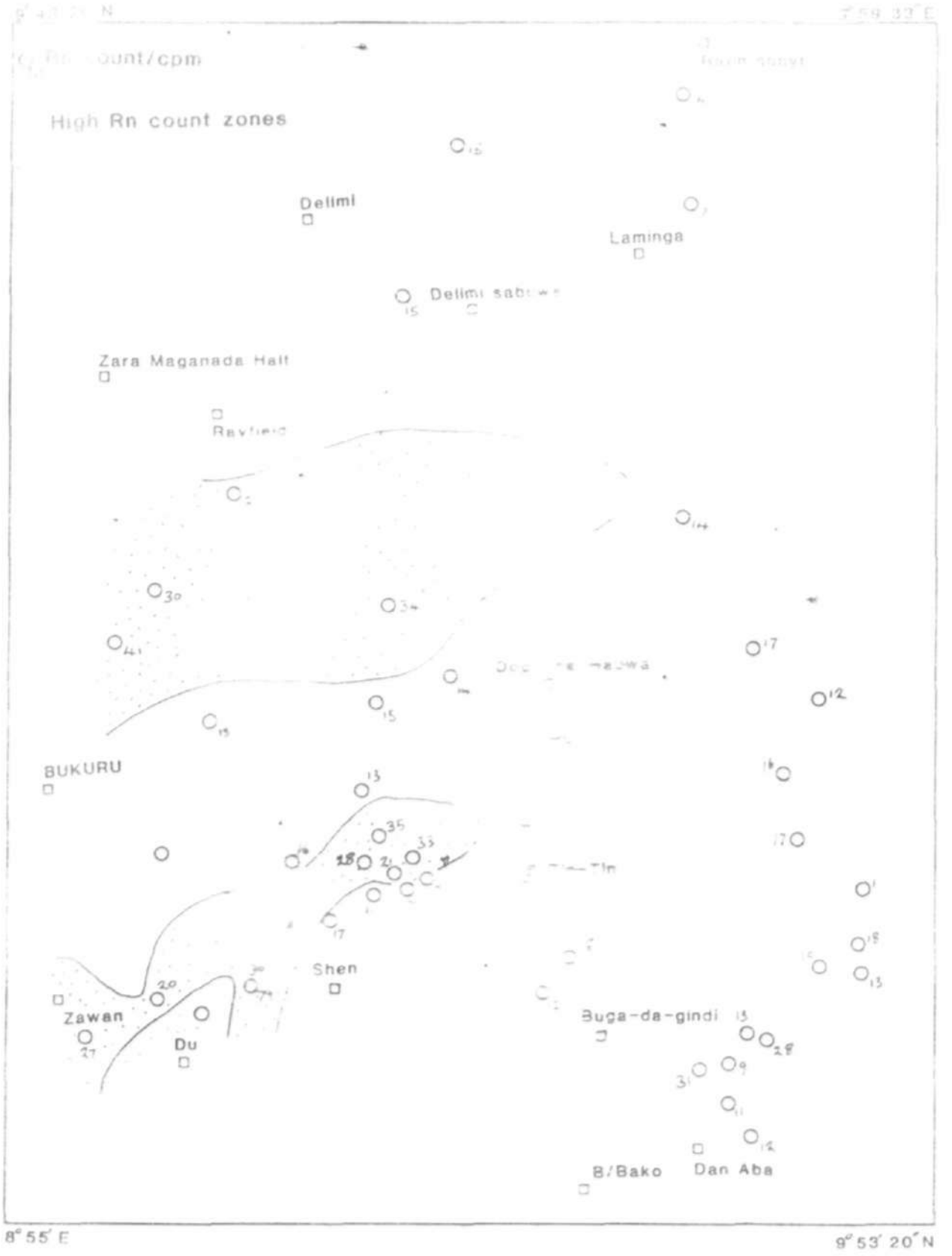


FIGURE 9.17 Rn distribution in Jos Plateau soils

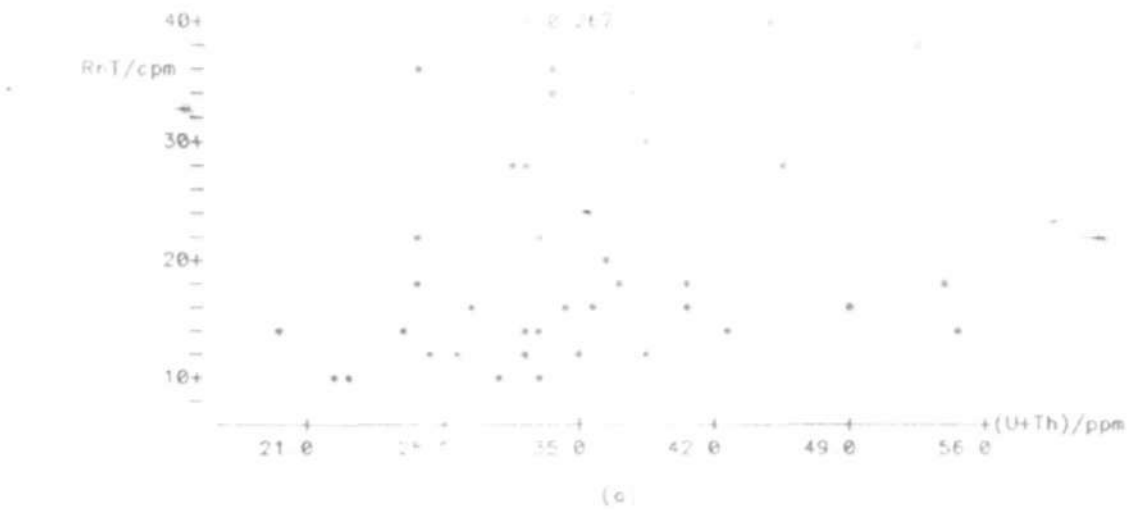


FIGURE [illegible] Correlation of total soil Rn activity (RnT) with [illegible] soil U and Th (U+Th) (a) and rock U and [illegible] (b)

plots of soil Rn against the sum of U and Th (U+Th), both in the soils and the associated rocks. The generally low correlations in these plots indicate the influence of factors other than the U and Th content of the soil, on the Rn activity. However, the correlations are significant enough to suggest some influence. Due to the similarity in the correlation coefficient between Rn and soil U+Th concentrations on the one hand, and the rock U+Th concentrations on the other, it is difficult from these plots to to determine the main contributor to the Rn activity. However, Figure 9.19 which shows plots of Rn activity against the U and Th content of the soil, indicates that Rn activity is more correlated with Th than U. Similar plots for the associated underlying rocks (Figure 9.20) have the same character, that is Rn activity is more associated with Th than U. This may reflect the importance of ^{220}Rn in the total Rn activity. Again these plots show similar correlation coefficients between Rn and U and Th in both the soils and the rocks. In Figures 9.21 and 9.22 are shown plots of ^{222}Rn against soil and rock U abundances and ^{220}Rn against soil and rock Th abundances, respectively. These clearly demonstrate a closer association of ^{220}Rn with Th than of ^{222}Rn with U. Importantly, too, is the absence of any significant correlation between ^{222}Rn and U in the soil, whereas they are significantly correlated in the rock. It thus appears that there is greater contribution of ^{222}Rn from U in the underlying rocks than from the soil itself. Therefore, soil ^{222}Rn is not supported by soil U. This further

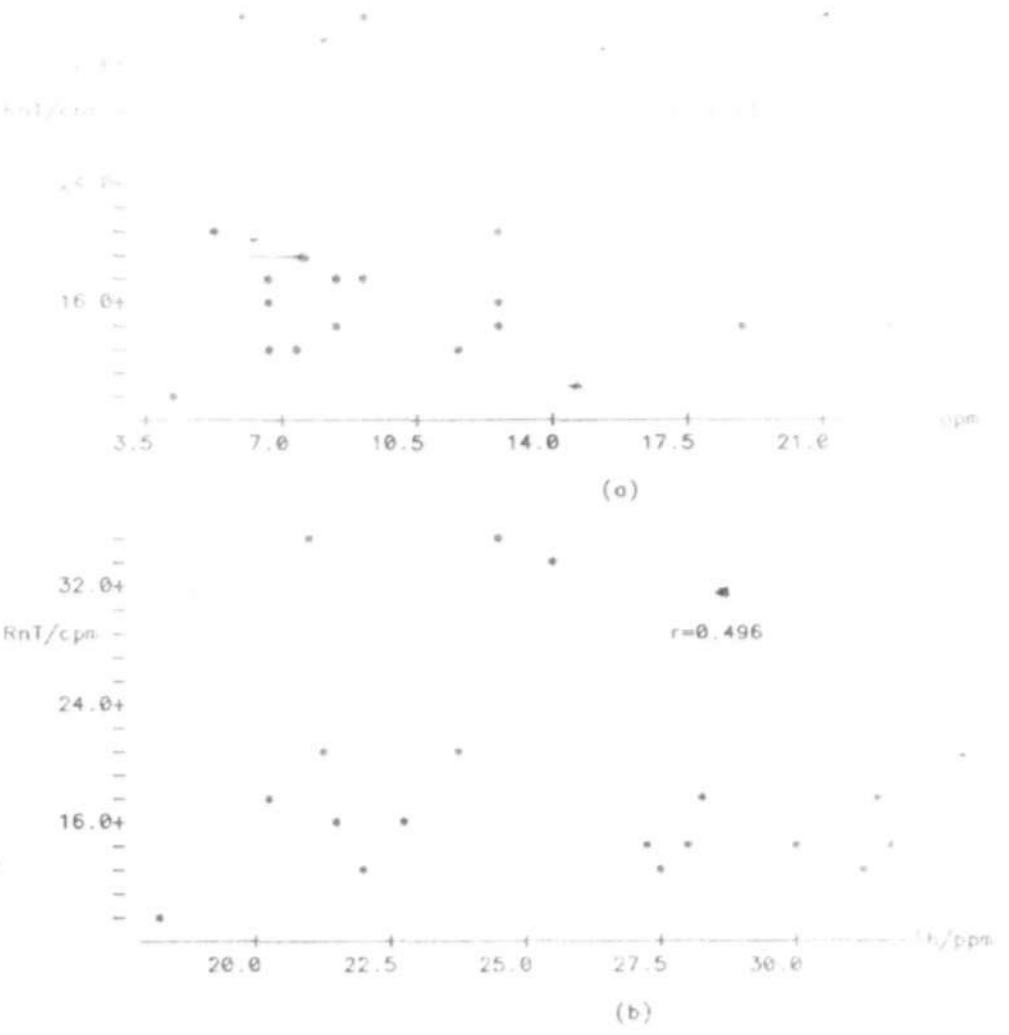


FIGURE 9.19 Correlation of total soil Rn activity (RnT) with soil U (a) and soil Th (b)

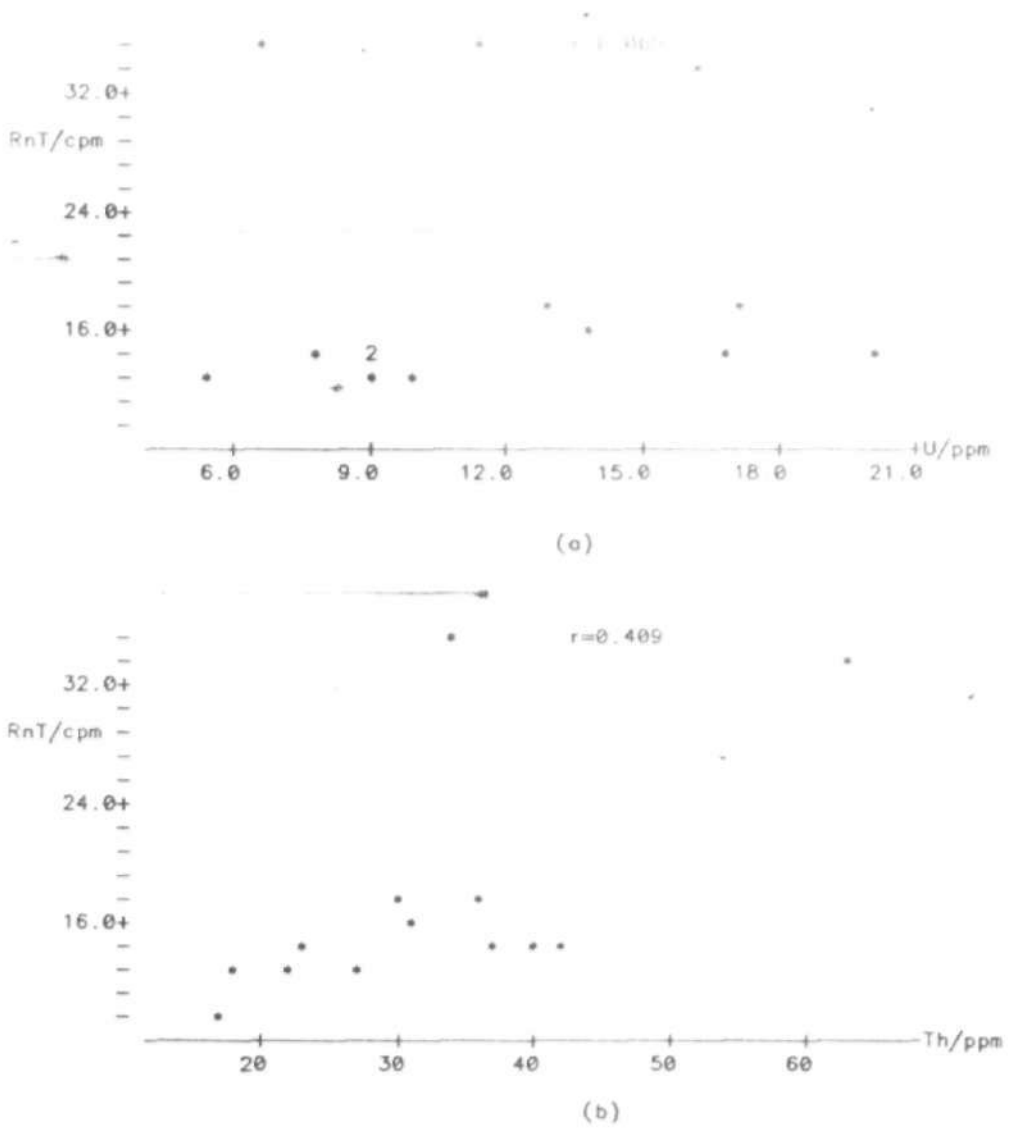
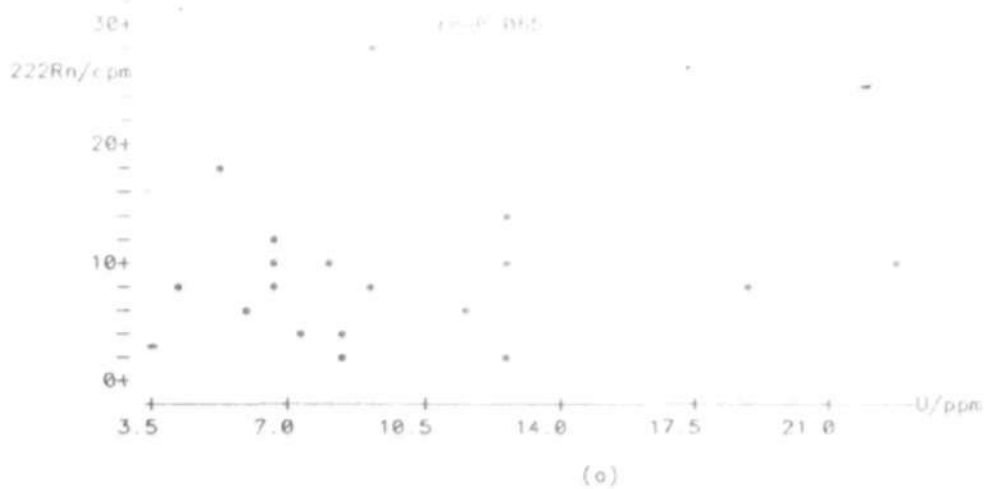


FIGURE 9.20 Correlation of total soil Rn activity (RnT) with rock U (a) and Th (b)



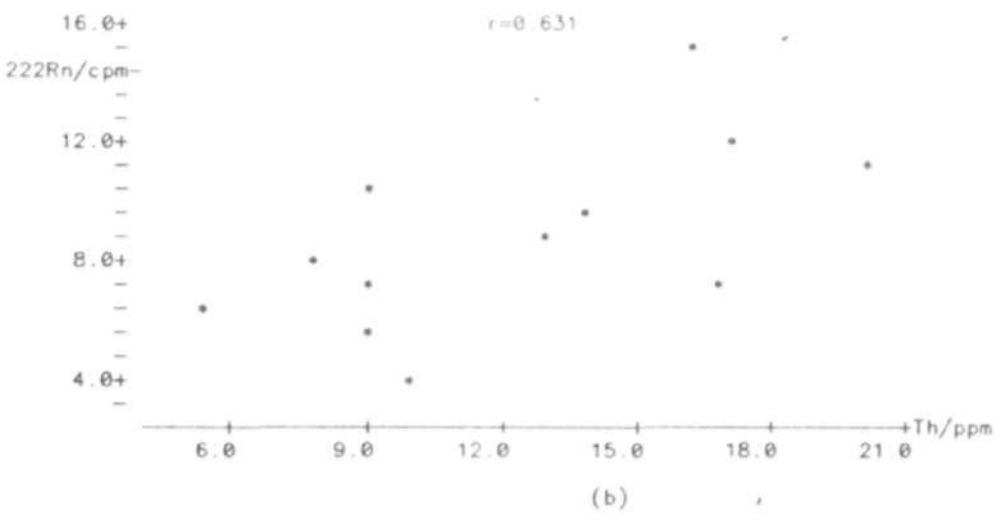


FIGURE 9.21 Correlation of 222Rn activity with soil U (a) and rock U (b)

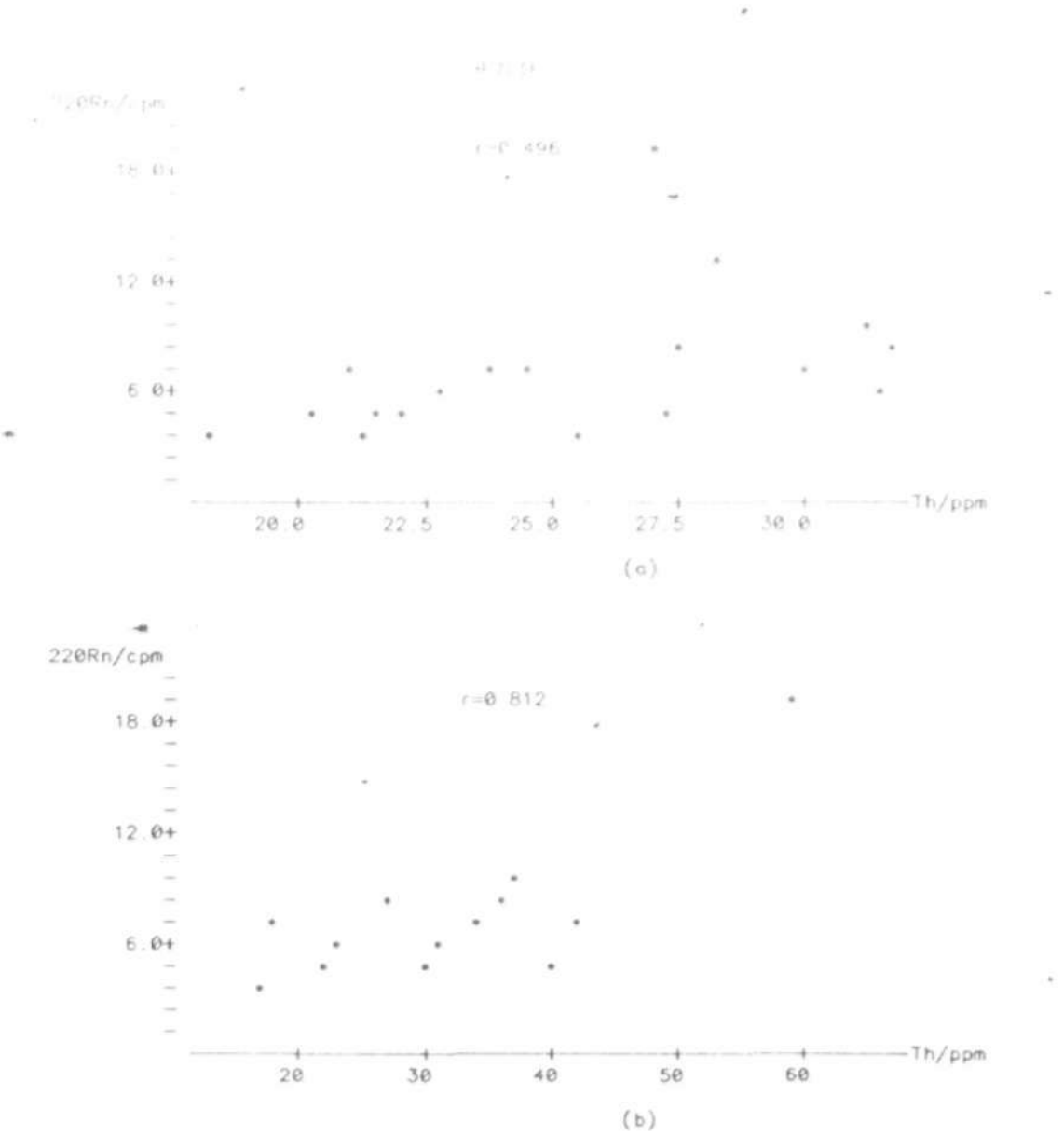


FIGURE 9.22 Correlation of 220Rn activity with soil Th (a) and rock Th (b)

indicate the presence of newly-precipitated U in the soil, that is U which has not had enough time to reach equilibrium with ^{226}Ra. Th, on the other hand, possibly occurring in resistate minerals, is able to support most of the ^{220}Rn activity. Also, because the Th decay series contains daughters with relatively short half-lives, it needs only a little time to reach secular equilibrium (Chapter 7).

In general, therefore, the results of the soil Rn survey appear to suggest that ^{222}Rn is associated more with U in the underlying rocks than with U in the soil. Soil ^{222}Rn activity in the region can thus be used to indicate variations in the abundance of U at depth. However, any Rn survey in the region has to take into consideration the contribution due to ^{220}Rn.

That soil Rn is correlated with the underlying rocks implies that some active upward transport is taking place. This may either be ^{222}Rn occurring as a gaseous phase, or ^{226}Ra in solution. The former explanation is more probable as atmospheric pumping is likely to be present, while the latter would mean an upward movement of groundwater supported either by a gravitational head or a thermal head (Durrance, 1983). In view of the active formation of lateritic soils in the area a general upward movement of groundwater can not occur.

9.8 Conclusions

Investigation of U in the lateritic soils of the Jos Plateau were undertaken with the aim of identifying the effect of deep weathering on geochemical mobility. Conclusions reached are derived from chemical analyses on 43 soil samples, mostly from the B horizon of the soil profile, and a soil gas Rn survey of the Jos - Bukuru complex. The chemical analyses show that accompanying an increase in the concentration of Fe and Al during lateritization, the elements, Ti, Mg, Ni, Cu, As, W, Pb, Cr, Zr, Sn and V became enriched in the soil relative to the associated parent granites, while Si, Ca, Na, K, Zn, Ga, Th, U, ba, La, Ce, Rb, Y, Nb and Cs are depleted. Apparently both Mg and Ti are significantly concentrated by the processes that concentrated Fe^{3+}, as well as by their occurrence in resistate minerals which have evaded alteration. Ti, in particular, is thought to be precipitated in the secondary mineral anatase. Evidence of intense leaching during the weathering is provided by the almost complete removal of Ca and Na. The elements V, Cr, Ni, Zr, As, La and Rb have been most greatly affected by the soil-forming process. Cr, Ni and Zr remain concentrated in resistate minerals, while As and Cu become sorbed onto organo-metallic complexes. The significant introduction of V into the soil indicates the scavenging power of the solutions involved in the weathering processes. Because of the high V abundance, it is thought that secodary vanadates have been formed.

Indeed the relatively high U content of the soils, and a significant correlation of U with V, suggest that secondary vanadates such as carnotite and tyuyamunite are present.

The depth distributions of the elements within the soil show an increase of Fe, Si, Ti and Na with increase in depth, while Al, Mg and K decrease. Of the trace elements, Cr, Ce, W, Ni and As show an increase, while Zn, Ga, Pb, Th, U, La, Rb, Nb, Cs, Sn and Ba decrease with increasing depth. However, a marked depletion of most of the elements occurs within the first 35cm of the soil profile. This is the likely extent of the elluviation zone. The few elements that show an increase in this zone are probably held in organic complexes. Local variations in the chemical composition of the soils associated with the different rock types are also present. In particular, the elements Si, Ca, Na, K, Pb, Th, U, Cr, Ce, Zn, Sn, and V show these variations very clearly. Of interest in this respect are the higher V and U contents of the soils associated with the medium-grained granites. It is in these soils that the possible occurrence of secondary vanadates is most likely.

There is only a slight depletion of U in the soil relative to its parent rocks. U in the soils is not associated entirely with resistate accessory minerals. This indicates the importance in the soils of U-bearing secondary minerals and U adsorbed onto secondary Fe oxides. It also appears that the Rare Earth minerals which host U in the granite, have been very susceptible to weathering.

^{222}Rn activity in the soil is mainly controlled by the U

content of the underlying rocks. In view of the strong correlation between ^{222}Rn in the soil and the U of the underlying rock, it is believed that soil ^{222}Rn activity is a better indicator of U at depth than the U content of the soil itself. This supports the view that secondary U in the soil is freshly precipitated, so that the U decay series has not had enough time to achieve secular equilibrium. The results suggest that where the need arises, and with proper environmental control, ^{222}Rn survey can be applied to delineate U occurrences in the region. However, any such surveys should take into consideration the contribution due to ^{220}Rn.

CONCLUSION AND REMARKS

The research work presented in this thesis was carried out with the aim of determining the abundance and distribution of U in the Nigerian Younger Granites and the kaolinised granites of South-West England, particularly to investigate the mobility of U during the low-temperature alteration processes of kaolinisation and weathering. The work also aimed at determining the relationship between gamma-ray activity and the amount of U present in order to facilitate the future use of gamma-ray surveys for U exploration in these environments. The work mainly involved samples from the granites and soil of the Jos - Bukuru Younger Granite complex in Nigeria and a kaolinised pit on Bodmin Moor in South-West England. Techniques applied in the study included in-situ and laboratory gamma-ray spectrometry, XRF analysis, soil Rn gas survey, alpha autoradiography, and alpha-particle spectrometry, with other methods used in an adjunct capacity where necessary.

The area of the Nigerian Younger granites has high gamma-ray activity, as revealed by an airborne gamma-ray survey which in 1971 covered most of northern Nigeria. The survey showed a number of anomalous zones of high activity associated with the Younger Granites. Often, these anomalies have been found to be caused by high levels of U (Uwah, 1985; Dewu, 1986). In Contrast, in South-West England, an airborne gamma-ray survey over the region

showed low activity over the kaolinised granites with high activity restricted to areas of unaltered granite. For this reason, among others, it was generally believed that kaolinisation caused U to be leached out of the granites.

Gamma-ray spectrometry was one of the first techniques used in the study of these materials. Measurement on 1.76MeV emission of ^{214}Bi, the 2.62MeV emission of ^{208}Tl and the 1.46MeV emission of ^{40}K indicated that laboratory results gave consistently lower U and Th values than the in-situ results. This investigation suggested that in order to utilise laboratory measurements, a suitable conversion factor has to be determined. Calculations based on data obtained in this study showed that for the DISA 400 spectrometer, this factor is about 1.8.

However, the problem of using data from gamma-ray spectrometry to obtain reliable analyses of Th and U still persists if disequilibrium is present in the U decay series. To overcome this difficulty, this study investigated various schemes which have been proposed to identify recent U mobilisation. In particular, it was found that use of the Disequilibrium Factor introduced by Durrance (1983) could be very helpful in identifying recent U mobilisation carried out in the field. Generally, the results from this investigation suggest that with proper data management and good geochemical control, data from four-channel gamma-ray spectrometry can be used to obtain accurate abundances of the radioelements in granitic rocks.

Taking into account these considerations, the results of gamma-ray spectrometric determinations of the Nigerian Younger Granites gave average values of 17.51ppm U, 47.00ppm Th and 4.11% K, but considerable variations were found between specific sites. Investigations of the equilibrium condition of the U and Th decay series in the granites suggested that while Th is largely in equilibrium, the U series showed some evidence of being disturbed.

The abundances of U, Th and K in the granites was also determined by chemical analyses. U and Th are present in the Nigerian granites with an average Th:U ratio of 2.9. Study of the abundance data indicates that the concentrations of U and Th are generally controlled by magmatic activity. Both elements increase with fractionation as indicated by increasing SiO_2, the igneous differentiation index, and Rb:Sr and K:Rb ratios. However, late- and post-magmatic processes have greatly modified the occurrence of U. Because U has been mobilised, there is possibility of vein-controlled U mineralisation in the granites and economic U mineralisation in the surrounding environment. Indeed, it may be the case that these granites are the source of U mineralisation in the Bauchi Plains, where U has been deposited in old river channels, just like the alluvial Sn deposits associated with the granites.

The importance of primary U-bearing minerals in controlling the abundance of U in the Nigerian granites is shown by the concomitant decrease of its major associates (Zr, Ti, Ce, La) in

the common accessory minerals, with an increase in fractionation. This means that most of U must be partitioned into minerals such as uraninite, uranothorite and complex NB-Ta-Ti-Y oxides. The fact that this investigation of the mineralogical distribution of U in the granites has shown the importance of these minerals in accounting for a large proportion of U in the granites is, therefore, not suprising. However, accessory minerals which also contain U in the granites are zircon, allanite and sphene. Mass-balance calculations have demonstrated that these accessory minerals make up about 15% of the whole-rock U, with about 40% accounted for by uranothorite. Evidence from this study suggest that most of the remaining U is held in uraninite. Although no uraninite was recorded in this investigation, sites which were once probably occupied by this mineral have been identified. The fact that uraninite is now missing is probably because the samples were collected from the surface and had been affected by weathering. Certainly, the widespread occurrence of secondary deposits with high alpha activity contain redistributed U.

The redistribution of U during weathering is shown by the soils associated with the Nigerian granites.

On average, U was found to be depleted in the soils relative to the granites, but is still rather high. An average of 7ppm U was recorded in the soil. Most of this U was found to be held in minerals of secondary origin. These were derived especially from the Rare Earth minerals, which appear to have been very susceptible

to weathering. The U released was deposited within carnotite and tyuyamunite, but also adsorbed onto secondary Fe and Al oxides, and clay minerals.

That U in the soil may be young, and out of secular equilibrium in the decay series above ^{226}Ra, was shown by the results of a soil Rn gas. The soil Rn was found to be correlated more with U in the underlying rocks than with the soil U. The results of U decay series disequilibrium studies were found to support the recent origin of U in the soil: ^{238}U and ^{230}Th activities indicating that soil formation occurred within the last 80,000 years and is probably an ongoing process. It is interesting that not only is U separated from its daughters but some fractionation between ^{238}U and ^{234}U also occurred during soil formation. This is consistent with widespread dispersed U mineralisation in the granites.

Investigations into the effects of kaolinisation in the granites of South-West England on U revealed a number of important features concerning the processes which brought about the formation of the china clay deposits in the region. As a measure of the degree of kaolinisation, it was found that the density of samples provided an excellent quantitative scale which was easily applied. Using this scale, chemical analyses showed that U, and many other elements, become depleted with progressive kaolinisation. These results also showed that the processes which led to kaolinisation occurred in two major phases. The characteristic products of these

phases suggest the operation of separate types of hydrothermal circulation.

Although the low gamma-ray activity of the kaolinised granites would appear to indicate low radioelement concentrations in the granites. However, the chemical analyses of this material have shown that, although the U, Th and K are depleted relative to fresh granite, the decrease in each element is not sufficient to explain the low activity. Consequently while gamma-ray spectrometric analyses gave average values of 2.12ppm U, 3.14ppm Th and 0.97% K, the values from chemical analyses were 9ppm U, 7ppm Th and 5.59% K. Although these results still indicate high U in the kaolinised granites, the amount of U lost during kaolinisation was substantial. Given the processes characteristic of hydrothermal circulation, the evidence suggests that large U ore deposits should be found near areas of kaolinisation. However, the few minor occurrences of U mineralisation known to be in the vicinity of the kaolinised granites are not enough to account for the estimated amounts of lost U. Previously it has been suggested that most of the U must have been deposited in small vein-lets in the rock mass, rather than as ore bodies, or that the deposits have yet to be discovered. However, the U in the kaolinised granites is of recent origin, (less than 110,000 years) which suggests that kaolinisation is partly young and an on-going process. During kaolinisation U is being leached by the descending limbs of hydrothermal circulation cells, but most is temporarilly adsorbed

onto the newly-formed clay minerals before being reworked as more water passes through the system. Although this process of reworking of U must have been occurring prior to 110,000 years ago, it is impossible to say for precisely how long. Nevertheless, from the extent of alteration now known to be modern, it is unlikely to have operated for a long period in the past. It is quite possible that the china clay deposits are a product of the Tertiary and Quarternary ages. There are two important implications for this conclusions:

(1) The fate of the U lost from the areas of kaolinisation is probably precipitation in the zones affected by the rising limbs of the modern hydrothermal circulation cells. With these cells operating at comparatively low temperature (Durrance, 1983) it is in turn, likely that the resulting ore deposits are forming at a depth of about 2 km. At such depths they would not be detectable by present-day survey results.

(2) Deep alteration of the granites and isostatic uplift of the kaolinised zones (Durrance and Bristow, 1986), is a relatively rapid phenomenon. Episodic movement on minor faults in the vicinity of the altered zones can, therefore be expected. The NW-SE trending faults which control much of the kaolinisation in the South-West England, by determining the positions of the positions of the descending limbs of the hydrothermal circulation cells, could be reactivated by this adjustment and, consequently, be maintained as highly permeable pathways.

The other aspect of interest which has emerged from this work concerns the possible recovery of U from the kaolinised granites, as by-product, in the china clay mining process. This will need further study of the mechanisms involved in holding U onto clay surfaces. Processing of the kaolinised granites in the production of china clay mainly involves mechanical separation of the clay from other mineralogical components. This means that the U adsorbed onto clay surfaces persists into the china clay product. The only chemical process that may remove U is one which is applied only in certain circumstances. That is where Fe must be stripped out in order to improve the colour of the clay in the final refining processes. Thus that part of the U in the kaolinised granites which has been adsorbed onto clay minerals becomes incorporated into the end-product of the china clay (ceramic, paper coating etc), unless it is removed during the manufacture of these end-products. In this respect, it is interesting to note that investigation of waste dumps from china clay processing did not reveal any significant radioactivity. Therefore, most of the U held onto the clay fractions must have remained in the china clay. Even if it is only one-fourth of the U in the kaolinised granites it is a substantial amount.

Appedix 4.1: Detection limits of the elements for XRF analysis (Philips PW1400 X-ray spectrometer); Department of Geology, University of Exeter)

Element	Limit(ppm)
Nb	4
Zr	2
Y	2
Sr	2
Rb	2
V	1,36,80*
Cr	2,12,43*
Mn	2
Ba	14
La	10
Ce	11
U	2
Th	4
Pb	4
As	1
Ga	1
Zn	2
Cu	1
Ni	1
Cs	2
Sn	4

*.....36pp at 0.2% TiO_2

80ppm at 2.0% TiO_2

**.....2ppm at 0ppm V

12ppm at 100ppm V

43ppm at 500ppm V

Appendix 6.1: Disequilbrium Factor (ψ) for kaolinised granites.

Sample	TC/cpm	ψ
BMP1	2507	3.59
BMP2	2432	3.33
BMP3	2379	3.16
BMP4	2317	3.12
BMP5	2343	3.26
BMP7	2654	3.71
BMP8	2747	3.99
BMP9	2561	3.45
BMP10	2537	3.43
BMP11	2797	3.20
BMP12	2440	3.44
BMP13	2437	3.34
BMP14	2113	2.68
BMP15	2364	3.18
BMP16	2408	3.26
BMP17	2486	3.47
BMP18	2437	3.37
BMP19	2623	3.41
BMP20	2486	2.85
BMP21	2205	2.86
BMP22	2471	3.30
BMP23	2139	2.51
BMP24	2332	2.76
BMP25	2321	3.21
BMP26	2132	2.74
BMP27	2802	2.99
BMP28	2282	3.00
BMP29	2540	3.25
BMP30	2313	3.34
BMP31	2604	3.54
BMP32	2304	3.24
BMP33	2386	3.34
BMP34	2476	3.36
BMP35	2748	2.96
BMP36	2874	3.04
BMP37	2442	3.45
BMP38	2394	3.27
BMP39	2322	3.23
BMP40	2409	3.16
BMP41	2437	3.13
BMP42	2195	3.11
BMP43	2255	3.05
BMP44	2452	3.33
BMP45	2443	3.53
BMP46	2357	3.31
BMP47	2602	3.37
BMP48	2307	3.26
BMP49	2483	3.44
BMP50	2650	3.68
BMP51	2656	3.45

Continue.....

Appendix 6.1, Continued.

BMP52	2565	3.71
BMP53	2690	3.35
BMP54	2676	3.29
BMP55	2617	3.55
BMP56	2387	3.40
BMP57	2579	3.31
BMP58	2544	3.16
BMP59	2080	2.79
BMP60	2295	2.98
BMP61	2222	2.62
BMP62	2738	3.88
BMP63	2223	2.90
BMP64	2571	3.39
BMP65	2612	3.14
BMP66	2518	3.54
BMP67	2466	3.35
BMP68	2431	3.32
BMP69	2453	3.52
BMP70	2458	3.53

Appendix 7.1: Procedure for the recovery of U and Th from rock samples for alpha spectrometry

(a) Pressure digestion of sample powders[1]

1. Dry sample powder at 110°C overnight then transfer to a dessicator and leave for 10 minutes
2. Place 0.4g of the powder in a PTFE beaker and pipette 0.75ml Conc. HCl[2] and 0.75 conc. HNO_3 into a beaker.
3. Add 6-7ml HF from a ploypropylene graduated cylinder.
4. Assemble digestion bomb and place in an oven at 110°C for 2 hours.
5. Remove from oven and allow to cool for at least half an hour.
6. Evaporate almost to dryness under an infra-red lamp[3].
7. Wash residue with deionised water into a volumetric flask making up the solution to 100ml.
8. Transfer the solution to a polypropylene bottle.

0.4g of sample powder is now dissolved in 100ml of deionised water.

Notes: 1. sample powders were obtained as described in Section 4.3

2. Analar grade acids were used.
3. Before this stage the solution may be washed with a little deionised water into a different PTFE beaker to prevent heat damage and preserve the good fit of the first beaker in the bomb.

(b) Preparation of ion exchange columns

1. Plug the bottom of a burette with glass wool.
2. Add 30ml of resin. Pack by pouring a suspension of resin particles in deionised water and allowing to settle slowly by agitating with a glass rod.
3. Plug the top of the column with glass wool
4. generate the column by eluting with 150ml 0.1M HCl followed by two lots of 75ml of either 9M HCl, (for the chloride column packed with Amberlite resin), or 7M HNO_3, (for the nitrate column packed with Dowex resin)
5. Add sample.

(c) Ion exchange separation of U and Th.

Spiking:

1. Add 1.0 ml of tracer solution[1].
2. transfer the spiked sample solution to a 250ml beaker washing the bottle with 6M HCl into the beaker. Place on a hot plate at $80^{o}C$ under an infra-red lamp and evaporate to dryness.

Solvent extraction:

3. If the residue appear to contain excessive Fe, that is, if it has a yellow colour, wash with 25ml, 6M Hcl, 5ml at a time, into separation funnel and add an equal amount of the solvent

M.I.B.K.[2]. Mix thoroughly by shaking, allow the solvent and acid to separate and run the acid off into a beaker.

Separation of U (with Pa and Fe^{3+}), from Th, (with other cations):

4. Wash the sides of the beaker with 10ml 9M Hcl and evaporate to dryness again. The residue is now transferred to the chloride (Amberlite), column for Th recovery in 10ml 9M HCl added as one 5ml and two 2.5ml lots, washing down the sides of the beaker with the last 2.5ml.
5. Follow the sample through the column with 10ml 9M HCl added in 1ml or 2ml lots to flush all the Th through. Collect in a beaker.
6. Prepare the column for U recovery by adding 0.1M Hcl, 1ml at a time, when the level of 9M Hcl drops to the level of glass wool above the resin. As the 0.1M Hcl percolates down through the column, the colour of the resin changes from dark brown to pale yellow-brown. When the colour change reaches the bottom of the column, change the collection beaker.
7. Continue to add 0.1M HCl as three lots of 1ml followed by one lot of 2ml and two lots of 10ml. This allows full U recovery.
8. After recovery of Th and U solutions evaporate each to dryness.

Preparation of nitrate column:

9. Prepare nitrate (Dowex) column for separation of Th from other cations and U (plus Pa), from Fe^{3+} by eluting the resin with 7M

HNO_3 until there is no Cl^- present. The absence of Cl^- is confirmed by adding a few drops of acid from the column to an equal amount of $AgNO_3$ solution. The presence of Cl^- will be indicated by by formation of a white precipitate.

Separation of Th from other cations:

10. Add the residue from step 8 to the column in 10ml 7M HNO_3 added as one 5ml and two 2.5ml lots, washing down the sides of the beaker with the last 2.5ml. Continue to add 7M HNO_3 to the column as two lots of 1ml, one lot of 2.5ml and three lots of 10ml to flush all other cations from the resin. This is discarded.
11. Add 0.1M HCl to the column as two lots of 1ml followed by one lot of 2.5ml and two lots of 10ml to flush the Th from the resin to be collected in a beaker. Up tq 30ml 0.1M HCl may be added to ensures full Th recovery.
12. Add 5 drops of conc, $HClO_4$ to the solution in the beaker to remove any organic matter that might be present and evaporate to dryness.

Separation of U, (plus Pa), from Fe^{3+}:

13. To regenerate the nitrate column for separation of U, (plus Pa), from Fe^{3+} add 7M HNO_3 as two lots of 1ml, one lot of 2.5ml and several lots of 10ml until $AgNO_3$ test confirms absence of Cl^-, (step 9).

14. Pass U residue from step 8 through column as described for Th residue in steps 10 and 11.

15. As step 12

16. Proceed with electrodeposition as described in Section 7.5.4

Notes: 1 ^{236}U and ^{229}Th

2 It was found useful to mix M.I.B.K. with 6M HCl prior to separation to condition it.

(d) Resin and solvent specifications.

Amberlite resin CG-400 (Cl),

Chromatographic grade,

Type 1, 100-220 mesh.

Dowex resin,

BioRad analytical grade anion exchange resin;

AG1-X8. 100-200 mesh, chloride form.

BioRad laboratories, Richmond, California

Both are quaternary ammonium styrene resins of total capacity 3.2meq/dry g, 1.4meq/ml resin bed.

B.I.B.K. solvent,

iso-butyl methyl ketone, (4-methyl entan-2-one)

$(CH_3)_2CH.CH_2.CO.CH_3$.

British Drug House.

Appendix 7.2: Separation, electrodeposition, counting dates, and alpha-particle counts for samples analysed by alpha spectrometry.

(a) Dates:

Sample	Isotope	separation	electrodeposition	counting
JPS17	U	13.4.89	25.4.89	06.6.89
	Th	13.4.89	5.5.89	12.6.89
JPS42	U	13.4.89	25.4.89	18.5.89
	Th	13.4.89	8.5.89	15.5.89
BMP33	U	20.4.89	10.5.89	30.5.89
	Th	20.4.89	9.5.89	02.6.89
BMP36	U	20.4.89	10.5.89	22.5.89
	Th	20.4.89	12.5.89	26.5.89
JPR17	U	13.4.89	20.4.89	15.6.89
	Th	13.4.89	24.4.89	24.7.89
JPR42	U	03.7.89	05.7.89	07.8.89

(b) Counts:

Ch. No.	counts											
	JPS17		JPS42		BMP33		BMP36			JPR17	JPR42	
	ThP	UP	UP	ThP	UP	ThP	UP	ThP	UP	ThP	UP	Thp
479	1	2	-	-	-	-	-	-		11		2
480	3	7	-	-	-	-	-	-		17		3
1	13	3	-	-	-	-	-	-		55		4
2	18	-	3	-	-	-	-	2	0	71		5
3	23	-	4	-	-	-	-	8	3	65		2
4	14	4	7	8	-	-	-	10	1	6		8
5	4	6	3	4	-	-	-	4	0	3		2
6	-	4	-	4	-	-	-	22	2	2		3
7	-	6	-	-	-	-	-	4	2	1		7
8	-	1	-	-	-	-	-	-	6	4		1
9	-	-	-	-	-	-	-	-	3	1		-
490	4	-	-	-	-	-	-	-	3	1		-
1	9	-	-	-	-	-	3	-	3	4	2	-
2	12	-	-	-	-	-	2	-	8	2	10	-
3	34	-	3	-	2	-	13	7	15	16	29	-
4	37	-	7	-	3	-	16	20	38	18	65	-
5	36	4	11	5	7	2	8	38	51	19	38	-
6	59	15	14	4	7	6	18	42	35	17	74	-
7	93	27	15	2	16	10	32	44	69	50	136	-
8	135	35	27	4	12	5	45	82	137	62	225	-
9	106	34	56	13	28	10	29	157	111	45	137	-
500	44	63	79	20	5	20	9	127	24	7	27	-
1	11	148	30	10	30	18	4	35	3	1	0	-
2	6	167	4	3	3	10	-	-	1	1	1	-
3	-	42	-	-	162	5	-	-		1	1	-
4	-	7	-	-	-	-	-	-		2	3	-
5	-	544	-	-	-	-	-	-		2	2	-
6	-	-	-	-	-	-	-	-		0	2	-

Continue.....

Appedix 7.2, Continued.

7	-	-	-	-	-	-	-	-		5	1	-
8	-	-	-	-	-	-	-	-		6	1	-
9	-	-	-	-	-	-	-	-	9	6	0	-
510	-	-	-	-	-	-	-	-	7	2	7	-
1	-	-	-	-	-	-	-	-	8	2	3	-
2	-	-	-	-	-	-	-	-	11	9	6	-
3	14	-	-	-	-	-	-	-	12	6	5	-
4	24	-	-	-	-	-	-	9	23	16	11	-
5	46	-	-	-	-	-	18	21	28	16	15	-
6	81	-	-	-	-	-	16	41	67	49	32	-
7	157	8	31	3	19	2	99	89	178	130	125	-
8	260	15	87	8	45	7	210	261	489	230	218	-
9	476	28	297	23	117	19	273	633	664	248	278	-
520	512	76	523	33	303	26	184	926	474	230	218	-
1	610	204	432	53	377	23	400	740	749	490	381	-
2	1039	468	452	46	284	68	854	1128	1706	861	852	-
3	1325	420	1133	77	450	58	860	2299	2198	770	894	-
4	851	395	1745	152	1023	130	348	3235	902	196	308	-
5	176	837	1049	155	1281	205	62	1611	123	32	35	-
6	17	1632	202	94	483	242	6	212	3	4	6	-
7	2	1367	25	29	70	112	-	16	1	4	0	-
8	-	311	1	4	3	11	-	-	3	1	1	6
9	-	31	-	-	-	-	-	-	1	4	2	11
530	-	-	-	-	-	-	-	-	0	2	2	17
1	-	-	-	-	-	-	-	-		9	2	23
2	9	-	-	-	-	-	-	-		8	2	27
3	9	-	-	2	-	-	-	8		22	2	33
4	9	4	4	4	-	-	-	14	3	8	0	36
5	-	1	6	6	6	-	-	28	6	4	0	35
6	-	-	-	4	6	-	-	6	4	8	1	47
7	17	-	-	-	-	-	6	-		18	2	89
8	34	-	-	-	-	-	12	9		55	5	92
9	43	-	2	5	2	-	12	26	6	53	10	61
540	35	-	5	5	6	3	7	67	12	33	18	27
1	36	-	6	9	9	8	11	40	21	26	50	13
2	34	10	10	6	7	9	15	50	49	21	64	8
3	43	13	22	6	10	6	19	29	38	23	46	
4	42	21	27	3	19	4	13	36	25	39	67	
5	77	25	23	6	16	6	19	37	58	57	129	
6	118	43	38	4	8	10	13	101	133	93	213	
7	134	31	53	9	27	13	31	152	119	80	136	67
8	87	33	94	23	58	21	47	144	43	80	35	102
9	65	106	35	24	44	32	48	80	9	150	4	150
550	101	179	17	20	15	31	13	82	16	254	6	186
1	157	111	9	19	18	24	19	146	13	470	4	250
2	219	68	17	44	45	27	20	258	11	674	4	242
3	269	23	29	92	56	32	53	422	8	534	2	185
4	203	39	33	116	93	64	81	488	8	275	2	94
5	106	70	20	129	108	93	68	329	1	185	1	88
6	81	85	12	104	72	75	45	159		198		84
7	85	67	11	67	48	30	37	124		168		74

Continue.....

Appendix 7.2, Continued.

8	69	35	12	50	38	38	22	151		151	62
9	72	20	7	47	43	30	43	148	7	147	57
560	55	23	12	46	33	32	15	85	4	85	47
1	38	31	8	36	23	34	23	62	0	97	
2	54	15	6	32	18	23	15	59		137	
3	64	13	8	22	10	17	14	75		125	
4	55	8	5	14	17	11	20	113		69	
5	28	8	7	32	24	18	17	81		48	
6	19	9	2	27	21	11	11	41		26	
7	17	24	3	13	8	20	7	27		56	
8	33	17	1	16	5	14	6	36		98	
9	39	6	4	12	5	5	11	41		134	
570	49	7	7	7	7	11	11	83		102	
1	31	5	8	26	15	15	23	104		50	
2	11	11	3	34	35	18	13	49		9	
3	3	14		18	18	18	14	22		6	
4	2	15		5	5	17	5	5		0	
5	-	8		1	-	5		-		-	
6	-	2		2	-	6		-		-	
7	-	7		-	-	0		-		-	
8	-	4		-	-	-		-		-	
9	-	-		-	-	-		-		-	
580	-	-		-	-	-		-		-	
1	-	-		-	-	-		-		-	
2	-	-		-	-	-		-		-	
3	-	-		-	-	-		-		-	
4	-	-		-	-	-		-		-	
5	-	-		-	-	-		-		2	
6	-	-		-	-	-		-		6	
7	-	-		-	-	-		-		3	
8	8	-		-	-	-		-		2	
9	5	-		-	-	-		-		12	5
590	12	-		-	-	-		-		5	4
1	14	-		-	-	-		-		4	9
2	7	-		7	-	-		5		14	13
3	6	-		6	-	-		9		23	27
4	6	-		5	-	-		8	6	27	19
5	3	-		6	-	-		11	8	11	11
6	-	-		8	-	-		10	8	5	14
7	-	-		9	-	-		12	11	17	30
8	8	-		41	-	-		-	8	25	39
9	12	-		2	-	-		12	9	54	54
600	33	-		-	-	-		14	8	90	56
1	31	-		9	-	-		28	9	67	44
2	36	5		13	-	-		22	11	32	22
3	15	8		14	-	-		29	24	26	16
4	10	11		20	-	-		23	18	25	9
5	20	21		18	-	24		37	22	13	
6	22	14		19	-	14		31	4	11	
7	7	18		20	-	19		21	6	11	

Continue.....

Appendix 7.2, Continued.

8	8	14	15	-	21	-	-	5
9	2	10	10	-	14	-	-	2
610	-	8	7	-	3	-	-	-
1	-	7	3	-	6	-	-	-
2	-	1	5	-	3	-	-	-
3	-	-	-	-	-	-	3	-
4	8	-	-	-	-	-	7	-
5	12	-	-	-	-	-	4	-
6	18	-	-	-	1	-	-	-
7	16	-	-	-	12	-	-	-
8	13	-	-	-	2	11	-	-
9	15	-	-	-	2	19	-	-
620	18	4	4	-	5	21	7	-
1	19	5	9	-	6	20	15	-
2	28	12	7	-	10	16	17	108
3	40	10	5	-	8	19	10	-
4	38	12	8	-	12	20	8	-
5	40	12	8	-	10	21	11	-
6	52	16	9	-	7	26	20	147
7	60	24	10	-	14	38	22	-
8	51	13	13	16	12	46	23	-
9	54	12	24	20	22	40	19	-
630	54	20	15	26	14	40	15	-
1	103	21	19	19	24	51	37	-
2	151	23	24	22	19	72	48	-
3	165	17	34	39	25	126	73	-
4	213	28	43	58	38	152	68	828
5	281	45	50	71	66	203	96	-
6	132	61	54	98	70	249	56	-
7	78	83	73	134	101	192	15	-
8	11	114	67	109	121	72	3	-
9	11	158	50	43	83	19	-	-
640	-	110	8	9	75	8		-
1	-	42	6	5	18	-		-
2	-	16	1	3	3	-		-
3	-	4	4	7	-	-		-
4	-	-	-	2	-	-		-
5	-	-	-	-	-	-		-
6	-	-	-	-	-	-		-
7	-	-	-	-	-	-		-
8	-	-	-	-	-	-		-
9	-	-	-	-	-	-		-
650	-	-	-	-	-	-		-
1	-	-	-	-	-	-		-
2	-	-	-	-	-	-		-
3	-	-	-	-	-	-		-
4	-	-	-	-	-	-		-
5	-	-	-	-	-	-		-
6	-	3	-	-	-	-		-
7	-	7	-	-	1	-	0	-
						-	4	-

Continue.....

Appendix 7.2, Continued.

8	18	2	-	-	9	6	7	-
9	53	-	-	-	4	15	16	184
660	62	10	6	9	5	26	16	-
1	50	6	12	11	9	44	16	-
2	26	9	17	21	14	47	9	-
3	9	9	19	33	17	23	4	-
4	9	32	11	11	39	11	0	-
5	3	37	4	5	17	5		-
6	-	14	0	-	11	-		-
7	-	6	3	-	4	7		-
8	-	123	-	-	-	5		-
9	-	-	-	-	-	8	2	-
670	16	-	-	-	-	10	8	-
1	24	-	-	-	4	16	7	-
2	30	-	-	-	10	20	8	-
3	52	-	-	-	5	21	12	-
4	53	-	-	-	8	16	16	-
5	63	7	14	-	7	25	13	-
6	184	7	5	15	4	42	39	-
7	241	13	15	18	8	89	81	1073
8	345	25	20	32	23	168	97	-
9	263	20	43	79	33	279	72	-
680	108	38	76	147	65	207	25	-
1	28	70	80	150	91	106	16	-
2	9	149	52	74	134	45	2	-
3	-	155	40	25	80	23		-
4	-	85	20	13	55	7		-
5	-	34	9	6	21	-		-
6	-	19	2	-	8	-		-
7	-	7		-	3	-		-
8	-	1		-	-	-		-
9	-	-		-	-	-		-
690	-	-		-	-	-		-
1	-	-		-	-	-		-
2	-	-		-	-	-		-
3	-	-		-	-	-		-
4	-	-		-	-	-		-
5	-	-		-	-	-		-
6	-	-		-	-	-		-
7	-	-		-	-	-		-
8	-	-		-	-	-		-
9	-	-		-	-	-		-
700	-	-		-	-	-		-
1	-	-		-	-	-		-
2	-	-		-	-	-		-
3	-	-		-	-	-		-
4	-	-		-	-	-		-
5	-	-		-	-	3		-
6	-	-		-	-	7		-
7	-	-		-	-	7		-

Continue.....

Appendix 7.2, Continued.

8	-	-	-	-	-	-
9	-	-	-	-	-	-
710	-	-	-	0	-	-
1	4	-	-	3	-	-
2	4	-	-	0	-	-
3	9	-	-	-	-	53
4	20	-	-	-	0	-
5	13	-	-	-	3	-
6	9	-	-	-	1	-
7	-	-	-	-	7	-
8	-	-	-	-	4	-
9	-	-	-	-	0	-
720	-	-	-	-	-	-
1	-	-	-	-	-	-
2	-	-	-	-	-	-
3	5	-	-	-		-
4	-	-	-	-		-
5	-	-	-	-		-
6	-	-	-	-		-
7	-	-	-	-		-
8	4	-	-	-		-
9	9	-	-	-		-
730	3	-	-	-		-
1	-	-	-	-		-
2	-	-	-	-		-
3	19	-	-	-		-
4	30	-	-	-	6	-
5	48	-	-	-	17	-
6	68	-	-	-	23	-
7	183	2	14	7	45	-
8	269	8	20	16	98	1100
9	367	15	43	17	95	
740	258	16	78	31	39	
1	112	36	116	22	32	
2	57	64	132	110	23	
3	47	133	73	102	13	
4	14	190	55	119	0	
5	-	116	38	64		
6	-	55	14	44		
7	-	36	7	28		
8	-	26	0	13		
9	-	11		-		

UP and ThP refer to U and Th planchet, respectively.

Appendix 8.1 Procedure for the determination of the density of kaolinised granite samples.

1. Dry overnight in an oven at 100^{O}C.
2. Weigh in air (m_1)
3. Immerse sample in molten wax, making sure that the sample is waxed all over. Allow the wax to solidify.
4. Weigh waxed sample in air (m_2).
5. Weigh waxed sample in water (m_3).
6. Relative density is calculated by:

$$R.\ D. = m_1/((m_2-m_3)-(m_2-m_1/\rho_w)),$$

where ρ_w is the density of the wax.

Appendix 8.2: Procedure for determination of clay content in natural samples

1. Weigh 10g of sample (if not in powder form, it may have to be crushed) into a a marked 250ml beaker (a settling velocity of 2.5cm per hour).
2. Dissolve sample in water and make up the beaker to the top mark and stir the content.
3. Leave undisturbed for an hour.
4. Pour out the top 2.5cm of the sample solution into a weighted evaporating dish and fill up the beaker to the brim again and stir.
5. Evaporate the solution in the evaporating dish to dryness.
7. Repeat steps 4 and 5 until reasonable amount of clay is obtained (12 extractions were used in this study) for comparative clay content determinations or until all clay is extracted, for absolute content determinations.
8. Weigh evaporating dish after extraction to determine the amount of clay extracted.

REFERENCES

Adams, J.A. S., 1962, Radioactivity of the lithosphere. In: Nuclear Radiation in Geophysics. Israel, H. and Krebs, A. (Eds.), Springer-Varlag, Berlin.

Adams, J. A. S. and Gasparini, P., 1970, Gamma ray spectrometry of rocks. Methods in geochemistry and geophysics. Elsevier, New York.

Ahrens, L. H., 1965, Some observations on the uranium and thorium distributions in accessory zircon from granitic rocks. Geochim. Cosmochim. Acta. 29, 711-716.

Ahrens, L. H., 1954, The lognormal distribution of the elements. Geochim. Cosmochim. Acta. 5, 49-73.

Ahrens, L. H., Cherry, R. D. and Erlank, A. J., 1967, Observation on the Th-U relationship in zircons from granitic rocks and from kimberlites. Geochim. Cosmochim. Acta. 31, 2379-2387.

Alderton, D. H. M., 1978, Fluid inclusion data for the lead-zinc ores from SW England. Trans. Inst. Min. Metall. London 87, B132-B135.

Alderton, D. H. M., Pearce, J. A. and Potts, P. J., 1980, REE mobility during granite alteration: Evidence from SW England. Earth and Planet. Sci. Letts. 49, 149-165.

Alford, M. J., Hill, I. D., Rackham, I. J. and Tuley, P., 1979, The Jos Plateau: A survey of environment and land use. Dept. of Geography, Univ. of Durham occasional publ. 14.

Alter, H. W., 1978, Track Etch ratios to soil uranium and a new uranium abundance estimates. Symp. on the Natural Radiation

Anderson, D. H. and Hawkes, H. E., 1958, Relative mobility of the common elements in weathering of schist and granite areas. Geochim. Cosmochim. Acta. 14, 204-210.

Andrews, J. N. and Wood, D. F., 1972, Mechanism of radon release in rock matrices and entry into ground waters. Trans. Inst. Min. Metall. London 81, B198-B209.

Armstead, H. C. H., 1978, Geothermal Energy. Wiley, Bristol.

Asikaineu, M., 1981, State of disequilibrium between 238U, 234U, 226Ra and 222Rn in ground water from bedrock. Geochim. Cosmochim. Acta. 45, 201-206.

Baas Beckin, L. G. M., Kaplan, I. R. and Moore, D., 1960, Limits of the natural environment in terms of pH and oxidation - reduction potentials. J. Geol. 68, 243-284.

Bacon, M. P., 1978, Radioactive disequilibrium in altered mid-oceanic basalts. Earth Planet. Sci. Lett. 39,(2), 250-254.

Baes, F. C.(Jr.) and Mesmer, R. E., 1976, The hydrolysis of cations. Wiley, New York.

Ball, T. K. and Basham, I. R., 1979, Radioactive accessory minerals in granites from South-West England. Proc. Ussher Soc. 4, (3), 437-448.

Baranov, S. A., Zelenkov, A. G. and Kulakov, V. M., 1960, Fine structure of the 231-Pa alpha radiation and the energy level scheme of the 237-Ac nucleus. Bull. Acad. Sci. USSR Phys. Ser. Columbia Trans. 24.

Barbier, M. J., 1974, Continental weathering as a possible origin of vein-type uranium deposits. Mineral. Deposita. 9, 271-288.

Barretto, P. M. C., Clark, R. B. and Adams, A. S., 1972, Physical characteristics of radon-222 emanation from rocks, soils and minerals: Its relation to temperature and alpha dose. In: The Natural Radiation Environment II, Proc. Symp., Houston, Texas.

Barnes, H.L. and Czamanske, G. K., 1967, Solubilities and transport of ore minerals. In: Geochemistry of hydrothermal ore deposits. Holt, Rinehart and Winston, New York.

Barshad, I., 1954, Cation exchange in micaceos minerals II. Replacement of ammonium and potassium from vermiculite, biotite and montmorillonite. Soil Sci. 78, 57-76.

Basham, I. R. and Easterbrook, G. D., 1977, Alpha particle autoradiography of geological specimens by use of cellulose nitrate detectors. Trans. Inst. Min. Metall. London 86, B96-B98.

Basham, I. R., Ball, T.K., Beddos-Stephens, B. and Michie, U. McL., 1982a, Uranium bearing accessory minerals and granite fertility: 1 Methods of identification. Symp. U. Expl. Methods, NEA-IAEA, Paris.

Basham, I.R., Ball, T. K., Beddoe-Stephens, B. and Michie, U. McL., 1982b, Uranium bearing accessory minerals and granite fertility: 2 Studies from the British Isles.Symposium on uranium exploration methods, NEA-IAEA, Paris.

Basham, I. R., Vairinho, M. M. B and Bowles, J. F. W., 1982c, Uranium-bearing accessory minerals in the sao Pedro do Sull granite Portugal. In: Vein-type and similar Uranium Deposits in Rocks Younger than Protozoic. Proc. Tech. Comm. meetg., Lisbon, IAEA, Vienna.

Basset, W.A., 1960, Role of hydroxyl orientation in mica alteration. Bull. Geol. Soc. Am. 71, 449-456.

Bates, T.F., 19 , Interpretation of structure and genesis in the kaolinite group. In: Problems of clay and laterite genesis, Amer. Inst. Min. Metall. Engineers.

Batchelor, A. S., 1980, Unpub. summary of informal workshop on the Cornubian batholith. Camborne School of Mines, Cornwall.

Beer, K. E., 1952, The petrography of some of the riebeckite granites of Nigeria. Rep. Geol. Surv., U.K. Atom. Energy Div. 116, London, HMSO.

Beth, M., Enge, W. and Sermond, G., 1986, Some new aspects on etching of CR-39 plastic detector. Nuclear tracks 12, (1-6), 97-101.

Billings, M. P. and Keevil, N.B., 1946, Petrology and radioactivity of four Paleozoic magma series in New Hampshire. Bull. Geol. Soc. Am. 57, 797-828.

Black, J. H., 1979, Results of a multiple borehole pumping in low permeability granite. O.E.C.D. 1979, Paris.

Bloomer, J. R., Kuckes, A. F., Oxburgh, E. R. and Richardson, S. W., 1982, Heat flow studies in the Winterborne Kingston borehole, Dorset. Inst. Geol. Soc. report 81/3, 176-183.

Bowden, P., 1985, The geochemistry and mineralisation of alkaline ring complexes in Africa 8a review). Jour. Afr. Earth Sci. 3, (1/2), 17-39.

Bowden, P., Bennett, J. N., Whitely, J. E., Abaa, S. I., and Hadzigeogiou -Starrakis, P. K., 1981, Uranium in the Niger-Nigeria Younger granite Province. Mineral. Mag. 44, 379-389.

Bowden, P. and kinnaird, J. A., 1984, Geology and mineralization of

Bowie, S. H. U., 1954, Nuclear Emulsion Technique. In: Faul, H. (Ed.), Nuclear Geology. Wiley, New York.

Bowie, S. H. U., 1972, The status of uranium prospecting. In: *Uranium Exploration Handbook*, Bowie, S. H. U., Davis, M. and Ostle, D. (Eds.) Inst. Min. Metall., London.

Bowie, S. H. U., Ostle, D. and Campbell, C. B., 1973, Uranium mineralisation in N. Scotland, Wales, the Midlands and S. W. *England. Trans. Inst. Min. Metall. Lonodon* 82, B177-B179.

Boyle, R. W., 1970, Regularities in wall rock alteration phenomena associated with epigenetic deposits. In: Pouba, Z. and Stemprok, M. (Eds.), Problems of hydrothermal ore deposition, 233-260, Academia Kiado, Budapest.

Bouda, S., 1985, Mossbaeur effect and geochemical study of solution-mineralisation in surface environment of south west England. Ph.D. Thesis, Univ. of Exeter.

Brady, N. C., 1974, The nature and properties of soils. Macmillan London.

Brammal, A. and Harwood, H. F., 1923, The occurrence of rutile, brockite and anatase in Dartmoor. Mineralog. Mag., 20, 20-26.

Brammal, A. and Harwood, H. F., 1932, The Dartmoor granites: Their genetic relationships. Q. J. Geol. Soc. London 88, 171-237.

Bray, C. J., 1980, *Mineralisation, greisenisation and kaolinsation* at Goonbarrow china clay pit, Cornwall, U. K. Ph. D. Thesis, Univ. of Oxford.

Bristow, C. M., 1977, A review of the evidence for the origin of the kaolin deposit in S.W. England, Proc. 8th Intern. Kaolin Symp. and meeting on alunite, Madrid - Rome.

Bristow, C. M., 1988, Ball clays, weathering and climate. Proc. 24th Forum on the Geology of Industrial Minerals, South Carolina Geol. Surv. Columbia, S. C.

Bristow, C. M. and Exley, C.S., 1988, Kaolin deposits of the United Kingdom. In press.

Broda, E and Feather, N., 1947, The assigment of the slow-neutron-produced activities of thallium and the dual disintegration of radium E. Proc. Roy. Soc. London, 190A, 20-30.

Brown, G., 1953, the Dioctahedral analogue of vermiculite. Clay Min. Bull. 2, 64-69.

Brown, G. C., 1977, Mantle origin of Cordilleran granites. Nature, 265, 21-24.

Brown, G., C. and Mussett, A. E., 1981, The inaccessible Earth. Allen and Unwin, London.

Brown, H., Blake, W. J., Chodos, A. A., Kowahkowski, R., Mckinney, C. R., Neuerburg, G. J., Silver, L. T. and Uchiyama, A., 1953, Leaching studies of interstial material in igneous rocks (Abs.). Bull. Geol. Soc. Am. 64, 1400.

Burcham, W. E., 1963, Nuclear Physics, an Introduction. Longmans, London.

Butler, J. R., 1953, The geochemistry and mineralogy of rock weathering; (1) The Lizard area, Cornwall, Geochim. Cosmochim. Acta. 4, 157-178.

Butler, J. R., Bowden, P. and Smith, A.Z., 1962, K/Rb ratios in the evolution of the Younger granites of Northern Nigeria. Geochim. Cosmochim. Acta. 36, 89-100.

Butt, C. R. M. and Gole, M. J., 1985, Helium in soil and overburden gas as a exploration pathfinder - an assessment. J. Geochem. Explor. 24, 141-173.

Cameron, J., 1974, Mineralogical aspects and origin of the Uranium in the vein deposits of Portugal. IAEA, Vienna, TC-295/18, 349-370.

Caneer, W. T. and Saum, N. M., 1974, Radon emanomatry in uranium exploration. Min. Eng. 26, (5), 26-29.

Carroll, D., 1953, Weatherability of zircon. J. Sed. Pet., 23, 106-116.

Cartwright, B. G. and Shirk, E. K., 1978, A nuclear-track recording polymer of unique sensitivity and resolution. Nuclear instr. methods 153, 457-460.

Chappel, B. W. and White, A. J. R., 1974, Two contrasting granite types. Pacific Geol. 8, 173-174.

Chayes, F., 1964, Variance-covariance relation in some published Harker variation diagrams in volcanic suites. J. Petrol. 5, 219-237.

Clark, G. J., Gulson, B. L. and Cookson, J. A., 1979, Pb, U, Tl, Hf and Zr distribution in zircons determined by proton microprobe and fission track technique. Geochim. Cosmochim. Acta. 43, 905-918.

Clarke, D. B., 1981, The mineralogy of peraluminous granites: A review. Can. Min... 19, 3-17.

Clark, S. P. Jr. and Turekian, K. K., 1979, Thermal constraints on the distribution of long-lived radioactive elements in the earth. Phil. Trans. R. Soc. London A291, 269-275.

Collins, W. J, Beams, S. D., White, A. J. R and Chappel, B. M., 1982, Nature and origin of A-type granites with particular reference to South Eastern Australia. Contr. Miner. Petrol. 80, 189-200.

Coppens, R., 1649, Study of radioactivity in some rocks by photographic emulsions. Ph.D. Thesis, Paris.

Corfunke, E. H. P., 1969, The chemistry of uranium. Elsevier, New York.

Correns, C. W., 1960, Experimental chemical weathering of silicates. Clay Min. Bull. 4, 249-265.

Covett, G. J. S., 1983, Rock geochemistry in mineral exploration. In: Covett, G. J. S. (Ed.), Handbook of Exploration Geochemistry. Elsevier, New York.

Cox, K.G.,Bell,J.D. and Parnkhost, R.J.,1979, The interpretation of igneous rocks. George Allen and Unwin, London.

Cramer, J. J., 1982, Effects of rock-water interaction on radionuclide transport: At:waste management infor.mett.May '87, Winnipeg. AECL Tech. Record.TR201 pp277-88.

Cramer, J. J. and Nesbitt, H. W., 1983, Mass-balance relations and trace element mobility during continental weathering of various igneous rocks. In: Petrology of weathering and soils. Int. Symp., Centre Nat. Research Sci. Mem. 73, Paris.

Crowther, E. M., 1930, The relationship of climate and geological factors to the composition of the clay and the distribution of soil types. Proc. Roy. Soc. 107, 10-30.

Darnley, A. G., 1970, Airborne gamma-ray survey spectrometry. Trans. Can. Inst. Min. Metall. 73.

Darnley, A. G., 1972, Airborne gamma-ray survey techniques. In: Bowie, S. H. U., Davis, M. and Ostle, D. (Eds.). Uranium Exploration handbook, Inst. Min. Metall. London.

Darnley, A. G., Bristow, Q. and Donhoffer, D. K., 1969, Airborne gamma-ray spectrometer experiments over the Canadian Shield. In: IAEA, Nuclear techniques and mineral Resources, Vienna.

Dearman, W. R., 1963, Wrench-faulting in Cornwall and south Devon. Proc. Geol. Assoc. 74, 265-287.

Dewu, B. B. M., 1986, A geophysical ground follow-up to an aero-radiometric survey, Jos Plateau, Nigeria. M. Sc. Thesis, Ahmadu Bello Univ. Zaria.

Dewu, B. B. M., Omuetok, U. M., Umo, N. C. and Umo, C. C., 1984, Gravity and magnetics profile across the Nigerian Younger Granite. M. Sc. project, Ahmadu Bello Univ. Zaria.

Dodd, P. H. and Eschliman, D. H., 1972, Borehole logging techniques for uranium exploration and evaluation. In: Bowie, S. H. U., Davis M. and Ostle, D. (Eds.), Uranium Exploration Handbook. Inst. Min. Metall., London.

Donaldson, I. G., 1968, A possible model for hydrothermal systems and methods of studying such models. Proc. Ann. Conf. Hydraulics and Fluid Mechanics.

Durrance, E. M., 1983, Radiological indications of hydrothermal circulation in South East Devon. Ph. D. Thesis, Univ. of Exeter.

Durrance, E. M., 1985, Hydrothermal circulation and isostasy, with particular reference to the granites of Southwest England. In: High Heat Producing (HHP) granites, hydrothermal circulation and ore genesis. Inst. Min. Metall., London.

Durrance, E. M., 1986, Radioactivity in Geology: Princples and Applications. Ellis Horwood, Chichester.

Durrance, E., M., Meads, R. E., Brindly, R. K., and Stark, A. G. W., 1980, Radioactive disequilibrium in uranium-bearing nodules from the New Red Sandstone (Permian-Triassic) of southeast Devon. Proc. Ussher Soc. 5, 81.

Durrance, E. M., Bromley, A. V., Bristow, A. C., Heath, M. J. and Penman, J., 1982, Hydrothermal circulation and post-magmatic changes in granites of south-west England. Proc. Ussher Soc. 5, 304-320.

Durrance, E. M. and Heath, M. J., 1985, Thermal groundwater movement and radionuclide transport in south west England. Mineral. Mag. 49, 289.

Durrance, E. M. and Bristow, C. M., 1986, Kaolinisation and isostatic readjustment in south-west England. Proc. Ussher Soc. 6, 318-322.

Dyck, W., 1969, Development of uranium exploration methods using radon. Pap. Geol. Surv. Can., 69-46.

Dyck. W., 1972, Radon methods of prospecting in canada. In: S. H. U., Bowie, M. Davis and D. Ostle, (Eds.), Uranium Exploration Handbook, Inst. Min. Metall. London.

Dyck, W. and Smith, A. Y., 1968, Use of radon-222 in surface waters for uranium geochemical prospecting. Can. Min. J. 89, 100-103.

Dyck, W. and Cameron, E. M., 1975, Surface lake water uranium radon Survey of the Lineament Lake area, District of Manckenzie. Geol. surv. Can. Papers 75-1A, 209-212.

Eisenbud, L., Garvey, G. T. and Wigner, E. P., 1967, General principles of nuclear structure. In: Condon, E. W. and Ovishaw, H. (Eds.), Handbook of Physics. McGraw-Hill, New York.

Elder, J., 1981, Geothermal systems. Academic Press, London.

Evans, A. M., 1980, An introduction to ore geology. Geoscience Texts, vol. 2. Blackwell, Oxford.

Evans, R. D., 1955, The Atomic Nucleus. McGraw-Hill, New York.

Exley, C. S. and Stone, M., 1966, The granitic rocks of southwest of England. In: Hosking, K. F. G and Shrimpton, G. J. (Eds.), Present views on some aspects of the geology of Cornwall and Devon. R. Geol. Soc. Cornwall, 150th Anniv. vol. for 1964, 131-184.

Exley, C. S. and Stone, M., 1982, Hercynian intrusive rocks. In: Sutherland, D. S. (Ed.), Igneous rocks of the British Isles. Wiley London.

Exley, C. S., Stone, M. and Floyd, P. A., 1983, Composition and petrogenesis of the Cornubian batholith and post orogenic rocks in SW England. In: Hancock, P. L.(Ed.). The Variscan fold belt in the British Isles. Adam Hilger London.

Eyles, U. A., 1952, The composition and origin of Antrim laterites and bauxites. Mem. Geol. Surv. (Belfast).

Fano, U., 1953, Gamma-ray attenuation, Part 1 Basic processes. Nucleonics 11, 8-12.

Faul, H., 1954, (Ed.) Nuclear geology. John Wiley and Sons, New York.

Fehn, U, 1985, Post-magmatic convection related to high heat production in granites of southwest England: A theoretical study. in: High Heat Production (HHP) Granites, hydrothermal circulation and ore genesis. Inst. Min. Metall. London.

Fehn, U, Cathles, L. M. and Holland, H. D., 1978, Hydrothermal convection and uranium deposits in abnormally radioactive plutons. Econ. Geol. 73, 1556-1566.

Feth, J. H., Robertson, G. and Polzer, W., 1961, Sources of mineral constituents in water from granitic rocks, Sierra Nevada,California and Nevada, U. S. Geol. Surv. Water Supply Paper 1535-I.

Fews, A. P., 1982, A study of alpha particle tracks in CR-39 plastic. Ph. D. Thesis, Univ. of Bristol.

Fews, A. P., 1986, Fully automatated image analysis of alpha particle and proton etched tracks in CR-39. Nucl. Tracks 12, 221-225.

Ford, I. H., 1951, Radioactivity in rocks: an improvement in the photographic technique. Nature 167, 273-274.

Finney, G. D. and Evans, R. D., 1935, The radioactivity of solids determined by alpha-ray counting. Phys. Rev. 48, 503-511.

Frank, A. L., Ogura, K. and Benton, E. V., 1986, Fading of latent tracks in CR-39 due to environmental conditions. Nucl. Tracks 12, 83-86.

Fyfe, W. S., 1978, The evolution of the earth's crust: modern plate tectonics to ancient hot spot tectonics? Chem. Geol. 23, 89-114.

Garg, S. K. and Kassoy, D. R., 1981, Convective heat and mass transfer in hydrothermal systems. in: Rybach, L. and Muffler, L. J. P. (Eds.) Geothermal systems: principles and case histories. Pitman, Bath.

Gascoyne, M., 1977, U series dating of speleothems: An investigation of technique, data processing and precision. Tech. Mem. Dept. of Geol., McMaster Univ., 77-84.

Gascoyne, M., 1981, A simple method of uranium extraction from carbonate groundwater and its application to uranium-234/uranium-238 disequilibrium studies. Geochem. Explor. 14, 199-207.

Giblin, A. M., Batts, B. D. and Swaine, D. J., 1981, Simulation studies of uranium mobility in natural waters. Geochim. Cosmochim. Acta. 45, 699-709.

Giletti, B. J. and Kulp, J. L, 1955, Radon leakage from radioactive minerals. Am. Mineral. 40, 481-496.

Gingrich, J. E., 1984, Radon as a geochemical exploration tool. J. Geochem. Explor. 21, 19-39.

Gingrich, J. E. and Fisher, J. C., 1976, Uranium exploration using the Track-Etch methods. In: Exploration for uranium ore deposits. IAEA, Vienna.

Glasstone, S., 1967, Source book on Atomic Energy. D. Van. Nostrand Princeton.

Goldich, S. S., 1938, A study in rock weathering. J. Geol. 46, 17-58.

Gosh, P. K., 1927, The petrology of Bodmin moor granite (eastern part), Cornwall. Mineral. Mag. 21, 285-309.

Govindaratu, K. (Ed), 1984, Compilation of working values and sample description for 170 int. ref. samples of mainly silicate rocks and minerals. CNRS, VandVeure, Les Nancy.

Green, J., 1959, Geochemical tables of the elements for 1959. Bull. Geol. Soc. Am. 70, 1127-1184.

Gregory, R. G., 1987, Soil gas emanomatry and hydrothermal mineralisation in southwest England. Ph. D. Thesis Univ. of Exeter.

Grim, R. E., 1953, Clay mineralogy. McGraw-Hill, London.

Grim, R. E., 1962, Applied clay mineralogy. McGraw-Hill, London.

Halliday, D., 1950, Introductory Nuclear Physics. Wiley New York.

Hamilton, E. H., 1958, Distribution of radioactivity in rocks and minerals and the effect of weathering on determination of uranium. Nature 181, 697-698.

Hanson, R. O. and Stout, Perry R., 1968, Isotopic distribution of uranium and thorium in soils. Soil Science 105, 44-50.

Hargraves, R. B., 1976, Precambrian geologic history. Earth Planet. Sc. Lett. 193, 363-371.

Harrison, A. F. and Bocock, K. L., 1981, Estimation of Soil bulk density from loss on ignition values. J. Appl. Ecology 8, 919-927.

Harriss, R. C. and Adams, J. A. S., 1966, Geochemical and mineralogical studies on the weathering of granitic rocks. Amer. J. Sci. 264, 146-173.

Harvey, P. K., Taylor, D. M., Hendry, P. D., and Bancroft, F., 1973, An accurate fusion method for the analysis of rocks and chemically related materials by X-ray fluorescence spectrometry. J. X-ray Spectrometry 2, 33-44.

Hatch, F. M., Wells, A. K. and Wells, M. K., 1972, Petrology of the igneous rocks. George Allen and Unwin, London.

Hayase, I., 1953, The radioactivity of rocks and minerals studied with nuclear emulsion.
I. The study of radioactive minerals of the Tanakamiyama and Mikumo granite. Siga Pref. Japan: Memoirs Coll. Sci.

Heath, M. J., 1982, Uranium in the Dartmoor granite: Geochemical and radiological investigations in relation to the South West England geothermal anomaly. Ph. D. Thesis, Univ. of Exeter.

Heckter, M., 1934, Radiochemish obserflahesbestumung an Glass. Glastech. Berl. 12, 15-172.

Hee, A., Dervile, R. P. and Jarovoy, M., 1954, Determination of the radioactivity of the Quincy granite by the photographic method. Am. J. Sci. 252, 736-744.

Heins, T. and Enge, W., 1986, Oxygen effect on the etch rate in CR-39 plastic detector. Nucl. Tracks. 12, 87-89.

Heir, K. S. and Rogers, J. J. W., 1963, Radiometric determinations of thorium, uranium and potassium in basalts and in two magmatic differentiation series. Geochim. Cosmochim. Acta. 27; 137-154.

Helgeson, H. C., Garrels, R. M. and Mackenzie, F. T., 1969, Evolution of irreversible reactions in geochemical processes involving minerals and aquous solutions II Applications. Geochim. Cosmochim. Acta 33, 455-481.

Henderson, P., 1982, Inorganic geochemistry. Pergamon, London.

Henderson, P., 1984, General geochemical properties and abundances of the rare earth elements. in: Henderson P. (Ed). Rare Earth Element Geochemistry, developments in Geochemistry 2, Elsevier, Armsterdam.

Hostetler, P. B. and Garrels, R. M., 1962, Transportation and precipitation of uranium and vanadium at low temperatures with special reference to sandstone type uranium deposits. Econ. Geol. 57, 137-167.

Hurley, P. M., 1956, Direct radiometric measurement by gamma-ray scintillation spectrometer. Part I. Uranium and Thorium series in equilibrium. Bull. Geol. Soc. Am. 67, 395-404.

Hurley, P. M., and Fairbairn, H. W., 1957, Abundance and distribution of uranium and thorium in zircon, sphene, apatite, epidote and monzonite in granitic rocks. Trans. Am. Geophys. Union 38, 939-944.

Hyde, E. K., Pearlman, I and Seaborg, G. T., 1971, The nuclear properties of the heavy elements II. Detailed radioactivity properties. Dover, New york.

Ike, E. C., 1979, The structure petrology and geochemistry of the Tibchi Younger Granite ring complex. Ph. D. Thesis, Univ. of St. Andrews.

Ivanovich, M., 1982, Spectroscopic methods. In: Ivanovich, M. and Harmon, R. S. (Eds.), Uranium Series Disequilibrium, Application to Environmental Problems. Oxford Univ. Press, Oxford.

Jackson, N., 1960, Vacuum sublimation approaches for preparation of thin sources of alpha-active materials. J. Sci. Inst. 37, 169-171.

Jackson, N. J., Halliday, A. N., Shepherd, S. M. F. and Mitchell, J. G., 1982, Hydrothermal activity in the St. Just mining district, Cornwall, England. In: Evans, A. M. (Ed.), Metallization Associated with Acid Magmatism, Wiley, Chichester, 137-179.

Jackson, R. R. E, and Macleod, W. N., 1977, Geology of the Liruei, Banke and adjacent Younger Granite ring complexes. Bull. Geol. Surv. Nig. 33, 1-117.

Jaupart, C., 1985, On the average amount and vertical distribution of radioactivity in the continental crust.Thermal modelling in sedimentary basins, 1st Conference on expl. Res. of the Inst. Francai-Bu-Petrole, Carcas, France, 1985.

Jay, K. E. B., 1955, Atomic energy research at Harwell.

Jefferies, N. L., 1988, The distribution of uranium in the Carnmenellis pluton, Cornwall. Ph. D Thesis, Univ. of Exeter.

Jenny, H., 1941, Factors of soil formation, A system of quantitative pedology, McGraw-Hill, New York.

Jenny, H., 1950, Origin of soils: in Applied sedimentation; Trask, P.D. (ed.), Wiley, New York.

Johnson, N. M., Likens, G. E., Bormann, F. H. and Pierce, R. S., 1968, Rate of chemical weathering of silicate minerals in New

Katz, J. J. and Seaborg, G. T., 1957, The chemistry of the *actinide elements*. *Methuen, London.*

Keller, W. D., 1964, Processes of origin and alteration of clay minerals. In: Rich, C. J. and Kunze, G. W. (Eds.), Soil clay mineralogy, Univ. North Carolina Press.

Kigoshi, K., 1971, Alpha-recoil thorium-234: Dissolution into water and uranium-234/uranium-238 disequilibrium in nature. Science 173, 47-48.

Killeen, P. G. and Carmichael, C. M., 1970, Gamma-ray spectrometer calibration for field analysis of uranium, thorium and potassium. Can. J. Earth Sci. 7, 1093-1098.

Killeen, P. G. and Carmichael, C. M., 1976, Determination of radioactive disequilibrium in uranium ores by alpha-spectrometry. Geol. Survey paper 75-38. Canada Geol. Survey Commission.

Kinnaird, J. A., 1985, Hydrothermal alteration and mineralization of the alkaline anorogic ring complexes of Nigeria. J. Afr. Earth Sci. 3, 229-251.

Kinnaird, J. A., Batchelor, R. A., Whitley, J. E. and MacKENZIE, A. B., 1985, Geochemistry, mineralization and hydrothermal alteration of the Nigerian high heat producing granites. In: High heat production (HHP) granites, hydrothermal circulation and ore genesis, Inst. Min. Metall. London.

Knight, G. B. and Macklin, R. I., 1948, Half-life of UX$_1$ (Th$_{234}$). Phys. Rev. 74, 1540-1541.

Kohman, T. P., 1956, Extinct natural radioactivity: Possibilities

Kohman, T. P., 1956, Extinct natural radioactivity: Possibilities and potentialities. Annals. New York Academy of Science, 505-542.

Kohman, T. P., 1961, Chronology of nucleosynthesis and extinct natural radioactivity. J. Chem. Ed. 38, 73-82.

Kovach, E. M., 1944, An experimental study of radon content of soil-gas. Trans. Am. Geophys. Union. 25, 563-571.

Kovach, E. M., 1945, Meteorological influence upon the radon content of soil gas. Trans. Am. Geophys. Union 26, 241-248.

Kovach, E. M., 1946, Diurnal variations in the radon content of soil gas. Terr. Magnetism and Atmosph. Electricity 51, 45-46.

Kraner, H. W., Schoeder, G. L. and Evans, R. D., 1964, Measurements of the effects of atmospheric variables on radon-222 flux and soil-gas concentrations. In: Adams, J. A. S. and Lowder, W. M. (Eds.), The Natural Radiation Environment, Chicago Univ. Press, Chicago, 191-215.

Kronfield, J., 1974, Uranium deposition and thorium-234 alpha recoil. Exploration for extreme uranium-234/uranium-238 fractionation within the Trinity aquifer. Earth Planet. Sci. Lett 21, 327-330.

Ku, Teh-Lung, 1965, An evaluation of the U^{234}/U^{238} method as a tool for dating pelagic sediments. Geophys. Res. 70, 3457-3474.

Lally, A. E., 1982, Chemical procedures. In: Ivanovich, M. and Harmon, R. S. (Eds.), Uranium Series Disequilibrium Studies: Applications to environmental Problems. Oxford Univ. Press, Oxford.

Lally, A. E. and Eakins, J. D., 1978, Symp. Determ. radionuclides in biological materials. CEGB, London.

Lambert, I. B. and Heier, K. S., 1967, The vertical distribution of uranium, thorium and potassium in the continental crust. Geochim. Cosmochim. Acta. 31, 377-390.

Langmuir, D., 1978, Uranium solution-mineral equilibrium at low temperature with applications to sedimentary ore deposits. Geochim. Cosmochim. Acta. 42, 547-59.

Larsen, E. S., and Gottfried, D., 1960, Uranium and thorium in selected suites of igneous rocks. Amer. J. Sci. 258, 151-169.

Larsen, E. S.Jr. and George, Phair, 1954, The distribution of uranium and thorium in igneous rocks. In: Faul, H. (Ed.) Nuclear Geology. McGraw-Hill, Toronto.

Leake, B. E., Hendry, G. L., Kemp, A., Plant, A. G, harvey, P. K., Wilson, J. R., Coats, J. S., Ascott, J. W., Lunel, T., and Howarth, R. J., 1969, The chemical analysis of rock powders by automatic X-ray Fluorescence. Chem. 65., 7-86.

Lederer, C. M. and Shirley, V., 1978, Table of Isotopes, Interscience, New York.

Lederer, C. M., Hollander, J. and Perlman, I., 1967, Table of Isotopes. Wiley, New York.

Levinson, A. A., Bland, C. J., and Lively, R. S., 1982, Exploration for U deposits. In: Ivanovich, M. and Harmon, R. S. (Eds.), Uranium series disequilibrium studies, Application to environmental problems. Oxford Univ. Press, Oxford.

Loiselle, M. C., and Wones, D. R., 1979, Characteristics and origin of anorogic granites. Abst. 92nd G.S.A. ann. meetg., 11, 468.

Loughnan, F. C., 1969, Chemical weathering of the silicate minerals. Elsevier, New York.

Lovering, T. G., 1955, Progress in radioactive iron oxide deposits investigation. Econ. Geol. 50, 186-195.

Madansky, L. and Rosetti, F., 1956, Decay of Rn^{220} and Rn^{222}. Phys. Rev. 102, 464-465.

Mason, B., 1958, Principles of geochemistry. Wiley, New York.

Mason, B., 1960, Principles of geochemistry. Wiley, New York.

Mackay, R. A., 1949, The radioactive mineral resources of Nigeria. Geol. Surv. Gt. Britain, Atomic Energy Div., Report, 77.

Macleod, W. N., 1977, The geology of the Jos - Bukuru Younger Granite complex with particular reference to the distribution of columbite. Mem. Geol. Surv. Nig. 33.

Macleod, W. N., and Berridge, N. G., 1971, The Jos bukuru complex. In: Buchanan, M. S., Macleod, W. N., and Turner, D. C. (Eds). The Geology of the Jos Plateau. Bull. Geol. Surv. Nig. 2,(32), 67-84.

Macleod, W. N., Turner, D. C., and Wright, E.P., 1971, The geology of the Jos Plateau. Bull. Geol. Surv. Nig. 1, 118pp.

Maignien, R., 1966, Review of research on laterites. Natural resources research IV Unesco, Varllant - Carmanne, Paris.

Mero, J. L., 1960, Uses of gamma-ray spectrometer in mineral exploration. Geophysics 25, 1654-1676.

Merrill, G. P., 1906, A treatise on Rocks, Rock weathering and soils, Macmillan, New York.

Meyer, C. and Hemley, J. J., 1967, Wall rock alteration. In: Rybach, L. and Muffler, L. J. P. (Eds.) Geothermal systems:principles and case histories. Pitman, Bath.

Miller, J. M. and Loosemore, W. R., 1972, Instrumental techniques for uranium prospecting. In: Bowie, S. H. U., Davis, M. and Ostle, D. (Eds.), Uranium Prospecting Handbook. Inst. Min. Metall., London.

Mohanty, A. K., Iyanger, K. N. and Ajitanand, N. N, 1986, Automatic scanning of enlarged tracks in Lexan polycarbonate. Nucl. Tracks 12, 227-229.

Mohr, E. C. J., 1932, Soils of Equatorial Regions. Edwards Ann. Arbor.

Mohr, E. C. J. and Van Baren, F. A., 1954, Tropical soils. The Hague.

Moore, J. McM, 1982, Mineral zonation near the granitic batholith of south west England and some geothermal analogues. In: Evans, A. M. (Ed.) Metallization Associated with Acid Magmatism, Wiley, Chichester, 229-241.

Morse, R. H., 1970, The surficial geochemistry of radium, radon and uranium near Bancroft, Ontario, with applications to prospecting for uranium. Unpub. Ph. D. Thesis, Queens Univ., Kingston.

Morse, R. H., 1976, Radon counters in uranium exploration. In: Exploration for uranium ore deposits. IAEA Symp., Vienna, 229-239.

Mortland, M. M., 1958, Kinetics of potassium release from biotite. Soil Sci. Soc. Am. Proc. 22, 503-508.

Nesbitt, H. W., Morkovics, G. and Price, R. C., 1980, Chemical processes affecting alkalis and alkaline earths during continental weathering. Geochim. Cosmochim. Acta. 44, 1659-1666.

Neuerburg, A., 1955, Uranium in igneous rocks of the United states. Int. Conf. Peaceful Uses of Atomic energy 6, 264-274.

Nielson, K. K., Rogers, V. C., Mauch, M. L, Hartley, J. N. and Freeman, H. D, 1982, Radon emanation characteristics of uranium mill tailings. Uranium mill tailings management Proc. 5th Symp. Colorado, State Univ.

Nockolds, S. R. and Allen, R., 1953, The geochemistry of some igneous rock series. Geochim. Cosmochim. Acta. 4, 105-141.

Nurmia, M. and Karras, M., 1960, Natural radioactivity of samarium and neodynmium. Nature 190, 601.

Odumodu, L. O., 1983, Rainfall distribution, variability and probability in Plateau State, Nigeria. J. Climatology 3, 385-393.

Ollier, C., 1969, Weathering. Oliver and Boyd, Edinburgh.

Oshin, I. O., and Rahman, M. A., 1986, Uranium favourability study in Nigeria. J. Afr. Earth Sci 5, 167-175.

Osmond, J. K. and Cowart, J. B., 1982, Groundwater. In: Ivanovich, M. and Harmon, R. S. (Eds.), Uranium Series Disequilbrium Studies: Applications to Environmental Problems. Oxford, Oxford Univ. Press.

Ostrihansky, L ., 1976, Radiometric disequilibrium determinations 2. Radioactive disequilibrium investigations, Elliot Lake area, Ontario. Paper Geol. Surv. Can., 75-38, 19.

Parker, A., 1970, An index of weathering for silicate rocks. Geol. Mag. 107, 501-504.

Pastor, J., and Turaki, U. M., 1985, Primary mineralization in Nigerian ring complexes and its economic significance. J. Afr.

Patterson, C., Tilton, G. R., and Inghram, M., 1953, Concentration of uranium and lead and the isotopic composition of lead in meteoric materials. Phys. Rev. 92, 1234-1235.

Pedersen, C. P., Dunbier, J and Gingrich, J. E., 1980, Experience with the Track Etch method for uranium exploration in Northern Australia. In: Ferguson, J. and Goleby, A. B. (Eds.), Uranium in the Pine Creek geosyncline. IAEA, Vienna.

Peebles, P. J. E., 1968, Primeval element abundance. In: Ahrens, L. H. (ed.), Origin and distribution of the elements. Pergamon, Oxford.

Pendleton, R. L., 1953, Povisional map of soils and surface rock of the Kingdom of Siam, Bangkok.

Perkins, R. W., Thomas, C. W. and Nielsen, J. M., 1965, Measurements of airborne radionuclides and determinations of their physical characteristics. In: Proc of Conf. on Radioactive Fallout from Nuclear Weapons Tests, Washington, U. S. Atomic Energy Comm., Washintgton.

Pettijohn, F. J., 1949, Sedimentary rocks. Harper, New York.

Piccioti, E. and Wilgain, S., 1954, Thorium determination in deep sea sediments. Geochim. Cosmochim. Acta. 6, 197-207.

Pitcher, W. S., 1979, Comments on the geological environments of granites. In: Atherton, M.P. and Tarney, J. (Eds.), Origin of granite batholiths, geochemical evidence. Shira, Cheshire.

Pliler, R. and Adams, J. A. S., 1962, The distribution of thorium and uranium in a Pennsylvania weathering profile. Geochim. Cosmochim. Acta 26, 1137-1146.

Poldevaart, A., 1955, Chemistry of the earth's crust. In: Poldevaart, A. (Ed.), Crust of the Earth - A Symp. geol. Soc. Am. Spec. paper 62, 119-144.

Polynov, B. B., 1937, Cycle of weathering. Murby, London.

Poole, J. H. J. and Bremmer, J. W., 1949, Investigation of the distribution of radioactive elements in rocks by the photographic method. Nature 163, 130-131.

Price, P. B. and Walker, R. M., 1963, A simple method of measuring low uranium concentrations in natural crystals. Appl. Phys. Lett. 2, 23-25.

Prutkin, M. I. and Shashkin. V. L., 1966, Radon emanation from uraniferous ores and minerals immersed in liquid. Atomnaya Energiya 22, (2), 140-141. (Engl. Trans.).

Ragland, P. C., 1964, Autoradiographic investigations of naturally occuring materials. In: Adams, J. A. S. and Lowder, W. M. (Eds.) The natural radiation environment. Univ. Chicago Press, Chicago.

Ragland, P. C., Billings, G. K., and Adams, J. A. S., 1967, Chemical fractionation and its relationship to the distribution of thorium and uranium in a zoned granite batholith. Geochim. Cosmochim. Acta. 31, 17-33.

Rankama, K., and Sahama, Th. G., 1949, Geochemistry. Chicago univ. press, Chicago.

Reiche, P., 1943, Graphic representation of chemical weathering. Jour. Sed. Petrology 13, 58-68.

Reimer, G. M., Derton, E. H., Friedman, I. and Otton, J. K., 1979, recent developments in uranium exploration using the U. S. geological survey's mobile helium detector, Jour. Geochem. Explor.

Rich, R. A., Holland, H. D. and Peterson, U., 1988, Hydrothermal Uranium deposits. Elsevier, Amsterdam.

Rich, C. I. and Obenshain, S. S., 1955, Chemical and clay mineral properties of a red and yellow podsolic soil derived from muscovite schist. Proc. Am. Soil Sci. 19, 334-339.

Ridland, G. C., 1945, Use of the Geiger-Muller counter in the search for pitchblende-bearing veins at Great Bear Lake, Canada. Trans. Am. Inst. Min. Metall. Eng. 164, 117-124.

Ries, H, 1908, Clays: Their Occurrence, Properties and Uses. Wiley, New York.

Richardson, K.A.,1963, Thorium, uranium and potassium in the Conway granite, New Hampshire, U.S.A. In: Adams, J. A. S. and Lowder, W.J. (Eds.), Natural radiation environment, Univ. of Chicago press, Chicago.

Robinson, G. W., 1951, Soils, their origin, constitution and classification. Murby, London.

Rogers, J. J. W. and Ragland, P. C., 1961, Variation of thorium and uranium in some selected granitic rocks. Geochim. Cosmochim. Acta. 25, 99-109.

Rogers, J. J. W., and Adams, J. A. S., 1963, Lognormality of thorium in the Conway granite. Geochim. Cosmochim. Acta. 27, 475-783.

Rose, A. W. and Korner, L. a., 1979, Radon in natural waters as a guide to uranium deposits in Penynsylvania. In: Watterson, J. R. and Theobold, P. K. (Eds.), Geochemical Exploration, 1978, Ontario, Ass. Explor. Geochem.

Rosholt, J. N., 1959, Natural radioactive disequilibrium of the uranium series. U. S. Geol. Surv. Bull., 1084-A

Ruxton, B. P., 1968, Measures of the degree of chemical weathering of rocks. J. Geol. 76, 518-527.

Sand, L. B., 1956, On the genesis of residual kaolin. Am. Mineral. 41, 28-40.

Seidel, A., 1965, Solubilities: Inorganic and metal organic Compounds. Am. Chem. Soc. 2, 1383.

Senftle, F.E., Farley, T. A. and Stieff, L. R., 1984, A theoretical study of alpha star populations in loaded nuclear emulsions. Geochim. Cosmochim. Acta. 6, 197-207.

Shaw, D. M., 1968, A review of K:Rb fractionation trends by covariance analysis. Geochim. Cosmochim. Acta. 32, 573-601.

Sheppard, S. M. F., 1977, The Cornubian batholith: D/H and O^{16}/O^{18} studies of kaolinite and other alteration minerals. J. Geol. Soc. London 133, 573-591.

Sheppard, J. J., Miller, M. F., Scrivener, R. C., and Derbyshire, D. P.F., 1985, Hydrothermal fluid evolution in relation to minerals zonation in southwest England with special reference to the Dartmoor-Bodmin area In: High Heat Production (HHP) granites, hydrothermal circulation and ore genesis. Inst. Min. metall., London 345-364.

Short, N. M., 1961, Geochemical variation in four residual soils. J. Geol 69, 534-571.

Siegbahn, K. (Ed.),1965, Alpha-, Beta- and gamma-ray spectroscopy. Interscience, New York.

Siever, R., 1957, The silica budget in the sedimentary circle. Am.

Silver, L. T., Woodhead, J. A. and Williams, I. S., 1982, Primary mineral distribution and secondary mobilisation of uranium and thorium in radioactive granites. Procedings on Peaceful Uses of Atomic Energy. IAEA, Vienna.

Simpson, P. R., Plant, J, and Cope, M. J., 1977, Uranium abundance and distribution in some granites from northern Scotland and southwest England as indicators of uranium provinces. Proc. Int. Symp. Inst. Min. Metall., London, 126-139.

Singh, N. P., Singh, M. and Singh, S., 1986, Uranium and thorium analysis in geological samples using plastic track detectors. Nucl. Tracks 12, 883-886.

Smith, A. Y. and Dyck, W., 1969, The application of radon methods to geochemical exploration for uranium. Annual Meeting., Can. Inst. Min. Metall, Montreal.

Smyth, C. H., 1913, The relative mobilities of the chemical constituents of rocks. J. Geol. 21, 105-120.

Spiegel, M. R., 1961, Theory and Problems in Statistics - Scaum's outline series. McGraw-Hill, New York.

Staatz, M. H., Conklin, N. M. and Brownfield, I. K, 1977, Rare earths, thorium and other minor elements in sphene from some plutonic rocks in west-central Alaska. J. Res. U. S. Geol. Surv 5, 623-628.

Stephen, J., 1952, A study of rock weathering with reference to the soils of the Malvern Hils. J. Soil Sci. 3, 20-33.

Stephens, F. S. Jr., Asaro, F. and Perlman, I., 1957, Odd-Parity Rotational Bands in Even-Even Nuclei. Phys.. Rev. 107, 1091-1094.

Stone, M., 1975, Structure and petrology of the Tregonning-Godolphin granite, Cornwall: Proc. Geol. Assoc. 86, 155-170.

Stuckless, J. S. and Van Trump G. Jr., 1982, An evaluation of uranium content in zircon from igneous rocks of the contiguous United States as an aid to exploration and resource assessment. Proc. Peaceful Uses of Atomic Energy, Vienna.

Swardt, A. M. J. De, 1950, Recent erosion surfaces on the Jos Plateau. Proc. Int. W. Afr. Conf. III, Ibadan.

Talvitie, N. A., 1972, Electrodeposition of actinides for alpha spectrometric determinations. Anal. Chem. 44, (2), 280-283.

Tammemagi, H. Y. and Smith, N. L., 1975, Terrestrial heat flow and heat generation in south west England. J. Geol. Soc. London 131, 415-427.

Tanner, A. B., 1964, Radon migration in the ground: A review. In: Adams, J. A. S. and Lowder, W. M. (Eds.), Natural Radiation Environment. Chicago Univ. Press, Chicago, 161-190.

Taylor, S. R., 1964, Abundance of chemical elements in the continental crust: A new table. Geochim. Cosmochim. Acta. 28, 1278-1285.

Thurber, D. L., 1962, Anomalous U-234/U-238 in nature. J. Geophys. Res. 67, 4518.

Titayeva, N. A., Taskayev, A. I., Ovchenkov, V. Ya, Aleksakhin, R. M. and Shuktomova, I. I., 1973, Behaviour of uranium and thorium isotopes in crystalline rocks and surface waters in a cold climate. Geochem. Internat. 10, 1146-1151.

Turekian, K. K., 1977, Geochemical distribution of the elements. In: Encyclopadia of science and technology, McGraw-Hill, New York, 627-630.

Turekian, F. K. and Wedepohl, K. H., 1961, Distribution of the elements in the major units of the earth crust. Bull. Geol. Soc. Am. 72, 175

Uwah. E. J, 1984, Investigation of radiometric anomalies by Nuclear and other methods (A case study of the Sokoto basin of Nigeria). Unpub. Ph. D. Thesis, Ahmadu Bello Univ. Zaria.

Vinogradov, A. P., 1962, Average content of chemical elements in the major types of igneous rocks of the Earth's crust. Geochemistry 7, 641-664.

Vogt, J. H. L., 1931, On the average composition of the Earth's crust with particular reference to the contents of phosphoric and titanic acid. Skr. Nor. Vidensh. Akad. Oslo 1, 1-48.

Walker, G. F., 1949, Decomposition of biotite in the soil. Min. Mag. 28, 693-708.

Wheildon, J., Francis, M. F., Ellis, J. R. L. and Thomas-Betts, A., 1980, Exploration and interpretation of the S.W. England geothermal anomaly. In: Strub, A.S.and Ungemah, P. (eds). Advances in European geothermal research: Proc. second int. seminar on results of European community geothermal energy research, Strasbourg,

White, D. E., Hem, J. D. and Waring, G. A., 1963, Data of geochemistry. Chemical composition of subsurface waters. U.S. Geol. Surv. Prof. Paper 440-F.

Whitefield, J. M., Rogers, J. J. W. and Adams J. A. S., 1959, The relationship between the petrology and the thorium and uranium contents of some granitic rocks. Geochim. Cosmochim.. Acta. 17, 248-271.

Wollast, R., 1967, Kinetics of the alteration of K-feldspar in buffered solutions at low temperature. Geochim. Cosmochim. Acta. 31, 635-648.

Wollenberg, H., Kunzendorf, H. and Rose-Hansen, J. (1971), Isotope-excited X-ray fluorescence analysis for Nb, Zr, and La+Ce on outcrops in the Ilimansaq intrusion, south Greenland. Econ. Geol. 16, 1048-1060.

Yagoda, H., 1946, Localization of uranium and thorium minerals in polished section. Part 1: Alpha ray emission pattern. Am. Mineral. 31, 87-124.

Young, A., 1980, Tropical Soils and soil survey. Interprin., Malta.

Zaghloul, Z. M., 1958, Radioactive accessory zircons of Land's End granite, south-west England. Unpub. Ph. D. Thesis, Univ. of Bristol.

Ziemens, K. E., 1943, Surface area determination and diffusion measurements by means of radiometric inert gases. Ztschr. Phys. Chem. 192, 1-55.

KAS[illegible]RARY
AH[illegible]
ZARIA. [illegible]ERSITY